University of Stavanger

Faculty of Science and Technology

MASTER'S THESIS

Study program/Specialization: Offshore Technology- Marine and Subsea Technology	Spring semester, 2013 Restricted access
Writer: Christer Eiken	………………………………………… (Writer's signature)
Faculty supervisor: Professor Ove Tobias Gudmestad External supervisor(s): Odd Reidar Boye (IKM Testing)	
Title of thesis: Pre-commissioning hose operations on the Valemon field in the North Sea	
Credits (ECTS): 30	
Key words: Marine pre-commissioning operation, Valemon field in the North Sea, flexible hose, OrcaFlex, static and dynamic analysis	Pages: 108 + enclosure: 265 Stavanger, 14.06.2013. Date/year

Master Thesis

Pre-commissioning hose operations on the Valemon field in the North Sea

by

Christer Eiken

June 2013

University of Stavanger

N-4036 Stavanger

Abstract

Marine operations for the offshore industry worldwide have been carried out for several decades and for each operation one has to consider which environmental conditions one can operate under. All operations should be performed in a safe and efficient manner; therefore an analysis for every specific operation with field specific conditions should be carried out to be able to define the operation limiting criteria's. Pre-commissioning hose operations are relatively unusual marine operations which require applying the relevant flexible riser regulations.

Attention is given to a pre-commissioning operation which consists of flooding, cleaning and gauging of the 22" gas pipeline from the Huldra platform to the Valemon platform in the North Sea. The aim of the study is to find the optimum hose configuration and define the limiting criteria for this operation.

Two hose types will be considered, where experimental testing is carried out for one of the hoses (6" Oilflex Super hose) to identify unknown parameters to achieve a more accurate analysis. For the other hose type, adequate information was available to carry out analysis. Thereafter standard flexible riser configurations are considered as potential hose configurations for this operation and appropriate configurations are selected qualitatively for further evaluation using the computer software OrcaFlex. In Orcaflex, the remaining configurations will be considered for representative environmental loads from the Valemon field. Based on these loads, an optimum model will be selected.

The free hanging configuration for the 4" Bunkerflex STH gave the highest operating limiting criterions for this pre-commissioning operation compared with different lazy wave configurations. The critical limitations were too high compression load and too high curvature for the hose, mainly in the splash zone, under the selected environmental cases. The operation limiting criteria is in addition to the environmental loads dependent on the arrangement on deck.

The operation can be carried out during a weather window with up to H_s = 2.15 m without violating the identified limitations.

Key words: Marine pre-commissioning operation, Valemon field in the North Sea, flexible hose, OrcaFlex, static and dynamic analysis

Acknowledgements

First, I would like to thank Prof. Ove Tobias Gudmestad, my faculty supervisor, for all his guidance and help during this Master Thesis. I consider it as an honor to work with him during my master study at the University of Stavanger.

I would also like to thank the following persons:

- Subsea Engineering Manager Odd Reidar Boye, my external supervisor, at IKM Testing for contribution of Master Thesis topic and his guidance during the study.
- Pipeline Engineer Espen Svendsen for his contribution during the experimental hose testing and during the OrcaFlex analysis.
- My good friend and PhD student Ole Erik Vestøl Endrerud for his help and guidance of how to solve a scientific problem.
- My friend and student colleague Maria Nikolaevna Urycheva for good academic discussions and understandings during the study.
- My student colleagues Tesfalem Keleta, Jihan Herdiyanti, Sadjad Karegar at IKM Ocean Design for good academic discussions during the study.
- Fadil Maksutaj for allowing me to perform experimental hose testing at the IKM Testing workshop at Bærheim.
- Foreman Svein Jan Landsnes for help and guidance during my hose testing.
- Equipment Engineer Knut Bjerkan for logistics of equipment used during my experimental hose testing.

Finally, I would like to thank everybody else who helped me during this Master Thesis, and a special thanks to IKM Testing and IKM Ocean Design for sharing information, and providing offices, workshop, equipment and software at my disposal.

Sincerely,

Stavanger, 9th June 2013

____

Christer Eiken

Table of Contents

List of Figures

List of Tables

List of Abbreviations

API	American Petroleum Institute
BR	Bend Radius
COG	Centre Of Gravity
DNV	Det Norske Veritas
HAZID	Hazard Identification Study
HAZOP	Hazard and Operability Study
ID	Inner Diameter
LRFD	Load and Resistance Factor Design
MBR	Minimum Bending Radius
NCS	Norwegian Continental Shelf
OS	Oilflex Super
OD	Outer Diameter
RAO	Response Amplitude Operator
RFO	Ready For Operation
ROV	Remotely Operated Vehicle
TDP	Touch Down Point
ULS	Ultimate Limit State
VIV	Vortex Induced Vibrations

List of Symbols

Latin symbols

a	Moment arm
a_c	Acceleration
a_r	Fluid acceleration relative to the body
a_w	Fluid acceleration relative to earth
a_{wave}	Wave amplitude
A	Area
A_e	External cross sectional area of pipe
A_i	Internal cross sectional area of pipe
AE	Axial stiffness
c	Phase velocity
C_A	Added mass coefficient
C_D	Drag coefficient
C_m	Inertia coefficient
$C(p,c)$	System damping load
d	Water depth
ds	Hose element length
e	Damping coefficient of the line
F	Axial load
$F(p,v,t)$	External load
F_w	Fluid force
F_x	Force in x-direction
g	Gravitational acceleration
h	Arc height
H	Wave height
H_s	Significant wave height
k	Curvature
k_{BX}	Curvature Bunkerflex hose
K_c	Keulegan-Carpenter number
k_{OS}	Curvature Oilflex Super hose
$K(p)$	System stiffness load
L	Length
L_i	Length from hose start to any given point
L_o	Unstretched length
L_s	Segment length
M	Moment

$M(p,a)$	System inertia load
OP_{LIM}	Limiting operational environmental criteria
OP_{WF}	Forecasted operational criteria
p	Position vector
p_e	External pressure
p_i	Internal pressure
R	RAO amplitude
R_c	Characteristic resistance
R_d	Design resistance
R_{dBXC}	Design resistance Bunkerflex hose compression
R_{dBXT}	Design resistance Bunkerflex hose tension
R_{dOSC}	Design resistance Oilflex Super hose compression
R_{dOST}	Design resistance Oilflex Super hose tension
R_e	Reynolds number
S	Wave steepness parameter
S_b	Bending stiffness
t	Time
T	Wave period
T_C	Estimated maximum contingency time
T_e	Effective tension
T_h	Horizontal force on seabed
T_{POP}	Planned operation period
T_R	Operation reference period
T_t	Top tension
T_{tw}	True wall tension
u_c	Surface current speed
u_r	Current speed 3 m above sea
U_R	Ursell number
v	Velocity
v_r	Fluid velocity relative to the body
V	Volume of body
w	Arc width
w_a	Apparent weight per unit length
W_e	External fluid weight per unit length
w_h	Hose weight per unit length
w_i	Internal fluid weight per unit length
x	Horizontal distance from TDP
X	Vessel displacement
z	Height above seabed

Greek symbols

α	Factor accounting for uncertainty in weather forecast
β	Angle with the vertical
β_w	Direction of propagation
γ_E	Environmental load effect
γ_m	Material resistance factor
γ_{SC}	Safety class roductionesistance factor
δ	Displacement
Δ	Mass of fluid displaced by the body
ε	Total mean axial strain
η	Expansion factor of a segment
λ	Wave length
θ	Angle to the x-axis
Θ	Phase function
ν	Poisson ratio
ξ_a	Free surface elevation
ρ	Water density
ρ_{sea}	Seawater density
ρ_{tw}	Treated water density
ψ	Non dimensional roughness number
φ	Phase
ω	Wave frequency

Chapter 1. INTRODUCTION

1.1 Background

Marine operations have been, and still are, very important for the development of the oil and gas industry worldwide. New fields have to be developed and existing fields needs to be maintained. In Norway, offshore production facilities have been developed on the Norwegian Continental Shelf (NCS) over the last 40 years and have given valuable experiences on how to perform safe and efficient marine operations.

On the NCS structures are exposed to harsh environmental conditions. Safety is crucial to avoid devastating consequences, and the demand for top quality engineering is high. Different kinds of marine operations on different locations have different sets of requirements. Vessel characteristics, environmental conditions and seasonal characteristics are parameters that determine the operability. Smart solutions and innovative thinking may increase operability and reduce the cost of marine operations.

Analysis of operation with implementation of actual met-ocean data results in limitations for the operation. By identifying critical parameters makes it possible to increase operability time.

1.2 Problem statement

We will study an operation that is dependent on the use of hoses for transfer of fluids between a vessel and a platform. The hose configuration for a marine operation can be arranged in several different ways. Every specific operation has to consider different kind of configurations based on vessel type, duration of the operation, hose properties, equipment to be used, arrangement on deck and relevant hydrodynamics for the location. What is the best configuration for this specific marine operation?

So far no one has developed an offshore standard for application of hoses for marine operations. However, because flexible risers have similarities with hoses, the regulations for flexible risers can be applied.

Although each operation has to be treated separately, a comparison of requirements in similar areas can also be useful for future operations.

1.3 Purpose and scope

This research focuses on a marine operation that will be carried out on the Valemon field by IKM in 2013. The aim is to make an accurate analysis for this particular application in this specific field. Different kind of hose configurations will be investigated for this operation. Some relevant configurations will be discussed theoretically, while some recommended configurations will be considered both in a static and a dynamic analysis. The dynamic analysis will define the optimum configuration and based on this configuration, the operation limiting criteria for the operation will be defined. These criteria are specific for the planned equipment and are based on the relevant regulations. Vessel data will be as for the Skandi Inspector vessel. The analysis should conclude on how the operation can be carried out with respect to relevant regulations.

Scope of the thesis:

- Experimental testing of a relevant hose to gather input data for the analysis (6" Oilflex Super);
- Consider the metocean design basis for the Valemon field in the analysis;
- Study the relevant standards to be able to create operational requirements for the models;
- Describe the equipment used in the operation;
- Discuss general configurations that is used for similar operations;
- Analyse appropriate configurations with software programs;
- Discuss and evaluate results;
- Find an optimum model and limitations for the operation.

1.4 Limitations

- The waves are considered to approach at ±45° from the bow;
- The currents are considered to approach the vessel from the stern, starboard side, bow and port side;
- Wind loads are not considered in the analysis;
- Fatigue analysis is not considered;
- Vortex induced vibrations (VIV) is not included;
- Torsion is not considered;
- Installation phase is not considered in the analysis.

1.5 Thesis organization

Chapter 2 (Design basis) presents Valemon field data, requirements to standards, operational aspects and limiting criteria, hose parameters and environmental data to be considered in the further analysis.

Chapter 3 (System description) gives an introduction to the equipment which will be used for the operation. This involves vessel type, reel, chute and hose types considered for this operation. This chapter also gives a description of pigging activities.

Chapter 4 (Operation) contains pre-commissioning operations in general and a description of the specific pre-commissioning operation that will be carried out on the Valemon field. In addition, a theoretical comparison between flexible pipe and hose is performed. General riser configurations will be identified and considered as hose configurations for the operation and evaluated.

Chapter 5 (Theoretical basis for hydrodynamic loads) addresses the relevant wave theory for this field and also considers hydrodynamic loads.

Chapter 6 (Analysis) gives an introduction to the software program OrcaFlex, which is used for the analysis and describes how the specific model is built up for this operation. This chapter also addresses theoretical static analysis. In addition, static and dynamic analyses for the two different hoses are carried out for several configurations in OrcaFlex. A section about verification and validation for the selected models is included, before the influence of current is considered for the optimum configuration. Finally, the operational requirements for the operation are defined.

1.6 Research methodology

The objective of this thesis is defined in chapter 1.3. This will be accomplished by the following methodology:

- First the operational requirements for the vessel and hose will be defined according to Det Norske Veritas (DNV) rules and regulations. DNV is chosen because they have established basic requirements on the NCS.
- Experimental testing will be carried out on one of the hoses (6”Oilflex Super) to find unknown parameters. This is done to find missing parameters needed in OrcaFlex to be able to create a representative model. Different hose samples will be tested in compression, tension and bending with different methods. These tests are carried out to identify axial stiffness in compression/tension and bending stiffness.
- Thereafter relevant hose configurations will be identified for the operation. Suitable configurations will be selected qualitatively based on simplicity, operation time and mobilising/ demobilising. These selection criterions are emphasised because the marine operation duration is less than 48 hours.
- Then the recommended configurations will be investigated more in detail with numerical software for the 4” Bunkerflex STH hose and the 6” Oilflex Super hose. This will tell which hose is most suitable for the different configurations. The optimum hose configuration will be able to be used in the worst weather conditions. This is done because the software can determine under which conditions and how the operation can be carried out. Computer modelling is carried out with the computer program OrcaFlex, which is a marine dynamics program for static and dynamic analysis of offshore systems. OrcaFlex software is chosen because it can consider site specific conditions and calculate relevant load effects during the operation. It is also the only relevant software program accessible for this thesis. The loads will be compared with the operation requirements, and are based on safety factors from DNV. The model is only valid for use of the Skandi

Inspector operating on the Valemon field. This is because RAO data for the vessel will be implemented in the analysis, and representative environmental conditions for the Valemon field are used. Statoil gives the meteocean data for the Valemon field. The methodology could be applied to other fields and vessels, however.

- The model will be compared with an OrcaFlex analysis for a 6” Bunkerflex hose carried out by IKM. This is to check that the model corresponds and acts in the same manner as the one carried out by an OrcaFlex specialist in IKM. The model will be verified with *animation*, *comparison to other models* and *face validity*. *Animation* is a part of the dynamic analysis in OrcaFlex where the model’s operational behaviour is displayed graphically as the model moves through time [1]. *Comparison to other models* is used to check the model corresponds with results from other validated models. *Face validity* is also used to ask an OrcaFlex specialist whether the models behaviour is reasonable [1].
- The optimum hose configuration will be exposed for current in different directions to identify potential critical current directions.

Below, in Figure 1.1 a methodology chart for the study is given.

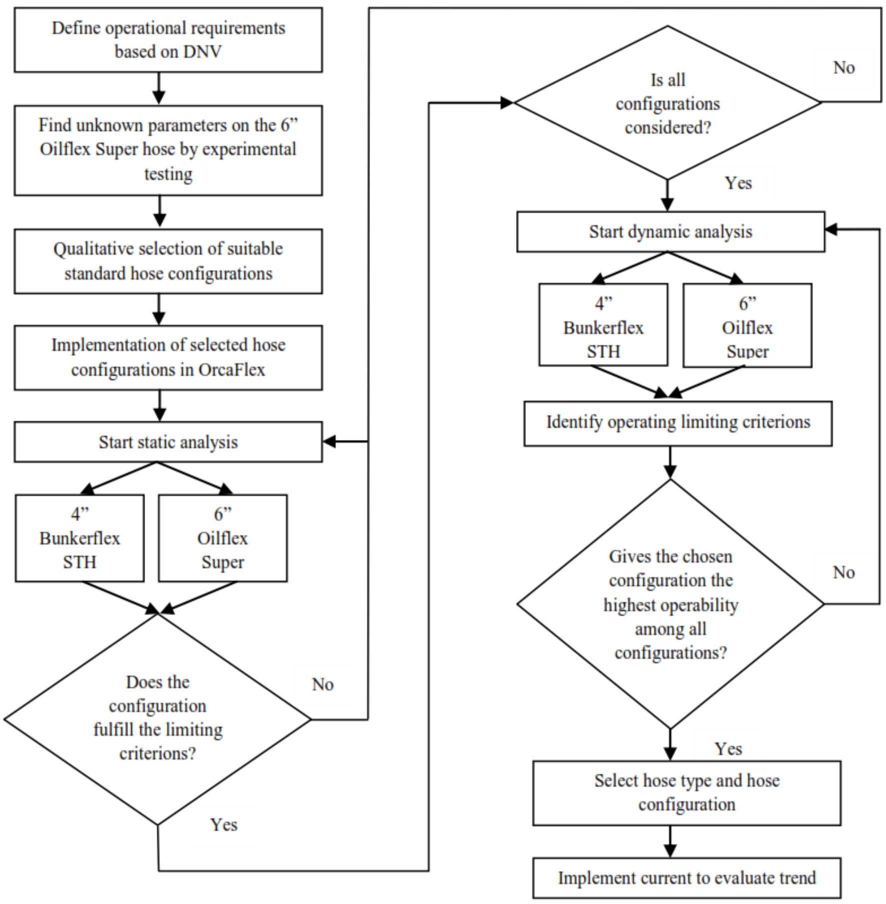

Figure 1.1 Methodology chart for Master Thesis

Chapter 2. DESIGN BASIS

IKM will perform a pre-commissioning operation on the Valemon field in the summer season of 2013. For this operation the DNV design codes, standards and regulations will be used. The details of the design basis are only valid for the pre-commissioning operation on the Valemon Field.

This chapter will discuss the Valemon field in general, the requirements to standards used for this operation, operational aspects and limiting criteria, hose parameters, and environmental data applied for the analysis.

2.1 The Valemon field

The Valemon field is a gas and condensate field located in the northern part of the North Sea. The field was first discovered in 1985 and is still under development. The production is planned to start in 2014.

The recoverable reserves in the Valemon field are estimated to be 33.5 mill Sm^3 oil equivalents. The development concept is a wellhead platform that will be remotely controlled from the Kvitebjørn platform via a power cable and a fibre optic cable. The structure is a four legged jacket structure that was installed in 2012. The wellhead platform will only be manned during drilling, work-over and pigging activities. Drilling and work-over activities will be performed with a jack up rig from 2012 to 2014. The water depth is about 135 metres and the reservoir is characterized with high pressure and temperature, and is laying approximately 4000 metres below the seabed.

The process facilities will consist of a simple separation process where the gas and condensate will be separated into unstable condensate and rich gas. The unstable condensate will be transported to the Kvitebjørn platform with a new 8" pipeline. The rich gas will be exported with a new 22" pipeline to the Heimdal platform. The 22" pipeline will be tied in to the existing Huldra-Heimdal pipeline before the rich gas is further treated at the Heimdal platform.

The Kvitebjørn platform is located 14 km east of the Valemon field, while the Huldra platform is located approximately 27 km South-East for the Valemon platform. Below, in Figure 2.1, a map of the northern part of the North Sea is shown.

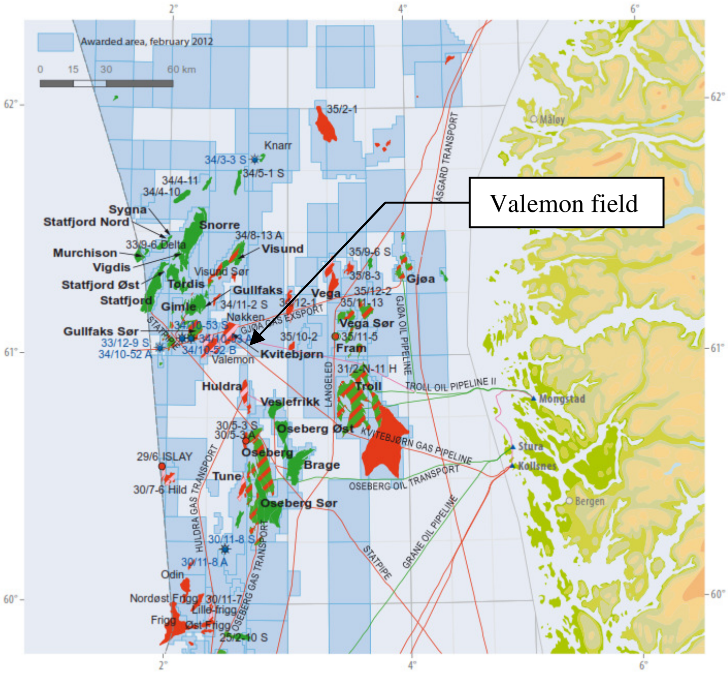

Figure 2.1 Fields and discoveries in the northern part of the North Sea [2]

2.2 Standard requirement

Marine operations and dynamic riser design methodology, considerations and calculations are based on standards and recommended practices according to DNV. The following standards and recommended practices have been applied in this thesis:

- DNV-OS-F201 (2010) – *Dynamic Risers*
- DNV-OS-H101 (2011) – *Marine operations, General*
- DNV-OS-H102 (2012) – *Marine Operations, Design and Fabrication*
- DNV-OSS-302 (2010) – *Offshore Riser Systems*
- DNV-RP-C205 (2007) – *Environmental conditions and environmental loads*

It is worth to mention that DNV service documents consist of the following types of documents [3]:

- *Service Specifications* which give procedural requirements.
- *Standards* which give technical requirements.
- *Recommended practices* which give guidance.

2.3 Operational aspects and limiting criteria

The planned schedule for the operation is as follows:

- Installation of the hose from the vessel to seabed is estimated to take 4 hours.
- Pigging from Huldra to Valemon is estimated to take 26 hours.
- Pull up hose is estimated to take 2 hours.

The duration of marine operations shall be defined by an operation reference period, T_R [4]:

$$T_R = T_{POP} + T_C \qquad \textbf{(2-1)}$$

where

T_R = Operation reference period [hours]

T_{POP} = Planned operation period [hours]

T_C = Estimated maximum contingency time [hours]

As discussed above, T_{POP} is estimated to be 32 hours. The T_C shall cover [4]:

- General uncertainties in the planned operation time, T_{POP}
- Possible contingency situations that will require additional time to complete the operation.

As mentioned, the estimated pull up time is specified to be 2 hours. However, the contingency situations are not assessed in detail. According to DNV [4], the reference period should then normally at least be taken as twice the planned operation period.

$$T_R \geq 2 \times T_{POP} \qquad \textbf{(2-2)}$$

Marine operations with a reference period (T_R) less than 96 hours and a planned operation time *(*T_{POP}*)* less than 72 hours may normally be defined as weather restricted [4]. The pre-commissioning operation is thus a weather restricted operation, based on:

$$T_R \geq 2 \times 32 = 64 \text{ hours} \qquad \textbf{(2-3)}$$

Weather restricted operations use specified values, while unrestricted operations are based on statistical data [5].

The limiting operational environmental criteria, OP_{LIM}, shall be established and be clearly described. According to DNV, the OP_{LIM} [4] shall not be taken greater than the minimum of:

a) The environmental design criteria.
b) Maximum wind and waves for safe working- (e.g. at vessel deck) or transfer conditions for personnel.
c) Equipment (e.g. ROV and cranes) specified weather restrictions.
d) Limiting weather conditions of diving system (if any).
e) Limiting conditions for position keeping systems.
f) Any limitations identified, e.g. in HAZID/HAZOP, based on operational experience with involved vessel(s), equipment, etc.
g) Limiting weather conditions for carrying out the identified contingency plans.

The ROV has a limitation at a significant wave height, H_S= 4 m. The OP_{LIM} criteria will be analysed in Chapter 6.

There are uncertainties in monitoring and forecasting of environmental conditions. Based on this, DNV [4] recommends to define a forecasted operational criteria as:

$$OP_{WF} = \alpha \times OP_{LIM} \tag{2-4}$$

where

OP_{WF} = Forecasted operational criteria [hours]

α = Factor accounting for uncertainty in weather forecast

In the North Sea and the Norwegian Sea the α-factor should normally be selected according to relevant tables as given in Table 2.1 [4].

Table 2.1 α-factor for waves, base case [4]

Operational period [h]	Design Wave height [m]						
	$H_S = 1$	$1 < H_S < 2$	$H_S = 2$	$2 < H_S < 4$	$H_S = 4$	$4 < H_S < 6$	$H_S \geq 6$
$T_{POP} \leq 12$	0.65	Liner Interpolation	0.76	Liner Interpolation	0.79	Liner Interpolation	0.80
$T_{POP} \leq 24$	0.63		0.73		0.76		0.78
$T_{POP} \leq 36$	0.62		0.71		0.73		0.76
$T_{POP} \leq 48$	0.60		0.68		0.71		0.74
$T_{POP} \leq 72$	0.55		0.63		0.68		0.72

Arrangements for receiving weather forecasts at regular intervals prior to, and during the marine operations shall be made [4]. The weather forecasts shall be area/route specific [4].

DNV categorise weather forecast into three levels [4];

- Level A
- Level B
- Level C

The pre-commissioning operation is categorised into weather forecast level C. In weather forecast level C it is not required to have a meteorologist on site, but one independent weather forecast source is required. The α-factor may change as a result of changes in forecast level, or seasonal variations.

2.4 Hose parameters

The 4” Bunkerflex STH and the 6” Oilflex Super hoses have different characteristics. In this sub chapter the hose data and design factors will be identified. In addition hose restrictions for the analysis will be defined.

2.4.1 Hose data

The hose data are essential for the analysis. Below in Table 2.2 some key data for the 4” Bunkerflex STH hose are represented, while in Table 2.3 some key data from the 6” Oilflex Super hose are listed. These hose types are described more in details in Chapter 3.4.

Table 2.2 Hose data for 4" Bunkerflex STH [6]

ID [inch]	ID [mm]	OD [mm]	Working pressure [bar]	Burst pressure [bar]
4”	102	127	30	90
Minimum Bend Radius (MBR) [mm]	Empty mass of hose in air [kg/m]	Empty mass of hose in seawater [kg/m]	Water filled mass of hose in air [kg/m]	Water filled mass of hose in seawater [kg/m]
1000	6.5	-6.5	14.7	1.7

Table 2.3 Hose data for 6” Oilflex Super [6]

ID [inch]	ID [mm]	OD [mm]	Working pressure [bar]	Burst pressure [bar]
6”	152.4	187	40	160
Minimum Bend Radius (MBR) [mm]	Empty mass of hose in air [kg/m]	Empty mass of hose in seawater [kg/m]	Water filled mass of hose in air [kg/m]	Water filled mass of hose in seawater [kg/m]
1525	13.42	-14.73	31.66	3.51

2.4.2 Design factors

According to DNV [7], the riser system (which in our case will be categorised as a hose system) shall be classified into different safety classes based on the failure consequences.

The material resistance factor governs the ultimate limit design (ULS), since fatigue is not considered in the scope. The safety class of a hose depends on [7]:

- The hazard potential of the fluid in the hose, i.e. fluid category;
- The location of the part of the hose that is being designed;
- Whether the hose is in operating or temporary state.

The fluid in the hose is filtrated, inhibited and dyed sea water which will be categorised into Category A as a typical non-flammable water-based fluid [7]. In general, the internal fluid in a pipe is categorised from class A to E where class E is most toxic.

The location of the hose will be categorised into Location 1, which is an area where no frequent human activity is anticipated [7]. The locations are separated between class 1 and 2. The Huldra field is normally not manned and is remotely operated from Veslefrikk B, which is 16 km away [2]. It is also assumed in this thesis that the horizontal distance to the Huldra platform exceeds 500 m during the pre-commissioning operation.

The operation is also defined as a temporary operation.

This results, with respect to safety class requirements, into a categorization as low. According DNV [7], this is when failure implies low risk of human injury and minor environmental and economic consequences. This results in a safety class resistance factor, γ_{SC} = 1.04.

The loads to be considered in hose systems are classified into different load categories [7]:

- Pressure (P) loads;
- Functional (F) loads;
- Environmental (E) loads;
- Accidental (A) loads.

This operation consists of all load categories described above. Therefore the highest load effect will be chosen, which is the environmental load effect, γ_E = 1.3.

The limit state category for this operation is selected as ULS. This results in a material resistance factor, γ_C = 1.15. Below, in Table 2.4 the selected design factors for this operation are listed.

Table 2.4 Design factors

Factor	Class	Value
Safety class factor, γ_{SC}	Low safety class	1.04
The environmental load effect, γ_E	ULS	1.3
Material resistance factor, γ_C	ULS, ALS	1.15

2.4.3 Hose restrictions

The design resistance is according DNV [7], based on Load and Resistance Factor Design (LRFD) method. The design resistance is defined as:

$$R_d \leq \frac{R_c}{\gamma_{SC}\gamma_E\gamma_m} \qquad \textbf{(2-5)}$$

where

R_d = Design resistance

R_c = Characteristic resistance

The characteristic resistance on the two different hoses are different. The 4” Bunkerflex STH hose has a characteristic resistance 78.5 kN in tension [8]. This leads to:

$$R_{dBXT} = \frac{78.5\ kN}{1.04 \times 1.3 \times 1.15} = 50.5\ kN \qquad \textbf{(2-6)}$$

The 6” Oilflex Super hose has a characteristic resistance 155.0 kN in tension [9]. This leads to:

$$R_{dOST} = \frac{155.0\ kN}{1.04 \times 1.3 \times 1.15} = 99.7\ kN \tag{2-7}$$

Formula (2-5) can also be applied for determine maximum compression load. Based on [8], the 4” Bunkerflex STH hose can withstand a characteristic resistance up to 5.88 kN in compression. This leads to:

$$R_{dBXC} = \frac{5.88\ kN}{1.04 \times 1.3 \times 1.15} = 3.78\ kN \tag{2-8}$$

Some samples of the 6” Oilflex Super hose were exposed to loads up to 11.28 kN during the experimental testing and no plastic deformation is observed on the hose structure. To be conservative, this will be taken as the characteristic resistance for the analyses. This leads to:

$$R_{dOSC} = \frac{11.28\ kN}{1.04 \times 1.3 \times 1.15} = 7.25\ kN \tag{2-9}$$

The curvature of the hose, k, is defined as:

$$k = \frac{1}{MBR} \tag{2-10}$$

Also the curvature for the two hoses is different. The 4” Bunkerflex STH hose has a MBR equal 1000 mm. This leads to:

$$k_{BX} = \frac{1}{1} = 1\ \frac{rad}{m} \tag{2-11}$$

The 6” Oilflex Super hose has a MBR at 1525 mm. This leads to:

$$k_{OS} = \frac{1}{1.525\ m} = 0.656\ \frac{rad}{m} \tag{2-12}$$

The following parameters are based on experimental testing:

- Axial stiffness in tension;
- Axial stiffness in compression and;
- Bending stiffness.

Parameters for the 4” Bunkerflex STH hose were obtained by IKM [8], while a test for the 6” Oilflex Super is carried out during this thesis and is attached in Appendix A. The values for axial stiffness in tension and the bending stiffness are based on internal pressure 5 barg, while the axial stiffness in compression is based on 0 barg internal pressure. Below, in Table 2.5 the parameters are listed.

Table 2.5 Parameters obtained from experimental testing

Hose type	Axial stiffness in tension	Axial stiffness in compression	Bending stiffness
4” Bunkerflex STH	700 kN	40 kN	0.2 kNm^2
6” Oilflex Super	850 kN	75 kN	1.4 kNm^2

It should be noticed that the bending stiffness is significantly higher for the 6” Oilflex Super hose compared with the 4” Bunkerflex STH hose. This can be explained by bigger wall thickness and diameter of the Oilflex Super hose.

In Table 2.6 is given an overview of the hose restrictions for the operation.

Table 2.6 Overview of hose restrictions for the operation

Restriction	4” Bunkerflex STH		6” Oilflex Super	
Design resistance in tension	R_{dBXT}	50.5 kN	R_{dOST}	99.7 kN
Design resistance in compression	R_{dBXC}	3.78 kN	R_{dOSC}	7.25 kN
Curvature	k_{BX}	1.0 rad/m	k_{OS}	0.656 rad/m

2.5 Environmental data

The metocean design basis for the Kvitebjørn and Valemon fields is delivered by Statoil and is used as the environmental data input. The environmental data should be representative for the geographical area or site and operation [4]. In this thesis environmental parameters such as wind, ice, earthquake, marine growth, and temperature are not considered in the analysis.

2.5.1 Wave

The waves have a significant effect on the behaviour of the vessel and the hose during operation. The waves are in this thesis assumed to hit the vessel bow with ±45°.

The wave height interval on the scatter diagram is from 0 to 28 m for a period of 100 years. However, since this is a temporary operation and not a design study, it is not necessary to investigate all wave heights and wave periods. The operation is planned during summer season (June-August).

Based on the monthly and annual sample distributions of non-exceedance of significant wave heights [10] it is less than 2% probable that H_S >4 m during the summer season (June-August). Therefore the upper wave height in this thesis is defined as 8 m. In comparison with winter season (December-February), the sample distributions show that it is 30 to 37% probable that H_S>4 m. These data can be seen in Table 2.7 below.

Table 2.7 Monthly and annual sample distributions of non-exceedance (%) of significant wave heighs (H_S) at the Valemon field [10]

H_s [m]	June	July	August	December	January	February
< 1	18.23	22.49	20.69	1.02	0.90	1.45
< 2	72.34	78.81	74.75	16.48	14.70	20.44
< 3	92.75	95.86	94.06	42.17	40.46	47.56
< 4	98.49	99.18	98.67	66.43	63.01	69.13
< 5	99.64	99.89	99.77	82.21	79.85	83.91
< 6	99.97	99.95	99.92	90.80	89.31	92.83
< 7	99.98	99.99	99.98	95.90	94.83	96.88
< 8	99.98	100.00	99.98	98.41	97.77	98.94

The wave period interval depends on the wave height. It is suggested in this thesis to select the wave periods based on minimum 1% probability of occurrence for the relevant wave heights. Periods having less than 1% probability are not considered as typical weather conditions at the site. The selected wave heights and wave periods are listed in Table 2.8 below.

Table 2.8 Selected wave periods based on scatter diagram [10]

Wave height, H [m]	Wave period, T [s]
2	4-14
3	4-15
4	5-15
5	6-15
6	6-15
7	6-15
8	7-15

2.5.2 Current

The current conditions are dominated by the Atlantic inflow waters which follow the western slope of the Norwegian Teench south-eastwind into the North Sea [10]. The current has a major effect on both the behaviour of the vessel and the hose configuration during operation. The current data are not from the Valemon field, but from various nearby locations. In this thesis, the currents are assumed to hit the vessel from:

- 0° direction (the astern)
- 90° direction (the starboard side)
- 180° direction (the bow)
- 270° direction (the port side)

The different directions are chosen with a 90° interval. The waves occur in a large range of directions at the Valemon field, so a current analysis from the suggested directions is recommended. The vessel will head against the waves during operation.

Based on [11], the 10 years wave is used for temporary conditions, while 100 years wave is the basis for the design. The same approach will be considered for currents.

Below in Table 2.9 is shown estimates of extreme omni-directional current speed at the Valemon field. These current speeds occur with an annual probability of exceedence (10^{-1}) according to Statoil [10].

Table 2.9 Estimates of extreme omni-directional current speed at the Valemon field [10].

Parameter	Value
Surface current speed, u_c	1.15 m/s
Current speed, u_r, 3 m above seabed	0.65 m/s

Due to lack of seasonal data, the estimates of extreme omni-directional current speeds from the design basis are considered to be too conservative for the operation. The hose configuration will most probably change shape to a large extent if using these values. It is therefore suggested to use a current speed that occurs with less than 5% probability and is based on direct measurements from the site. Below in Table 2.10, a current velocity for the operation is suggested. This velocity is also conservative and is not based on seasonal conditions.

Since the pre-commissioning operation will be carried out during summer seasonal conditions, the currents will probably be even less. However, this current velocity will be used in the analysis. A constant current profile will be assumed in the analysis.

Table 2.10 Current data [10]

Parameter	Value
Surface current speed, u_c	0.30 m/s

Chapter 3. SYSTEM DESCRIPTION

The objective of this chapter is to give a basic understanding of some of the equipment needed to carry out the planned pre-commissioning operation at the Valemon field in the North Sea. This chapter discuss the vessel, the reel, the chute, the two different hoses considered, pigging activities and other equipment for the operation.

3.1 Vessel

The vessel selected for the operation is the Skandi Inspector, which is an offshore support vessel, built by ULSTEIN in 1979. The support vessels normally include survey, standby, inspection, and installation assistance (e.g., monitoring) [12]. Skandi Inspector is defined as a Multi-Role ROV Survey and Construction Support Vessel [13].

Skandi Inspector is a quite small vessel, which is rented for relatively cheap day rate since there are a lot of comparable vessels in the market. Some considerable aspects of importance of support vessels are [14]:

- The horizontal wind, wave and current loads;
- The wave frequencies effect on the vessel's motions and accelerations;
- The vertical relative motions of the vessel and;
- Station keeping ability.

Station keeping ability refers to positioning that keeps the vessel at the right position during an operation. Skandi Inspector is equipped with both mooring equipment and a DP2 system. DP2 stands for dynamic positioning with dual redundancy. For this pre-commissioning operation, only the DP2 system will be used since the vessel can be allowed to move relatively much during operations. Even though anchoring reduces the probability of drift off, anchoring will not be considered because it will result in a more time demanding and costly operation. Below, in Figure 3.1 the Skandi Inspector vessel is shown. In addition, some key vessel data are listed in Table 3.1 below.

Figure 3.1 Skandi Inspector vessel [15]

Table 3.1 Vessel parameters for Skandi Inspector [13]

Dimensions [m]	
Length	80.77
Breadth	18.00
Draft (maximum)	4.97
Freeboard (summer)	2.13
Deck area	36 x 15 (540m^2)
Weight [tonnes]	
Mass	3345 Gross, 1004 Net
Displacement (maximum)	4740

3.2 Reel

A reel is a drum used for storage of flexible pipes or hoses in long lengths. The reel rotates normally around a horizontal axis and is used for loading and unloading of hose in an operation. Reeling helps to provide a safe operation and a safe working environment on deck. One reel that can be selected for this operation is the HHD-09 reel. This reel is delivered by IKM and is shown below in Figure 3.2. Some key data of the reel is presented below in Table 3.2.

One of the most important characteristics of the reel is the inner diameter (ID) drum. The ID shall exceed the MBR for the hose. Even though the ID of the drum is less than the MBR of the hose, it is possible to build out the ID of the drum. This can be done with one or several layers of "dummy" hoses placed on the reel, before loading the reel with the planned hose.

A reel should be fitted with the following facilities [16]:

- Fully controllable braking;
- Manual override for automatic tensioning devices;
- Back tensioning facility, e.g., for re-reeling.

Figure 3.2 Reel HHD-09 [17]

Table 3.2 HHD-09 reel data [17]

Data	
Break	Hydraulic
Emergency	Hose cutter on pressurized hydraulic accumulator
Dimensions unit [m]	
Length	6.00
Width	3.45
Height	3.75
Dimensions drum [m]	
ID drum	1.84
OD drum	3.02
Width drum	3.65
Weight [tonnes]	
Mass	22.0 (without hose installed)

3.3 Chute

A chute is a device that ensures safe transportation of the hose from the reel and over the vessel side and then into the sea. One chute that can be selected for this operation based on a 4" hose is the chute shown below in Figure 3.3, where the key dimensions are listed below in Table 3.3. This chute is delivered by IKM. The type of chute has to be reconsidered if the 6" Oilflex Super hose is more suitable for the operation.

Figure 3.3 Chute-14 [18]

Table 3.3 Chute-14 data [18]

Data	
Unit Identification	Chute-14
Dimensions [m]	
Length	4.12
Breadth	1.60
Height	2.53
Bending radius	1.20
Weight [tonnes]	
Mass	2.0

One of the most important characteristics of the chute is the bending radius. The bending radius should be equal or higher than the MBR of the selected hose. It is not recommended to do any modifications with the chute to increase the bending radius as with the reel.

This pre-commissioning operation can also be carried out with a vertical lay installation through the vessel moonpool.

In practice, the chute is often flushed with water during operation to reduce the friction against the hose. Also, there may be fixed strops fastened, to prevent the hose from jumping out of the chute.

3.4 Hose

The primary function of the hose is to transport the medium on deck safe and reliable during the pigging operation.

Previously one similar pre-commissioning operation has been carried out by IKM with a 4" Bunkerflex STH hose. For the operation on the Valemon field this 4" Bunkerflex STH hose will be compared with a 6" Oilflex Super hose to evaluate which one gives the highest operation limiting criteria's for the operation. In Appendix A there is a report from a test carried out to find mechanical properties of the 6" Oilflex Super hose. A comparable test report has been prepared previously by IKM Testing for the 4" Bunkerflex STH [8].

3.4.1 4" Bunkerflex STH

The Bunkerflex STH hose application is mainly suction and discharge of fuel, oil and chemicals [6]. Below in Figure 3.4, a Bunkerflex STH illustration is shown.

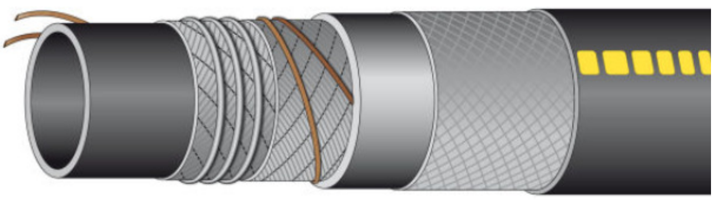

Figure 3.4 Bunkerflex STH hose illustration [6]

The Bunkerflex STH is a flexible rubber hose. The inner rubber layer is black nitrile rubber, while the second layer is a reinforcement layer, which consists of synthetic cords with a double steel helix and double ground wire. The outer cover is black neoprene rubber [6]. The synthetic cords are composed of several layers where each layer has the synthetic fibres braided. The hose is marked with a yellow, helical stripe in the longitudinal direction. Basic hose data for the 4" Bunkerflex STH hose are presented in the Design basis in Table 2.2.

3.4.2 6" Oilflex Super

The Oilflex Super hose main application is suction and delivery of oil-containing products and liquid mud (drilling mud) [6]. Below in Figure 3.5 a Oilflex Super hose illustration is shown.

The Oilflex Super is a flexible rubber hose. The inner rubber layer is black nitrile rubber, while the second layer is a reinforcement layer, which consists of synthetic cords and a steel double helix. The outer cover is black ozone and weather resistant neoprene rubber [6].

The synthetic cords are composed of 6 layers where each layer has the synthetic fibres braided. The hose is marked "TESS OILFLEX SUPER" in a longitudinal blue stripe. Basic hose data for the 6" Oilflex Super hose are presented in the Design basis in Table 2.3.

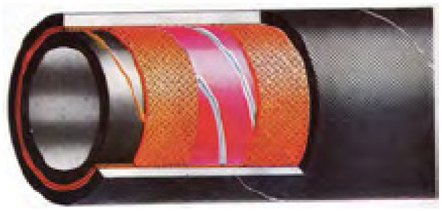

Figure 3.5 Oilflex Super hose illustration [6]

3.5 Pigging

Pigging is in general performed to protect assets and optimize the efficiency of the pipeline. Pigging is carried out in different phases of a pipeline life cycle. In the early stages pigging is used during construction. Later in the operation life cycle pigging is used for inspection, maintenance and repair, while in late life it is used for decommissioning.

In this thesis, pigging will be used for flooding, cleaning and gauging during the pre-commissioning operation. This is basically to fill the pipeline with water to perform hydrotesting or tie in, remove debris from the installation of the pipeline and to check the pipeline integrity. In this sub chapter pig types and pigging operations will be discussed briefly. This chapter is based on [19].

3.5.1 Pig types

Today there are over 350 pigs of all types, a large number of specialist services and several thousand related products [19]. The selection of pig type for different operations depends on a number of factors. The most important factors are the objective of the pigging plus the conditions for the pipeline such as pipeline length, diameter, internal coating etc. This often results in custom-made pigs, specially customised for the operation.

In this study only utility pigs will be considered, since this is the only relevant pig type for the pre-commissioning operation. Other typical pig types are; magnetic pigs, plugging pigs, gel pigs, and intelligent pigs.

Utility pigs are most often divided into cleaning pigs, which removes debris inside a pipeline and sealing pigs that can be used for separating fluids. There are often made by-pass holes in the cleaning pigs to prevent accumulation in front of the pig. Cleaning and sealing pigs are provided in four different forms [19]:

- Mandrel pigs
- Foam pigs
- Solid cast pigs
- Spherical pigs

Mandrel pigs are made up of a number of component parts, which are mounted on a body tube so that they may be replaced or re-configured as the need arises [19]. There are different configurations on the sealing devices, depending whether the pigs are unidirectional or bidirectional. The main difference between cleaning mandrel pigs and sealing mandrel pigs is that the sealing pigs do not have any cleaning elements assembled, plus the position of the seal discs are more critical on sealing pigs. Bidirectional mandrel pigs will be used for the Valemon project.

Foam pigs are made of open cell polyurethane foam [19]. The main advantage with foam pigs compared with the other types is that they are cheap and have a flexible body shape. Because of this flexible body shape the pig rarely gets stuck. The main disadvantage is the relatively low efficiency of the pigging and the service life of the pig.

Solid cast pigs are usually made of polyurethane and these pigs are moulded in one piece. The solid cast pigs are in general cheaper and lighter compared with mandrel pigs.

Spherical pigs are made in a number of different elastomers [19]. The two most used materials for spheres are polyurethane and neoprene. The main advantage for polyurethane is that it has a good tear resistance, while neoprene is resistant against wide temperature ranges. The main advantage with spheres compared with the other pig types is their ability to pig through complex pipelines. This makes them the most versatile of all pig types.

3.5.2 Pigging operations

Pigging operations can be carried out either by a single pig or with several pigs. Several pigs in one pipeline run are often referred to as a pig train. Most often pigging operations are performed with a pig train, which also is the case for the pre-commissioning operation considered in this thesis. The set up of the train depends on the objective of the pigging operation. The pigs have the ability to separate different fluids or gases in the train. Based on this a pig train makes it possible to group different chemicals such as filtrated water and nitrogen gas in a certain order.

Pig traps are the equipment used for inserting and launching pigs into an operating pipeline and for subsequently receiving and removing them from the pipeline [19]. Pig traps are often separated into pig launchers and pig receivers. Facilities for launching and receiving can be located onshore, offshore topside or offshore subsea. The layout of the pig traps varies depending on pig type, pig size, number of pigs etc. Onshore and offshore-topside traps are intended for operational pigging, while subsea traps are more related to the construction phase. Subsea traps are most often installed as pipe components on the seabed, with the pig train already installed. The pig traps often have pig signallers installed, which are able to verify that the pig reaches this position.

The driving medium inside the pipeline may vary depending on the operation. It is often preferred to use an incompressible fluid as a drive force for pigging, since it give more control over the speed and reduce wear on the pig. Gas as a driving medium requires higher safety considerations.

Pigs are most effective if they run at a constant speed. If the pig is driven too slow, it will not run smoothly through the pipeline, which may lead to leakages or by pass. Pigs will not be effective if the run is at too high a velocity [19]. The velocity also influences the sealing effect the pig has against the pipe wall. The distance between the pigs is important to prevent collision.

There are at present no recognized national or international standards for the design, construction or operation of pigs or pigging systems [19].

3.6 Other equipment

The goal of the main *pump* is to give energy to the liquid to cause it to move through a pipeline by overcoming the resistance of friction and changes in elevation [20]. A *chemical injection pump* gives energy to the chemicals from the chemical tank to the main flow.

The main *tank* should store filtered water, while the *chemical tank* contains green chemicals that will be provided in the water flow in addition to the filtrated water.

The *filter* is inserted to separate certain substances in the flow.

Chapter 4. OPERATION

Today there are a lot of different methods and designs available to carry out a pre-commissioning operation. The solutions are all based on the objectives and the requirements of the operation.

This chapter will discuss different pre-commissioning operations, the pre-commissioning operation on the Valemon field, similarities and differences between use of hoses and flexible pipes, potential failure modes, general riser/hose configurations used in the industry, and suitable riser/hose configurations for a pre-commissioning operation.

4.1 Pre-commissioning operations

Pre-commissioning, also known as for RFO (ready for operation), covers all activities from performance of the acceptance pressure test, normally part of the scope of the installation contractor, up to filling the competed pipeline with the product, and the commencement of product transportation [21]. Below, some pre-commissioning operations are described briefly:

Flooding is an operation that consists of filling the pipeline with water to perform hydro testing or facilitate tie-in [21]. Pumping one or several pigs through the pipeline with water carries out the flooding in a controlled manner. The water is firstly run through a filter followed by adding chemicals to the flow before entering the pipeline. This process is carried out to prevent corrosion and other impurities inside the pipeline.

The *cleaning* operation consists of removing debris inside the pipeline with several pig runs. With line lengths up to several hundred meters, it is particular important to remove the remaining debris such as water and rust. Most often the cleaning operation is carried out with a pig train consisting of mandrel pigs with water as the driving medium.

Hydro testing is pressurising the pipeline to verify its strength and tightness. This operation is carried out when the pipeline is water filled. This procedure starts with pressuring the water up to a specified leak test pressure. Afterwards the temperature has to stabilise for a certain time before the following holding period starts. During the holding period, the pressure is monitored. If the pressure drop overruns the allowable pressure drop, the leak must be identified and repaired. If the pressure drop is within its boundaries, the test will be approved.

Gauging is an operation that checks if there any dents in the line pipe wall after hydro testing, which could induce failure in the long term, or obstruct the passage of cleaning or batching pigs

[21]. For this purpose gauging pigs and intelligent pigs are run through the pipeline during water filling. The intelligent pigs are equipped with sensors measuring the internal diameter, while gauging pigs are equipped with a metal plate to detect possible irregularities. The metal plate is most often made of a “soft” material such as aluminium, which deforms when it hits any obstacles. The plate itself is often divided into segments to deform easily. This decreases the probability of the pig to get stuck and reduces the chance that the plate will damage the internal surface of the pipeline.

De-watering consist of removing the remaining water during or after cleaning operation. The pigs are most often driven by compressed air and the remaining water is most often discharged to sea after being diluted through a diffuser head.

Drying operations consist of removing the remaining water inside the pipeline after de-watering. Normally tree methods are used for drying:

- Methanol/glycol swapping
- Hot air drying
- Vacuum drying

These methods can be used separately or in combination. The first method, methanol/glycol swapping, involves methanol or glycol between the pigs that remove the remaining water from the pipeline. A pig train is run through the pipeline by compressed air. The second method, hot air drying, transforms the liquid to vapour by adding hot air into the system. The third and last method, vacuum drying, lowers the pressure in the system. This results in lower boiling pressure for the remaining water.

De-watering and drying activities are particular important for gas pipelines because any remaining water may react with the gas. The combination of water, high pressure and low temperature can form gas hydrates inside the pipeline that can result in plugging of pipeline and reduced functionality of the valves.

Nitrogen purging is the process when the air inside the pipeline is replaced by nitrogen. To prevent any internal corrosion between pre-commissioning and operation it is customary to fill the pipeline with a non-corrosive gas, such as nitrogen [21]. This is the last stage of the pre-commissioning operations. It is of great importance that the nitrogen content is sufficiently high to prevent corrosion. The amount of nitrogen is monitored.

Even though there are different pre-commissioning operations, some of these operations can be combined in one operation i.e. cleaning, flooding and gauging. The pig train may be up to several hundred meters, all depending on the purpose of the operation. Below, in Figure 4.1, an example of a pig train consisting of several mandrel pigs is shown. This train can be used for flooding, cleaning and gauging operations.

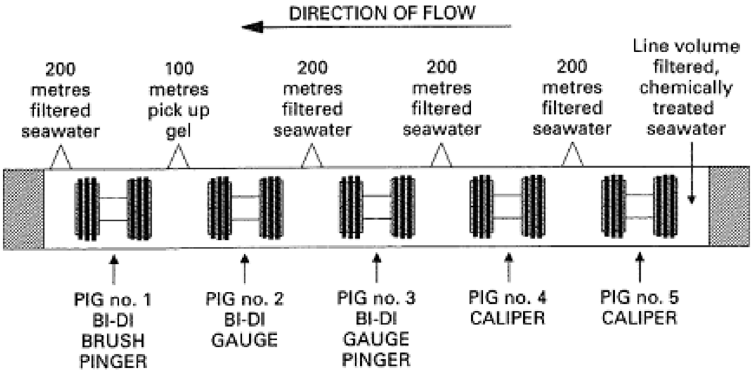

Figure 4.1 Example of pig train used for flooding, cleaning and gauging [20]

4.2 The pre-commissioning operation

The IKM pre-commissioning operation considered for this thesis is flooding, cleaning and gauging of the 22" gas pipeline from the Huldra platform to the Valemon platform. The objective of the operation is to prepare the pipeline for tie in with the Valemon riser.

The pipeline has been installed with subsea traps assembled. Initially the pipeline is air filled. The subsea launcher is pre-installed with 2 cleaning pigs and 2 gauging pigs. Pig tracking devices are pre-installed on the pigs which makes it possible to trace them during the operation.

The Skandi Inspector vessel will supply the pigs with filtrated, inhibited and dyed water as the driving medium. The inhibited water is not harmful to the environment and the dyed water is used to easily detect potential leakages in the system. The fluid will be transported from the vessel deck through a hose and down to the pipeline. First, the fluid is treated by a filter which separates certain substances in the flow before the fluid will be stored in a break tank. Then a pump transports the fluid and chemicals are added into the flow. This is done by a chemical tank and a chemical injection pump. Now the fluid is treated to enter the pipeline. This combined flow enters the reel on deck, where the fluid is transported through a hose down to the pig launcher. A chute ensures safe transportation from the vessel deck and into the sea. An illustration of this is shown below in Figure 4.2. The same medium will be used to separate the pigs in the pig train.

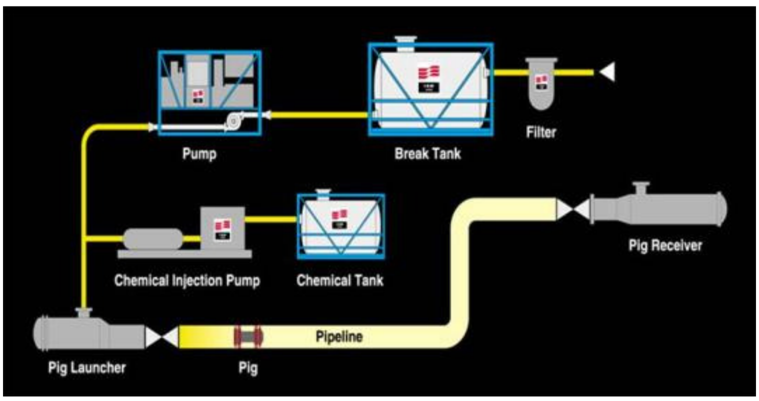

Figure 4.2 Overview of equipment used for the pre-commissioning operation [22]

First the hose is spooled from the reel with an internal pressure of 5 barg over the chute into the sea. This is performed in a controlled manner. The hose contains fluid during the whole installation period. During the operation the hose configuration is monitored subsea with assistance from an ROV. When the hose is lowered in exact position it will be connected to the pipeline with the help of the ROV. The installation of the hose from the vessel down to the pipeline is estimated to take 4 hours.

Now the pigging can start. It is important to maintain control of the hose configuration to ensure a safe operation. The pig train will run with a speed of 0.3 m/s from the pig launcher subsea close to Huldra platform to the Valemon platform. First inhibited seawater will be injected in front of the first pig to lubricate the pipeline for increased cleaning effect.

Then the pigs will be launched with a distance of 250 m between each other. This distance is measured by pigging transponders. An ROV should verify pig launch and receipt in both ends of the pipeline. The pigging time is estimated to be 26 hours.

After the pigs have reached the subsea receiver, the hose can be disconnected. This is done with the help of an ROV. The hose is then spooled back to the surface and this part of the pre-commissioning operation is complete.

Weather conditions evaluations are carried out through the operation to assure that the hose configuration maintains its planned shape. Bad weather may temporary stop the operation, and the hose will be spooled back to vessel. If the installation should be aborted, the estimated pull up time is 2 hours. The hose can also be cut from the vessel deck.

Below, in Figure 4.3 a field layout of the Valemon, Kvitebjørn, Huldra and Heimdal platforms are shown.

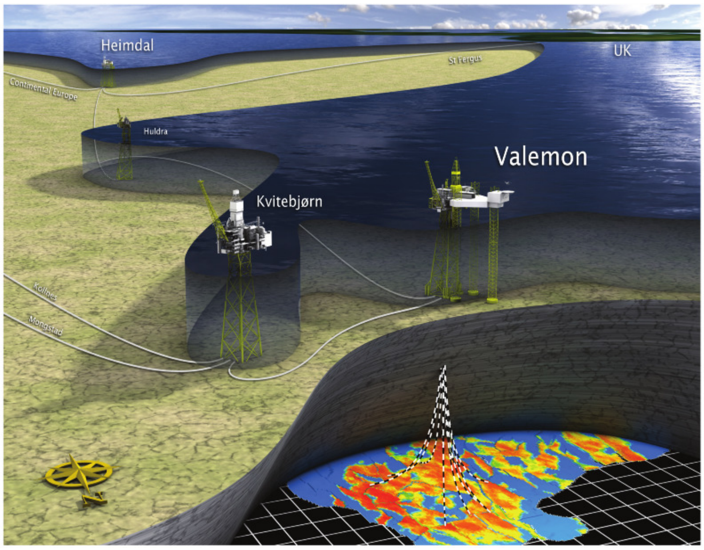

Figure 4.3 Field layout of Valemon, Kvitebjørn, Huldra and Heimdal [2]

4.3 Flexible steel pipe vs. hose

Currently there are no regulations for the use of hoses in operations on the NCS. Therefore it is necessary to compare them with current regulations. Based on this, the hoses will be compared with flexible pipelines. A hose has several similarities with a flexible pipe. The construction and build up of flexible pipe and hose differs from contractor to contractor, depending on the objective of the operation. Flexible pipes and hoses are further discussed and compared in the following sub topics.

4.3.1 Flexible steel pipe

The main characteristics of a flexible pipe is its low relative bending to axial stiffness [12]. This characteristic is achieved through the use of a number of layers of different materials in the pipe wall fabrication [12]. When the pipe body is compounded of different layers, the layers are able to slip relative to each other during different loading conditions. This slipping effect between different layers results in low bending stiffness.

Flexible pipes are most often divided into:

- Bonded pipes
- Unbounded pipes

In bonded pipes, different layers of fabric, elastomer, and steel are bonded together through a vulcanization process [12]. The use of bonded pipes is in general restricted to short lengths.

Unbounded pipes are built up with separate layers such as steel armour layers and polymer sealing layers. A typical cross section of an unbounded pipe is shown below in Figure 4.4. The steel armour provides strength, while polymer sealing layers provide fluid integrity. The space between the internal polymer sheath and the external polymer sheath is known as the pipe annulus [12]. The type, number and sequence of the different layers depend on the design requirements. Below some of the main components of the unbounded flexible pipe are discussed briefly.

The *carcass* is the inner steel layer of the flexible pipe that should prevent collapse caused by external overpressure. The *internal polymer sheath* is a layer that provides internal fluid integrity. The *pressure armour* should resist hoop stress on the pipe caused by internal pressure. The *anti-wear layers* reduce the friction between the armour layers placed in the flexible pipe. These tapes, or anti wear layers, increases the service life of the flexible pipe by reduced wear. The *tensile armour* and *armour wire layer* should withstand tension load on the pipe. There are applications where several tensile armour layers are used, for instance in deep water operations. The *anti-birdcaging layer* is to prevent the wires from twisting out of their present configuration [12]. The *external polymer sheath* protects the armour wires during installation and act as a barrier against seawater.

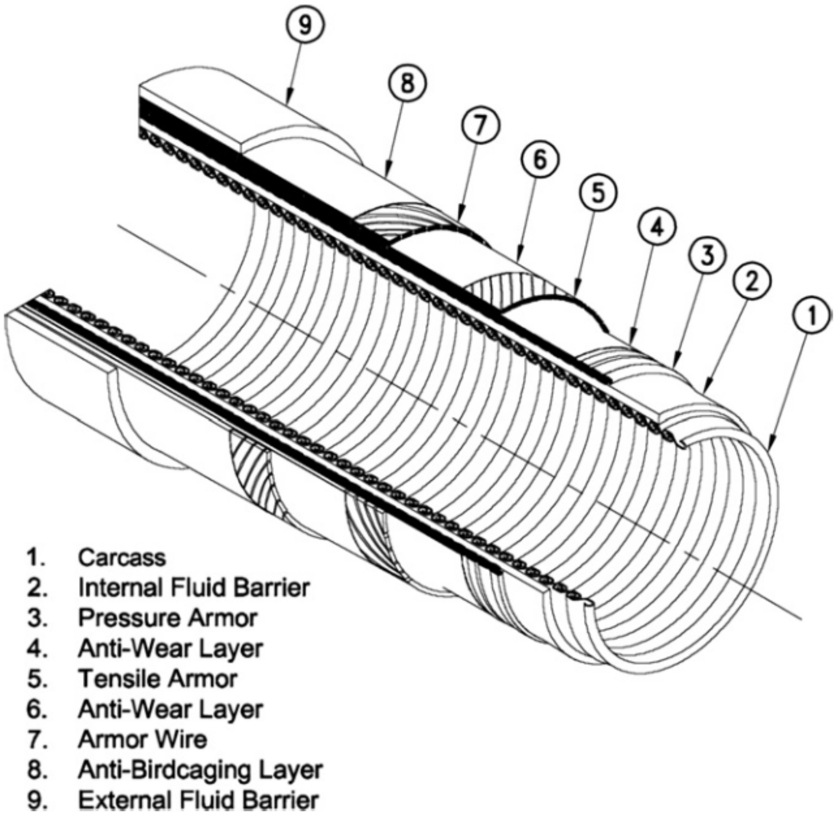

Figure 4.4 Typical cross section of an unbounded flexible pipe [12]

4.3.2 Hose

As for the flexible steel pipe, the hose is built up by a number of layers in different materials. These layers are shown below in Figure 4.5 for the Bunkerflex STH hose.

The *inner rubber layer* is a layer that provides internal fluid integrity. The *steel helix* and the *braided synthetic fibres* should have a resisting effect on internal and external pressure. In addition, they should resist tensile loads on the hose. The steel helix will also contribute to resist torsion loads. The *ground wire* should serve special electrical applications. The *outer rubber layer* should act as a barrier against seawater.

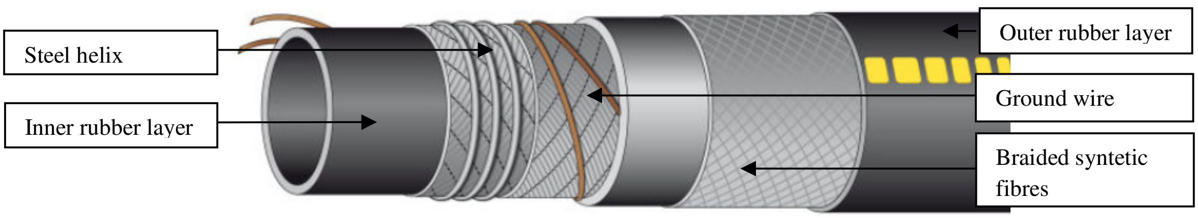

Figure 4.5 Bunkerflex STH hose build up [6]

4.3.3 Discussion

As discussed above, there are some similarities between a flexible riser and a hose build up. Both types are easy to install, flexible, and can be manufactured in long continuous lengths. The purpose of the different layers is generally the same, even though the hose build up does not contain a carcass layer.

Flexible pipes can also be classified as shown in Table 4.1 below. It can be seen that the smooth pipe does not contain internal carcass in the build up structure. This makes the smooth flexible pipe and hose comparison even more convincing. It should also be noted that there are more structural layers described in Figure 4.4 compared with Table 4.1. Table 4.1only considers the main structural layers, while Figure 4.4 considers the structural layers more detailed.

Table 4.1 Classification of standard, unbounded flexible pipes [21]

Main structural layer	Product family I (smooth pipe)	Product family II (rough bore)	Product family III (rough bore)
Internal carcass		X	X
Inner liner/ Internal polymer sheath	X	X	X
Pressure armour	X		X
Intermediate sheath/ Anti-wear layers	X*		
Tensile armour	X	X**	X
Outer sheath/ External polymer sheath	X	X	X

* The use of an intermediate sheath is optional
** The cross-wound tensile armour may be applied with a lay angle close to 55° to balance radial and axial loads

The general differences between a flexible steel pipe and a hose are quite obvious. The flexible steel pipe has several steel layers, which results in a stronger and more robust structure. The hose on the other side can withstand a higher curvature and is significantly lighter than the flexible pipe.

4.3.4 Failure modes for flexible pipe

Before an analysis, it is important to identify potential failure modes for the intended application. Below, the most common failure modes are listed [16]:

- Collapse
- Burst
- Tensile failure
- Compressive failure
- Overbending
- Torsional failure
- Fatigue failure
- Erosion
- Corrosion

4.3.5 Failure modes for the pre-commissioning operation

Not all failure modes are considered equally important considering the specific operation. Below some of the failure modes are discussed briefly;

Collapse can occur caused by lack of internal carcass or lack of sufficient internal pressure in the hose. The consequence of this is reduced flow and potential damages on hose. Even though the hose collapse, it is possible to maintain the shape by increasing the working pressure. An inspection needs to be carried to ensure functionality of the hose before pressurising. Collapse is not considered among the most important failure mode for this operation.

Burst may also be a potential failure mode, but since the working pressure in our case will not exceed 10 barg, this failure mode does not seem probable. The given burst pressure for the 4" Bunkerflex STH hose is 90 barg, while the burst pressure for the Oilflex Super hose is 160 barg. Based on this, burst is not considered to be among the most critical failure modes for this operation.

Tensile failure and compressive failure can occur during the operation. Large vessel motions result in large tension and compression forces on the hose. The tension load will be considered especially in the following areas;

- Hang off point/chute
- Sag bend/ potential s-curve
- Touch Down Point (TDP)

The reaction forces are dependent on the system arrangement and hose configuration in the sea. This will be discussed later for different configurations in Chapter 4.4.

Overbending is also an important failure mode for this operation. Since the hoses are quite flexible it is important that the MBR is not lower than its limitation. Too small radius may cause the hose to be damaged. The overbending will specially be considered in the following areas;

- Hang off point/chute
- Potential slamming against the vessel hull
- Sag bend/ potential s-curve
- TDP

The overbending is dependent on the system arrangement and hose configuration in the sea. More details about this will be discussed for different configurations in Chapter 4.4.

Torsional failure can be an important failure mode for this operation if large vessel rotations occur. If the vessel loses its positioning the hose will either be de-coupled or cut. To limit the thesis scope, torsion is not considered in the analysis.

Fatigue failure is not considered as an important failure mode since the operation is short and defined as temporary. In addition, fatigue is not considered in the thesis scope.

Erosion is not considered as a relevant failure mode since the fluid will only contain filtrated water with green chemicals. No sand or other impurities will be absent in the fluid.

Corrosion is not considered as an important failure mode since the inner and outer layer of the hose is rubber. If there are any injuries on the hose, the hose has to be reeled back and repaired. Since the filtrated water is dyed it is easier to observe potential leakages.

4.4 General configurations

Today there are a number of standard riser configurations that may be applied depending upon the application. The configuration should be analysed both for a static case and for a dynamic case. The following aspects shall be taken into account when selecting configuration [23]:

- Global behaviour and geometry
- Structural integrity, rigidity and continuity
- Cross sectional properties
- Means of support
- Material
- Costs

Even though these configurations are for flexible risers, the same configurations can be applied for hose configurations. Preferably the selection of configuration should be performed taking site-specific environmental conditions into account. Different factors such as water depth, hang off location, vessel RAO, hose parameters and environmental data are of great importance for the analysis. This information will increase the accuracy for the analysis, which gives a better indication of which configuration is most suitable. A well designed hose configuration is safe and provides compliancy to vessel motions in a cost effective manner [16].

It is important that the configuration have sufficient flexibility to allow for relatively large drift off from the vessel. Below, in Figure 4.6 it is shown standard flexible riser configurations, while in Figure 4.7 it is shown some alternative riser configurations. These configurations will be considered as potential hose configurations for our pre-commissioning operation.

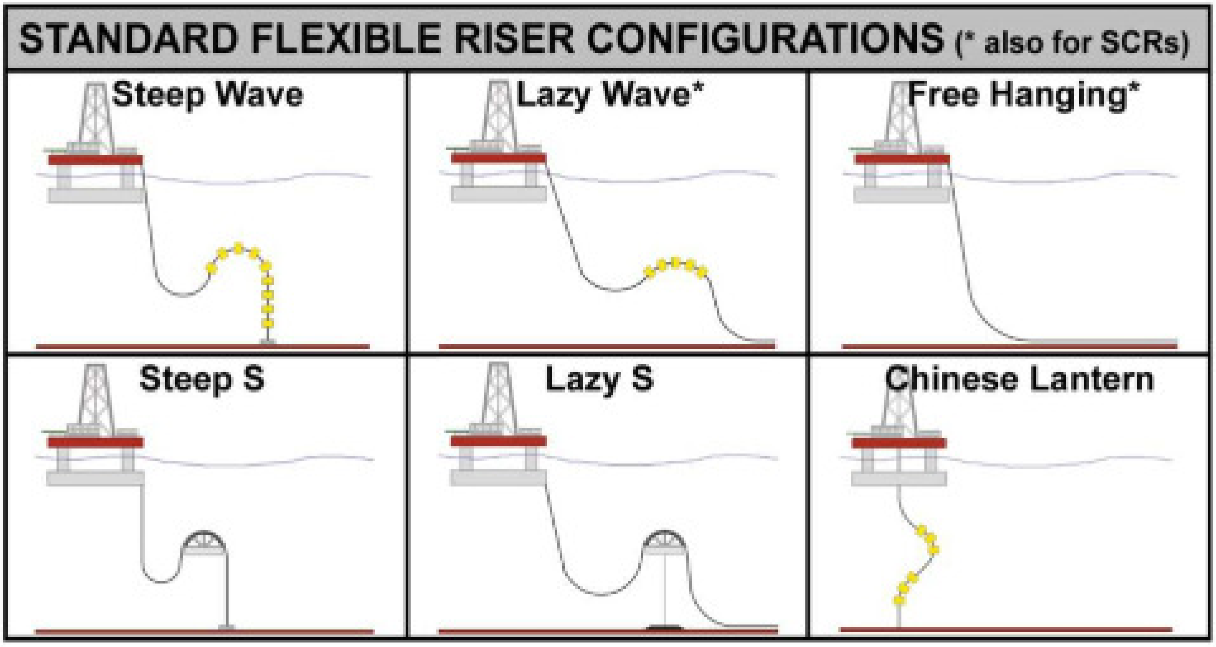

Figure 4.6 Standard flexible riser configurations [24]

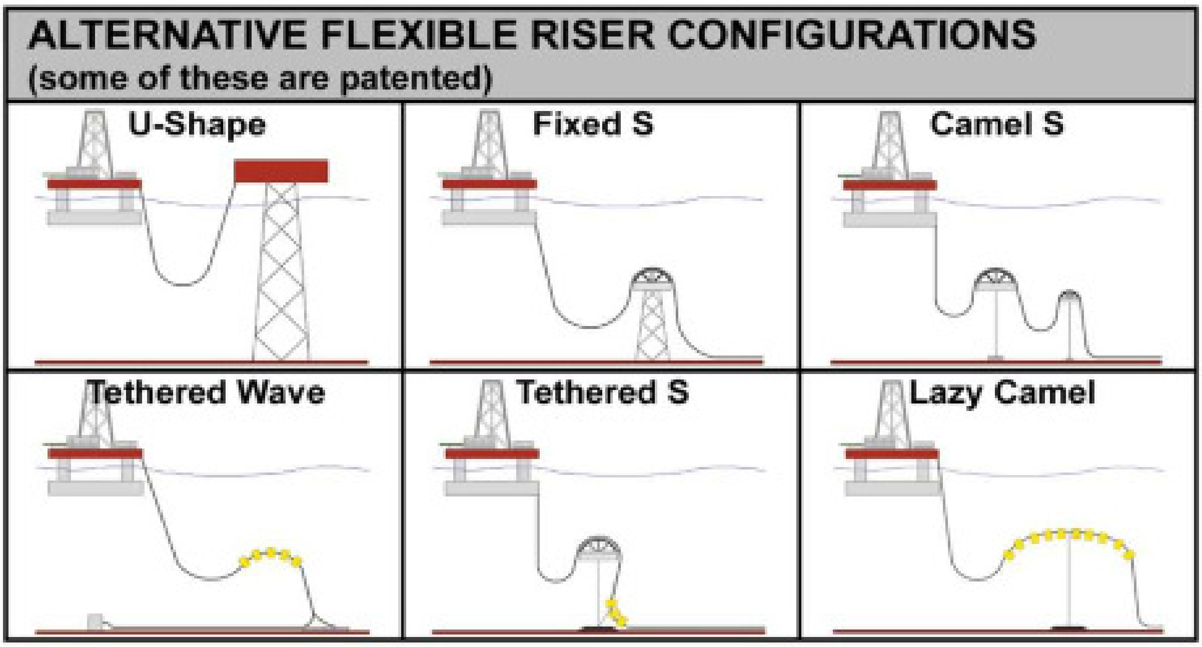

Figure 4.7 Alternative flexible riser configurations [24]

4.4.1 Free hanging

The free hanging configuration has the simplest shape and is the cheapest solution. It does not require any additional subsea equipment installed in the sea or on the seabed. Based on this the free hanging configuration has the shortest mobilisation/demobilisation time of all configurations considered.

Since there is no support from buoyancy modules or seabed structures during operation, this leads to high tension and compression loads on the hose. Buckling and over bending are potential consequences of this effect. The hang off point at the vessel and the TDP area on the seabed are critical areas for this configuration. In general, this configuration is not preferred for deep-water operations since the weight of the hose is increasing with increased water depth. This increased weight results in increased tension at the hang off point.

4.4.2 Lazy S and Steep S configurations

The Lazy S shape configuration has a subsea buoy which is positioned by e.g. chains [23]. The Steep S configuration has a subsea buoy which is fixed to a structure on the seabed.

The subsea buoy reduces the loads in both the hang off point and the TDP. The load reduction effect depends on where the buoy is located and the size of it. A subsea buoy has generally a positive effect on the hose loading since it absorbs the tension variation induced by the floater. This results in a reduced tension at the hang off point plus a small variation in tension in the TDP [23]. In the case of large vessel motions, Steep S configuration is often preferred in front of Lazy S shape. Meanwhile, the Steep S riser buoy is more susceptible to torsional instability than the Lazy S solution [16].

Lazy S and Steep S have proper shape from an engineering point of view, but the installation for both is complex and time demanding. Both configurations require subsea equipment installed in addition to the subsea buoy. A time demanding operation offshore results in high cost.

4.4.3 Lazy wave, Steep wave and Pliant wave configurations

In the wave type configurations, buoyancy and weight are added along a longer length of the riser, to decouple the vessel motions from the TDP of the riser [23]. Wave configurations, in general are more compliant to environmental loading than the S configurations. While the increased compliancy to vessel motions of the wave configurations is a definite advantage, the compliant nature of the riser configuration itself to environmental loading and particularly to cross loading makes riser interference with adjacent risers or structures an important design consideration [16].

Lazy wave configuration requires less subsea equipment installed compared with Steep wave. Steep wave configuration requires a subsea base and a subsea bend stiffener to operate and is more suitable than the Lazy wave configuration if the fluid density changes. If the fluid density changes, the global behaviour change more in a Lazy wave configuration compared with a Steep wave configuration. The buoyancy modules need to be tightened to the riser to avoid slippage. If slippage occurs, the configuration may lose its shape, which can result in unacceptable loadings to the riser.

The Pliant wave configuration is a modification of the Steep wave configuration. The difference compared with Steep wave is that a subsea anchor controls the TDP. The tension in the riser is transferred to the anchor or clump weight and not the TDP [23]. The riser touches down on the seabed in a similar way as the Lazy wave configuration, except that the TDP is controlled by an anchor or clump weight.

The pliant wave configuration is well suited for changes in fluid densities and vessel motions. The installation of this configuration is complex and time demanding.

4.4.4 Chinese lantern

The Chinese lantern configuration is built up with buoyancy modules fastened certain positions along the hose. The Chinese lantern is quite similar to the steep wave configuration, but the placement of the buoyancy modules and TDP are different.

4.4.5 Alternative flexible riser configurations

None of the alternative flexible riser configurations will be described in detail, since the configurations are too complex to be considered for this temporary operation.

4.5 Selection of configurations

Based on the basic configurations described above, it should be possible to eliminate some of the configurations qualitatively before moving to the analysis part. The configuration selection is based on the pre-commissioning operation described in chapter 4.2. Calculations must be carried out for the specific water depth to enable one to state which configuration is the optimum for this operation.

As mentioned, a well designed riser configuration is safe and provides compliancy to vessel motions in a cost effective manner [16]. Other considerations to account for are the surroundings during operation. The hose will not interfere with other equipment during operation. The fluid density will not change during this operation. The selected configurations for further analysis are therefore described below.

4.5.1 Free hanging

The driving factors for this configuration are that the configuration is simple, cheap and are quick to mobilise/demobilise. The main disadvantage is potential high loads on the hose.

For this hose operation the water depth does not exceed 122 m. This is the water depth close to the Huldra platform. This is not particularly deep, so the free hanging configuration will be considered in further analysis.

4.5.2 Lazy wave configuration

The main advantage for this configuration is the ability to reduce the high loads on the hose during operation. In addition it is carried out with limited subsea equipment.

The wave configuration is preferred in front of S shape configurations since they are generally more compliant to environmental loading and less subsea equipment is required during operation. The Pliant wave configuration is, however, not considered for further analysis because it requires installing more subsea equipment compared with Lazy wave. The Chinese lantern is not preferred as it is a more complex design compared with the Lazy wave configuration.

This operation is considered as a temporary operation, so the demand for additional equipment should be limited. This favours the choice of buoyancy modules in front of subsea buoys.

The main purpose of the *buoyancy modules* is to achieve a certain lazy wave configuration, which results in load reduction on the hose. A number of buoyancy modules are needed to be fastened over a section of the hose to achieve the chosen configuration. The buoyancy modules are most often air cans or syntactic foam modules.

The reaction loads on the hose depend on number, size, position and distance between the buoyancy modules. The reaction loads are also dependent on the hose weight, water depth, and the offset. This will be considered further in Chapter 6.

The buoyancy modules need to be fastened tightly enough to avoid slippage on the hose in addition not to damage the outer layer of the hose. Slippage may result in unwanted change in configuration, while external injury on hose layer may result in seawater ingress to the system. Below, in Figure 4.8 is shown a buoyancy module. It can be observed that the clamp first needs to be fastened on the hose, before the buoyancy module is bolted together.

Damage to one single buoyancy element should not result in unacceptable loss of buoyancy for the system as a whole [16].

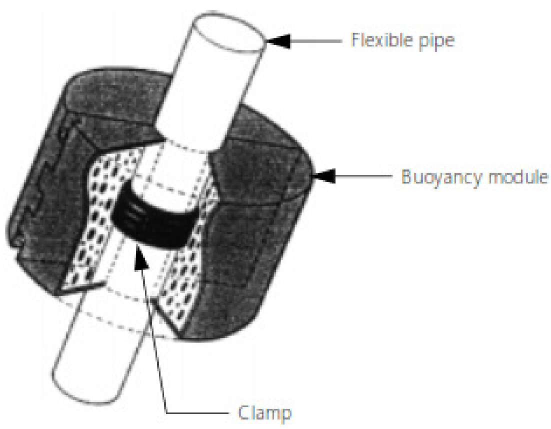

Figure 4.8 Example of a buoyancy module for wave configurations [16]

Chapter 5. THEORETICAL BASIS FOR HYDRODYNAMIC LOAD CALCULATION

For this pre-commissioning operation, the hose is exposed for different environmental loads which are mainly waves and current. Ocean surface loads cause periodic loads on the hose which will affect the operability for the operation. In this chapter, a short introduction to wave theory and hydrodynamic loads is presented.

5.1 Wave theory

Waves can be generated in different ways such as from tides, wind, earthquake etc. In this study only waves generated by the interaction between wind and the sea surface will be considered, since this is the most relevant for the operation.

Wind generated waves can be classified into two basic categories: sea and swell [14]. Sea waves are driven by local wind and have an irregular form, while swell waves can travel over long distances where the winds are calm and have more regular form [14].

A *regular* travelling wave is propagating with permanent form. It has a distinct wave length, wave period and wave height. In irregular or random waves, the free surface elevation $\xi_a\ (x,y,t)$ is a random process [25].

Even though the wind generated waves are more irregular, the superposition principle can be applied to represent an irregular wave form by adding different regular wave components. This gives a more representative presentation of actual waves. A simple illustration of this superposition principle can be seen in Figure 5.1 below.

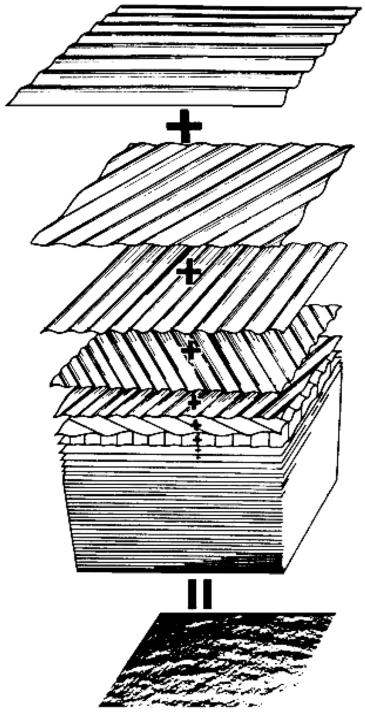

Figure 5.1 A sum of many regular waves makes an irregular sea [14]

For the further analysis, only regular wave theory will be applied since regular waves are recommended for sensitivity analysis [16].

Below in Figure 5.2 regular wave profile is shown at a fixed time, while in Figure 5.3 a regular wave profile is shown at a fixed location. It should be noticed that the origin is placed at the still water level. The d represents the water depth, the λ represents the wave length, the ξ represents the surface of the wave, the ξ_a represents the free surface elevation and the T represents the wave period. The highest point of the wave is called its crest and the lowest point on its surface is the trough [14].

Based on the assumption of regular waves, the wave number, k_w (rad/m), and the wave angular frequency, ω (rad/s), can be expressed as follows:

$$k_w = \frac{2\pi}{\lambda} \tag{5-1}$$

$$\omega = \frac{2\pi}{T} \tag{5-2}$$

The face speed, or phase velocity is given by:

$$c = \frac{\lambda}{T} \tag{5-3}$$

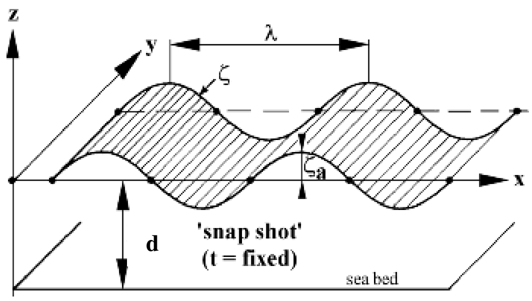

Figure 5.2 Regular wave definitions at a fixed time [14]

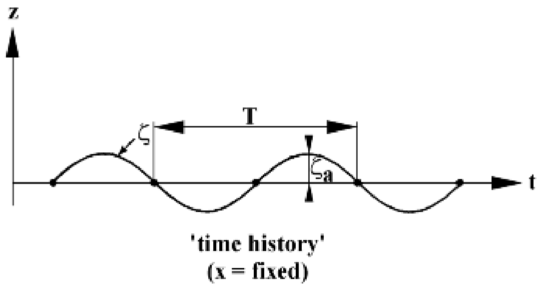

Figure 5.3 Regular wave definitions at a fixed location [14]

The wave frequency is important for the operation, since different vessels have different RAO's which will influence the vessel motions which will affect the hose behaviour in the sea. The phase velocity is also an important parameter to consider, for example by comparing the wave velocities with the current velocities on the field.

The choice of regular wave theory is based on DNV recommendations [25]. The choice of wave theory is determined by three wave parameters:

- Wave height (*H*)
- Wave period (*T*)
- Water depth (*d*)

Below in Figure 5.4 ranges of validity for various wave theories are shown.

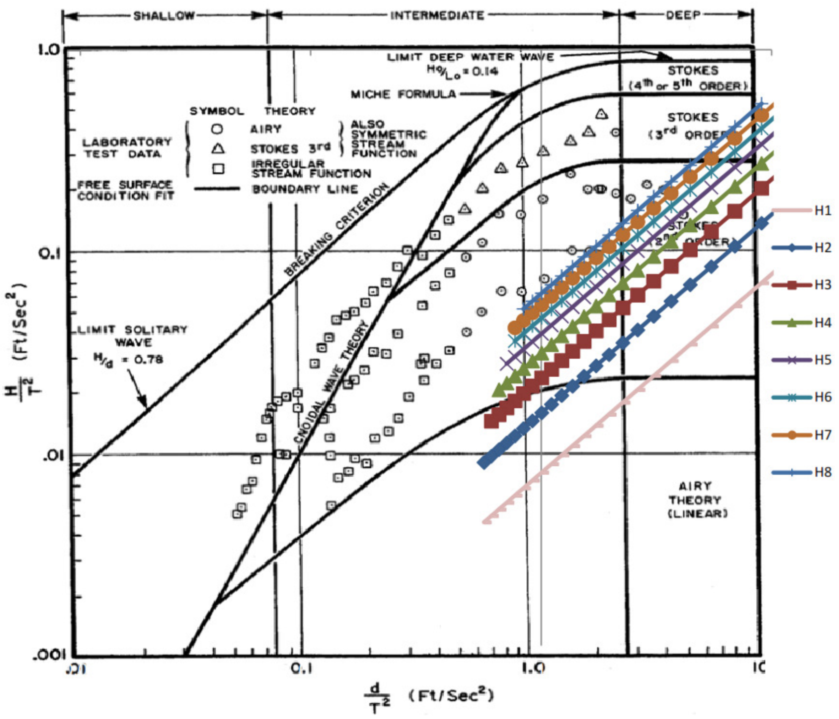

Figure 5.4 Ranges of validity for various wave theories [25]. H1 to H8 represents wave heights from 1 to 8 metres.

The relevant site conditions are plotted directly into this diagram. H1 – H8 represents wave heights from 1 m to 8 m. It should also be noted that the axes are in feet, not in metres. Based on the plot above, the Stoke wave theory can be recommended.

Another method to verify the wave theory is to calculate the wave steepness parameter (*S*) and the Ursell number (U_R).

According DNV [25], the parameters are defined as follows:

$$S = 2\pi \frac{H}{gT^2} \tag{5-4}$$

$$U_R = \frac{H\lambda^2}{gT^2} \tag{5-5}$$

where

λ = Wave length

g = Gravitational acceleration

The criterion for the Stoke wave theory is that $S < S_{max}$ and $U_R < 30$. The maximum crest to wave height ratio for a Stokes wave is 0.635 [25]. Both these criterions are met within the chosen interval. Based on this, *Stokes wave theory* is selected based on DNV [25] for the analysis.

Stokes wave expansion is an expansion of the surface elevation in powers of the linear wave height *H* [25]. A first-order Stokes wave is identical to a linear wave, or Airy wave [25].This can be expressed as:

$$\xi_a(x, y, t) = \frac{H}{2} cos\Theta \tag{5-6}$$

where

Θ = Phase function

This phase function can be expressed as

$$\Theta = \mathrm{k_w(xcos\beta_w + ycos\beta_w) - \omega t} \tag{5-7}$$

where

β_w = is the direction of propagation, measured from the positive x-axis.

For the second-order Stokes waves, the wave crests are increased by $(1 + \frac{\pi H}{2\lambda})$ and wave troughs become wider with a factor $(1 - \frac{\pi H}{2\lambda})$.

The third-order Stokes theory considers the dependence of a phase velocity on the wave height [25].

The fifth-order Stokes theory will be used in further modeling since this is the only applicable Stokes theory implemented in OrcaFlex software. This wave theory sub chapter is to a large extent written based on [14] and [25].

5.2 Hydrodynamic loads

During the analysis, hydrodynamic (wave and current) loads will be considered. Wave forces acting on the hose can be calculated based on the Morison's equation for slender cylinders since the hose diameter is much less than the wave length.

The Morison's equation is a combination of an inertial term and a drag term. The general form of Morison's equation is given below [26]:

$$F_x = \rho C_m V a_c + \frac{1}{2} \rho C_D A v|v| \tag{5-8}$$

where

F_x = force in x direction

ρ = density of water

C_m = inertia coefficient

V = volume of body

a_c = acceleration

C_D = drag coefficient for the body

v = velocity

However, equation (5-8) can be modified to take account of the movement of the body. This results in two inertia components and one drag component. This can be expressed as [27]:

$$F_w = (\Delta a_w + C_A \Delta a_r) + \frac{1}{2} \rho C_D A V_r |V_r| \tag{5-9}$$

where

F_w = fluid force

Δ = mass of fluid displaced by the body

a_w = fluid acceleration relative to earth

C_A = added mass coefficient for the body

a_r = fluid acceleration relative to the body

V_r = fluid velocity relative to the body

A = drag area

As mentioned, the Morison's equation contains three main components, where the Δa_w expression often is referred to as the *Froude-Krylow* component. The $C_a \Delta a_r$ expression is often referred to as the *added mass* component, while the $\frac{1}{2}\rho C_d A V_r|V_r|$ is often referred as the *drag* component. In case the body does not move, a_r is equal to a_w and the total inertia force can be calculated as:

$$F_i = \Delta(1 + C_A)a_w \tag{5-10}$$

When the body moves, the resulting wave force will depend on the direction of the body motion relative to the flow.

The selection of C_D and C_A should consider the variation as a function of [25]:

- Reynolds number, R_e;
- Keulegan-Carpenter number, K_c;
- Non dimensional roughness number, ψ

Below in Table 5.1 possible coefficients for the hoses are listed. Alternatively the selection of C_D and C_A can be based on American Petroleum Institute (API) standards. The API choice of hydrodynamic coefficients is different compared with the DNV recommendations. For further reading about Morison's equation about its assumptions and limitations, the hydrodynamic coefficient consideration and discussion of API and DNV regulations it is recommended to Techet [26], DNV [25] and Gudmestad and Moe [28] respectively.

Table 5.1 Selected hose coefficients [25]

Coefficient	Value
Drag coefficient, C_D	1.2
Added mass coefficient, C_A	1.0

Chapter 6. ANALYSIS

The analysis should cover all relevant configurations and load conditions. The aim should be to establish limiting criteria for the operation and to determine the optimum model and technical solution for the operation. To be able to do this, it is required to identify the critical load variables during operation. Are the compression forces, tension forces or the curvature on the hose most critical? And are the critical limitations the same for both hose types?

This chapter will discuss the OrcaFlex software which will be used for the analysis, the OrcaFlex model build up for this particular case, theoretical static analysis for effective tension and curvature, the static analysis in OrcaFlex, the dynamic analysis in OrcaFlex for regular waves, the verification and validation of the models, the dynamic analysis in OrcaFlex for regular waves with current loads and finally we will define the operational requirements for the operation.

6.1 OrcaFlex software

Today, there are several programs that can be used to analyse static and dynamic behaviour of marine applications. Some well-known software tools are OrcaFlex, Flexcom and Riflex. OrcaFlex was selected since this program is capable of modelling the problem with appropriate accuracy and was accessible.

This sub chapter discuss OrcaFlex in general, the line model build up, the static and the dynamic analysis, the vessel motions and RAO, the coordinate systems and the direction conventions used. This chapter is to a large extent written based on the OrcaFlex manual [27].

6.1.1 General

OrcaFlex is a user-friendly software program that helps students and engineers to become capable of solving complex marine cases. OrcaFlex is a marine dynamics program for static and dynamic analysis of a wide range of offshore systems, including all types of marine risers, global analysis, moorings, installation and towed systems [27].

The model build up consists of several standard objects such as vessel(s), line(s), shape(s) etc. A number of input parameters and coefficients can be selected to the model to make it representative.

OrcaFlex is a fully 3D non-linear time domain finite element program that builds a mathematical computer model of the system. This model is capable of dealing with large deflections of the flexible from the initial configuration [27]. The analysis is shown in a graphical view, so potential errors may be detected visually during the analysis.

In addition, OrcaFlex has a spread sheet that can be linked to Microsoft Excel. This link makes it possible to create batch script files, which is a number of different OrcaFlex files that are based on a set of defined input parameters (e.g. environmental loads). After a number of different load cases have been established, a number of resulting output loads can be calculated. Outputs for this particular operation will be discussed later.

The results can be given in both graphs and tables for different periods such as the static case, a specified period, or the complete simulation period. There are a number of output variables which can be identified, such as;

- Positions
- Motions
- Angles
- Forces
- Moments
- Stresses
- Stains

6.1.2 Line model build up

Orcaflex uses a finite element model (FEM) to calculate the actions on the line. This is expressed mathematically by dividing the line into different segments. OrcaFlex takes segments from the actual line and divide them into nodes and segments to create a "discretised" model. The segments and nodes are numbered and starts from "End A" and ends at "End B". The transition from an actual line over to the discretised model is clearly illustrated by Figure 6.1 below.

The node models the mass, buoyancy and drag properties from the actual line segments. Each node is effectively a short straight rod that represents the two half segments either side of the node [27]. Based on this build up, the forces and moments are applied on the nodes, and not on the segments.

The segments only model the axial, torsional and bending properties from the actual line segments. Each property is built up with a spring and a damper concept, as shown in Figure 6.2. The axial stiffness is measured with a spring and damper that is placed on the centre of the segment. The placement is the same for the torsional properties, while the bending properties are represented by rotation on each side of the node, spanning between the node's and the segment's axial direction [27]. Figure 6.2 shows more details of the line model compared to Figure 6.1, but the principles are the same.

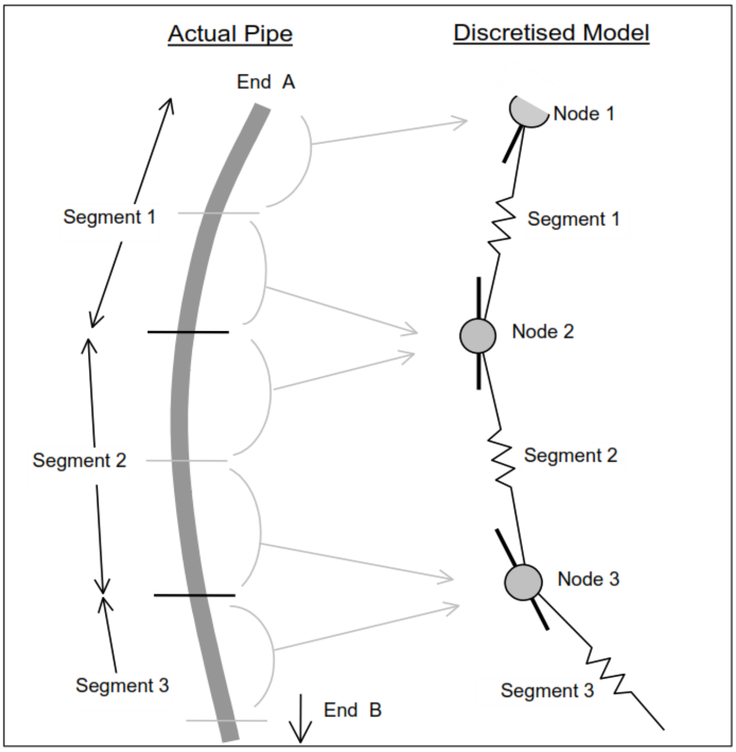

Figure 6.1 OrcaFlex line model [27]

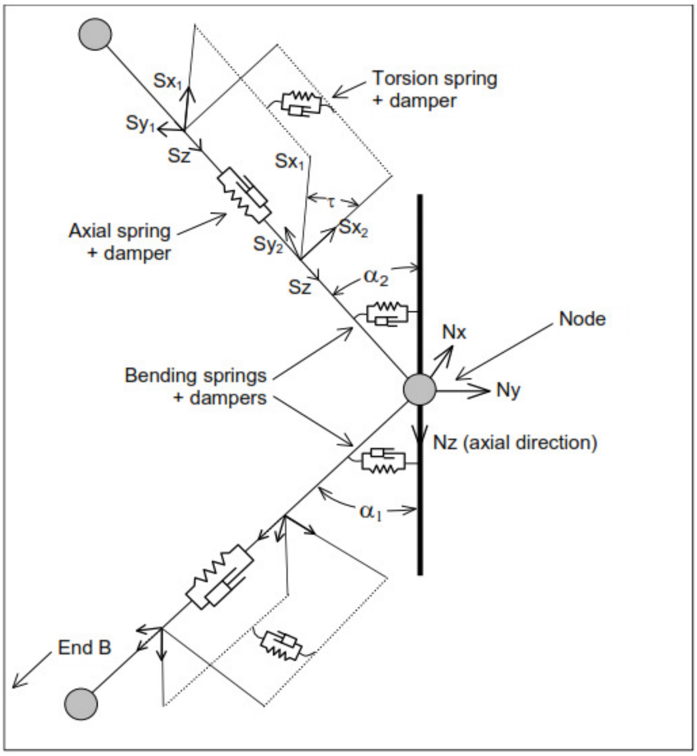

Figure 6.2 Detailed representation of the OrcaFlex line model [27]

6.1.3 Static and dynamic analysis

When the model build-up is accomplished, OrcaFlex is able to calculate both the statics and the dynamics of the system. First a static calculation has to be completed, before starting on the dynamic analysis. The dynamic analysis is completed when the dynamic simulation is completed. OrcaFlex calculates the forces and moments in five stages, respectively in the following order: tension forces, bend moments, shear forces, tension moments and total load. Details about each stage can be found in the OrcaFlex manual [27].

To be able to complete the analysis of the static equilibrium, three iterative stages have to be completed. First, the initial positions for the floating structures (vessel and buoy) are calculated. Second, the equilibrium for each line that is connected to the floating object is calculated. Third, and last, the out of balance load acting on each free body is calculated and a new position for the body is estimated [27]. The static analysis is complete when the out of balance loads are within the specified tolerance (which is close to zero). The static equilibrium for each line is based on the assumption that the line ends are fixed. However, it may happen that the static calculations do not convergence to a stable equilibrium. If this is the case, the choice of line method should be reconsidered, or the convergence parameters should be adjusted.

The dynamic analysis is a time simulation of the motions of the model over a specified period of time, starting from the position derived by the static analysis [27]. The time and simulation stages for an OrcaFlex model are shown in Figure 6.3 below.

Firstly, the build-up sequence starts. This is where the dynamics starts to affect the system until they occur at full value. This sequence therefore smoothen the transition from static to full dynamic motion. The build-up sequence starts at the same time as the set global time origin. When the build-up sequence is completed, a simulation time origin is defined. This means that the build-up time is defined as negative time, which is 10 s in Figure 6.3 below. The remaining build up stages, depend on the simulation time chosen. In Figure 6.3 below, Stage 1 and Stage 2 consist of one wave period each that is 15 s (for this case). After the two stages are completed, the simulation time is completed after 30 s. For some special cases, it may be beneficial to define a wave train time origin and/or time history origin different than the simulation time origin. This may be beneficial if the simulation time is long.

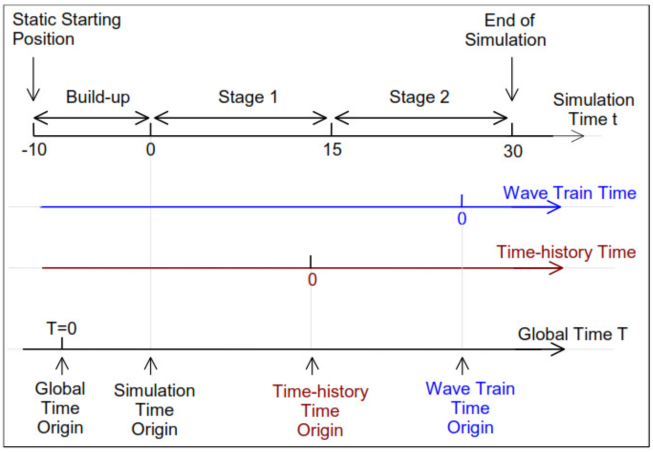

Figure 6.3 Time and simulation stages for OrcaFlex model [27].

The calculation performed in the dynamic analysis is based on the equation of motions. This equation can be solved by either explicit or implicit integration. The equation of motion OrcaFlex solves is [27]:

$$M(p, a_c) + C(p, v) + K(p) = F(p, v, t) \tag{6-1}$$

where

$M(p,a)$	= system inertia load
$C(p,c)$	= system damping load
$K(p)$	= system stiffness load
$F(p,v,t)$	= external load
p	= position vector
v	= velocity vector
a_c	= acceleration vector
t	= simulation time

The explicit integration scheme is forward Euler with a constant time step [27]. The initial conditions are based on the static analysis, which allows us to calculate the forces and moments that are acting on each free body and node in the system. Equation (6-1) can be rearranged to a local equation of motion for each free body and each line node.

$$M(p)a_c = F(p, v, t) - C(p, v) + K(p) \tag{6-2}$$

Equation (6-2) can be solved for a_c for each load step as long as the initial conditions are known. This results in that the positions and orientations for all nodes and free bodies can be calculated for the system. Small integration time steps are often required to get a stable simulation.

The implicit integration scheme uses the Generalised-α integration scheme [27]. The difference is that the system is solved at the end of each time step, instead of the start of each time step. The implicit integration methodology requires an iterative solution method.

6.1.4 Vessel motions and RAO

For different vessels, the motions can be defined by displacement RAO's. Each displacement RAO consists of a pair of numbers that define the vessel response, for one particular degree of freedom, to one particular wave direction and period [27]. The two numbers are an amplitude, which relates the amplitude of the vessel motion to the amplitude of the wave, and a phase, which defines the timing of the vessel motion relative to the wave [27].

In general, the RAO's are typically given as a set of tables describing vessel response in six degrees of freedom. It should be noted that RAO's are given for regular wave heights, as function of periods. In Figure 6.4 the six degrees of motions for a vessel are defined.

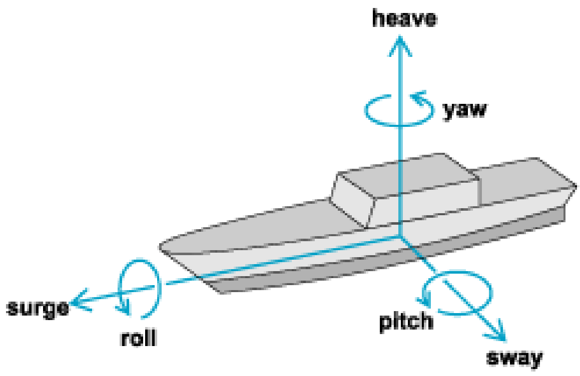

Figure 6.4 The six degrees of motions of a vessel [29]

Surge, sway and heave are often separated into translational motions, while roll, pitch and yaw are separated into rotational motions. The translational motions are given in unit lengths, while the rotational motions are given in degrees in Orcaflex.

The vessel displacement for each degree of freedom is calculated as [27]:

$$X = Ra_{wave}\cos(\omega t - \varphi) \tag{6-3}$$

where

X = Vessel displacement

a_{wave} = Wave amplitude

ω = Wave frequency

t = Time

R = RAO amplitude

φ = Phase angle

6.1.5 Coordinate system

The coordinate systems may often be defined dissimilar in different software. Therefore a separate chapter is dedicated to this important theme. It is always necessary to get familiar with the respective coordinate systems before starting an analysis. In OrcaFlex, it is important to separate between the global coordinate system and the local coordinate system. The coordinate system described in this chapter will be used as basis for all further discussions. All the coordinate systems in this thesis are right handed.

OrcaFlex uses one global coordinate system and a number of local coordinate systems. The *global coordinate system* is characterized with capital letters GXYZ, where G is the global origin and GX, GY and GZ are the global axes directions. The *local coordinate system* is categorized with Lxyz, where L is local origin and Lx, Ly and Lz are local axes directions. The following global coordinate system is used consistently:

- GX is positive to bow
- GY is positive port side
- GZ is positive upwards

OrcaFlex uses a number of local coordinate systems, generally one for each object in the model. Typically the origin is at a selected fixed point on the object and the axes are in special fixed directions, such as the surge, sway and heave directions of the vessel [27].

Whenever data or results are coordinate system dependent, they are referred to as being either global-relative or object-relative [27]. The position of objects and sea conditions are most often given relative to global axes. Below, in Figure 6.5 an example of different coordinate systems are shown.

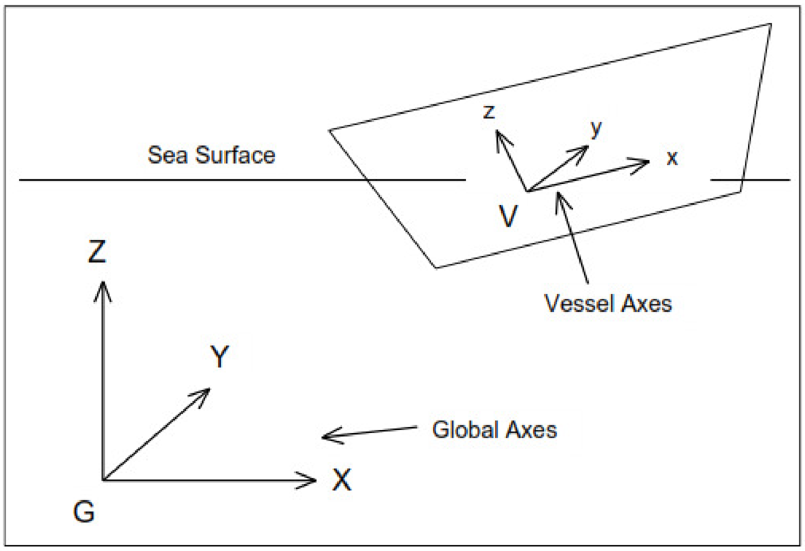

Figure 6.5 Coordinate systems [27]

6.1.6 Direction conventions

OrcaFlex defines the directions and headings by giving the azimuth angle of direction, in degrees, measured positive from the x-axis towards the y-axis [27]. This is illustrated in Figure 6.6 below.

The direction of the environmental load is specified from the direction the load is progressing, relative to the global axis, while the vessel heading is specified as the local vessel direction relative to the global axis. This means that the environmental load from head seas, are progressing from a 180° direction. In addition, the vessel heading relative to the global axis also is 180° relative to global axis. This is shown in Figure 6.6.

However, these directions are sometimes defined relative to global axes and sometimes to the local object axes [27]. The azimuth and declination angles are defined as follows: [27]:

- Azimuth is the angle from the x axis to the projection of the direction onto the xy plane. The positive x axis direction therefore has Azimuth= 0°, and the positive y axis direction has Azimuth = 90°.
- Declination is the angle the direction makes with the z axis. Therefore declination is 0° for the positive z-direction, 90° for any direction in the xy plane, and 180° for the negative z direction.

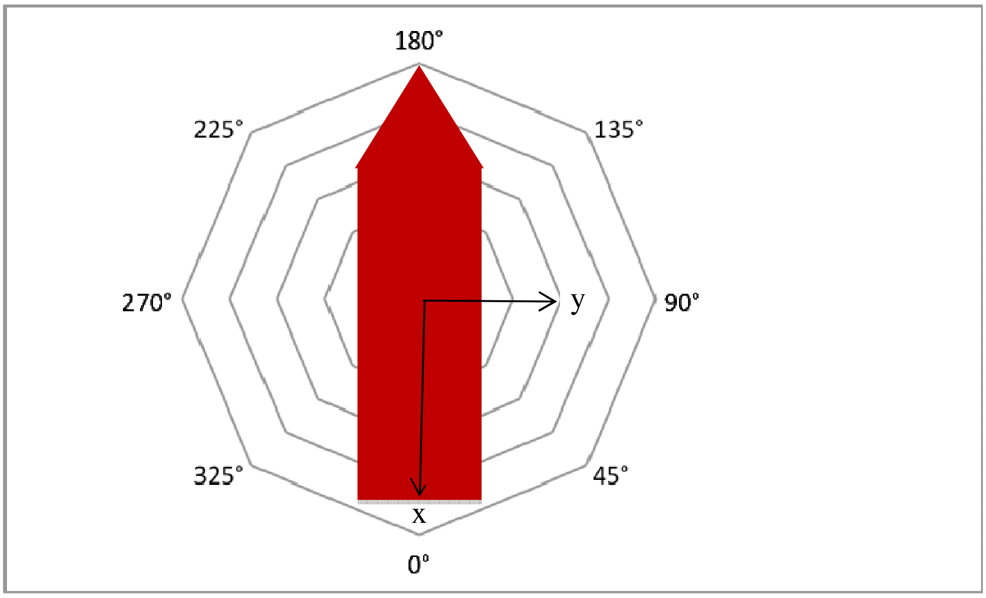

Figure 6.6 Directions relative to axes

6.2 The OrcaFlex model

It is important to show how the model is build up and draw attention to differences between the different models in the analysis. This chapter show some illustrations of general components in the model and illustrate free hanging and lazy wave configurations in OrcaFlex. In addition, some assumptions for modelling are stated.

6.2.1 General components

The general components should represent the equipment used for the operation. This can be done in different ways. Below, in Figure 6.7 is shown a top view of a free hanging model showing the X-Y positioning of the hose on the seabed. It is clear that the bottom location of the hose is moved in a positive Y direction away from the vessel. This is done to reduce the probability of slamming effects on the vessel. The white points on the hose show contact between the hose and a surface, in this case the seabed.

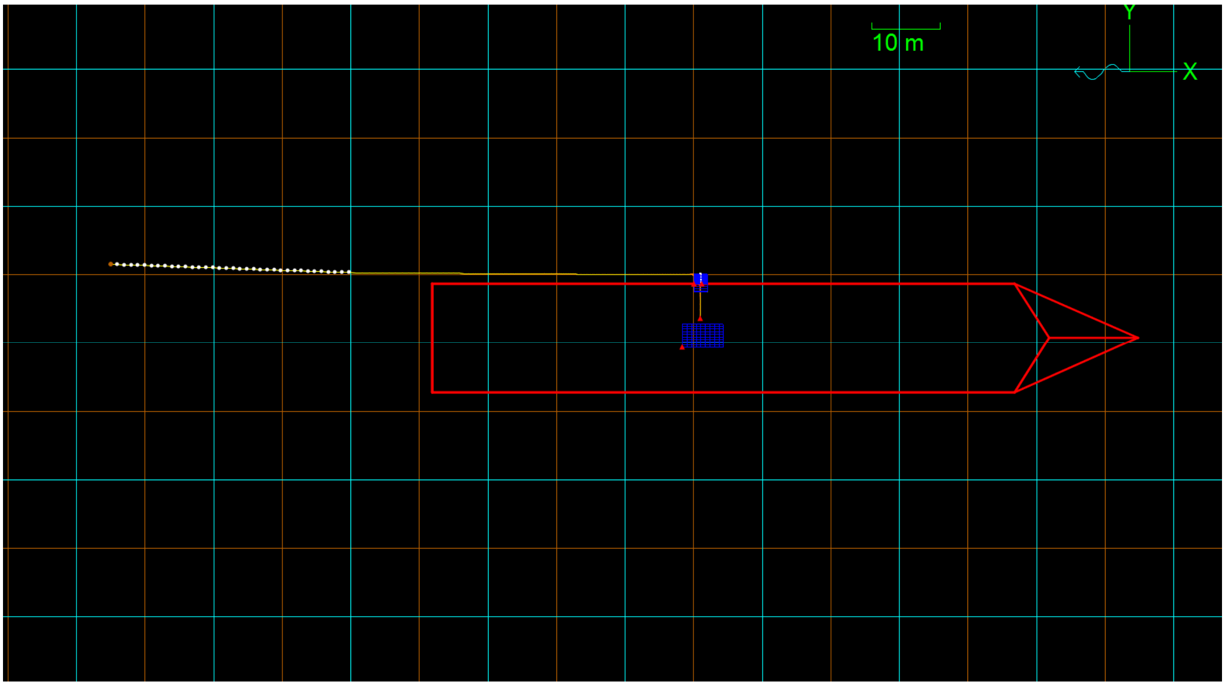

Figure 6.7 X-Y view of the model

The construction of the chute is important. The radius shall be equal or exceed the MBR of the applied hose. This requires two different chute diameters for the two different hose types. The chute radius differs as shown in Table 6.1. In addition, vertical walls on the chute are added to reduce the movement of the hose in the X direction. These walls are added to make the chute as similar as possible to the real chute design used in the operation. Below in Figure 6.8 the model is shown from the stern. The white points show contact between the hose and the chute. The chute also ensures a sufficient distance between the vessel and the hose during the operation.

Table 6.1 Chute dimensions for different hoses

	4" Bunkerflex STH	6" Oilflex Super
Chute radius	1200 mm	1600 mm

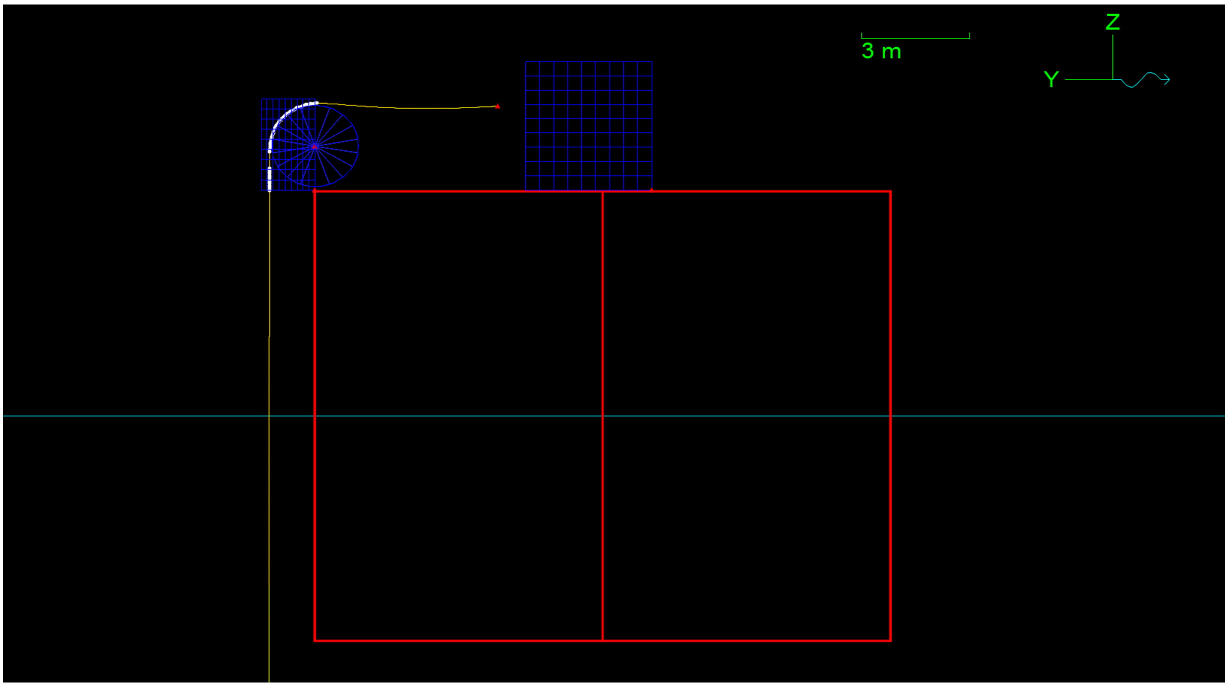

Figure 6.8 Y-Z view of the model

The modelled chute is built up by one cylinder and two blocks in OrcaFlex. The hose will lie smoothly over the cylinder, while the two blocks limit the movement of the hose in the X direction. This model build up is shown below in Figure 6.9.

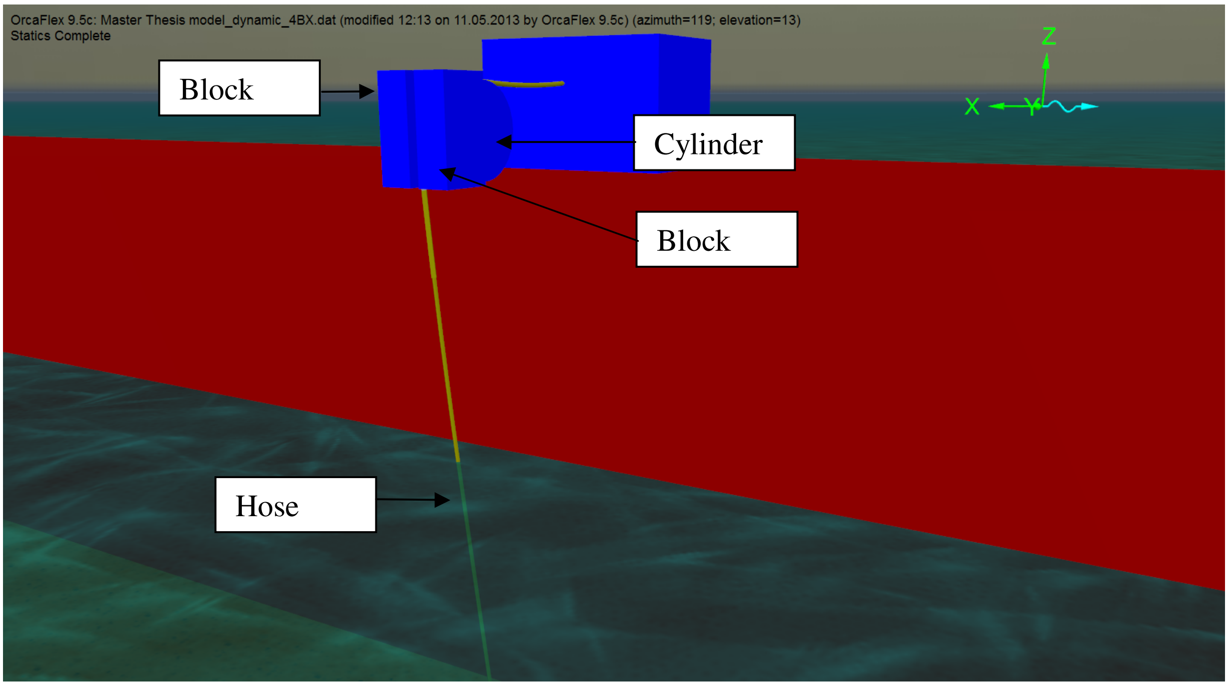

Figure 6.9 Chute modelled in OrcaFlex

6.2.2 Arrangement on deck

The arrangement of the equipment on deck is important to consider when the operating weather window should be determined. By smart engineering, the operability window can be increased for this operation.

Whenever possible, the chute should be placed at half of the length of the vessel in the longitudinal (X-axis) direction. This position has a minimum pitch motion, which will lead to minimum reaction forces in the hose. In this case, horizontal installation is preferred to vertical installation. This results in maximum effect from the roll motion of the vessel whenever the chute is placed on the deck. Normally the bow is placed against the waves, however, which will result in limited roll motion.

The reel should be placed in line with the chute and centralized at the half of the vessel width. The placement in line with the chute is to assure that the external loads such as bending and tension are kept at a minimum before entering the chute. When the reel is centralized at the half of the width, it improves vessel conditions such as stability.

The vessel deck on the Skandi Inspector vessel is 36 m long and 15 m wide as mentioned in Chapter 3.1. This gives limitations where to place the chute and the reel in the longitudinal direction. Below in Figure 6.10 a suggestion for the arrangement on deck is shown. It leaves 1 m space between the reel and the housing.

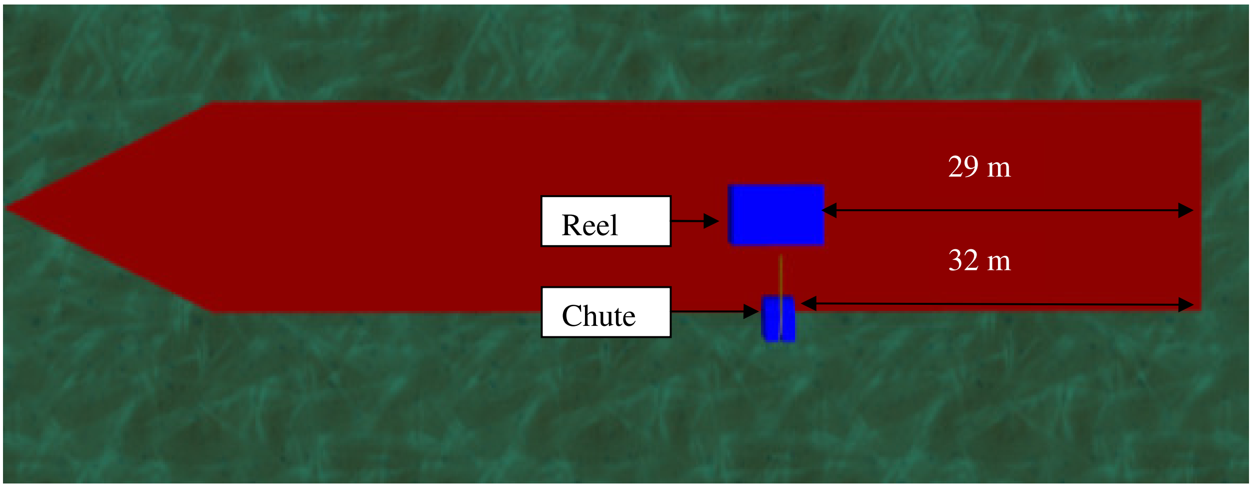

Figure 6.10 Arrangement on deck

Bend limiters and bend restrictors are not considered as a part of the equipment used for the installation. It may, however, be a recommendation to include such if the curvature is the critical load (bending).

6.2.3 Free hanging configuration

The first model to be analysed is a free hanging configuration of the hose. The free hanging configuration is shown below in Figure 6.11. The hang off point is where the hose leaves the chute, while the offset is the horizontal distance from the hang off point to the TDP.

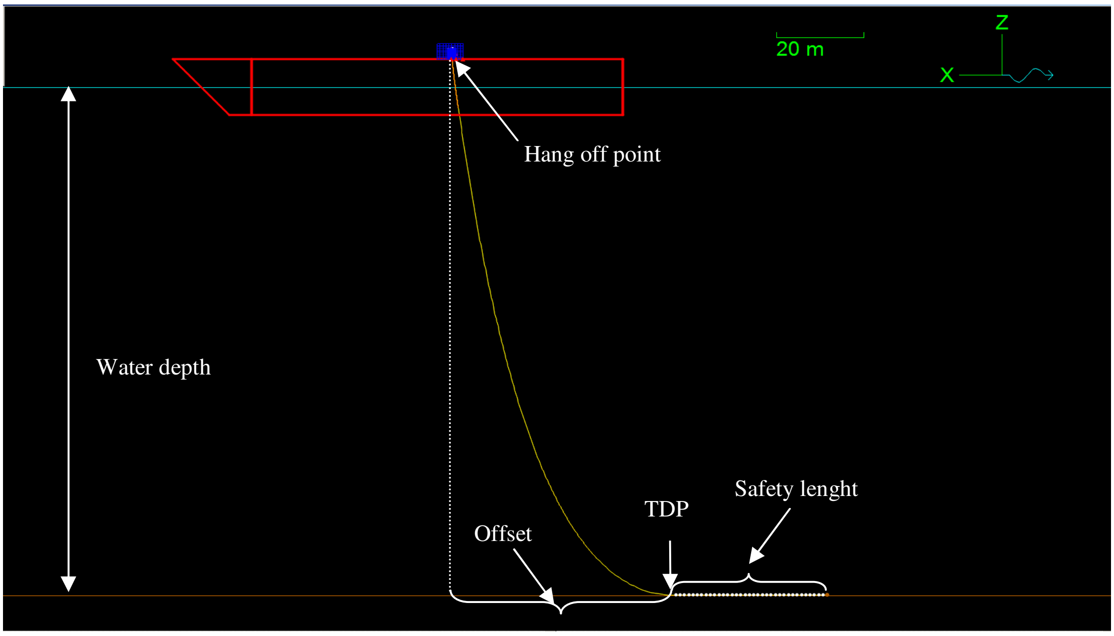

Figure 6.11 Free hanging model in OrcaFlex

6.2.4 Lazy wave configuration

The second model to be analysed is a lazy wave configuration of the hose. The lazy wave configuration is shown below in Figure 6.12. The hang off point is where the hose leaves the chute. The distance to the floatation point is defined as the distance between sea level and the highest point on the hose that is lifted up by buoyancy modules. The lazy wave height is the vertical distance of the lazy wave shape.

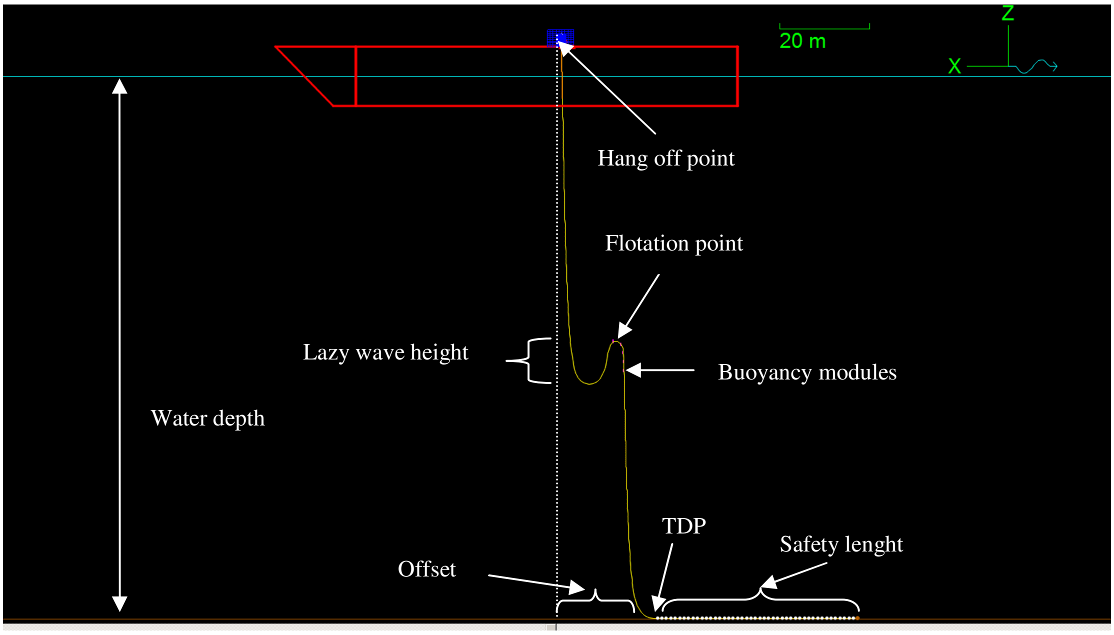

Figure 6.12 Lazy wave model in OrcaFlex

6.2.5 Assumptions for modelling in OrcaFlex

To simplify the pre-commissioning operation into a model, some reasonable assumptions need to be stated. The input values are defined in the Design basis and a short summary of the assumptions are given below:

Vessel

- Mass = 3345 tonnes
- Length= 80.77 m
- Width = 18 m
- The reel is located 29 m from the stern
- The chute is located 32 m from the stern
- RAO data for the Skandi Inspector vessel
- Centre Of Gravity (COG) for Skandi Inspector vessel is not implemented

Direction convention

- Surge: Positive forward
- Sway: Positive to port
- Heave: Positive upwards
- Roll: Positive starboard down
- Pitch: Positive bow down
- Yaw: Positive bow to port

Hose

- 4” Bunkerflex STH (ref Design basis)
- 6” Oilflex Super (ref Design basis)
- Length
  - Free hanging configuration = 190 m
  - Lazy wave configuration = 210 m
- Offset
  - Free hanging configuration = 51 m
  - Lazy wave configuration = 20 m
- Treated water density, ρ_{tw} = 1000 kg/m^3
- The hose “lay down length should/ safety length” is at least 20 m from the TDP to the pipeline to prevent large tension and compression forces in the hose
- Fatigue and VIV not considered in the analysis

Buoyancy modules

- OD = 217 mm
- Length= 0.5 m
- Weight= 10 kg/module in air

Environmental conditions

- Stokes wave theory applied
- Water depth 122 m
- Environmental loads will hit the vessel ± 45° from the vessel bow
- Wave heights and wave periods (ref Design basis)
- Seawater density, ρ_{sea} = 1025kg/m^3

Seabed geotechnical data

- Assume flat bottom
- Seabed friction coefficient = 0.5

6.3 Theoretical static analysis

The aim of the static analysis is to determine the initial static geometry of the hose configuration [16]. The parameters to be selected are typically [16]:

- Hose length
- Hose weight
- Buoyancy requirements
- Location of seabed TDP

As discussed in Chapter 4, there are several potential failure modes for the operation. The most critical analyses output with respect to operation limitations are considered to be effective tension and curvature of the hose. The effective tension determines possible tensile and compressive failures, while the curvature determines occurrence of overbending of the hose.

6.3.1 Effective tension

When considering effective tension for this operation, the buoyancy of the hose has to be discussed. The well known Archimedes law states that when a body is wholly or partially immersed in a fluid, it experiences an upward force equal to the weight of fluid displaced [30]. This upward force is also referred to as the buoyancy force and acts at the centroid of the object. The effective tension will be formulated based on the Archimedes law. However, to adopt Archimedes law, the following points should be taken into consideration [30]:

- The law can be applied directly only to pressure fields that are completely closed
- The law says nothing about internal forces or stresses

The Archimedes law can be derived from the principle of superposition [30]. The superposition principle makes it possible to calculate the internal forces for different structures. Therefore the superposition principle will be applied to the hose structure, and is shown below in Figure 6.13.

The figure shows a pipe which will be considered as a hose. The hose including its content is considered to be submerged in water. Furthermore, the figure shows the forces acting on the hose segment, the internal fluid and the external fluid separately. Since a closed pressure field exists, the principle of superposition along with the Archimedes principle can be applied to calculate the effective tension of the hose.

A hose segment is shown curved and in equilibrium under the combined influence of hose weight, internal pressure, external pressure, and the true wall tension acting in the hose wall [30]. The resultant lateral force acting on the hose due to the internal and external pressure is zero because the forces are counterbalancing each other. An axial force is required to hold the true weight of the hose. This axial force is acting on the wall of the hose and is referred to as true wall tension.

The resultant forces acting on the internal fluid is only in the axial direction. Whereas the resultant lateral force acting on the internal fluid due to pressure is zero because the forces are counterbalancing each other. This resultant axial force is given as the product of internal pressure and the internal cross section of the hose. This force is equivalent to the weight of the fluid in the hose. Similarly, the external fluid is only subjected to an axial force. This axial force is equal to the product of external pressure and external hose cross section.

The resultant axial force is calculated by adding the axial force acting on the hose wall and the internal fluid, subtracting the axial force acting on the external fluid (displaced fluid). This resultant axial force is equivalent to the effective tension.

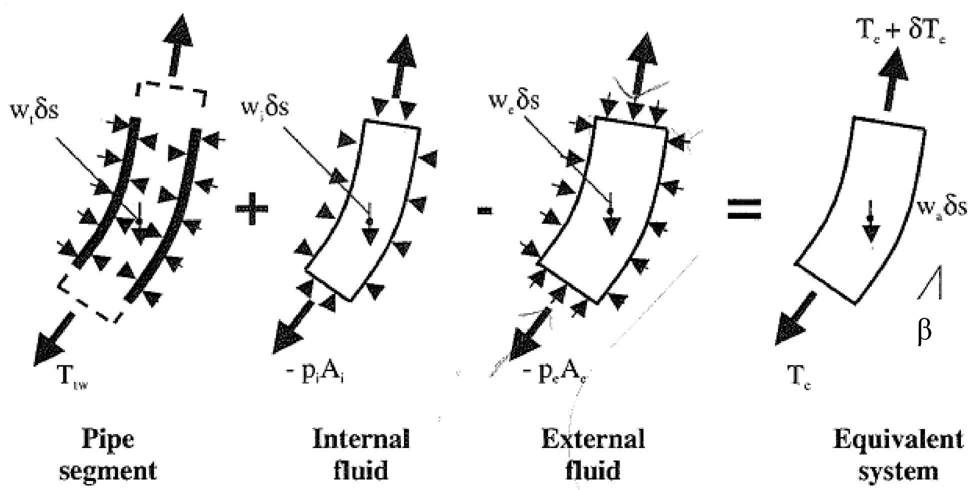

Figure 6.13 Hose with internal and external fluids - equivalent force systems [30]

The effective tension is mathematically formulated as follows [30]:

$$T_e = T_{tw} + (-p_i A_i) - (-P_e A_e) \tag{6-4}$$

where

T_{tw} = True wall tension

p_i, p_e = Internal and external pressures

A_i, A_e = Internal and external cross-sectional areas of the pipe

The equation for the apparent weight (w_a) is defined as [30]:

$$w_a = w_h + w_i - w_e \tag{6-5}$$

where

w_a = Apparent weight per unit length

w_h = Hose weight per unit length

w_i = Internal fluid weight per unit length

w_e = External fluid weight per unit length

The effective tension and apparent weight are related. For a hose element of length *ds,* resolution of forces in the axial direction gives [30]:

$$\frac{dT_e}{ds} = w_a \cos\beta \tag{6-6}$$

where

ds = Hose element length

β = Angle with the vertical

Equation (6-6) shows that with small angles $dT_e/ds = w_a$.

The effective tension can be calculated by two different methods. The first method is based on equation (6-4). The second model can, according to [30], be calculated as the effective tension at any point along a riser. This can be calculated by considering the equilibrium of the segment between the point and the riser top end, taking into account the riser top tension and the segment's apparent weight.

The second method will be used in this thesis for some manual calculations. The top tension (T_t) is defined as follows for the static case:

$$T_t = w_a \times L_s \times g \tag{6-7}$$

where

T_t = Top tension

L_s = Segment length

g = Gravitational acceleration

For the pre-commissioning operation, it should be noticed that the apparent weight depends whether the hose is hanging in the air or is submerged in water. The apparent weight will also depend on hose type for this operation.

The effective tension can be calculated as:

$$T_e = T_t - w_a \times L_i \times g \quad \textbf{(6-8)}$$

where

L_i = Length from hose start to any given point

Now, the true wall tension (T_{tw}) can be calculated based on equation (6-4). This sub chapter is to a large extent written based on Sparks [30].

6.3.2 Curvature

The hose shape is assumed to follow a catenary model. This model can be expressed as [23]:

$$z = \frac{T_h}{w_a}(cosh\frac{xw_a}{T_h} - 1) \quad \textbf{(6-9)}$$

where

x = horizontal distance from TDP

z = height above seabed

T_h = horizontal force at seabed

The curvature is defined as follows [23]:

$$k = \frac{w_a}{T_h}cosh\frac{xw_a}{T_h} \times \cos\theta \quad \textbf{(6-10)}$$

Where

θ = angle to the x-axis

Based on (6-10), the maximum curvature will be at the TDP. This results in:

$$k_{max} = \frac{w_a}{T_h} \quad \textbf{(6-11)}$$

6.3.3 Free hanging static analysis - Effective tension

The effective tension in the static case will be calculated to identify how the effective tension changes due to hose length and will ensure that the effective tension is below the hose restrictions. The effective tension for the two different hose types will change as a result of different parameters.

The boundary conditions for the case considered in Figure 6.14 are the hose length at 6 m and the hose length at 130 m. These boundaries are highlighted with a black vertical dashed line below in Figure 6.14. These boundaries are chosen to able to use linear theory for manual calculations. Non-linear theory is required if the bends in the configuration should be considered.

It is shown that the 6” Oilflex Super hose is exposed to higher effective tension compared with the 4” Oilflex Super hose. It should also be mentioned that the trend changes along the hose length. The hose is lowered into the sea with lengths of approximately 15 m; therefore there is a changed trend. This change of the surrounding environment for the hose is highlighted with a vertical blue line below. From 0 m to 15 m the hose is surrounded by air, while from 15 m to 190 m the hose is surrounded by seawater.

The calculated effective tension will be compared with the effective tension calculated by OrcaFlex for a static free hanging configuration to check if the approximation assumed in this chapter is acceptable. The same methodology can be used for the lazy wave configuration, but buoyancy modules/effects should be implemented in the calculations.

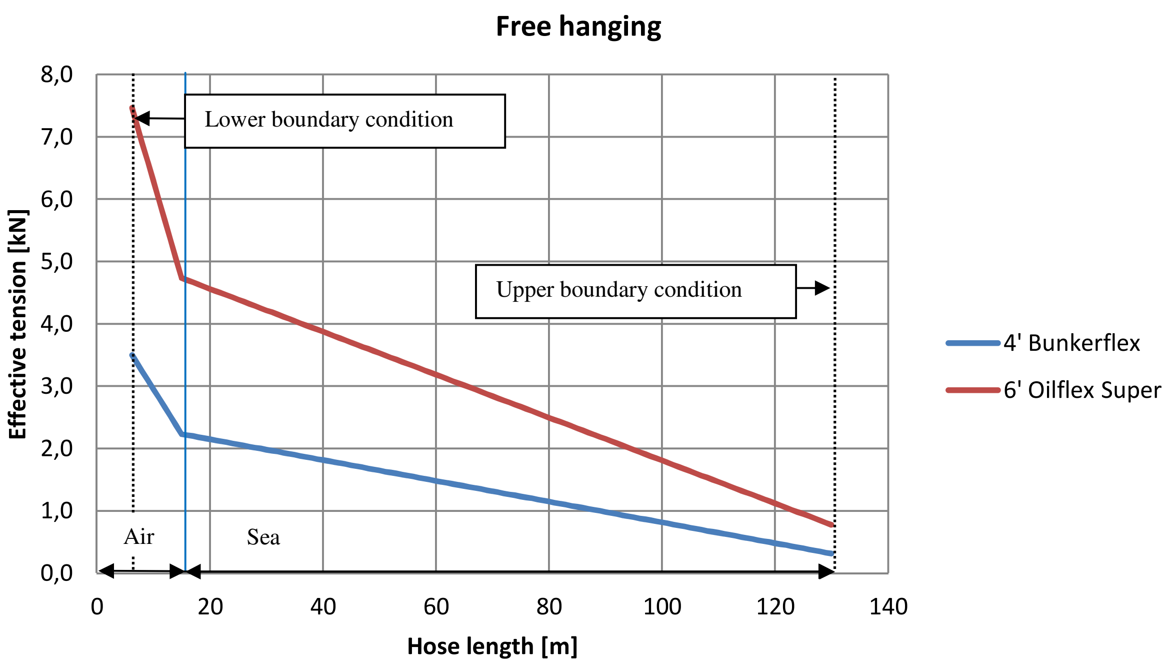

Figure 6.14 Manual calculation of effective tension for free hanging configuration

6.3.4 Free hanging static analysis - Curvature

Firstly, let us assume some input parameters for the analysis for the 4" Bunkerflex STH:

- x = 51 m
- θ = 84.9 °

Top tension can be calculated from (6-7). This results in:

$$T_t = w_a \times L_s \times g \ = 3500.1\ N$$

After the top tension is defined, T_h can be calculated as follows:

$$T_h = T_t\ \cos(84.9°) = 313.7\ N$$

Based on (6-9) the free hanging shape can be calculated. This results in Figure 6.15 as shown below. It is important to emphasise that this shape is from the sea level to the TDP.

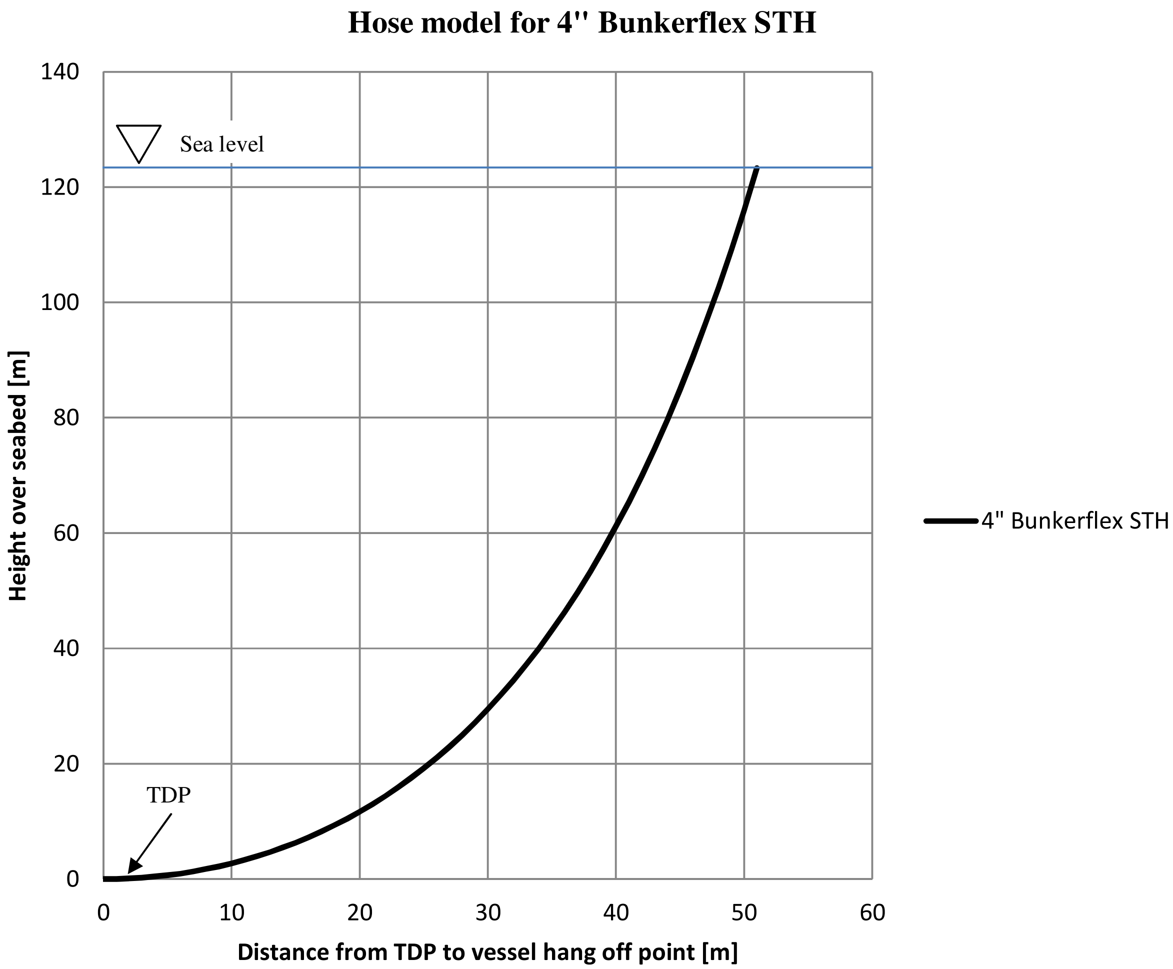

Figure 6.15 Free hanging configuration shape for 4" Bunkerflex STH - manual calculation

Based on (6-11), the maximum curvature is then defined as:

$$k_{max} = \frac{1.7\ \frac{kg}{m} \times 9.81\frac{m}{s^2}}{313.8\ N} = 0.053\ \frac{rad}{m}$$

The same methodology for T_t, T_h and k_{max} can be used for the 6" Oilflex Super hose. This results in values as given in Table 6.2:

Table 6.2 Static summary results for 6" Oilflex Super hose

Parameter	Value
T_t	7467.4 N
T_h	669.4 N
k_{max}	0.051 rad/m

In the lazy wave configuration, buoyancy modules need to be included in the calculations.

6.4 OrcaFlex static analysis

The static analysis is first carried out before applying dynamics to the system. The static analysis determines the relationship between the vessel position and connection point, which in this case is the pipeline on the seabed. The output will be the curvature and the effective tension for the system. This is the first step to see whether the relevant configurations will be considered further for dynamic analysis. Below in Figure 6.16, a flow chart that shows the methodology for static analysis will be used in this thesis is given.

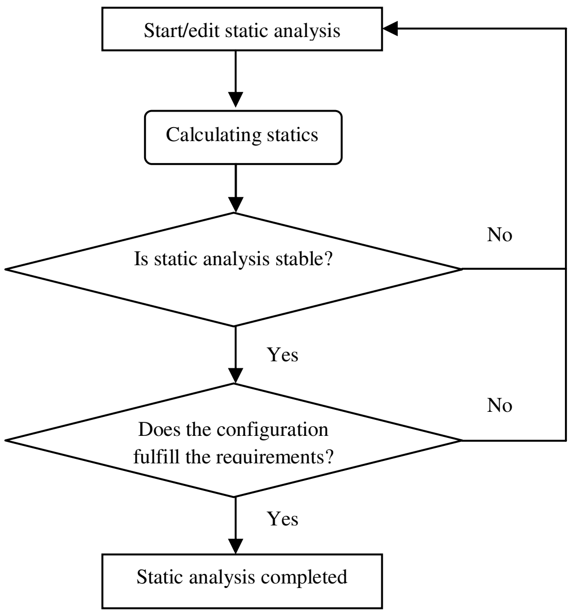

Figure 6.16 Flow chart for static analysis

6.4.1 Free hanging configuration

The free hanging configuration shall be analysed for both hose types. A graph for effective tension vs. arc length for the 4” Bunkerflex STH is shown below in Figure 6.17. The arc length (hose length) is shown on the X-axis, while the effective tension is shown on the Y-axis. The graph gives an indication of where the maximum loads are located. As predicted previously in the thesis, the maximum effective tension is located at the hang off position located close to the chute. The effective tension decreases with the arc length for this configuration.

In addition, a graph for curvature vs. arc length is shown in Figure 6.18. The arc length is shown on the X-axis, while the curvature is shown on the Y-axis. The graph shows that the maximum curvature is located in the chute area. This seems realistic for the static case. It can be seen that the curvature after the chute is decreasing until the sag bend occurs. There is a small curvature (less than 0.1 rad/m) where the sag bend starts and down to the TDP of the hose. The curvature is below its critical limitation. Similar graphs for the 6” Oilflex Super hose can be found in Appendix B – Static results.

For both hose types, the configuration is within the requirements. Below, in Table 6.3 the output of the graphs is summarised.

Table 6.3 Maximum effective tension and maximum curvature for both hose types in free hanging configuration (static case)

Hose type	Maximum effective tension	Allowable effective tension	Maximum curvature	Maximum allowable curvature
4” Bunkerflex	3.6 kN	50.5 kN	0.8 rad/m	1.0 rad/m
6” Oilflex Super	9.7 kN	99.7 kN	0.63 rad/m	0.656 rad/m

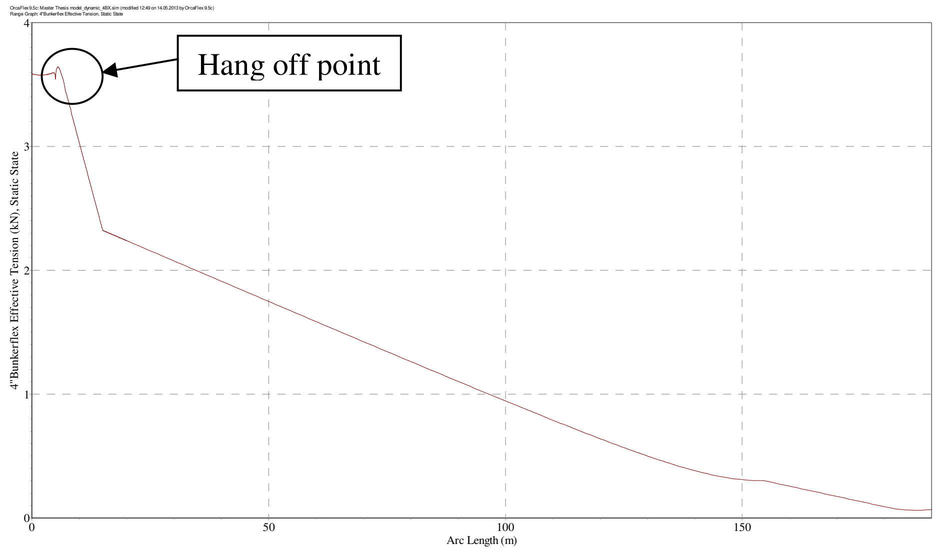

Figure 6.17 Effective tension vs. arc length for 4" Bunkerflex STH hose for free hanging (static case)

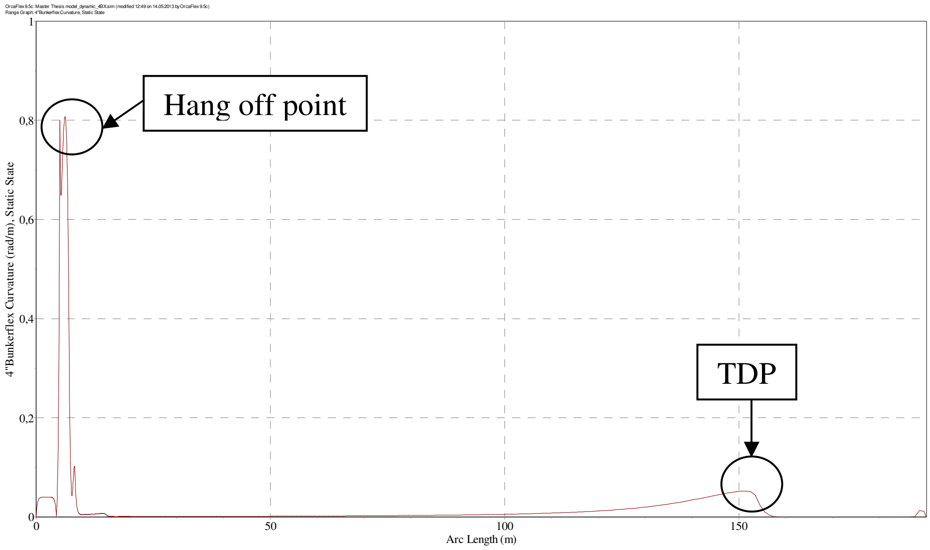

Figure 6.18 Curvature vs. arc length for 4" Bunkerflex STH hose for free hanging (static case)

6.4.2 Lazy wave configuration

As discussed in Chapter 4, the reaction loads on the hose depend on a different set of parameters such as:

- Size of buoyancy modules
- Flotation point position
- Number of buoyancy modules
- Distance between buoyancy modules

The size of the buoyancy modules are as listed in chapter 6.2.5.

A sensitivity analysis will be performed in OrcaFlex to determine the minimum number of buoyancy modules required for different flotation point positions. It is assumed that the distance between the buoyancy modules will be placed with an interval from 1-5 m.

Two criteria's are suggested to be able to define the minimum number of buoyancy modules:

- The bending radius on the hose > MBR of the hose
- The height of the lazy wave has to be positive

Positive height of the lazy wave is shown below in Figure 6.19, where the buoyancy modules makes a small top in the configuration, while negative height of the lazy wave is shown below in Figure 6.20 where the top is absent.

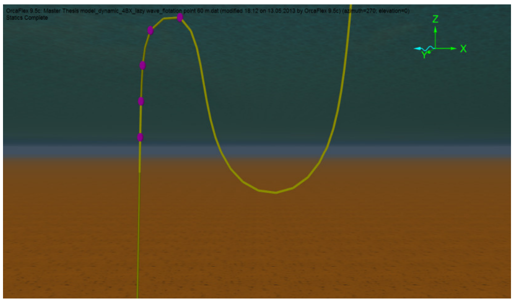

Figure 6.19 Positive lazy wave height

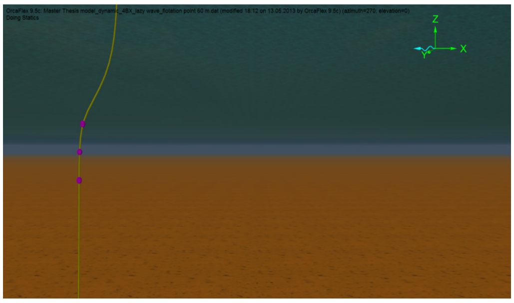

Figure 6.20 Negative lazy wave height

The output of the static buoyancy analysis will be to identify how the discussed parameters affect the minimum number of buoyancy modules required. The upper limit of the floatation point is selected to be 20 m. A floatation point with less distance to the sea level may cause interference between the hose and the vessel. The interval chosen between the floatation points is selected to be 20 m based on the water depth. The deepest floatation point was selected to be 80 m from the sea level. A floatation point deeper than 80 m may result in that the buoyancy modules can interfere with the seabed.

Based on Table 6.4 it can be observed that the flotation point for the hose has a significant effect on minimum required buoyancy modules. In this particular case, the distance between the buoyancy modules has no effect on the 4” Bunkerflex STH hose. However, the distance between the modules of the 6” Oilflex Super hose are of importance based on the two suggested criteria’s above. However, if the distance between the buoyancy modules is 1 m, this may increase the probability for high curvature in the given configuration. However, an increased distance between buoyancy modules resulted in decreased positive lazy height. Therefore the distance between the buoyancy modules will be chosen to be 2 m in the dynamic analysis. This also corresponds to IKM procedures.

The floatation point will be chosen based on the results from the free hanging dynamic analysis and different case studies carried out for the lazy wave model.

If the buoyancy modules are placed relatively close to the vessel they reduce the tension/compression forces from the vessel on the hose, which reduces the movement at the TDP. However, if the buoyancy modules are positioned close to the TDP, the movement at the TDP reduces even more. The limiting variable will be identified in the dynamic analysis.

The minimum number of buoyancy modules required at different flotation points is also plotted in Figure 6.21 based on the hose length in the static case. From Table 6.4 and Figure 6.21 it is seen that the 6” Oilflex Super hose requires significantly higher amount of buoyancy modules. This is realistic since both the bending stiffness and hose weight are higher for the 6” Oilflex Super hose. After having identified the minimum amount of buoyancy modules required for the different models, it is a requirement that damage to one single buoyancy element should not result in unacceptable loss of buoyancy for the system as a whole [16].

Table 6.4 Minimum number of buoyancy modules for different floatation points with different distance between modules

	4" Bunkerflex STH				6" Oilflex Super			
Minimum number of buoyancy modules	Flotation point below sea level [m]							
	20	*40*	*60*	*80*	*20*	*40*	*60*	*80*
1 m distance between	7	6	5	4	15	13	10	7
2 m distance between	7	6	5	4	15	13	10	7
3 m distance between	7	6	5	4	15	13	10	7
4 m distance between	7	6	5	4	15	13	10	7
5 m distance between	7	6	5	4	16	13	10	8

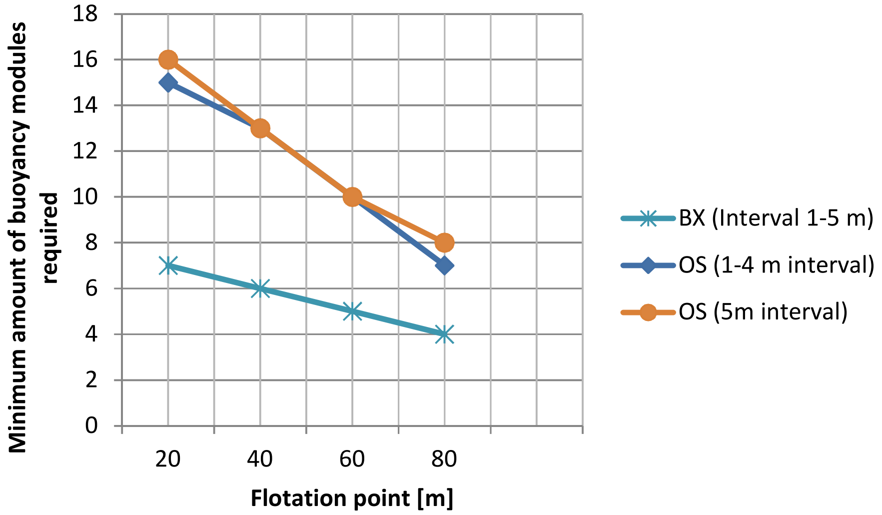

Figure 6.21 Minimum required buoyancy modules required based on different flotation point

A graph for effective tension vs. arc length for the 4" Bunkerflex STH with floatation point at 60 m is shown below in Figure 6.22. The arc length is shown on the X-axis, while the effective tension is shown on the Y-axis. The graph gives an indication of where the maximum loads are located. As predicted previously in the thesis, the maximum effective tension is located in the hang off position located close to the chute. The effective tension decreases until it reaches the buoyancy modules. After the buoyancy modules the effective tension is again quite low until it reaches the TDP where a small peak occurs.

In addition, a graph for curvature vs. length is shown in Figure 6.23. The arc length is shown on the X-axis, while the curvature is shown on the Y-axis. The graph shows that the maximum curvature is located in the chute area. This seems realistic for the static case.

It can be seen that the curvature after leaving the chute is decreasing until the buoyancy modules occur. There is a curvature (up to 0.75 rad/m) where the buoyancy modules are located. After the buoyancy modules the curvature decreases until the curvature again rises in the TDP area. The curvature is below its limitation. Similar graphs for the 6" Oilflex Super hose can be found in Appendix B – Static results.

For both hose types, the configuration is within the defined requirements. Below, in Table 6.5 the output of the graphs for both hose types are summarised.

Table 6.5 Maximum effective tension and maximum curvature for both hose types in lazy wave configuration floatation point 60 m (static case)

Hose type	Maximum effective tension	Allowable effective tension	Maximum curvature	Maximum allowable curvature
4” Bunkerflex	2.5 kN	50.5 kN	0.82 rad/m	1.0 rad/m
6” Oilflex Super	5.2 kN	99.7 kN	0.62 rad/m	0.656 rad/m

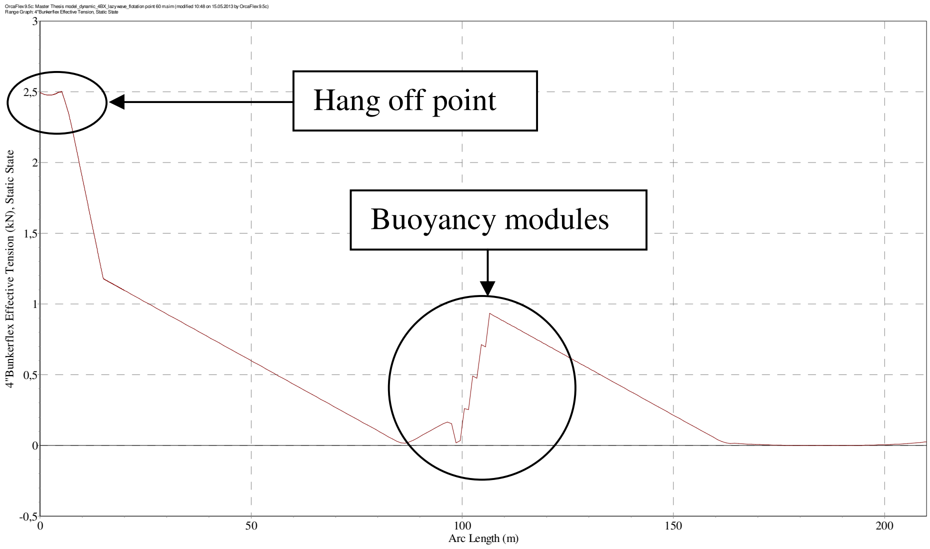

Figure 6.22 Effective tension vs. arc length for 4" Bunkerflex STH hose for lazy wave configuration (static case)

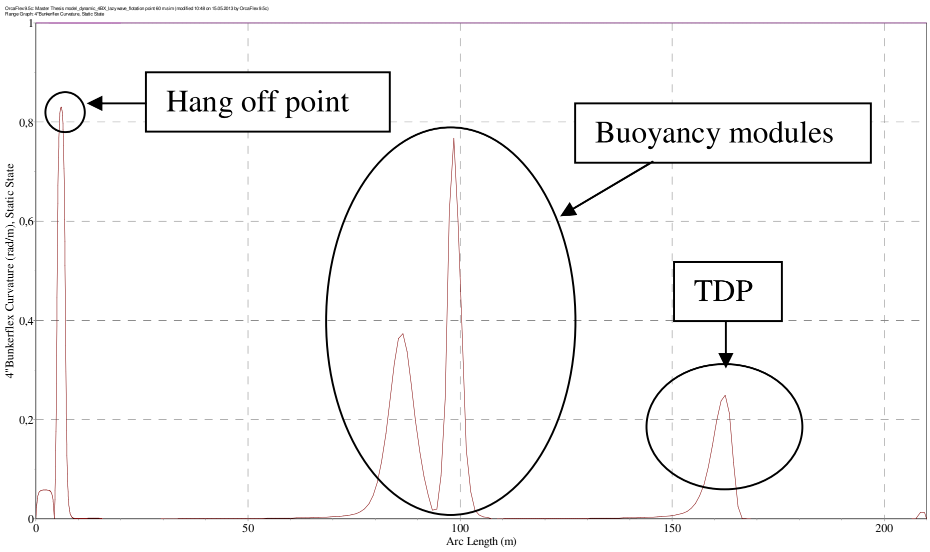

Figure 6.23 Curvature vs. arc length for 4" Bunkerflex STH hose for lazy wave configuration (static case)

6.4.3 Discussion static results

It is shown that the maximum effective tension is higher for the 6" Oilflex Super hose for both configurations compared with the 4" Bunkerflex STH. This seems realistic since the 6" Oilflex Super is the heaviest hose dry and when submerged in water. The curvature is lower for the 6" Oilflex Super hose for both configurations. This seems realistic since the maximum curvature in the static case is placed in the chute area for both configurations, and the size of the chute is larger for the 6" Oilflex Super hose.

It should be specified that the number of buoyancy modules in the analysis are not selected based on minimum required amount of buoyancy modules. According to [16] the configuration should maintain its shape if minimum one buoyancy module loses its function. While analyzing the minimum required amount of buoyancy modules, a trend was showing that when the distance between the buoyancy modules increase, it resulted in a decreasing effect on the height of the lazy wave. In some cases, this lead to an increased amount of buoyancy modules required. The required number of buoyancy modules also depends on where the offset is located. Longer offset between the vessel and TDP, requires more buoyancy modules.

It should also be mentioned that we should not place too many buoyancy modules on the hose. This may result that too much of the hose floats, which again leads to shorter distance between the TDP and the pipeline connection, also called the "safety length". The distance from the TDP to the pipeline should be sufficient, to prevent high tension/compression forces in the end connection. The number of buoyancy modules will be based on a smooth curve which has a significant height of the lazy wave, and to assure a sufficient safety length for all configurations.

The free hanging configuration and the lazy wave configuration will be chosen based on sensitivity analyses in OrcaFlex. The sag bend in the free hanging configuration is clearly within its requirements. This sag bend curvature would be more dominant if the water depth was deeper. A flotation point close to the vessel resulted in reduced tension and compression forces at the hang off point, while a flotation point close to the seabed results in less curvature for the TDP. All static models are within their requirements w.r.t. the maximum effective tension and curvature. This results in that each model can be considered for dynamic analysis.

Below in Figure 6.24 and Figure 6.25 is shown a comparison of the effective tension for manual calculations against OrcaFlex calculations for the 4" Bunkerflex STH hose and 6" Oilflex Super hose, respectively. Both calculations follow the same trend, but it seems like the OrcaFlex calculations are slightly more conservative. The formulas and assumptions for the manual calculations are given in chapter 6.3.1, while OrcaFlex [27] have a different approach to the problem. The effective tension in OrcaFlex is calculated based on the wall tension, $T_{tw\text{-}OrcaFlex}$, which is calculated as follows [27]:

$$T_{tw-OrcaFlex} = EA\varepsilon - 2\nu(P_eA_e - P_iA_i) + \frac{EAe(\frac{dL}{dt})}{L_o} \tag{6-12}$$

The first term is the contribution from axial stiffness, the second term is the contribution from external and internal pressure (via the Poisson ratio effect) and the third term is the axial damping contribution [27]. The variables are given by:

EA = Axial stiffness of line

ε = Total mean axial strain $(L_s\text{-}\eta L_o)/(\eta L_o)$

L_s = Instantaneous length of segment

η = Expansion factor of segment

L_o = Unstretched length of segment

v = Poisson ratio

e = damping coefficient of the line

dL/dt = rate of increase of length

This is most probably the reason why the OrcaFlex curve has a slighter higher values compared with the manual theory used from Sparks [30].

The calculated curvature (0.053 rad/m) for free hanging configuration corresponds to the maximum curvature for the free hanging configuration.

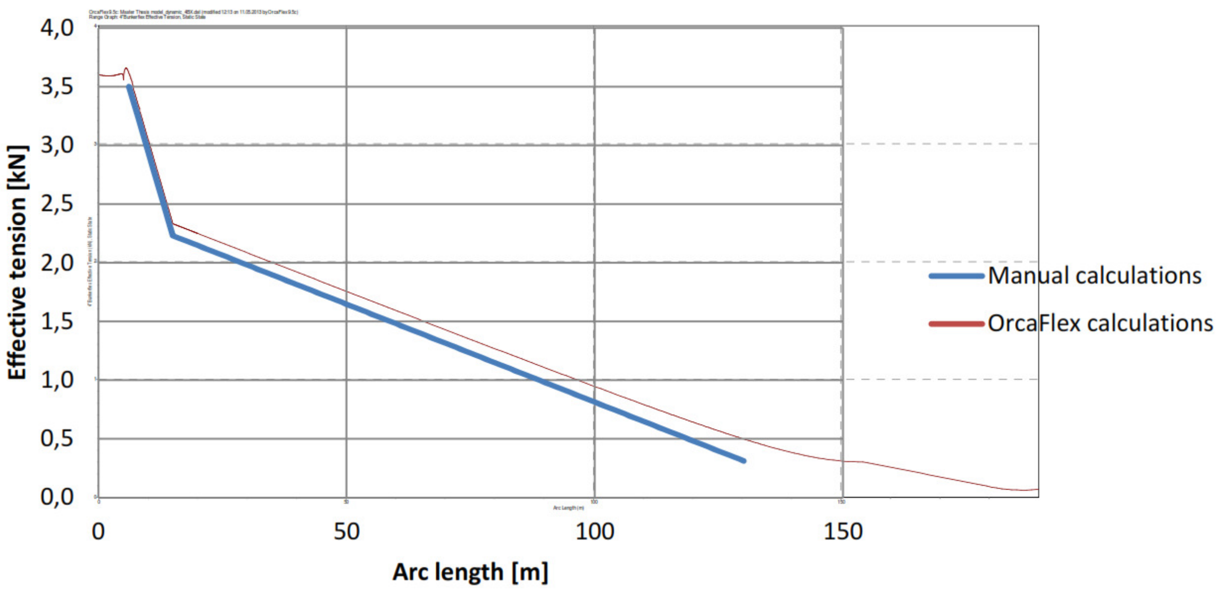

Figure 6.24 Comparison of effective tension for manual calculations vs. OrcaFlex calculations for the 4'' Bunkerflex STH

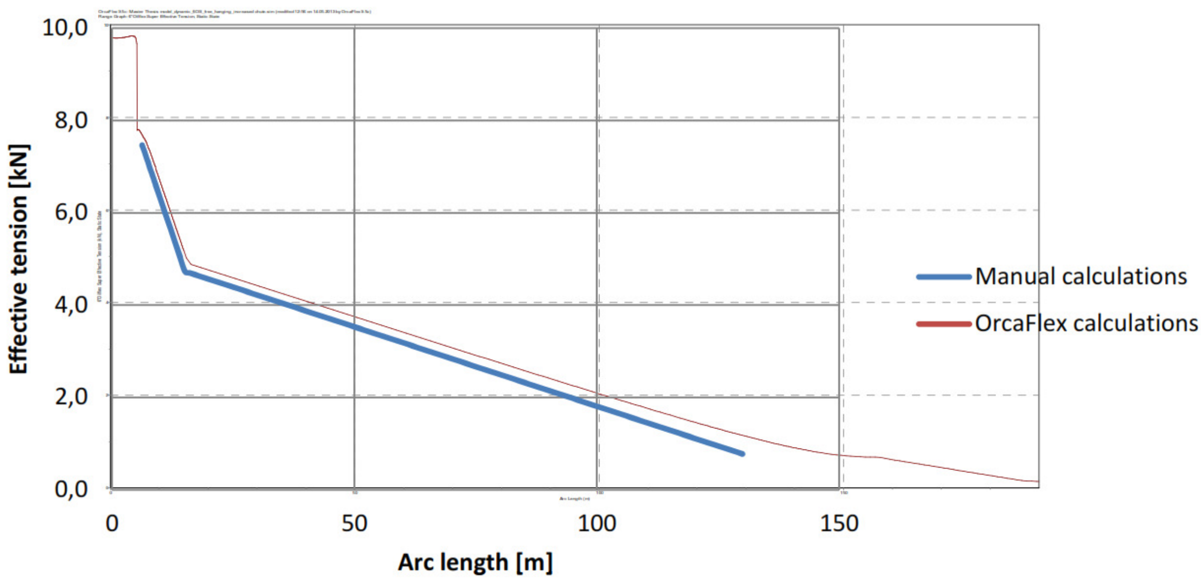

Figure 6.25 Comparison of effective tension for manual calculations vs. OrcaFlex calculations for the 6" Oilflex Super

6.5 OrcaFlex dynamic analysis - regular waves

Dynamic analysis applies dynamics to a static configuration [31]. The dynamic analysis will show how the model will react during different environmental loads. It is recommended that initially the regular wave approach should be used in parametric studies [16].

Below in Figure 6.26 a flow chart for the dynamic analysis for regular waves is shown. All the results will be attached in Appendix C – Dynamic results.

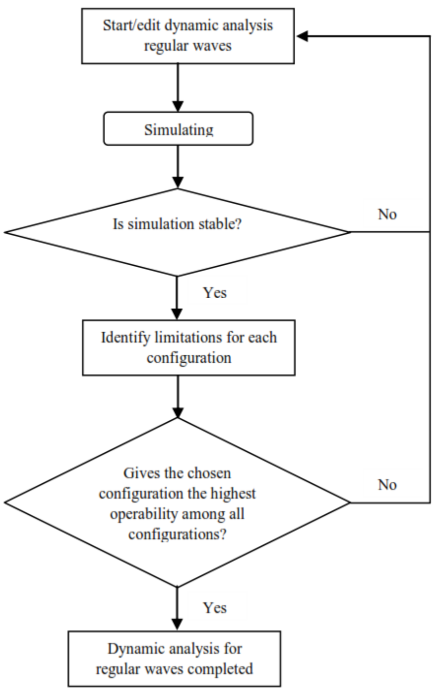

Figure 6.26 Flow chart for dynamic analysis - regular waves

6.5.1 General

For the dynamic analysis, the graphs in chapter 6.4 will be implemented in column charts. The output from the charts will be:

- Maximum effective tension
- Minimum effective tension
- Maximum curvature

This implementation is carried out to get a better overview of the environmental cases selected. Each different environmental load case is given a specific name. One example is T06dir135H7, which can be split up in three parameters:

- T06 = Wave period is 6 s
- Dir135= Wave direction is 135°
- H7 = Wave height is 7 m

Below in Figure 6.27 an example of an effective tension graph is shown. In the chart title it is first written which variable that is analysed, which in this case is effective tension. Then the direction of the waves is identified, followed by the given wave heights. This chart title makes it easy to navigate in all the different graphs in Appendix C – Dynamic results. The red line shows the limitation for compression load for the system, which is 3.78 kN for the 4" Bunkerflex STH hose. There will also be a red limit line if the effective tension is close to, or exceeds the maximum effective tension for the given hose type. It can be seen that the environmental load for the T07dir135H6, the T07dir135H7 and the T08dir135H7 case overruns the limitation. This is shown with three circles in Figure 6.27.

In Figure 6.28 the curvature for different environmental load cases are shown. The chart title build up is the same as for effective tension. The red line shows the curvature limitation for this hose type, which is 1.0 rad/m for the 4" Bunkerflex STH hose. It can be seen that the environmental load for the T09dir180H7 case overruns the limitation in this case.

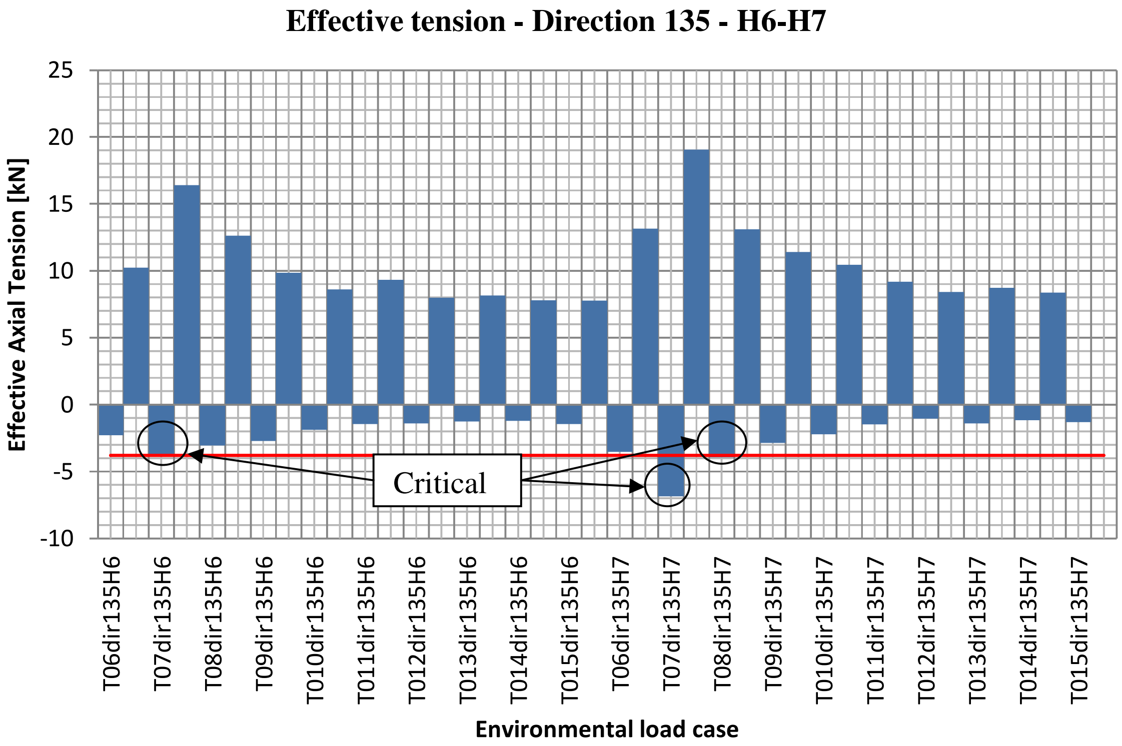

Figure 6.27 Example of graph showing effective axial tension for different environmental load cases

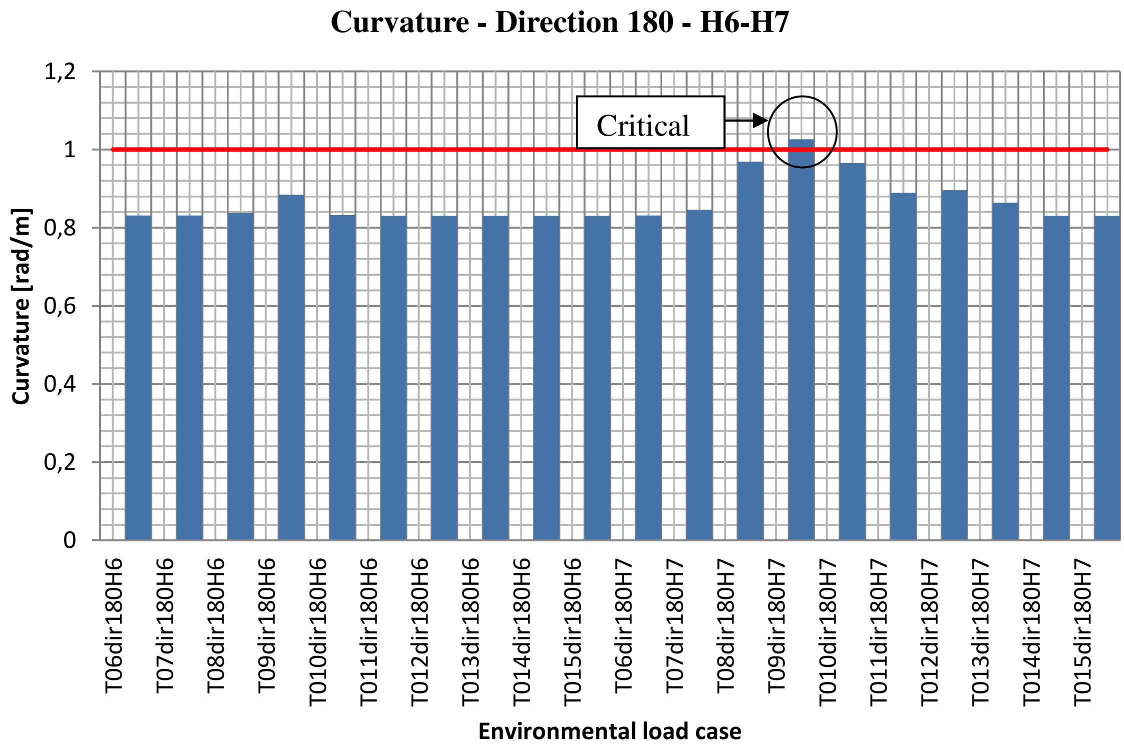

Figure 6.28 Example of graph showing curvature for different environmental load cases

To summarise all the different environmental load cases for a model, a typical wave rose is used to show the wave height limitation for different directions for the particular model. Below in Figure 6.29 an example of a wave rose is shown. The numbering system from 0-315 shows the direction the waves hit the vessel, while the numbers 0-8 shows the wave height limitation for this model. For this illustration, it can be observed that the vessel can operate in up to 4 m maximum wave height when the waves hit the vessel from 135° direction, and up to 6 m for a wave height from 180° direction, while it can operate in up to 7 m wave height from 225° direction. The wave rose do not consider wave periods, just maximum wave heights.

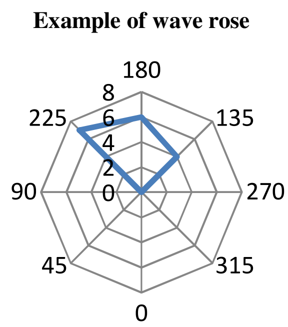

Figure 6.29 Example of wave rose

The last type of charts which is called a limitation plot is shown in Figure 6.30 In comparison with the wave rose illustration, this graph shows both the limiting wave height and wave period for the different wave directions. The area above the graph lines shows an area of wave heights and wave periods that is not accepted or evaluated in this thesis. To be conservative, wave heights higher than 8 m are not considered for this pre-commissioning operation. The area below the graph lines is considered acceptable for this operation. The vertical dotted line shows the wave periods that are considered for the analysis, where the lower limit is 4 s and the upper limit is 15 s (ref Design Basis).

The limitation plot actually summarises all the column charts for one model in one graph. Below it is highlighted three points circled with dotted lines. The wave rose in Figure 6.29 shows the wave limitations for the model to be:

- 4 m for 135°
- 6 m for 180°
- 7 m for 225°

This can also be observed based on the limitation plot. But if the wave period increases from 6 s to 8 s, the wave limitation would change. This is shown with the two circles in Figure 6.30. This results in that the vessel can operate in following conditions:

- 6 m for 135°
- 6 m for 180°
- 8 m for 225 °

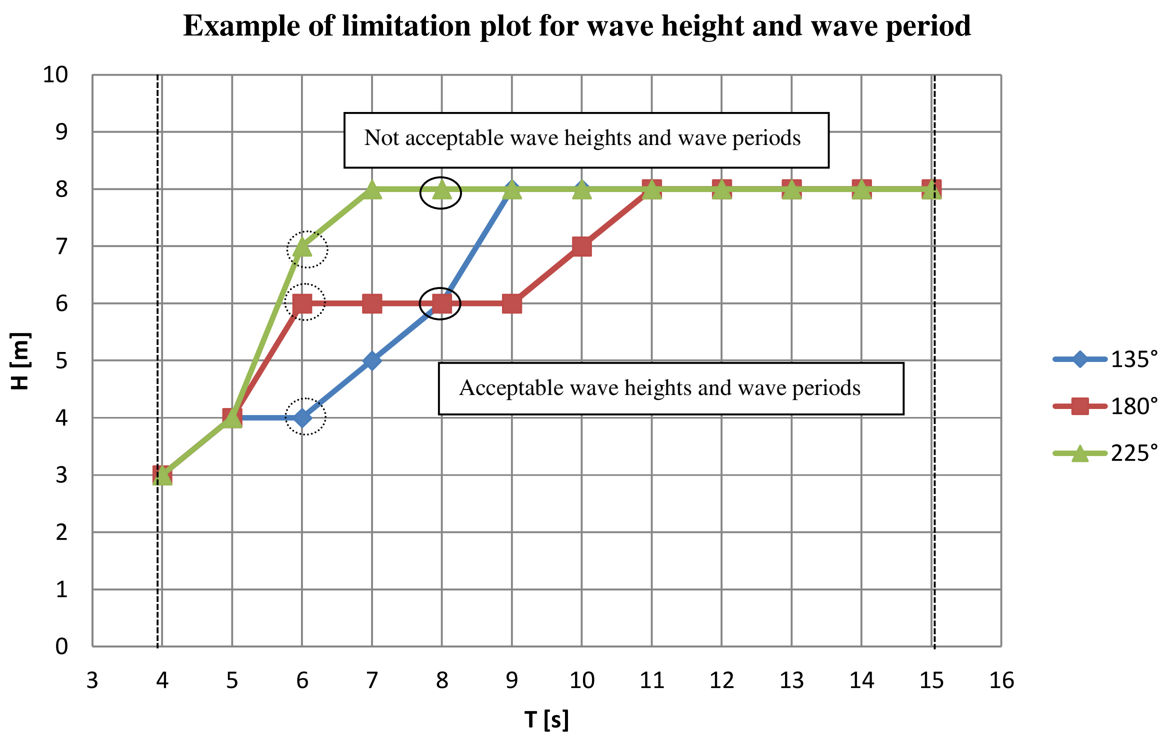

Figure 6.30 Example of limitation plot

6.5.2 Free hanging configuration

All the dynamic results for the free hanging configuration can be found in Appendix C – Dynamic results. Below in Figure 6.31 a summary of the results are presented in wave rose format for each hose type. The wave roses show that the 4” Bunkerflex STH hose can operate under higher wave heights compared with the 6” Oilflex Super.

For the 4” Bunkerflex STH hose it is the curvature which is the limiting criteria, except from the waves coming from a direction 225°. Here compression loads is the limiting criteria. Curvature is also the limiting criteria for the 6” Oilflex Super hose, except for the waves coming from a direction 135°. Here compression loads is the limiting criteria.

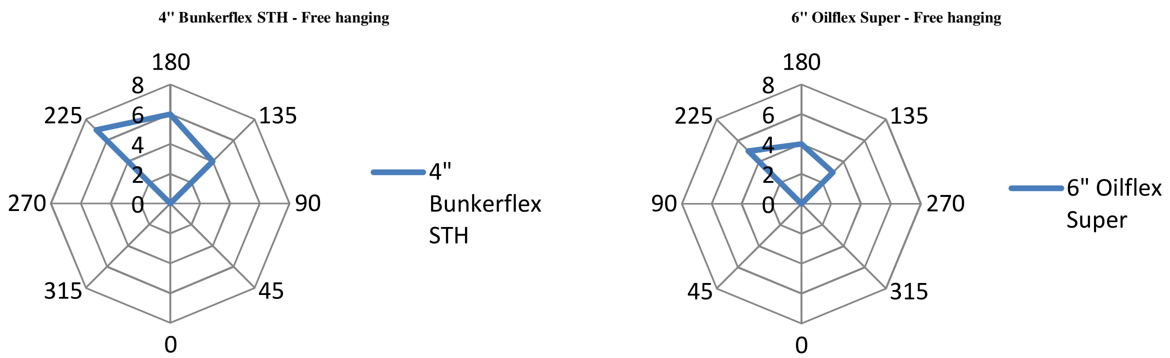

Figure 6.31 Free hanging configuration dynamic results for both hose types

The maximum tension does not at any stage approach critical value, while the maximum compression limit and the maximum curvature do. This is shown by dynamic range graphs in Figure 6.32 and Figure 6.33 for the particular case of T07dir135H7. In general, the highest tension is located along the hang off point and the water level. The maximum compression is found at the varying TDP. The highest curvature is also found on the sea surface, and not at the TDP. It should also be noticed that the graphs for the dynamic cases show the minimum, maximum and average/mean load during the simulation. The allowable tension graph is not shown in Figure 6.32 since this is higher than 20 kN. In addition, an allowable curvature line is shown in Figure 6.33.

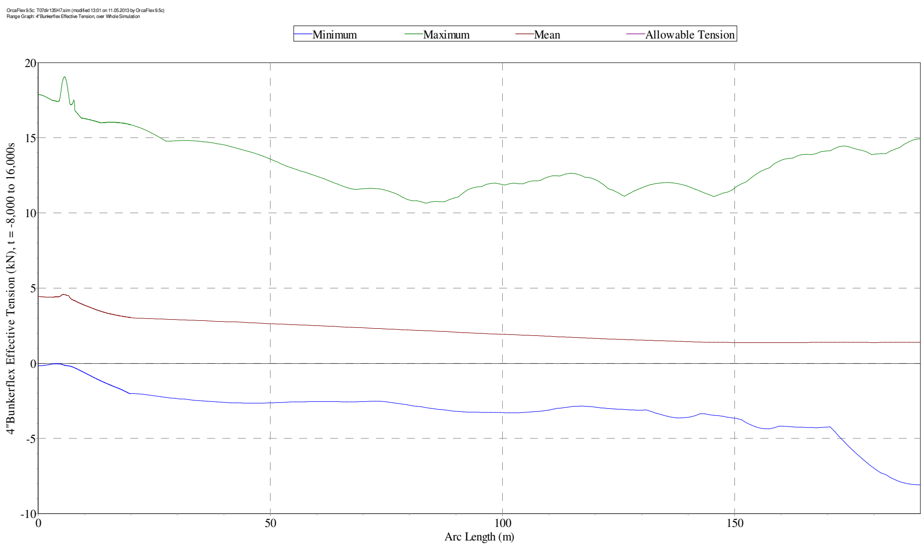

Figure 6.32 Dynamic graph for effective tension for case T07dir135H7

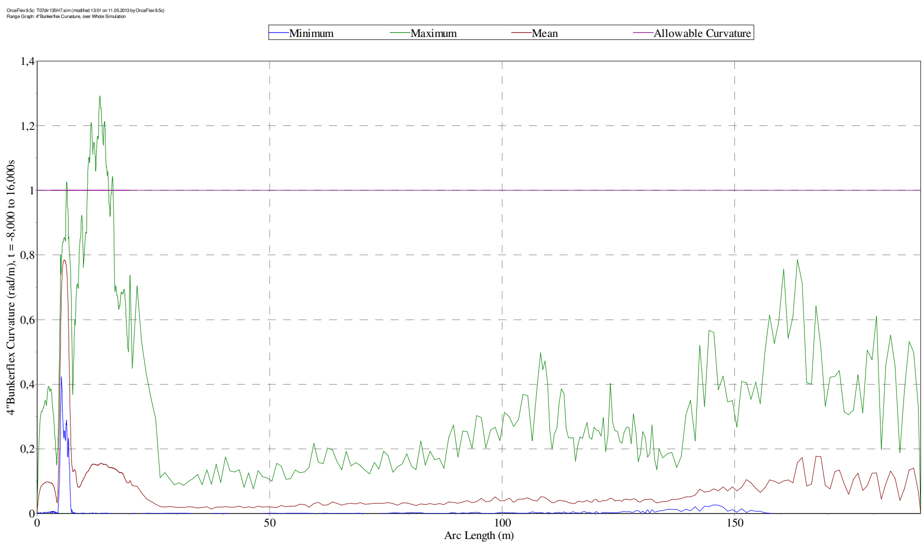

Figure 6.33 Dynamic graph for curvature for case T07dir135H7

6.5.3 Lazy wave configuration

All the dynamic results for the lazy wave configuration can be found in Appendix C – Dynamic results. Below, in Figure 6.34, a summary of the results are presented in wave rose format for each hose type. The wave roses show different operability conditions, depending on floatation point and hose type.

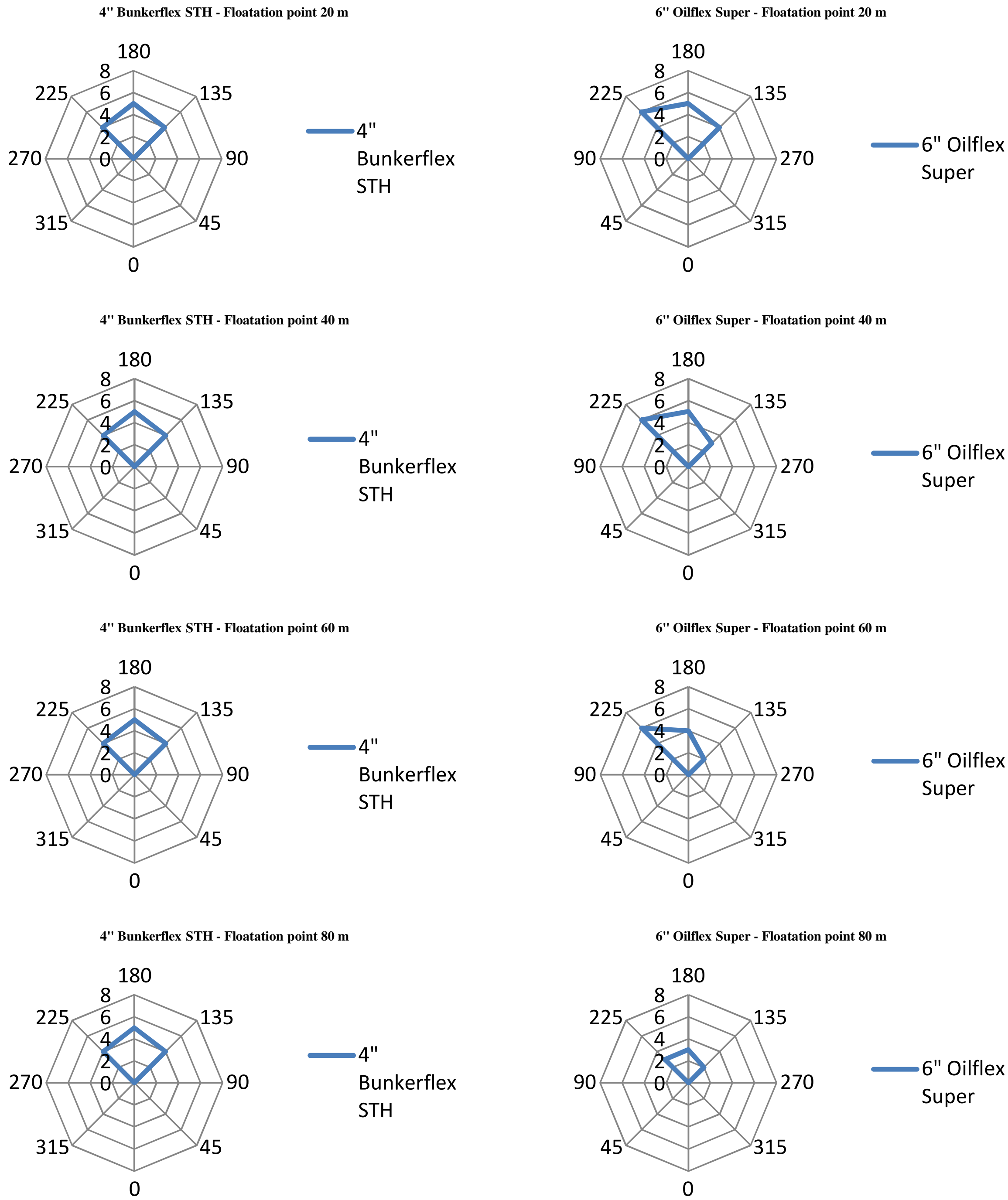

Figure 6.34 Wave roses for lazy wave configuration at different floatation points

The maximum tension does not at any stage approach critical value, which is reasonable since the lazy wave configuration reduces the tensions compared with the free hanging hose. As for the free hanging configuration, the maximum compression and maximum curvature are the limiting criterias for the lazy wave configuration. For all floatation points for both hose types it is the curvature that is the first limiting criteria.

This is shown in the dynamic graphs in Figure 6.35 and Figure 6.36. In general, the highest tension is located along the hang off point and the water level. The maximum compression is placed at the upper end of the hose, because the buoyancy modules reduce the movement of the hose. The highest curvature is also placed around the sea surface. It should also be noticed that the graphs for the dynamic cases show the minimum, maximum and average loads found during the simulation. The allowable tension graph is not shown in Figure 6.35 since this is higher than 20 kN. In addition, an allowable curvature line is shown in Figure 6.36.

The 4” Bunkerflex STH hose has the same limitations for different flotation points with respect to wave heights in the analysis, while the 6” Bunkerflex STH hose have different wave limitations for different floatation points. At a floatation point at 20 m, the 6” Oilflex Super hose seems more suitable compared with the 4” Bunkerflex STH. At floatation points from 40 m, 60m, and 80 m the 4” Bunkerflex STH hose seems more suitable to use with respect to maximum allowable wave height during operation.

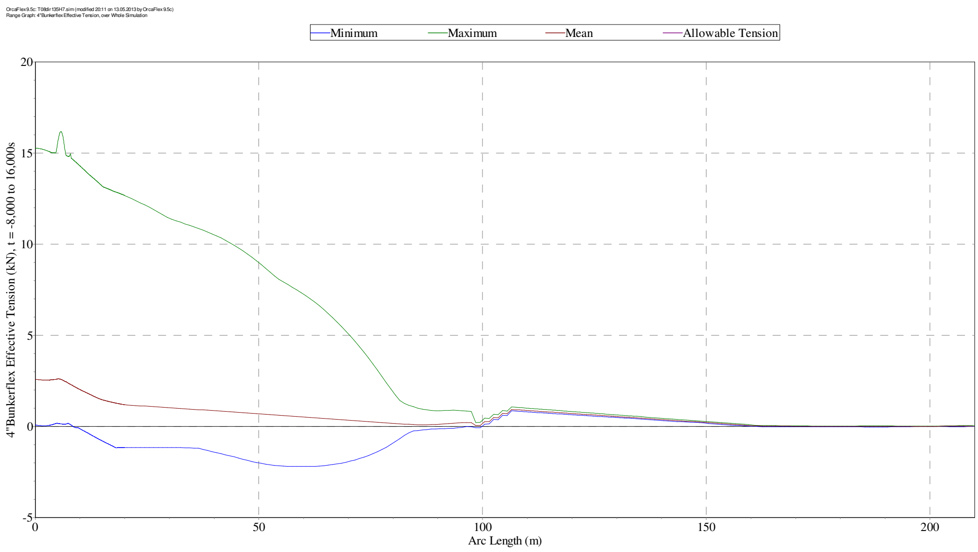

Figure 6.35 Dynamic range graph for effective tension for lazy wave configuration (floatation point 60 m) for case T08dir135H7

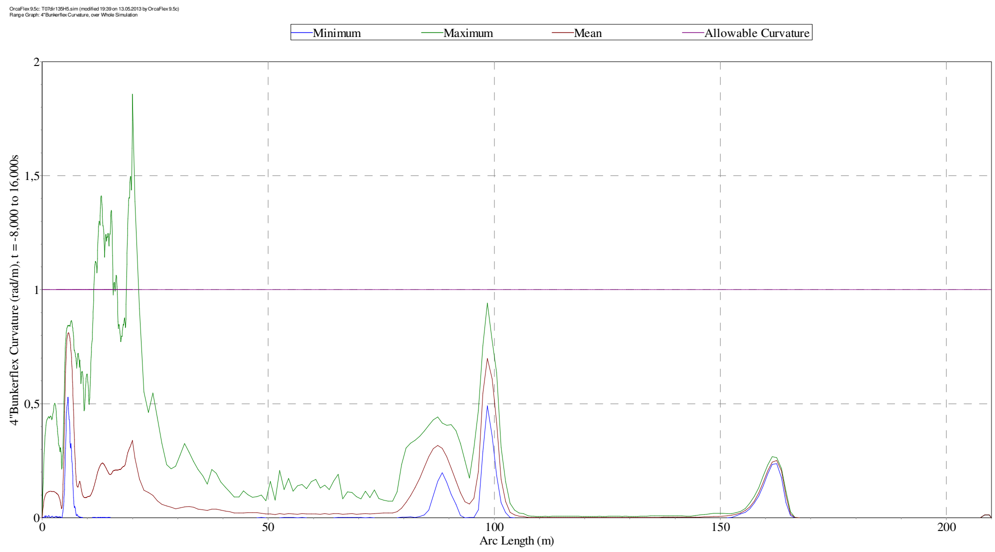

Figure 6.36 Dynamic range graph for curvature for lazy wave configuration (floatation point 60 m) case T08dir135H7

6.5.4 Discussion dynamic results

The 4" Bunkerflex STH is less exposed for tension and compression loads compared with the 6" Oilflex Super hose. In general, the curvature is the limiting criteria for all configurations except for the 4" Bunkerflex STH free hanging configuration and the 6" Oilflex Super free hanging configuration where the compression load exceeds the limitation when the waves hit the vessel from 225° and 135° directions, respectively.

The operability of the vessel is in general lowest when the waves hit the vessel from 135° direction. The main reason is that the chute is placed on the port side of the vessel. This arrangement results in maximum load reactions on the system when waves hit the vessel from starboard quartering sea (135° direction).

When the waves hit the vessel from the 135° direction, the vessel experiences mainly heave, roll and pitch motions. The negative pitch motion of the bow section will impose a compression force on the hose which is placed behind the transversal midline of the vessel (ref arrangement on deck chapter), while the positive pitch motion of the bow will impose a tensional force on the hose. The worst case scenario for the operation is simultaneous negative roll, negative pitch and negative heave for this arrangement. This alternating tension and compression stresses on the hose may result in fatigue.

The waves which hit the vessel from 180° and 225° direction have similar effect on the hose, but they are in general less critical than the waves from the 135° direction. However, if the chute was placed on the starboard side, the waves from the 225° direction would most probable be the most critical waves. If the chute arrangement was placed into the mono hull, the hose configuration would most likely be able to carry out the operation in the same wave conditions regardless of whether the waves hit the vessel from 135° or 225°.

The combination of wave heights and wave periods is also strongly connected to the results. The wave height limitation for different configurations is shown below in Table 6.7, while the critical periods, in general, are from 6 to 8 s. It may be concluded that the higher the magnitude (wave height) is for the same period, the bigger is the tension and compression stresses on the hose, which most often results in a critical curvature in the splash zone. Shorter wave periods will increase the acceleration of the vessel motions and the hose will be subjected to alternative compression and tensional stresses in a shorter time interval. The limitation plot for each model show that the period decides the wave height the vessel can operate under. However, the selection of hose and configuration will only be based on operability under wave heights.

At the splash zone, the hose experiences the highest curvature based on the alternating tension and compression loads as discussed above. How resistant the system is against wave heights from the selected directions seems to depend on the hose type. Some key parameters for each hose are listed below in Table 6.6. The different hose parameters are compared to easily get an understanding of how they are compared with each other in values and factors, to easily see the relationship between them.

Table 6.6 Key parameters for both hose types

Parameter	4" Bunkerflex		6" Oilflex Super	
Axial stiffness in tension	700 kN	1.0	850 kN	1.21
Axial stiffness in compression	40 kN	1.0	75 kN	1.88
Bending stiffness	0.2 kNm^2	1.0	1.4 kNm^2	7.0
Curvature limitation (maximum)	1.0 rad/m	1.0	0.656 rad/m	0.656
Water filled mass of hose in seawater	1.7 kg/m	1.0	3.51 kg/m	2.06

The splash zone leads to varying buoyancy on the hose caused by the waves which deteriorates the conditions for the operability in form of increased curvature. The 4" Bunkerflex STH hose seems in general most resistant against starboard quartering seas and head seas, while the 6" Oilflex Super seems in general most resistant against port quartering seas. However, for different configurations each case has to be considered separately. Therefore it is recommended to refer to Table 6.7 for the different configurations.

Free hanging is the configuration that can operate during the highest regular waves for the 4" Bunkerflex STH hose. This hose allows for the highest curvature, which is the dominant limiting criterion for this configuration. The offset of the free hanging configuration is higher compared with the lazy wave configuration, which is assumed to be a dominant factor whether the vessel can operate or not. It is assumed that the friction between the hose and sea bottom would be sufficient to withstand horizontal forces acting on the system.

It should also be mentioned that the hose type affects the trend for the different floatation points for lazy wave configurations. For the 4" Bunkerflex STH hose, the wave limitations is the same for all floatation points, while the wave limitations differs for each floatation point for the 6"

Oilflex Super hose. The most probable reason for the differences is the inertia of the system. In general, the deeper the floatation point is placed, the heavier the hose section will be between the hang off point and the floatation point. This results in more movement of mass caused by the vessel motions. Because of inertia, the hose may move upwards, while the vessel moves downwards. This results into bending of the hose that causes a critical curvature around the wave surface/splash zone. The lazy wave should also have sufficient height to ensure that the configuration maintain its original shape during the operation.

The two hose types will be considered separately. The submerged weight of the 6” Oilflex Super is more than 2 times bigger than for the 4” Bunkerflex STH hose, while the axial stiffness in compression for the 6” Oilflex Super is less than 2 times bigger than for the 4” Bunkerflex STH. The 6“ Oilflex Super will, as discussed, experience larger forces acting on the system compared with the 4” Bunkerflex STH. In a dynamic system, this would result that the 6” Oilflex Super would be more vulnerable to compression loads, which can result in buckling. Even though the bending stiffness is much higher on the 6” Oilflex Super, the allowable curvature is less.

The free hanging configuration would not experience the same trend as for the floatation points for the lazy wave configurations. This is most likely explained by the choice of offset and the “safety length” on the seabed. The vessel will cause large movement of the TDP, which will be less than the critical requirements. The TDP for the lazy wave configuration will not be exposed to large motions. The offset for the lazy wave configuration was chosen less than for the free hanging configuration to be able to design the lazy wave shape similar for the different floatation points and to be able to use the same hose length for different floatation points. It is of great importance that the “safety length” is sufficient on the seabed for the free hanging configuration, to assure that the hose does not get pulled away from the connection point, which is the pipeline. From a practical point of view, large movements in the TDP are undesired for long time operations.

Below in Table 6.7 an overview of the dynamic analysis results for regular waves is listed. It is shown that the 4” Bunkerflex STH hose for free hanging has the highest operability based on the suggested limitations. The vessel can operate in the following conditions:

- 4 m wave height from 135°
- 6 m wave height from 180°
- 7 m wave height from 225°

It must be noted that these operational limits must be transferred to applicable significant wave heights in an actual wave situation. The H_s value can be found by dividing the maximum operating wave height by the factor 1.86.

Table 6.7 Overview of the dynamic analysis results (maximum operating wave height) for regular wave

Hose type	Floatation point	Waves from 135°	Waves from 180°	Waves from 225°
4” Bunkerflex STH	Free hanging	4	6	7
	20 m	4	5	4
	40 m	4	5	4
	60 m	4	5	4
	80 m	4	5	4
6” Oilflex Super	Free hanging	3	4	5
	20 m	4	5	5
	40 m	3	5	6
	60 m	2	4	6
	80 m	2	3	3

6.5.5 Selected model for further analysis

The selected configuration for current analysis will be the free hanging configuration for the 4” Bunkerflex STH hose. This model can operate under the highest wave conditions. Below, in Figure 6.37 a plot showing the limitation for the selected configuration is shown.

From the plot, each line has a dip for certain periods. This dip represent a critical period for the given wave direction.

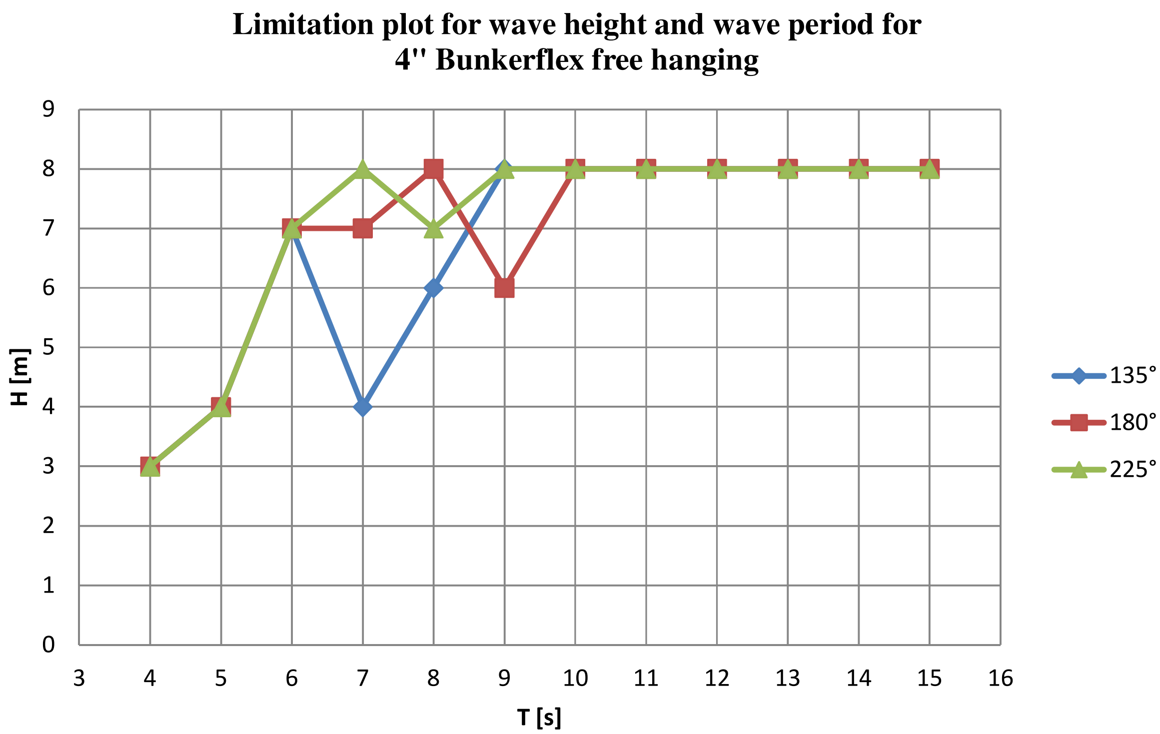

Figure 6.37 Limitation plot for the selected model for the analysis, H is the maximum wave height for the operation

6.6 Verification and validation of the simulation models

6.6.1 General

Verification and validation of the models are essential to ensure that representative models are applied. This is important to be able to carry out a safe and efficient operation. The verification and validation of the OrcaFlex model is inspired by Sargent [1] and Balci [32].

Model verification is defined as "ensuring that the computer program of the computerized model and its implementation are correct", while *model validation* is defined as the "substantiation that a model within its domain of applicability possesses a satisfactory range of accuracy consistent with the intended application of the model [1]. But since a model is an abstraction, perfect representation is never expected. Therefore the accuracy should not be considered as "perfectly accurate" or "totally inaccurate", but it should be judged on a scale defined by nominal scores such as excellent, very good, satisfactory, deficient, and unsatisfactory [32].

In this thesis a decision making approach called independent verification and validation is used. This approach uses a third party to decide whether the simulation model is valid [1]. This approach is chosen to give the model higher credibility. When verification and validation is conducted by an independent (third) party and it is concluded that the simulation model is valid, there is much greater likelihood that others will accept the model as valid and results from the model as being "correct" [1].

The methodology for verification and validation to the model development process is shown below in Figure 6.38. This model is based on Sargent simplified version of the model development process [1]. The *pre-commissioning operation* is the situation to be modelled, and the *theoretical model* is a logical representation of the operation. The *OrcaFlex static model* is the theoretical model implemented in the software program. The theoretical model is developed through an *analysis and modelling phase*, while the Orcaflex static model is developed through a *computer programming and implementation phase* [1]. The framework for the pre-commissioning operation will be developed through a *dynamic analysis phase*.

Theoretical model validation is defined as determining that the theories and assumptions underlying the conceptual model are correct and that the model representation of the problem is "reasonable" for the intended purpose of the model [1]. *OrcaFlex static model verification* should assure that the input parameters are representative for the model. *Operational validation* is defined as determining that the model's output behaviour has a satisfactory range of accuracy for the model's intended purpose over the domain of the model's intended applicability. *Design basis* should address the necessary limitations and input parameters to create a representative model.

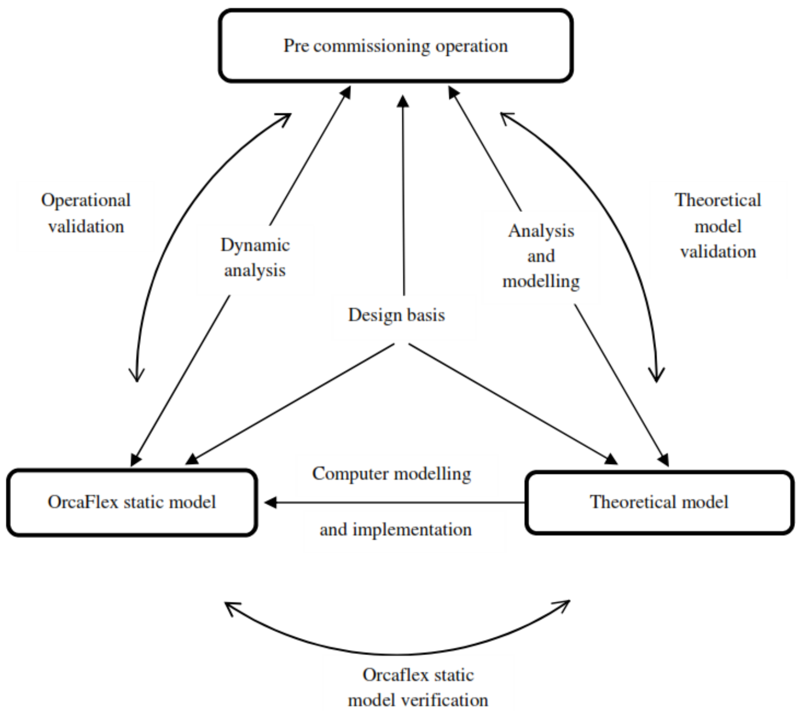

Figure 6.38 Simplified version of the model development process [1]

Usually, it requires several models before one representative model can be validated and verified.

The validation techniques used for this thesis are [1]:

- Animation
- Comparison to other models
- Face validity
- Historical data validation
- Parameter variability-sensitivity analysis

The *animation* is carried out in the graphical window in OrcaFlex, where both static and dynamic cases are modelled. The *comparison to other models* will be used to see if the trend is the same for the model and another validated model by IKM. The *face validity* will be used to check that the output is reasonable. The *historical data validation* is implemented from the design basis valid for the specific field where the operation will be carried out, which will result in an accurate analysis. The *parameter variability-sensitivity analysis* has been run for a number of different environmental cases to identify the sensitivity of the operation under different wave heights, wave periods and wave directions for all hose configurations considered.

To obtain a high degree of confidence in a simulation model and its results, comparisons of the model's and system's output behaviour for several different sets of conditions are usually required [1]. This behaviour can be explored either qualitatively or quantitatively. In the qualitatively analysis, the directions of the output's behaviour is examined and also possibly whether the magnitudes of the results are "reasonable" [1]. In quantitative analysis, both the directions and the precise magnitudes of the output's behaviour are examined [1]. The quantitative analysis is most often based on parameter variability-sensitivity analysis as discussed above.

The approach for comparing the simulation model output behaviour to the system output behaviour for regular waves is by using column charts to be able make a subjective decision. Based on these graphs, the results from each environmental load case will be evaluated subjective. The operational wave height will be based on the maximum wave height the vessel can operate from the given wave direction.

After the animation phase, the face validity and the parameter variability sensitivity analysis are done; it is important to compare the output results with other validated models to see whether the trend is the same for both models. The most critical environmental load cases will be identified in both models, to see whether the trend is the same for both models.

6.6.2 Differences in the models

One model is suggested by IKM to validate the model used in the thesis. This is an analysis for a 6" Bunkerflex hose where some parameters have been assumed. However, this model has some different characteristics that are listed below:

- Water depth = 140 m
- MBR = 1200 mm
- Vessel RAO = Skandi Carla
- Vessel dimensions = Skandi Carla
- Axial stiffness = 1050 kN
- Bending stiffness = 0.684 kNm^2
- Wave theory = Dean Stream 10^{th}
- Offset = 35 m
- Chute design
  - Radius = 1.2 m
  - Location = 20.9 m from the stern
  - Side support built up

Even though there are some different input parameters, the main trend for different environmental load cases should be sufficient to validate the model. It should be mentioned that the axial stiffness and the bending stiffness for the 6" Bunkerflex hose were assumed based on scaling.

6.6.3 Free hanging configuration

The free hanging configuration will be used as basis to validate the model. The lazy wave configurations are built up through the free hanging configuration, only the offset point and hose length are changed. The results are presented in form of wave roses in Figure 6.39 below:

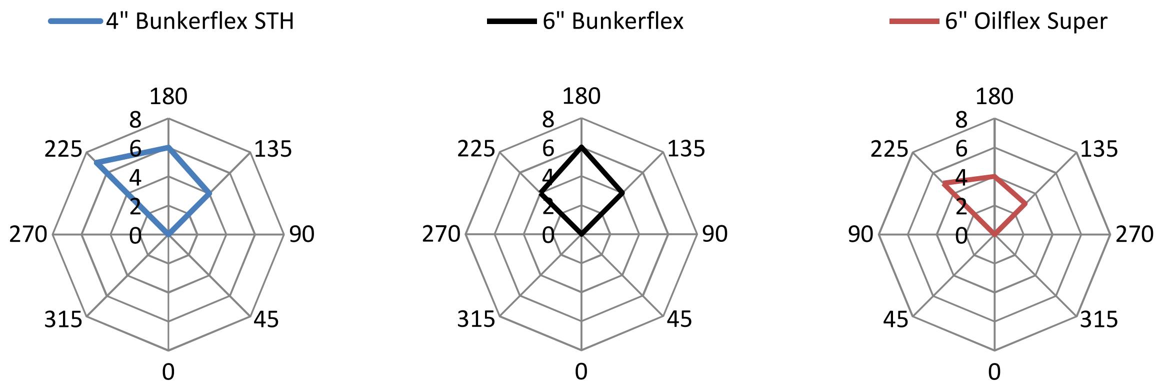

Figure 6.39 Comparison of free hanging model results for validation

6.6.4 Discussion

At first, the results may look slightly different compared with each other. The operability restrictions for the 6” Bunkerflex are more similar to the operability restrictions on the 4” Bunkerflex STH hose rather than for the 6” Oilflex Super. This is reasonable, however, since the build-up layers are slightly different for the Bunkerflex hose compared with the Oilflex Super hose.

In addition, the wave height limitation for the 6” Bunkerflex is almost the same as the wave height limitations for different floatation points for the lazy wave 4” Bunkerflex STH configuration. The only difference is that the 6” Bunkerflex can operate in 6 m waves compared with 5 m waves from the 180° direction. The offset between the lazy wave configuration and the 6” Bunkerflex free hanging is approximately the same. Again, it seems like the offset has a significant effect on when the vessel can operate in the allowable weather window, and when it cannot.

The animations in OrcaFlex do not show any errors in the graphical window. The trend is the same considering wave periods, but not the same wave heights. This is reasonable since there are some key differences between the input parameters. The critical wave periods identified from the 6” Bunkerflex hose analyses are from 6 to 8 s, which is the same as for the 4” Bunkerflex STH hose and the 6” Oilflex Super hose. All the parameter sensitivity analyses also show that the critical periods basically are from 6 to 8 s. The vessel has the highest response when encountered by waves with 6 to 8 s periods, most probably because the corresponding wave frequency of these waves is close to the Eigen frequency of the vessel. Support vessels in general have natural periods around 6 to 8 s, depending on different factors such as mass, geometry etc.

Since the water depth between the models differs, this would result in different tension and compression forces and therefore result in higher curvature. However, the MBR for the 6” Bunkerflex is 1200 mm, which results in an allowable curvature of 0.83 rad/m. The 6” Bunkerflex allows for a higher curvature compared with the 6” Oilflex Super hose. The vessel’s

RAO and vessel dimensions are taken from the support vessel Skandi Carla, which is relatively similar to the Skandi Inspector vessel. The axial stiffness for the 6” Bunkerflex hose was scaled up to 1050 kN in the analysis, which is a higher stiffness compared with the other two hoses. The bending stiffness was also scaled up to 0.684 kNm^2. This bending stiffness is higher than for the 4” Bunkerflex STH but lower than for the 6” Oilflex Super hose. As long as the axial stiffness and bending stiffness are scaled, and not tested, these should not be considered as representative values. Dean Stream 10^{th} order wave theory was used for the comparison model, while Stokes theory was applied for the other models.

In addition, the chute radius is 1.2 m for the 4” Bunkerflex STH and the 6” Bunkerflex, while the chute radius is 1.6 m for the 6” Oilflex Super to satisfy curvature requirements. The side supports are also designed differently. In this thesis, the side support is built up by rectangular blocks on each side (ref chapter 6.2.1); while it is built up by two cylindrical shapes in the validated model. The chute is placed at a distance of 20.9 m away from the stern. This is closer to the stern compared with the other two models, which makes the model more vulnerable against pitch motions. The offset is also less, which may affect the result of the analysis significantly.

Below, in Table 6.8 some of the key parameters for the different configurations are listed. The different hose parameters are compared to easily get an understanding of how they are compared with each other in values and factors, to easily see the relationship between them.

To summarise, the analysis seems to have a very good accuracy, even though some different input parameters have been used. The comparison shows that the 4” Bunkerflex STH hose can allow the highest curvature, which also gives the highest operability. In addition, the same wave periods are critical for the operation.

Table 6.8 Overview of key parameters in different configurations

Parameter	4” Bunkerflex		6” Bunkerflex		6” Oilflex Super	
Axial stiffness	700 kN	1.0	1050 kN	1.5	850 kN	1.21
Bending stiffness	0.2 kNm^2	1.0	0.684 kNm^2	3.42	1.4 kNm^2	7.0
Curvature	1.0 rad/m	1.0	0.83 rad/m	0.83	0.656 rad/m	0.656
Offset	50 m	1.0	35 m	0.7	50 m	1.0

6.7 OrcaFlex dynamic analysis - current

The current load is an important hydrodynamic load to consider in addition to the waves in a dynamic analysis. This is done to evaluate the hose behaviour under combined wave and current loads which may affect the operability.

In this sub chapter, the current load will only be discussed for the selected free hanging configuration for the 4” Bunkerflex STH hose. The current load will be applied from 4 different directions for the same regular wave heights and wave periods as analysed in chapter 6.5.

6.7.1 General

The same column charts and wave roses as explained in Chapter 6.5.1 will be considered in the current analysis. The current direction will be specified on each environmental load case. As mentioned in the Design Basis, a constant current profile will be used for the dynamic analyses. It should be noticed that OrcaFlex, in the case of constant current profile, uses a constant current profile up to all levels above still water level.

It is generally accepted practice to vectorially superpose the current velocity on the velocity resulting from the waves before calculating the drag force [14].The simple summation of the wave and current forces at the end of computation would lead to underestimated loads since:

$$U_p^2 + u_p^2 < (U_p + u_p)^2 \tag{6-13}$$

So the current velocity will be superposed on the wave velocity vectorially and will be treated further as a single flow velocity.

6.7.2 Free hanging configuration

All the dynamic results with current loads included for the free hanging configuration can be found in Appendix D – Dynamic results - current.

Below, in Figure 6.40 a summary of the results is presented in wave rose format for each current direction. The wave roses show that the operability is dependent on the current direction. The static and dynamic shape of the hose is changed caused by the current loads acting on the system.

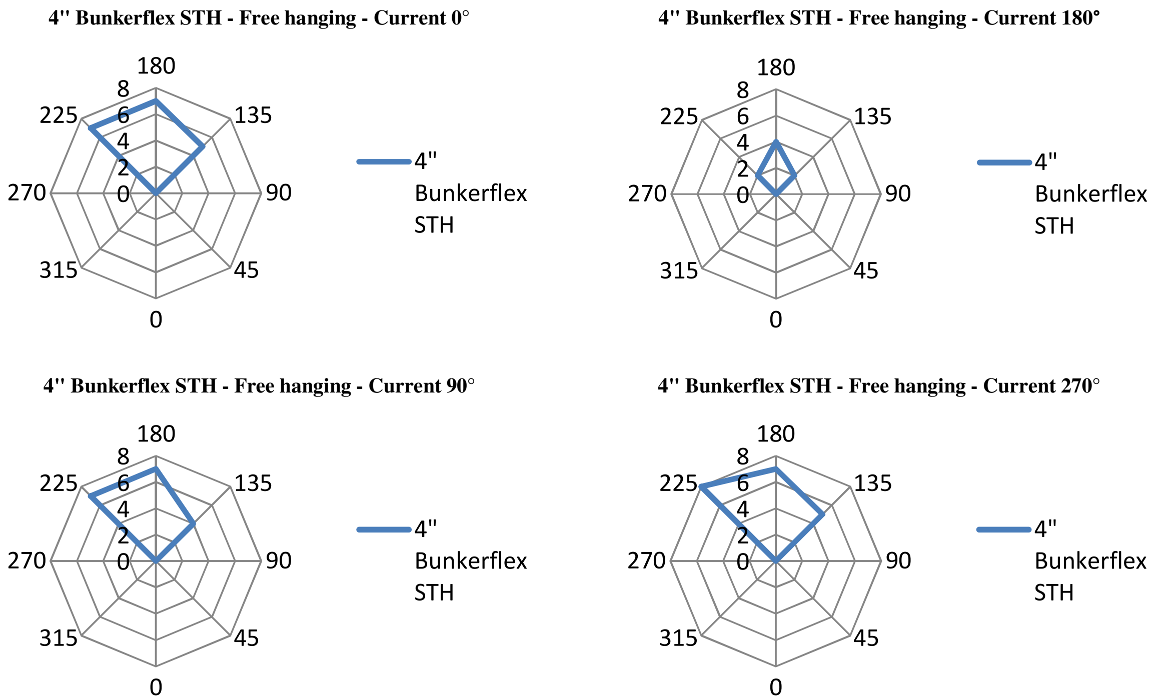

Figure 6.40 Wave roses for free hanging configuration for different current directions

6.7.3 Discussion dynamic results - current

Based on the assumptions for the current profile and velocity, the current has effect on the hose behavior which influences the operability for the vessel.

The curvature was the main limitation for the hose in the dynamic analyses without current loads, while the compression is more dominating when current loads are included. The critical compression forces occur at the splash zone or close to the TDP, while the critical curvature occurs in the splash zone. However, the limitation trend is still the same, showing that the waves from the 135° direction are the most critical for the operability for all current directions.

For the different environmental load cases, it is beneficial that the current load acts from the 0° or 270° directions. This current actually increases the operability for the vessel. This is reasonable since the current force acts against the heading seas. The remaining resultant force acting on the hose reduces and results in a less curvature at the splash zone. The operability limitation for this current direction has changed from curvature to compression in the 135° wave direction.

The worst case scenario is when the current hits the bow (180° direction). Here the current load increases the flow velocity acting on the system. This results in an increased resultant force which gives higher curvature of the hose that leads to lower operability. The limitations for this current direction are both critical compression and curvature.

When the current acts on the port side (270°) or the starboard side (90°), the operability also varies. The current on the starboard side is more critical than from the port side, since the current from the port side compensate some of the wave forces acting on the system from the most critical wave direction (135° direction). As discussed in Chapter 6.5.4, this is mainly caused by the arrangement on deck.

In general, it is assumed that current will influence both the direction and the velocity of the waves. If we consider waves from the 180° direction, the current from 0° direction will simply reduce the velocity of the waves. This is a relatively small change, since the velocity is small compared with wave velocity. However, if a current from either 90° or 270° direction occurs it will change both the wave direction and the wave velocity. The current from 270° direction changes wave directions to less critical than if they were from waves from a 180° direction.

To conclude, we can say that it is better if the current hits the stern or port side of the vessel and worse if the current hits the bow of the vessel. The hose is more resistant against current from the port side compared with starboard side because of the arrangement on deck.

Below in Table 6.9 an overview of the dynamic analysis results for regular waves is listed with different current directions.

Table 6.9 Overview of the dynamic analysis results (maximum operating wave height) for regular wave with different current directions

Current direction	Waves from 135°	Waves from 180°	Waves from 225°
0°	5	7	7
90°	4	7	7
180°	2	4	2
270°	5	7	8

Seasonal variations of environmental conditions are not taken into account. The seasonal variations might give a different current profile than considered. The aim of the current analysis is to identify the trend, showing which current directions are most critical and that they change the operability. One practical problem with the current from the 270° direction is that a slamming effect can occur. This might result in external damages of the hose; therefore the hose should be monitored during operation. The current analysis will not be considered in next sub chapter, which defines the operational requirements.

6.8 Operational requirements

Based on the analysis in this chapter, the OP_{LIM} can be identified as H = 4 m. The H_S for this operation can then be identified as follows:

$$H_S = \frac{H}{1.86} = 2.15\ m \quad \textbf{(6-14)}$$

Based on this, the OF_{WF} can be found. Normally the weather for the North Sea can be predicted for typically 3 days [11].

$$OF_{WF} = \alpha * OP_{LIM} \quad \textbf{(6-15)}$$

Since $2 < H_s < 4$ linear interpolation is required to select α factor. This results in:

$$\alpha = \alpha_1 + (\alpha_2 - \alpha_1) * \left(\frac{H_s - H_{s\,2\,m}}{H_{s\,4\,m} - H_{s\,2\,m}}\right) = 0.711 \quad \textbf{(6-16)}$$

When the α factor is selected, the OP_{WF} can be expressed as:

$$OF_{WF} = 0.711 * 2.15\ m = 1.53\ m \quad \textbf{(6-17)}$$

As mentioned in the Design Basis, the α factor represents uncertainty in both monitoring and forecasting in marine operations. This factor decreases when the T_{POP} increases. However, this uncertainty is dependent on the month when the operation is carried out. Normally, in the summer season the α-factor should be higher compared with the winter season, since the uncertainty is less because of more stable high pressure situation. Based on equation (6-15), it is obvious that the change in α factor affects the OP_{WF}. So the chosen α factor is conservative when the operation is carried out in the summer season, in particular during constant high pressure situations.

Chapter 7. CONCLUSION AND FURTHER RECOMMENDATIONS

7.1 Conclusion

The objective of this Master Thesis is to find the best hose configuration and to define operation limiting criteria's with the use of the software program OrcaFlex for a specific pre-commissioning operation which will be carried out during the summer season on the Valemon field in the North Sea.

Some conclusions from the thesis work are:

- The 4" Bunkerflex STH hose is, in general, more suitable for free hanging configuration and lazy wave configurations compared with the 6" Oilflex Super hose for this specific operation. The main reason is that the 4" Bunkerflex STH hose can allow higher curvature, which most often is the limiting criterion for the dynamic analysis. The critical curvature occurs in the splash zone as a result of varying buoyancy and inertia for the system and not at the Touch Down Point (TDP) which may be expected. The 4" Bunkerflex STH hose is around two times lighter than the 6" Oilflex Super and this results in less movements of mass during vessel motions. The maximum compression is the other limiting criteria that also occur in the splash zone, while the maximum tension does not at any stage approach critical value.
- The location of the equipment on deck affects which wave direction that is critical for the operation. Since the hang off position of the hose is on the port side of the vessel behind the transversal midline, the waves coming from starboard quartering seas are the most critical. The most critical vessel motion during the operation is a combination of negative heave, negative pitch and negative roll motion.
- The critical wave heights the vessel can operate in depends mainly on hose type and hose configuration, while the critical wave periods are in general wave periods from 6 to 8 s. This is where the Skandi Inspector vessel has highest response due to the waves.
- The highest regular waves the vessel can operate in without overrun the limitations is H = 4 m from starboard quartering seas, H = 6 m from head sea and H = 7 from port quartering seas for the selected environmental load cases. The limitations are selected

based on the worst wave period considered for the system. However, the operability is also dependent on the wave period, so different wave period than the critical ones affect the weather window operability.

- The current load affects the vessel's operability, where a current that acts towards the bow is the most critical case, while currents that act towards the stern and port side are the most beneficial currents. The current acting from the port side is more operability friendly compared with the current acting from the starboard side because of the arrangement on deck.

The configuration which gives the highest operability is a *free hanging configuration* for the 4" Bunkerflex STH hose that can operate up to H_s = 2.15 m, without crossing any limitations.

7.2 Recommendations for further work

To increase the operability for the operation while the same level of safety is kept, some recommendations for further work are suggested.

- Carry out experimental testing on both the 4" Bunkerflex STH and the 6" Oilflex Super to investigate if the Minimum Bending Radius (MBR) can be reduced when the working pressure during operation (5 barg) is significantly lower compared with allowable working pressure. In addition, perform an experimental compression test with internal pressure at 5 barg to validate that the compression limit is representative for both hose types.
- Seasonal variations in environmental loads should be gathered and included in the analysis. This will give more representative current considerations during operation.
- Perform a sensitivity analysis for different environmental cases which considers:
    - The distance from the hang off point for the hose to the TDP;
    - The selected coefficients (drag and added mass coefficient);
    - Position of hang off point on the vessel;
    - Vertical lay installation through the moonpool.
- Irregular sea analysis can be considered for the critical load cases to evaluate the cases more accurately.
- Carefully select relevant α-factor for the operation taking the actual weather condition into account.
- Run a special case analysis with added mass modules in the upper part of the hose, and a lazy wave shape at the bottom with an increased distance from the hang off point from the vessel to the TDP to increase the operability. The added mass modules may reduce the curvature the hose get exposed for in the splash zone, while the lazy wave shape would prevent large movement in the TDP. This may potentially result in increased operability.

These following suggestions will improve the quality of the analysis which will give a more representative model for this case, and for similar operations in the future.

References:

1. Sargent, R.G., (2007). *Verification and validation of simulation models*. Proc. Winter Simulation Conference, New York, USA, pages 124-137.
2. Hansen, J.Ø. and Rasen, B., (2012). *Facts 2012*. Issued by Norwegian Ministry of Oil and Energy, Oslo, Norway, pages 64-114.
3. DNV-OSS-302 (2010). *Offshore Riser Systems*. Hovik, Norway, pages 2-3.
4. DNV-OS-H101 (2011). *Marine Operations, General*. Hovik, Norway, pages 18-34.
5. DNV-OS-H102 (2012). *Marine Operations, Design and Fabrication*. Hovik, Norway, page 16.
6. TESS. *Hoses - Services - MRO*. Available from: http://tess.no/en/products/. (Accessed 2013)
7. DNV-OS-F201 (2010). *Dynamic Risers*. Hovik, Norway, pages 14-29.
8. IKM, (2008). Test Report - 4" Bunkerflex and 4" Manuli Mechanical Test. Not published, IKM, Stavanger, Norway.
9. TESS, (2012). Personal communication (E-mail), Dusavik, Stavanger, Norway.
10. Statoil, (2010). Kvitebjørn and Valemon Fields Metocean Design Basis. Not published, Statoil, Stavanger, Norway.
11. Gudmestad, O.T., (2012). *Marine Operation Window,* University of Stavanger, Lecture notes from course on: Marine Operations.
12. Bai, Y. and Bai, Q., (2010). *Subsea Engineering Handbook*. Kidlington, Oxford, UK: Elsevier, pages 147-888.
13. Fugro. *Skandi Inspector*. Available from: http://search.fugro.com/search?site=fugrocom&btnG=Search&entqr=0&ud=1&sort=date%3AD%3AL%3Ad1&output=xml_no_dtd&oe=UTF-8&ie=UTF8&client=fugro&proxystylesheet=fugro&q=skandi+inspector. (Accessed 9th April 2013)
14. Journee, J.M.J. and Massie, W.W., (2001). *Offshore Hydrodynamics*. Delft University of Technology, pages 1-1 - 12-28.
15. Vesseltracker.com. *Skandi Inspector*. Available from: http://www.vesseltracker.com/en/ShipPhotos/761430-Skandi-Inspector-7905285.html. (Accessed 8th April 2013)
16. API 17B (2002). *Recommended Practice for Flexible Pipe*. API, Dallas, USA, pages 14-102.
17. IKM. *HHD-09*. Available from: http://www.ikm.no/files/testing/utstyrskatalog/HHD-09_no.pdf. (Accessed 8th April 2013)
18. IKM. *Chute-14*. Available from: http://www.ikm.no/files/testing/utstyrskatalog/CHUTE-14_no.pdf. (Accessed 8th April 2013)

19. Cordell, J. and Vanzant, H., (2003). *The Pipeline Pigging Handbook*. Houston, Texas, USA.
20. Kennedy, J.L., (1993). *Oil and Gas Pipeline Fundamentals*. Tusla, Oklahoma, USA: PennWell Publishing Company, pages 105-106.
21. Braestrup, M.W., et al., (2005). *Design and Installation of Marine Pipelines*. Oxford, UK: Blackwell Science Ltd.
22. IKM, (2013). *Overview of equipment used for pre-commissioning operation*. Not published, IKM, Stavanger, Norway.
23. Bai, Y. and Bai, Q., (2005). *Subsea Pipelines and Risers*. Kidlington, Oxford, UK: Elsevier Ltd, pages 363-678.
24. Karunakaran, D., (2012). *Riser Technology,* University of Stavanger, Lecture notes from course on: Pipeline and Risers.
25. DNV-RP-C205 (2007). *Environmental Conditions and Environmental Loads*. Hovik, Norway, pages 24-119.
26. Techet, A.H. *Morrison's Equation*. 2004 Available from: http://web.mit.edu/13.42/www/handouts/reading-morrison.pdf. (Accessed 28th May 2013)
27. Orcina. *OrcaFlex Manual, Version 9.6a*. Available from: http://www.orcina.com/SoftwareProducts/OrcaFlex/Documentation/OrcaFlex.pdf. (Accessed 28th April 2013)
28. Gudmestad, O.T. and Moe, G., (1996). *Hydrodynamic Coefficients for Calculation of Hydrodynamic Loads on OffshoreTrussStructures*. Great Britain: Elsevier Science Limited, pages 745 - 759.
29. Answers.com. *Ship powering, maneuvering, and seakeeping*. Available from: http://www.answers.com/topic/ship-powering-maneuvering-and-seakeeping. (Accessed 1st April 2013)
30. Sparks, C.P., (2007). *Fundamentals of Marine Riser Mechanics*. Tusla, Oklahoma, U.S.A.: PennWell Corporation, pages 21-38.
31. Karunakaran, D., (2012). *Pipeline Installation*, University of Stavanger, Lecture notes from course on: Pipeline and Risers.
32. Balci, O., (2010). *Golden Rules of Verification, Validation, Testing and Certification of Modeling and Simulation Applications*. Blacksburg, Virginia, U.S.A.: Virginia Polytechnic Institute and State University, pages 1-7.

Appendix A – Test report

Test Report – Tess Oilflex Super 6”- Mechanical Test

Project No.:	286658	**Project Name:**	6” Oilflex Super - mechanical test

Table of Contents

Project No.: 286658 **Project Name:** 6” Oilflex Super - mechanical test

List of Figures

List of Tables

Project No.:	286658	Project Name:	6” Oilflex Super - mechanical test

1 Introduction

1.1 Background

This test report is carried out as a part of a Master Thesis written for IKM and the University of Stavanger. The title of the thesis is: Pre-commissioning hose operations on the Valemon field in the North Sea.

The thesis focuses on the limited wave conditions for a pre-commissioning marine operation that will be carried out on the Valemon field in the North Sea by IKM in 2013. One of the considerations is to evaluate if a 4” hose or a 6” hose is most suitable for this specific operation.

1.2 Objective

Different tests are carried out to find hose properties that currently are not available. The hose characteristics to be investigated are axial stiffness in compression, axial stiffness in tension and bending stiffness. These are important properties that influence the static and dynamic behaviour of the hose in the sea. IKM Testing will use the results for execution of the offshore pre-commissioning operations.

These hose properties derived from the different tests will be used as input parameters in OrcaFlex for static and dynamic analysis. Previously those parameters were assumed.

Hose samples from 6” Oilflex Super have been tested. This report summarizes hose data, hose description, test set ups, test results, conclusions and give recommendations how to improve the tests. Similar testing has been carried out previously for a 4” Bunkerflex STH hose.

1.3 Abbreviations

Abbreviation	Explanation
ID	Inner diameter
BR	Bend Radius
MBR	Minimum Bend Radius
OD	Outer diameter
OS	Oilflex Super

2 Hose Data

Basic data on the 6” Oilflex Super:

- ID = 152.4 mm
- OD = 187 mm
- Working Pressure = 40 barg
- Empty mass of hose in Air = 13.42 kg/m
- Empty mass of hose in Seawater = - 14.73 kg/m(buoyant)
- Water filled mass of hose in Air = 31.66 kg/m
- Water filled mass of hose in Seawater = 3.51 kg/m
- MBR = 1525mm = 0.656 rad/m

Project No.:	286658	**Project Name:**	6” Oilflex Super - mechanical test

3 Hose Description

Oilflex Super hose is a hose used for suction and delivery of oil containing products and liquid mud (drilling mud) [1].

The Oilflex Super is a flexible rubber hose. The inner rubber layer is black nitrile rubber, while the second layer is a reinforcement layer, which consists of synthetic cords and a steel double helix. The outer cover is black ozone and weather resistant neoprene rubber [1].

The synthetic cords are composed of 6 layers where each layer has the synthetic fibres braided. The hose is marked “TESS OILFLEX SUPER” in a longitudinal blue stripe. Below, in Figure 3.1 the different build up layers of the OilFlex Super is illustrated.

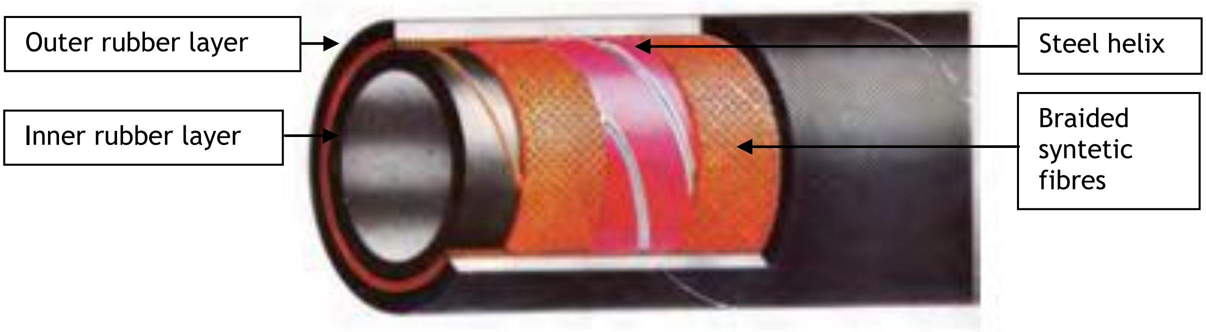

Figure 3.1 Oilflex Super build up layers [1]

IKM Testing has carried out an earlier analysis of a 4” Bunkerflex STH hose. This is also a hose used for suction and delivery of oil containing products and liquid mud (drilling mud) [1].

The Bunkerflex STH is a flexible rubber hose. The inner rubber layer is black nitrile rubber, while the second layer is a reinforcement layer, which consists of synthetic cords with a double steel helix and double ground wire. The outer cover is black neoprene rubber [1].

The synthetic cords are composed of several layers where each layer has the synthetic fibres braided. The hose is marked with a yellow, helical stripe in the longitudinal direction. Below, in Figure 3.2 the different build up layers of the Bunkerflex STH is illustrated.

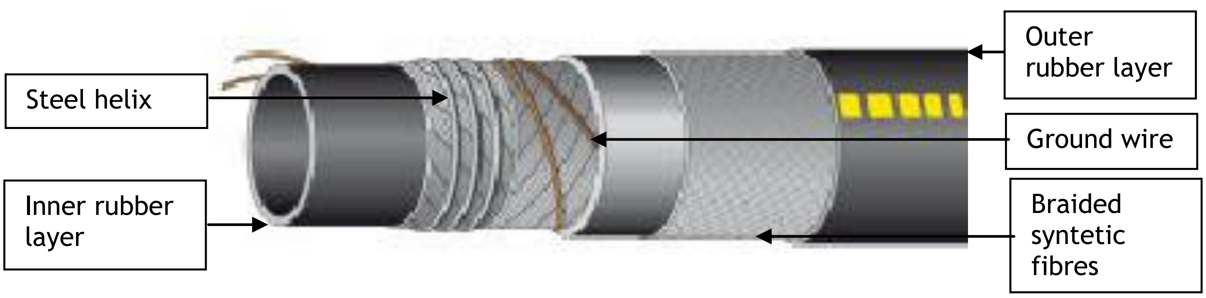

Figure 3.2 Bunkerflex STH build up layers [1]

Project No.:	286658	Project Name:	6” Oilflex Super - mechanical test

4 Theoretical formulas

4.1 Compression

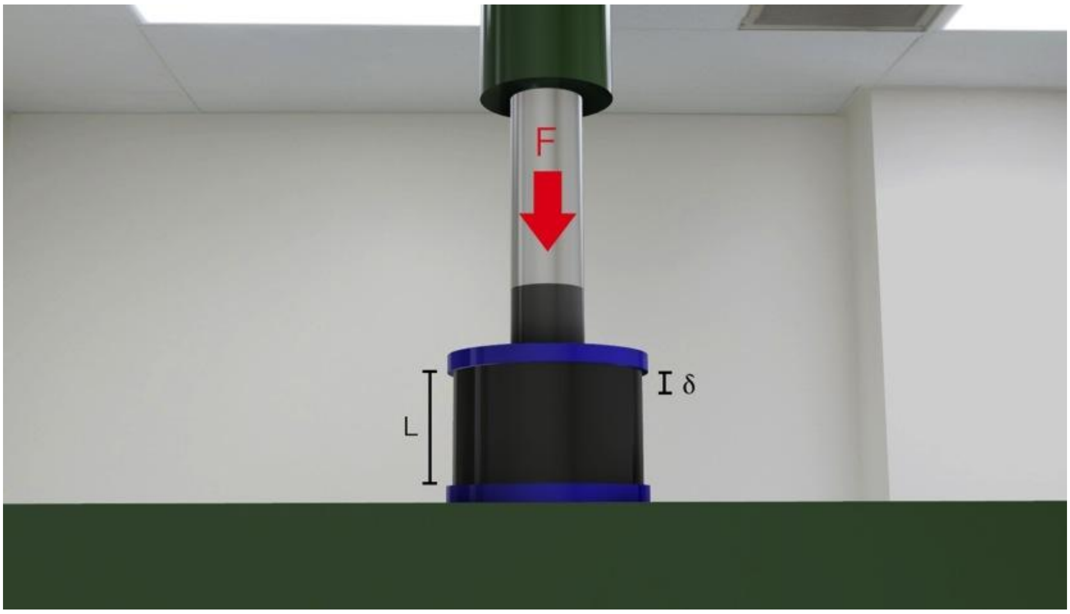

Figure 4.1 Parameters measured to find axial stiffness in compression

$$\text{Axial stiffness in compression} = \text{AE} = -\frac{FL}{\delta} \tag{4-1}$$

Where;
F = Axial load [kN]
L = Length [mm]
δ = Displacement [mm]

4.2 Tension

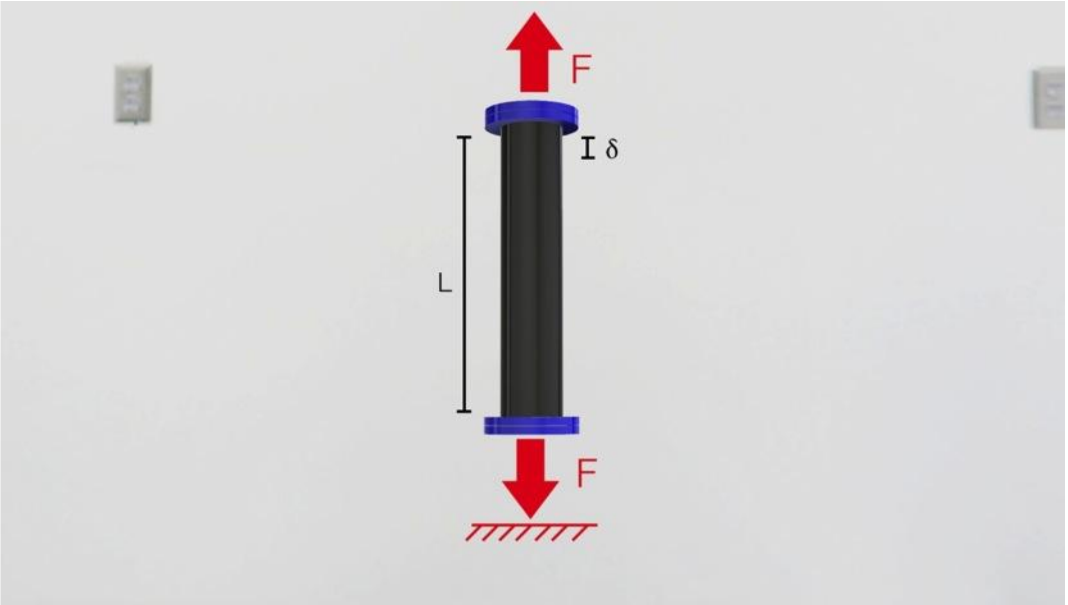

Figure 4.2 Parameters measured to find axial stiffness in tension

$$\text{Axial stiffness in tension} = \text{AE} = \frac{FL}{\delta} \qquad (4\text{-}2)$$

Where;

F = Axial load [kN]
L = Length [mm]
δ = Displacement [mm]

4.3 Bending

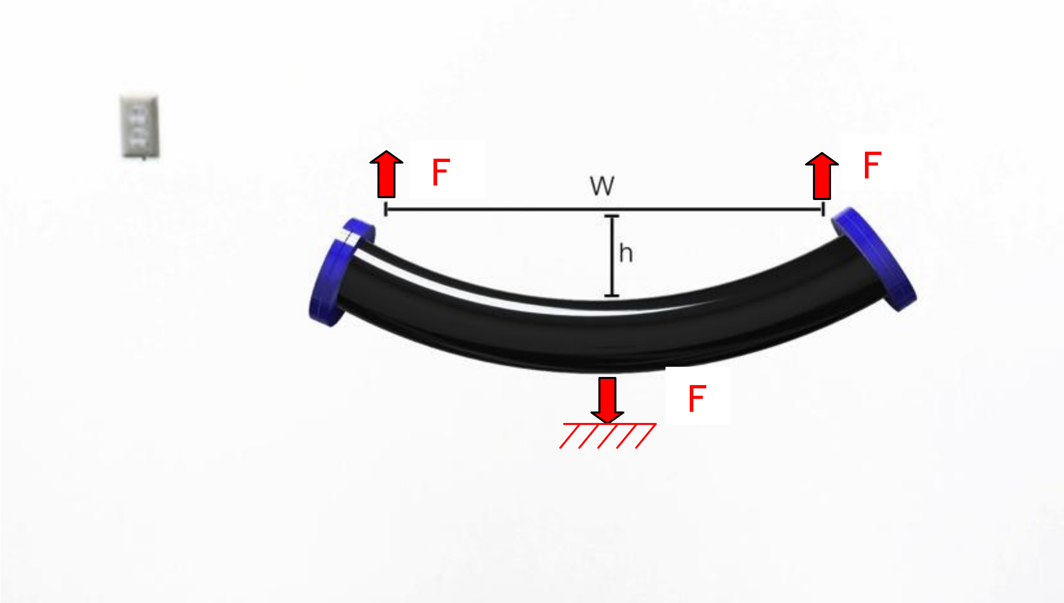

Figure 4.3 Parameters measured to find axial stiffness in compression

$$\text{Bending } radius = BR = \frac{h}{2} + \frac{w^2}{8h} \quad (4\text{-}3)$$

Where;

h = arc height [mm]

w = arc width [mm]

$$Curvature = k = \frac{1}{BR} \quad (4\text{-}4)$$

$$\text{Moment} = \text{M} = \text{F} * \text{a} \quad (4\text{-}5)$$

Where;

F = axial load [kN]

a = moment arm [mm]

$$\text{Bending stiffness} = \text{S}_\text{b} = \frac{M}{k} \quad (4\text{-}6)$$

5 Test Setup

5.1 Compression test

The purpose of the test is to find the axial stiffness in compression plus document and observe the behaviour of the hose test samples as they are exposed to increased axial loads.

The 6” hose sample was placed in a pressure bench and the equipment was positioned as shown in Figure 5.1. Compression load on each sample were carried out with a load steps of 50 kg. For each of those steps the strain was measured with the digital caliper, which was fastened to the hose sample. The different hose sample lengths were from 155-181mm. The initial distance between the caliper ends was 90 mm on each sample.

Each sample was tested 10 times within the same load steps. The purpose of testing the sample several times is to investigate if subsequent loads would lead to any changes in mechanical properties. It is also carried out to see if there is any variation of trend in the results.

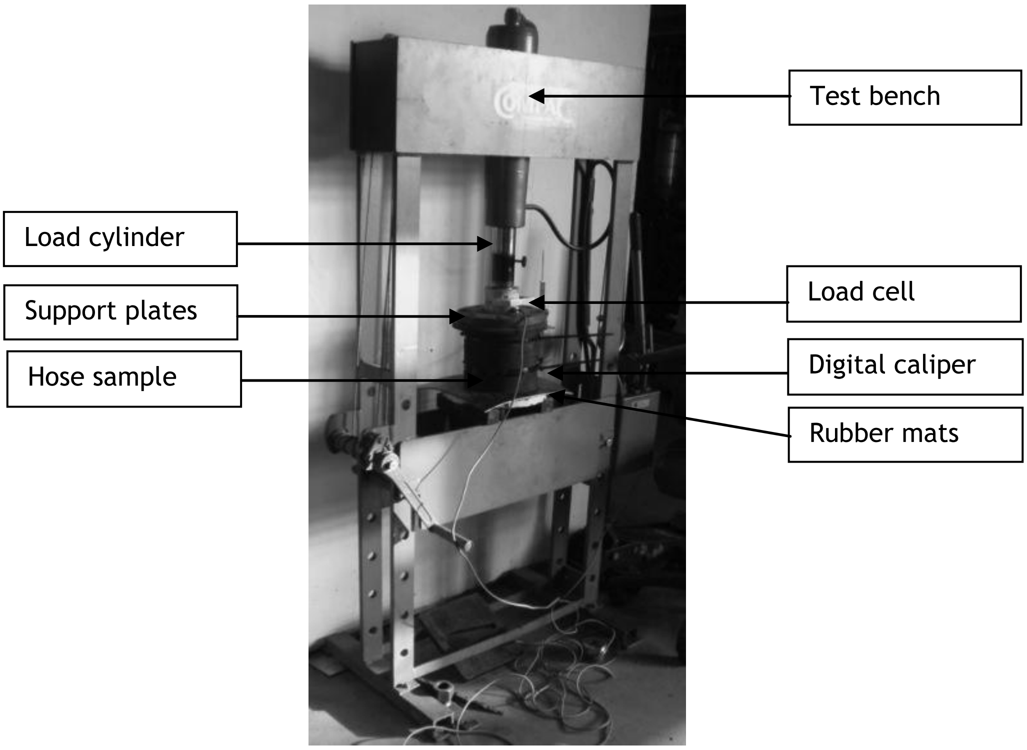

Figure 5.1 Test set up for axial compression

During the testing it was observed that the hose specimen length was shortened. The load value measured by the load cell was decreasing with time. This reduction in load could take up to one minute before it was stable. To be consistent the load was measured with 5-10 s intervals after the desired load had occurred.

Below in Figure 5.2 and Figure 5.3 there are close view photos before the loading sequence, while in Figure 5.4 and Figure 5.5 it is shown close view photos during the loading sequence. Notice that the hose in Figure 5.2 is initially longer than in Figure 5.4. In addition, it is possible to see in Figure 5.3 that the inside of the hose is less plastically deformed compared with Figure 5.5.

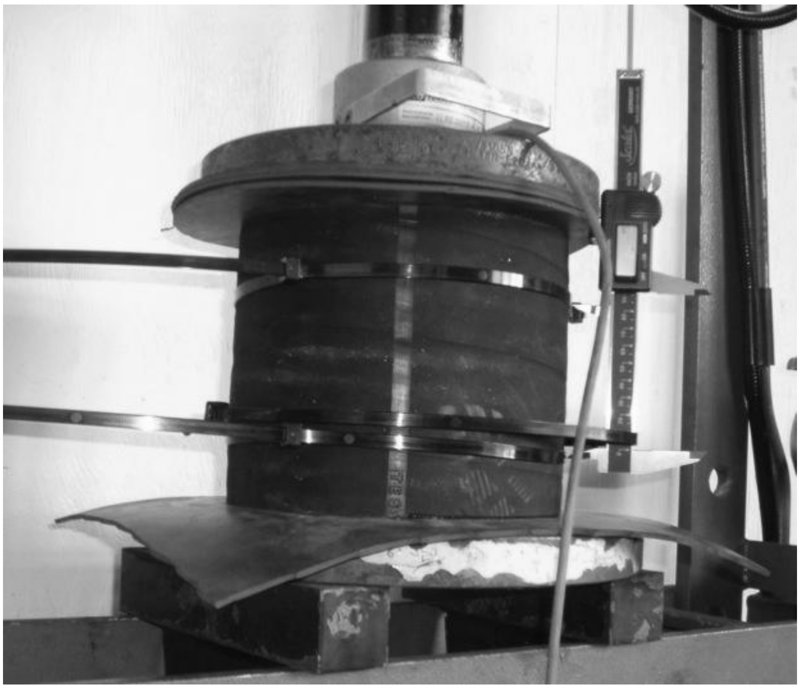

Figure 5.2 Close view of hose on test bench before loading sequence

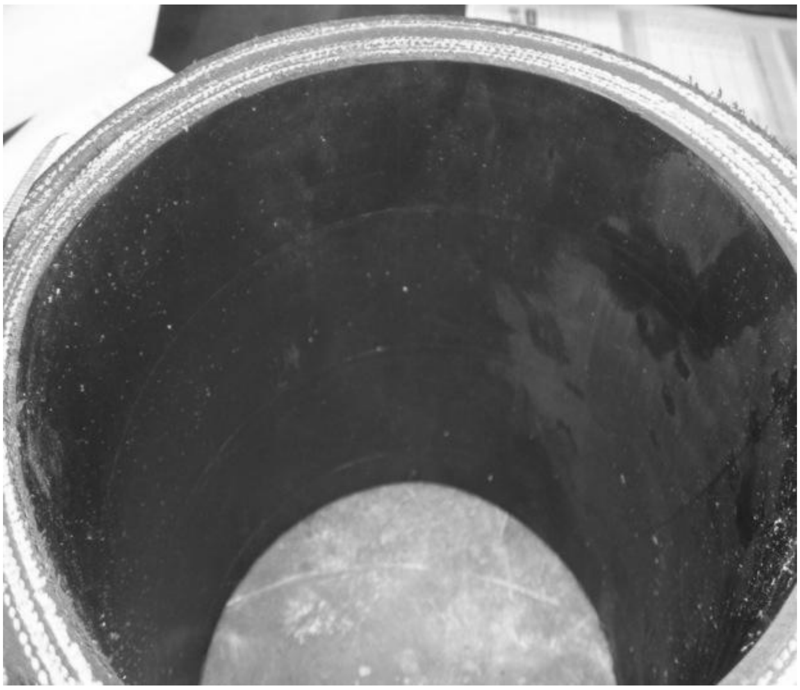

Figure 5.3 Close view of hose before loading sequence

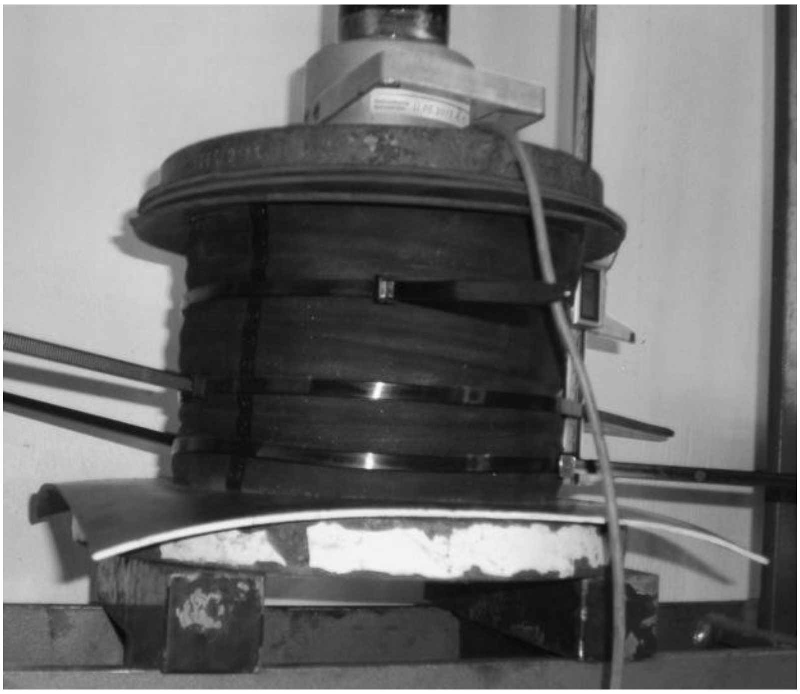

Figure 5.4 Close view of hose on test bench during loading sequence

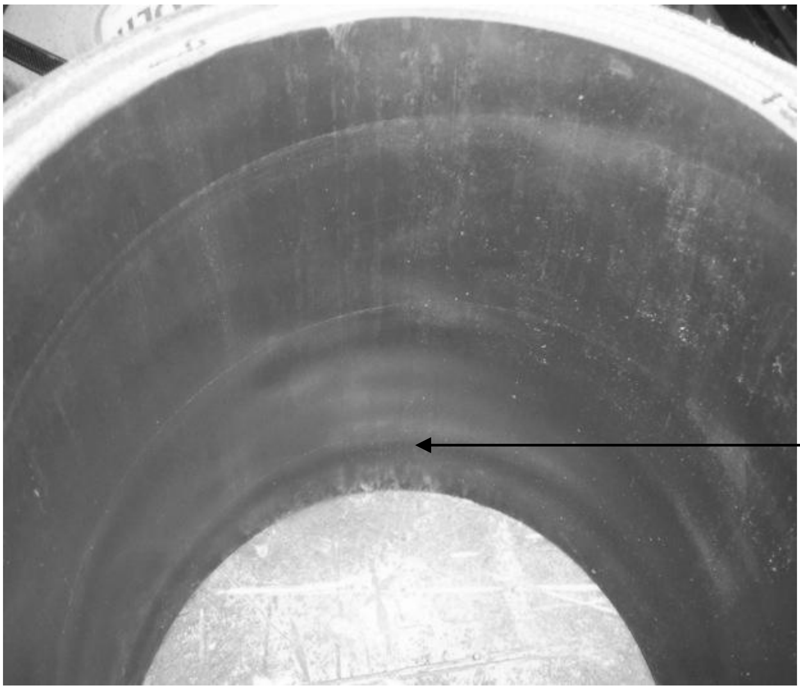

Plastic deformation inside the hose sample

Figure 5.5 Close view of hose after laoding sequence

5.2 Axial Tension Test

The purpose of the test is to find the axial stiffness in tension plus document and observe the behaviour of the hose test samples as they are exposed to increased axial loads for different pressures.

The hose sample was delivered with end terminations so flanges could be assembled. The rubber hose length for this test was 807mm, while the total length without the end flanges was 1500 mm.

The 6” hose sample was fixed to the ground and lifted with a chain hoist. The arrangement of the equipment was placed as shown in Figure 5.6. Initially the hose had a curvature shape. The curvature of the hose is discussed later in Chapter 7.3. The load on each sample was carried out with a load step of 100 kg. For each of these steps the strain was measured with minimum two digital calipers, which were fastened to the hose sample. Caliper 1 was placed on the inner bending radius side of the hose, while caliper 2 and caliper 3 were located on the outer bend radius side of the sample. The upper loading for tension was limited to 3500 kg since this was maximum weight at disposal. The initial distance between each caliper is described in Appendix 2. Tension loads were applied for 0 barg, 2 barg, 5 barg, 10 barg and 20 barg. To be consistent, the load was measured with 5-10 s intervals after the desired load was applied.

As for the compression test the sample was tested 10 times to investigate if there were changes in mechanical properties, and also to see the trend for the results.

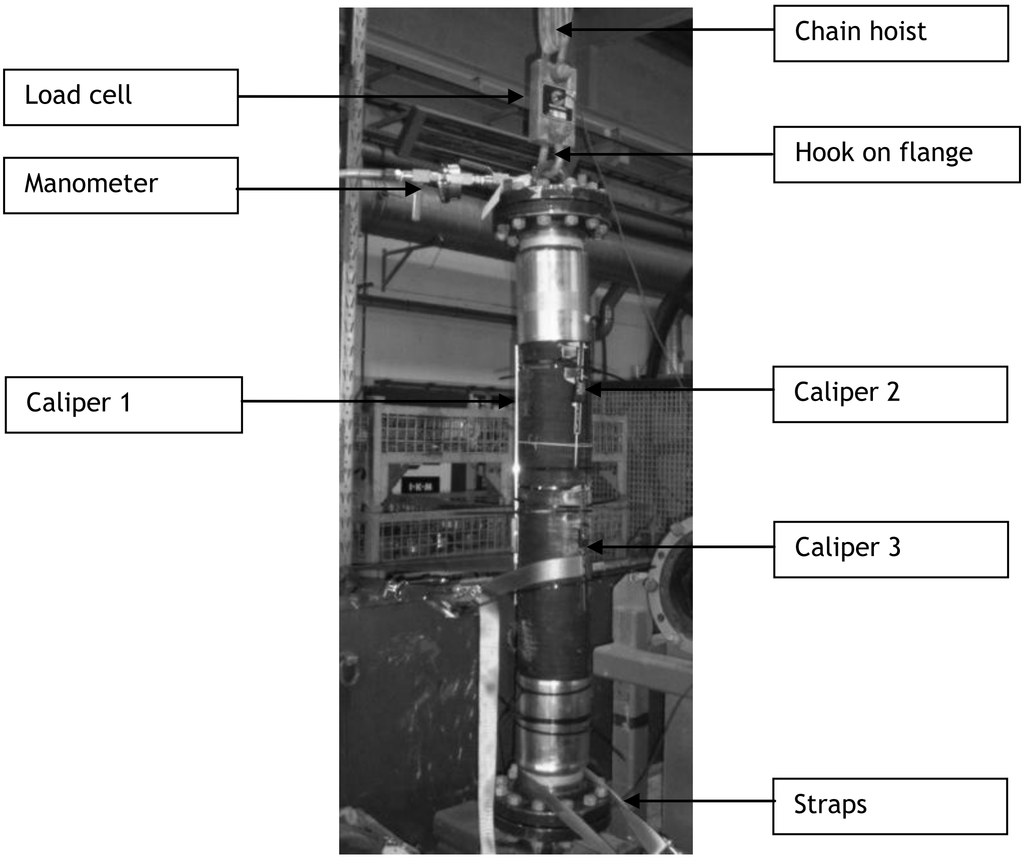

Figure 5.6 Test set up for axial tension

The hose sample was water filled during the testing. This is a more safe method of performing pressure testing compared with air filled and it is more relevant for its application. During water filling of the hose it is important to remove as much air as possible before pressurizing to make the pressure stable. Below, in Figure 5.7 the gasket is shown which seals off the water.

Figure 5.7 Gasket between hose and flange

During testing it was observed that the hose specimen length was increased. As for the compression test the load value measured by the load cell was decreasing with time. This reduction in load could take up to one minute before it was stable. It seemed like this decreasing rate of load enhanced with increased load.

Below, in Figure 5.8 there are shown a close view of the top of the test sample.

Figure 5.8 Close view of the top of the test sample

Project No.:	286658	Project Name:	6” Oilflex Super - mechanical test

Below in Figure 5.9 and Figure 5.10 there are shown how the calipers are fastened to the hose with the help of bricks.

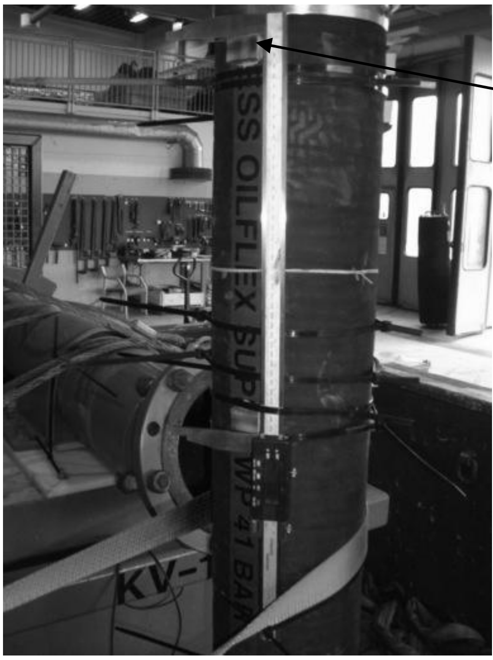

Figure 5.9 Close view of how caliper 1 is fastened

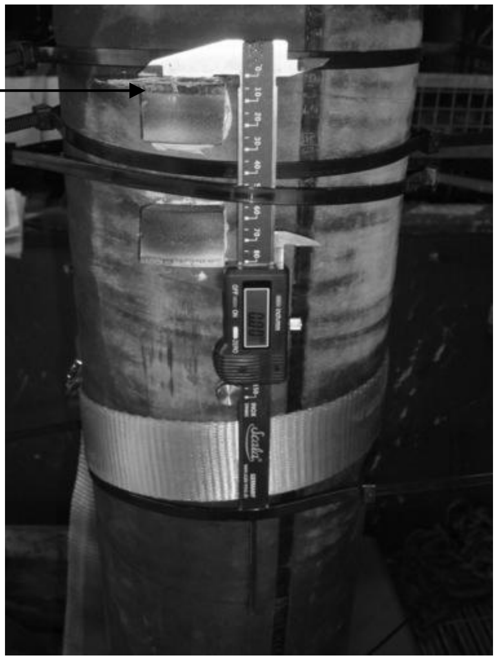

Figure 5.10 Close view how caliper 3 is fastened

Below in Figure 5.11 there is a close view of the bottom of the hose sample.

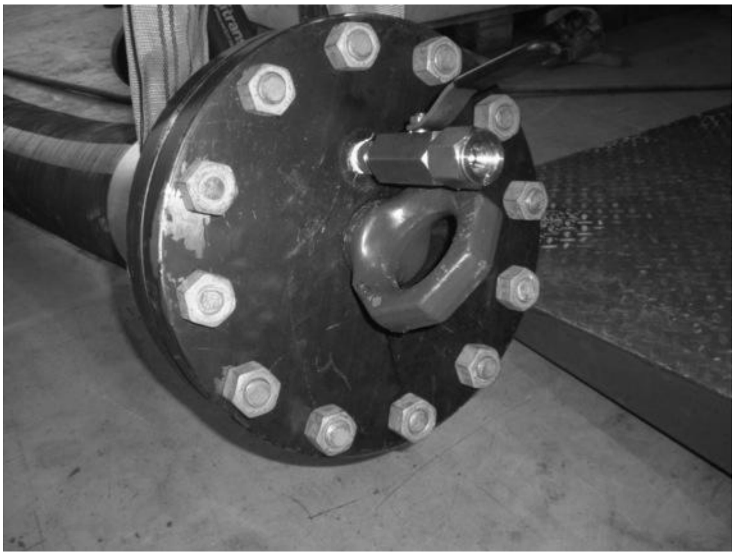

Figure 5.11 Close view of the bottom of the hose sample

5.3 Bending Stiffness Test

The purpose of the test is to find the bending stiffness under different pressures. The test should also document and observe the behaviour of the hose test samples during testing.

The rubber hose length for this test was 916 mm. The tensile load cell was fixed to the ground and fastened with a strap on the middle of the hose sample. The hose was lifted with two support straps with a distance between 900 mm. These support straps are fastened to a spreader bar, which is connected to a chain hoist by straps. The arrangement of test is shown in Figure 5.12 below.

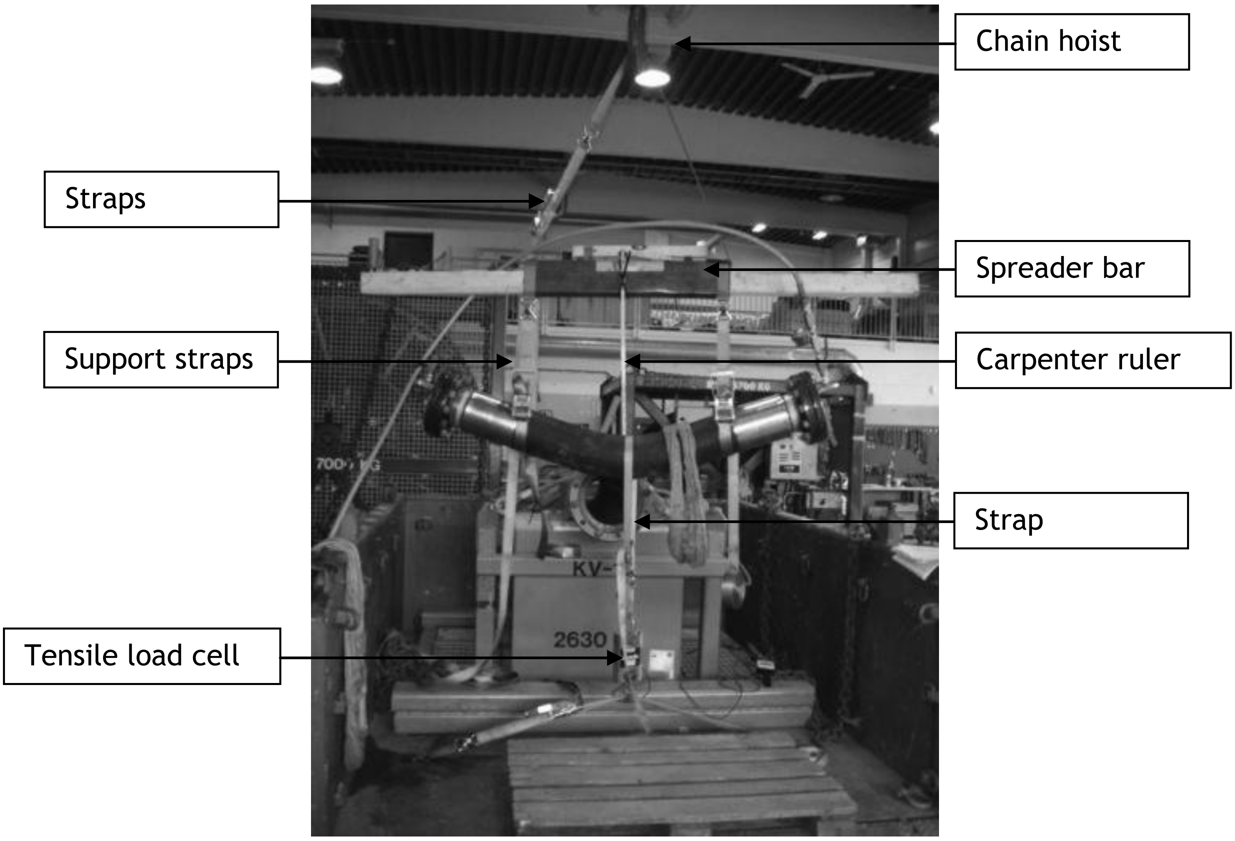

Figure 5.12 Test set up for bending stiffness

The bending was controlled by the sag bend and the load was measured in load steps of 10 mm on the carpenter ruler. The last load step was measured 5 mm since the upper limit was limited to 65mm because the MBR is given 1525mm (see Chapter 2). For each of those steps the strain was measured with one carpenter ruler, which was placed on the middle of the hose sample. The initial distance between the hose and spreader bar was 500 mm. Tension loads were applied for 0 barg, 2 barg, 5 barg, 10 barg and 20 barg. Each test was carried out 3 times for each pressure. The measurements are listed in Appendix 3. The hose sample was water filled before testing.

The length of the spreader bar needed to be adjusted before testing. After the cut was carried out it resulted in sharp edges as shown in Figure 5.13. To assure that the straps did not fail it was treated against sharp edges. This is shown in Figure 5.14 below. In addition rubber mats were placed to lower the probability of failure for the strap. This is shown below in Figure 5.15.

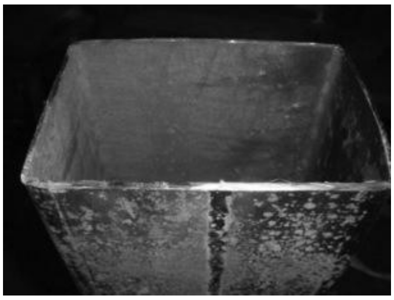

Figure 5.13 Spreader bar after cutting

Figure 5.14 Spreader bar after treatment

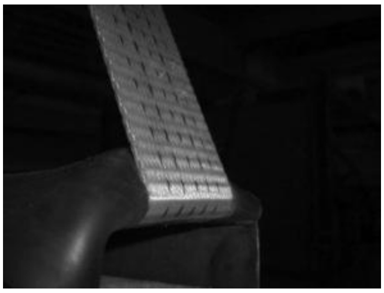

Figure 5.15 Rubber mats to prevent failure of strap

During testing it was observed that the lift needed to be centralized over the middle point of the hose so it lifts with the same force on both sides of the hose. To assure that the lift was carried out correct a level was located both on top of the hose and spreader bar before each lift. This is showed in Figure 5.16.

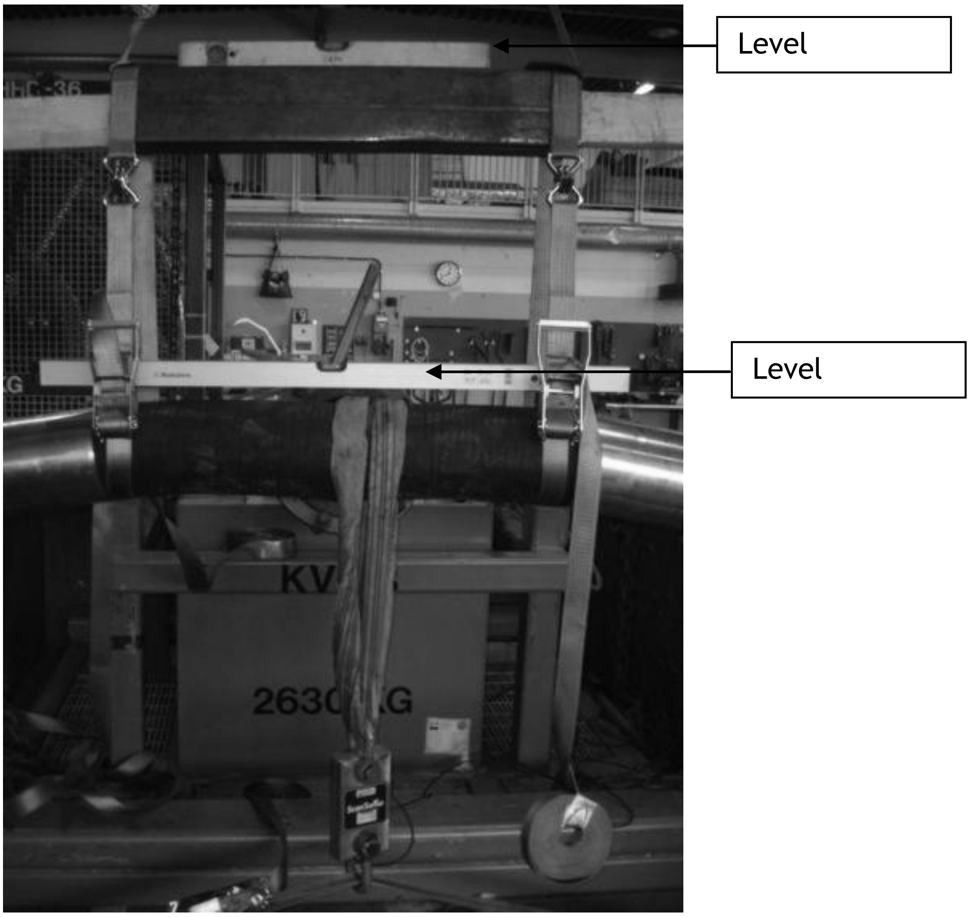

Figure 5.16 Levels on top of hose and spreader bar before lifting

6 Results

6.1 Axial Compression

Axial stiffness in Figure 6.1 to Figure 6.3 is derived from the basic formula shown in equation 4.1.

If a curve is denoted S1OS 3rd it gives the following information;

- S1= Sample 1
- OS= Oilflex Super hose
- 3rd= Third series of load steps

6.1.1 Sample 1

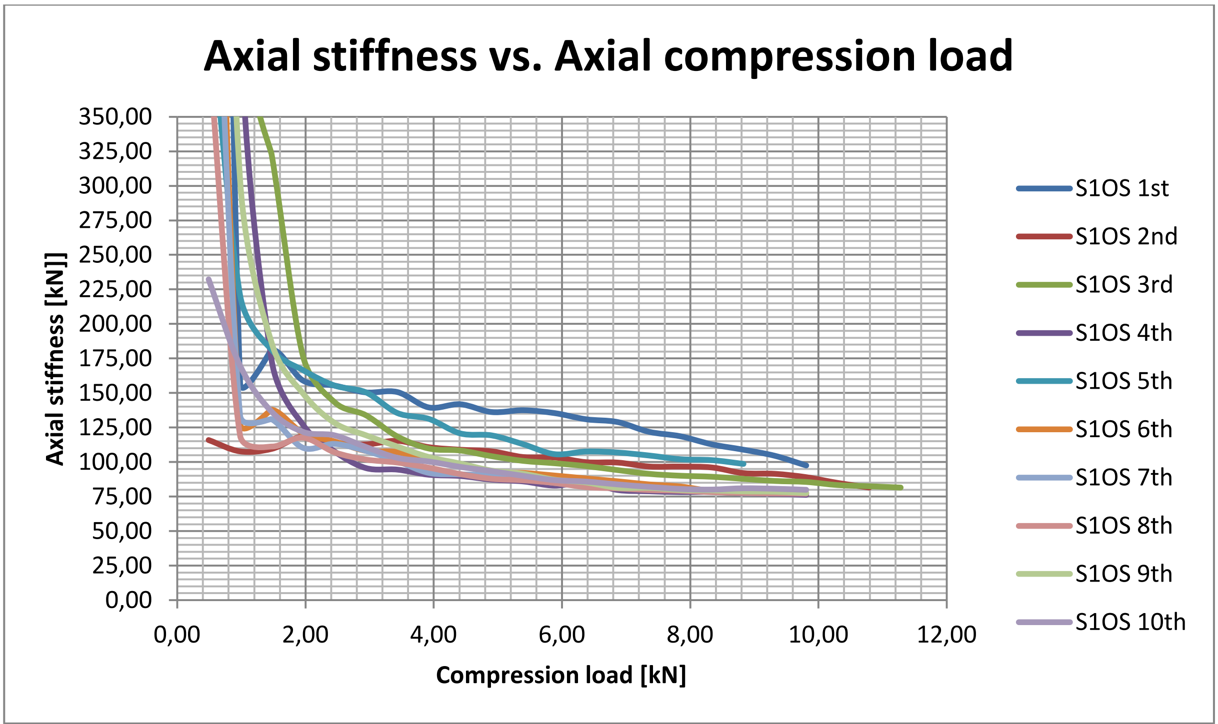

Figure 6.1 Axial stiffness in compression for sample 1

From Figure 6.1 it is seems like most of the data follows the same trend. It is reasonable that the first samples in general have higher axial stiffness compared with the later ones.

It is worth mention some characteristics from Figure 6.1;

- S1OS 2nd curve has a different trend compared to the others below 2.00 kN. This is most likely errors during testing where the first measurements are significantly higher compared with the other measurements.
- S1OS 5th was tested the day after. This is probably the reason for higher value on the axial stiffness.

The axial stiffness stabilizes at 75 kN for this sample.

An observation is that the hose shortens during the test. After one test is completed, the hose sample tries to maintain its original shape. The measurements after each tests indicates that the length of the hose is time dependent. The sample length measurements differ depending if you measure 1 or 5 min after the compression load.

Therefore the axial load will be decreased in the next sample. This reduction is to see if the same trend continues. This sample was loaded up to 11.28 kN during one test. In Appendix 1 all measurements from sample 1 are listed.

6.1.2 Sample 2

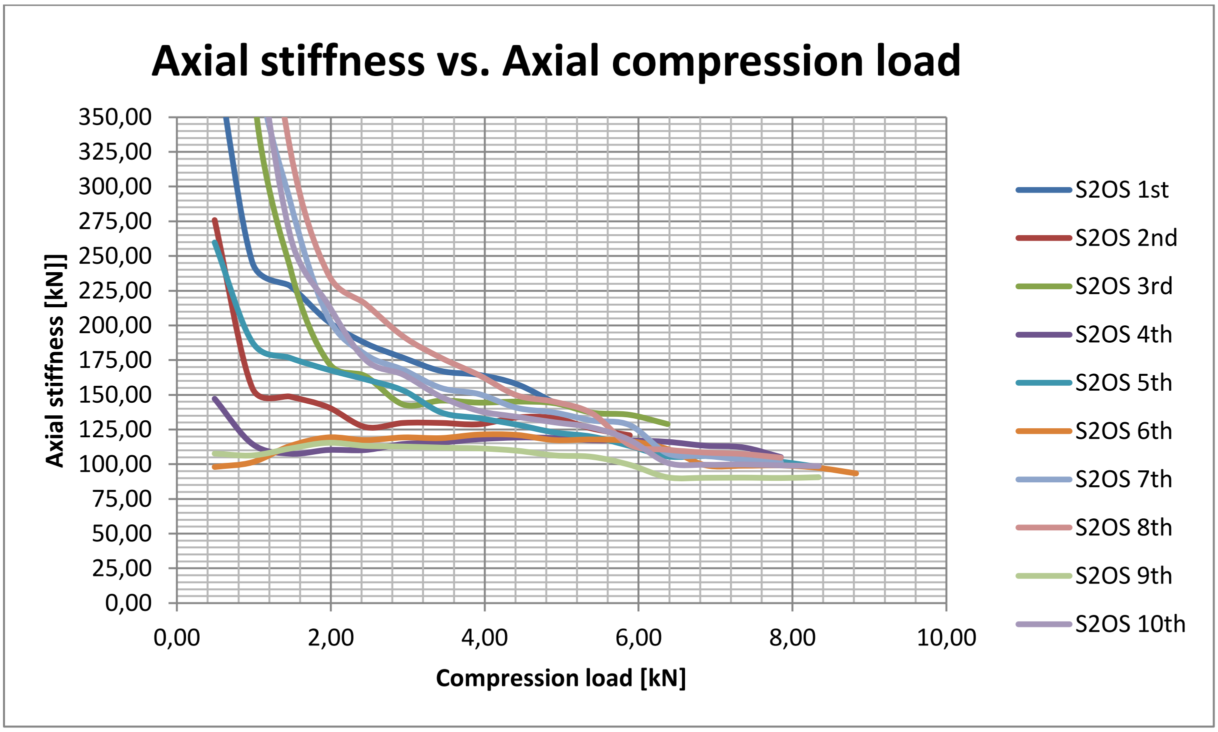

Figure 6.2 Axial stiffness in compression for sample 2

From Figure 6.2 it seems like most of the data follows the same trend as Figure 6.1.

It is worth mention some characteristics from Figure 6.2;

- S2OS 6th and S2OS 9th have a different trend compared with the others up to 2.00 kN. This is most likely error during testing where the measurements are significantly higher compared with the other measurements.
- S2OS 4th follow the same trend as the other curves, but have some lower axial stiffness compared with the others before 4.00 kN.

The axial stiffness has its most critical value at 85 kN for this sample.

On sample 1 it was an indication that the sample was plastically deformed after 8.83 kN. Therefore the upper load for compression during this test was 8.83 kN. Even though the load is less, the same elastic behaviour occurs for this sample. When the load is removed, it tries to maintain its original shape, and as time goes by the sample is stretching back to its original length. The hose is measured at 4 points before and after each load step.

Again, the time interval for the measurements is important. The measurements differ depending on time after loading. Therefore, in sample 3 the load will be limited up to 7.36 kN to see if the same trend continues.

In Appendix 1 all measurements from sample 2 are listed.

6.1.3 Sample 3

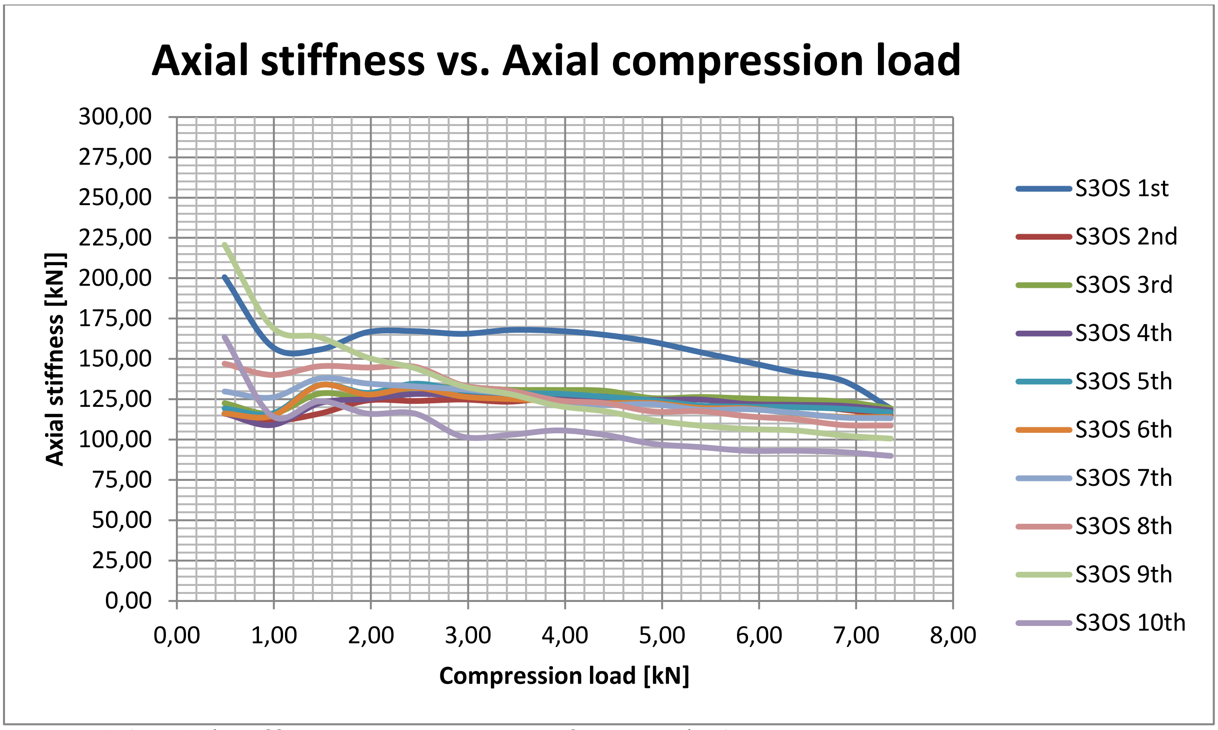

Figure 6.3 Axial stiffness in compression for sample 3

From Figure 6.3 it seems like the curves follow one certain value compared with Figure 6.1 and Figure 6.2.

It is worth mention some characteristics from Figure 6.3;

- S3OS 1st, S3OS 9th and S3OS 10th follow the same trend as in Figure 6.1 and Figure 6.2. The remaining curves tend to have a more stable value on the different load sequences.
- After 4.0 kN all curves decrease to a certain value.

The axial stiffness has its most critical value at 90 kN for this sample.

On sample 2 it was indication that the sample was plastically deformed after 7.36 kN. Therefore the upper load for compression during this test is 7.36 kN. Even though the load is less, the same elastic behaviour occurs for the sample. When the load is removed, the sample tries to maintain its original shape, and as time goes by the sample is stretching against its original length. The hose is measured at 4 points before and after each load step. Again the time interval for the measurements is important. The measurements differ depending on time after loading.

In Appendix 1 all measurements from sample 3 are listed.

6.2 Axial tension

Axial stiffness in Figure 6.4 to Figure 6.6 is derived from the basic formula shown in equation 4.2.

If a curve is denoted C1OS 3rd it gives the following information;

- C1= Caliper 1
- OS= Oilflex Super hose
- 3rd= Third series of load steps

Only the graphs from caliper 2 and caliper 3 are represented below. A discussion of representative caliper measurements is carried out in chapter 7.3.

6.2.1 0 barg

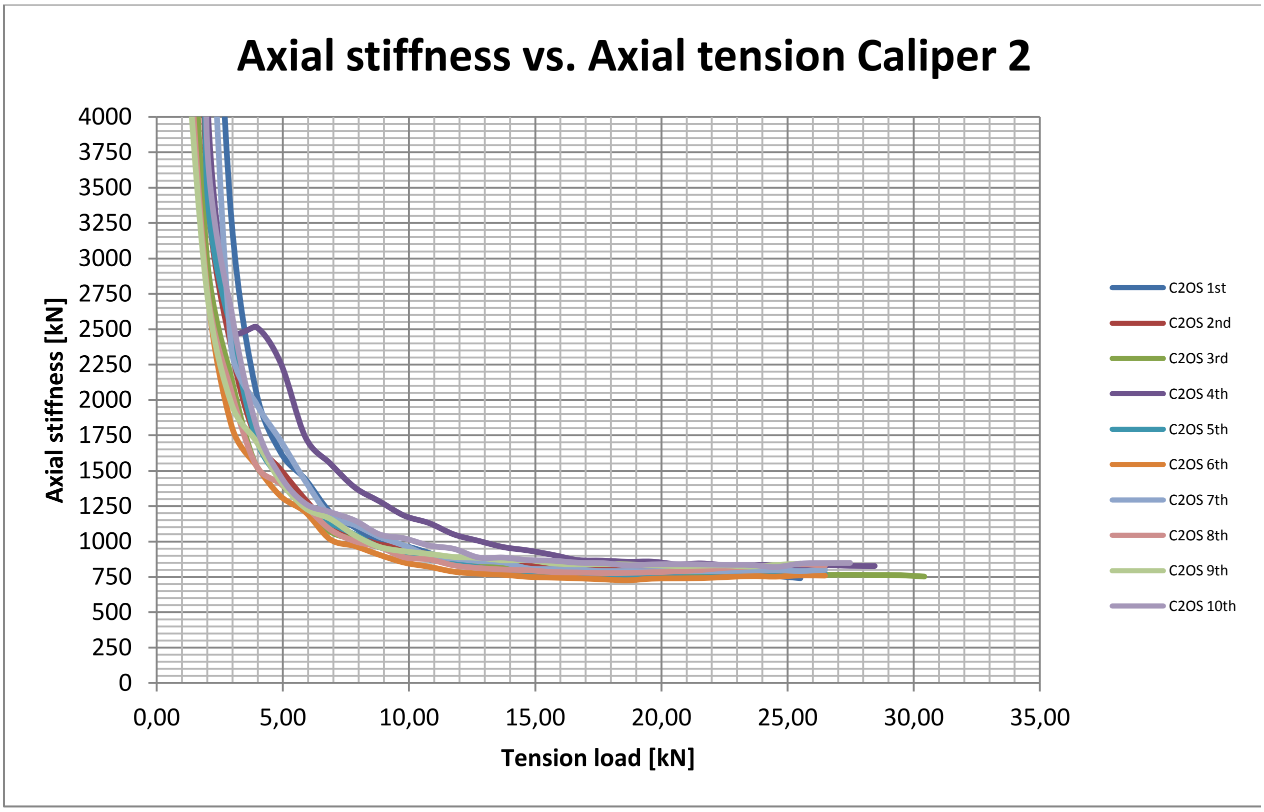

Figure 6.4 Axial stiffness in tension for 0 barg

From Figure 6.4 it is seems like most of the data follows the same trend. It is reasonable that the first samples in general have higher axial stiffness compared with the latest ones.

It is worth mention some characteristics from Figure 6.4;

- C1OS 4th curve has a different trend compared to the others. This is most likely errors during testing where the first measurements are significantly lower compared with the other measurements.

The axial stiffness stabilizes at 750 kN for this sample.

An observation is the hose length increases during the test. After one test is completed, the hose sample tries to maintain its original shape. The measurement after each test indicates that the length of the hose is time dependent. Therefore it was necessary to adjust the distance between the bricks to maintain the initial distance the same at each test. This distance was adjusted with straps and tape.

Therefore the axial load will be decreased in the next sample. This is to see if the same trend continues. This sample was loaded up to 33.6 kN during one test. In Appendix 2 all measurements from 0 barg are listed.

It was suggested that it would be more reliable data if there was one more caliper in addition to the two others, to be able to see which one of the result that proved to be most accurate.

6.2.2 2 barg

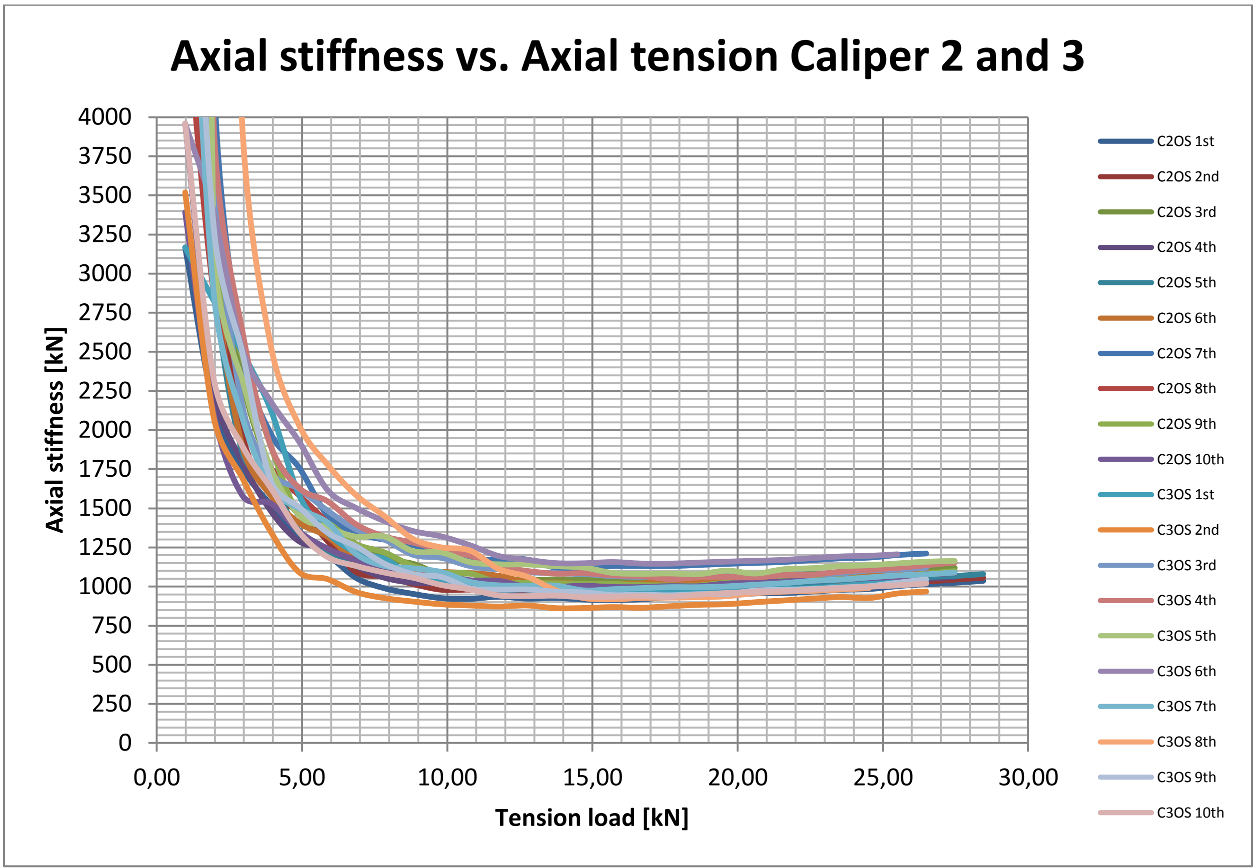

Figure 6.5 Axial stiffness in tension for 2 barg

From Figure 6.5 it is seems like most of the data follows the same trend.

It is worth mention some characteristics from Figure 6.5;

- C3OS 2nd curve has a different trend compared to the others. This is most likely errors during testing where the first measurements are significantly higher compared with the other measurements.

The most critical axial stiffness is 850 kN for this sample.

After one test is completed, the hose sample tries to maintain its original shape. Therefore it was necessary to adjust the distance between the bricks to maintain the initial distance the same at each test. This distance was adjusted with straps and tape. This sample was loaded up to 29.43 kN during all tests, which will be the same in the next test. In Appendix 2 all measurements from 2 barg are listed.

It is also worth mention that all data for the 2 barg test was tested the day after the 0 barg test.

6.2.3 5 barg

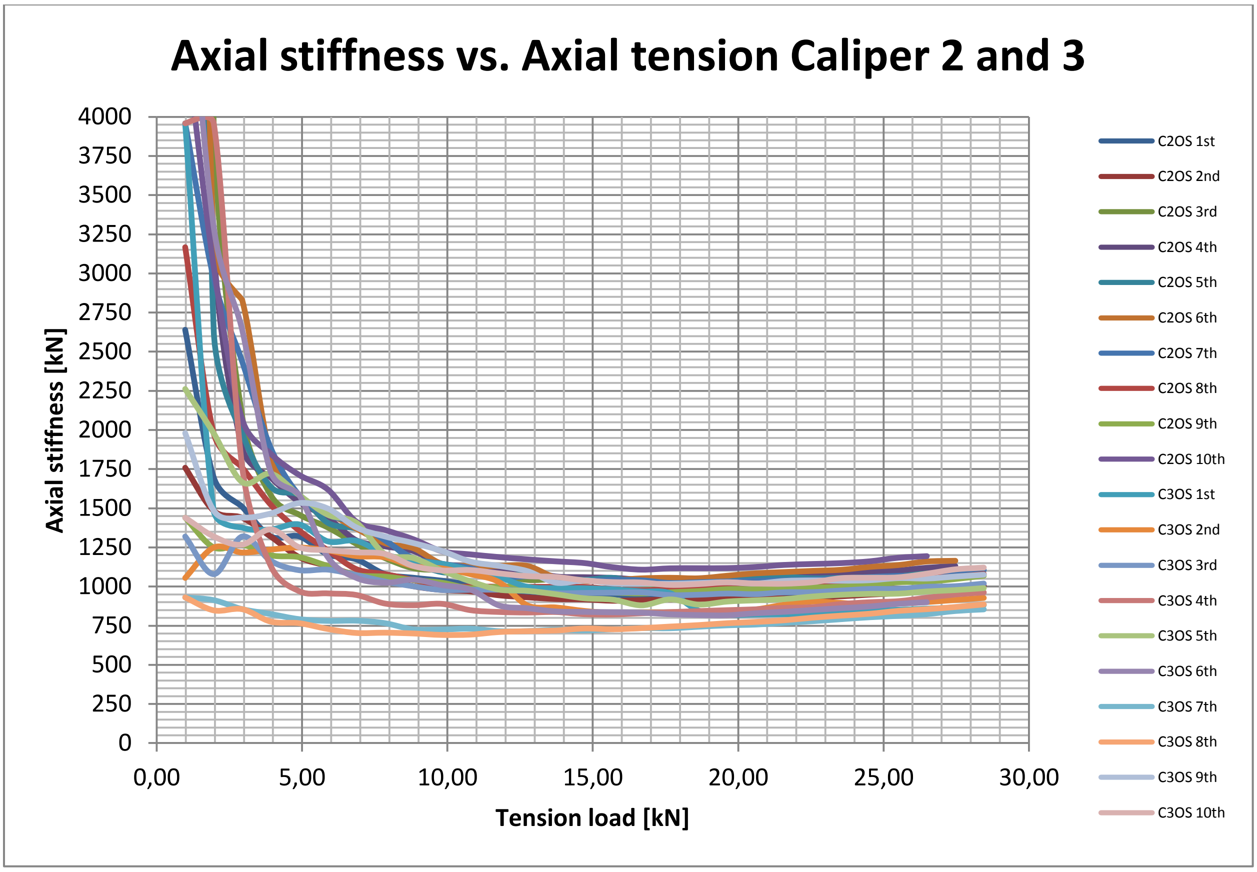

Figure 6.6 Axial stiffness in tension for 5 barg

From Figure 6.6 it is seems like most of the data follows the same trend.

It is worth mention some characteristics from Figure 6.6;

- C3OS 7th and C3OS 8th curve have a different trend compared to the others. This is most likely error during testing where the first measurements are significantly higher compared with the other measurements. A statement supporting this is that both C3OS 9th and C3OS 10th curve are significantly higher. If not C3OS 9TH and C3OS 10TH would be significantly higher, this deviation would be a new trend.
- C3OS 2nd and C3OS 3rd have a different trend compared with the other before 3.00 kN, which is most probably due to uncertainties in measurements.

The most representative axial stiffness is 850 kN for this sample if C3OS 7th and C3OS 8th are neglected. If C3OS 7th and C3OS 8th are not neglected, the critical axial stiffness would be 700 kN. In theory the axial stiffness should increase when the pressure is increased as the case have been for 0 barg and 2 barg.

During 5 barg pressure the hose sample had a tendency to straighten up in initial state before loading.

After one test is completed, the hose sample tries to maintain its original shape. Therefore it was necessary to adjust the distance between the bricks to maintain the initial distance the same at each test. This distance was adjusted with straps and tape. This sample was loaded up to 29.43 kN during all tests, which will be the same in the next test. In Appendix 2 all measurements from 5 barg are listed.

It is also worth mention that all data for the 5 barg test was tested the same day as the 2 barg test. This may also lead to higher interval between the curves compared with 0 barg and 2 barg results.

6.2.4 10 barg

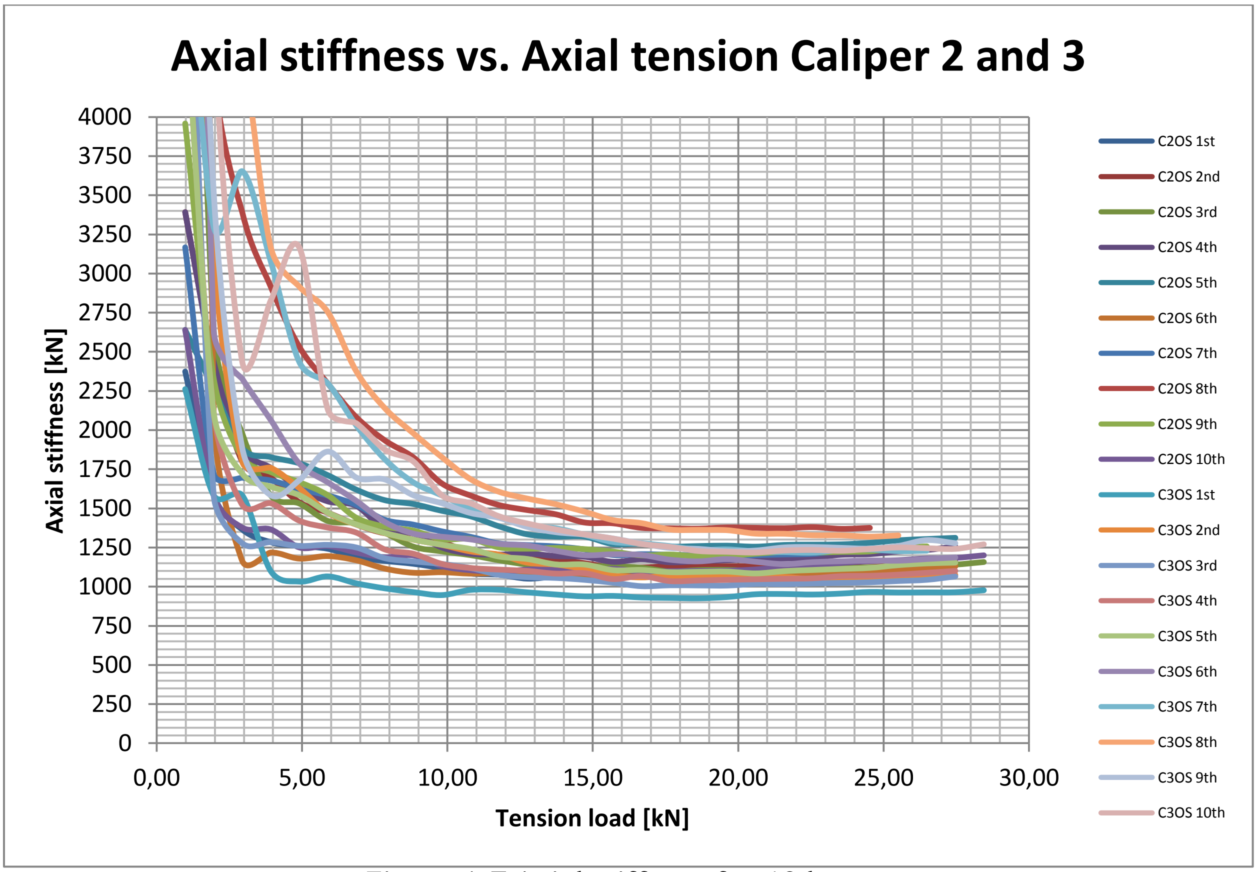

Figure 6.7 Axial stiffness for 10 barg

From Figure 6.7 it is seems like most of the data follows the same trend.

It is worth mention some characteristics from Figure 6.7;

- C3OS 1st has lower axial stiffness compared with the other curves. The trend on the previous tests shows that the axial stiffness normally is highest during the first tests. Since this is the lowest value during all tests, the measurements in this test can probably be neglected.

- C3OS 7th, C3OS 9th and C3OS 10th curve have a different trend compared to the others. This is most likely error during testing where some of the measurements seem to be close to one another. These variations are for tension load under 6.00 kN, so the main trend is the same.

The most representative axial stiffness is 1000 kN for this sample if C3OS 1st is neglected. If C3OS 1st is not neglected, the critical axial stiffness would be 900 kN.

As for 5 barg pressure the hose sample had a tendency to straighten up in initial state before loading.

After one test is completed, the hose sample tries to maintain its original shape. Therefore it was necessary to adjust the distance between the bricks to maintain the initial distance the same at each test. This distance was adjusted with straps and tape. This sample was loaded up to 29.43 kN during all tests, which will be the same in the next test. In Appendix 2 all measurements from 10 barg are listed. It was also noticed that it occurred some sounds when the load from the 10 barg hose was removed. The hose sample has increased its total length after this load sequence. This may indicate on plastic deformation.

It is also worth mention that all data for the 10barg test was tested the day after the 5 barg test.

6.2.5 20 barg

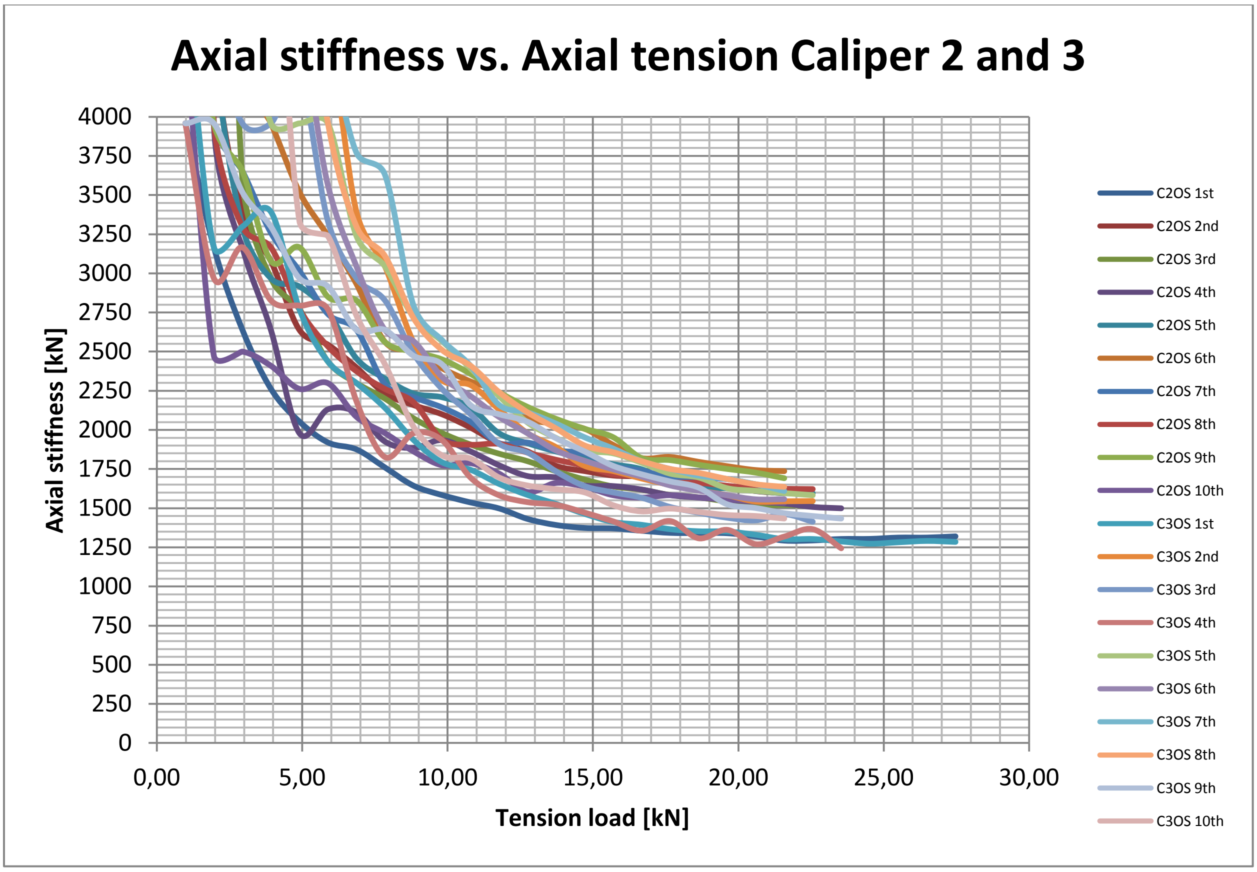

Figure 6.8 Axial stiffness for 20 barg

From Figure 6.8 it is seems like most of the data follows the same trend.

It is worth mention some characteristics from Figure 6.8;

- C2OS 1st and C3OS 1st have a higher tension load (kN) compared with the others. After applying 29.43 kN it indicated that the hose was plastically deformed. Therefore the following load steps stopped on 24.5 kN.

The most representative axial stiffness is 1300 kN for this sample. As for 5 barg and 10 barg pressure the hose sample had a tendency to straighten up in initial state before loading.

After one test is completed, the hose sample tries to maintain its original shape. Therefore it was necessary to adjust the distance between the bricks to maintain the initial distance the same at each test. This distance was adjusted with straps and tape. In Appendix 2 all measurements from 20 barg are listed.

It is also worth mention that all data for the 20 barg test was tested the next day after the 10 barg test. It was also noticeable that the OD increased significantly when the hose was pressurized up to 20 barg. The increase in diameter was up to 3mm.

6.3 Bending Stiffness

Bending stiffness in Figure 6.9 and Figure 6.10 are derived from basic formula shown in equation 4.6.

The measurements are given in Appendix 3. If a curve is denoted 0 barg it gives the following information;

- 0 barg = Test is carried out with 0 barg

Each test is carried out 3 times at for each pressure. The test results are summarized in Figure 6.9 below. Each curve is taken from the most critical measurements.

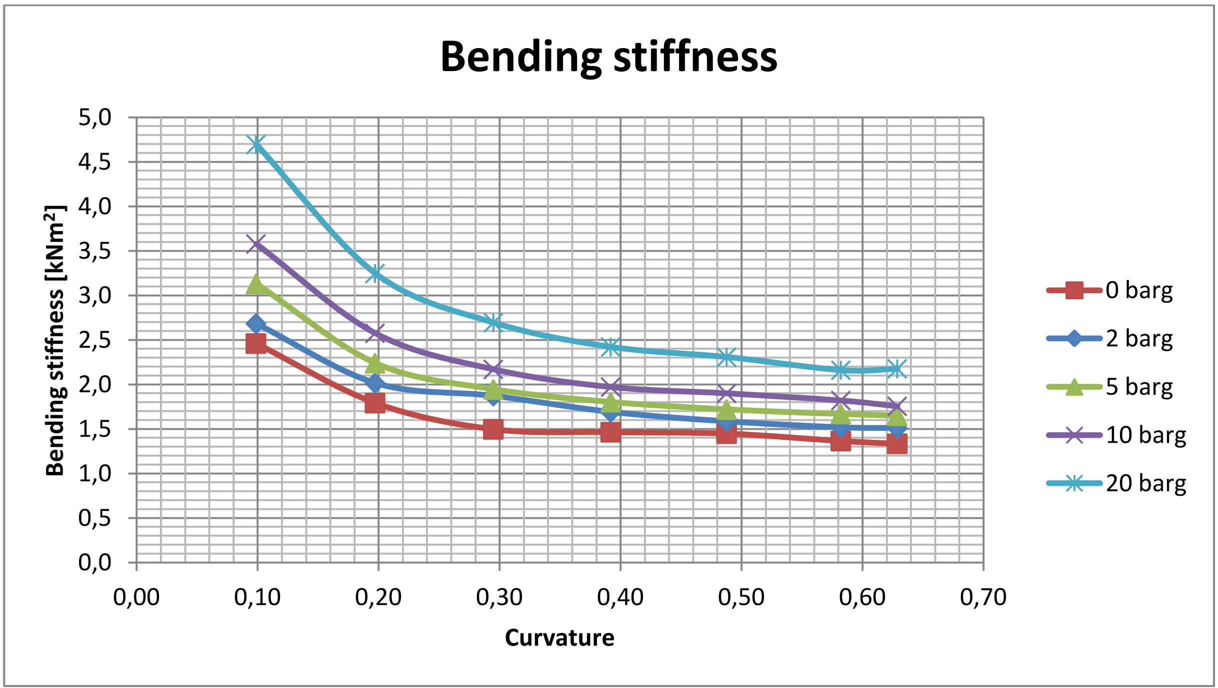

Figure 6.9 Bending stiffness with initial curvature

From the graph it seems like all results follow the same trend. The curvature is limited to 0.65 rad/m. The reason for this is because the minimum bending radius is given as 1525 mm.

It was decided to take additional tests, to see if the bending stiffness had the same trend if the given MBR was decreased. Those results are given in Figure 6.10.

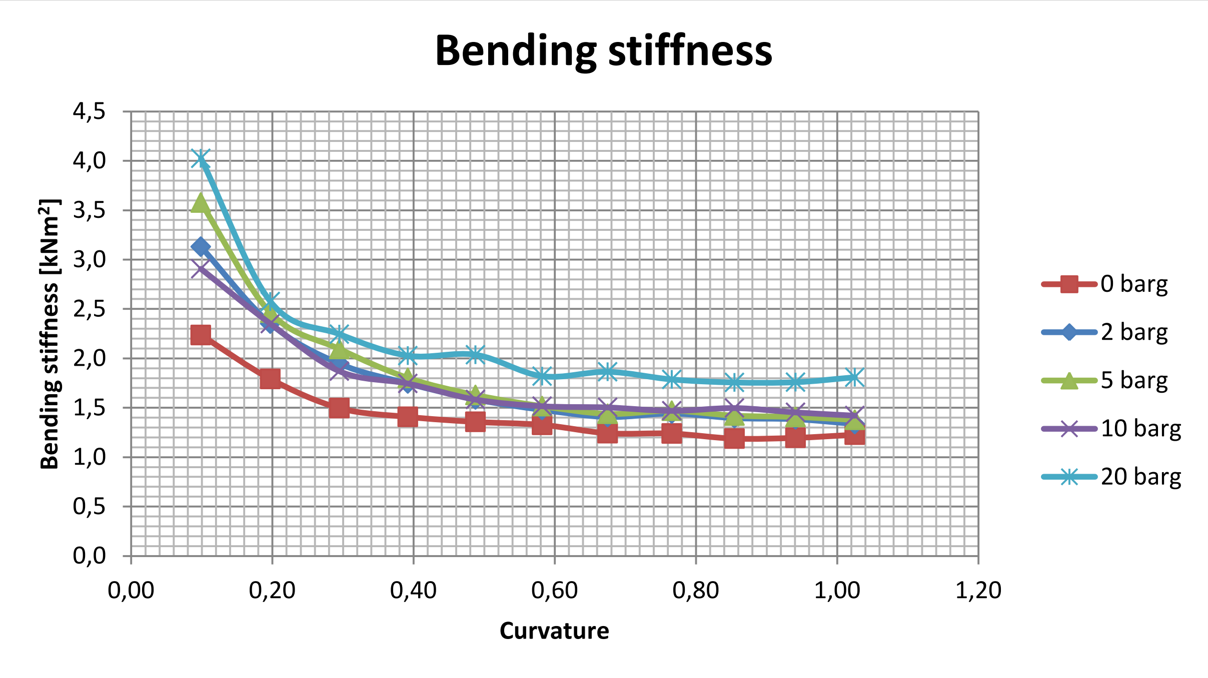

Figure 6.10 Bending stiffness with with increased curvature

From Figure 6.10 it seems that the curves follow the same trend as for Figure 6.9. When the curvature increases the bending stiffness decreases. It is observed that bending stiffness below critical bending radius is relatively stable.

The bending stiffness in Figure 6.10 is a little bit lower compared with Figure 6.9. This is probably since the same hose sample is used during both tests. If a new hose sample was used, the bending stiffness up to a curvature of 0.65 should been the same for both cases.

7 Discussion

7.1 General

When deciding which axial stiffness or bending stiffness to use for analysis, it is important to be aware of which load area that is critical for the particular operation. As a rule of thumb in engineering, it is usual to take the most conservative value since the consequence for failure may be high.

The loading sequence is dependent on when the load results are measured. The load from the chain hoist decreases as the hose deforms. Therefore it is recommended to use same interval for each reading and loading. For this experiment the loading was measured 5-10 s after load was applied.

All the results are dependent on the time interval between each test. The hose itself contains different layers that have different properties. After the hose is unloaded the elastic properties may change the hose back to its original shape, which is time dependent. It may also partly go back to its initial shape if the applied load was too high. It was noticed creeping behaviour of the hose at each test.

There are uncertainties related to the measurements and tests, but the outcome of the results is approximately values. From the results it can be seen that the stiffness is somewhat randomly spread, therefore the selected stiffness plot can be selected as min, average or max depending in what is the most conservative for the given application. The straps will be stretched, which may cause some inaccuracy. Based on the results the use of digital caliper and carpenter ruler are considered as satisfactory measurements.

7.2 Axial compression

The results showed different axial stiffness on the tree different samples. One factor to consider is that the initial length of the hose samples differs, even though the initial distance between the caliper gaps is the same. The critical axial stiffness is suggested to be the minimum value calculated based on measurements. This minimum axial stiffness for different samples is summarized in Table 7.1 below.

Table 7.1 An comparison of axial stiffness of each sample.

Hose sample	Sample length	Caliper gap	Compression load range	Minimum axial stiffness
1	155	90 mm	0.49 – 11.28 kN	75 kN
2	161	90 mm	0.49 – 8.83 kN	85 kN
3	180	90 mm	0.49 – 7.36 kN	90 kN

It is also important to notice that the compression load on these three samples varies. This may also be one important part that results in different axial stiffness. The hose may have been plastically deformed when the load on sample 1 was applied up to 11.28 kN.

When the load is removed, the hose tries to maintain its original shape. The hose may have been temporary deformed. After 10 min the hose length has increased compared with 1 min after testing. The hose had increased with 1-2 mm. Another factor worth mention is that the hose samples needed to be cut before testing, because of uneven surface in both ends. The surface was tried to be cut as plane as possible, but still there were some difference when measuring the surface at different locations. To reduce this effect rubber mats were placed between the hose and the flanges. Below, in Figure 7.1 it is showed how uneven the hose sample was before cutting.

Figure 7.1Cut of hose before experiment

7.3 Axial tension

It was assumed that the axial stiffness in tension would change based on the internal pressure. This was also the outcome of the testing.

The initial caliper gap was tried to be hold at a given distance during all tests to be able to compare the results better.

The first and most important to consider is the initial curvature of the hose. This curvature is shown in Figure 7.2 below. The curvature is natural since the hoses normally are placed on a reel. This curvature influences the axial tension. The orientation of the hose is dependent of the results.

Figure 7.2 Initial curvature of the hose sample

This curvature was expected to decrease due to applied load and increased internal pressure, which also was the case. Below, in Figure 7.3 the initial curvature of the hose is shown, while hanging in the chain hoist.

Figure 7.3 Initial curvature of the hose hanging in the chain hoist

This curvature was tried adjusted with the help of straps. An illustration of this can be seen in the test set up shown in Figure 5.6. The hose was strapped at the bottom of the hose sample and one on the middle to make it even with the level. A close view of the level on the bottom flange is shown in Figure 7.4 after strapping.

Figure 7.4 Bottom flange in level before loading

When the hose is stretched with the chain hoist, the compression side will stretch more than the tension side on the hose sample. This results in different axial stiffness when the displacement is measured at two different positions. The axial stiffness during 2 barg for caliper 1 is shown below in Figure 7.5.

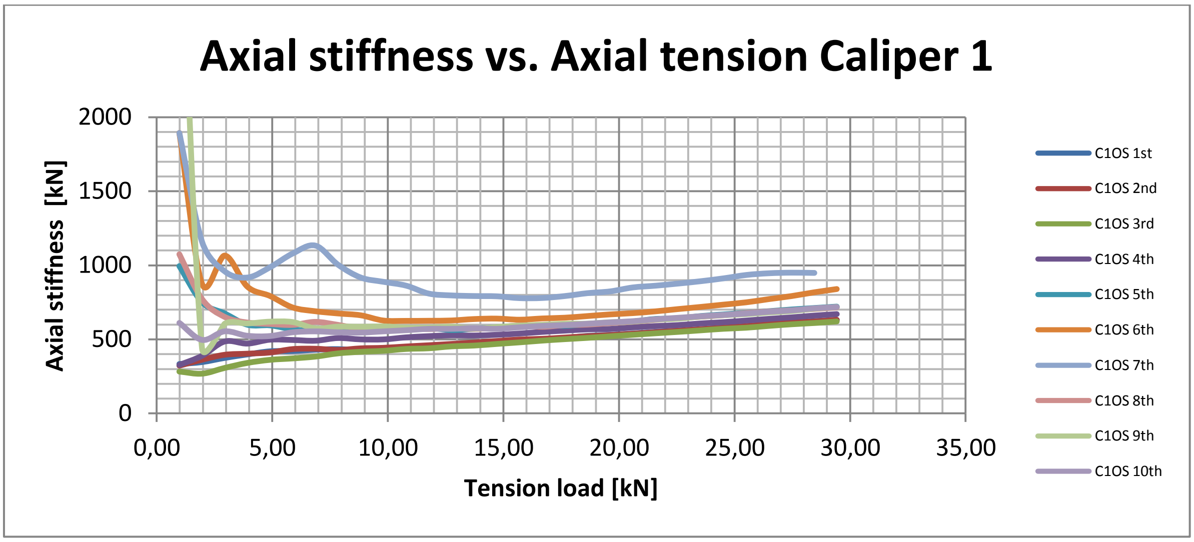

Figure 7.5 Axial stiffness for caliper 1 during 2 barg

For caliper 1 the trend during low pressure is that the axial stiffness increases with increased tension load. This is most probably due to huge displacement on caliper 1 during testing. Compared with figure 6.5 the trend on caliper 2 and 3 is that the axial stiffness evens out after a certain tension load.

From the results from caliper 1 the trend is that when the internal pressure increases the curvature decreases initially. This results in a decreasing trend of the axial stiffness that can be seen in Figure 7.6 below. Now the trend for the axial stiffness is the same as for caliper 2 and 3. By this reason it is recommended that the hose sample does not have any curvature when axial stiffness should be found.

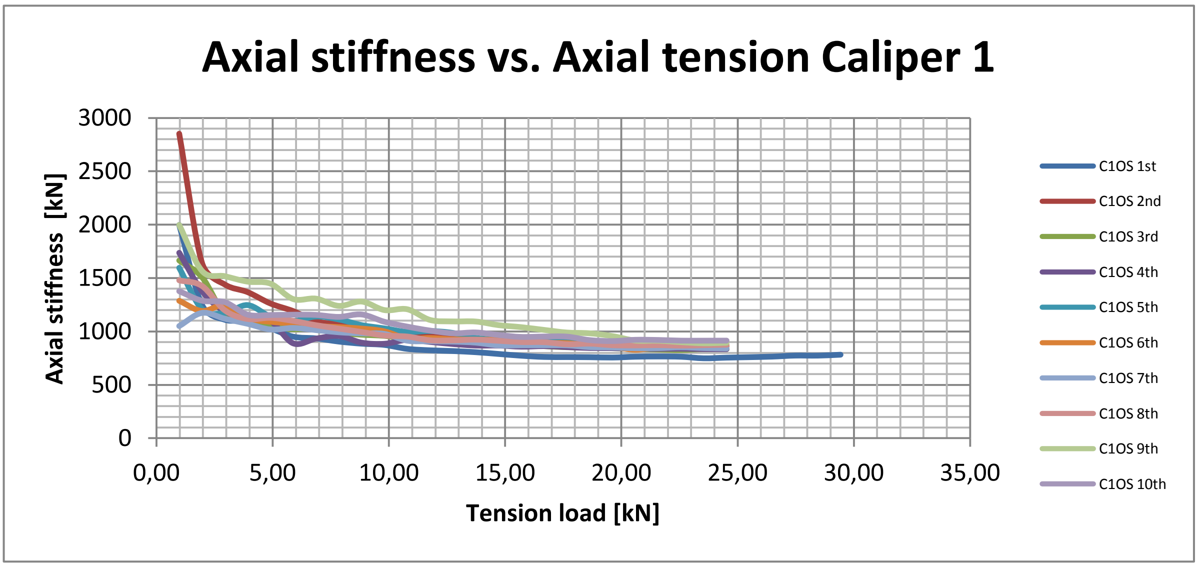

Figure 7.6 Axial stiffness for caliper 1 during 20barg

Even the hose sample was strapped in level with bottom flange and straightens the middle part of the hose, it was not completely in level at the top flange as shown in Figure 7.7. The top flange was in level after loading the hose with 7.85 kN. This is shown in Figure 7.8.

Figure 7.7 Top flange before lifting

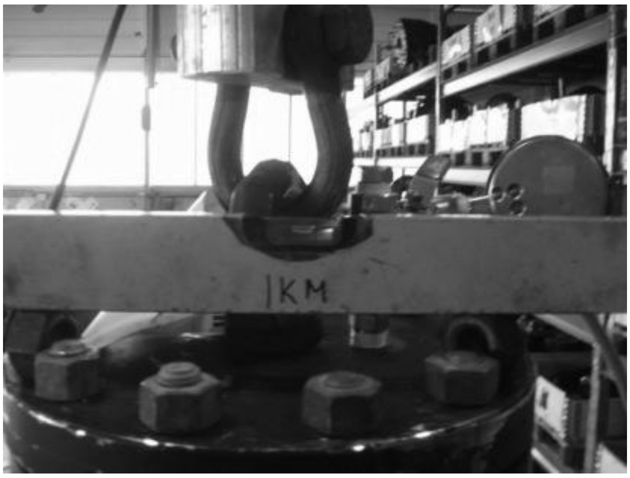

Figure 7.8 Top flange during lifting

The critical axial stiffness is tension is suggested to be the representative minimum value. The most critical axial stiffness for different pressures is listed in Table 7.2 below. The axial stiffness for the case of 5 barg is discussed in chapter 6.2.3, while the axial stiffness for 10 barg is discussed in chapter 6.2.4. In these two cases the minimum value is not chosen, because there are most likely errors in the measurements.

Table 7.2 Overview of representative axial stiffness

Pressure [barg]	Axial stiffness (from caliper 2 and 3)
0	750 kN
2	850 kN
5	850 kN*
10	1000 kN**
20	1300 kN

* ref chapter 6.2.3

** ref chapter 6.2.4

For each test it was carried out different loading intervals. All data are shown in Appendix 2.

Another observation was that the rubber length on the hose sample was increased during testing. The initial length was 807mm and after testing the rubber length had increased to 825 mm.

7.4 Bending stiffness

The bending stiffness is dependent on the curvature. The results showed a trend where the bending stiffness decreased with increased curvature. The critical bending stiffness is suggested to be the most critical value during testing.

Below, in Table 7.3 the critical bending stiffness for different pressures are summarized up to a curvature of 1.02 rad/m:

Table 7.3 Critical bending stiffness for different pressures for curvature up to 1.02

Pressure [barg]	Bending stiffness
0	1.2 kNm^2
2	1.3 kNm^2
5	1.4 kNm^2
10	1.45 kNm^2
20	1.75 kNm^2

The MBR is given 1525 mm. It is worth mention that this radius is given for the working pressure, which is 40 barg for Oilflex Super hose. Therefore it may be considered a less MBR when the internal pressure is less. This has to be discussed and evaluated within the company before considering any other MBR than 1525 mm.

If this kind of test should be representative it is important that the hose and spreader bar is level before lifting. Below in Figure 7.9 a level device is showed to assure correct initial conditions.

Figure 7.9 Level devive to assure correct initial conditions

8 Summary and conclusions

8.1 General

Compression tests, tension tests and bending tests have been carried out to find axial stiffness and bending stiffness for the 6” Oilflex Super hose.

During loading the hose has a tendency to creep under loading. This leads to that the applied load decreases with time. Therefore it is important that the hose loading measurements are measured within the same interval plus the hose should be unloaded a certain time before each test.

At this point it is possible to implement representative data for further OrcaFlex analysis. It is important to be aware of that none safety factors are included in the results.

8.2 Compression

Compression test results show a clear trend that the axial stiffness is going to a certain value when the compression load is increased.

8.3 Tension

Tension test was performed with internal pressures 0 barg, 2 barg, 5 barg, 10 barg and 20 barg. The tension test results show the same trend at different pressures. The trend is that the axial stiffness goes to certain value when the tension load is increased for all cases. The axial stiffness increases with increased pressure. One caliper measurements were disregarded since there was an initial curvature at this position. This caliper gave unreasonable results because the hose needs to be straightened before measurements.

8.4 Bending

Bending test was performed with internal pressures 0 barg, 2 barg, 5 barg, 10 barg and 20 barg.

The bending test results show the same trend at different pressures. For each pressure, the bending stiffness stabilizes when the loading increases. The bending stiffness enhances with increased pressure.

9 Evaluation and recommendations

9.1 Evaluation

9.1.1 Compression test

The test is considered representative and the given results will be used in further analysis.

9.1.2 Tension test

The measurements from caliper 1 were disregarded in the axial tension test, while the measurements from caliper 2 and caliper 3 were considered representative. To verify this statement an additional test set up was carried out. The same axial test set up was performed, but the measurements started when the hose was stretched with a load of 8.8 kN. This resulted that all calipers followed the same trend. The trend is that the axial stiffness goes from a high value to a certain value when the load is increased.

The test is considered representative and the given results will be used in further analysis.

9.1.3 Bending test

The test is considered representative and the given results will be used in further analysis.

In chapter 9.2 there are given recommendations how to improve the test set up for later analysis for other hose types.

9.2 Recommendations for future tests

9.2.1 Compression test

- Try to have the same length for each sample (because this is dependent on the axial stiffness if not the caliper measure the whole length of the sample)
- Measure with the caliper over the entire length of the sample (more accurate)
- The sample cross-section length should have the same initial length at each point.

9.2.2 Tension test

- Use strain gauges instead of digital calipers. This will measure strain in both longitudinal and cross direction
- Straighten up the hose initially before performing loading. This would decrease the potential curvature on the hose, and would result in more similar results between the calipers.

9.2.3 Bending Test

- Use strain gauges in addition to carpenter ruler. Then it is possible to measure the compression and tension on the hose during bending.

Project No.:	286658	Project Name:	6” Oilflex Super - mechanical test

References:

[1] TESS 2012, page 91- 93 Available from: http://tess.no/en/2012/06/25/products/. (Accessed 21st March 2013)

Appendix 1: Measurements from compression tests

Sample 1

Initial caliper gap: 90 mm

Hose length: 155 mm

Table A. 1 Measurements from compression test - Sample 1

Load [kg]	Strain [mm]									
	1st	2nd	3rd	4th	5th	6th	7th	8th	9th	10th
50	0,03	0,381	0,01	0,01	0,1	0,06	0,07	0,11	0,05	0,19
100	0,56	0,82	0,2	0,2	0,4	0,69	0,66	0,74	0,29	0,52
150	0,73	1,21	0,41	0,76	0,73	0,96	1,01	1,19	0,71	0,97
200	1,11	1,49	1	1,39	1,06	1,46	1,6	1,5	1,18	1,45
250	1,42	1,94	1,54	2,05	1,42	1,92	1,95	2,06	1,72	1,85
300	1,76	2,35	1,98	2,77	1,76	2,45	2,45	2,6	2,22	2,39
350	2,05	2,68	2,61	3,27	2,28	2,88	3,07	3,1	2,78	3
400	2,53	3,19	3,22	3,89	2,69	3,51	3,83	3,68	3,41	3,52
450	2,8	3,65	3,67	4,42	3,29	4,07	4,36	4,35	4,02	4,12
500	3,24	4,1	4,24	5,06	3,7	4,77	4,88	5,02	4,71	4,73
550	3,53	4,69	4,82	5,65	4,3	5,27	5,54	5,59	5,31	5,4
600	3,91	5,13	5,35	6,39	5,01	5,87	6,24	6,24	6,08	6,1
650	4,38	5,75	5,92	6,73	5,33	6,51	6,91	7,01	6,74	6,69
700	4,79	6,21	6,57	7,75	5,78	7,18	7,48	7,63	7,6	7,38
750	5,43	6,85	7,25	8,4	6,32	7,9	8,14	8,3	8,15	8,08
800	5,95	7,31	7,85	9,03	6,92	8,58	8,79	8,91	8,86	8,78
850	6,65	7,82	8,41	9,58	7,4	9,48	9,52	9,59	9,45	9,38
900	7,29	8,65	9,06	10,27	8,05	10,01	10,24	10,23	10,1	9,82
950	8,02	9,18	9,73	10,89		10,73	10,8	10,84	10,69	10,41
1000	9,05	9,93	10,33	11,59		11,41	11,39	11,44	11,39	11,06
1050		10,94	11,14							
1100		11,93	11,79							
1150			12,47							

Sample 2

Initial caliper gap: 90 mm

Hose length: 161 mm

Table A. 2 Measurements from compression test – Sample 2

Load [kg]	Strain [mm]									
	1st	2nd	3rd	4th	5th	6th	7th	8th	9th	10th
50	0,11	0,16	0	0,3	0,17	0,45	0	0	0,41	0,06
100	0,36	0,57	0,05	0,77	0,47	0,87	0,11	0,1	0,83	0,2
150	0,58	0,89	0,34	1,23	0,75	1,17	0,32	0,25	1,19	0,5
200	0,87	1,25	0,73	1,6	1,05	1,48	0,61	0,54	1,53	0,82
250	1,18	1,74	1,27	2	1,37	1,88	1,07	0,93	1,95	1,26
300	1,5	2,04	1,62	2,31	1,73	2,22	1,48	1,23	2,35	1,61
350	1,85	2,38	2,16	2,67	2,25	2,6	1,84	1,61	2,76	2,08
400	2,15	2,74	2,42	2,99	2,65	2,91	2,28	2	3,17	2,55
450	2,52	2,97	2,75	3,33	3,09	3,28	2,64	2,42	3,62	2,96
500	3,06	3,31	3,04	3,71	3,59	3,76	3,14	2,95	4,15	3,39
550		3,86	3,37	4,14	4,05	4,12	3,54	3,35	4,61	3,84
600		4,38	3,86	4,52	4,68	4,54	4,03	3,88	5,32	4,51
650			4,23	4,94	5,43	5,17	4,48	5,04	6,33	5,68
700			4,79	5,45	5,83	6,22	5,74	5,6	6,84	6,2
750				5,9	6,33	6,69	6,25	6,11	7,32	6,63
800				6,71	6,93	7,12	6,84	6,58	7,83	7,12
850					7,65	7,7	7,4	7,17	8,27	7,6
900						8,5				

Sample 3

Initial caliper gap: 90 mm

Hose length: 181 mm

Table A. 3 Measurements from compression test - Sample 3

Load [kg]	Strain [mm]									
	1st	2nd	3rd	4th	5th	6th	7th	8th	9th	10th
50	0,22	0,38	0,36	0,38	0,37	0,38	0,34	0,3	0,2	0,27
100	0,56	0,79	0,76	0,81	0,76	0,77	0,7	0,63	0,52	0,77
150	0,85	1,14	1,03	1,08	0,99	0,99	0,96	0,91	0,81	1,07
200	1,06	1,42	1,4	1,41	1,37	1,38	1,31	1,22	1,17	1,52
250	1,32	1,78	1,67	1,72	1,64	1,67	1,66	1,52	1,53	1,9
300	1,6	2,12	2	2,08	2,03	2,09	2,02	1,98	1,99	2,6
350	1,84	2,5	2,36	2,41	2,4	2,47	2,41	2,37	2,41	3
400	2,11	2,79	2,7	2,77	2,75	2,85	2,87	2,84	2,92	3,34
450	2,41	3,13	3,05	3,15	3,14	3,24	3,27	3,24	3,38	3,86
500	2,75	3,52	3,51	3,54	3,55	3,6	3,62	3,76	3,94	4,53
550	3,15	3,88	3,84	3,89	4,01	4,06	4,1	4,13	4,47	5,09
600	3,58	4,29	4,22	4,34	4,4	4,44	4,46	4,63	4,97	5,69
650	4,05	4,69	4,6	4,72	4,78	4,94	4,93	5,1	5,43	6,16
700	4,53	5,21	5	5,11	5,19	5,42	5,44	5,67	6,03	6,7
750	5,55	5,74	5,54	5,6	5,66	5,81	5,85	6,09	6,58	7,36

Appendix 2: Measurements from tension tests

0 barg
Caliper 1 gap: 403.5 mm
Caliper 2 gap: 80.7 mm
Caliper 3 gap: 80.7 mm

2 barg
Caliper 1 gap: 405.5 mm
Caliper 2 gap: 80.7 mm
Caliper 3 gap: 80.7 mm

5 barg
Caliper 1 gap: 405.5 mm
Caliper 2 gap: 80.7 mm
Caliper 3 gap: 80.7 mm

10 barg
Caliper 1 gap: 405 mm
Caliper 2 gap: 80.7 mm
Caliper 3 gap: 80.7 mm

20 barg
Caliper 1 gap: 407 mm
Caliper 2 gap: 80.7 mm
Caliper 3 gap: 80.7 mm

Table A. 4 Measurements from tension test – 0 barg

	Strain [mm]																													
	1st			2nd			3rd			4th			5th			6th			7th			8th			9th			10th		
	Caliper			Caliper			Caliper			Caliper			Caliper			Caliper			Caliper			Caliper			Caliper			Caliper		
Load [kg]	1	2	3	1	2	3	1	2	3	1	2	3	1	2	3	1	2	3	1	2	3	1	2	3	1	2	3	1	2	3
100	0,95	0		0,21	0		0,4	0		0	0		0,71	0		0,6	0		0,27	0		0,5	0		0,72	0		0,65	0	
200	2,34	0		1,31	0		1,66	0		0,2	0		2,02	0		1,8	0		0,91	0		1,61	0		1,59	0		1,9	0	
300	3,62	0,03		2,69	0		2,92	0		0,94	0		3,08	0		2,63	0		1,25	0		2,3	0		2,17	0		2,98	0,01	
400	4,86	0,05		3,81	0,03		4,15	0,05		1,87	0,01		4,02	0,02		3,49	0,06		1,63	0,03		2,62	0,06		2,72	0		3,85	0,08	
500	6,04	0,12		4,9	0,11		5,17	0,13		2,94	0,09		5,07	0,11		3,96	0,14		1,93	0,07		3,03	0,14		3,17	0,08		4,32	0,15	
600	7,5	0,23		5,99	0,2		6,25	0,22		3,68	0,19		5,79	0,19		4,58	0,26		2,35	0,2		3,42	0,23		3,56	0,17		4,92	0,26	
700	8,51	0,34		6,96	0,32		7,42	0,36		4,1	0,22		6,55	0,32		5,07	0,36		2,57	0,28		3,82	0,36		3,97	0,28		5,37	0,38	
800	9,34	0,44		7,69	0,42		8,14	0,45		4,61	0,28		7,18	0,44		5,65	0,48		2,73	0,37		4,09	0,45		4,26	0,37		5,83	0,5	
900	10,47	0,59		8,53	0,55		9,07	0,58		4,87	0,41		7,83	0,58		6,12	0,59		2,99	0,5		4,38	0,57		4,7	0,5		6,14	0,59	
1000	11,32	0,72		9,3	0,71		10,19	0,74		5,19	0,51		8,33	0,7		6,79	0,78		3,32	0,67		4,71	0,73		5,11	0,64		6,46	0,69	
1100	12,32	0,88		9,98	0,84		10,9	0,86		5,69	0,63		8,84	0,83		7,18	0,9		3,56	0,78		5,01	0,87		5,43	0,75		6,84	0,83	
1200	12,93	0,98		10,61	0,97		11,63	0,99		6,09	0,74		9,4	0,99		7,63	1,05		3,86	0,92		5,3	0,99		5,9	0,91		7,15	0,93	
1300	13,45	1,12		11,16	1,08		12,24	1,11		6,5	0,87		9,85	1,11		8,06	1,21		4,18	1,06		5,73	1,16		6,38	1,07		7,49	1,06	
1400	14,15	1,29		11,91	1,22		12,95	1,24		6,98	0,98		10,45	1,27		8,43	1,35		4,68	1,23		6,05	1,27		6,71	1,19		7,79	1,17	
1500	14,63	1,42		12,5	1,35		13,12	1,42		7,48	1,13		10,89	1,4		8,84	1,51		5,09	1,35		6,58	1,43		7,01	1,3		8,15	1,34	
1600	15,22	1,55		13,07	1,48		14,18	1,51		7,91	1,26		11,38	1,55		9,11	1,64		5,52	1,47		7	1,56		7,38	1,42		8,39	1,43	
1700	15,65	1,66		13,64	1,6		14,76	1,65		8,42	1,4		11,89	1,7		9,41	1,76		6	1,58		7,35	1,68		7,64	1,52		8,7	1,55	
1800	16,27	1,81		14,32	1,72		15,31	1,78		8,76	1,52		12,17	1,81		9,8	1,9		6,68	1,76		7,67	1,79		7,97	1,64		8,95	1,65	
1900	16,73	1,94		14,72	1,81		15,79	1,9		9,05	1,66		12,53	1,95		10,06	2,02		7,15	1,87		8,05	1,92		8,2	1,73		9,23	1,77	
2000	17,21	2,06		15,24	1,93		16,17	2,02		9,36	1,82		12,98	2,11		10,09	2,14		7,59	1,98		8,37	2,03		8,58	1,87		9,45	1,87	
2100	17,6	2,14		15,72	2,05		16,53	2,12		9,56	1,92		13,12	2,18		10,25	2,27		7,94	2,1		8,68	2,14		8,87	1,98		9,67	2	
2200	18,04	2,24		16,05	2,13		16,94	2,24		9,84	2,03		13,46	2,31		10,42	2,4		8,49	2,2		9,01	2,24		9,14	2,07		9,83	2,08	
2300	18,48	2,35		16,53	2,25		17,39	2,36		9,97	2,12		13,68	2,42		10,63	2,47		8,88	2,3		9,32	2,33		9,4	2,17		10,02	2,17	
2400	18,9	2,49		16,96	2,37		17,76	2,46		10,29	2,26		14,03	2,54		10,87	2,57		9,26	2,41		9,58	2,41		9,71	2,28		10,23	2,27	
2500	19,34	2,61		17,28	2,45		18,19	2,6		10,41	2,34		14,37	2,65		11,12	2,67		9,63	2,5		9,88	2,48		10,02	2,39		10,46	2,37	
2600	19,67	2,71		17,62	2,55		18,56	2,72		10,74	2,47		14,68	2,73		11,33	2,75		9,98	2,6		10,08	2,53		10,31	2,48		10,71	2,47	
2700	20,04	2,83		18,08	2,69		18,92	2,83		11,01	2,56		14,89	2,79		11,58	2,83		10,33	2,69		10,36	2,6		10,53	2,57		10,92	2,61	
2800	20,44	2,99		18,52	2,77		19,14	2,91		11,32	2,66		15,23	2,9		11,94	2,95		10,65	2,78		10,6	2,67		10,81	2,69		11,12	2,63	
2900							19,52	3,01		11,77	2,77		15,53	2,99		12,16	3,02		11,03	2,9		10,86	2,74		11,08	2,75		11,33	2,71	
3000							19,91	3,11		12,06	2,85		15,84	3,09		12,46	3,13		11,27	2,97		11,06	2,86		11,27	2,81		11,52	2,8	
3100							20,22	3,21		12,48	2,96																			
3200							20,61	3,32		12,81	3,06																			
3300							21,02	3,43																						
3400							21,38	3,58																						

Table A. 5 Measurements from tension test – 2 barg

Load [kg]	Strain [mm]																													
	1st			2nd			3rd			4th			5th			6th			7th			8th			9th			10th		
	Caliper			Caliper			Caliper			Caliper			Caliper			Caliper			Caliper			Caliper			Caliper			Caliper		
	1	2	3	1	2	3	1	2	3	1	2	3	1	2	3	1	2	3	1	2	3	1	2	3	1	2	3	1	2	3
100	1,19	0	0	1,23	0	0	1,41	0	0	1,22	0	0	0,4	0	0	0,21	0	0	0	0	0	0,37	0	0	0,11	0	0	0,65	0	0
200	2,29	0,05	0	2,19	0,03	0	2,97	0	0	2,05	0	0	1,06	0,03	0	0,91	0	0	0,42	0	0	1,03	0	0	1,81	0	0	1,6	0	0
300	3,18	0,11	0	3,01	0,07	0	3,89	0,03	0	2,46	0,06	0,02	1,77	0,08	0,01	1,12	0	0	1,03	0	0,04	1,83	0,05	0	1,97	0,04	0	2,15	0,07	0
400	3,99	0,18	0,1	3,94	0,16	0,09	4,67	0,09	0,05	3,38	0,14	0,08	2,66	0,17	0,1	1,86	0,06	0	1,66	0,01	0,11	2,59	0,11	0	2,62	0,1	0,05	3,03	0,15	0,08
500	4,74	0,26	0,14	4,83	0,25	0,19	5,5	0,17	0,11	4	0,22	0,15	3,35	0,24	0,17	2,51	0,13	0,1	2,17	0,09	0,19	3,29	0,19	0	3,21	0,16	0,12	3,8	0,25	0,17
600	5,66	0,36	0,19	5,49	0,32	0,28	6,43	0,27	0,22	4,82	0,32	0,25	4,21	0,35	0,27	3,34	0,25	0,14	2,42	0,19	0,29	3,99	0,27	0,02	3,87	0,25	0,19	4,35	0,31	0,25
700	6,47	0,46	0,26	6,37	0,43	0,41	7,26	0,38	0,32	5,68	0,43	0,34	5,02	0,46	0,38	4,04	0,35	0,22	2,58	0,28	0,37	4,5	0,35	0,06	4,85	0,38	0,33	5,02	0,41	0,34
800	7,33	0,6	0,4	7,42	0,58	0,58	7,85	0,45	0,39	6,26	0,51	0,41	5,71	0,56	0,46	4,72	0,45	0,29	2,81	0,36	0,45	5,32	0,45	0,16	5,43	0,45	0,42	5,8	0,51	0,47
900	8,4	0,72	0,53	8,14	0,67	0,68	8,6	0,56	0,48	7,17	0,63	0,51	6,35	0,65	0,54	5,41	0,54	0,37	3,57	0,49	0,59	6,26	0,59	0,28	6,12	0,56	0,53	6,55	0,61	0,6
1000	9,15	0,83	0,65	8,97	0,78	0,82	9,41	0,67	0,58	7,97	0,75	0,6	6,94	0,73	0,6	6,35	0,68	0,49	4,34	0,59	0,7	6,96	0,69	0,39	6,77	0,65	0,63	7,17	0,71	0,7
1100	9,96	0,94	0,74	9,67	0,89	0,94	10,05	0,76	0,67	8,53	0,85	0,68	7,73	0,85	0,71	7,01	0,77	0,58	4,93	0,67	0,78	7,65	0,81	0,49	7,55	0,77	0,76	7,78	0,81	0,8
1200	10,63	1,03	0,89	10,36	0,97	1,05	10,85	0,88	0,79	9,16	0,93	0,77	8,28	0,93	0,78	7,64	0,86	0,67	5,54	0,75	0,87	8,37	0,92	0,6	8,23	0,87	0,88	8,35	0,89	0,9
1300	11,16	1,1	0,99	11,02	1,06	1,16	11,42	0,95	0,87	9,82	1,02	0,86	9,2	1,05	0,89	8,25	0,94	0,76	6,4	0,86	1	8,97	1	0,71	8,84	0,95	0,97	9,04	0,99	1,02
1400	11,81	1,2	1,08	11,63	1,15	1,26	12,15	1,05	0,98	10,6	1,13	0,98	9,75	1,13	0,97	8,75	1,02	0,84	7	0,95	1,1	9,75	1,12	0,85	9,72	1,08	1,12	9,67	1,07	1,13
1500	12,35	1,28	1,19	12,2	1,23	1,36	12,71	1,14	1,07	11,25	1,23	1,08	10,28	1,21	1,04	9,33	1,11	0,94	7,54	1,01	1,18	10,3	1,21	0,95	10,23	1,16	1,21	10,43	1,19	1,26
1600	13	1,38	1,29	12,75	1,31	1,44	13,26	1,21	1,16	11,81	1,31	1,17	10,83	1,3	1,12	10,07	1,23	1,06	8,06	1,08	1,26	10,71	1,28	1,03	10,74	1,24	1,29	10,93	1,27	1,35
1700	13,49	1,47	1,39	13,42	1,41	1,56	13,75	1,29	1,24	12,3	1,39	1,24	11,36	1,37	1,2	10,56	1,31	1,15	8,7	1,2	1,38	11,55	1,4	1,21	11,31	1,32	1,39	11,43	1,34	1,43
1800	14,07	1,55	1,49	13,97	1,5	1,65	14,27	1,37	1,32	12,82	1,46	1,33	12,11	1,49	1,31	11,09	1,4	1,24	9,2	1,27	1,45	12	1,49	1,34	11,83	1,4	1,48	11,99	1,43	1,53
1900	14,45	1,61	1,55	14,49	1,56	1,73	14,8	1,44	1,41	13,33	1,54	1,41	12,57	1,56	1,39	11,51	1,48	1,31	9,55	1,33	1,52	12,59	1,56	1,54	12,47	1,49	1,59	12,47	1,51	1,61
2000	15,02	1,69	1,64	15,04	1,64	1,83	15,26	1,51	1,49	13,97	1,63	1,51	13,06	1,63	1,46	11,91	1,55	1,37	9,81	1,4	1,59	13,03	1,65	1,71	12,92	1,57	1,67	12,93	1,58	1,69
2100	15,5	1,76	1,73	15,52	1,71	1,9	15,72	1,57	1,55	14,4	1,7	1,57	13,49	1,7	1,54	12,35	1,62	1,45	10,15	1,47	1,67	13,49	1,73	1,81	13,46	1,65	1,76	13,4	1,66	1,78
2200	15,92	1,82	1,8	15,96	1,78	1,97	16,16	1,64	1,63	14,85	1,77	1,64	13,74	1,73	1,58	12,71	1,69	1,52	10,3	1,53	1,74	13,84	1,79	1,88	13,81	1,7	1,83	13,75	1,71	1,84
2300	16,4	1,9	1,88	16,4	1,85	2,05	16,6	1,7	1,7	15,35	1,85	1,72	14,29	1,82	1,68	13	1,75	1,58	10,62	1,59	1,8	14,23	1,86	1,96	14,3	1,79	1,91	14,15	1,78	1,9
2400	16,81	1,96	1,95	16,8	1,91	2,11	17	1,77	1,77	15,72	1,91	1,77	14,54	1,86	1,71	13,29	1,81	1,64	10,9	1,65	1,86	14,6	1,94	2,04	14,6	1,83	1,95	14,54	1,84	1,97
2500	17,19	2,02	2,01	17,22	1,98	2,17	17,38	1,83	1,83	16,15	1,97	1,84	14,9	1,93	1,77	13,55	1,86	1,7	11,15	1,71	1,91	14,99	2,01	2,11	14,99	1,89	2,02	14,94	1,91	2,04
2600	17,57	2,09	2,08	17,57	2,04	2,23	17,85	1,91	1,91	16,5	2,03	1,88	15,24	1,98	1,82	13,8	1,92	1,76	11,35	1,76	1,97	15,25	2,05	2,15	15,43	1,96	2,09	15,32	1,97	2,1
2700	17,86	2,13	2,13	17,87	2,09	2,29	18,15	1,96	1,97	16,83	2,09	1,93	15,58	2,04	1,88	13,93	1,98	1,81	11,5	1,81	2,02	15,59	2,11	2,21	15,76	2,02	2,15	15,63	2,03	2,16
2800	18,21	2,18	2,18	18,19	2,15	2,39	18,48	2,01	2,01	17,18	2,14	1,98	15,89	2,09	1,93	14,07	2,04	1,86	11,78	1,87	2,07	15,99	2,18	2,28	16,12	2,08	2,21	16	2,09	2,22
2900	18,56	2,24	2,24	18,59	2,2	2,4	18,87	2,07	2,07	17,47	2,19	2,02	16,23	2,15	1,98	14,12	2,1	1,92	12,15	1,91	2,13	16,35	2,23	2,34	16,31	2,12	2,24	16,24	2,13	2,28
3000	18,92	2,29	2,3	18,89	2,25	2,45	19,19	2,12	2,12	17,8	2,24	2,06	16,56	2,2	2,04	14,22	2,15	1,97	12,59	1,96	2,18	16,68	2,28	2,4	16,62	2,16	2,27	16,6	2,19	2,33

Project No.: 286658 **Project Name:** 6” Oilflex Super - mechanical test

Table A. 6 Measurements from tension test – 5 barg

Load [kg]	Strain [mm]																													
	1st			2nd			3rd			4th			5th			6th			7th			8th			9th			10th		
	Caliper			Caliper			Caliper			Caliper			Caliper			Caliper			Caliper			Caliper			Caliper			Caliper		
	1	2	3	1	2	3	1	2	3	1	2	3	1	2	3	1	2	3	1	2	3	1	2	3	1	2	3	1	2	3
100	0,61	0	0	1,24	0	0	0,53	0	0	1,13	0	0	1,2	0	0	0,85	0	0	1,31	0	0	1,52	0	0	0,56	0	0	0,61	0	0
200	2,18	0,06	0,04	2,78	0,09	0,15	1,94	0	0,12	2,57	0	0,04	2,31	0	0,07	1,89	0	0	2,33	0,04	0,17	2,55	0,05	0,17	2,05	0,11	0,08	1,94	0	0,11
300	2,94	0,14	0,16	3,67	0,16	0,19	2,81	0,02	0,22	3,43	0,03	0,06	3,13	0,02	0,12	2,83	0,02	0	3,2	0,08	0,26	3,56	0,12	0,28	3,15	0,19	0,16	2,92	0	0,18
400	3,77	0,21	0,23	4,27	0,22	0,26	3,47	0,08	0,24	4,1	0,1	0,18	3,81	0,12	0,19	3,58	0,1	0,06	3,79	0,13	0,37	4,24	0,18	0,37	3,84	0,25	0,22	3,83	0,07	0,25
500	4,55	0,3	0,29	4,99	0,3	0,32	4,4	0,19	0,34	5,02	0,21	0,35	4,05	0,2	0,23	4,08	0,14	0,12	4,58	0,21	0,48	5,05	0,26	0,51	4,57	0,33	0,27	4,45	0,13	0,29
600	5,11	0,36	0,34	5,7	0,4	0,38	5,22	0,3	0,43	5,63	0,28	0,49	4,64	0,29	0,3	5,03	0,26	0,18	5,4	0,3	0,6	5,77	0,35	0,62	5,25	0,4	0,31	5,34	0,23	0,38
700	5,9	0,46	0,43	6,44	0,49	0,45	5,81	0,38	0,5	6,2	0,36	0,58	5,46	0,35	0,38	5,78	0,35	0,32	6,06	0,38	0,71	6,66	0,45	0,76	5,96	0,49	0,37	5,95	0,3	0,45
800	6,46	0,54	0,49	7,12	0,59	0,53	6,38	0,46	0,59	6,79	0,44	0,67	6,04	0,45	0,45	6,42	0,43	0,4	6,71	0,45	0,81	7,58	0,57	0,9	6,78	0,59	0,46	6,59	0,37	0,52
900	7,25	0,66	0,59	7,74	0,68	0,6	7,03	0,56	0,69	7,61	0,55	0,8	6,77	0,52	0,59	7,14	0,52	0,6	7,42	0,55	0,93	8,3	0,66	1,01	7,36	0,67	0,54	7,19	0,44	0,59
1000	7,88	0,75	0,68	8,51	0,79	0,7	7,87	0,67	0,79	8,18	0,63	0,9	7,41	0,61	0,67	7,84	0,62	0,75	8,37	0,67	1,09	9,05	0,76	1,13	8,09	0,76	0,62	8,1	0,56	0,7
1100	8,52	0,84	0,76	9,16	0,89	0,78	8,55	0,78	0,89	8,77	0,71	0,98	8,22	0,75	0,79	8,47	0,7	0,85	8,98	0,76	1,2	9,81	0,87	1,26	8,65	0,85	0,71	8,74	0,64	0,79
1200	9,22	0,94	0,86	9,85	0,98	0,88	9,14	0,86	0,97	9,58	0,83	1,12	9	0,87	0,92	9,34	0,83	0,91	9,63	0,85	1,3	10,45	0,95	1,37	9,51	0,96	0,82	9,36	0,73	0,86
1300	10,03	1,05	0,97	10,62	1,09	1	9,72	0,94	1,05	10,2	0,91	1,23	9,53	0,94	1,05	9,93	0,91	1,02	10,51	0,97	1,44	11	1,03	1,45	10,09	1,03	0,91	10,2	0,84	0,95
1400	10,8	1,16	1,11	11,25	1,19	1,26	10,37	1,03	1,14	10,82	1	1,33	10,23	1,04	1,14	10,52	0,98	1,13	11,09	1,04	1,55	11,59	1,11	1,55	10,66	1,11	1,01	10,76	0,92	1,04
1500	11,4	1,25	1,2	11,92	1,29	1,37	11,15	1,14	1,24	11,41	1,08	1,42	10,89	1,1	1,25	11,09	1,05	1,35	11,62	1,12	1,64	12,2	1,19	1,65	11,48	1,23	1,16	11,36	1	1,12
1600	12	1,34	1,28	12,55	1,38	1,5	11,64	1,21	1,32	12,1	1,19	1,54	11,4	1,2	1,37	11,68	1,2	1,47	12,28	1,22	1,76	12,78	1,27	1,73	12,03	1,31	1,22	11,96	1,08	1,22
1700	12,52	1,42	1,37	13,22	1,48	1,62	12,14	1,29	1,4	12,68	1,27	1,64	11,96	1,29	1,47	12,39	1,3	1,6	12,82	1,29	1,85	13,47	1,37	1,85	12,68	1,4	1,32	12,53	1,16	1,31
1800	13,22	1,52	1,47	13,71	1,56	1,71	12,59	1,37	1,48	13,15	1,35	1,72	12,44	1,35	1,62	12,93	1,37	1,7	13,33	1,37	1,94	14,02	1,46	1,94	13,27	1,49	1,4	13,07	1,24	1,39
1900	13,72	1,6	1,57	14,23	1,64	1,8	13,3	1,48	1,59	13,62	1,44	1,8	13,15	1,47	1,64	13,55	1,43	1,8	14,02	1,47	2,05	14,52	1,53	2,02	13,81	1,56	1,48	13,81	1,34	1,49
2000	14,41	1,7	1,87	14,79	1,72	1,89	13,78	1,56	1,67	14,03	1,51	1,88	13,59	1,52	1,79	14,05	1,5	1,9	14,52	1,54	2,13	15,07	1,61	2,1	14,23	1,63	1,55	14,36	1,43	1,56
2100	14,93	1,78	2,03	15,23	1,79	1,98	14,25	1,62	1,74	14,38	1,58	1,96	14	1,59	1,84	14,62	1,58	2,02	15	1,61	2,21	15,54	1,67	2,17	14,71	1,69	1,62	14,8	1,49	1,62
2200	15,37	1,85	2,12	15,66	1,86	2,04	14,67	1,68	1,83	14,74	1,65	2,04	14,46	1,66	1,91	15,08	1,63	2,13	15,5	1,68	2,3	16,11	1,76	2,25	15,51	1,77	1,71	15,27	1,56	1,71
2300	15,84	1,92	2,21	16,42	1,97	2,06	15,1	1,74	1,89	15,18	1,72	2,11	14,96	1,72	1,98	15,45	1,68	2,23	15,94	1,75	2,37	16,51	1,82	2,32	15,7	1,84	1,76	15,79	1,63	1,79
2400	16,36	2	2,31	16,82	2,04	2,1	15,47	1,8	1,97	15,64	1,79	2,19	15,38	1,79	2,03	15,83	1,74	2,29	16,36	1,82	2,44	16,87	1,88	2,37	16,14	1,91	1,83	16,23	1,69	1,85
2500	16,73	2,07	2,37	17,25	2,11	2,21	15,83	1,85	2,03	15,95	1,83	2,23	15,8	1,88	2,09	16,22	1,8	2,36	16,72	1,88	2,5	17,27	1,94	2,43	16,6	1,98	1,91	16,59	1,74	1,88
2600	17,09	2,12	2,43	17,64	2,17	2,33	16,25	1,92	2,09	16,26	1,89	2,29	16,18	1,95	2,16	16,62	1,86	2,42	17,1	1,94	2,56	17,6	2	2,49	16,98	2,04	1,98	16,98	1,8	1,95
2700	17,53	2,2	2,51	17,98	2,23	2,4	16,67	1,98	2,17	16,64	1,95	2,36	16,6	2,02	2,24	16,96	1,9	2,48	17,48	2	2,63	17,93	2,05	2,53	17,23	2,08	2,03	17,35	1,86	2,02
2800	17,98	2,26	2,58	18,3	2,27	2,46	17,03	2,04	2,22	16,95	2,01	2,39	16,9	2,08	2,29	17,3	1,95	2,54	17,87	2,07	2,69	18,28	2,1	2,59	17,55	2,15	2,11	17,67	1,91	2,05
2900	18,35	2,32	2,65	18,57	2,31	2,51	17,39	2,1	2,29	17,21	2,05	2,42	17,16	2,12	2,35	17,54	1,98	2,58	18,09	2,1	2,72	18,66	2,16	2,64	17,83	2,19	2,16	17,93	1,94	2,07
3000	18,66	2,37	2,69	18,86	2,36	2,56	17,69	2,14	2,33	17,54	2,1	2,47	17,48	2,18	2,4	17,9	2,04	2,64	18,46	2,15	2,78	18,94	2,2	2,68	18,14	2,22	2,21	18,23	1,99	2,12

Test Report – Tess Oilflex Super 6”- Mechanical Test

Project No.: 286658 **Project Name:** 6” Oilflex Super - mechanical test

Table A. 7 Measurements from tension test – 10 barg

Load [kg]	Strain [mm]														
	1st			2nd			3rd			4th			5th		
	Caliper			Caliper			Caliper			Caliper			Caliper		
	1	2	3	1	2	3	1	2	3	1	2	3	1	2	3
100	0,54	0	0	0,34	0	0	0,49	0	0	0,57	0	0	0,38	0	0
200	1,36	0	0,07	0,91	0	0	1,32	0,02	0	1,48	0	0	1,27	0	0
300	2,21	0,1	0,15	1,86	0,07	0,03	2,31	0,09	0,04	2,61	0,07	0,05	2,19	0,09	0,05
400	3,33	0,2	0,2	2,46	0,13	0,1	3,2	0,16	0,2	3,47	0,13	0,15	3,12	0,14	0,15
500	4,14	0,29	0,36	3,44	0,22	0,22	4,02	0,25	0,31	4,41	0,21	0,26	4,05	0,21	0,23
600	4,99	0,37	0,46	3,96	0,28	0,27	4,61	0,31	0,37	4,94	0,27	0,31	4,64	0,26	0,29
700	5,61	0,44	0,52	4,62	0,36	0,34	5,26	0,39	0,44	5,56	0,34	0,39	5,25	0,31	0,35
800	6,18	0,51	0,62	5,27	0,43	0,43	5,84	0,45	0,5	6,17	0,41	0,46	5,92	0,37	0,43
900	6,86	0,6	0,72	5,92	0,51	0,51	6,46	0,53	0,57	6,73	0,47	0,53	6,6	0,44	0,51
1000	7,54	0,68	0,82	6,52	0,59	0,59	7,24	0,63	0,67	7,55	0,58	0,64	7,22	0,51	0,59
1100	8,12	0,76	0,92	7,14	0,65	0,67	7,84	0,71	0,75	8,17	0,65	0,72	7,83	0,57	0,67
1200	8,8	0,85	0,97	7,8	0,74	0,75	8,48	0,79	0,83	9	0,76	0,83	8,5	0,64	0,75
1300	9,64	0,95	1,05	8,55	0,84	0,84	9,13	0,88	0,92	9,63	0,85	0,92	9,1	0,71	0,83
1400	10,22	1,03	1,15	9,14	0,92	0,92	9,88	0,97	1,03	10,19	0,92	1	9,89	0,8	0,93
1500	11,06	1,13	1,25	9,88	1,01	1,03	10,51	1,05	1,12	10,74	0,98	1,08	10,54	0,89	1,01
1600	11,58	1,19	1,35	10,47	1,08	1,11	11,01	1,12	1,2	11,38	1,06	1,17	11,16	0,96	1,11
1700	12,12	1,26	1,43	11,15	1,17	1,21	11,59	1,19	1,29	11,9	1,13	1,24	11,7	1,02	1,18
1800	12,7	1,34	1,53	11,91	1,27	1,33	12,16	1,27	1,39	12,62	1,23	1,36	12,4	1,12	1,29
1900	13,24	1,41	1,62	12,48	1,34	1,42	12,87	1,37	1,5	12,98	1,28	1,41	12,87	1,18	1,36
2000	13,95	1,49	1,71	12,97	1,4	1,48	13,37	1,43	1,57	13,71	1,37	1,53	13,5	1,26	1,45
2100	14,47	1,56	1,78	13,48	1,47	1,56	13,85	1,5	1,65	14,19	1,43	1,6	13,94	1,32	1,52
2200	14,92	1,62	1,83	13,96	1,54	1,63	14,4	1,58	1,73	14,64	1,49	1,67	14,39	1,38	1,59
2300	15,4	1,68	1,91	14,51	1,61	1,71	14,88	1,64	1,79	15,11	1,55	1,74	14,96	1,45	1,68
2400	16,04	1,76	2	15,1	1,68	1,79	15,31	1,7	1,87	15,54	1,61	1,81	15,37	1,5	1,73
2500	16,71	1,86	2,07	15,75	1,77	1,89	15,8	1,77	1,94	16,01	1,67	1,88	15,78	1,56	1,79
2600	17,11	1,91	2,13	16,22	1,83	1,96	16,21	1,83	2,01	16,36	1,71	1,93	16,18	1,62	1,85
2700	17,48	1,96	2,22	16,69	1,9	2,04	16,67	1,9	2,08	16,79	1,77	2	16,63	1,67	1,91
2800	17,83	2,01	2,3	17,14	1,95	2,1	17,06	1,95	2,14	17,16	1,81	2,06	16,92	1,71	1,95
2900	18,21	2,06	2,38	17,5	2	2,16	17,48	2,01	2,2	17,51	1,86	2,11	17,28	1,76	2
3000	18,54	2,1	2,43	17,88	2,05	2,21	17,74	2,05	2,23	17,82	1,89	2,16	17,63	1,81	2,06

Load [kg]	Strain [mm]														
	6th			7th			8th			9th			10th		
	Caliper			Caliper			Caliper			Caliper			Caliper		
	1	2	3	1	2	3	1	2	3	1	2	3	1	2	3
100	0,32	0	0	0,38	0	0	0,36	0	0	0,36	0	0	0,48	0	0
200	1,1	0	0	1,12	0	0	1,23	0	0	1,34	0	0	1,38	0,06	0,01
300	1,73	0,01	0,02	1,91	0	0	2,28	0	0,03	2,13	0	0,03	2,4	0,15	0,05
400	2,71	0,15	0,12	3	0,1	0,06	3,01	0,02	0,07	3,01	0,08	0,09	3,39	0,23	0,13
500	3,43	0,34	0,17	3,71	0,23	0,12	3,94	0,09	0,09	4,01	0,17	0,21	4,02	0,29	0,14
600	4,02	0,39	0,23	4,29	0,28	0,13	4,51	0,14	0,15	4,66	0,26	0,3	4,85	0,38	0,15
700	4,8	0,47	0,31	4,86	0,33	0,18	5,17	0,19	0,19	5,14	0,32	0,33	5,45	0,44	0,26
800	5,39	0,53	0,38	5,51	0,39	0,26	5,73	0,25	0,23	5,75	0,38	0,34	6,06	0,52	0,31
900	6,07	0,61	0,46	6,06	0,45	0,31	6,4	0,31	0,3	6,31	0,45	0,42	6,67	0,6	0,38
1000	6,85	0,71	0,56	6,7	0,52	0,39	7,01	0,38	0,37	7,1	0,55	0,47	7,19	0,66	0,44
1100	7,53	0,8	0,65	7,47	0,61	0,48	7,62	0,45	0,44	7,71	0,63	0,55	8,06	0,77	0,55
1200	8,07	0,87	0,72	8,09	0,68	0,57	8,24	0,52	0,52	8,33	0,7	0,62	8,75	0,86	0,62
1300	8,65	0,95	0,79	8,7	0,76	0,65	9,02	0,62	0,61	8,95	0,79	0,7	9,37	0,94	0,71
1400	9,25	1,02	0,87	9,35	0,84	0,74	9,7	0,7	0,69	9,46	0,85	0,77	9,91	1	0,79
1500	9,8	1,09	0,94	10,05	0,93	0,82	10,24	0,78	0,76	10,23	0,95	0,86	10,49	1,07	0,87
1600	10,55	1,19	1,03	10,63	1	0,91	10,83	0,85	0,83	10,78	1,02	0,94	11,09	1,15	0,95
1700	11,24	1,28	1,12	11,15	1,07	0,98	11,35	0,92	0,91	11,31	1,08	1,01	11,62	1,21	1,03
1800	11,68	1,34	1,18	11,79	1,15	1,07	12,07	1,01	1	11,83	1,15	1,09	12,31	1,3	1,12
1900	12,15	1,39	1,25	12,48	1,25	1,17	12,53	1,07	1,07	12,39	1,23	1,18	12,88	1,37	1,2
2000	12,89	1,49	1,35	12,98	1,31	1,24	13,18	1,15	1,16	13,03	1,32	1,27	13,44	1,44	1,29
2100	13,44	1,57	1,43	13,45	1,38	1,32	13,6	1,21	1,22	13,52	1,38	1,34	13,91	1,51	1,36
2200	13,86	1,62	1,48	13,96	1,45	1,41	14,03	1,27	1,28	14,05	1,46	1,42	14,38	1,57	1,43
2300	14,49	1,7	1,57	14,46	1,52	1,47	14,42	1,32	1,36	14,49	1,52	1,48	14,81	1,62	1,48
2400	14,98	1,78	1,66	14,92	1,58	1,55	14,88	1,38	1,42	14,93	1,57	1,52	15,21	1,67	1,54
2500	15,36	1,83	1,71	15,4	1,64	1,62	15,39	1,44	1,49	15,37	1,62	1,58	15,68	1,72	1,61
2600	15,78	1,89	1,77	15,85	1,7	1,69	15,78	1,49	1,55	15,79	1,69	1,65	16,06	1,77	1,66
2700	16,13	1,95	1,83	16,16	1,74	1,73	16,23	1,56	1,62	16,19	1,75	1,72	16,43	1,83	1,71
2800	16,58	2,01	1,9	16,54	1,8	1,79	16,62	1,61	1,67	16,6	1,81	1,76	16,85	1,88	1,78
2900	16,92	2,06	1,95	16,95	1,86	1,87				16,82	1,84	1,77	17,25	1,94	1,85
3000	17,24	2,1	2	17,3	1,9	1,93				17,18	1,89	1,86	17,53	1,98	1,87

Table A. 8 Measurements from tension test – 20 barg

	Strain [mm]																													
	1st			2nd			3rd			4th			5th			6th			7th			8th			9th			10th		
Load [kg]	Caliper			Caliper			Caliper			Caliper			Caliper			Caliper			Caliper			Caliper			Caliper			Caliper		
	1	2	3	1	2	3	1	2	3	1	2	3	1	2	3	1	2	3	1	2	3	1	2	3	1	2	3	1	2	3
100	0,2	0	0	0,02	0	0	0,24	0	0	0,23	0	0	0,25	0	0	0,31	0	0	0,38	0	0	0,27	0	0	0,2	0	0	0,29	0	0
200	0,64	0	0	0,28	0	0	0,53	0	0	0,58	0,01	0,04	0,66	0	0	0,67	0	0	0,68	0	0	0,56	0	0	0,51	0	0,04	0,62	0	0
300	1,08	0,06	0,05	0,73	0	0,01	1,03	0,04	0,03	1,01	0,06	0,08	1,02	0,03	0,02	0,96	0	0	1,07	0	0	1	0,03	0	0,79	0,03	0,06	0,94	0	0
400	1,45	0,1	0,1	1,11	0,05	0,04	1,42	0,04	0,07	1,41	0,1	0,1	1,28	0,07	0,03	1,42	0,03	0,03	1,49	0,06	0,01	1,43	0,08	0,01	1,09	0,06	0,09	1,38	0,07	0,03
500	1,94	0,15	0,12	1,46	0,09	0,07	1,89	0,11	0,1	1,82	0,15	0,14	1,75	0,12	0,08	1,83	0,07	0,07	1,96	0,1	0,05	1,77	0,12	0,04	1,38	0,1	0,12	1,73	0,16	0,04
600	2,52	0,21	0,14	1,9	0,14	0,1	2,35	0,16	0,12	2,7	0,24	0,17	2,18	0,16	0,12	2,23	0,11	0,1	2,32	0,13	0,08	2,18	0,15	0,08	1,84	0,13	0,16	2,07	0,19	0,07
700	2,99	0,27	0,2	2,35	0,18	0,12	2,71	0,2	0,13	3	0,26	0,2	2,45	0,19	0,14	2,66	0,14	0,13	2,76	0,17	0,09	2,64	0,2	0,1	2,14	0,18	0,19	2,42	0,23	0,1
800	3,53	0,33	0,26	2,92	0,24	0,14	3,24	0,26	0,19	3,34	0,3	0,29	2,87	0,23	0,16	3,07	0,18	0,14	3,22	0,21	0,13	3,11	0,25	0,12	2,58	0,2	0,24	2,81	0,28	0,19
900	4,06	0,38	0,31	3,37	0,28	0,21	3,71	0,31	0,24	4,02	0,37	0,39	3,39	0,29	0,22	3,5	0,22	0,2	3,66	0,26	0,16	3,61	0,3	0,18	2,81	0,25	0,27	3,1	0,31	0,22
1000	4,57	0,45	0,37	3,87	0,33	0,26	4,17	0,36	0,28	4,52	0,42	0,4	3,88	0,34	0,26	3,99	0,27	0,26	4,09	0,3	0,21	4,15	0,35	0,24	3,33	0,28	0,32	3,66	0,38	0,29
1100	5,25	0,53	0,45	4,47	0,39	0,34	4,72	0,42	0,35	4,77	0,45	0,45	4,41	0,39	0,32	4,71	0,34	0,33	4,81	0,38	0,24	4,61	0,4	0,28	3,64	0,34	0,36	4,2	0,44	0,36
1200	5,82	0,6	0,53	4,97	0,44	0,41	5,25	0,48	0,42	5,32	0,51	0,56	4,77	0,43	0,37	5,11	0,38	0,37	5,28	0,43	0,34	5,22	0,49	0,35	4,33	0,38	0,44	4,75	0,51	0,47
1300	6,36	0,67	0,59	5,42	0,49	0,45	5,77	0,54	0,49	5,89	0,58	0,65	5,26	0,48	0,43	5,61	0,43	0,44	5,74	0,48	0,4	5,66	0,54	0,41	4,75	0,42	0,49	5,28	0,58	0,56
1400	6,94	0,74	0,67	5,93	0,55	0,52	6,29	0,6	0,58	6,45	0,65	0,72	5,95	0,56	0,5	6,06	0,48	0,5	6,25	0,54	0,46	6,05	0,58	0,46	5,12	0,47	0,54	5,64	0,62	0,61
1500	7,59	0,83	0,75	6,53	0,62	0,6	6,75	0,66	0,64	6,91	0,7	0,78	6,49	0,62	0,58	6,52	0,53	0,57	6,89	0,62	0,55	6,56	0,64	0,53	5,66	0,53	0,61	6,19	0,69	0,7
1600	8,27	0,91	0,83	7,06	0,68	0,67	7,31	0,73	0,73	7,46	0,77	0,86	7	0,68	0,65	7,16	0,61	0,64	7,35	0,66	0,6	7,09	0,7	0,6	6,15	0,59	0,68	6,73	0,79	0,77
1700	8,92	0,98	0,92	7,72	0,76	0,76	7,88	0,8	0,82	7,88	0,82	0,95	7,5	0,74	0,72	7,63	0,66	0,72	7,8	0,72	0,66	7,54	0,76	0,67	6,7	0,65	0,76	7,12	0,81	0,83
1800	9,46	1,04	1,01	8,25	0,82	0,82	8,44	0,87	0,89	8,43	0,88	1,05	7,95	0,8	0,77	8,08	0,71	0,79	8,27	0,77	0,73	8,16	0,83	0,75	7,27	0,71	0,83	7,55	0,87	0,89
1900	10	1,11	1,08	8,79	0,88	0,89	8,93	0,93	0,96	8,99	0,95	1,06	8,51	0,86	0,84	8,74	0,79	0,86	8,9	0,85	0,8	8,56	0,88	0,81	7,73	0,77	0,9	8,25	0,95	0,99
2000	10,57	1,18	1,16	9,24	0,93	0,96	9,48	1	1,05	9,48	1,01	1,21	9,27	0,95	0,92	9,33	0,87	0,93	9,41	0,91	0,88	9,16	0,95	0,88	8,36	0,87	0,97	8,77	1,01	1,07
2100	10,99	1,24	1,23	9,72	0,99	1,03	10,03	1,06	1,13	10,02	1,07	1,22	9,77	1,02	0,98	10,13	0,91	1,01	9,96	0,98	0,95	9,64	1	0,95	9,18	0,92	1,09	9,09	1,05	1,11
2200	11,48	1,3	1,29	10,2	1,05	1,1	10,59	1,13	1,21	10,5	1,13	1,37	10,25	1,07	1,07	10,3	0,97	1,08	10,42	1,03	1,02	10,07	1,06	1,01	9,63	0,98	1,16	9,54	1,11	1,18
2300	12,04	1,38	1,37	10,69	1,11	1,18	11,13	1,2	1,28	10,97	1,19	1,38	10,67	1,13	1,13	10,74	1,03	1,15	10,79	1,08	1,08	10,58	1,12	1,08	10,22	1,04	1,24	10,04	1,17	1,25
2400	12,8	1,47	1,46	11,21	1,18	1,23	11,49	1,25	1,3	11,49	1,26	1,39	11,11	1,19	1,19	11,18	1,09	1,22	11,36	1,15	1,15	10,99	1,17	1,15	10,79	1,1	1,31	10,48	1,23	1,31
2500	13,23	1,53	1,52	11,67	1,24	1,28	11,97	1,31	1,4	11,98	1,32	1,59	11,57	1,24	1,25	11,57	1,14	1,27	11,89	1,22	1,23	11,39	1,22	1,21	11,18	1,17	1,38	10,91	1,29	1,38
2600	13,68	1,58	1,6																											
2700	14,11	1,64	1,68																											
2800	14,45	1,69	1,73																											
2900	14,97	1,75	1,78																											
3000	15,32	1,8	1,85																											

Appendix 3: Measurements from bending tests

Bending measurements within initial curvature

Table A. 9 Measurements from bending test - 0 barg

Deflection at centre [m]	Load [kg]		
	1st	2nd	3rd
0,01	110	120	100
0,02	160	170	160
0,03	200	220	220
0,04	260	270	270
0,05	320	310	320
0,06	360	360	360
0,065	380	380	380

Table A. 10 Measurements from bending test - 2 barg

Deflection at centre [m]	Load [kg]		
	1st	2nd	3rd
0,01	140	120	130
0,02	200	180	190
0,03	250	250	250
0,04	300	300	300
0,05	350	350	350
0,06	400	400	410
0,065	420	430	430

Table A. 11 Measurements from bending test - 5 barg

Deflection at centre [mm]	Load [kg]		
	1st	2nd	3rd
0,01	160	140	150
0,02	220	200	210
0,03	280	260	270
0,04	340	320	340
0,05	390	380	400
0,06	450	440	450
0,065	470	470	480

Table A. 12 Measurements from bending test - 10 barg

Deflection at centre [mm]	Load [kg]		
	1st	2nd	3rd
0,01	160	160	160
0,02	240	230	240
0,03	290	290	300
0,04	360	350	360
0,05	420	420	420
0,06	470	480	480
0,065	500	500	500

Table A. 13 Measurements from bending test - 20 barg

Deflection at centre [m]	Load [kg]		
	1st	2nd	3rd
0,01	210	210	210
0,02	300	300	290
0,03	360	370	360
0,04	430	440	430
0,05	520	520	510
0,06	570	590	570
0,065	610	630	620

Bending measurements with increased curvature

Table A. 14 Measurements from bending test - Increased curvature 0 - 20 barg

Deflection at centre [m]	Load [kg]				
	0 barg	2 barg	5 barg	10 barg	20 barg
0,01	100	140	160	130	180
0,02	160	210	220	210	230
0,03	200	260	280	250	300
0,04	250	310	320	310	360
0,05	300	350	360	350	450
0,06	350	390	400	400	480
0,07	380	430	440	460	570
0,08	430	500	510	510	620
0,09	460	540	550	580	680
0,1	510	590	600	620	750
0,11	570	620	640	660	840

Appendix 4: Data sheets:

TEO TEKNIKK AS

Proof report

Instrument Calibrated		Calibration Normals	
TYPE:	CLP-100	ID No.:	M 861503
Description:	Compression load cell	Description:	5103-C3 20K 30NT
Manufacture:	Scan Sense	Manufacture:	Revere
Serie No:	HM-101/ 9527	Last Calibrated:	2011.11.28
Range:	0-5000 Kg	Proof No:	MTmPX17977-K02
Accuracy:		Traceability	Sveriges Provnings-ock Forskningsinstitut

Calibrationresults at 20° C

Real Weight	Read Weight			Average deviation	Variance	Variance	variance of max. load
	test 1	test 2	test 3				
kg	kg	kg	kg	kg	kg	%	%
500	500	500	500	500	0	0,00	0,00
750	750	750	750	750	0	0,00	0,00
1250	1240	1240	1240	1240	-10	-0,80	-0,20
2000	1990	1990	1990	1990	-10	-0,50	-0,20
3000	2990	2990	2990	2990	-10	-0,33	-0,20
5000	4990	4990	4990	4990	-10	-0,20	-0,20

Calibrated: 11.05.2012
Arvid Stokkeland
Terje Obrestad
Even Obrestad Hægstad
Åge Obrestad

Åge Obrestad

Postadresse: 4365 NÆRBØ | Besøksadresse: Haavegen 196 | Telefon: 51 79 84 00 | Telefax: 51 79 84 01 | E-post: teo@teo.no | Internett: www.teo.no | Foretaksregisteret: NO 936 940 218 MVA

Project No.:	286658	**Project Name:**	6” Oilflex Super - mechanical test

CALIBRATION REPORT

CALIBRATED UNIT

RANGE LOW:	0	ton	PRODUCT:	LS-3110-TL
RANGE HIGH:	6	ton	REPORT NO.:	ScS-L-7782
TESTLOAD:	12	ton	SERIAL NO.:	25591
OUTPUT LOW:	0.000	TTL	ARTICLE NO.:	5TL006-PLW-211
OUTPUT HIGH:	6.000	TTL	ScS ORDER NO.:	53845
ACCURACY:	0.25	%FS	CUSTOMER PO.:	4424104-1
COLOUR CODE:				

CALIBRATION REFERENCE

CALIBRATION DEVICE:	1011 25t CSPM SN:236080-96
ACCURACY:	0,6% FS 2 STD
TRACEABILITY:	DNV-CAL011-1089-A/2011

CALIBRATION RESULTS

TEST1		TEST2		TEST3		ERROR
REF	UNIT	REF	UNIT	REF	UNIT	%FS
-0.001	0.001	-0.001	0.007	0.000	0.004	0.08 %
1.511	1.510	1.530	1.530	1.507	1.505	-0.02 %
3.000	3.000	3.030	3.028	3.034	3.033	-0.02 %
4.509	4.510	4.507	4.510	4.521	4.521	0.02 %
6.015	6.018	5.999	6.005	6.033	6.036	0.07 %

NOTE:

DATE: 06.06.2012 SIGN: E. Theigler APPROVED:

ScanSense

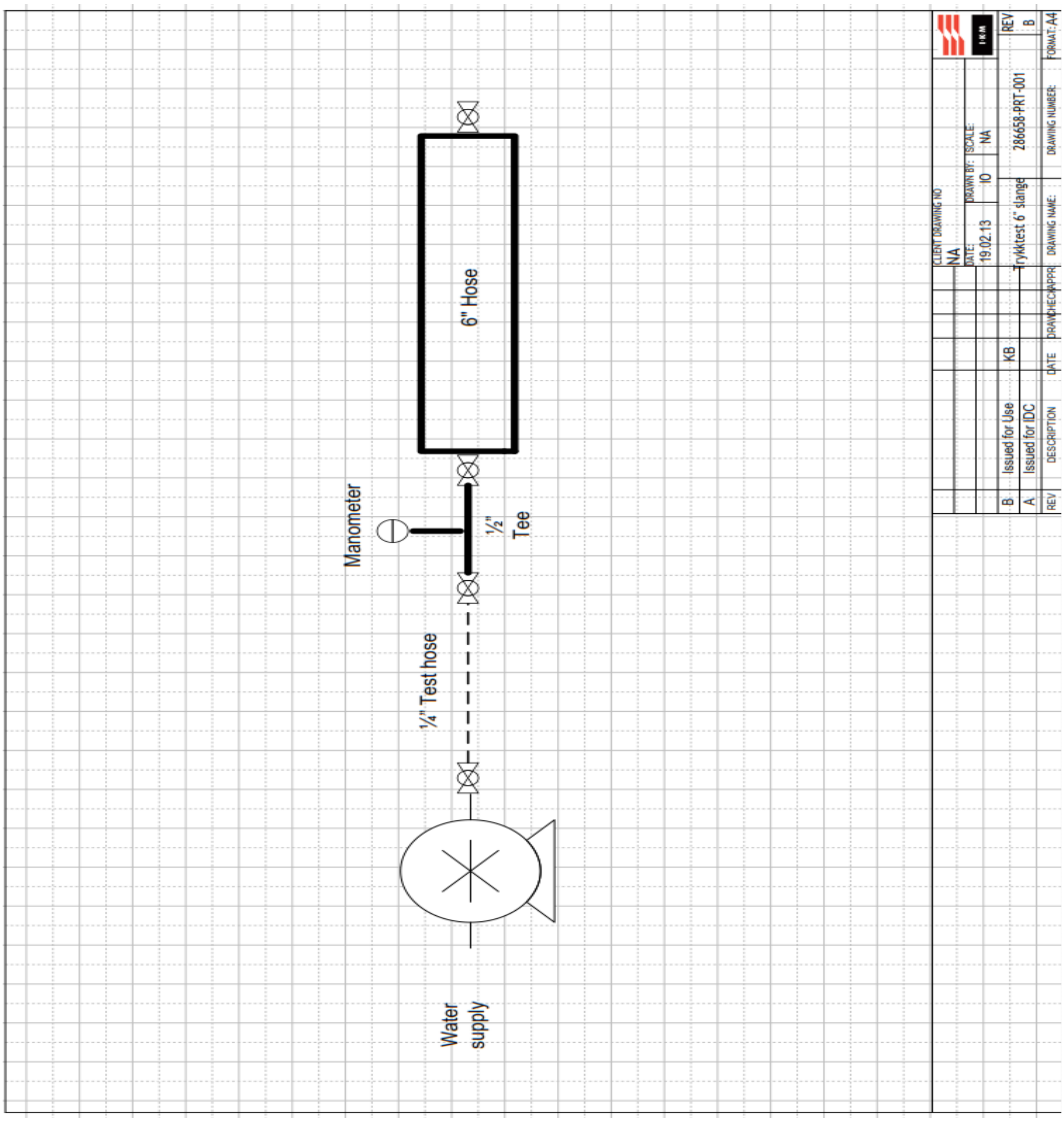
6" Hose
Manometer
½" Tee
¼" Test hose
Water supply
CLIENT DRAWING NO
NA
DATE:
19.02.13
DRAWN BY:
IO
SCALE:
NA
Trykktest 6" slange
286658-PRT-001
REV
B
FORMAT: A4
DRAWING NAME:
DRAWING NUMBER:
B
Issued for Use
KB
A
Issued for IDC
REV
DESCRIPTION
DATE

Appendix B – Static results

Table of Contents

List of Figures

Introduction

A detailed description of the graphs used in this Appendix is found in Chapters 6.4.1 and 6.4.2 in the main report.

4” Bunkerflex STH

Free hanging

Effective tension

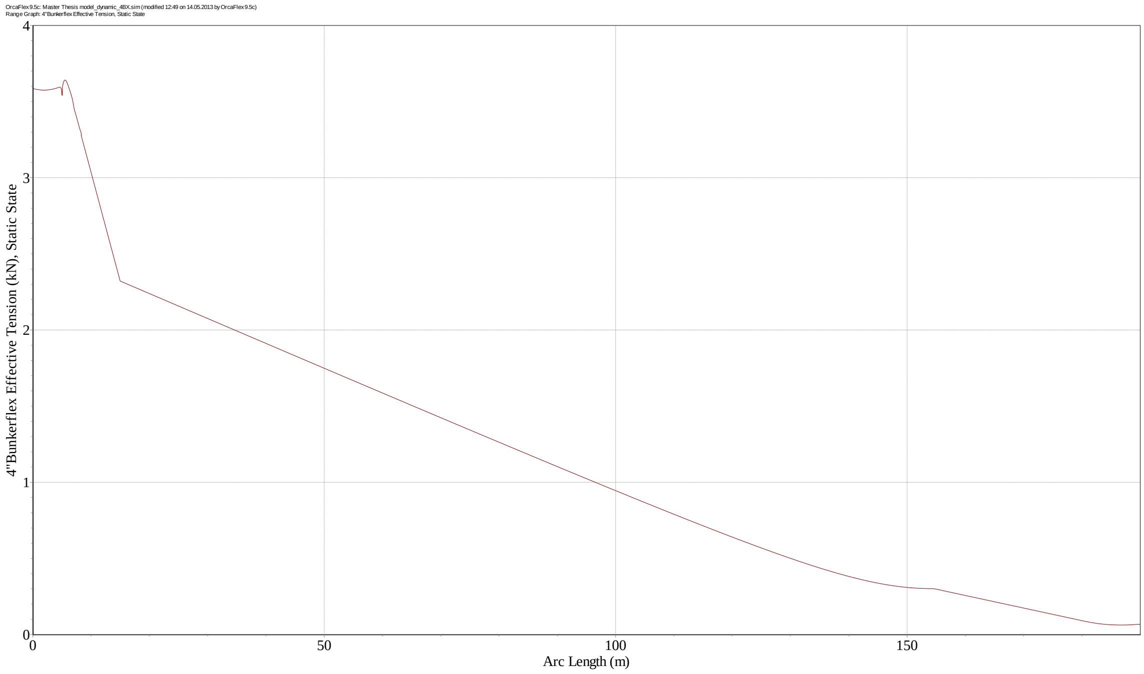

Figure B. 1 - 4” Bunkerflex STH - Free hanging - Effective tension

Curvature

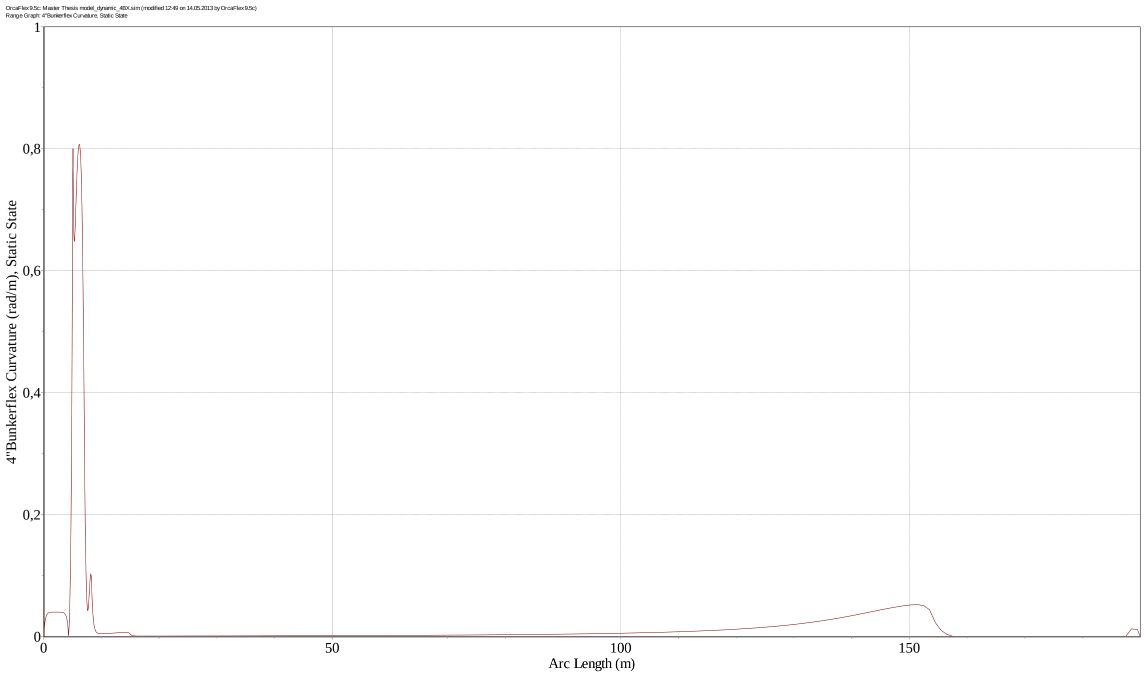

Figure B. 2 - 4" Bunkerflex STH - Free hanging - Curvature

Lazy wave – 20 m floatation point

Effective tension

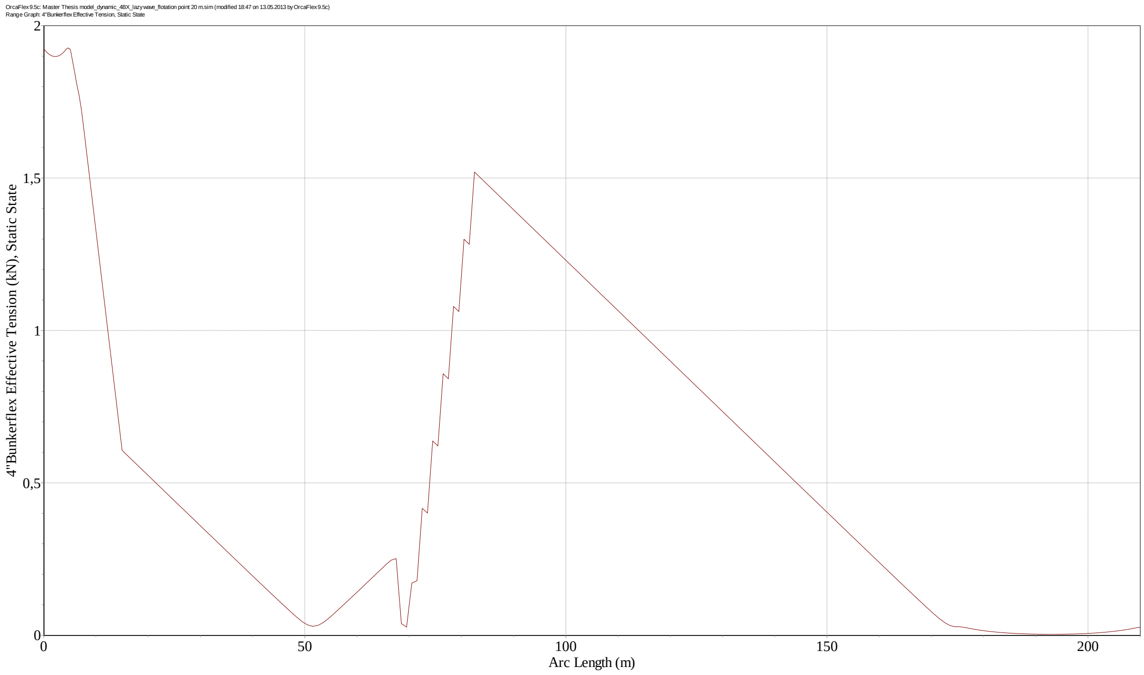

Figure B. 3 - 4" Bunkerflex STH - Lazy wave - 20 m floatation point - Effective tension

Curvature

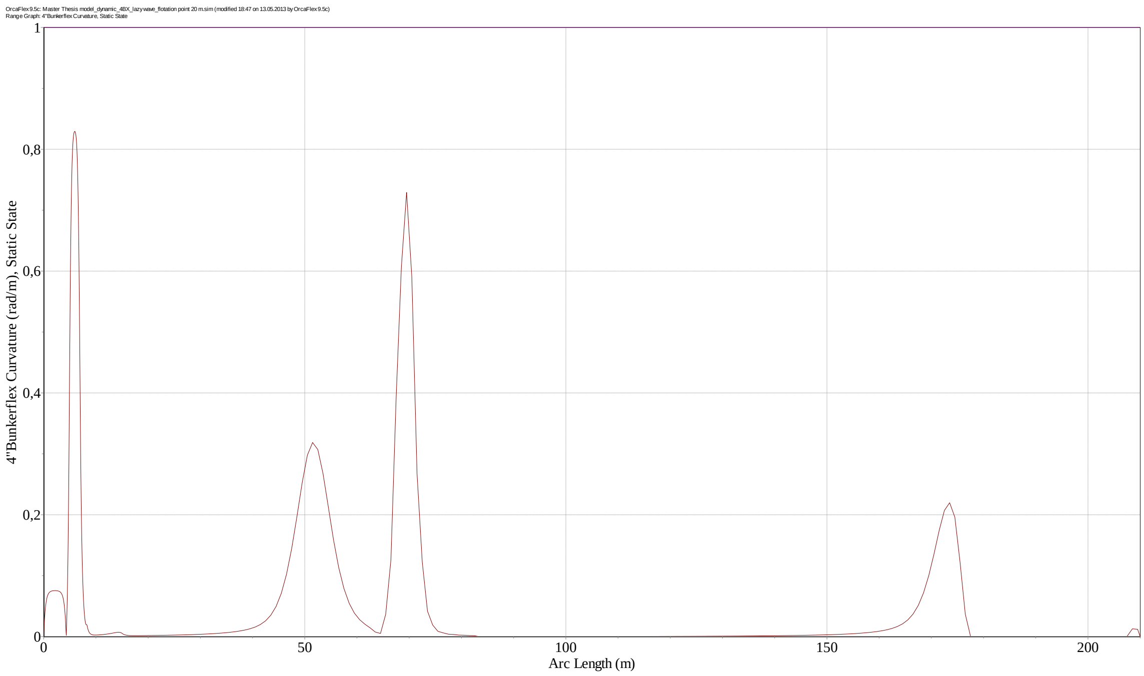

Figure B. 4 - 4" Bunkerflex STH - Lazy wave - 20 m floatation point - Curvature

Lazy wave – 40 m floatation point

Effective tension

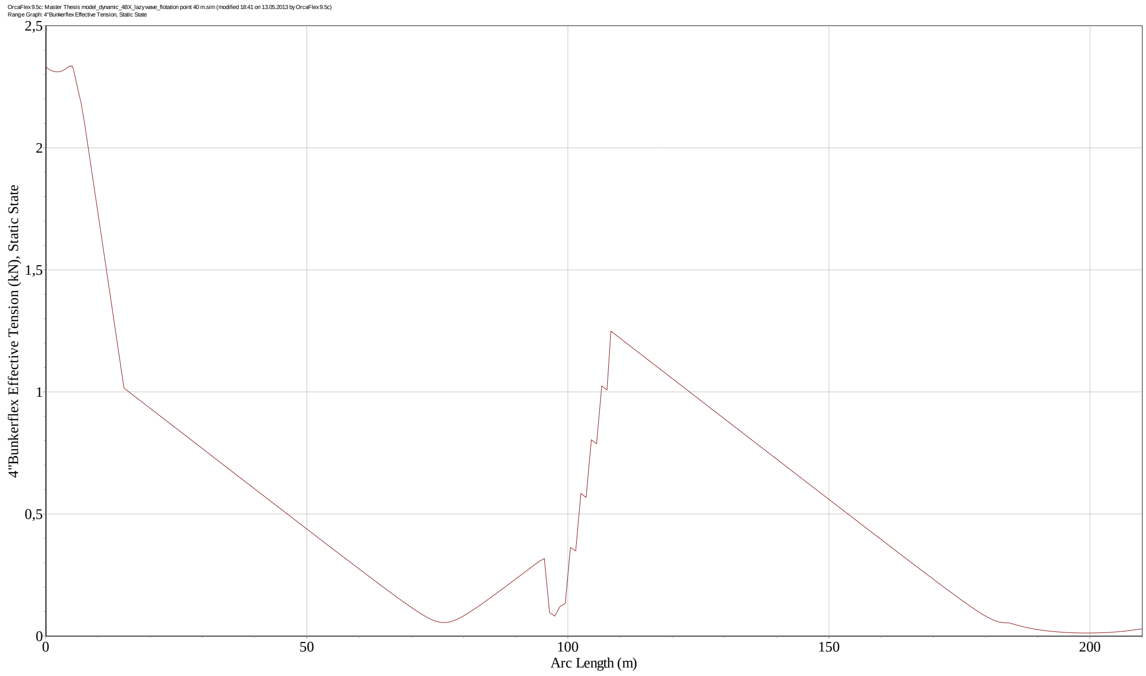

Figure B. 5 - 4" Bunkerflex STH - Lazy wave - 40 m floatation point - Effective tension

Curvature

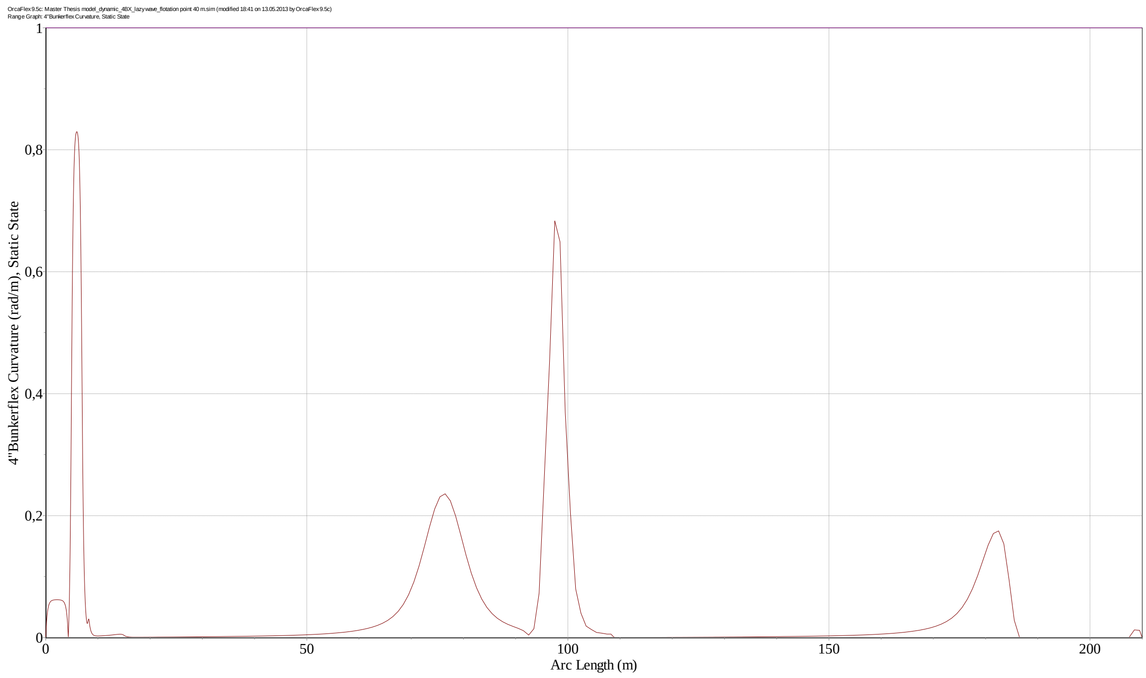

Figure B. 6 - 4" Bunkerflex STH - Lazy wave - 40 m floatation point - Curvature

Lazy wave – 60 m floatation point

Effective tension

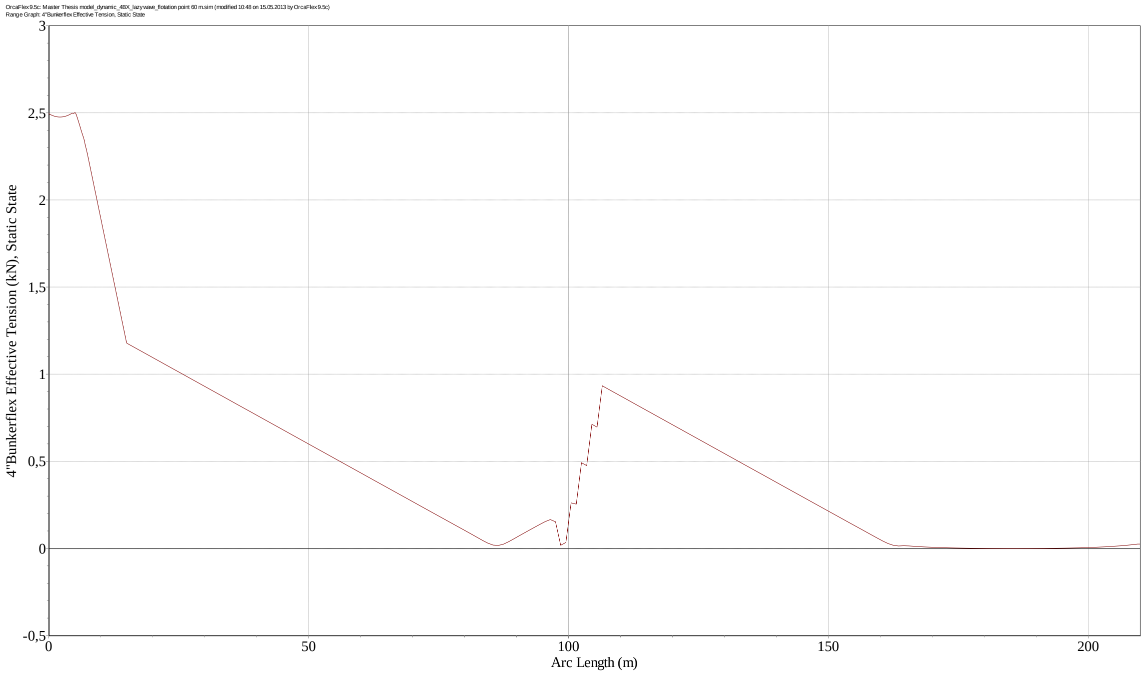

Figure B. 7 - 4" Bunkerflex STH - Lazy wave - 60 m floatation point - Effective tension

Curvature

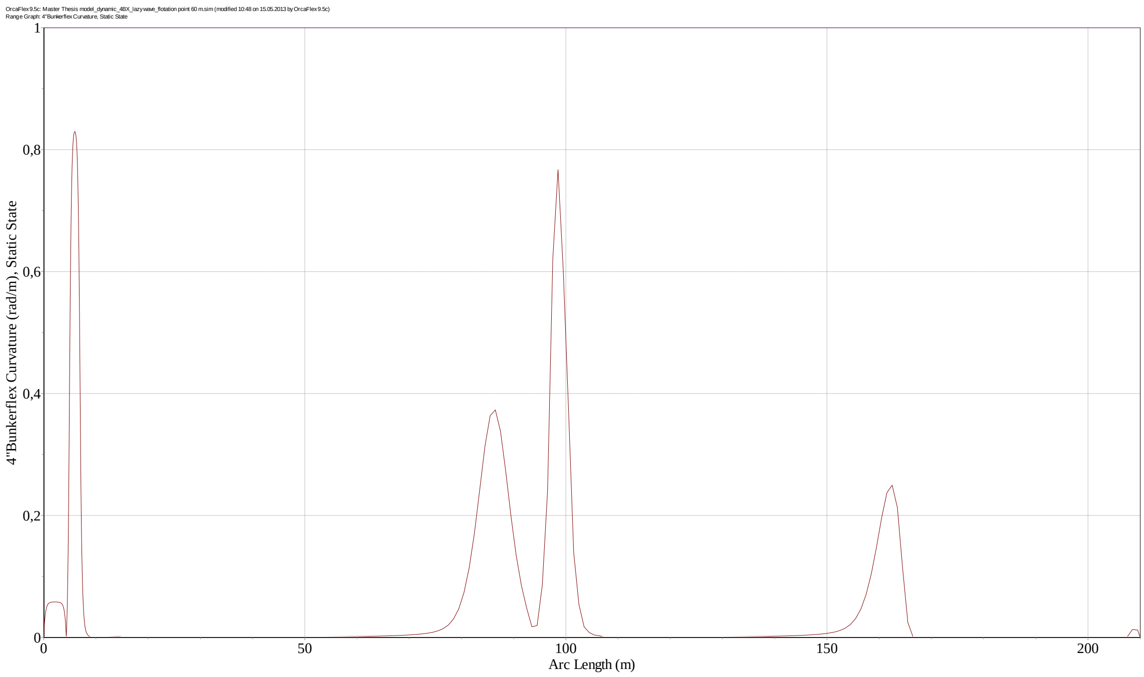

Figure B. 8 - 4" Bunkerflex STH - Lazy wave - 60 m floatation point - Curvature

Lazy wave – 80 m floatation point

Effective tension

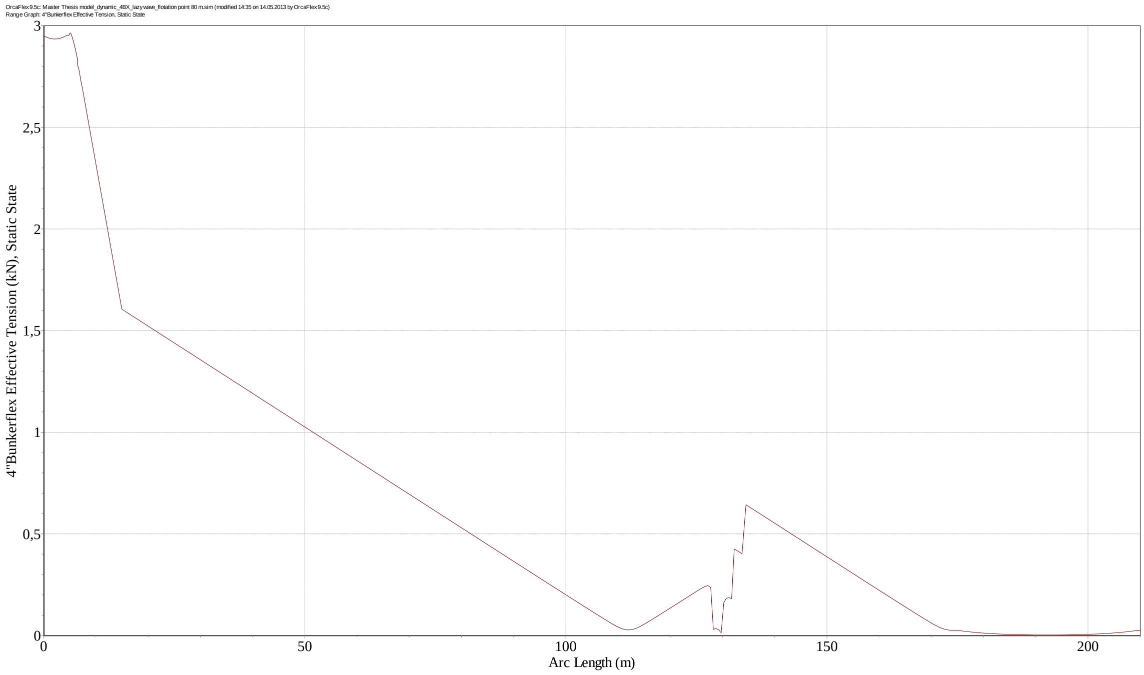

Figure B. 9 - 4" Bunkerflex STH - Lazy wave - 80 m floatation point - Effective tension

Curvature

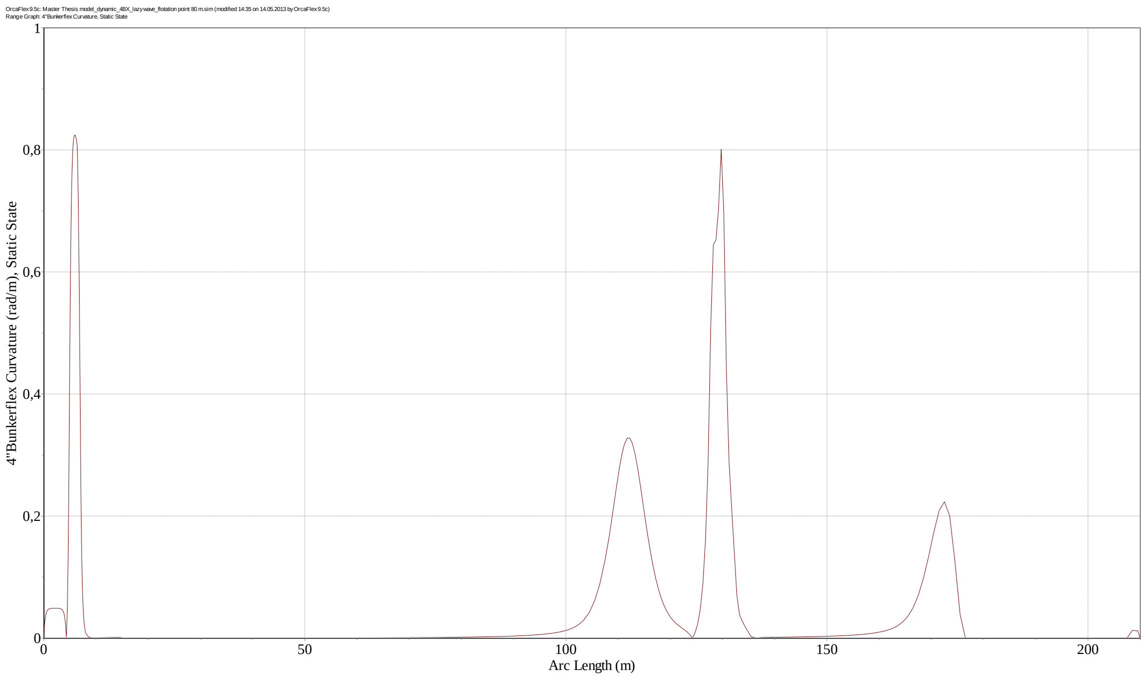

Figure B. 10 - 4" Bunkerflex STH - Lazy wave - 80 m floatation point - Curvature

6” Oilflex Super

Free hanging

Effective tension

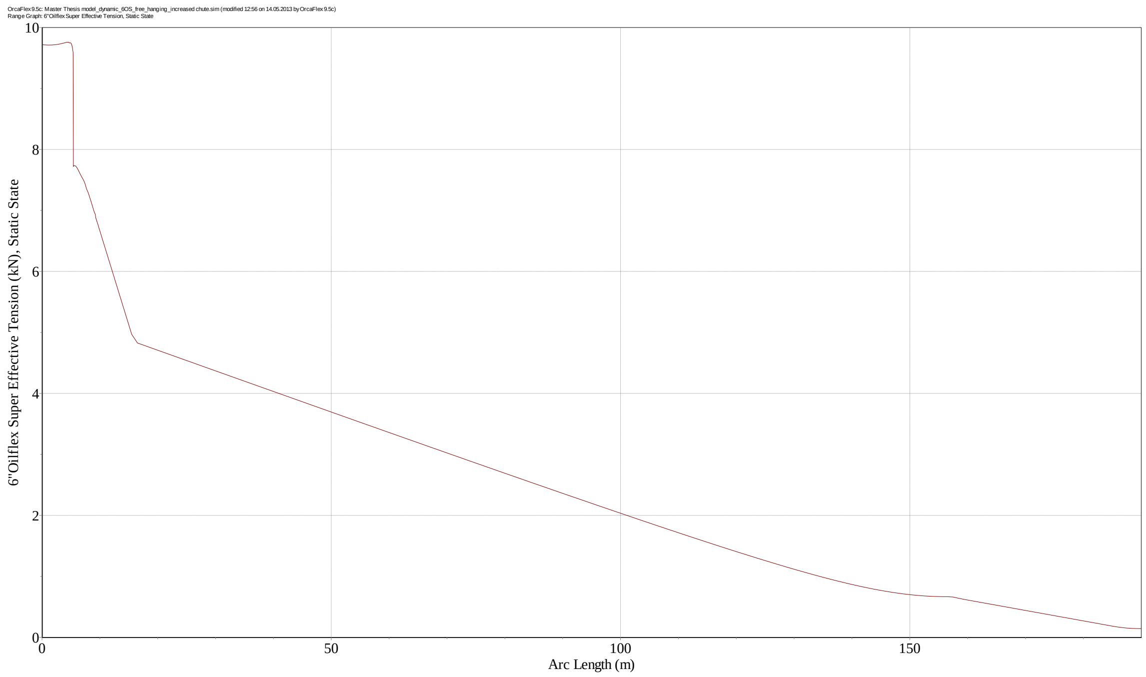

Figure B. 11 - 6" Oilflex Super - Free hanging - Effective tension

Curvature

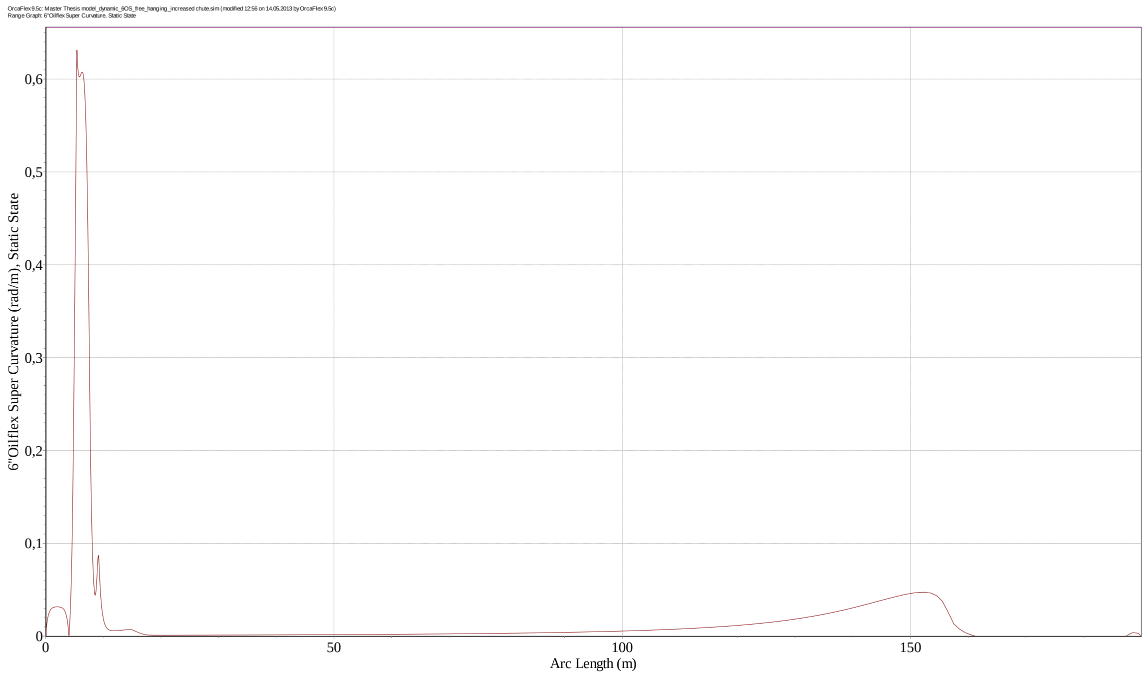

Figure B. 12 - 6" Oilflex Super - Free hanging - Curvature

Lazy wave – 20 m floatation point

Effective tension

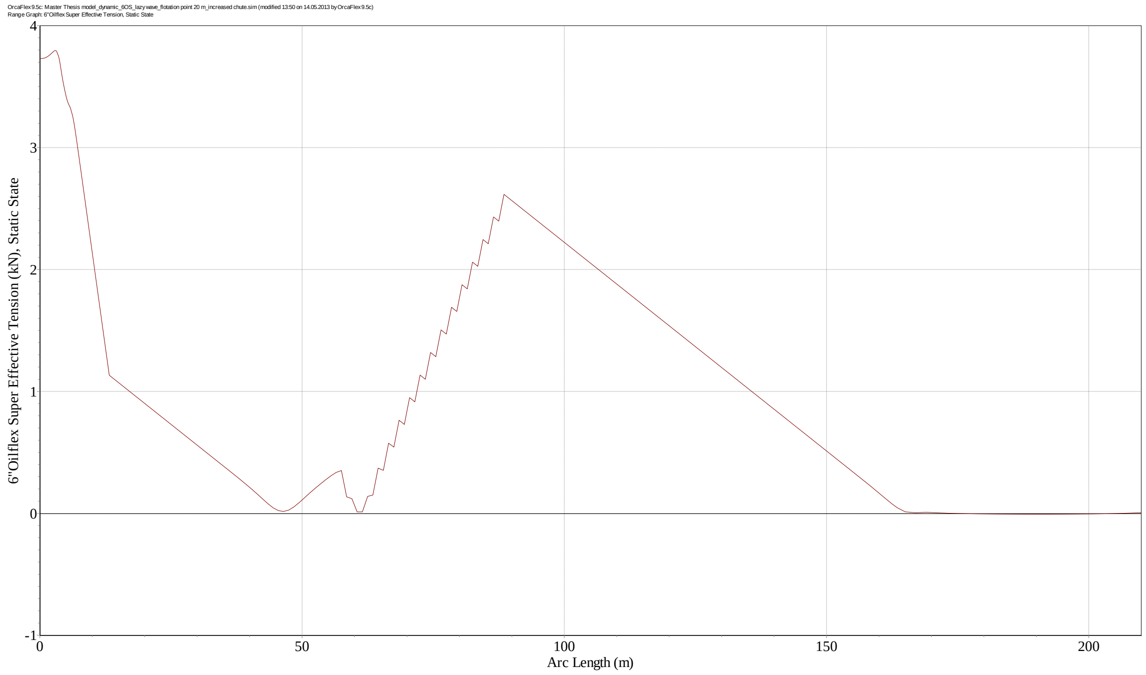

Figure B. 13 - 6" Oilflex Super - Lazy wave - 20 m floatation point - Effective tension

Curvature

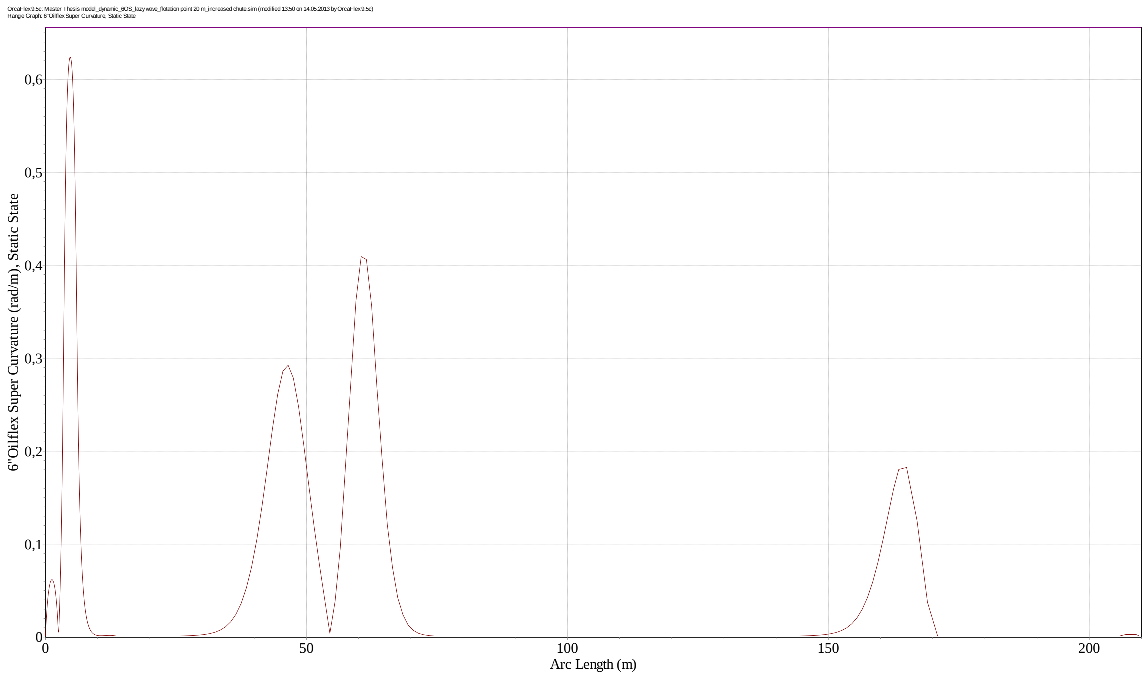

Figure B. 14 - 6" Oilflex Super - Lazy wave - 20 m floatation point - Curvature

Lazy wave – 40 m floatation point

Effective tension

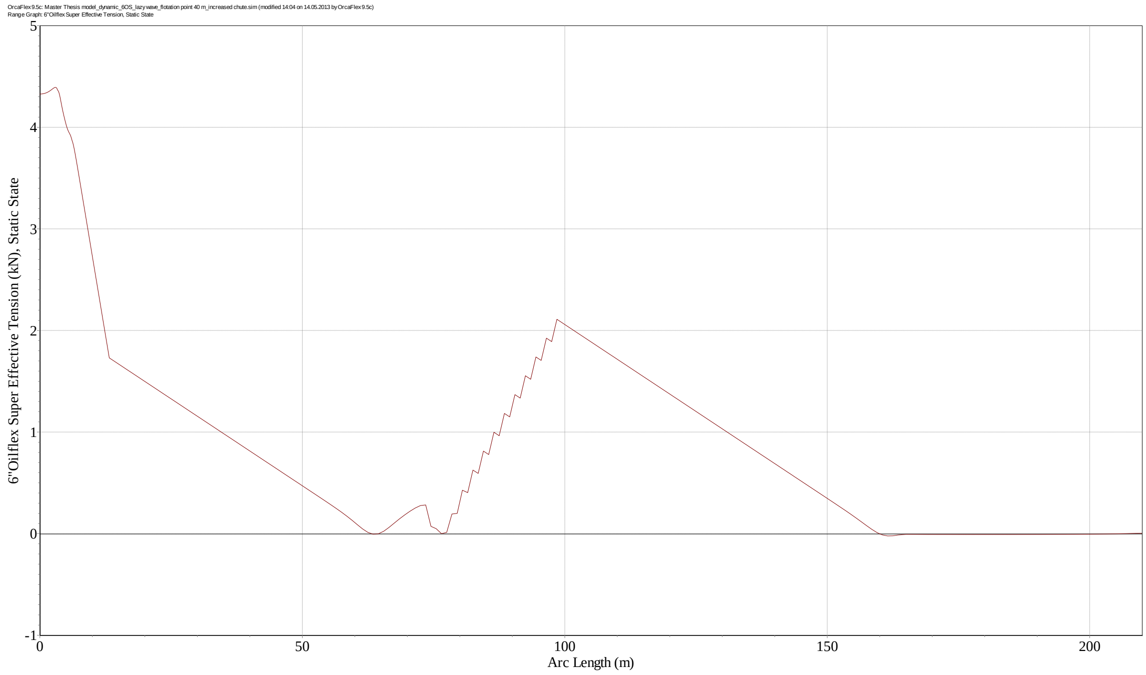

Figure B. 15 - 6" Oilflex Super - Lazy wave - 40 m floatation point - Effective tension

Curvature

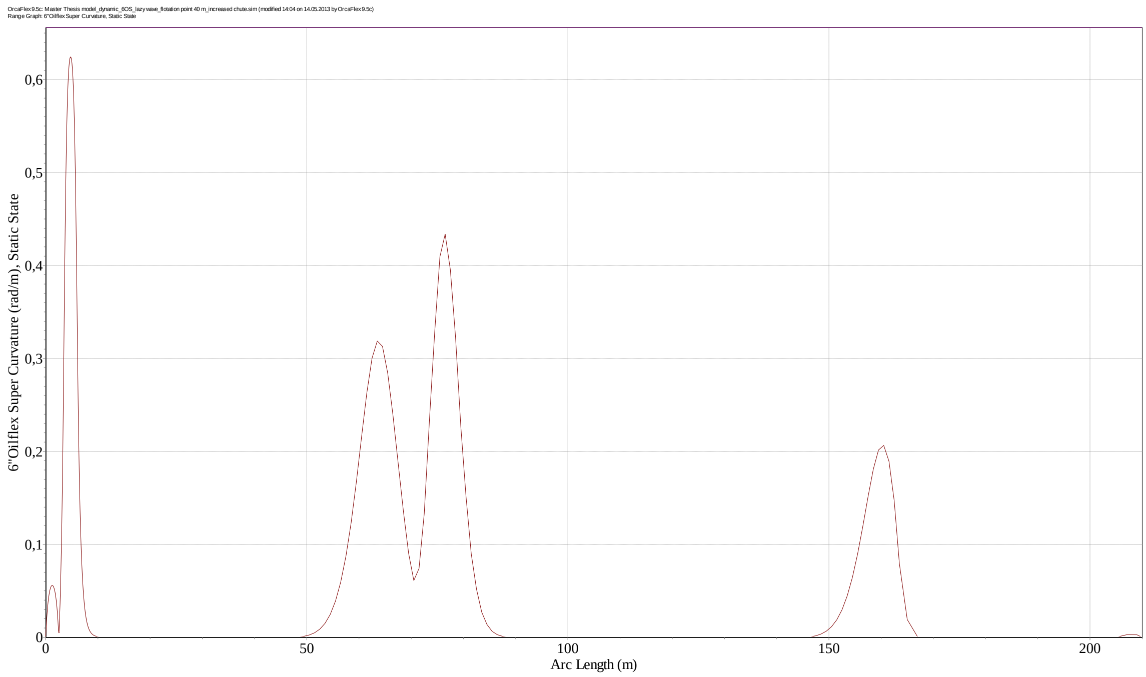

Figure B. 16 - 6" Oilflex Super - Lazy wave - 40 m floatation point - Curvature

Lazy wave – 60 m floatation point

Effective tension

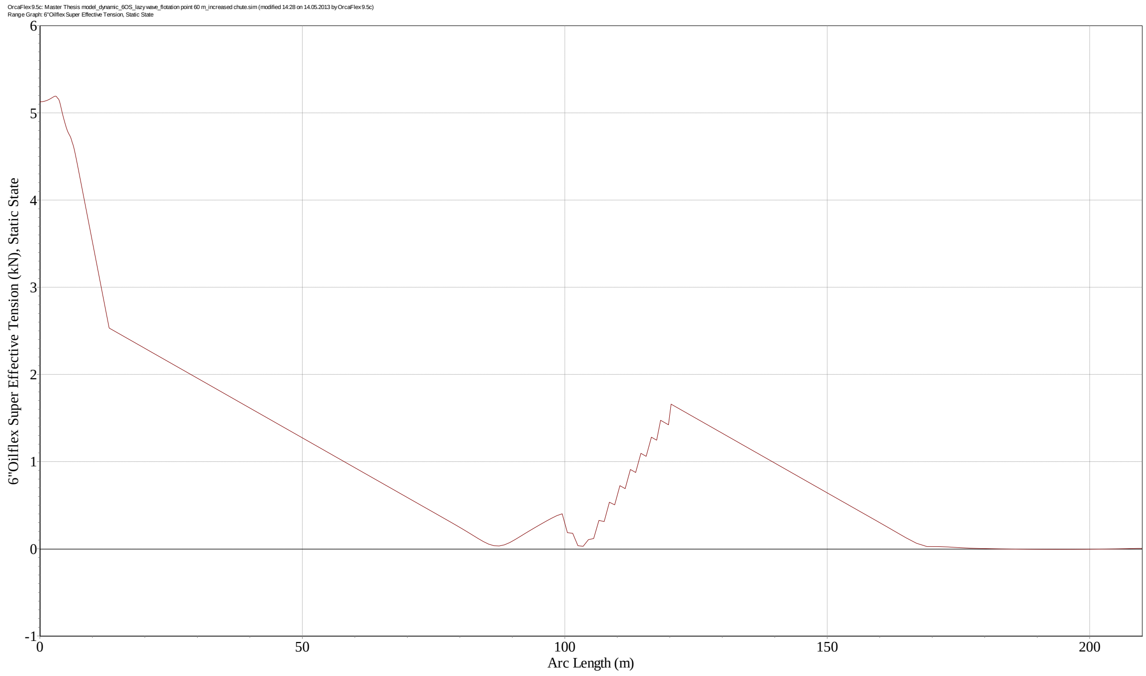

Figure B. 17 - 6" Oilflex Super - Lazy wave - 60 m floatation point - Effective tension

Curvature

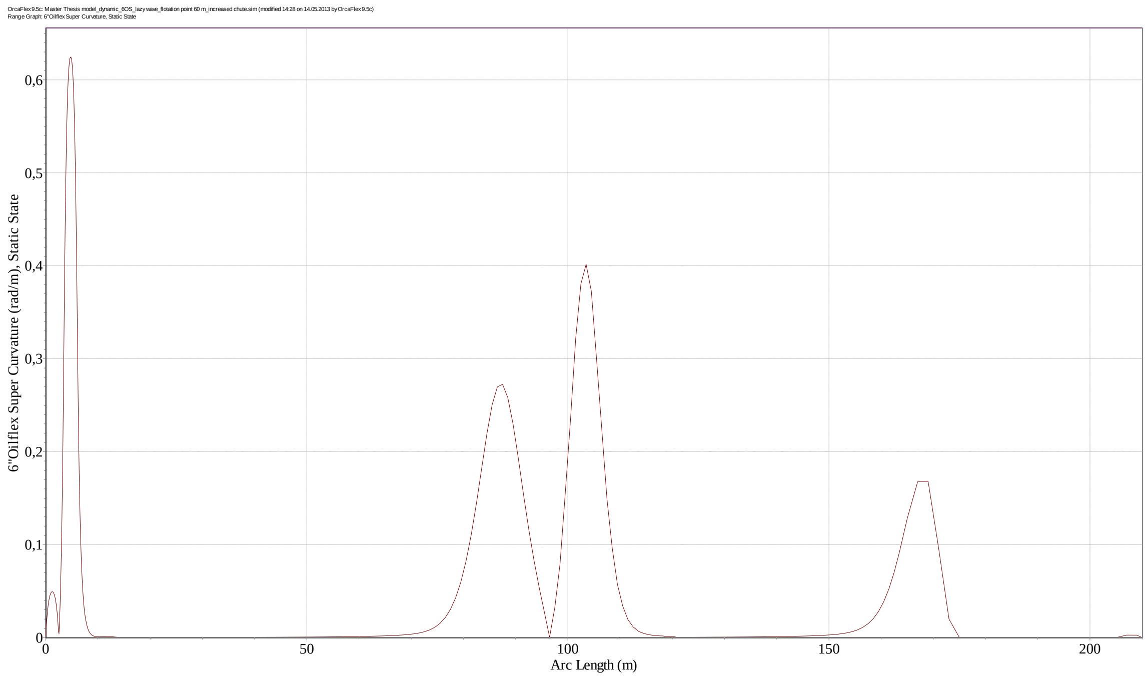

Figure B. 18 - 6" Oilflex Super - Lazy wave - 60 m floatation point - Curvature

Lazy wave – 80 m floatation point

Effective tension

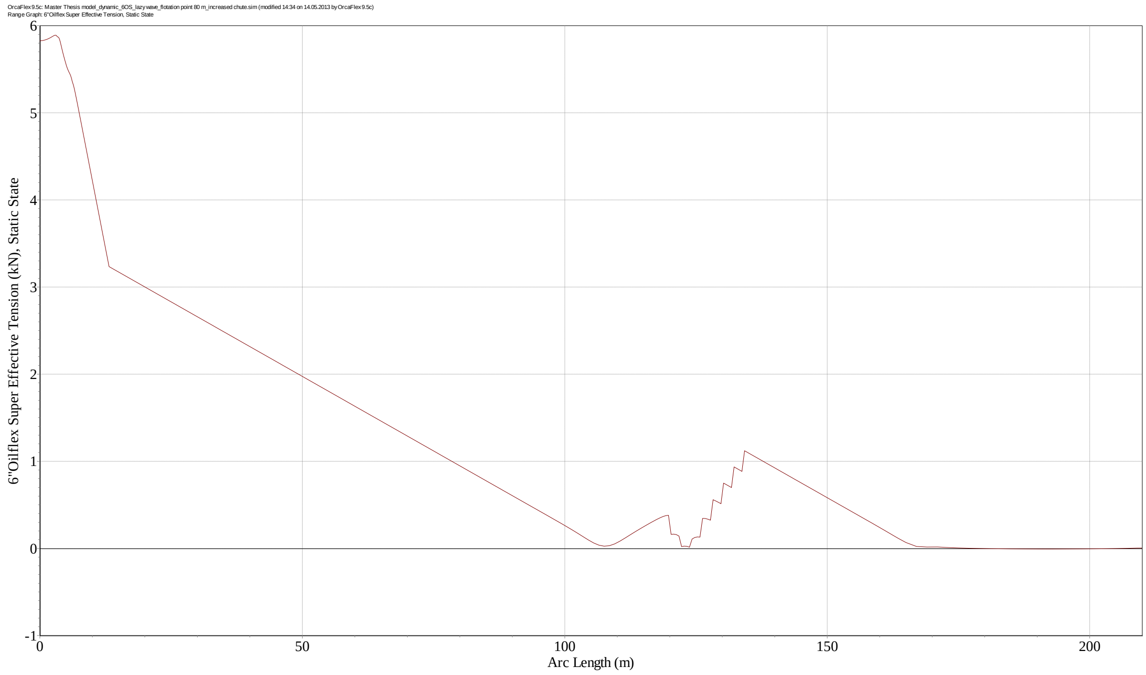

Figure B. 19 - 6" Oilflex Super - Lazy wave - 80 m floatation point - Effective tension

Curvature

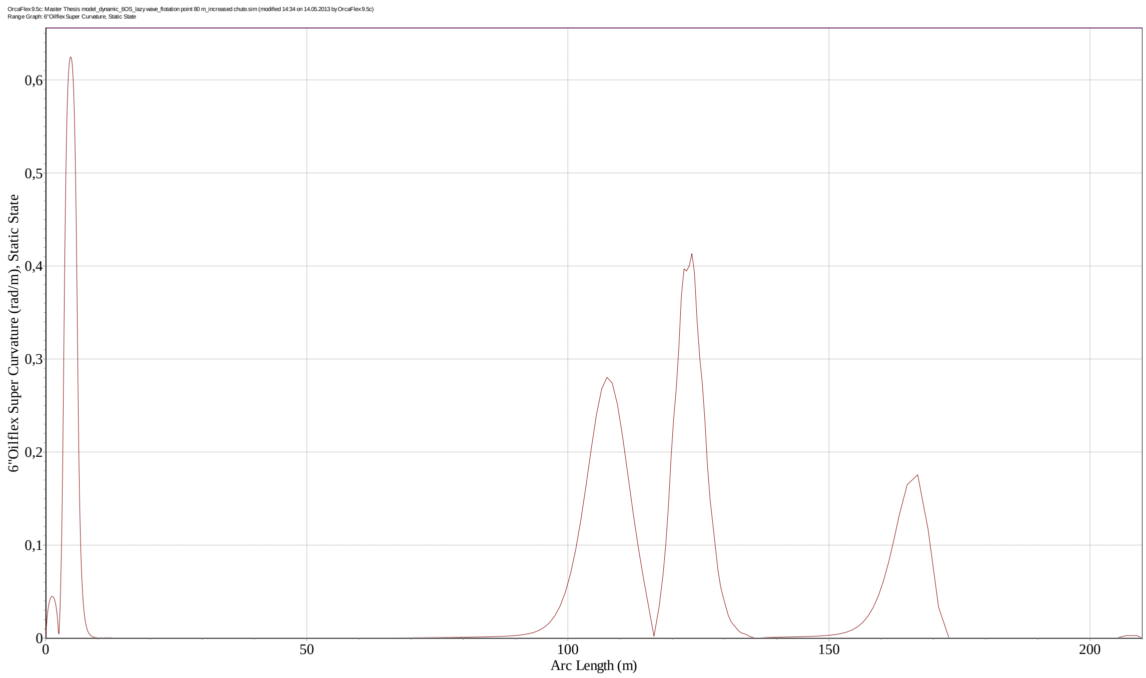

Figure B. 20 - 6" Oilflex Super - Lazy wave - 80 m floatation point - Curvature

Appendix C – Dynamic results

Table of Contents

List of Figures

Introduction

A detailed description of the graphs used in this Appendix is found Chapter 6.5.1 in the main report.

However, the direction conventions for the vessel are shown in Figure C. 1 below.

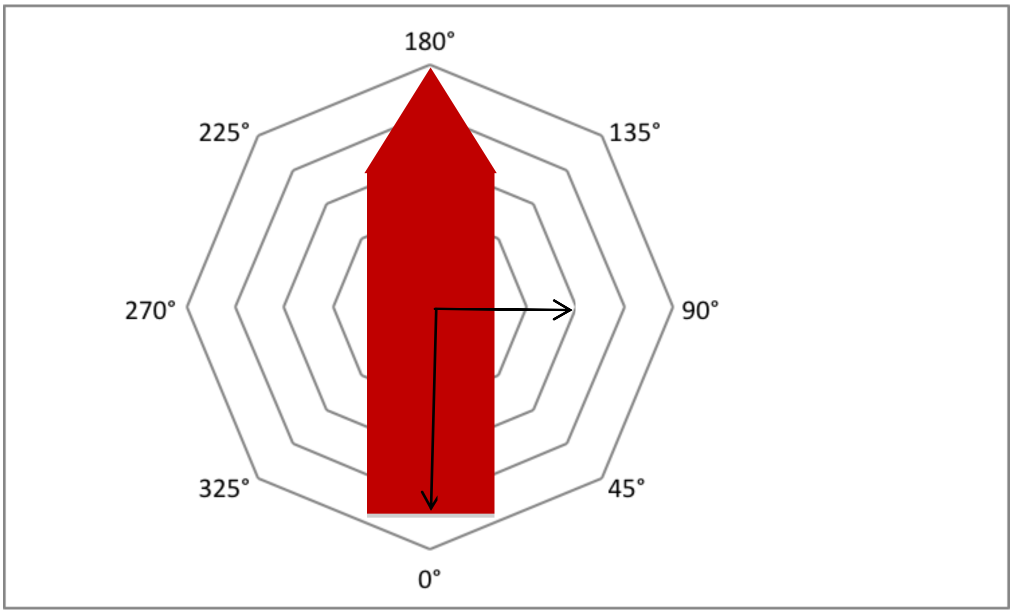

Figure C. 1 - Direction conventions for the vessel

4” Bunkerflex STH

Free hanging

Direction 135°

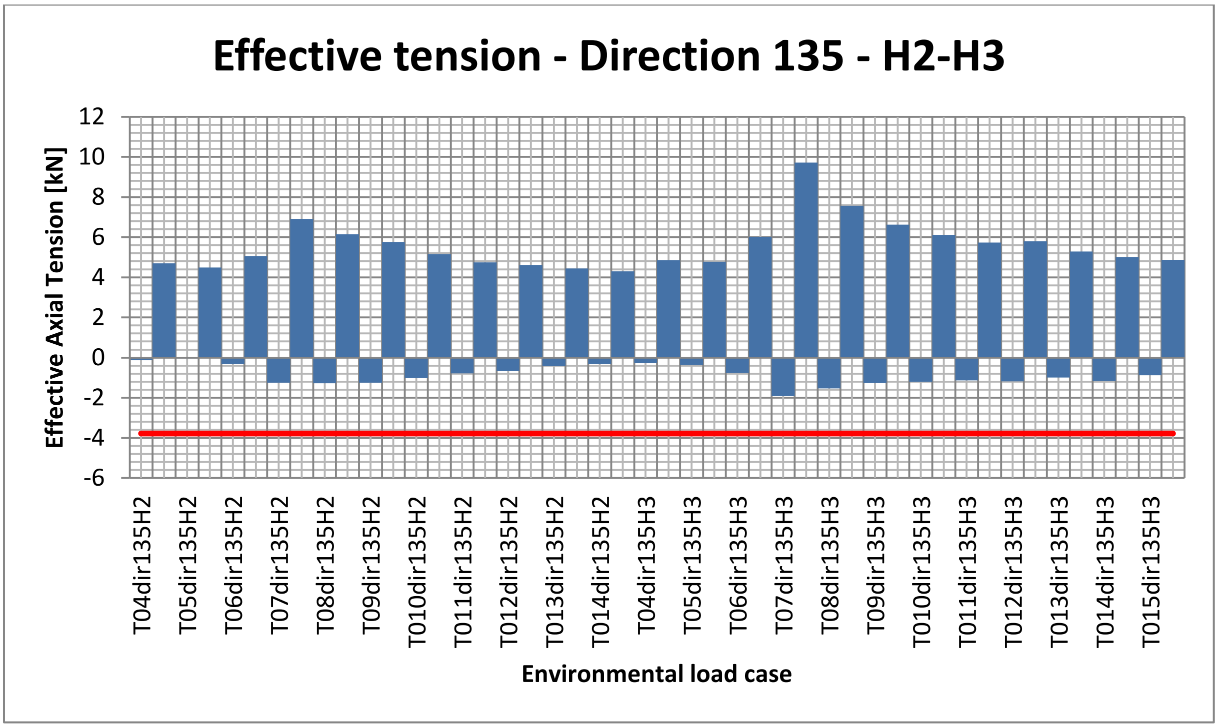

Figure C. 2 - 4” Bunkerflex STH – Free hanging – Effective tension – Direction 135° - H2-H3

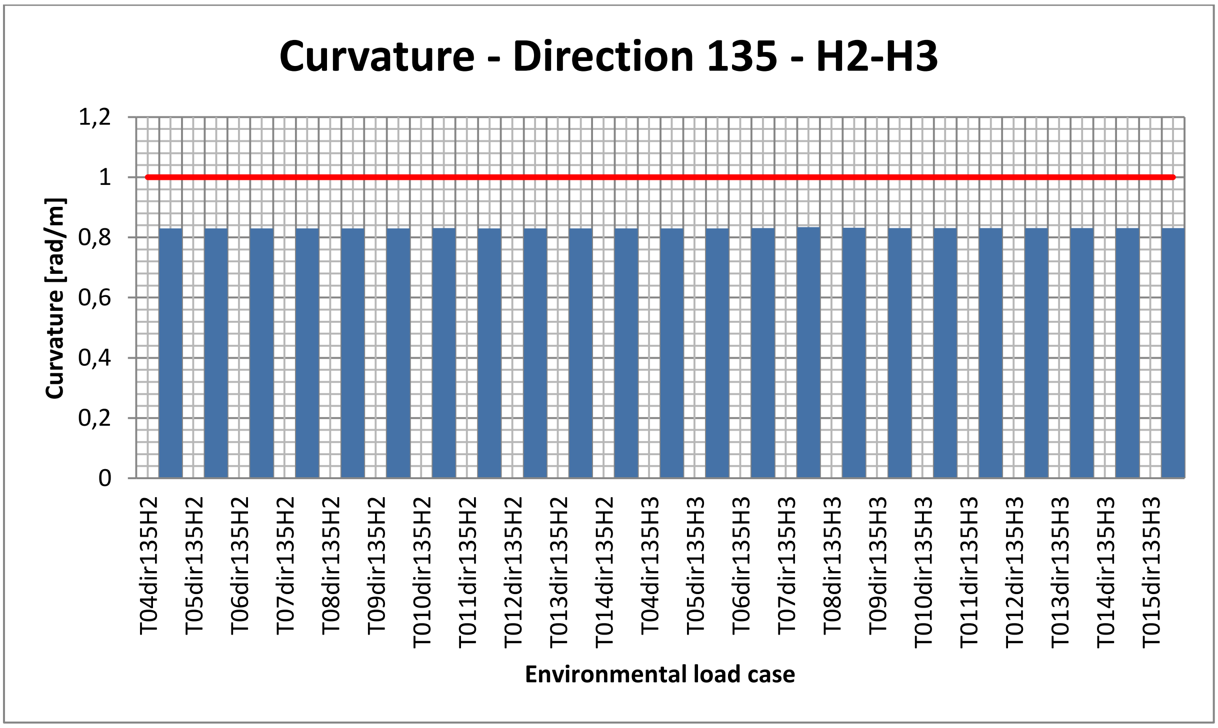

Figure C. 3 - 4” Bunkerflex STH – Free hanging – Curvature – Direction 135° - H2-H3

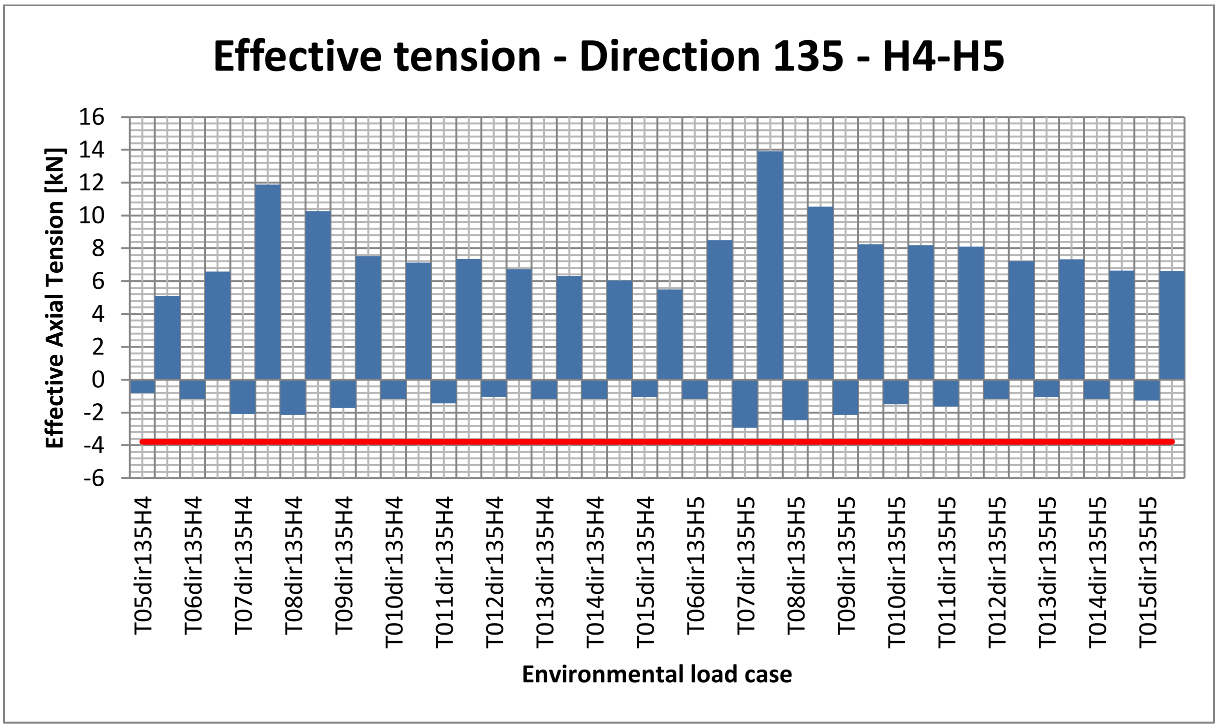

Figure C. 4 - 4” Bunkerflex STH – Free hanging – Effective tension – Direction 135° - H4-H5

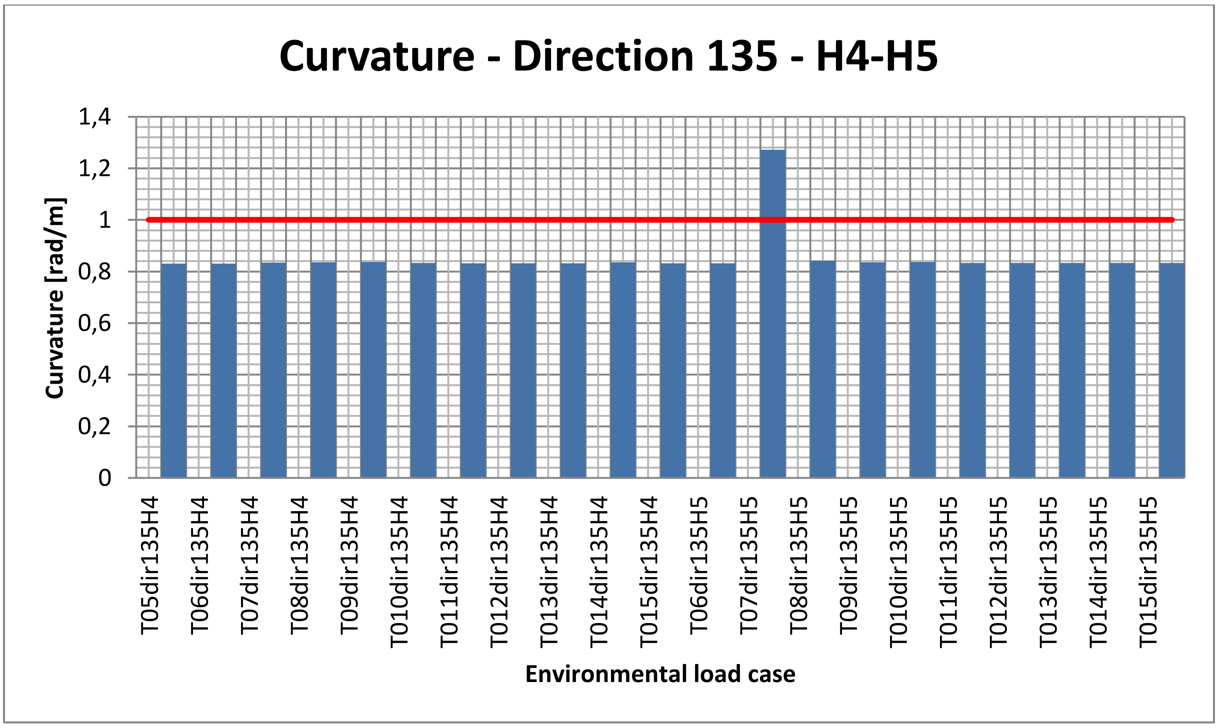

Figure C. 5 - 4” Bunkerflex STH – Free hanging – Curvature – Direction 135° - H4-H5

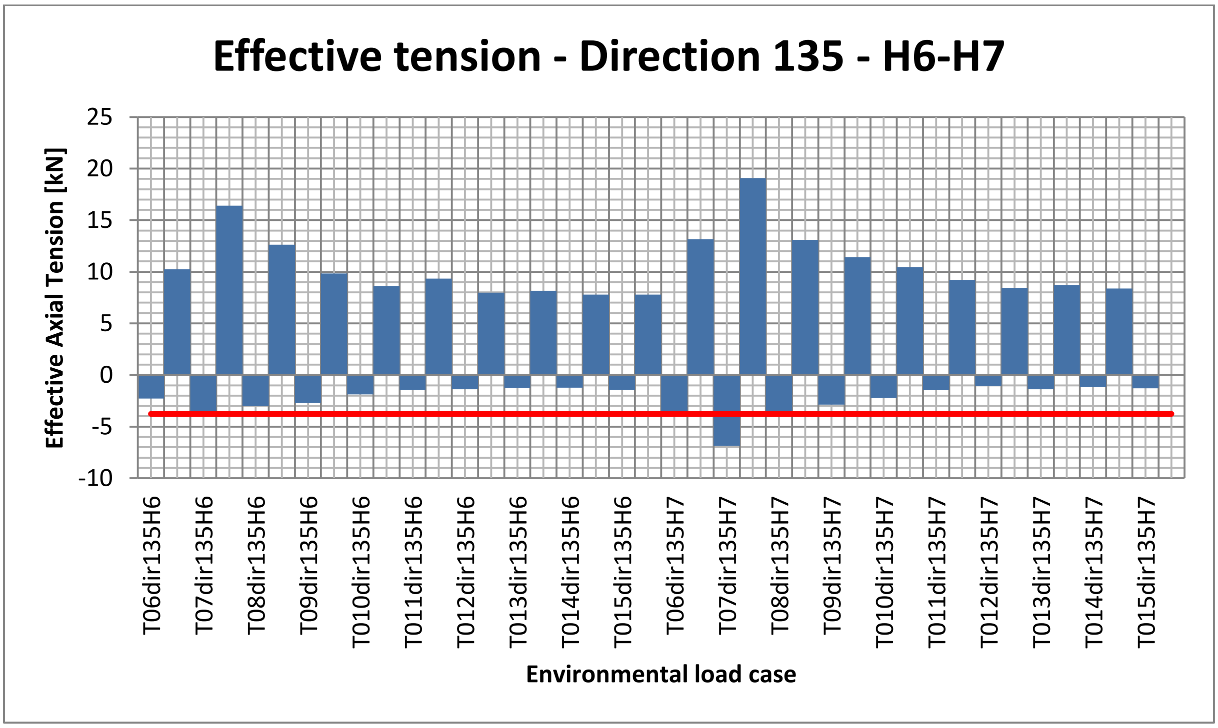

Figure C. 6 - 4” Bunkerflex STH – Free hanging – Effective tension – Direction 135° - H6-H7

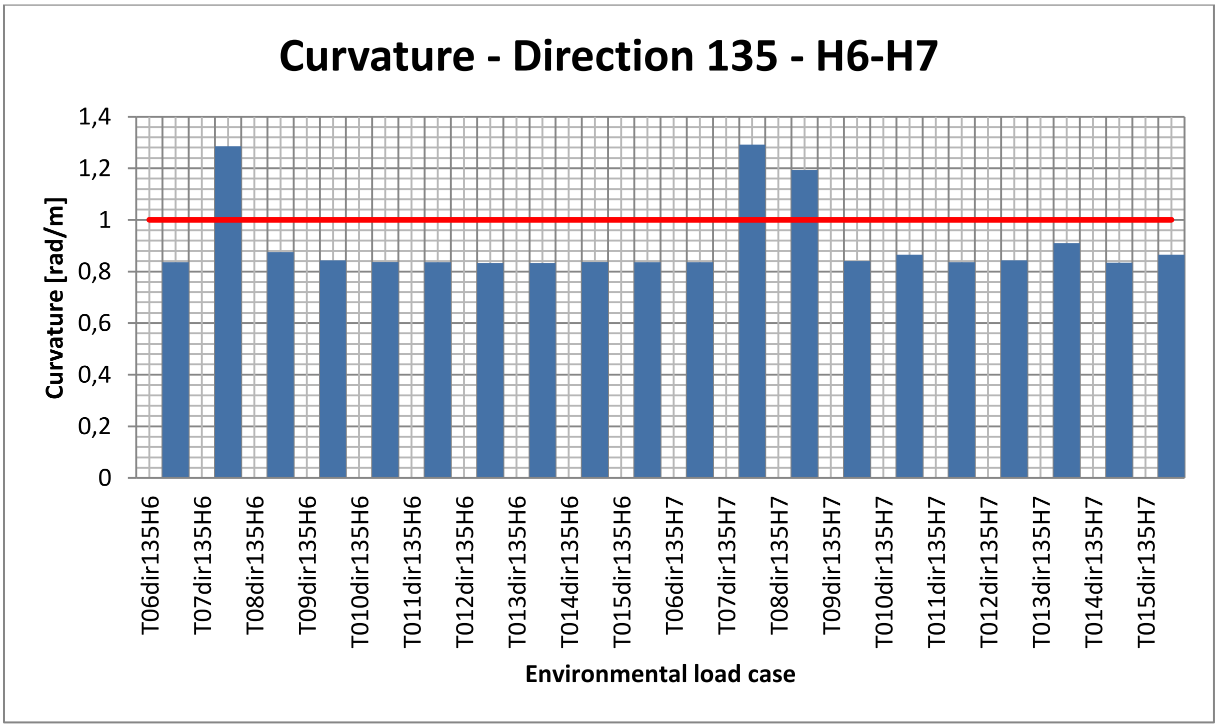

Figure C. 7 - 4” Bunkerflex STH – Free hanging – Curvature – Direction 135° - H6-H7

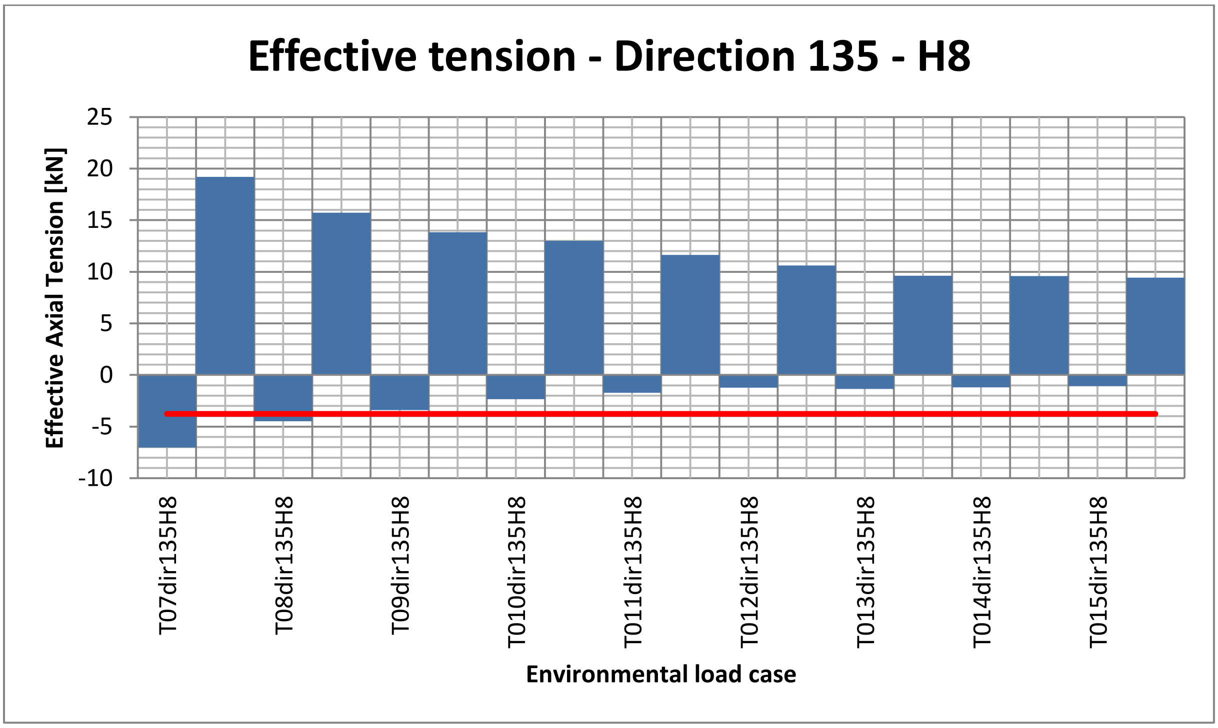

Figure C. 8 - 4” Bunkerflex STH – Free hanging – Effective tension – Direction 135° - H8

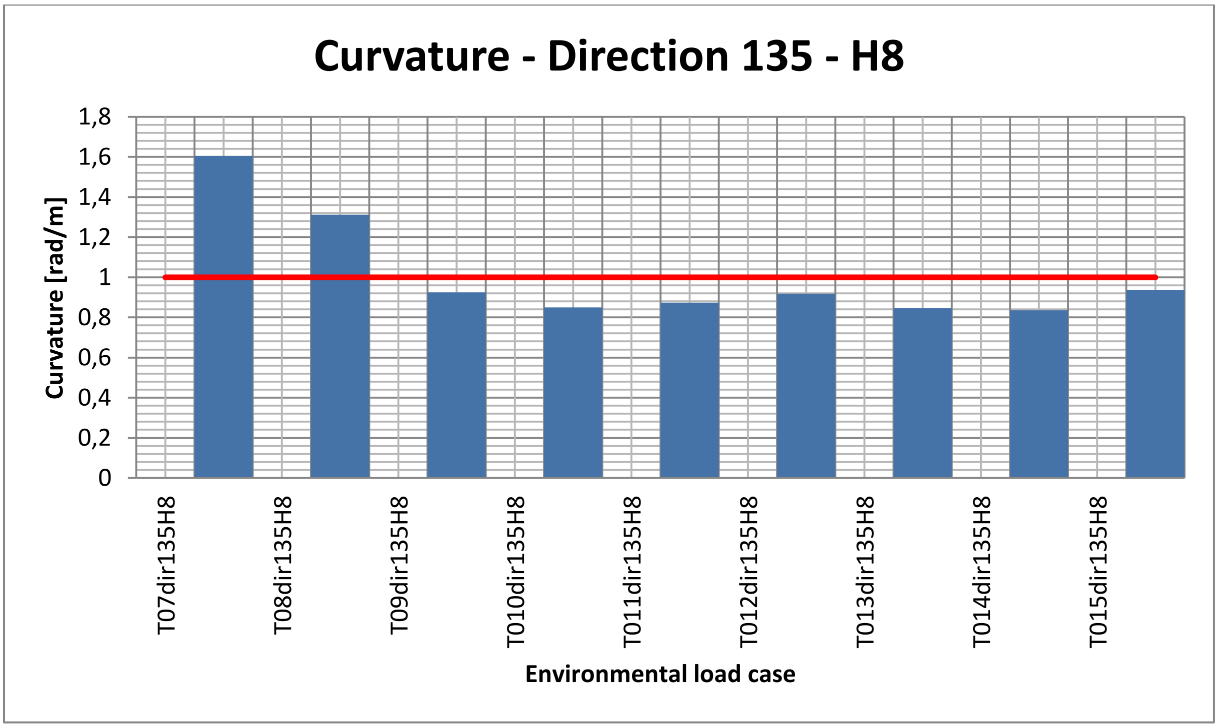

Figure C. 9 - 4” Bunkerflex STH – Free hanging – Curvature – Direction 135° - H8

Direction 180°

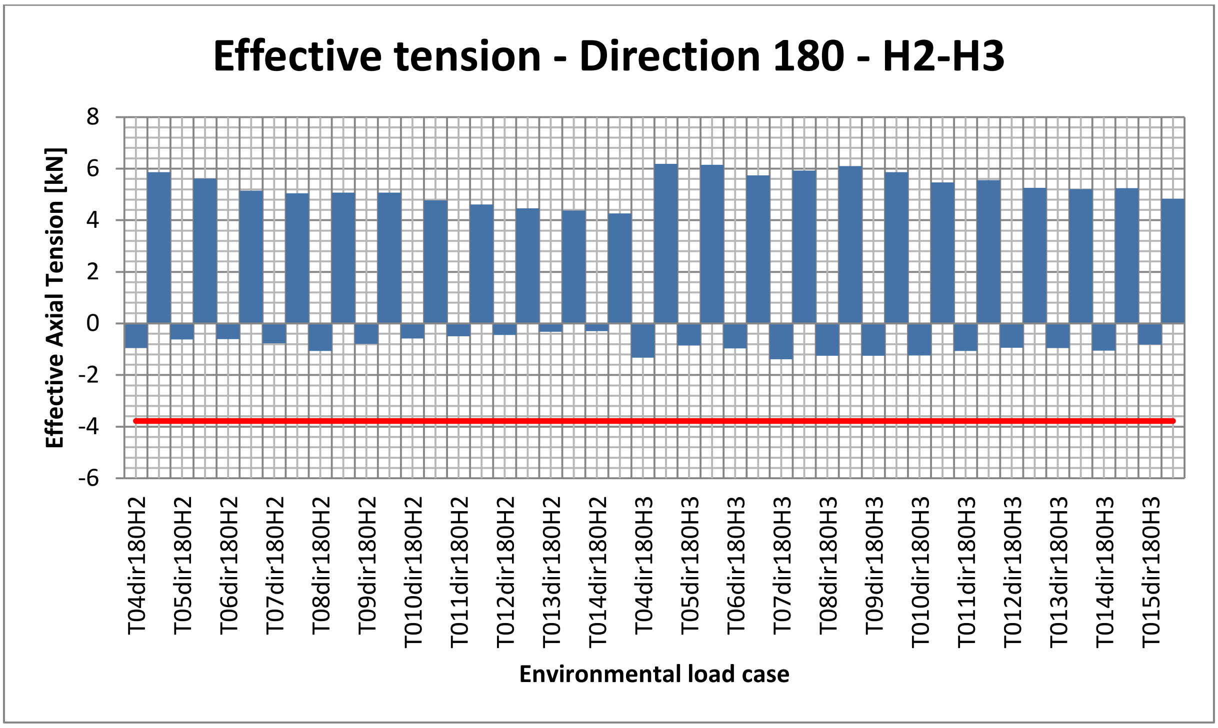

Figure C. 10 - 4” Bunkerflex STH – Free hanging – Effective tension – Direction 180° - H2-H3

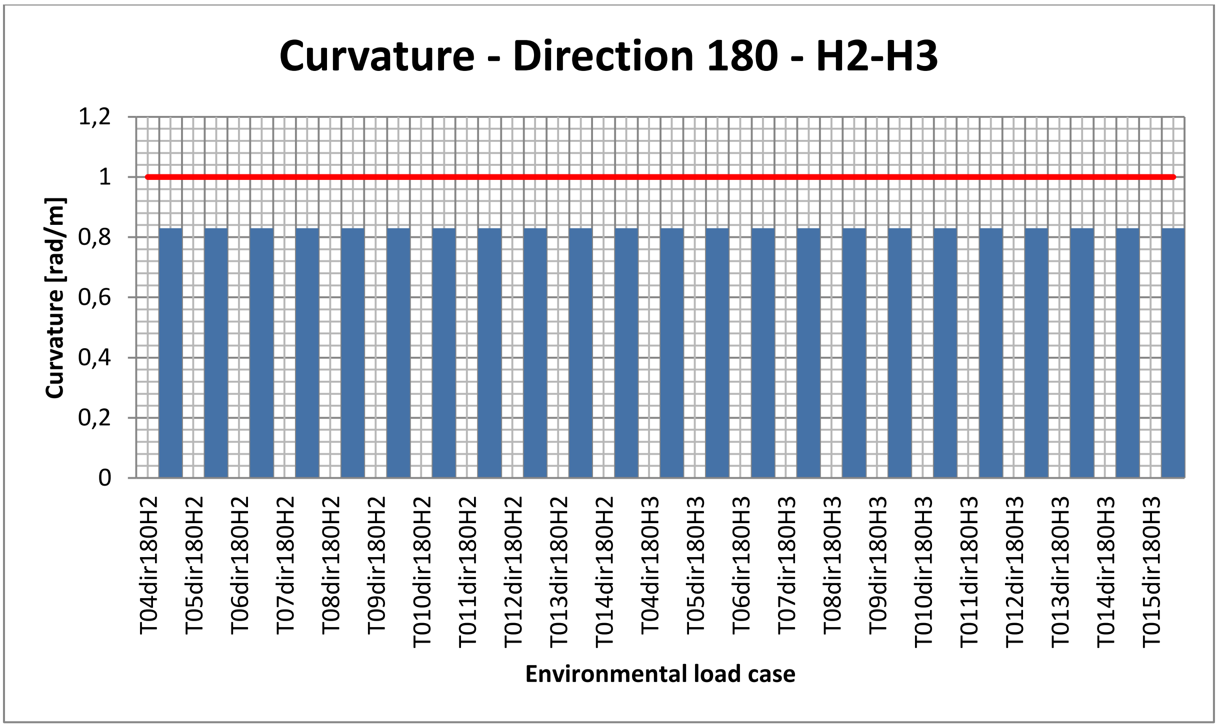

Figure C. 11 - 4” Bunkerflex STH – Free hanging – Curvature – Direction 180° - H2-H3

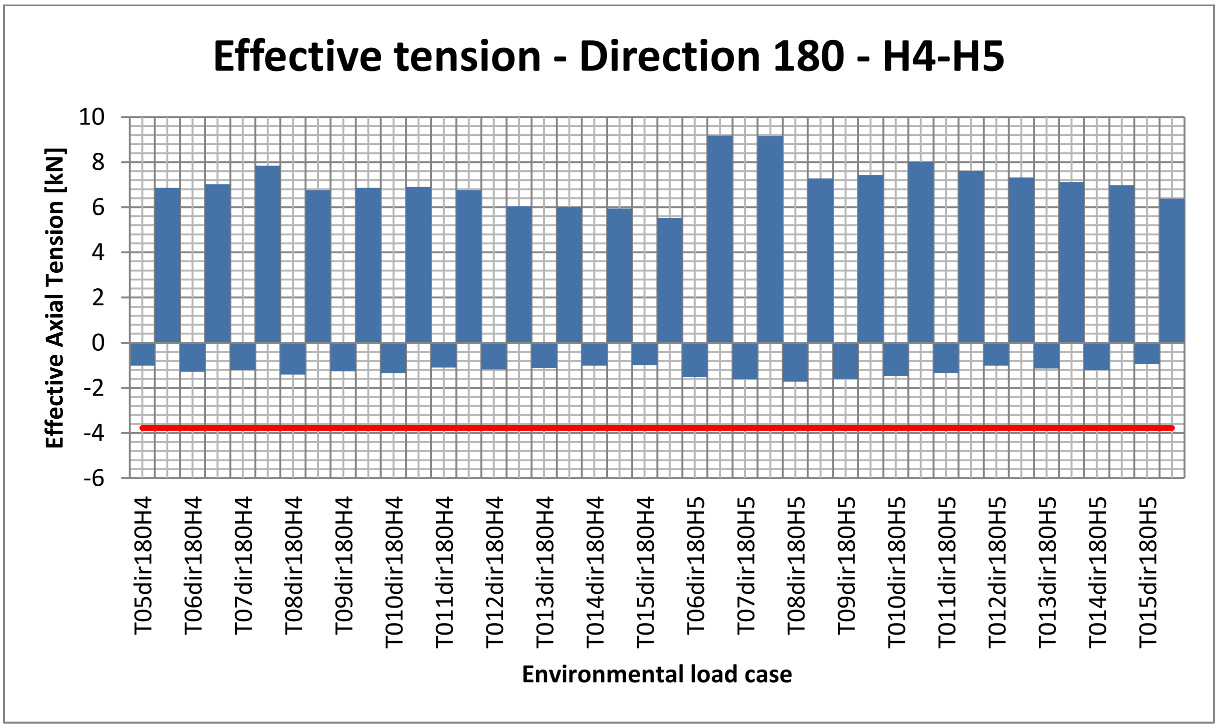

Figure C. 12 - 4" Bunkerflex STH – Free hanging – Effective tension – Direction 180° - H4-H5

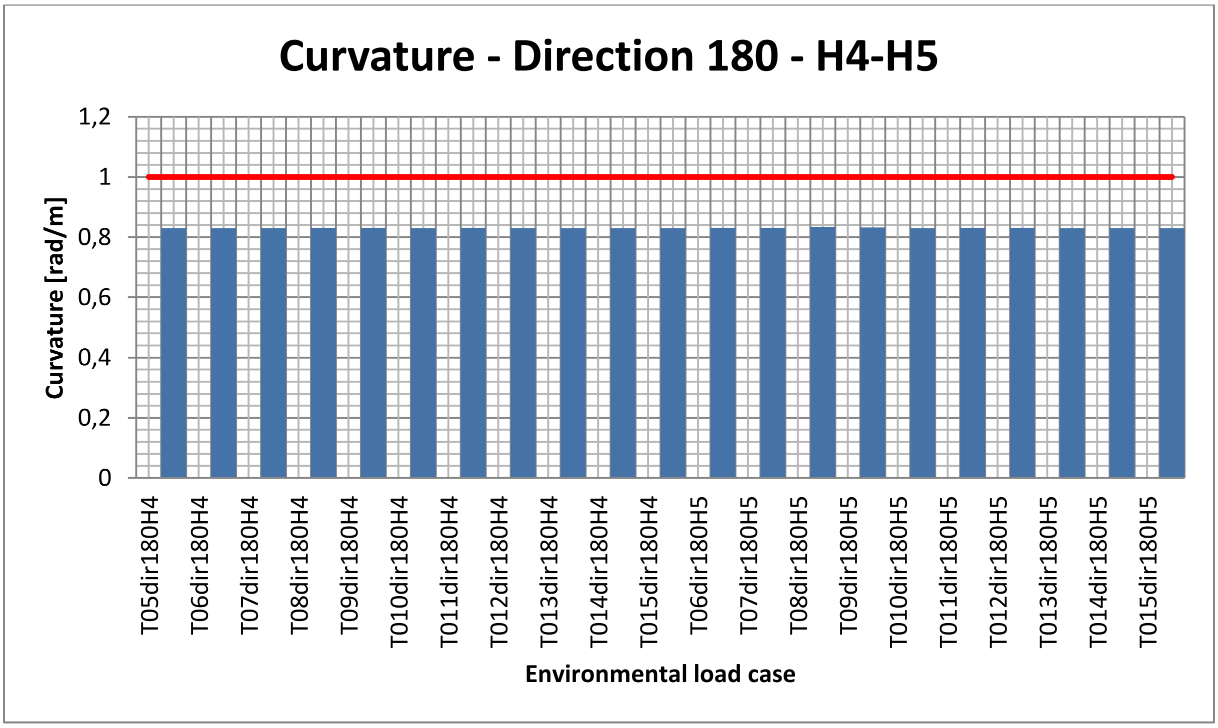

Figure C. 13 - 4" Bunkerflex STH – Free hanging – Curvature – Direction 180° - H4-H5

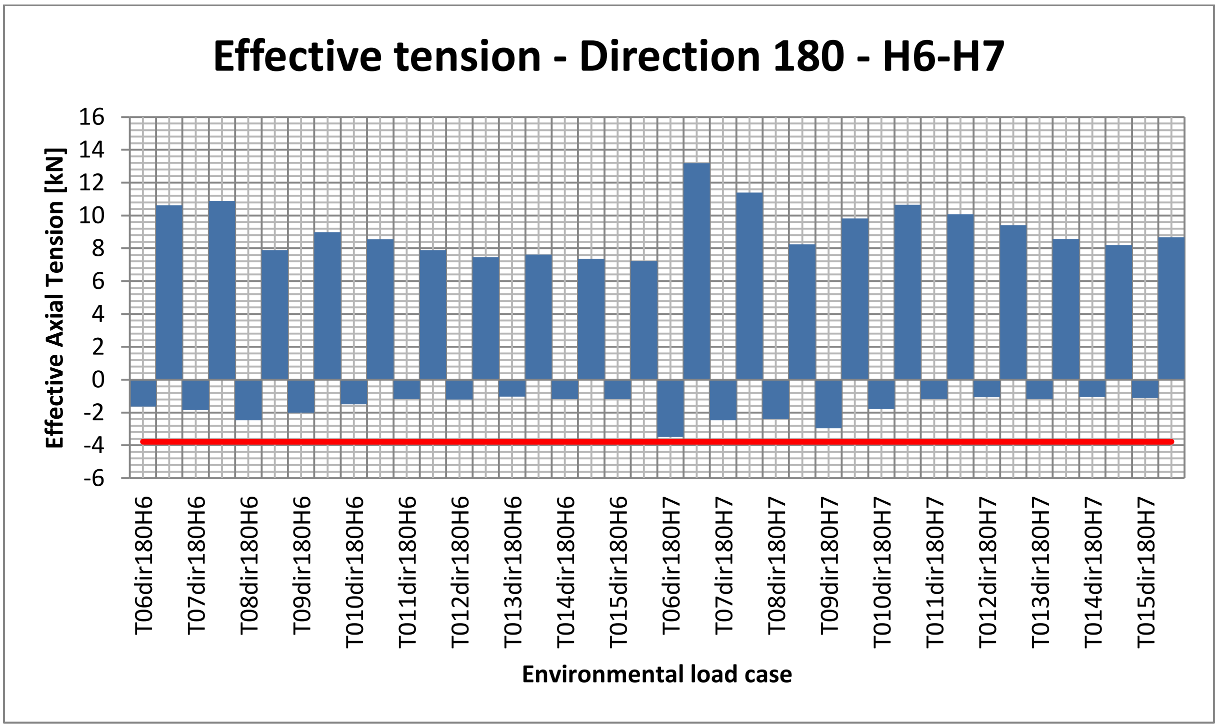

Figure C. 14 - 4” Bunkerflex STH – Free hanging – Effective tension – Direction 180° - H6-H7

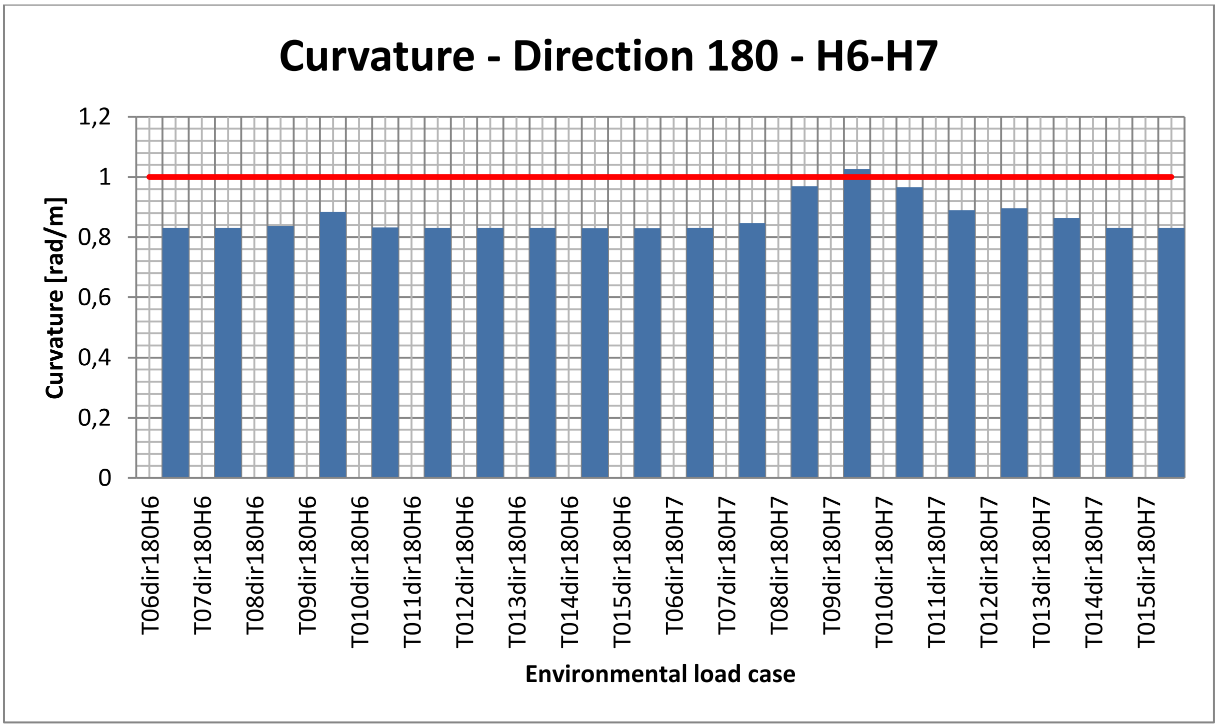

Figure C. 15 - 4” Bunkerflex STH – Free hanging – Curvature – Direction 180° - H6-H7

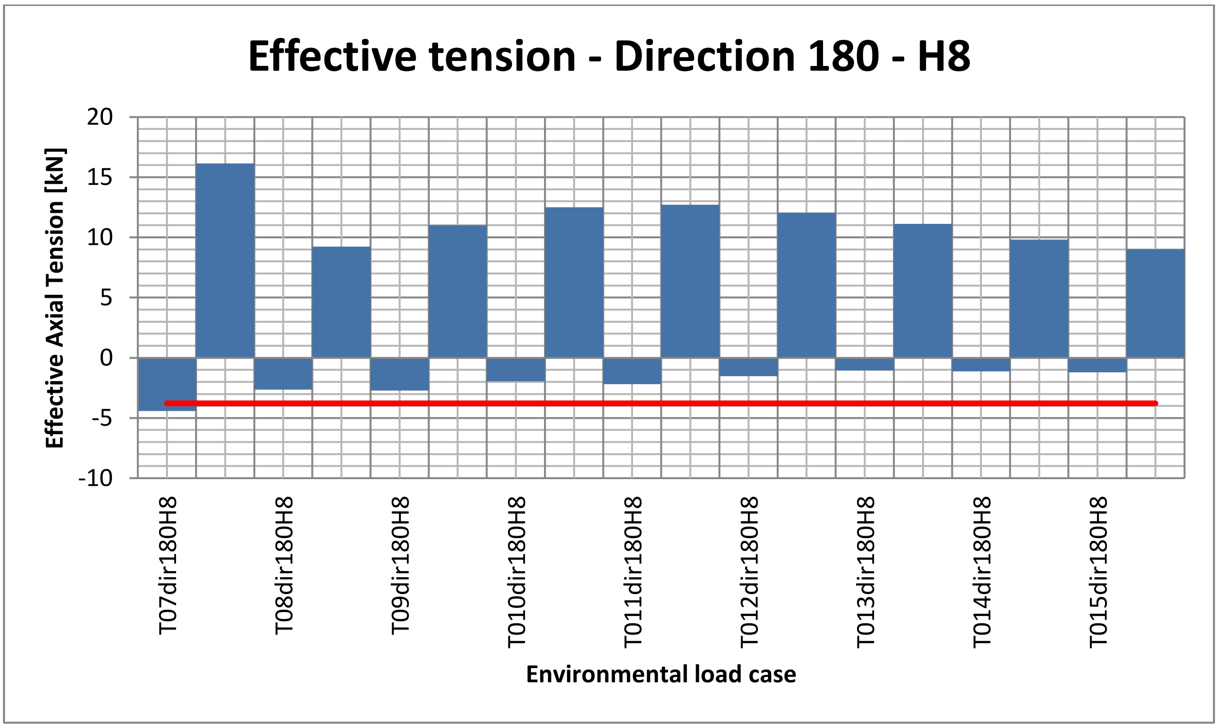

Figure C. 16 - 4” Bunkerflex STH – Free hanging – Effective tension – Direction 180° - H8

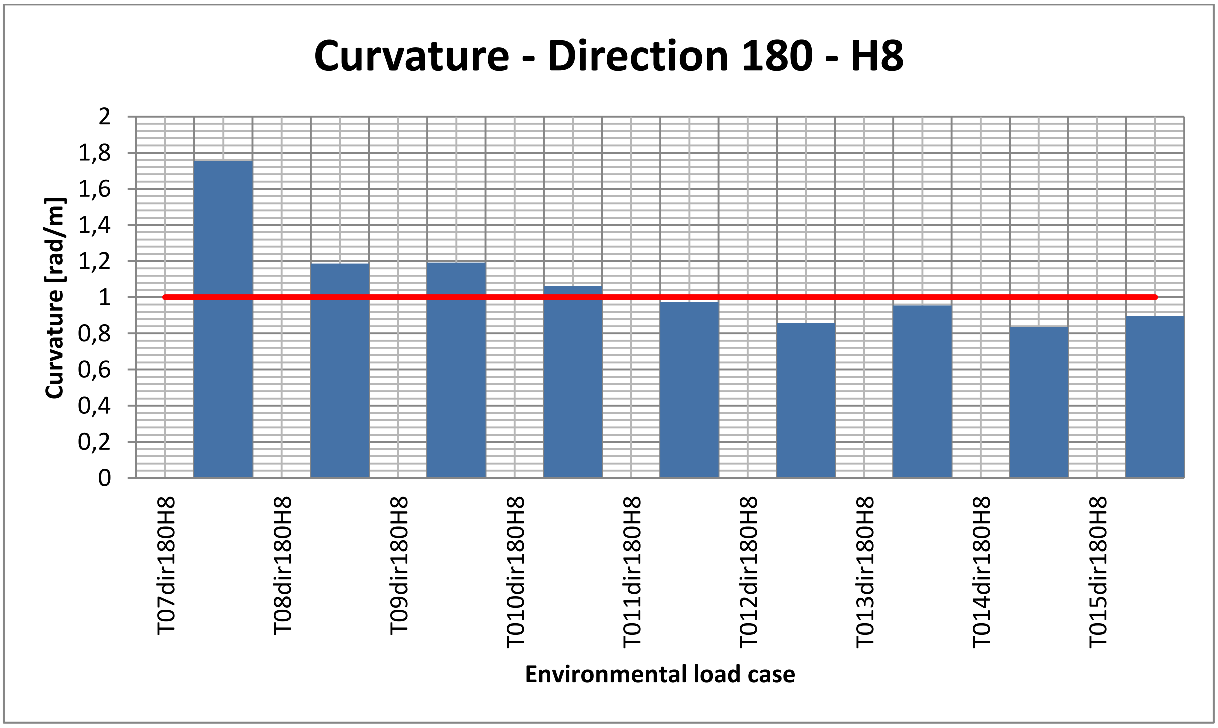

Figure C. 17 - 4” Bunkerflex STH – Free hanging – Curvature – Direction 180° - H8

Direction 225°

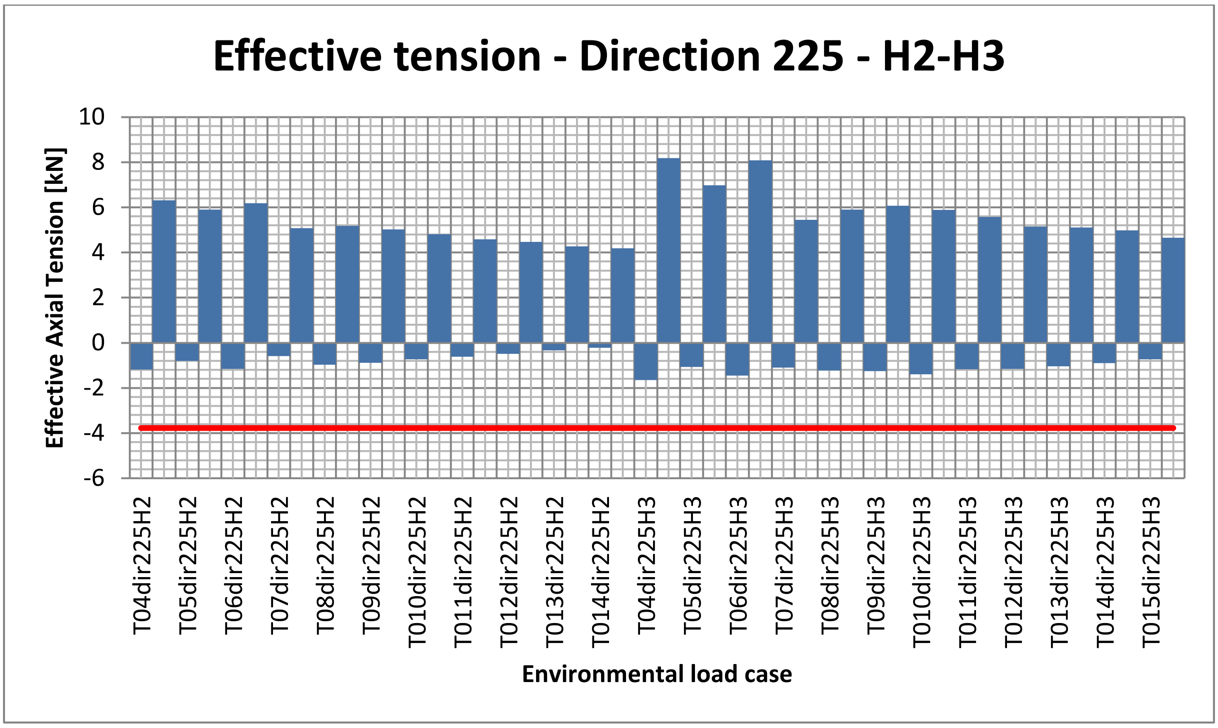

Figure C. 18 - 4” Bunkerflex STH – Free hanging – Effective tension – Direction 225° - H2-H3

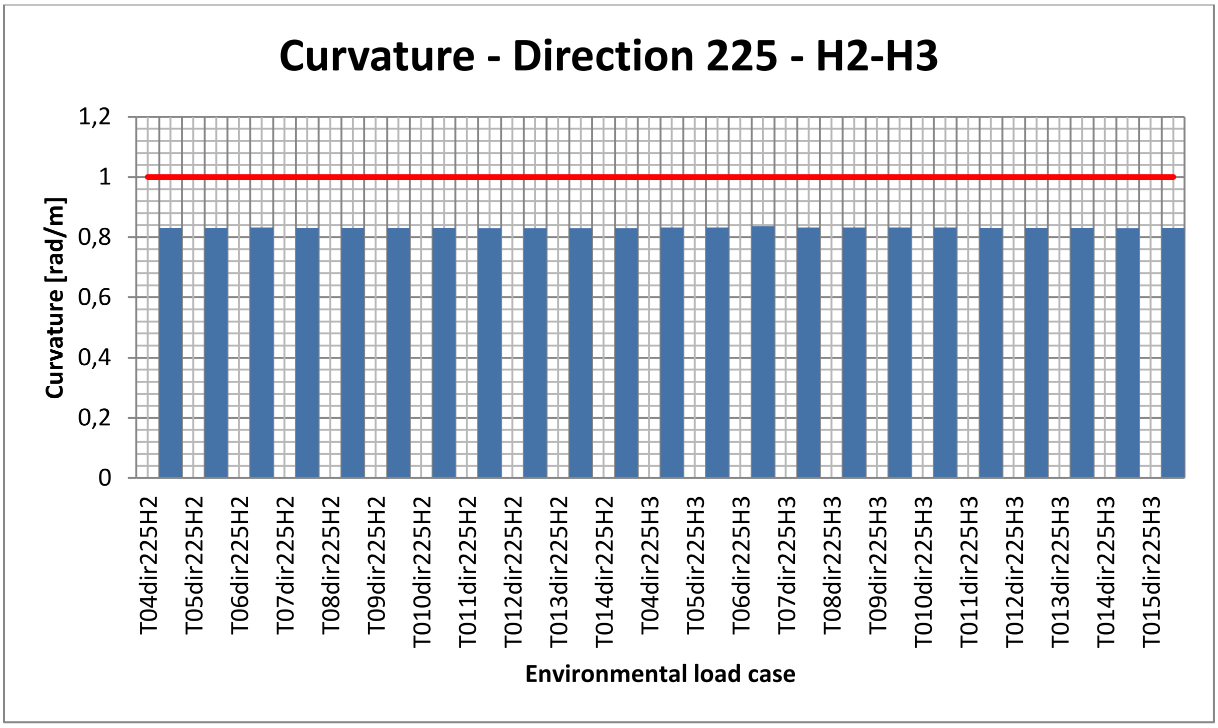

Figure C. 19 - 4” Bunkerflex STH – Free hanging – Curvature – Direction 225° - H2-H3

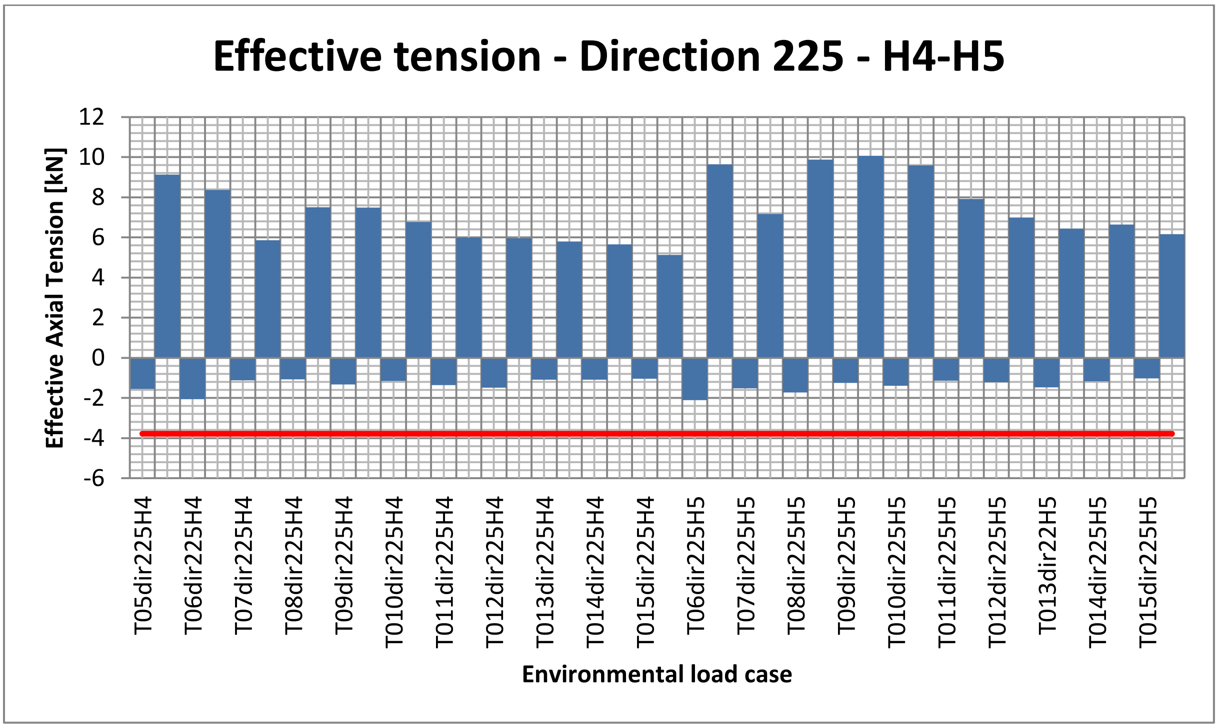

Figure C. 20 - 4” Bunkerflex STH – Free hanging – Effective tension – Direction 225° - H4-H5

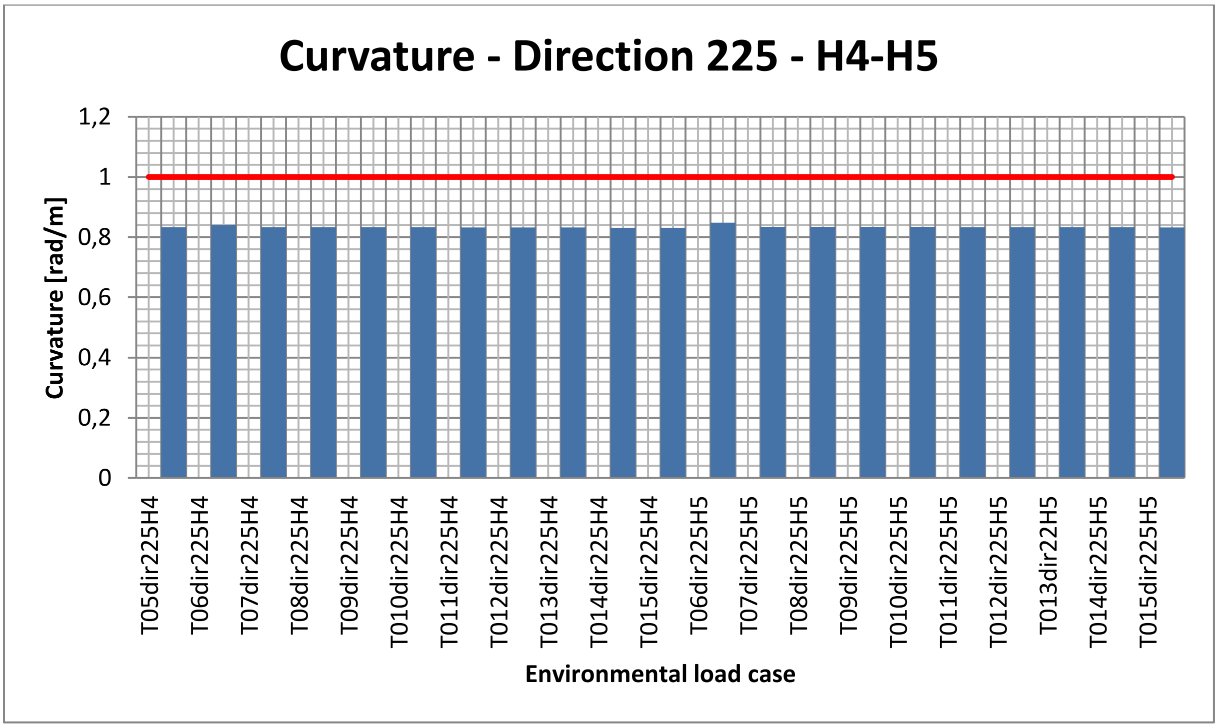

Figure C. 21 - 4” Bunkerflex STH – Free hanging – Curvature – Direction 225° - H4-H5

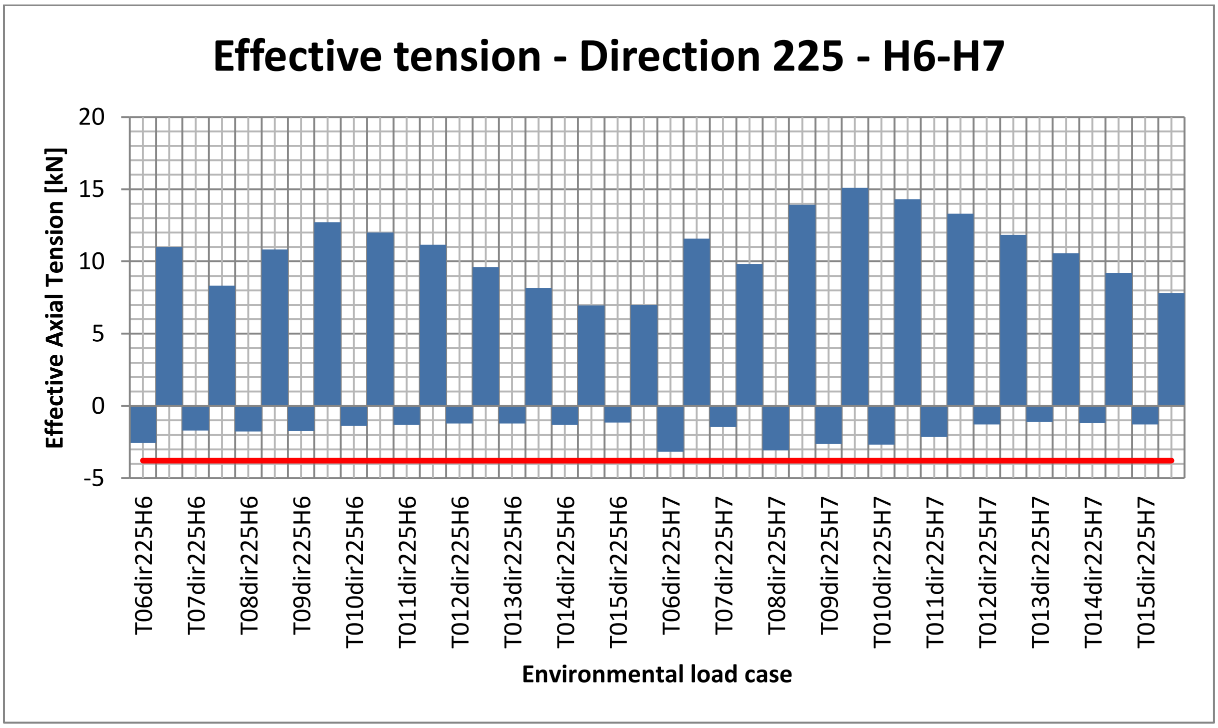

Figure C. 22 - 4” Bunkerflex STH – Free hanging – Effective tension – Direction 225° - H6-H7

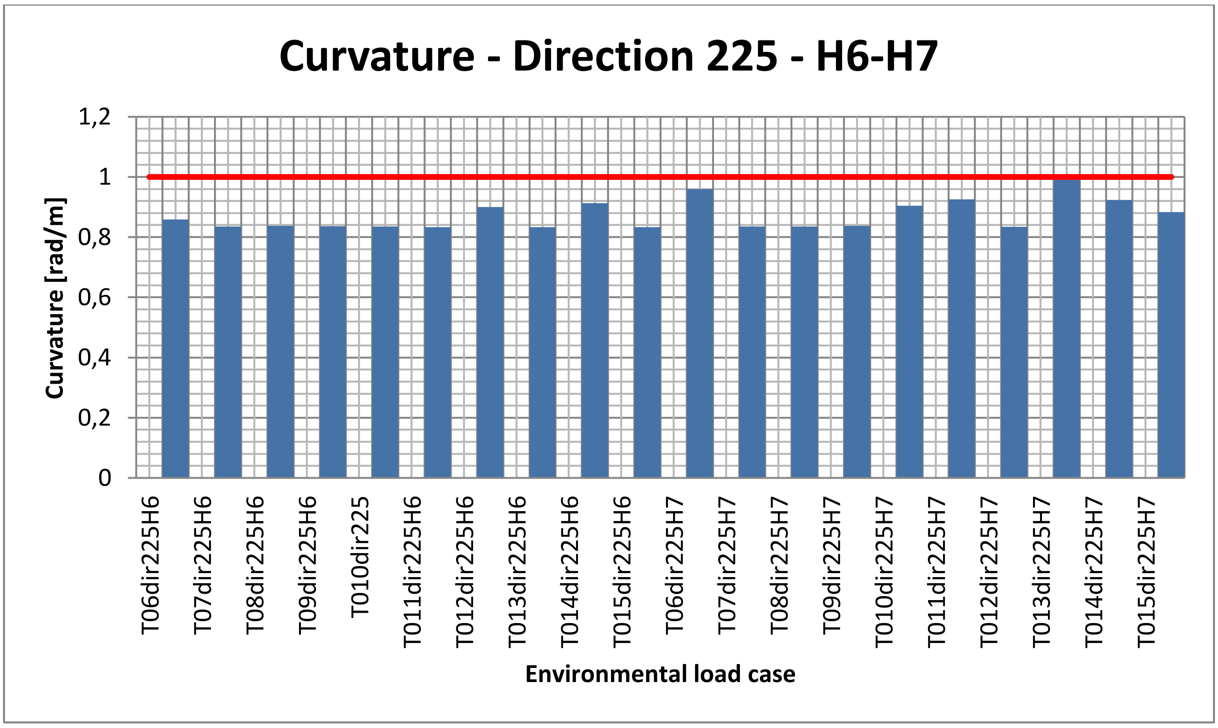

Figure C. 23 - 4” Bunkerflex STH – Free hanging – Curvature – Direction 225° - H6-H7

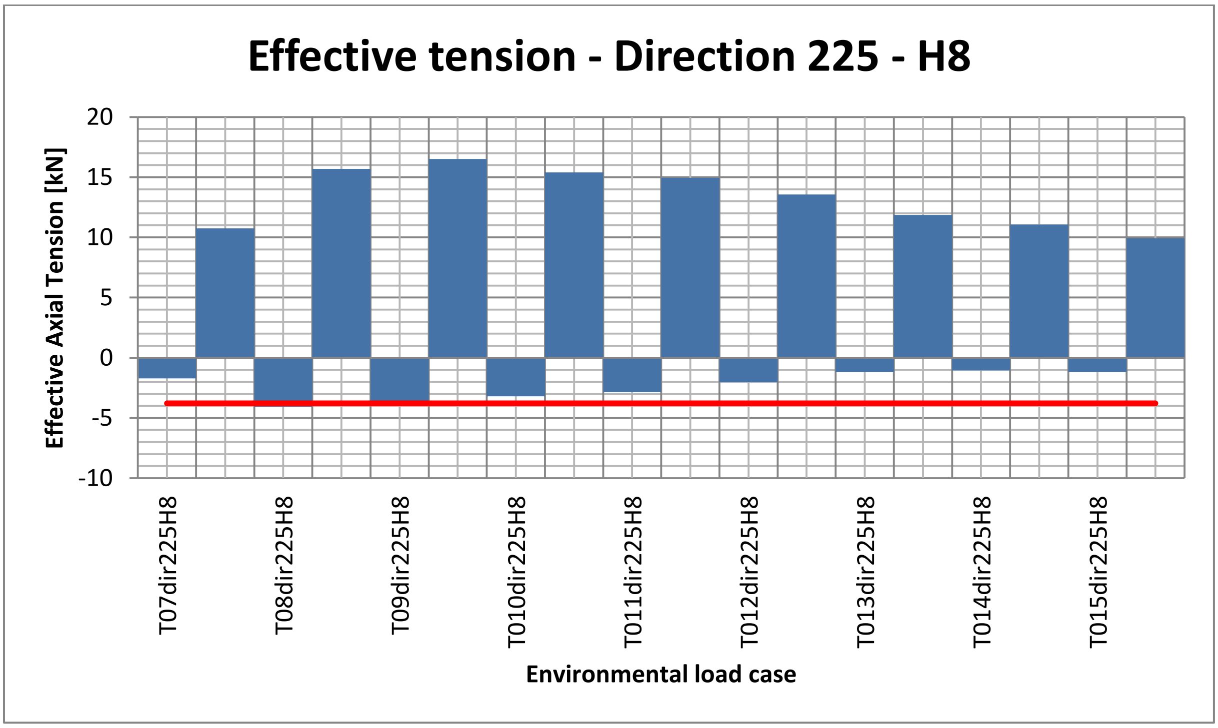

Figure C. 24 - 4” Bunkerflex STH – Free hanging – Effective tension – Direction 225° - H8

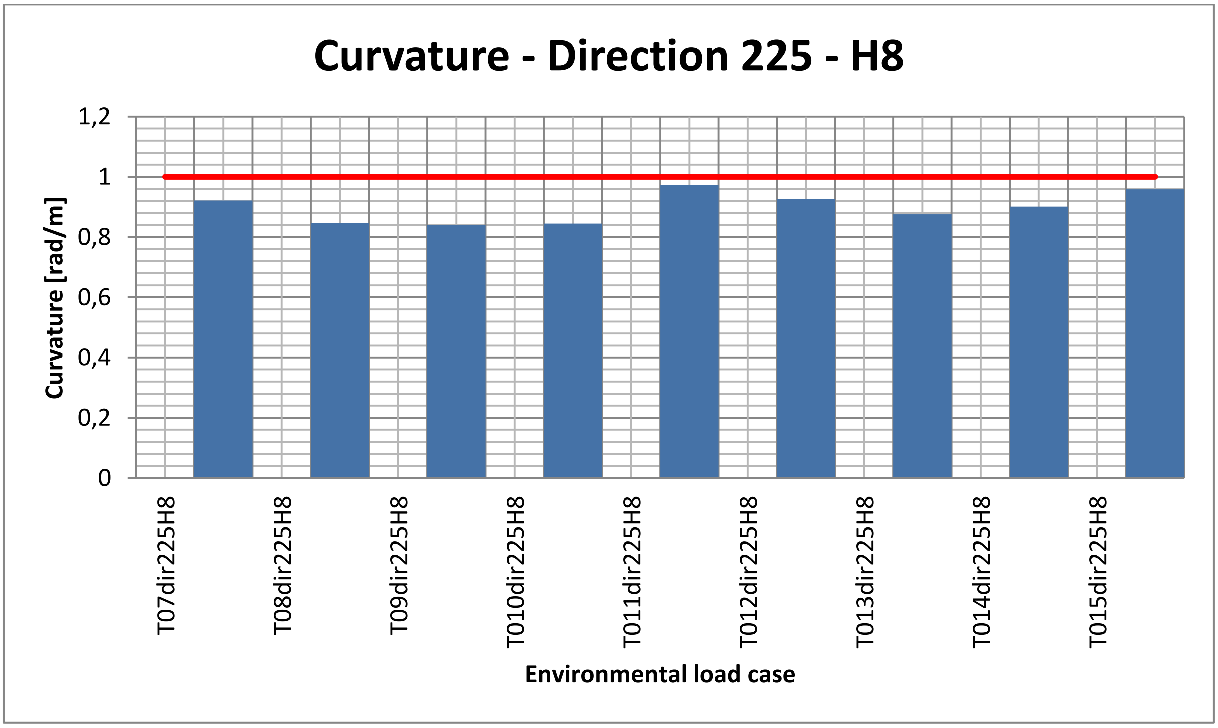

Figure C. 25 - 4” Bunkerflex STH – Free hanging – Curvature – Direction 225° - H8

Wave rose

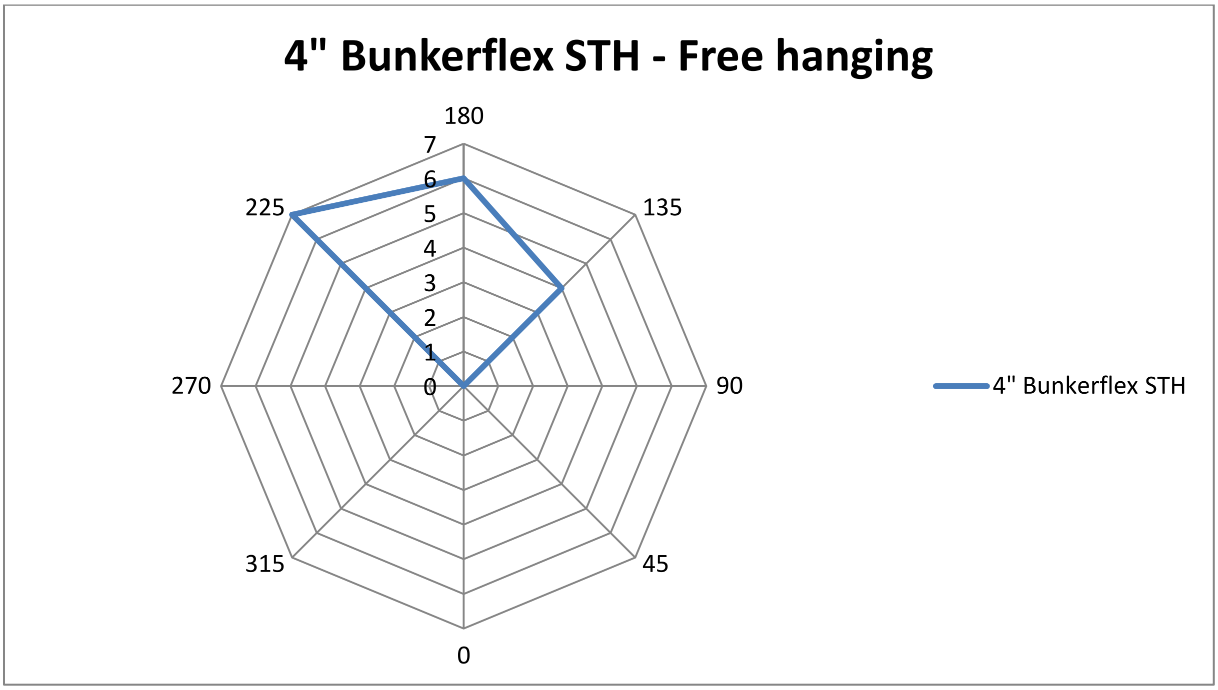

Figure C. 26 - 4” Bunkerflex STH – Free hanging – Wave rose

Limitation plot

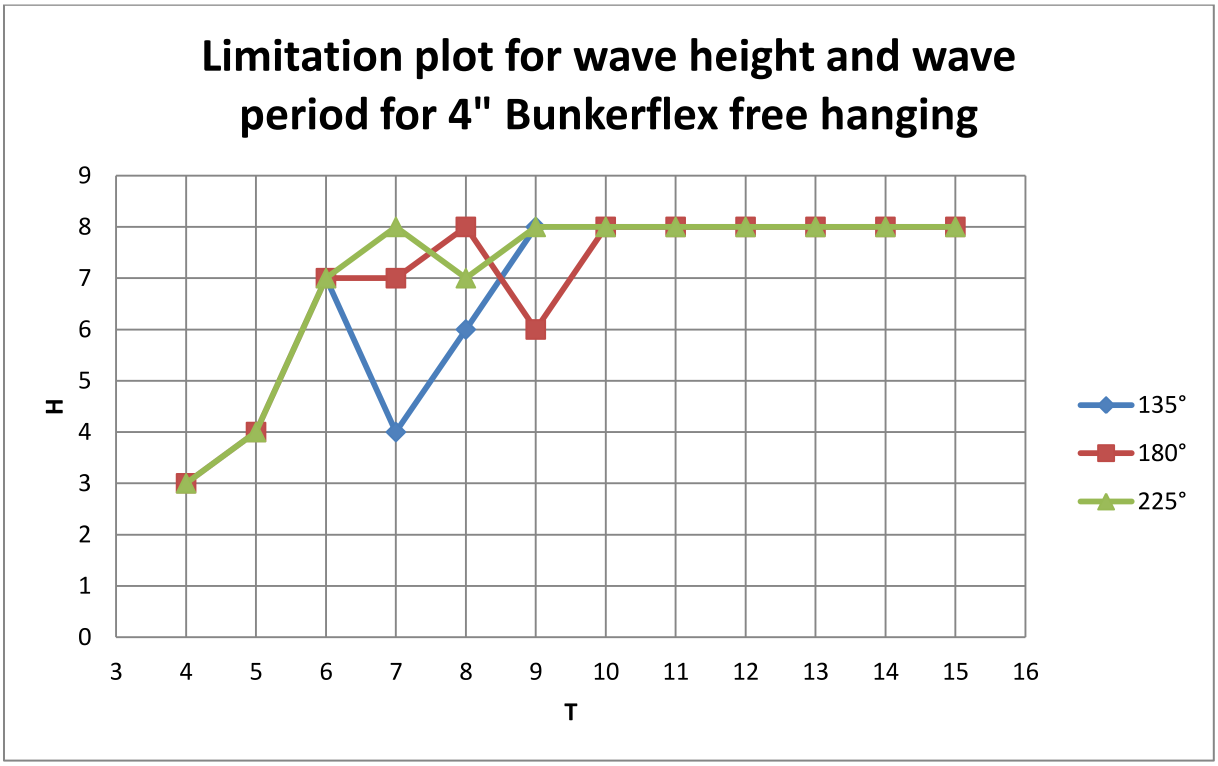

Figure C. 27 - 4” Bunkerflex STH – Free hanging – Limitation plot

Lazy wave – 20 m floatation point

Direction 135°

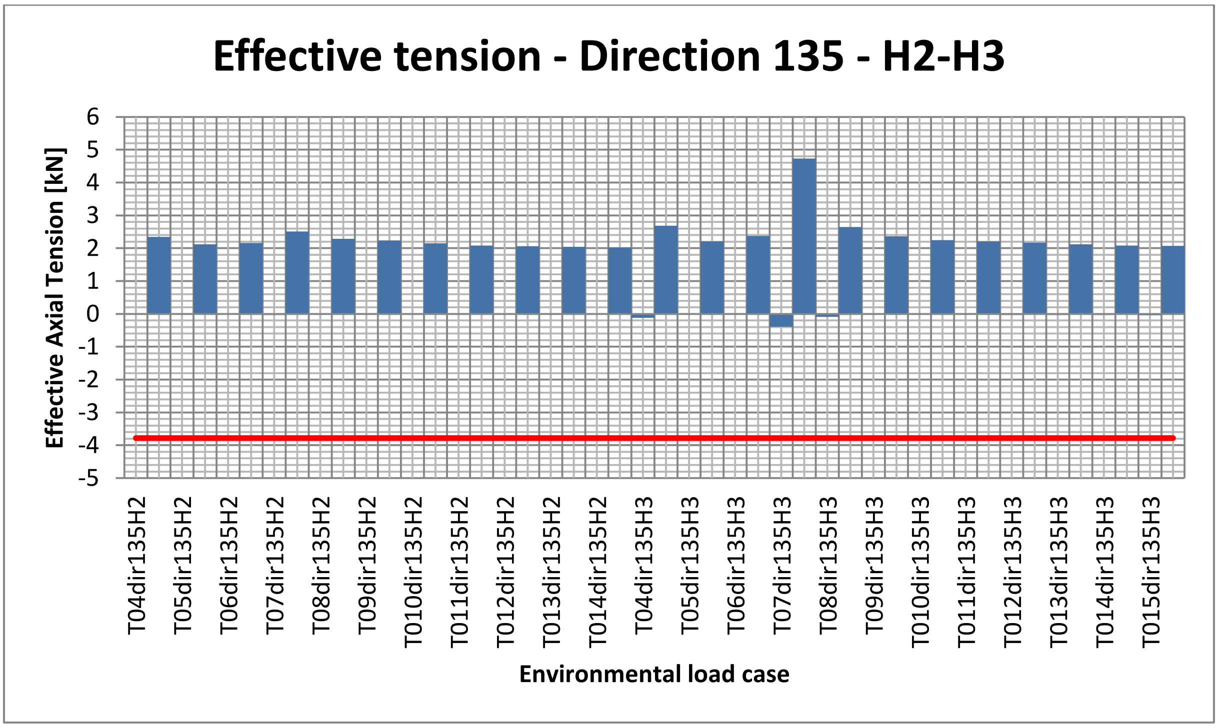

Figure C. 28 - 4” Bunkerflex STH – Lazy wave – 20 m floatation point – Effective tension – Direction 135° - H2-H3

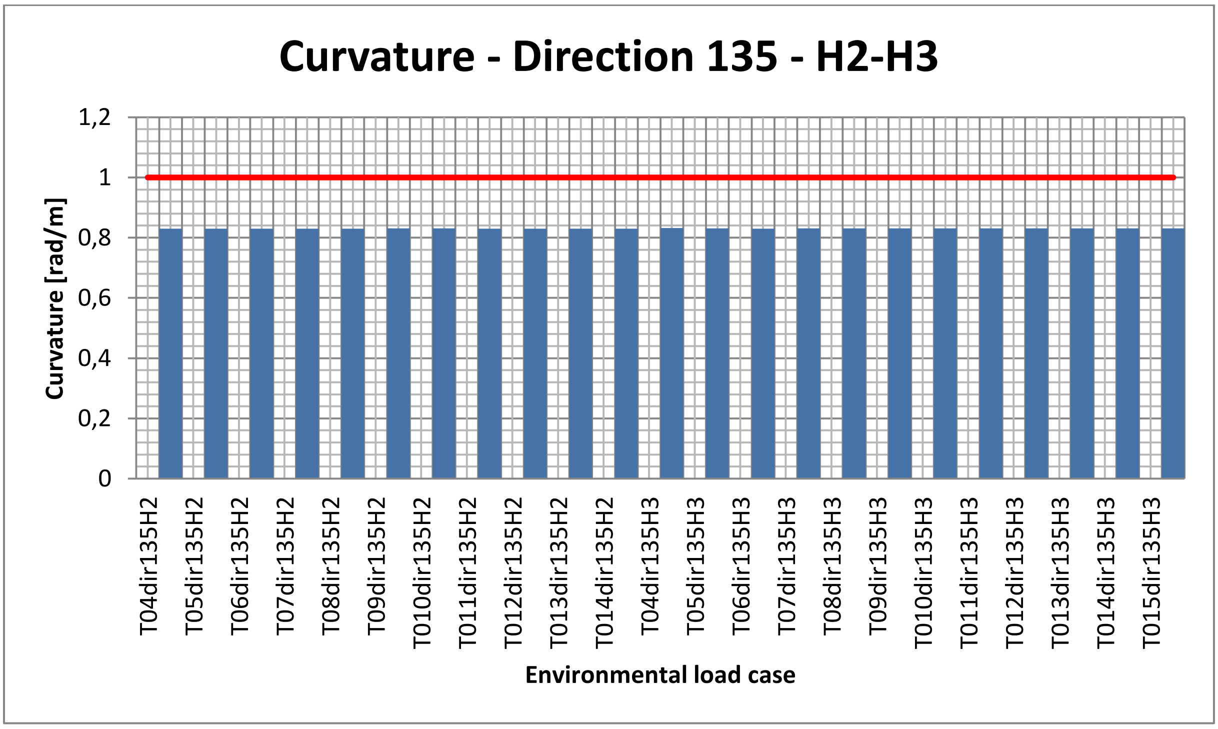

Figure C. 29 - 4” Bunkerflex STH – Lazy wave – 20 m floatation point – Curvature – Direction 135° - H2-H3

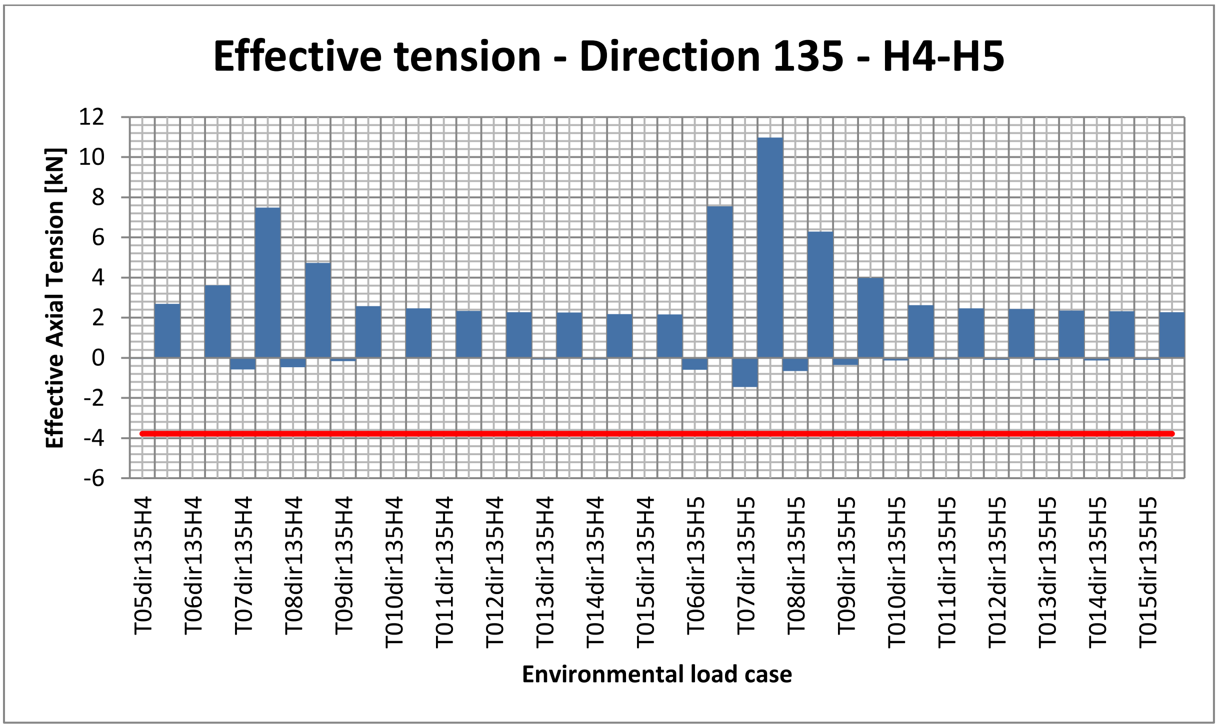

Figure C. 30 - 4” Bunkerflex STH – Lazy wave – 20 m floatation point – Effective tension – Direction 135° - H4-H5

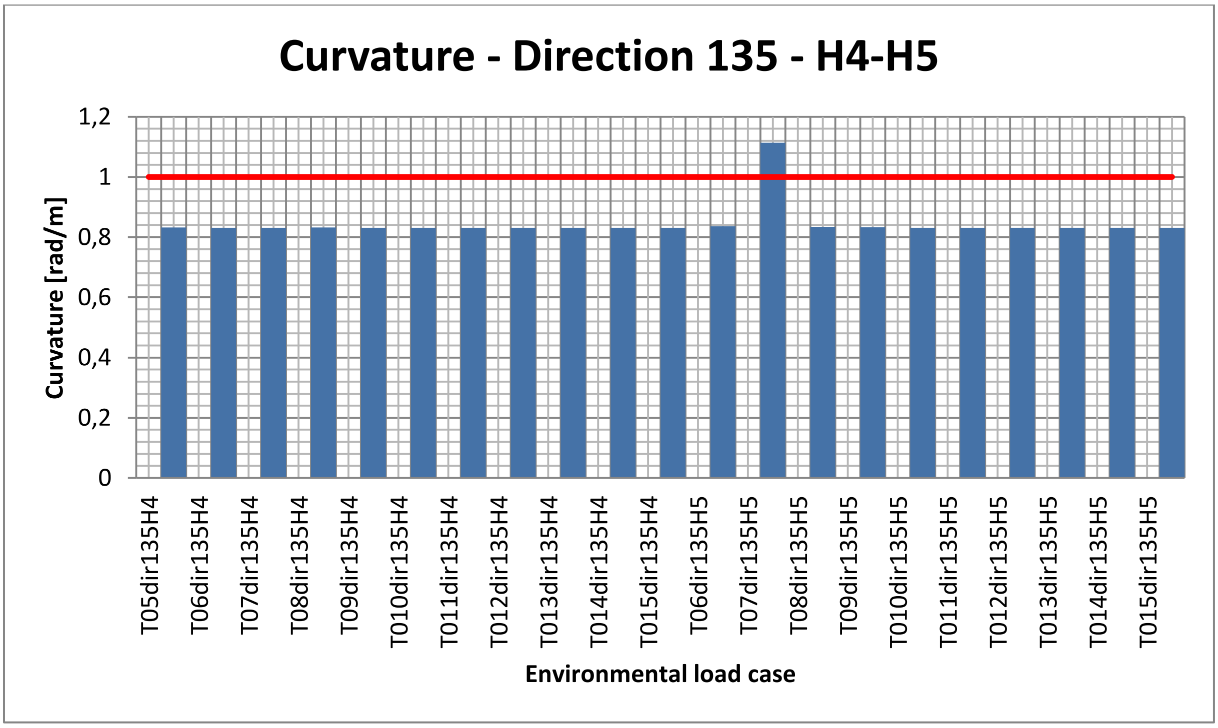

Figure C. 31 - 4” Bunkerflex STH – Lazy wave – 20 m floatation point – Curvature – Direction 135° - H4-H5

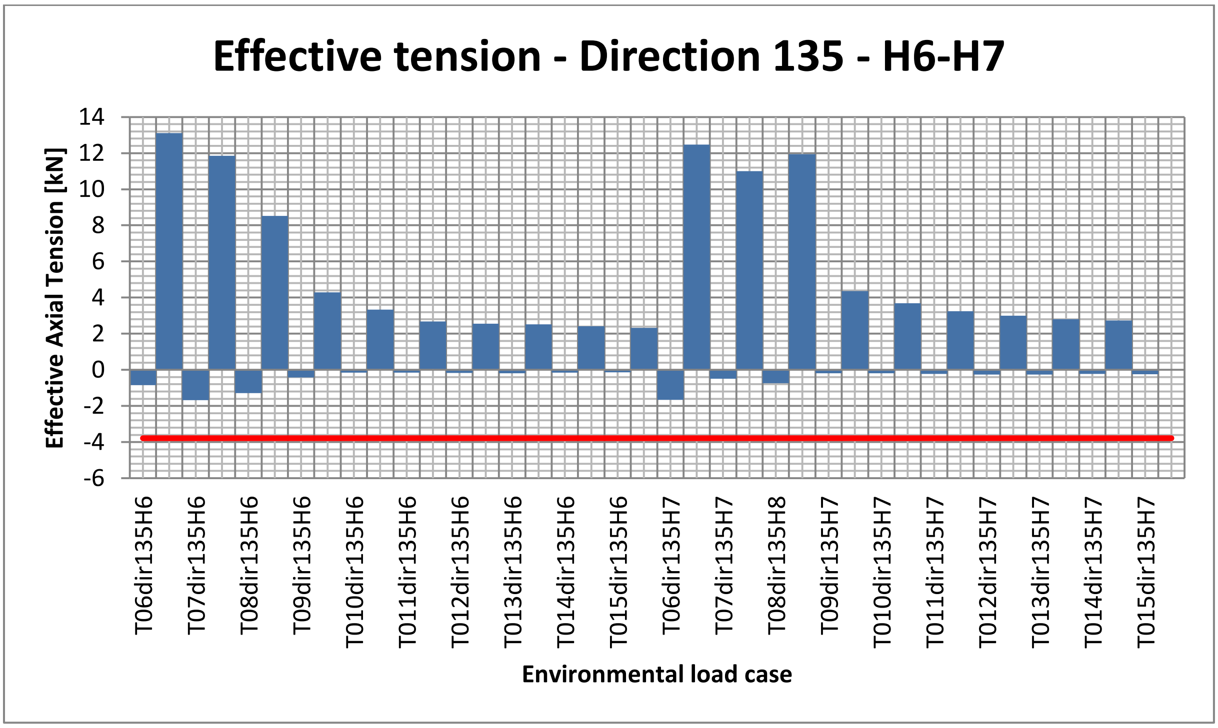

Figure C. 32 - 4” Bunkerflex STH – Lazy wave – 20 m floatation point – Effective tension – Direction 135° - H6-H7

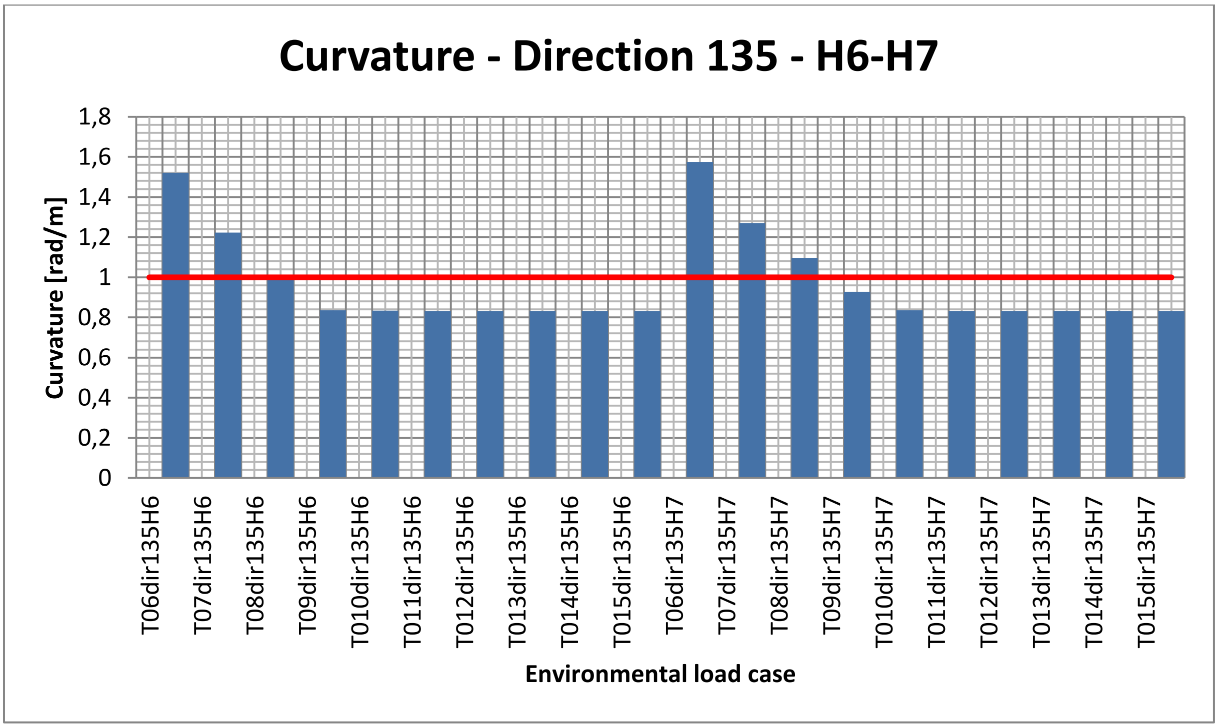

Figure C. 33 - 4” Bunkerflex STH – Lazy wave – 20 m floatation point – Curvature – Direction 135° - H6-H7

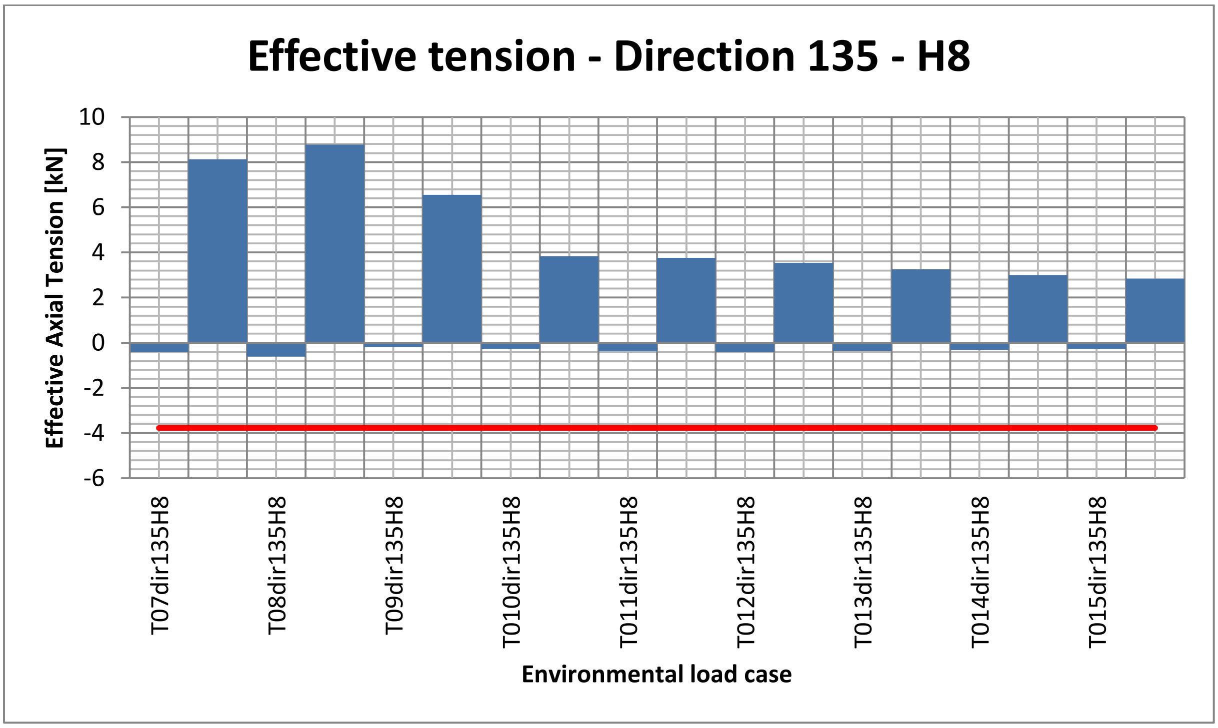

Figure C. 34 - 4" Bunkerflex STH – Lazy wave – 20 m floatation point – Effective tension – Direction 135° - H8

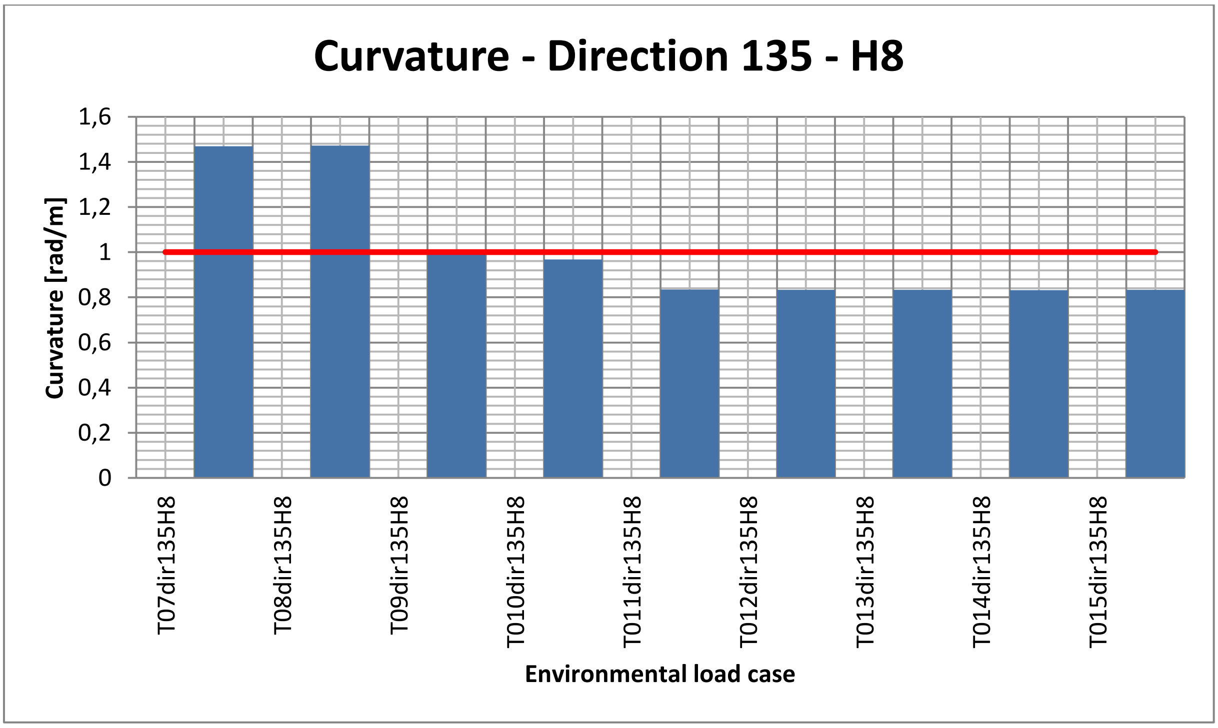

Figure C. 35 - 4" Bunkerflex STH – Lazy wave – 20 m floatation point – Curvature – Direction 135° - H8

Direction 180°

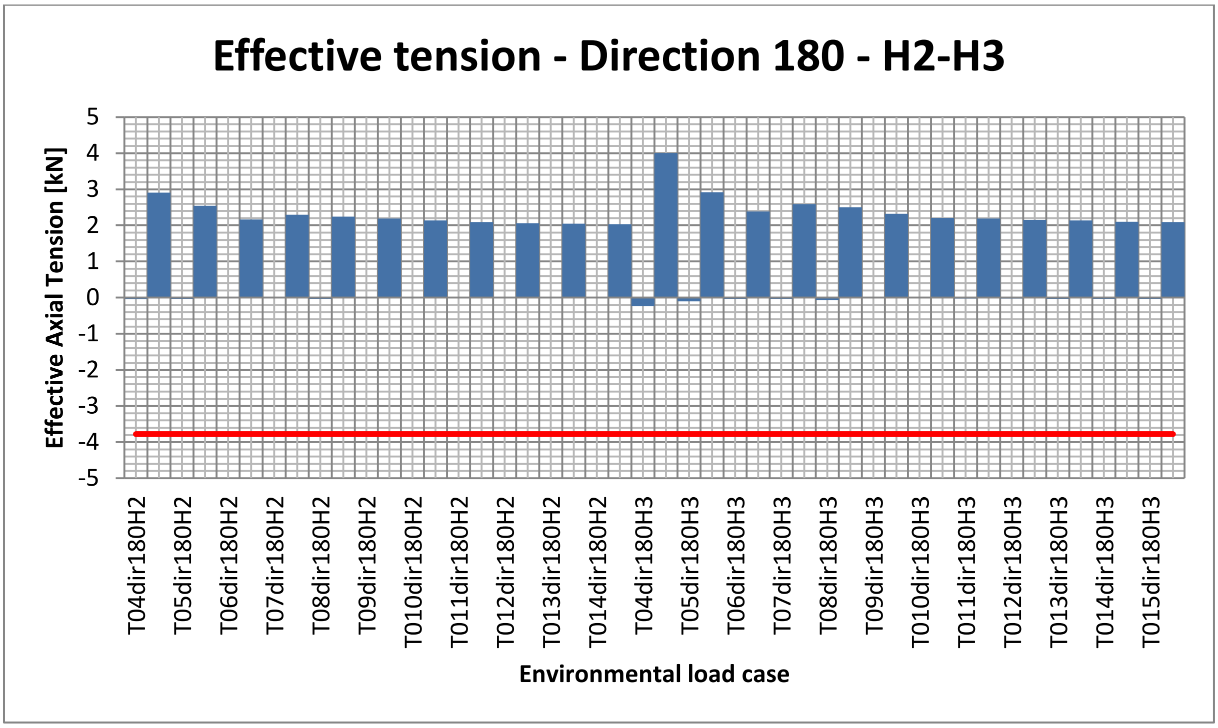

Figure C. 36 - 4” Bunkerflex STH – Lazy wave – 20 m floatation point – Effective tension – Direction 180° - H2-H3

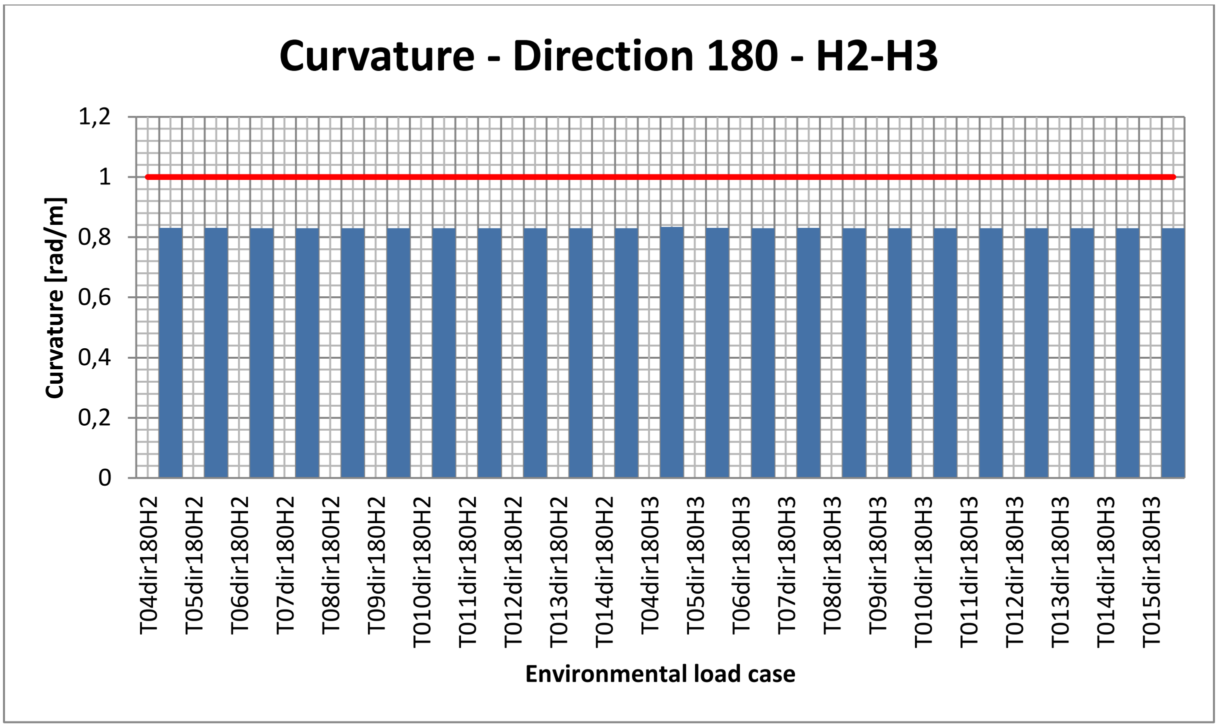

Figure C. 37 - 4” Bunkerflex STH – Lazy wave – 20 m floatation point – Curvature – Direction 180° - H2-H3

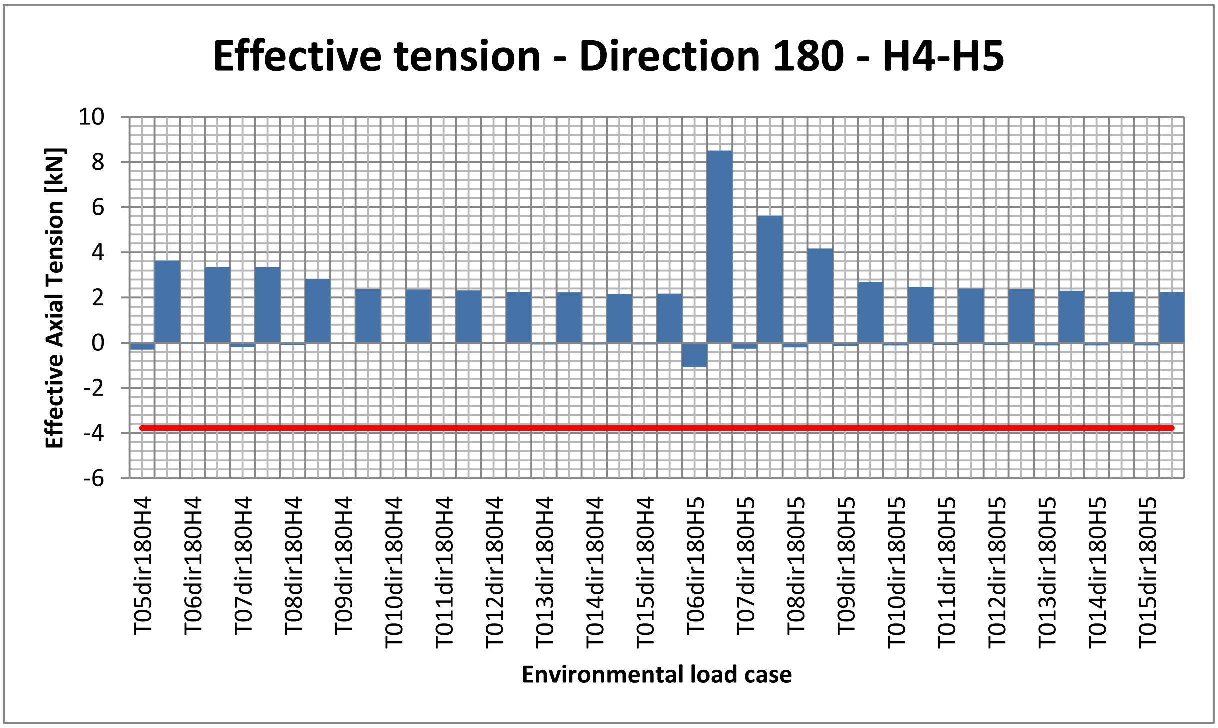

Figure C. 38 - 4” Bunkerflex STH – Lazy wave – 20 m floatation point – Effective tension – Direction 180° - H4-H5

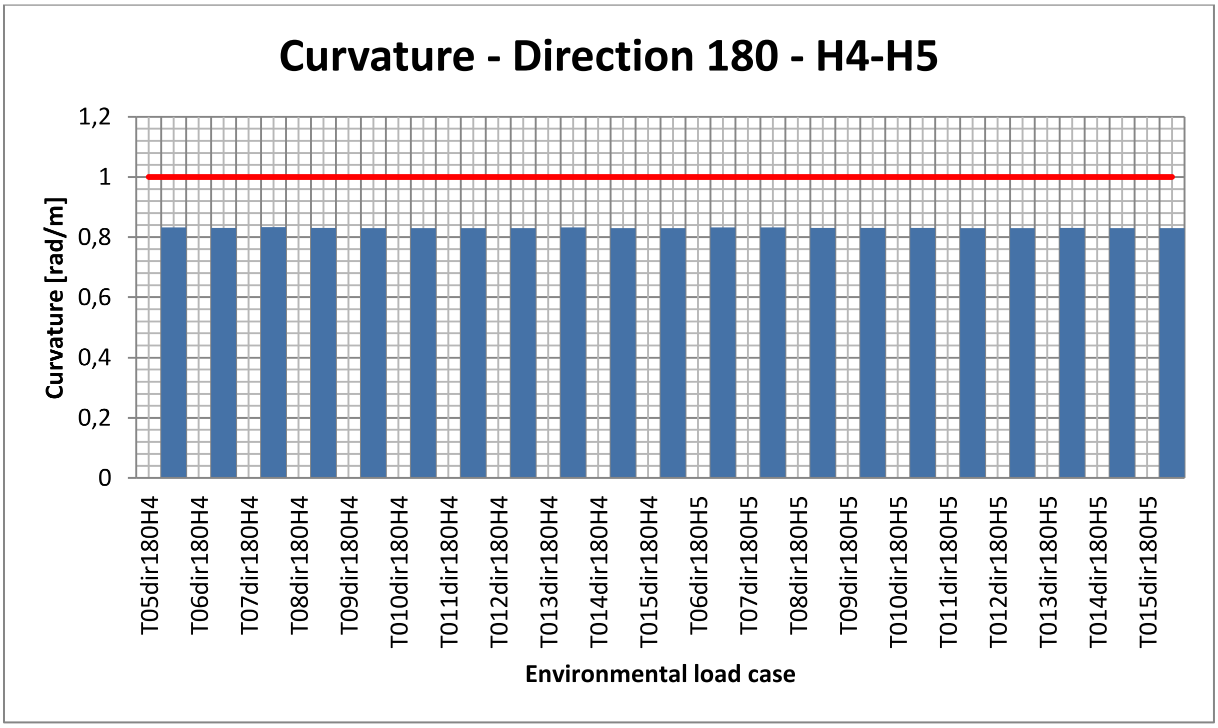

Figure C. 39 - 4” Bunkerflex STH – Lazy wave – 20 m floatation point – Curvature – Direction 180° - H4-H5

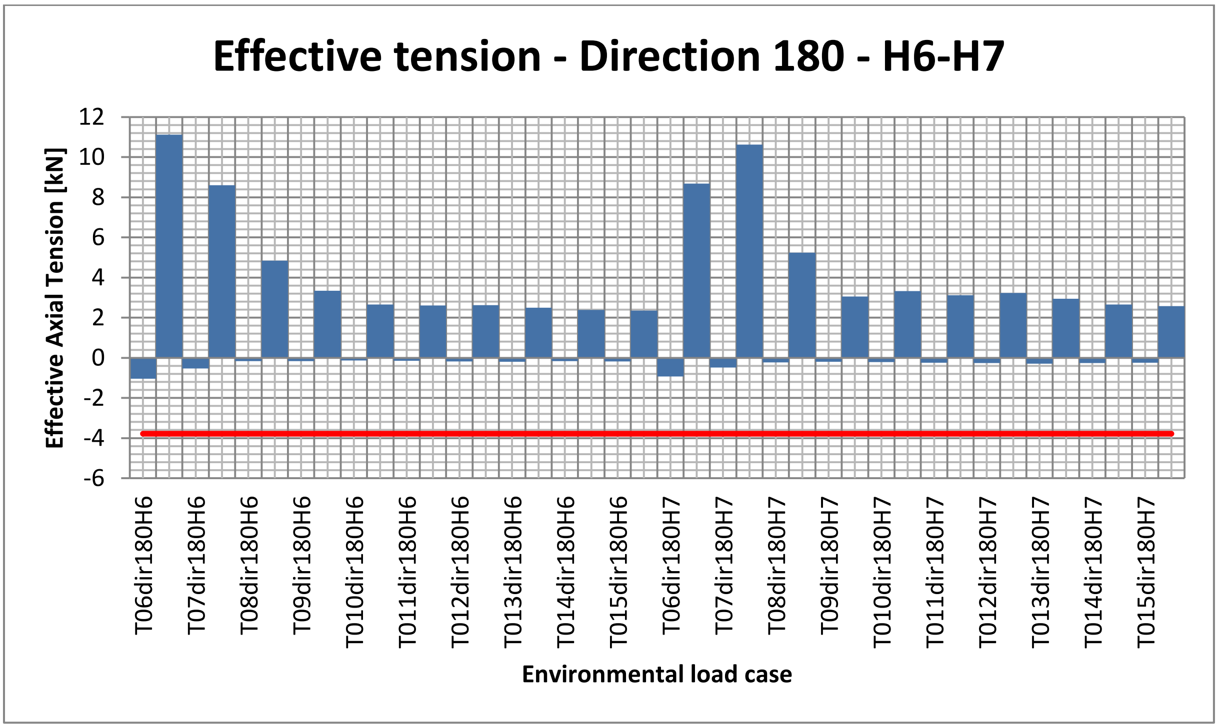

Figure C. 40 - 4” Bunkerflex STH – Lazy wave – 20 m floatation point – Effective tension – Direction 180° - H6-H7

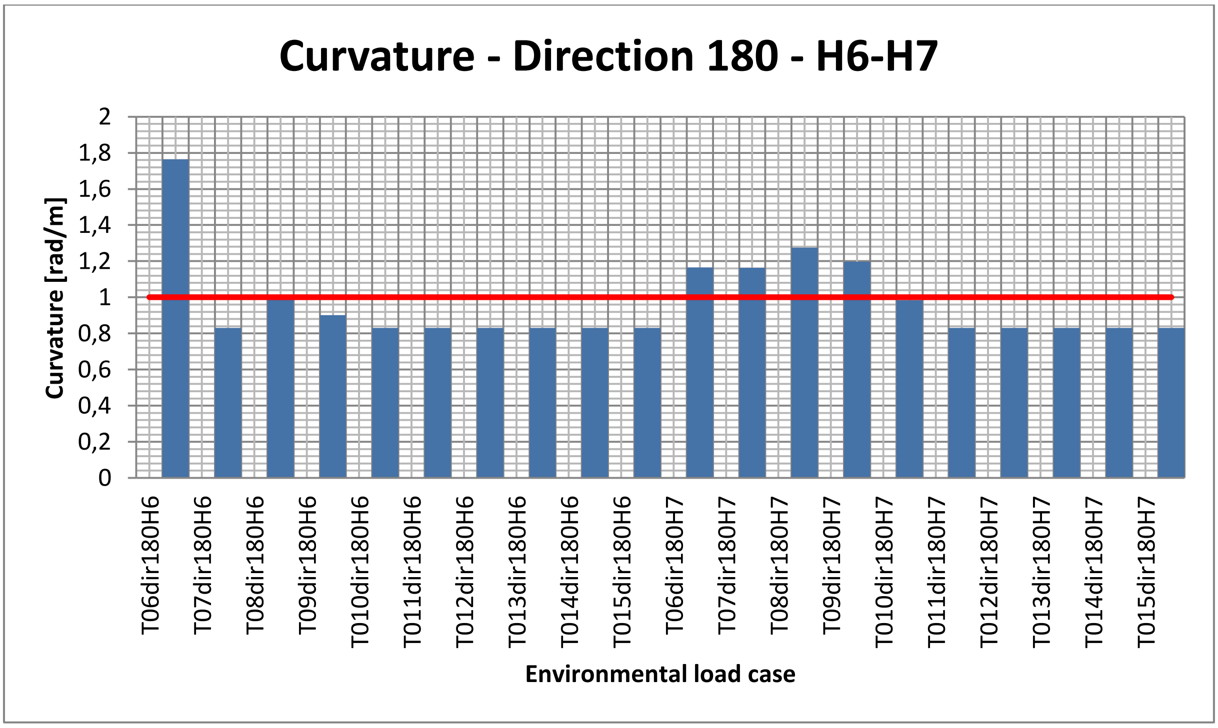

Figure C. 41 - 4” Bunkerflex STH – Lazy wave – 20 m floatation point – Curvature – Direction 180° - H6-H7

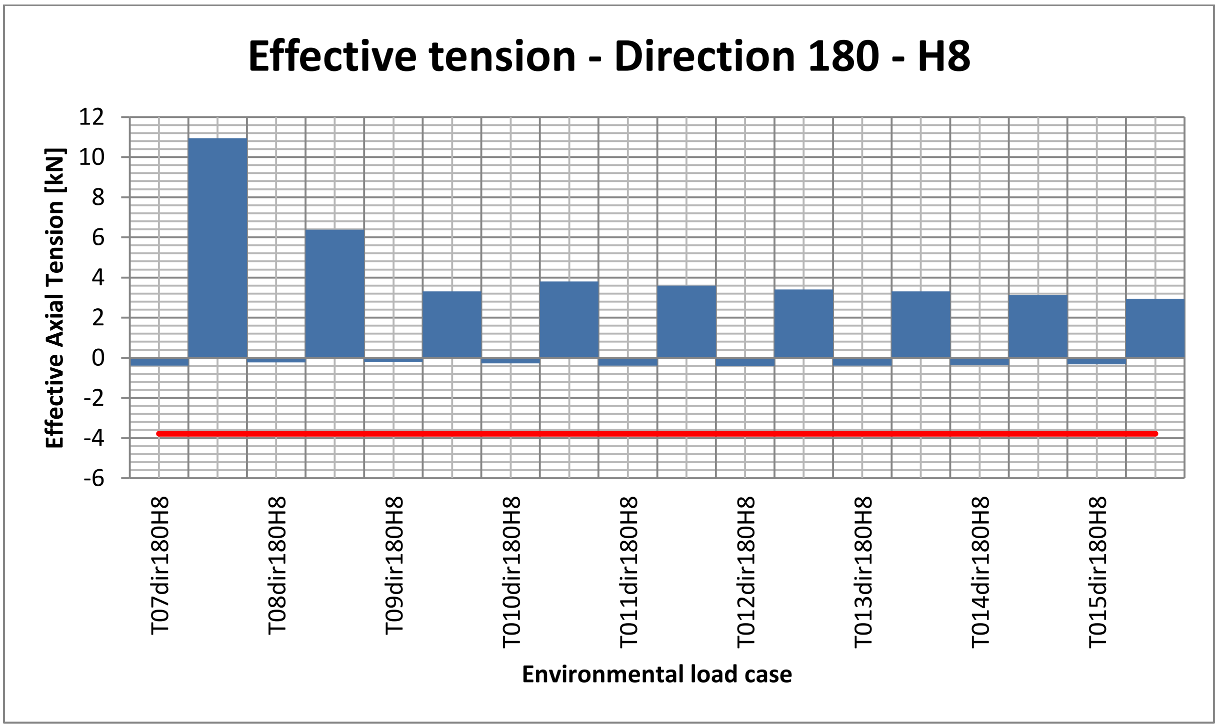

Figure C. 42 - 4” Bunkerflex STH – Lazy wave – 20 m floatation point – Effective tension – Direction 180° - H8

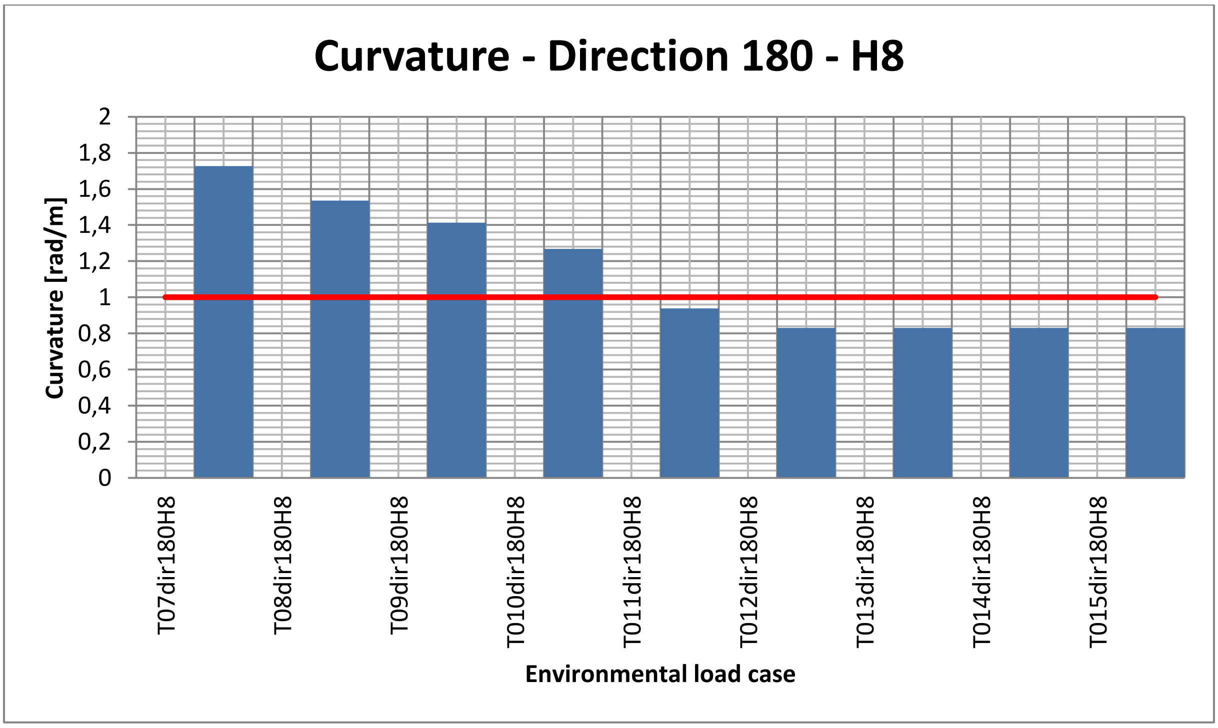

Figure C. 43 - 4” Bunkerflex STH – Lazy wave – 20 m floatation point – Curvature – Direction 180° - H8

Direction 225°

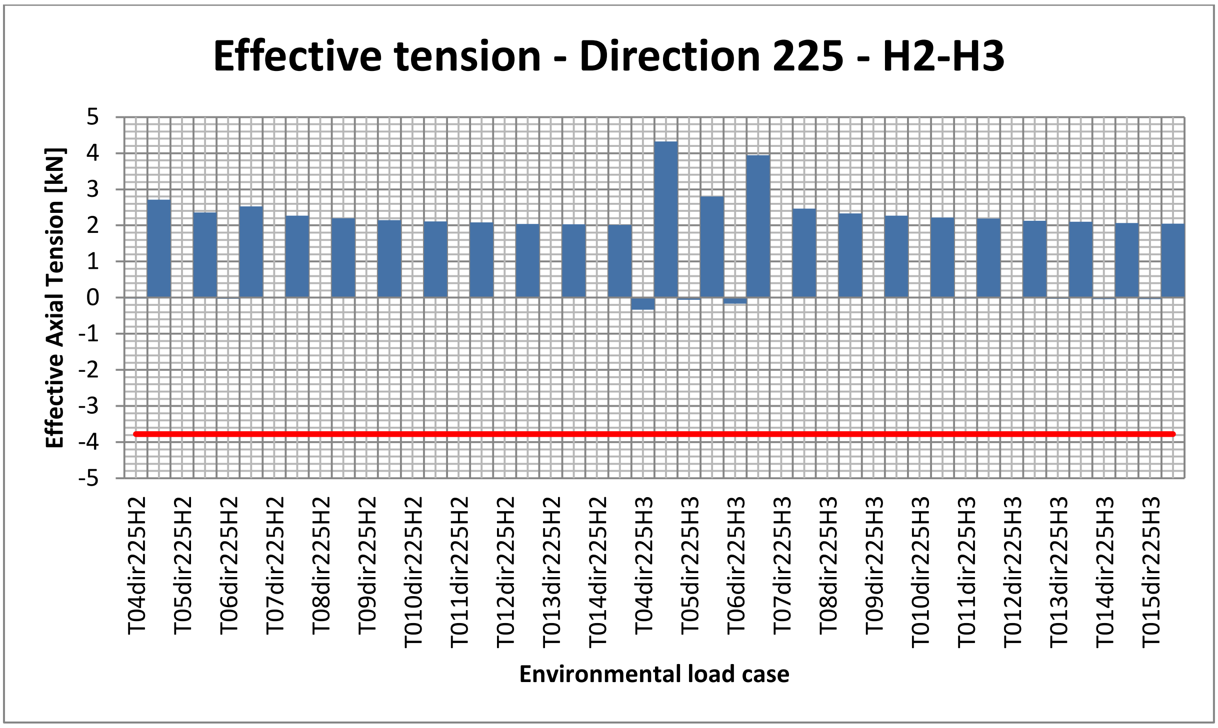

Figure C. 44 - 4” Bunkerflex STH – Lazy wave – 20 m floatation point – Effective tension – Direction 225° - H2-H3

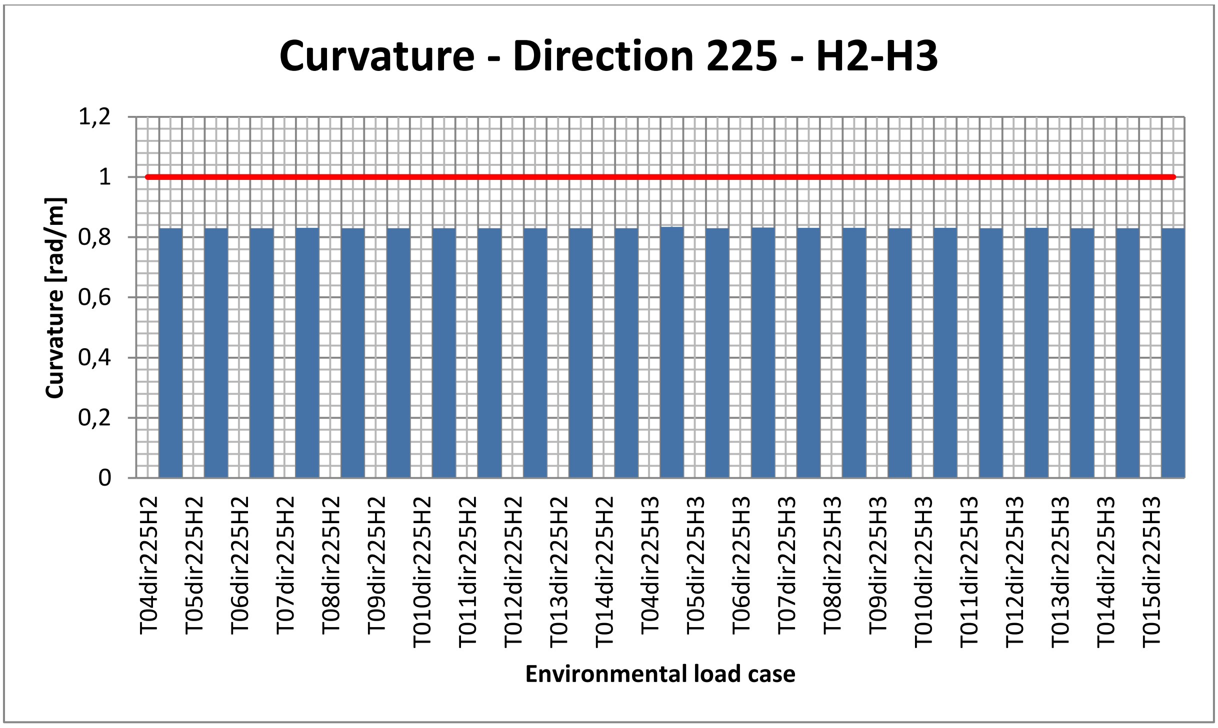

Figure C. 45 - 4” Bunkerflex STH – Lazy wave – 20 m floatation point – Curvature – Direction 225° - H2-H3

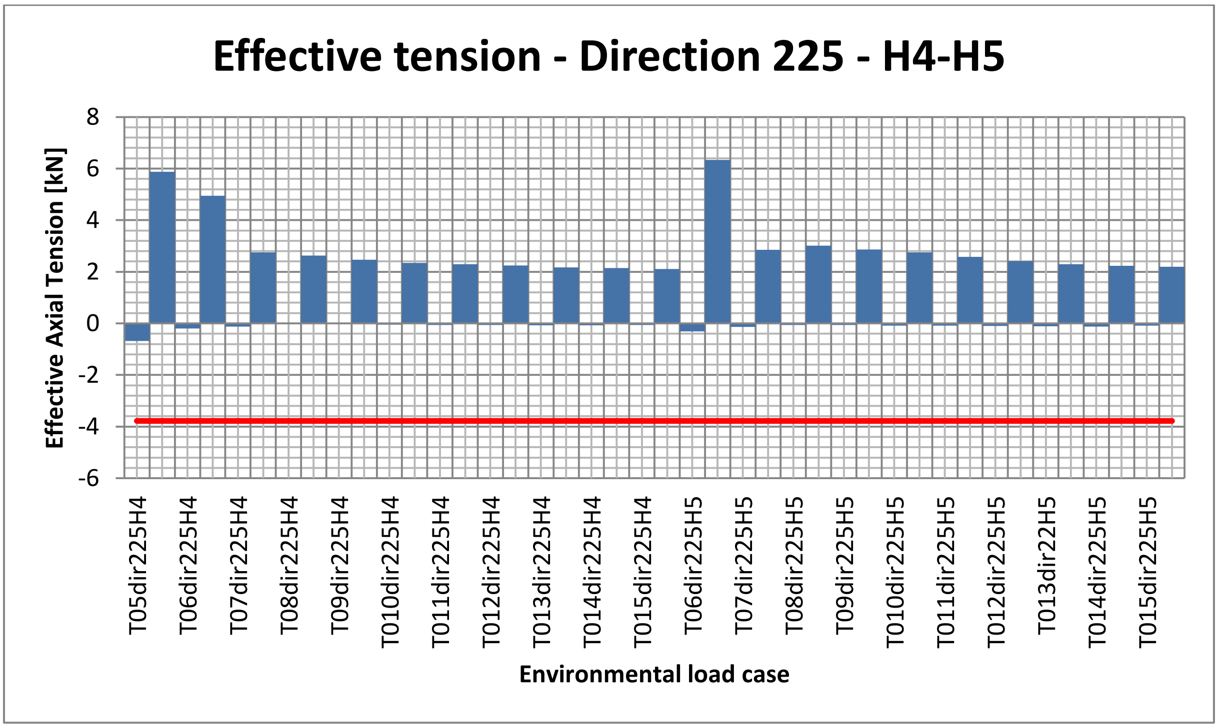

Figure C. 46 - 4" Bunkerflex STH – Lazy wave – 20 m floatation point – Effective tension – Direction 225° - H4-H5

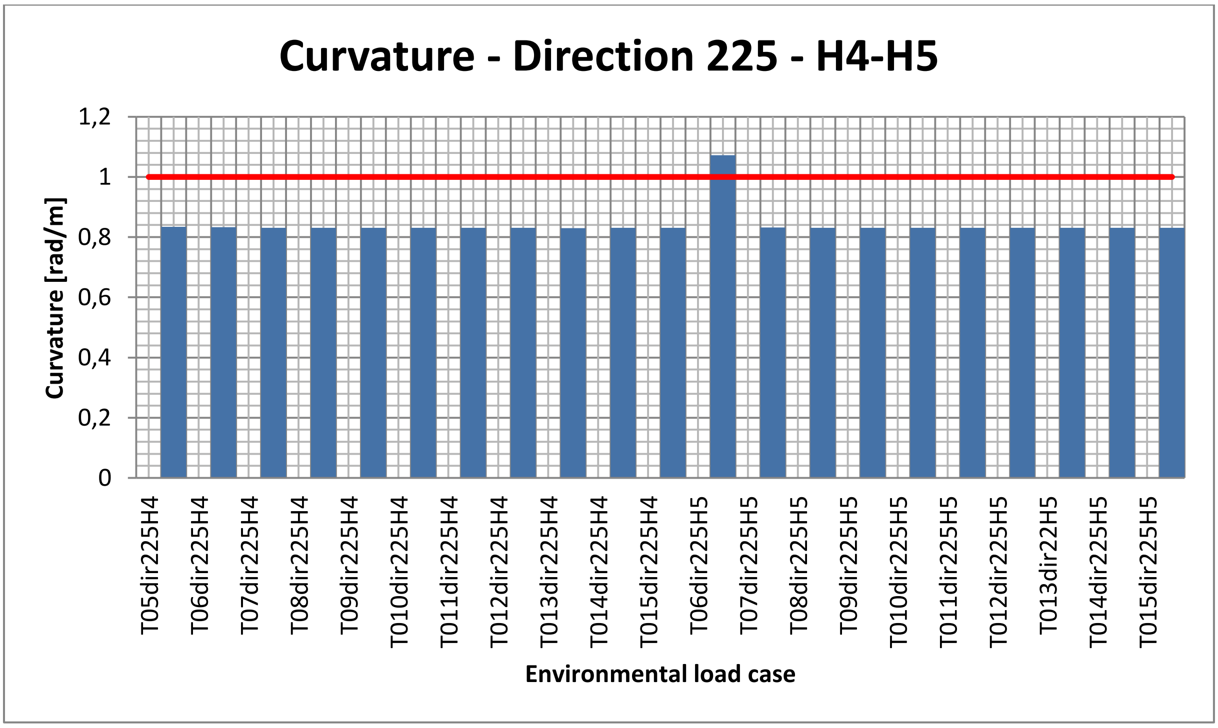

Figure C. 47 - 4" Bunkerflex STH – Lazy wave – 20 m floatation point – Curvature – Direction 225° - H4-H5

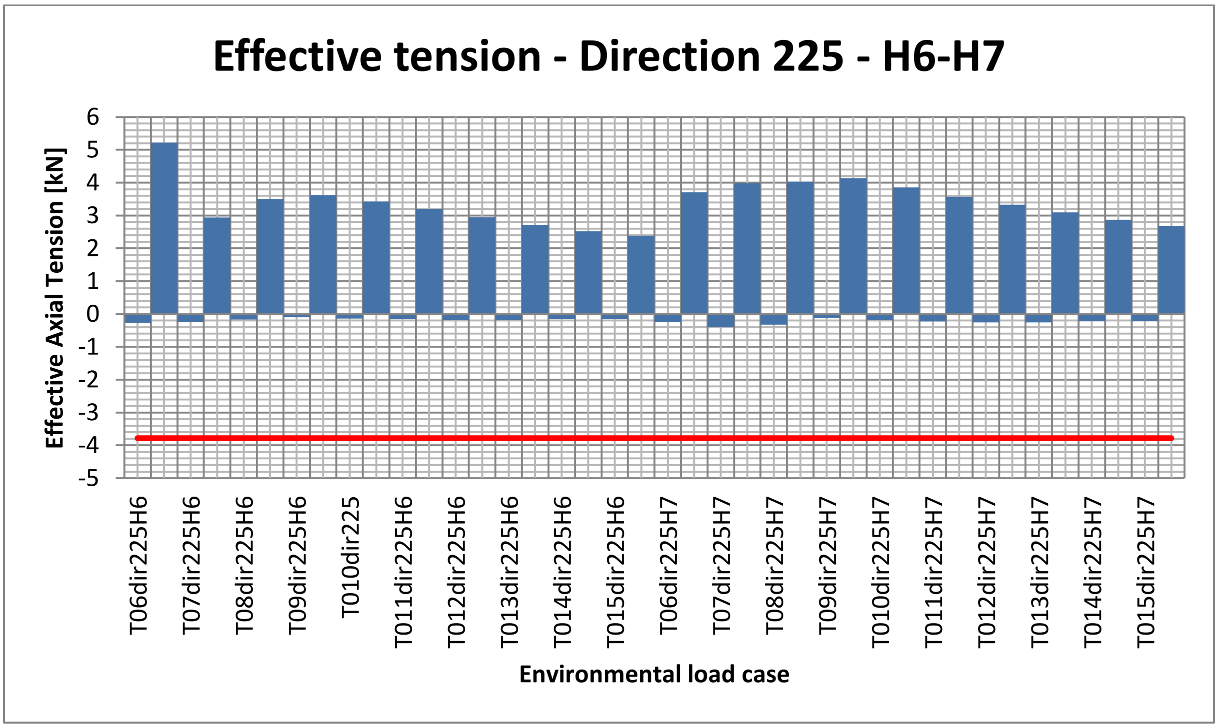

Figure C. 48 - 4" Bunkerflex STH – Lazy wave – 20 m floatation point – Effective tension – Direction 225° - H6-H7

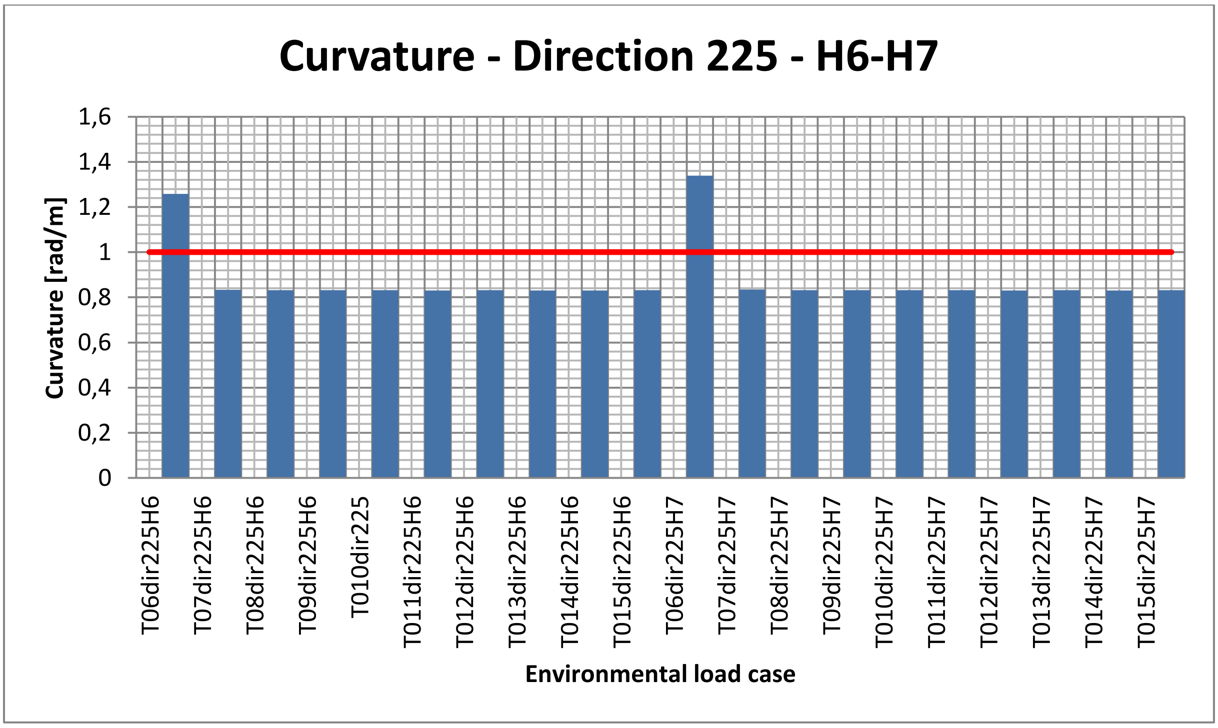

Figure C. 49 - 4" Bunkerflex STH – Lazy wave – 20 m floatation point – Curvature – Direction 225° - H6-H7

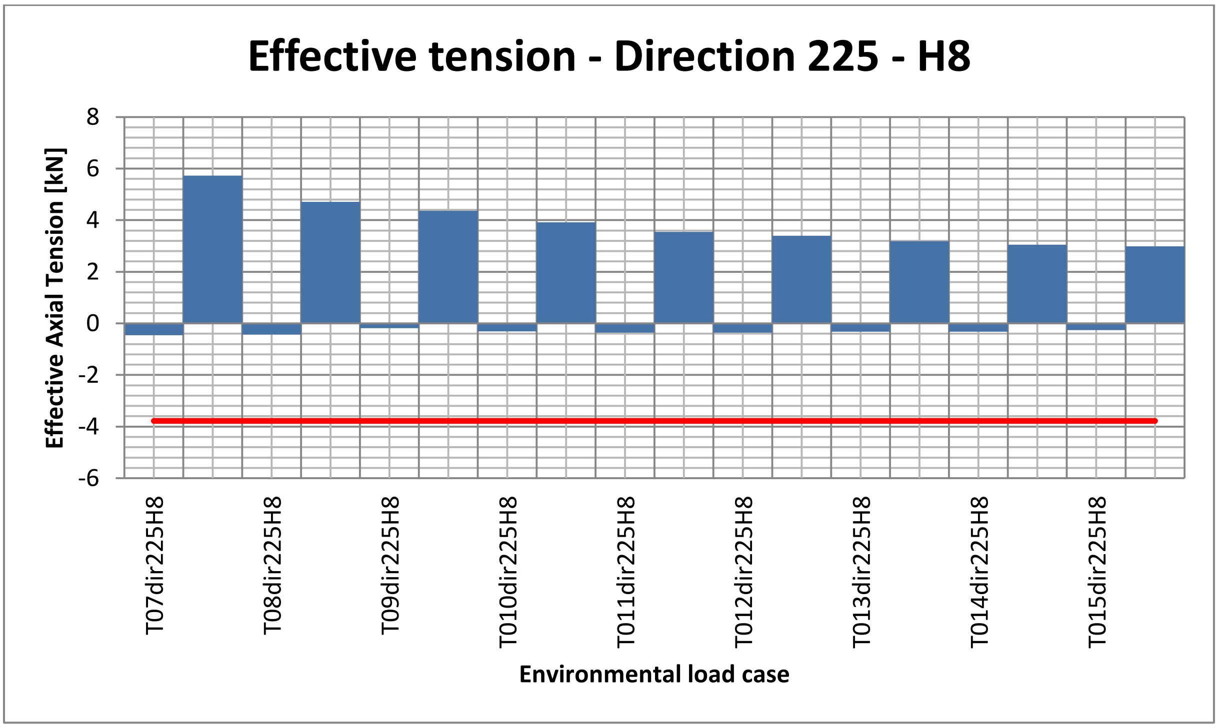

Figure C. 50 - 4” Bunkerflex STH – Lazy wave – 20 m floatation point – Effective tension – Direction 225° - H8

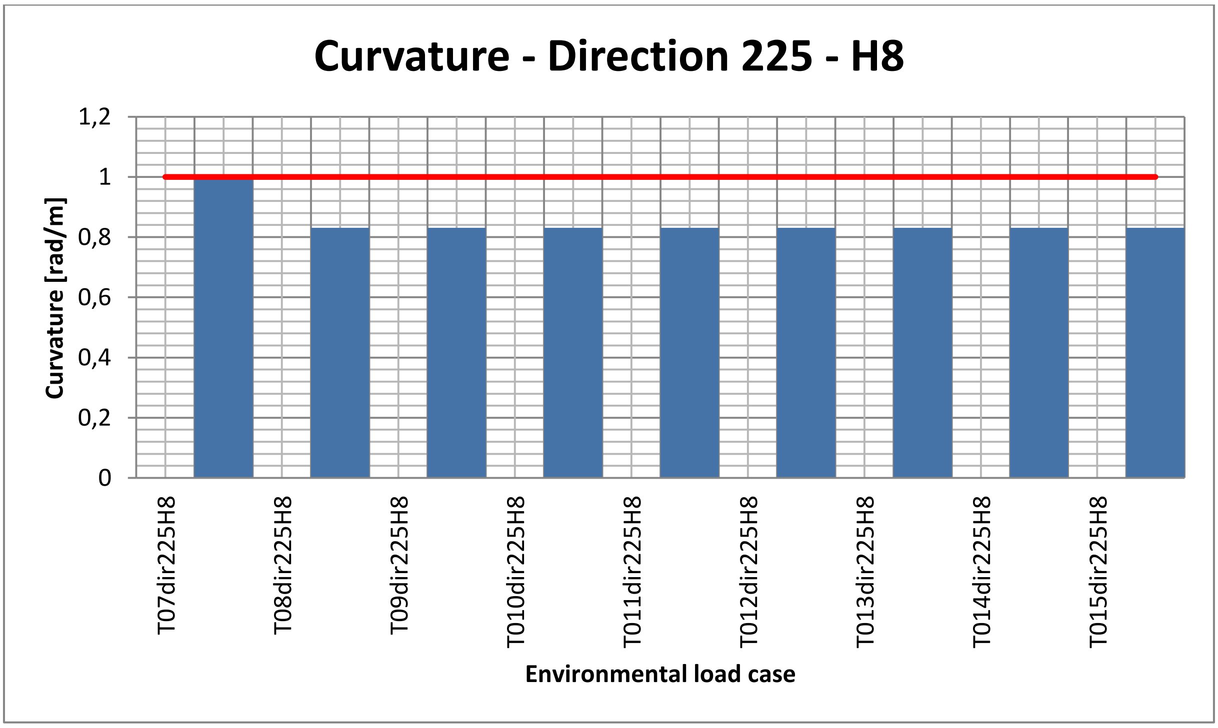

Figure C. 51 - 4” Bunkerflex STH – Lazy wave – 20 m floatation point – Curvature – Direction 225° - H8

Wave rose

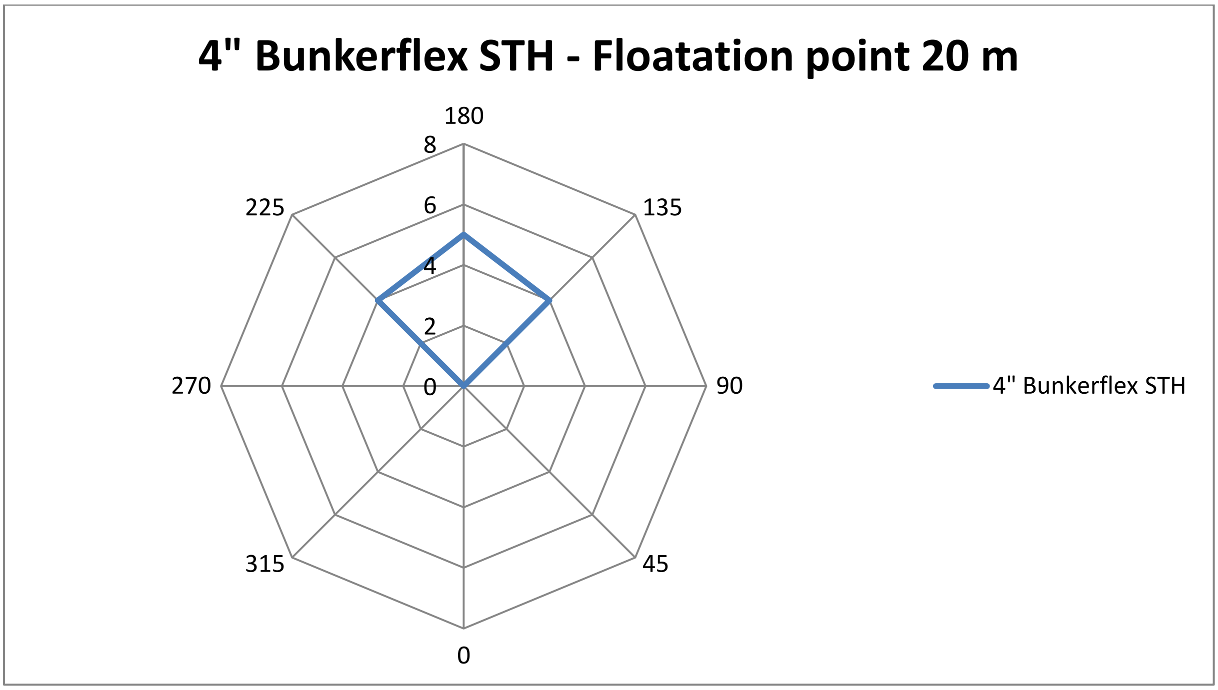

Figure C. 52 - 4” Bunkerflex STH – Lazy wave – 20 m floatation point – Wave rose

Limitation plot

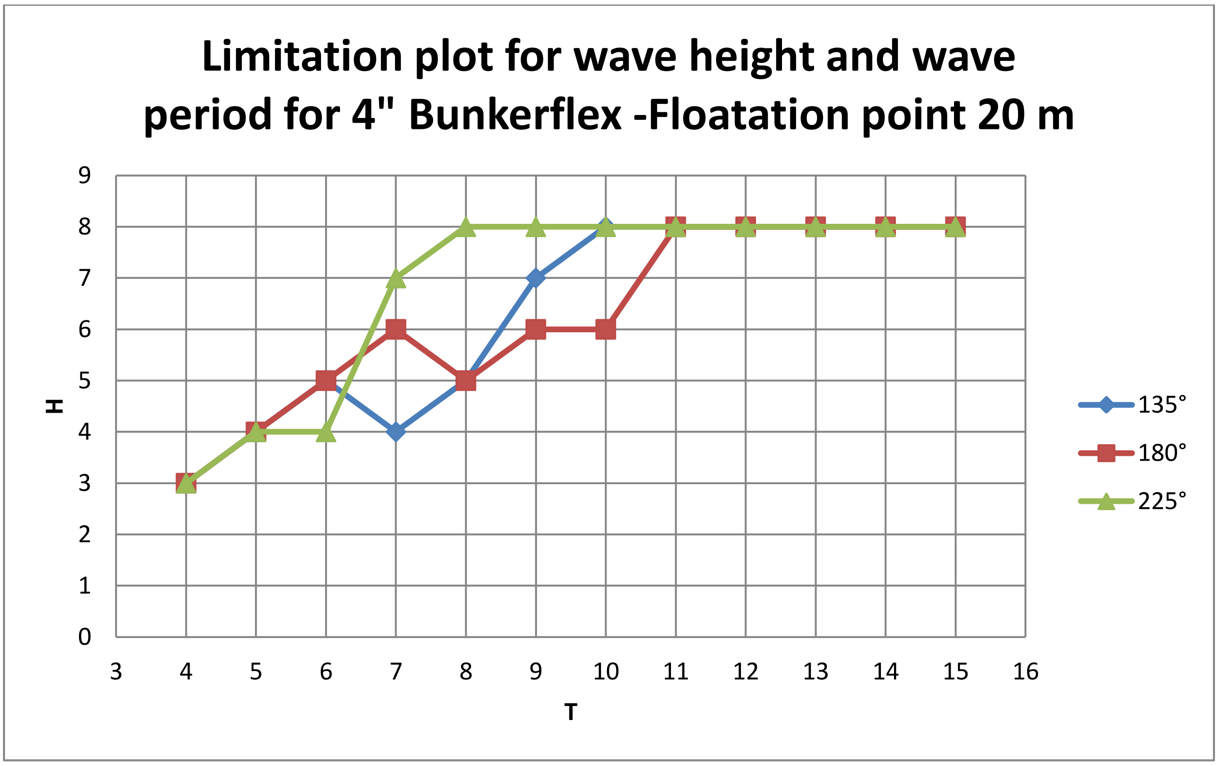

Figure C. 53 - 4” Bunkerflex STH – Lazy wave – 20 m floatation point – Limitation plot

Lazy wave – 40 m floatation point

Direction 135°

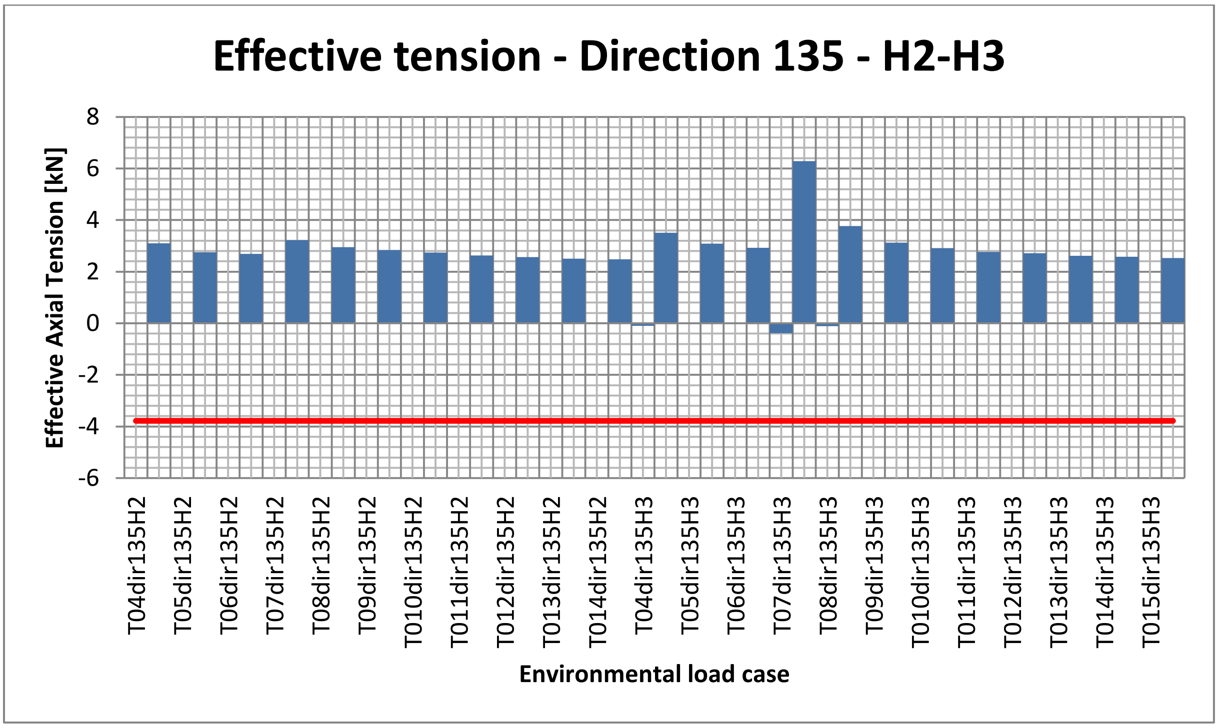

Figure C. 54 - 4" Bunkerflex STH – Lazy wave – 40 m floatation point – Effective tension – Direction 135° - H2-H3

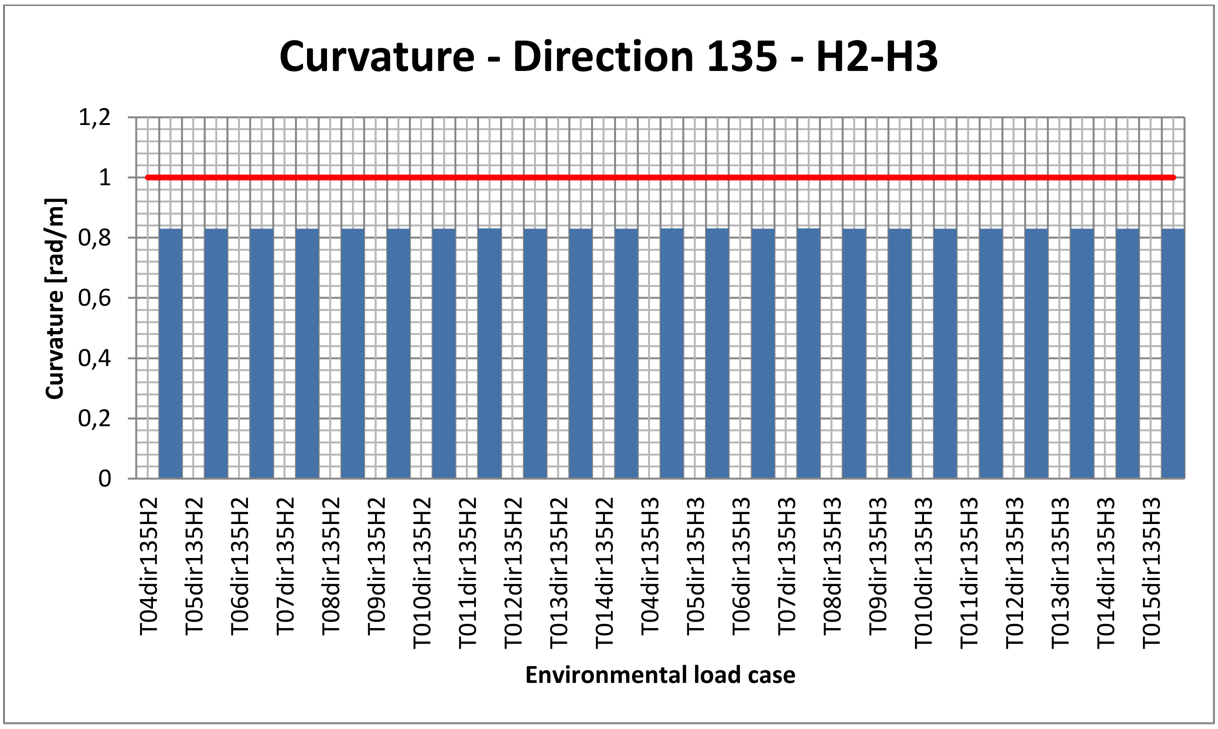

Figure C. 55 - 4" Bunkerflex STH – Lazy wave – 40 m floatation point – Curvature – Direction 135° - H2-H3

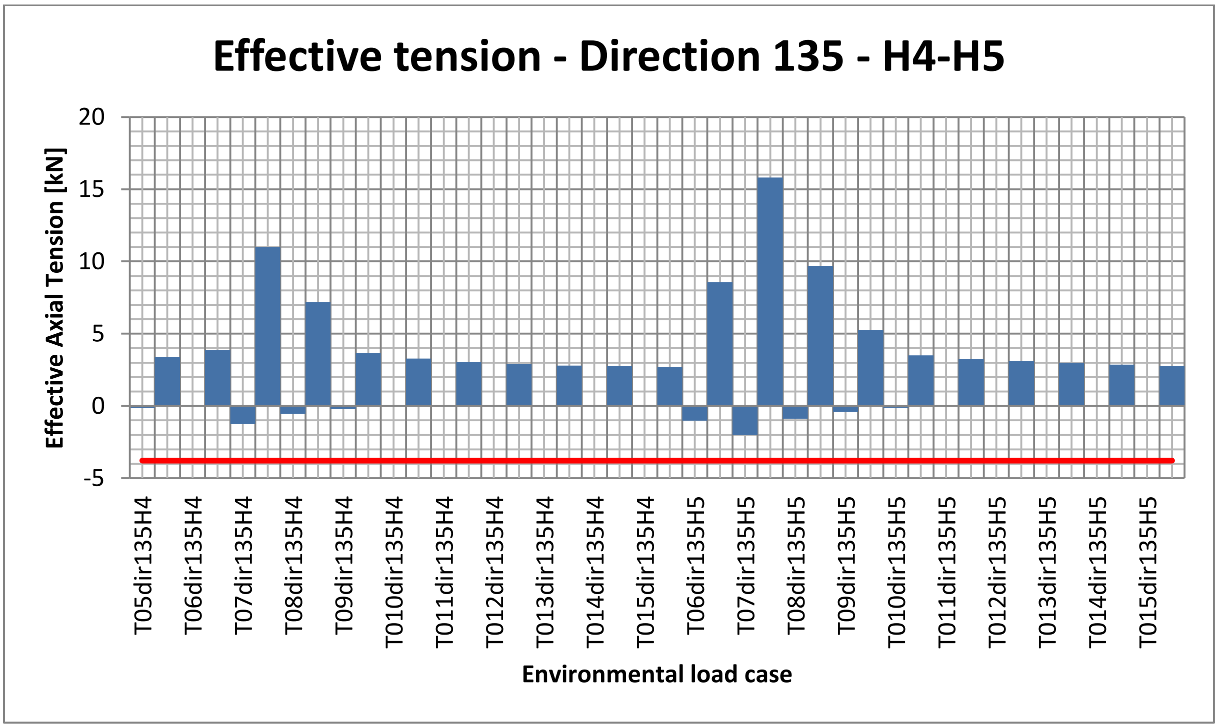

Figure C. 56 - 4” Bunkerflex STH – Lazy wave – 40 m floatation point – Effective tension – Direction 135° - H4-H5

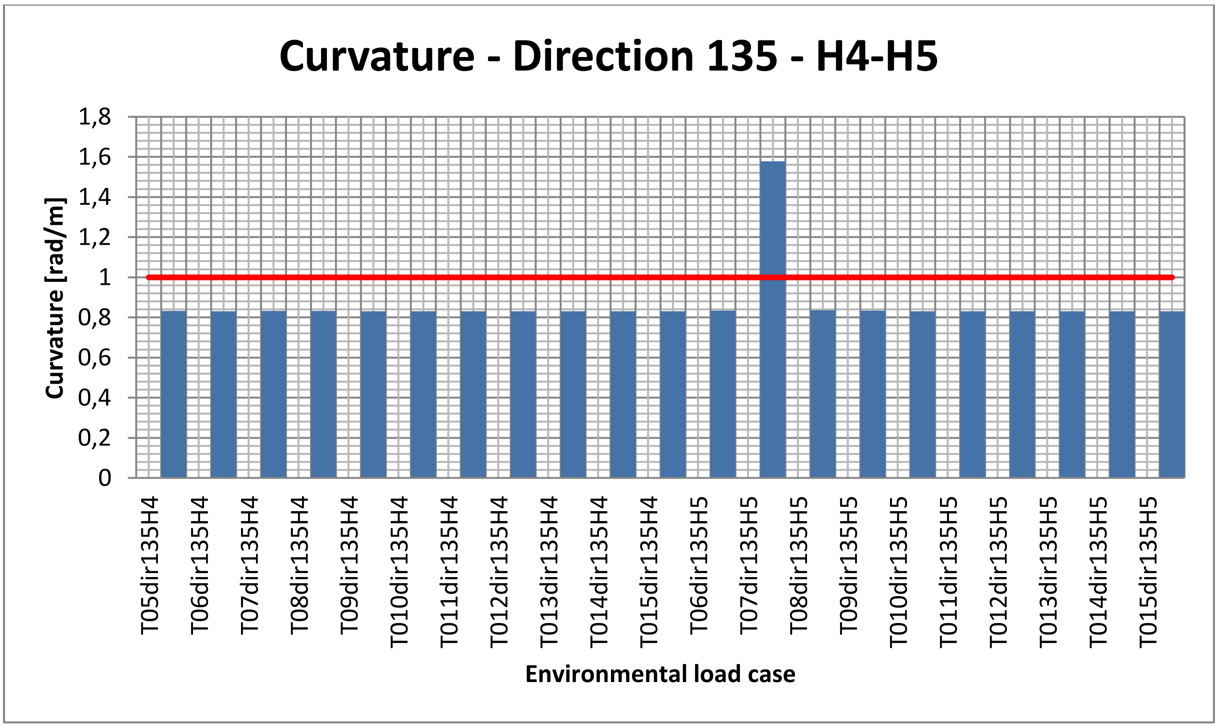

Figure C. 57 - 4” Bunkerflex STH – Lazy wave – 40 m floatation point – Curvature – Direction 135° - H4-H5

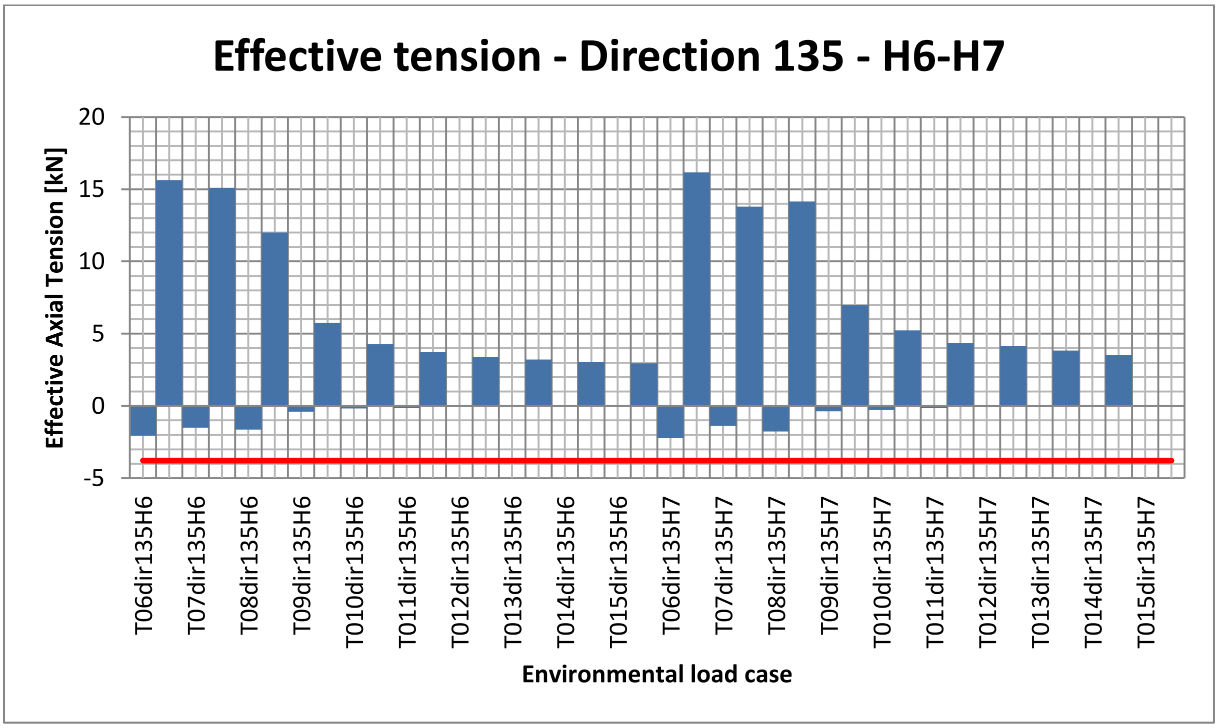

Figure C. 58 - 4” Bunkerflex STH – Lazy wave – 40 m floatation point – Effective tension – Direction 135° - H6-H7

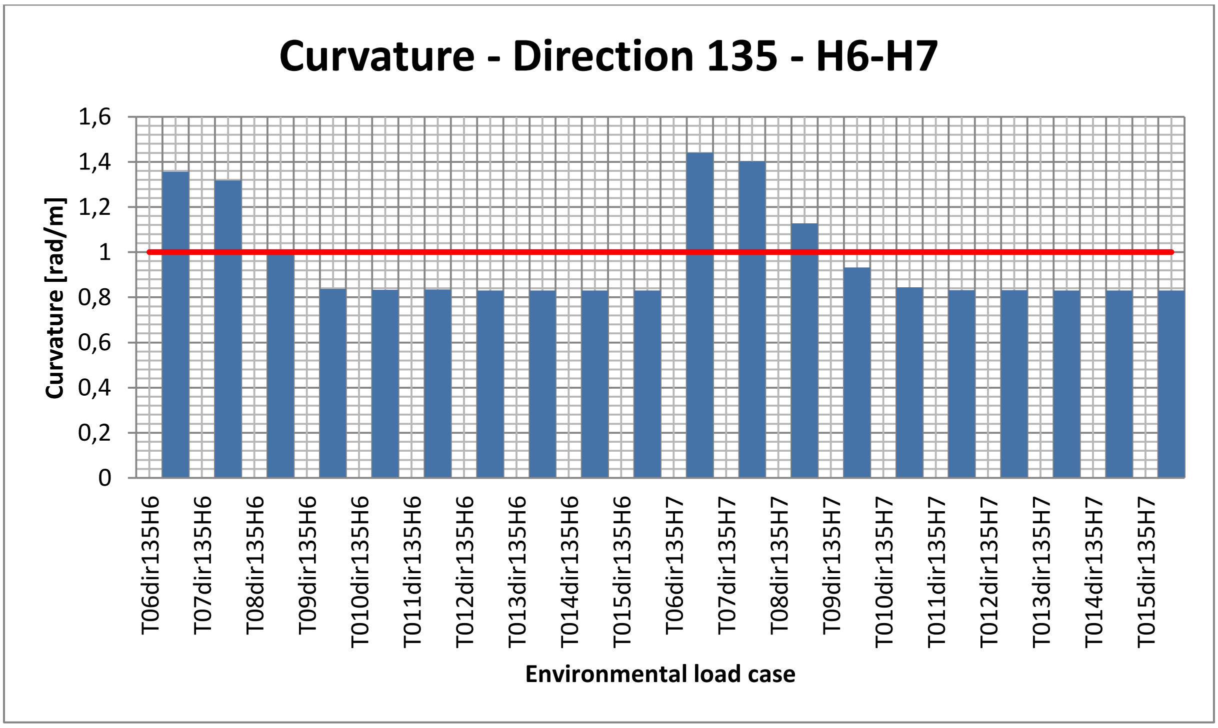

Figure C. 59 - 4” Bunkerflex STH – Lazy wave – 40 m floatation point – Curvature – Direction 135° - H6-H7

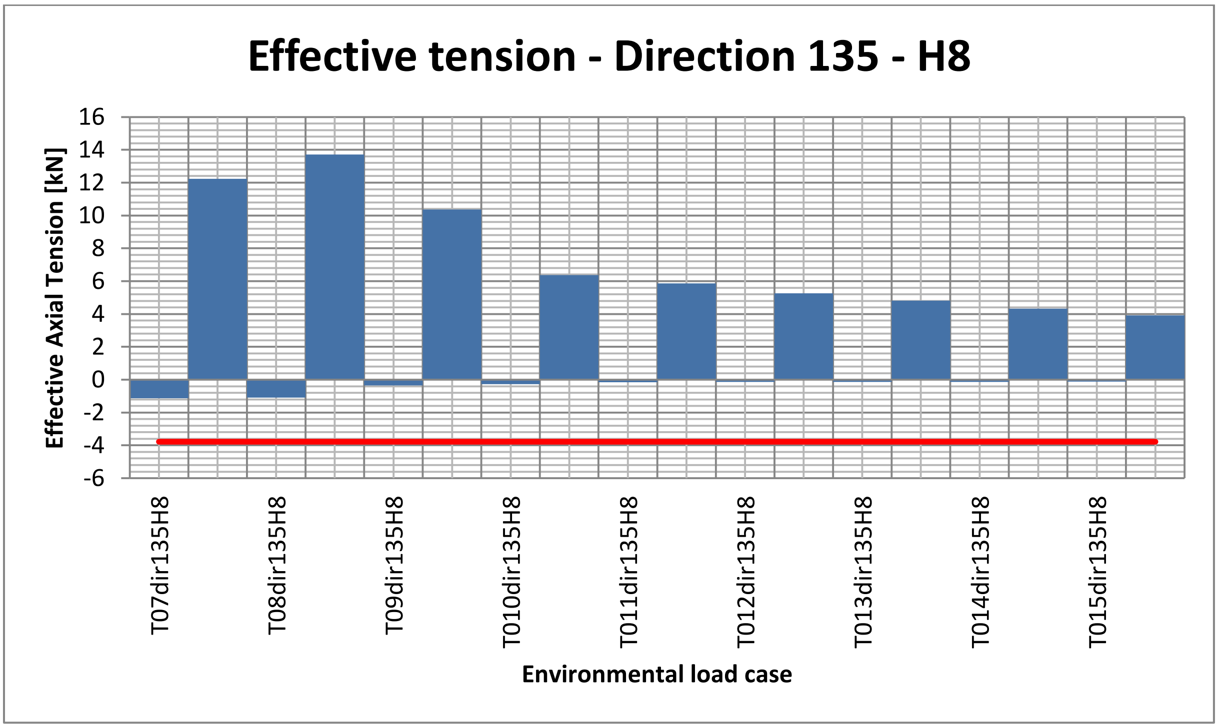

Figure C. 60 - 4” Bunkerflex STH – Lazy wave – 40 m floatation point – Effective tension – Direction 135° - H8

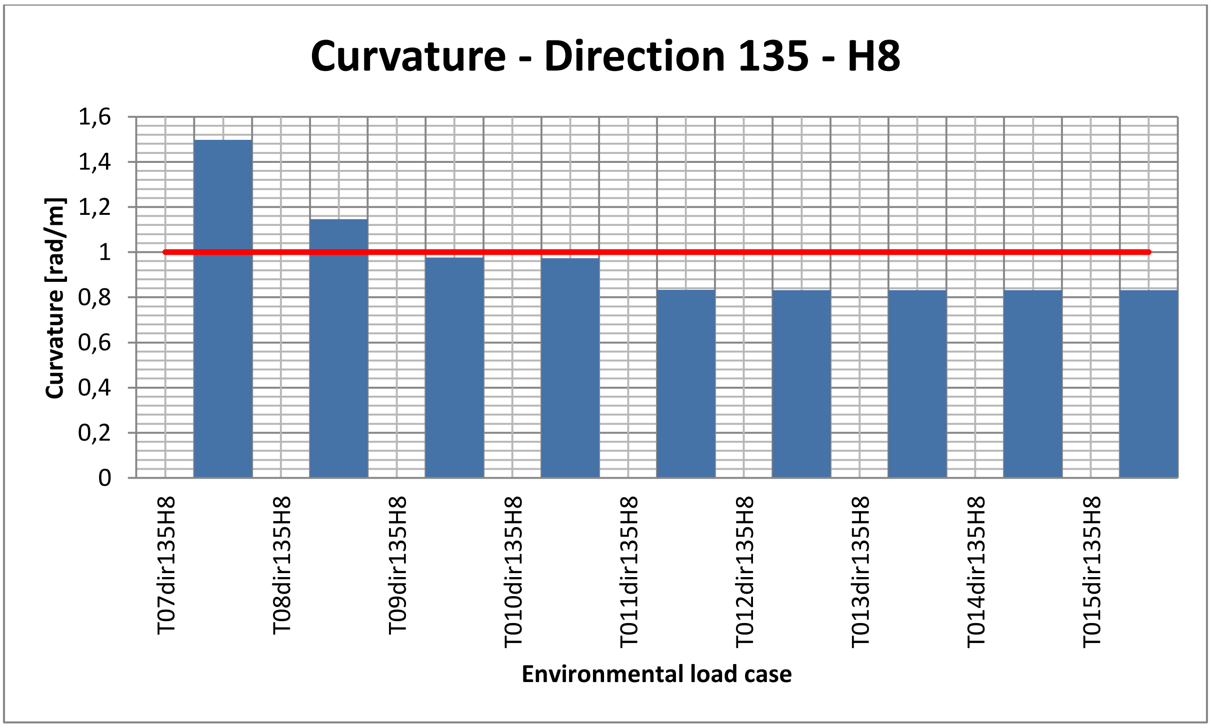

Figure C. 61 - 4” Bunkerflex STH – Lazy wave – 40 m floatation point – Curvature – Direction 135° - H8

Direction 180°

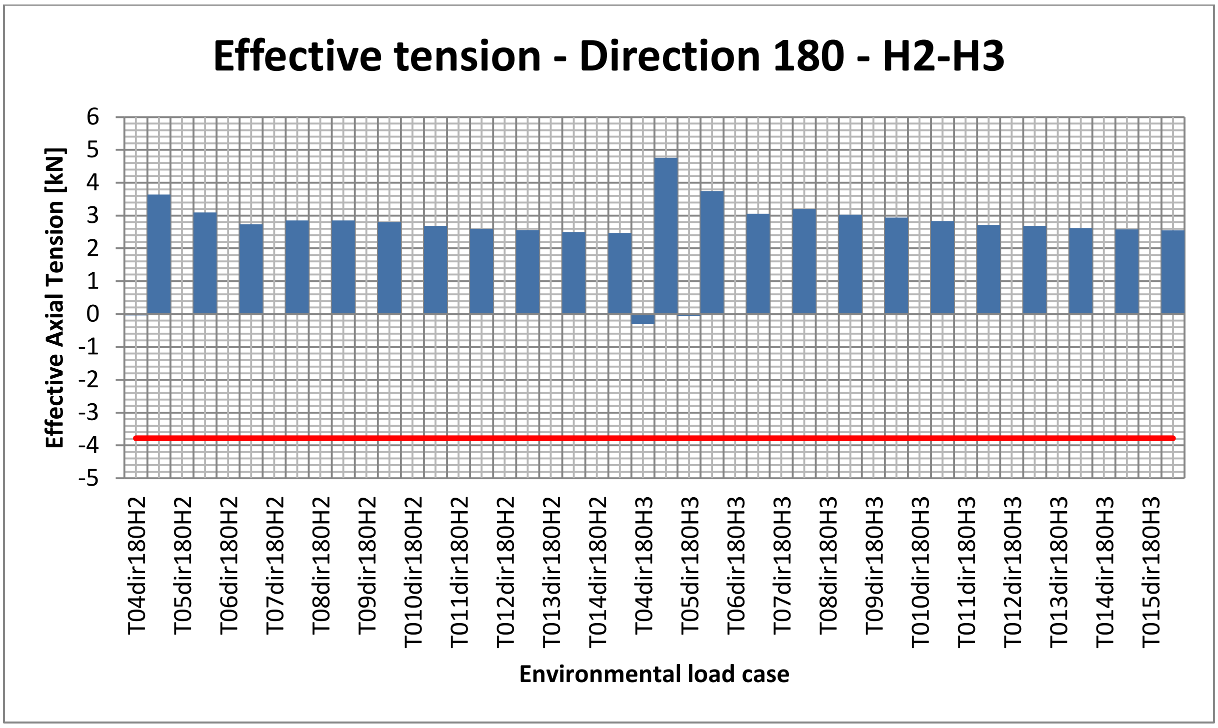

Figure C. 62 - 4" Bunkerflex STH – Lazy wave – 40 m floatation point – Effective tension – Direction 180° - H2-H3

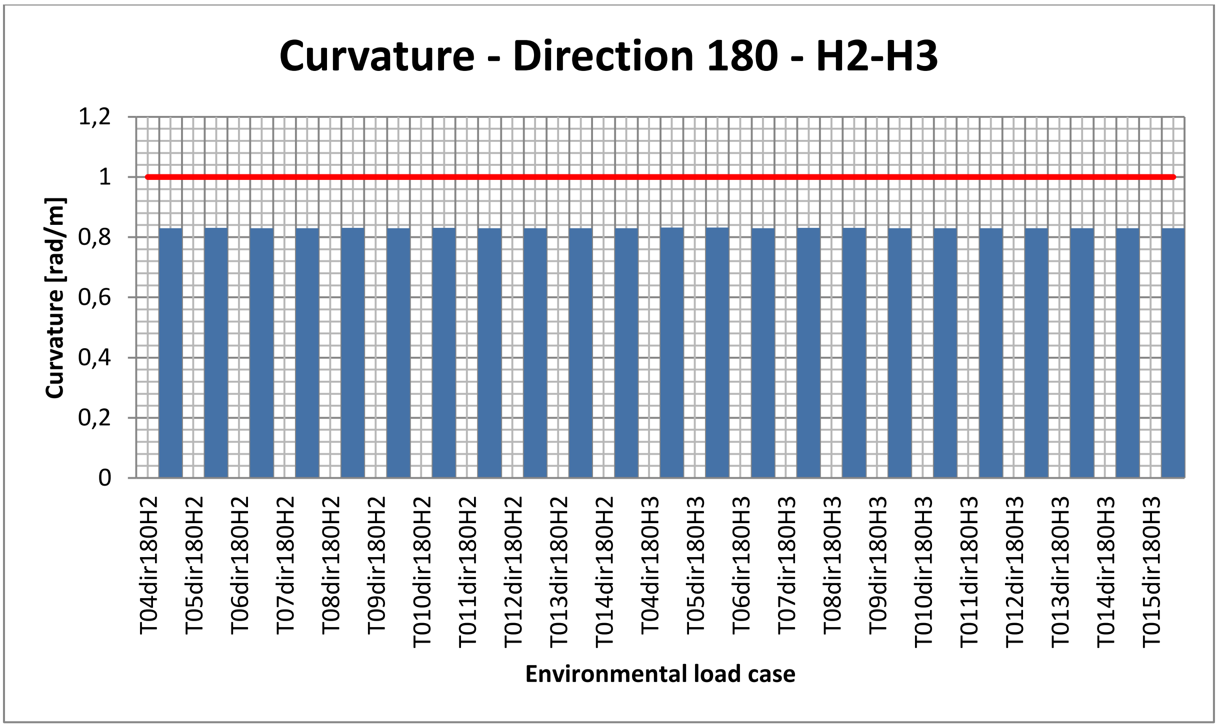

Figure C. 63 - 4" Bunkerflex STH – Lazy wave – 40 m floatation point – Curvature – Direction 180° - H2-H3

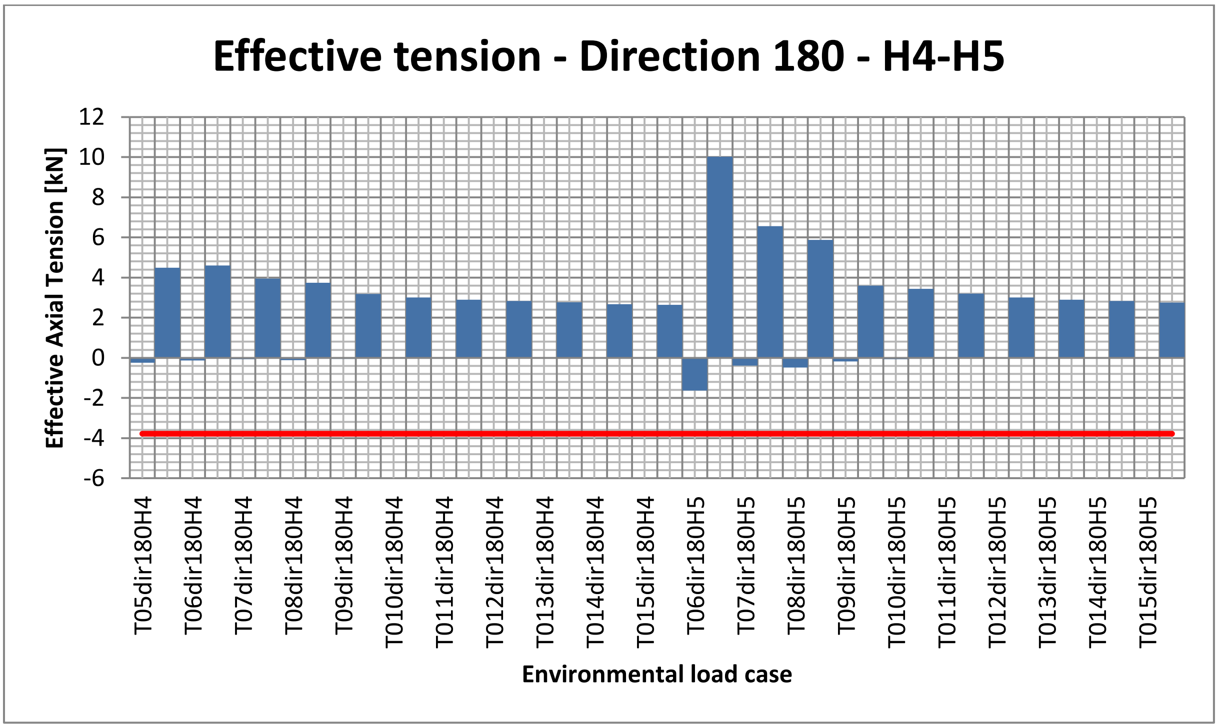

Figure C. 64 - 4” Bunkerflex STH – Lazy wave – 40 m floatation point – Effective tension – Direction 180° - H4-H5

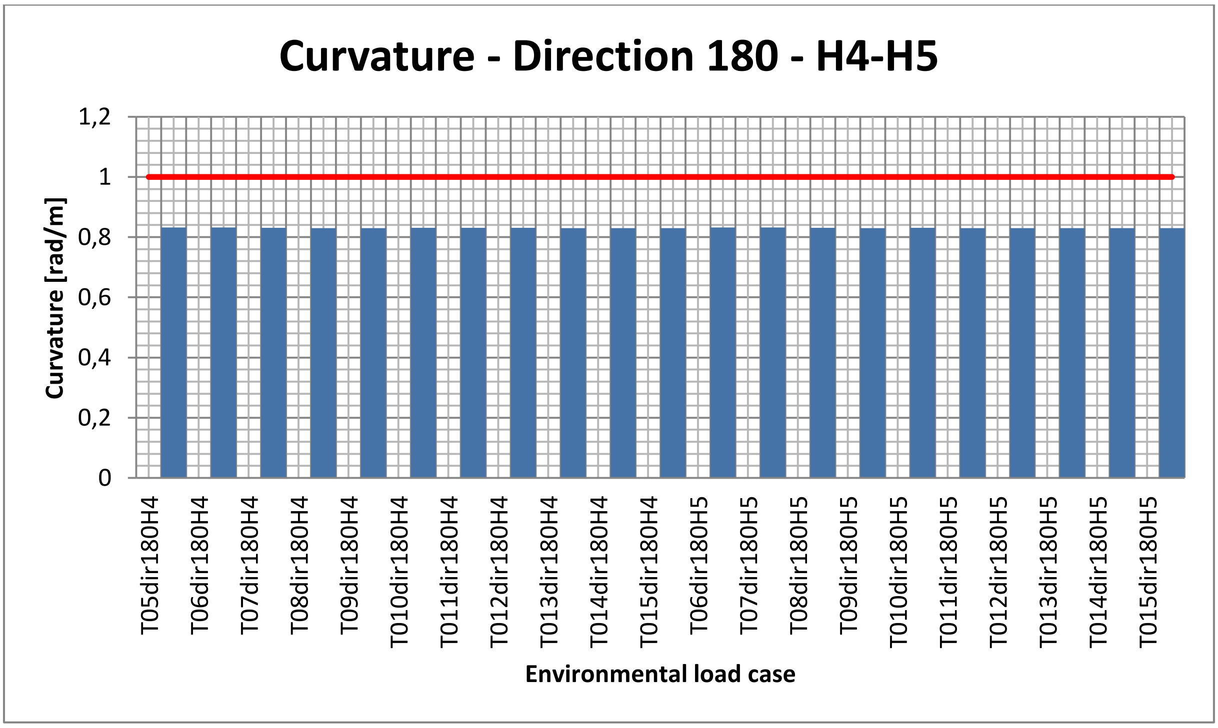

Figure C. 65 - 4” Bunkerflex STH – Lazy wave – 40 m floatation point – Curvature – Direction 180° - H4-H5

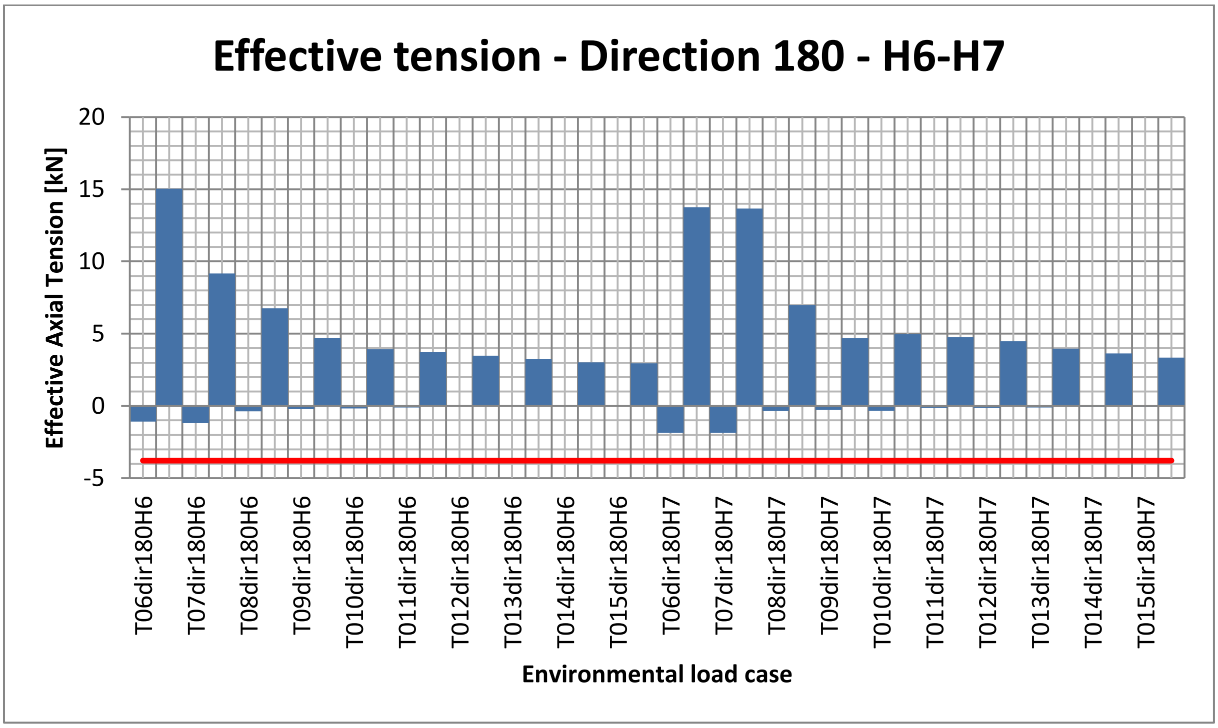

Figure C. 66 - 4" Bunkerflex STH – Lazy wave – 40 m floatation point – Effective tension – Direction 180° - H6-H7

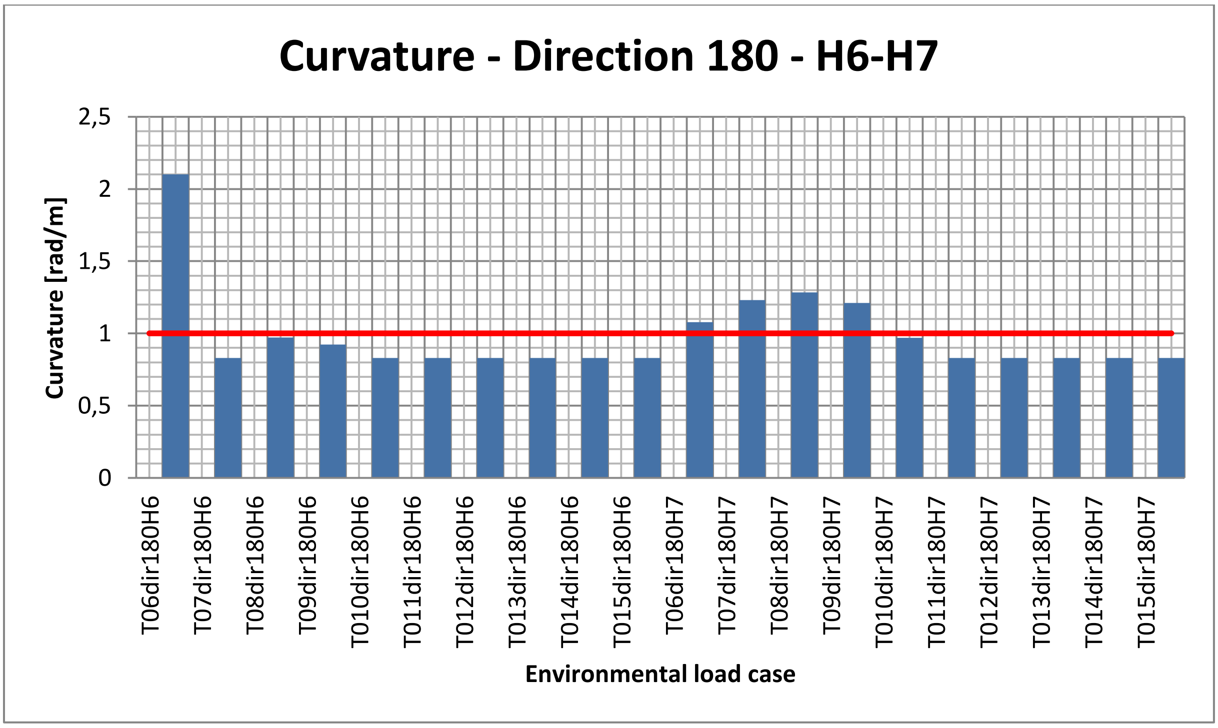

Figure C. 67 - 4" Bunkerflex STH – Lazy wave – 40 m floatation point – Curvature – Direction 180° - H6-H7

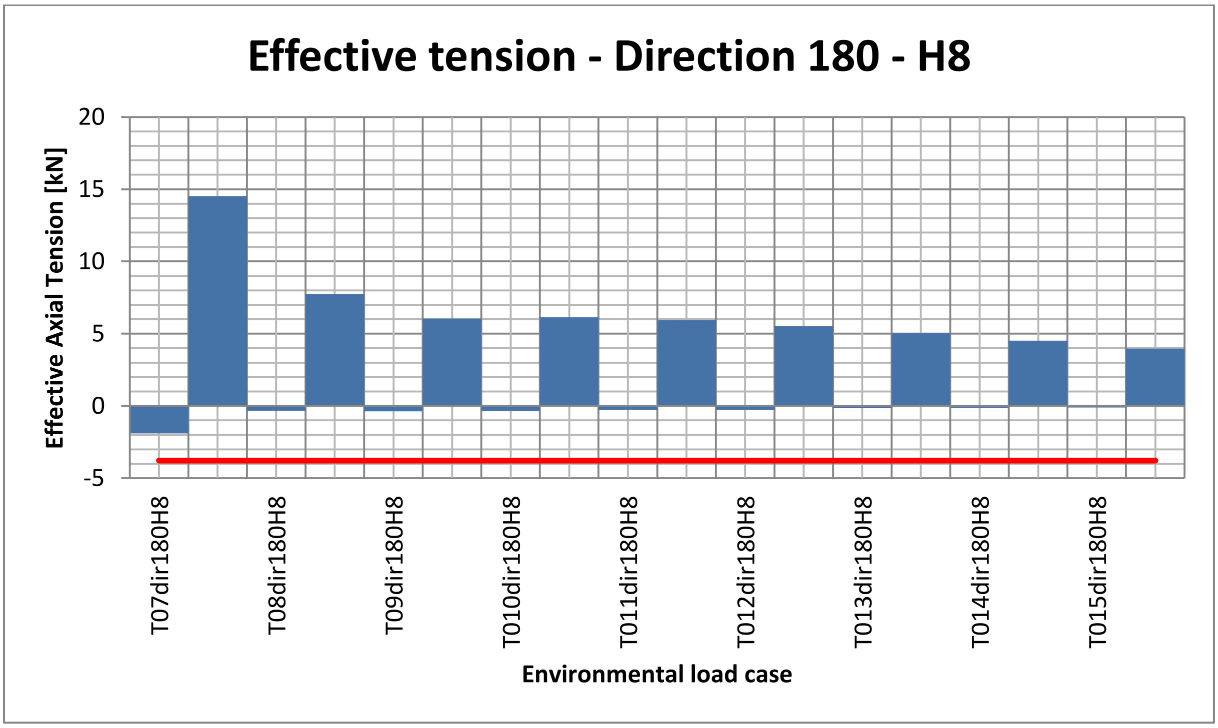

Figure C. 68 - 4" Bunkerflex STH – Lazy wave – 40 m floatation point – Effective tension – Direction 180° - H8

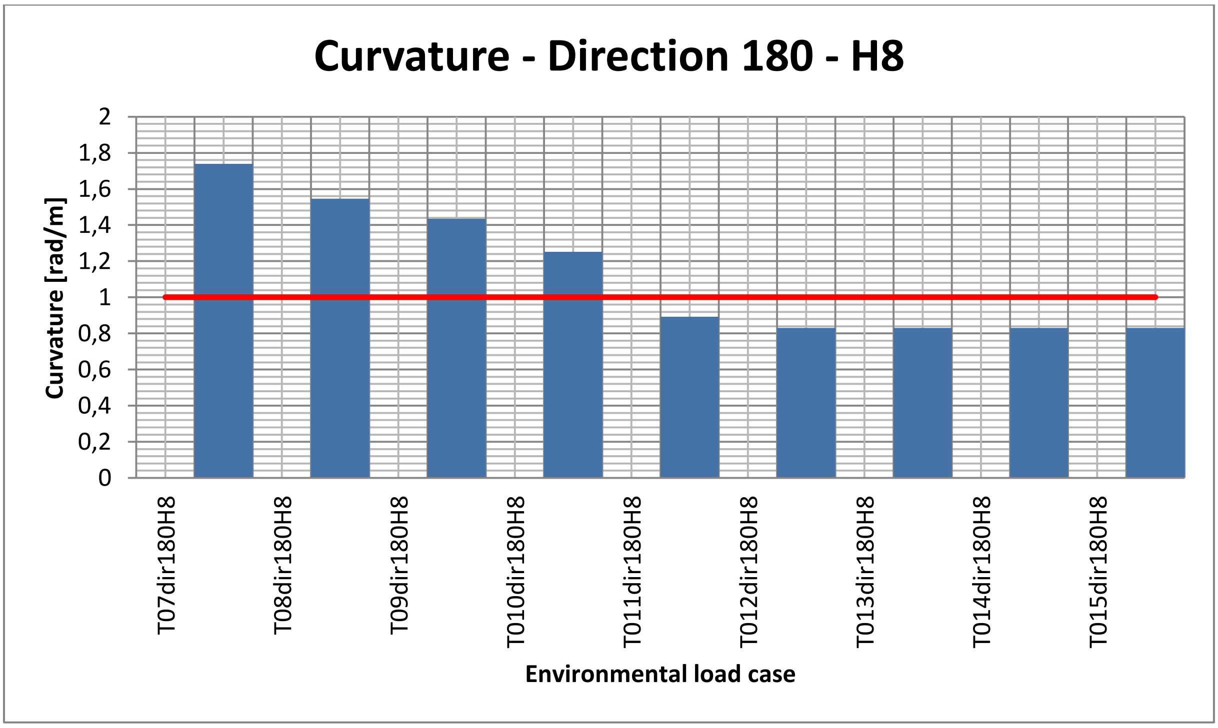

Figure C. 69 - 4" Bunkerflex STH – Lazy wave – 40 m floatation point – Curvature – Direction 180° - H8

Direction 225°

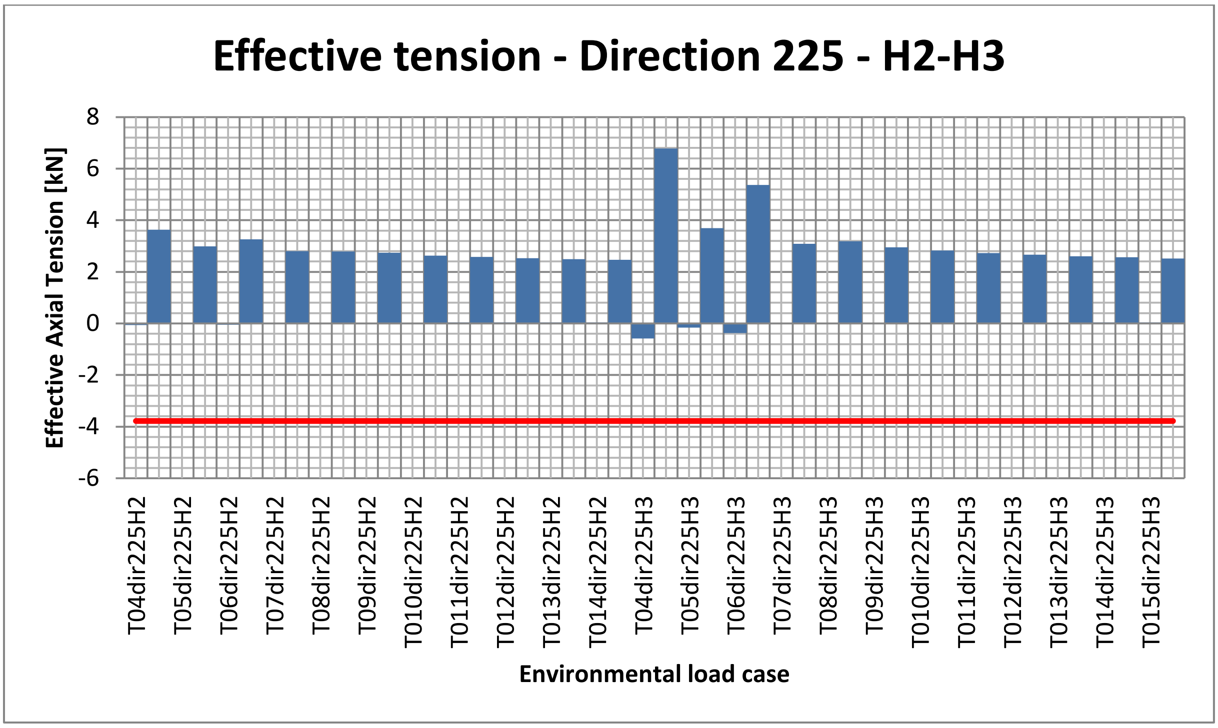

Figure C. 70 - 4” Bunkerflex STH – Lazy wave – 40 m floatation point – Effective tension – Direction 225° - H2-H3

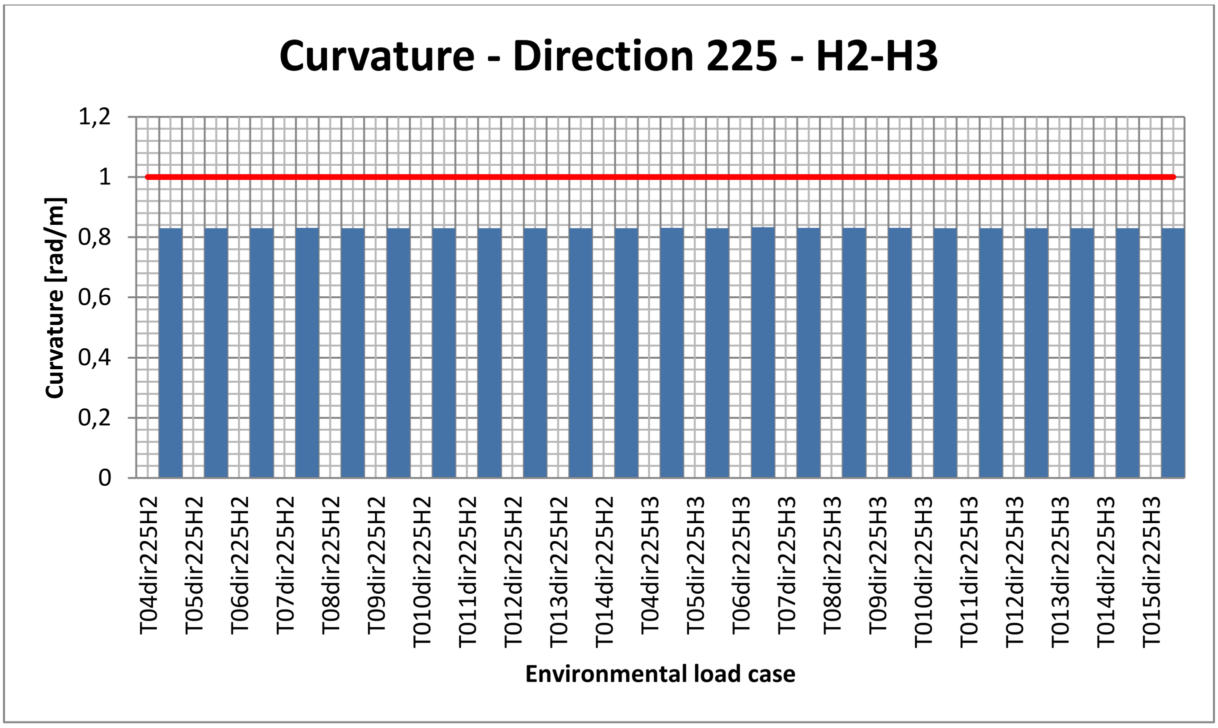

Figure C. 71 - 4” Bunkerflex STH – Lazy wave – 40 m floatation point – Curvature – Direction 225° - H2-H3

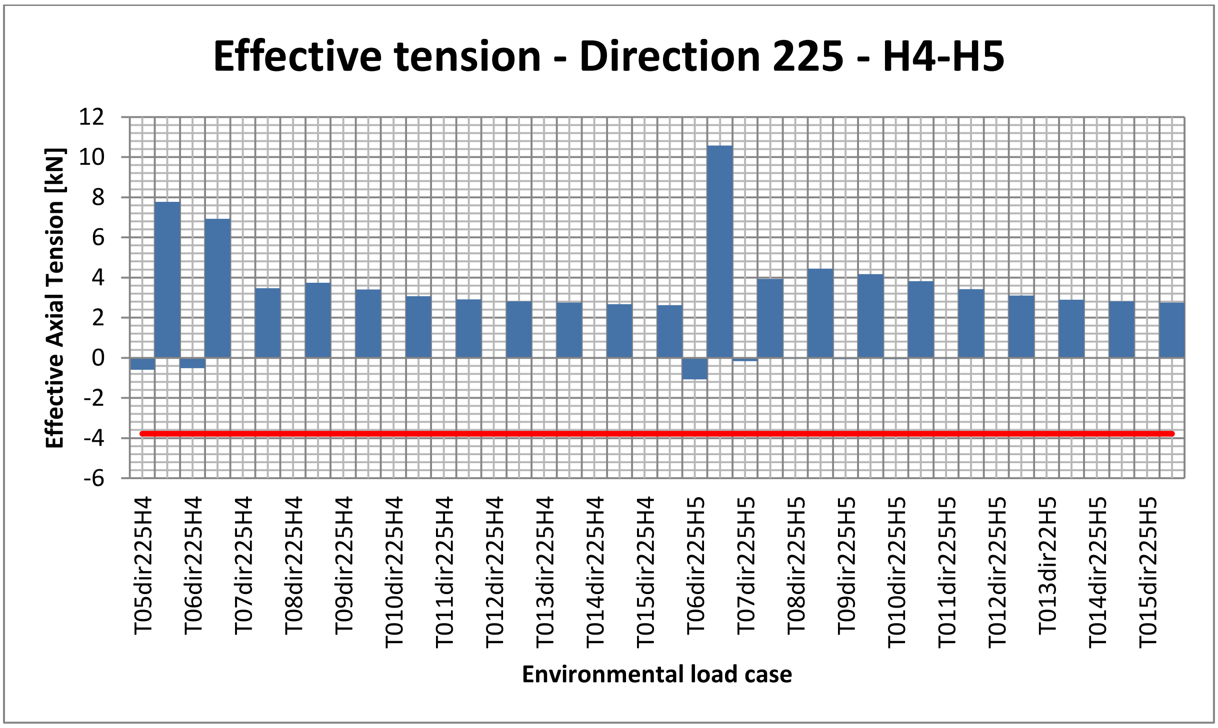

Figure C. 72 - 4” Bunkerflex STH – Lazy wave – 40 m floatation point – Effective tension – Direction 225° - H4-H5

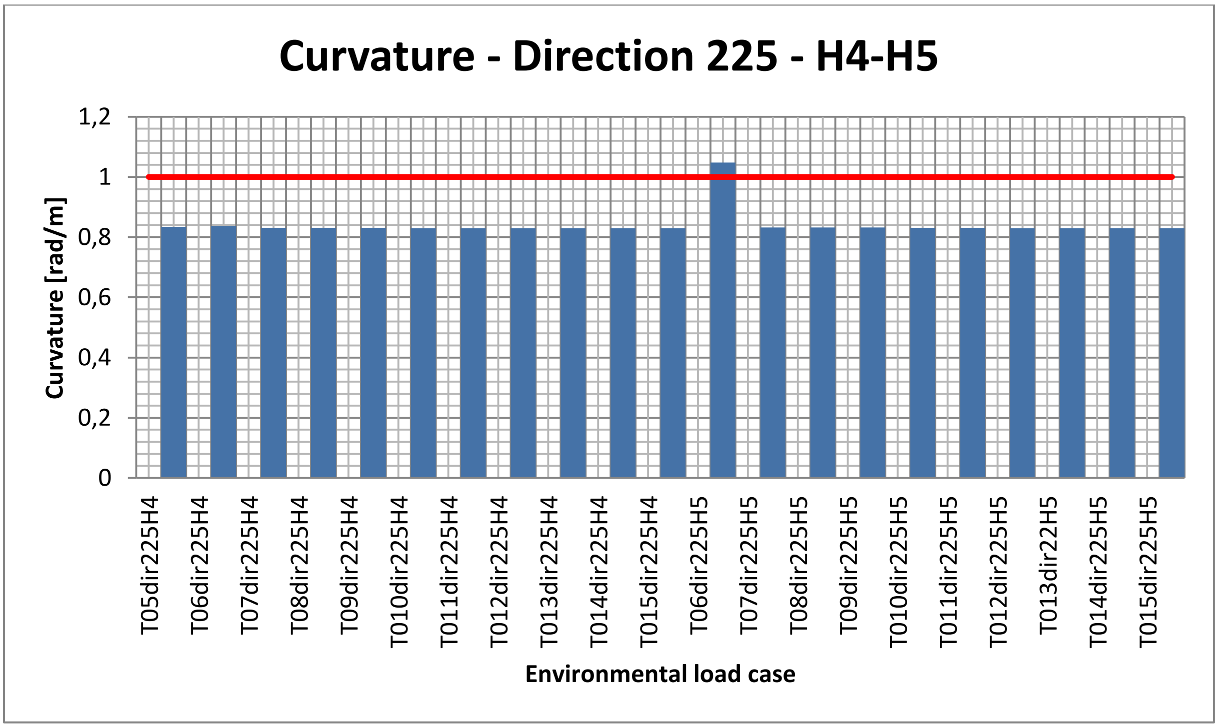

Figure C. 73 - 4” Bunkerflex STH – Lazy wave – 40 m floatation point – Curvature – Direction 225° - H4-H5

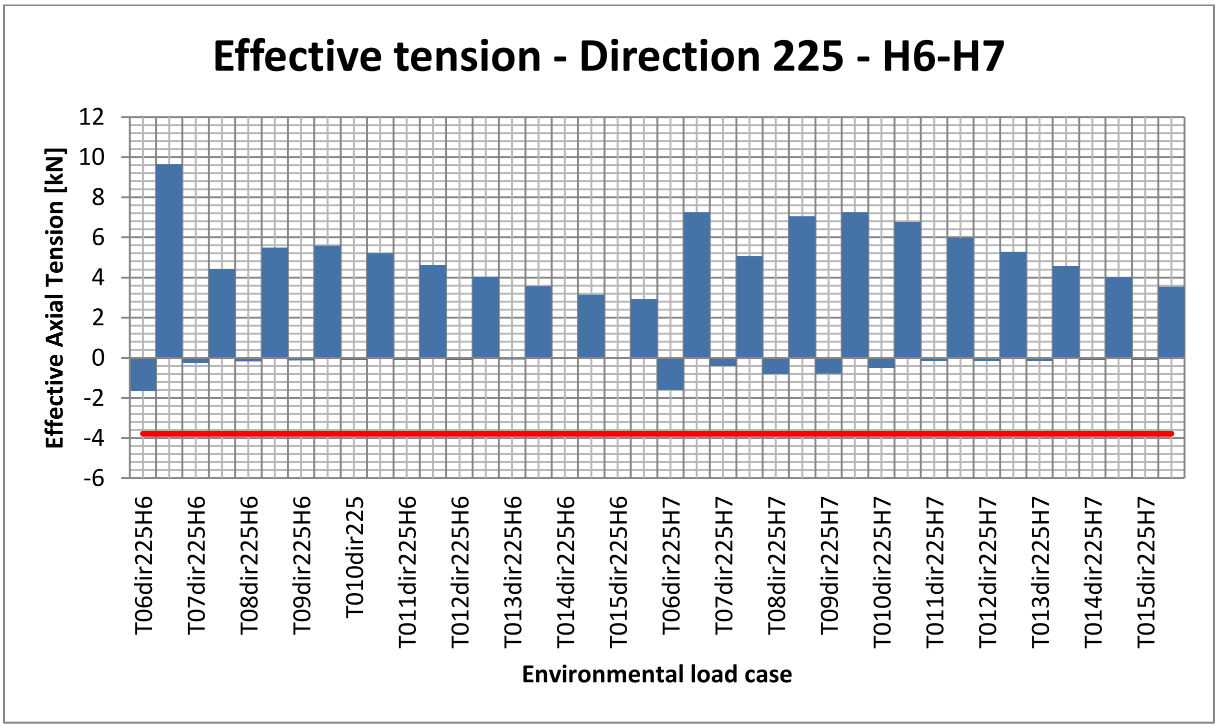

Figure C. 74 - 4” Bunkerflex STH – Lazy wave – 40 m floatation point – Effective tension – Direction 225° - H6-H7

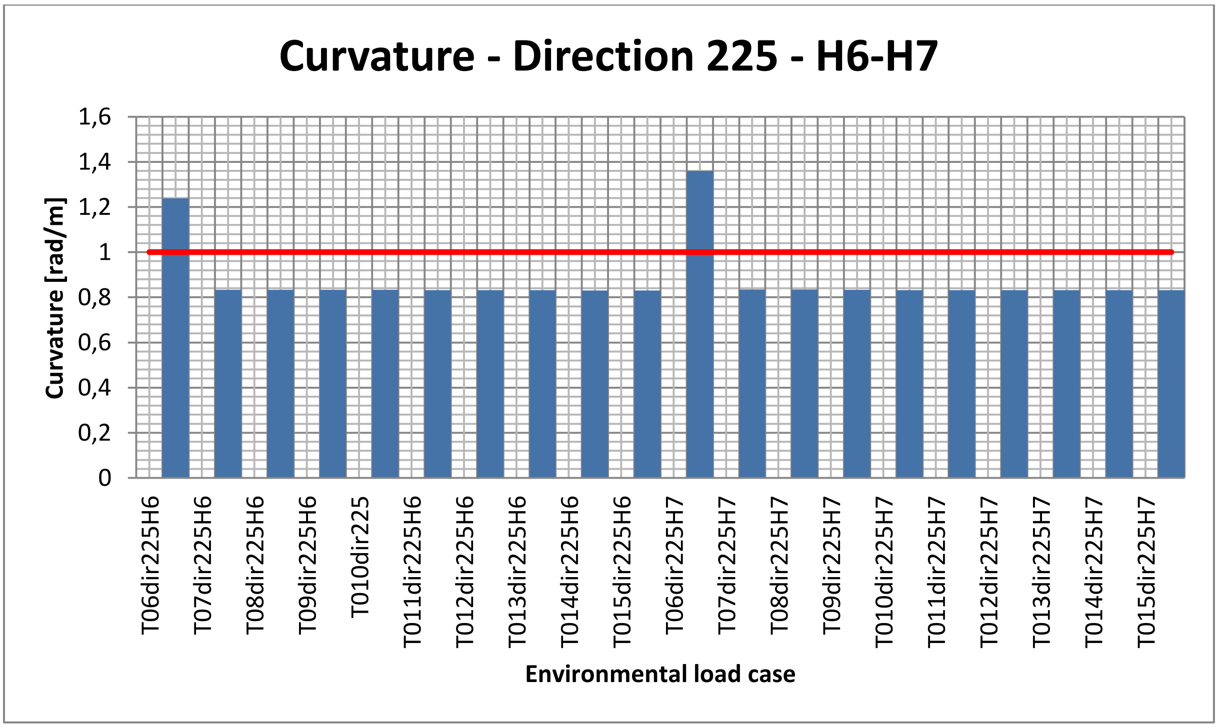

Figure C. 75 - 4” Bunkerflex STH – Lazy wave – 40 m floatation point – Curvature – Direction 225° - H6-H7

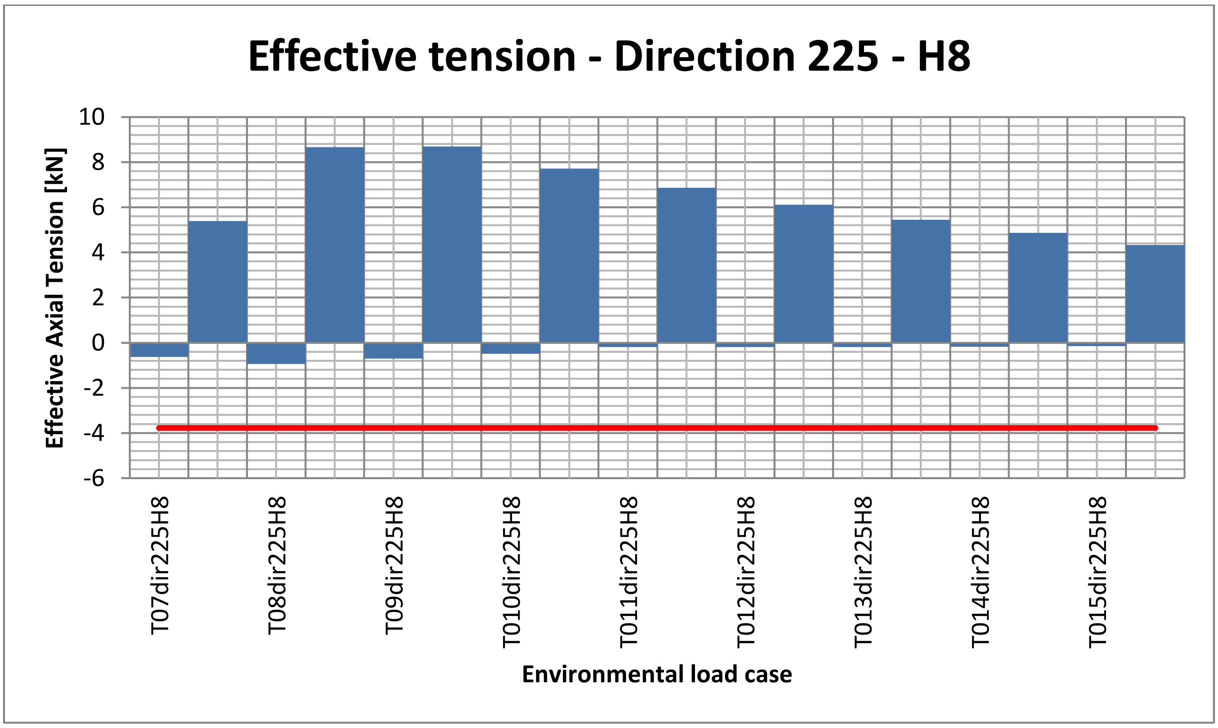

Figure C. 76 - 4” Bunkerflex STH – Lazy wave – 40 m floatation point – Effective tension – Direction 225° - H8

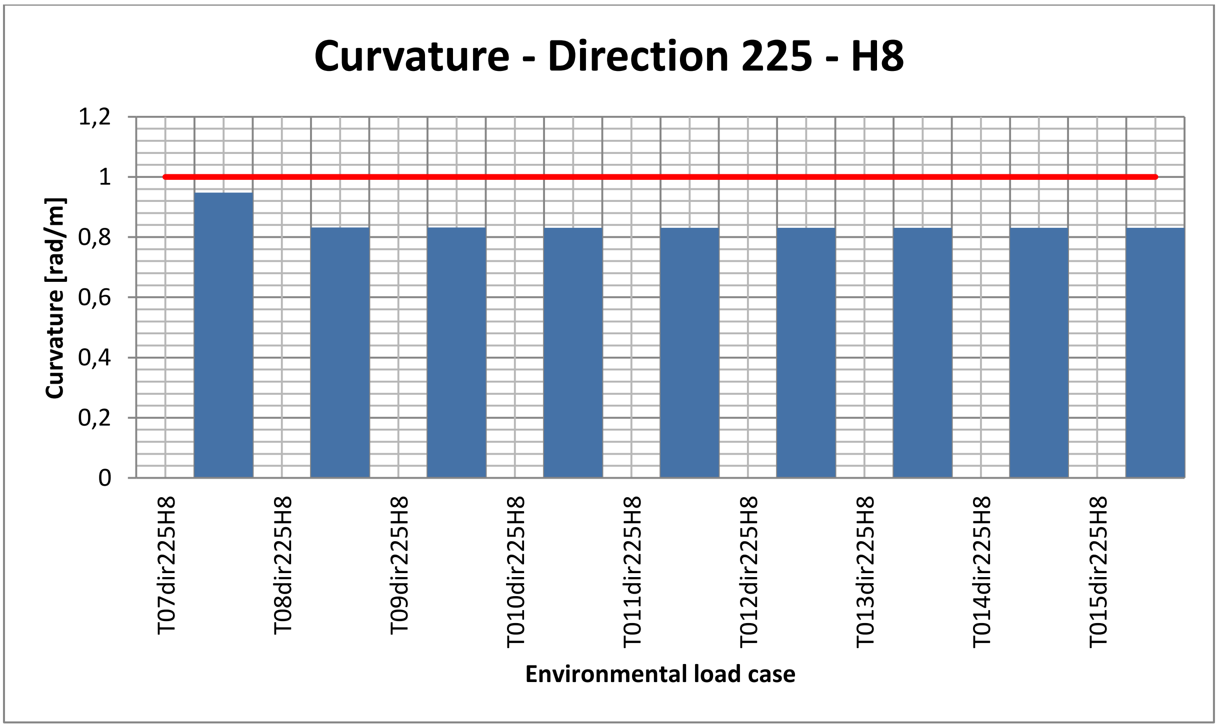

Figure C. 77 - 4” Bunkerflex STH – Lazy wave – 40 m floatation point – Curvature – Direction 225° - H8

Wave rose

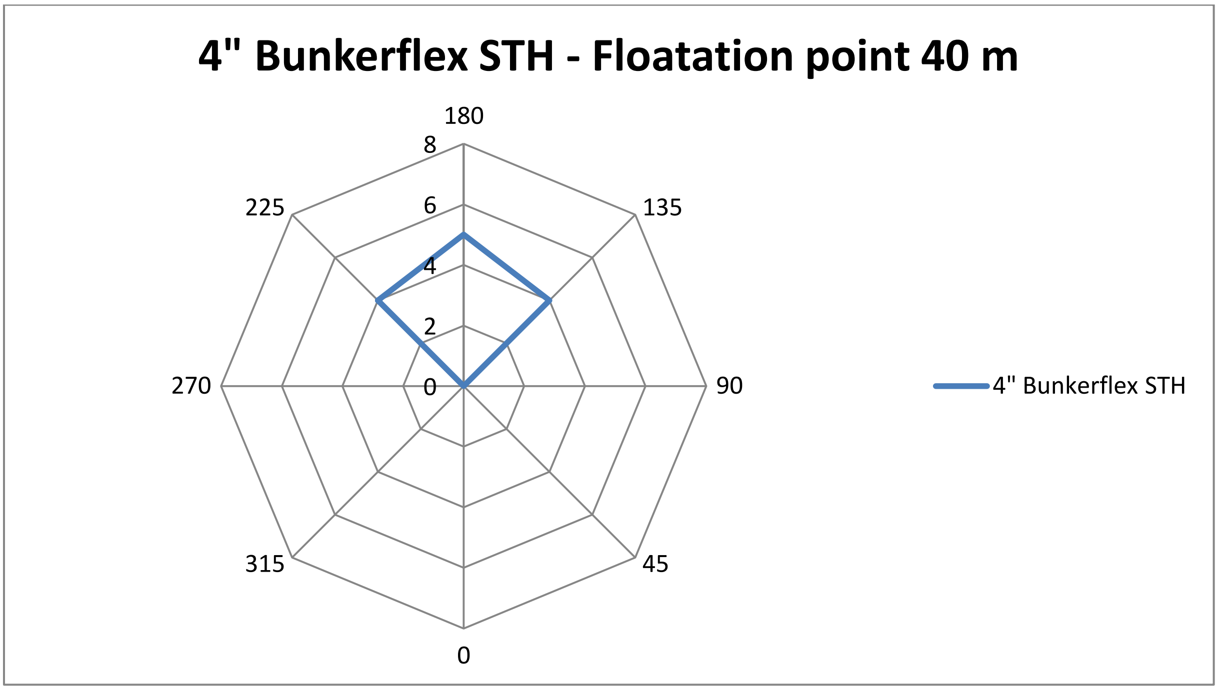

Figure C. 78 - 4” Bunkerflex STH – Lazy wave – 40 m floatation point – Wave rose

Limitation plot

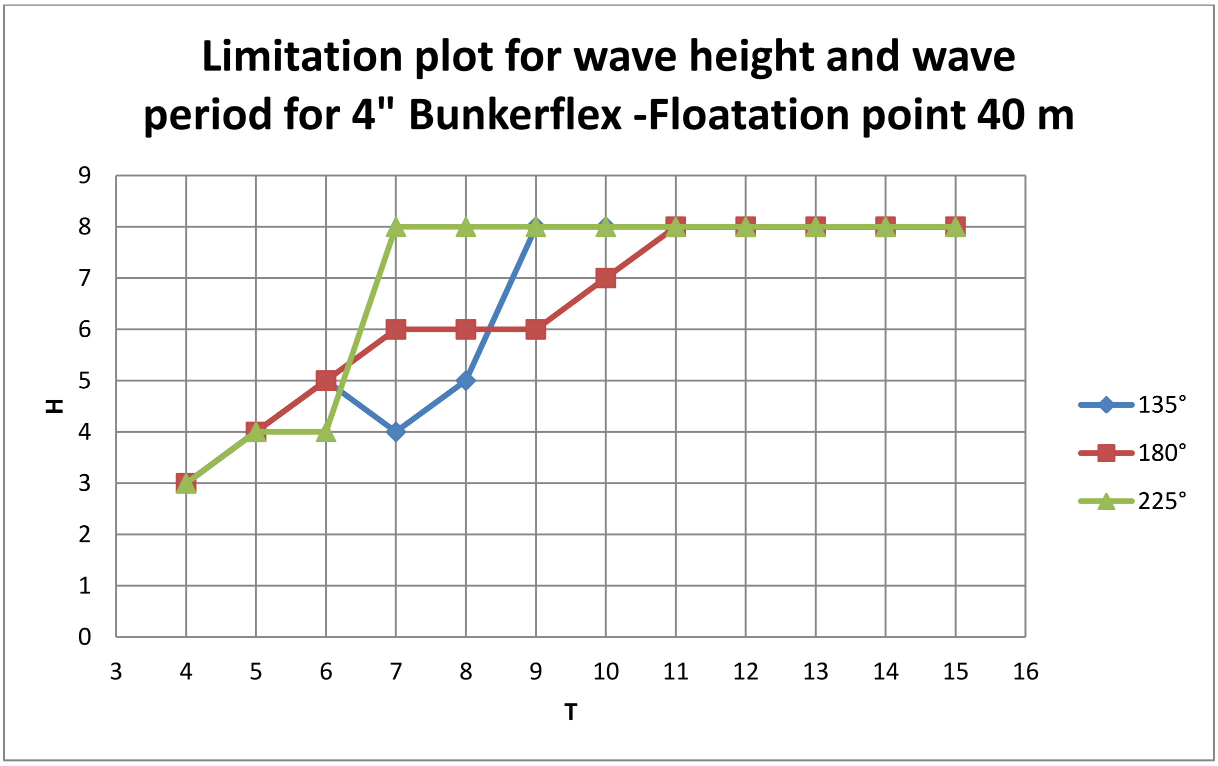

Figure C. 79 - 4” Bunkerflex STH – Lazy wave – 40 m floatation point – Limitation plot

Lazy wave – 60 m floatation point

Direction 135°

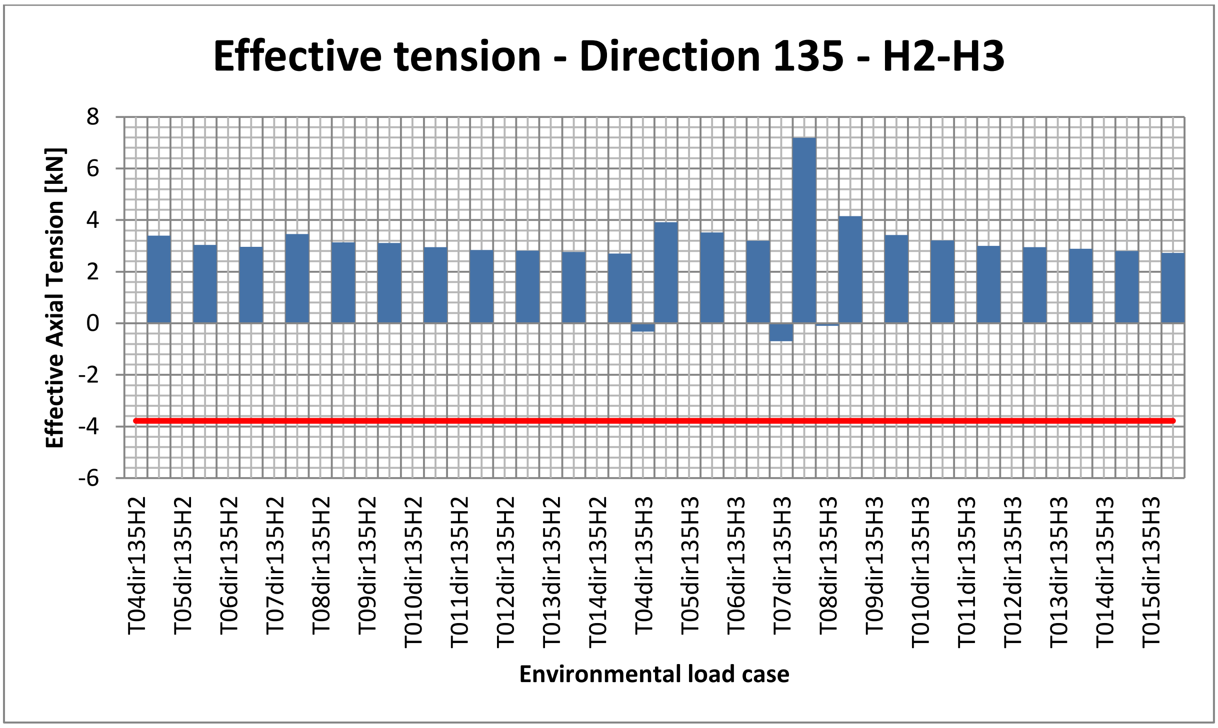

Figure C. 80 - 4” Bunkerflex STH – Lazy wave – 60 m floatation point – Effective tension – Direction 135° - H2-H3

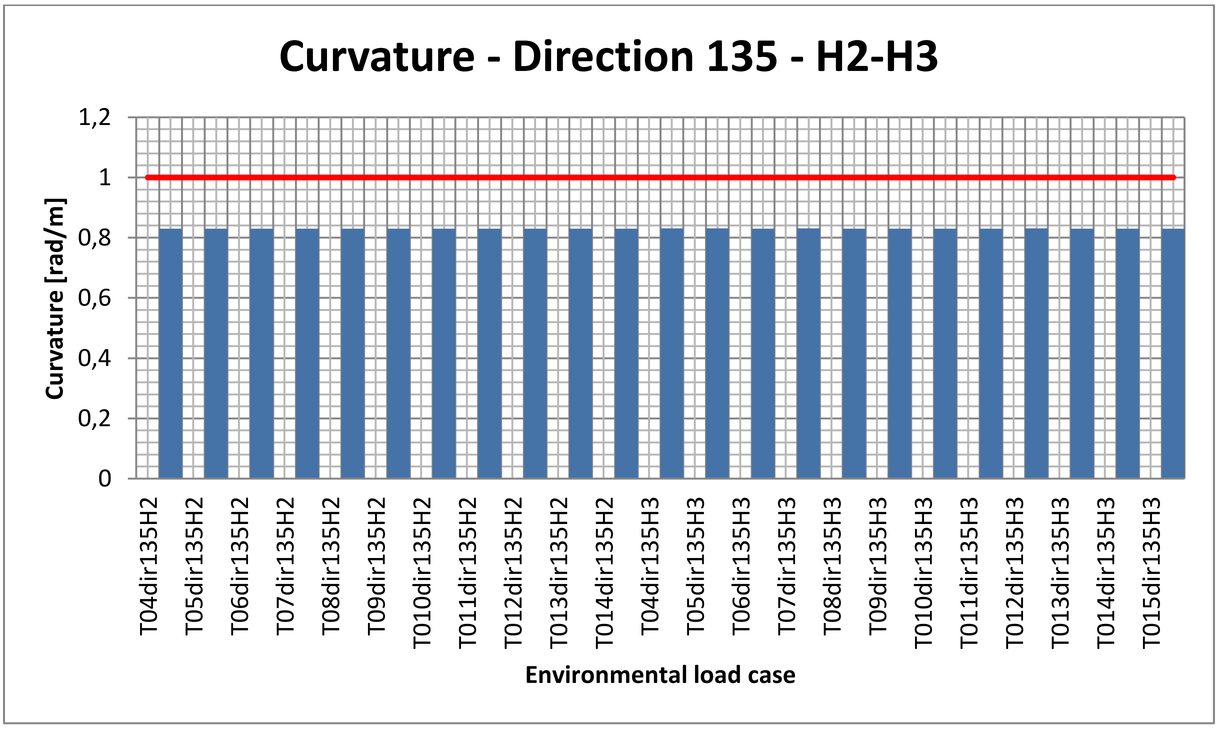

Figure C. 81 - 4” Bunkerflex STH – Lazy wave – 60 m floatation point – Curvature – Direction 135° - H2-H3

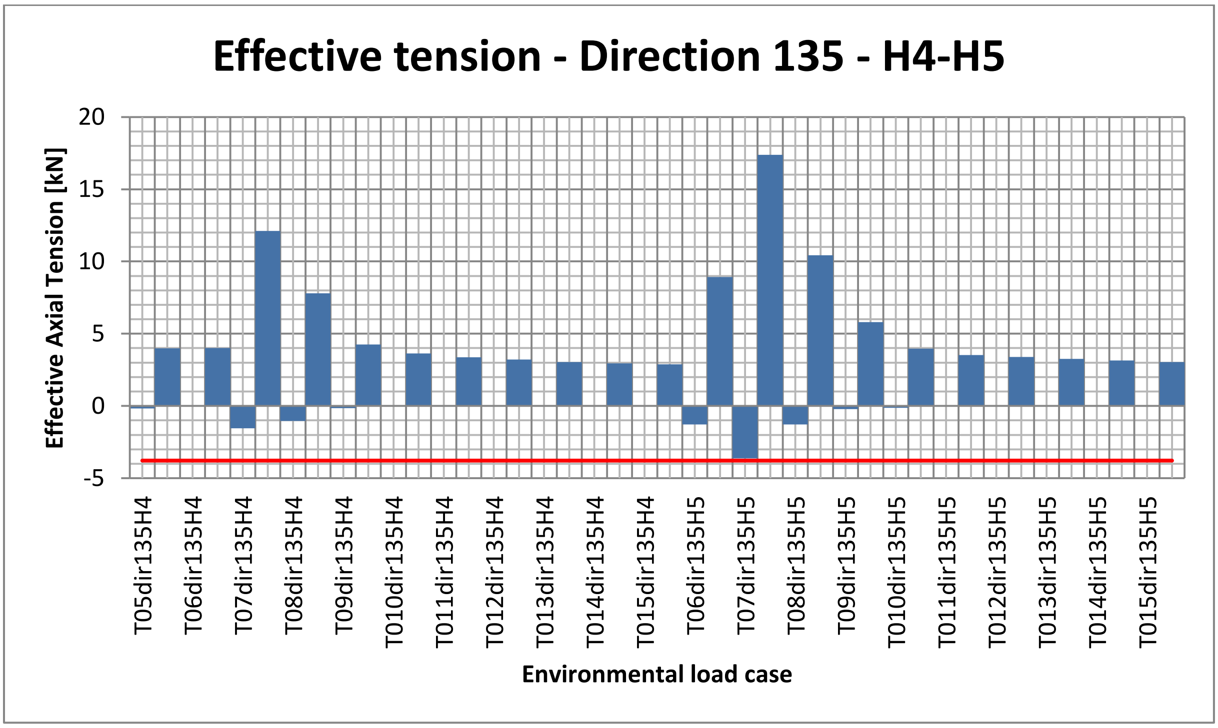

Figure C. 82 - 4” Bunkerflex STH – Lazy wave – 60 m floatation point – Effective tension – Direction 135° - H4-H5

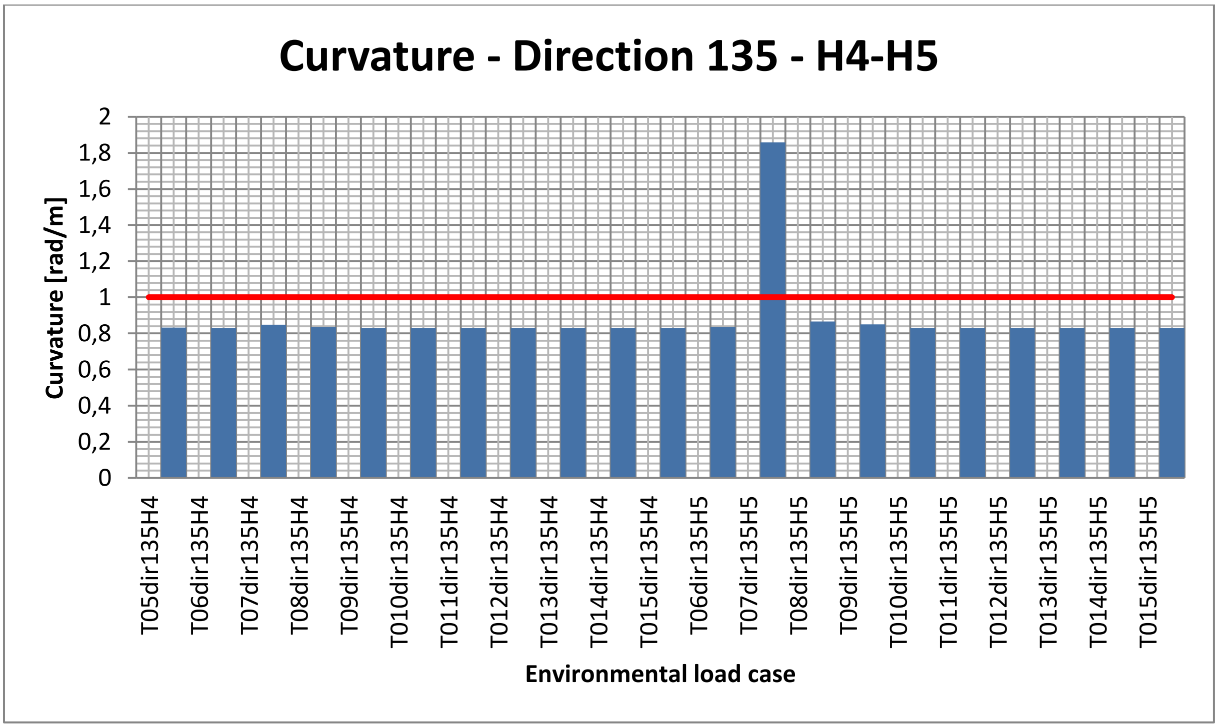

Figure C. 83 - 4” Bunkerflex STH – Lazy wave – 60 m floatation point – Curvature – Direction 135° - H4-H5

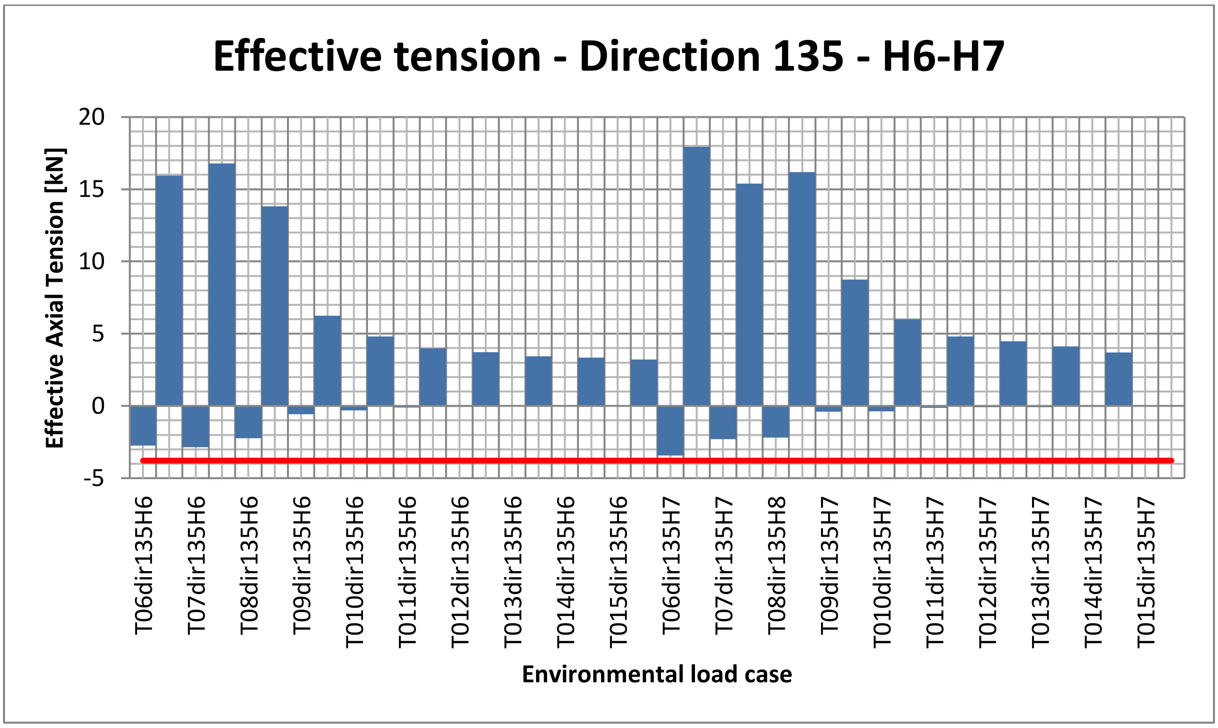

Figure C. 84 - 4" Bunkerflex STH – Lazy wave – 60 m floatation point – Effective tension – Direction 135° - H6-H7

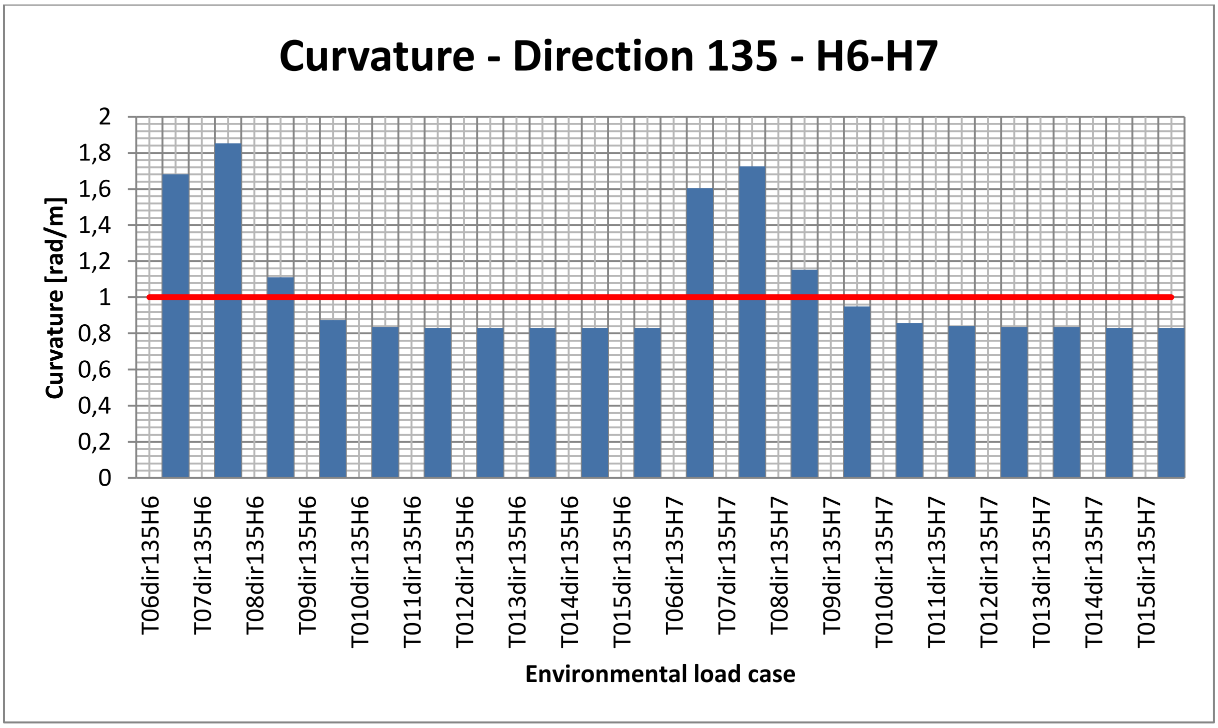

Figure C. 85 - 4" Bunkerflex STH – Lazy wave – 60 m floatation point – Curvature – Direction 135° - H6-H7

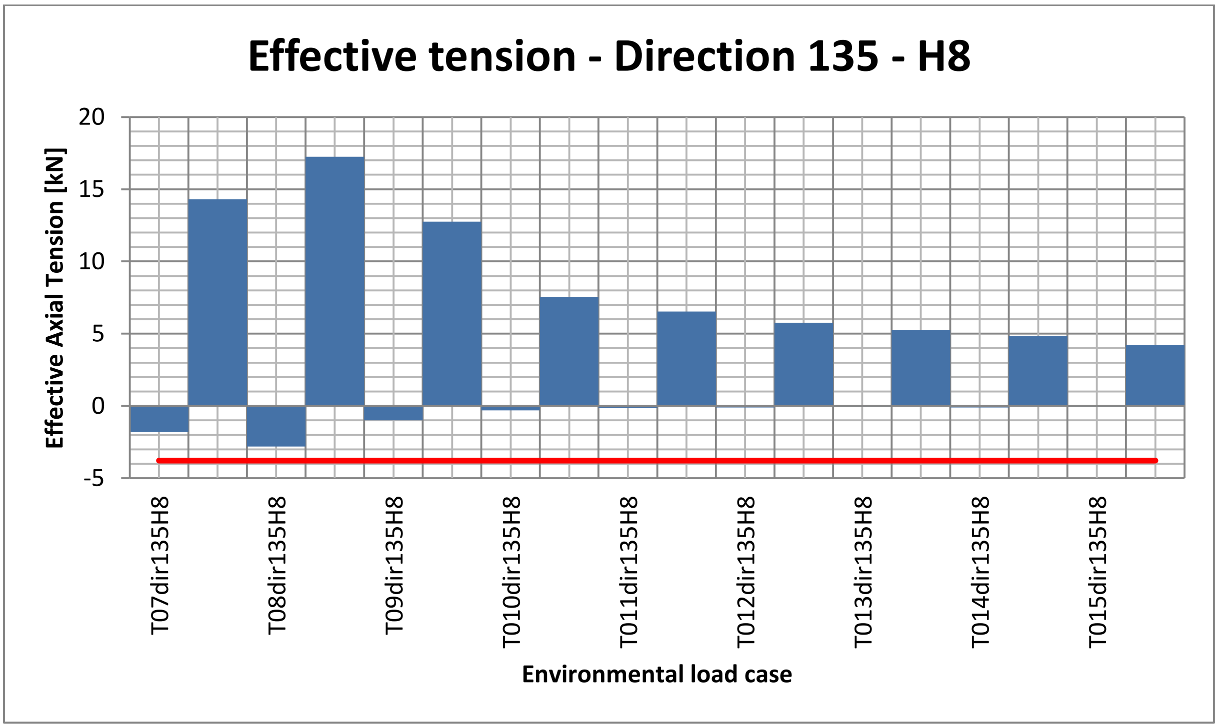

Figure C. 86 - 4” Bunkerflex STH – Lazy wave – 60 m floatation point – Effective tension – Direction 135° - H8

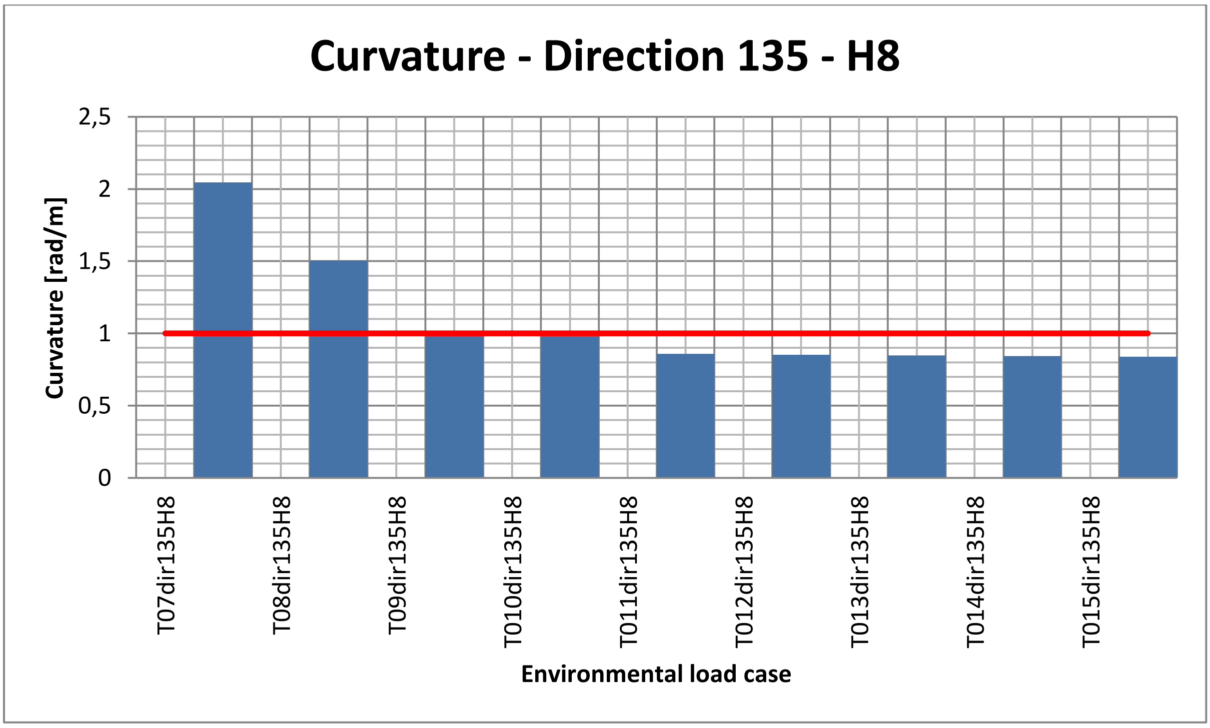

Figure C. 87 - 4” Bunkerflex STH – Lazy wave – 60 m floatation point – Curvature – Direction 135° - H8

Direction 180°

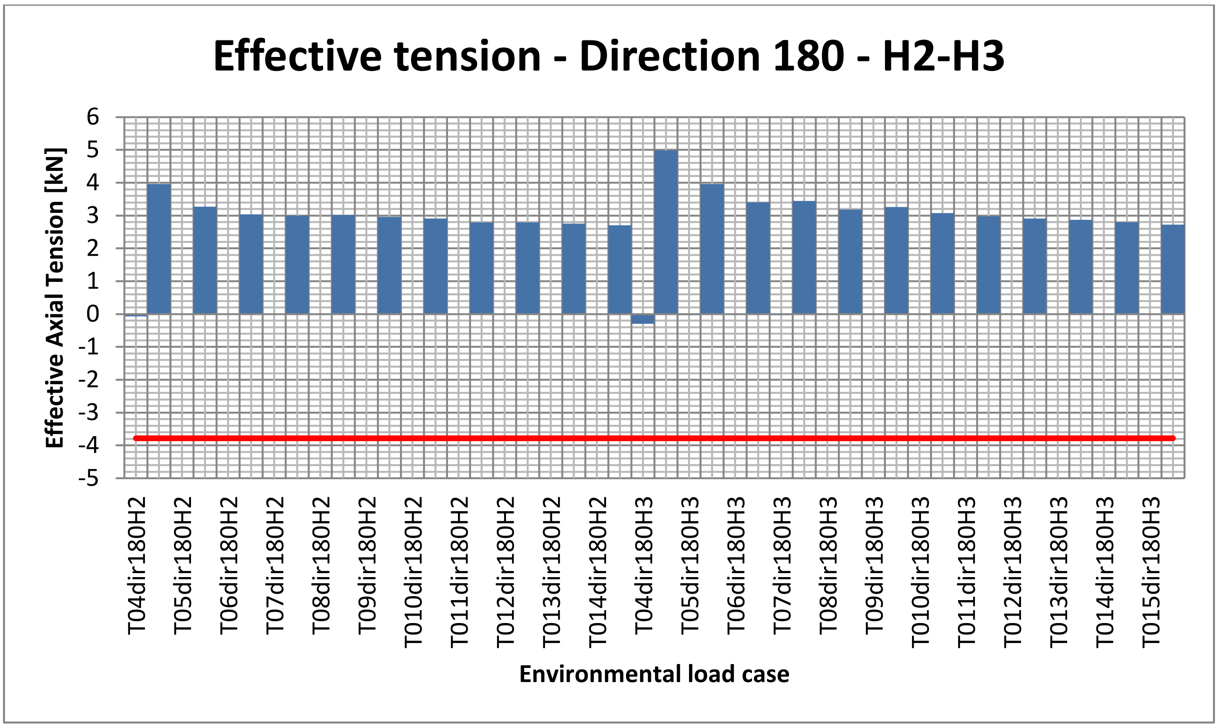

Figure C. 88 - 4” Bunkerflex STH – Lazy wave – 60 m floatation point – Effective tension – Direction 180° - H2-H3

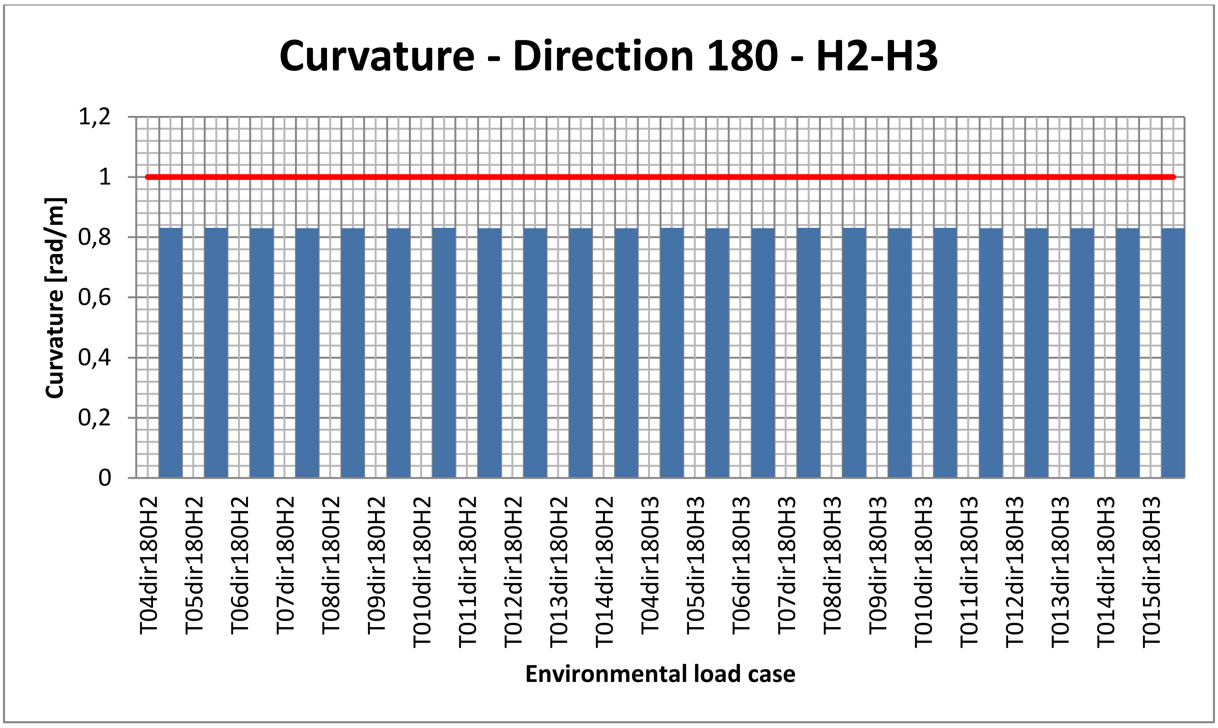

Figure C. 89 - 4” Bunkerflex STH – Lazy wave – 60 m floatation point – Curvature – Direction 180° - H2-H3

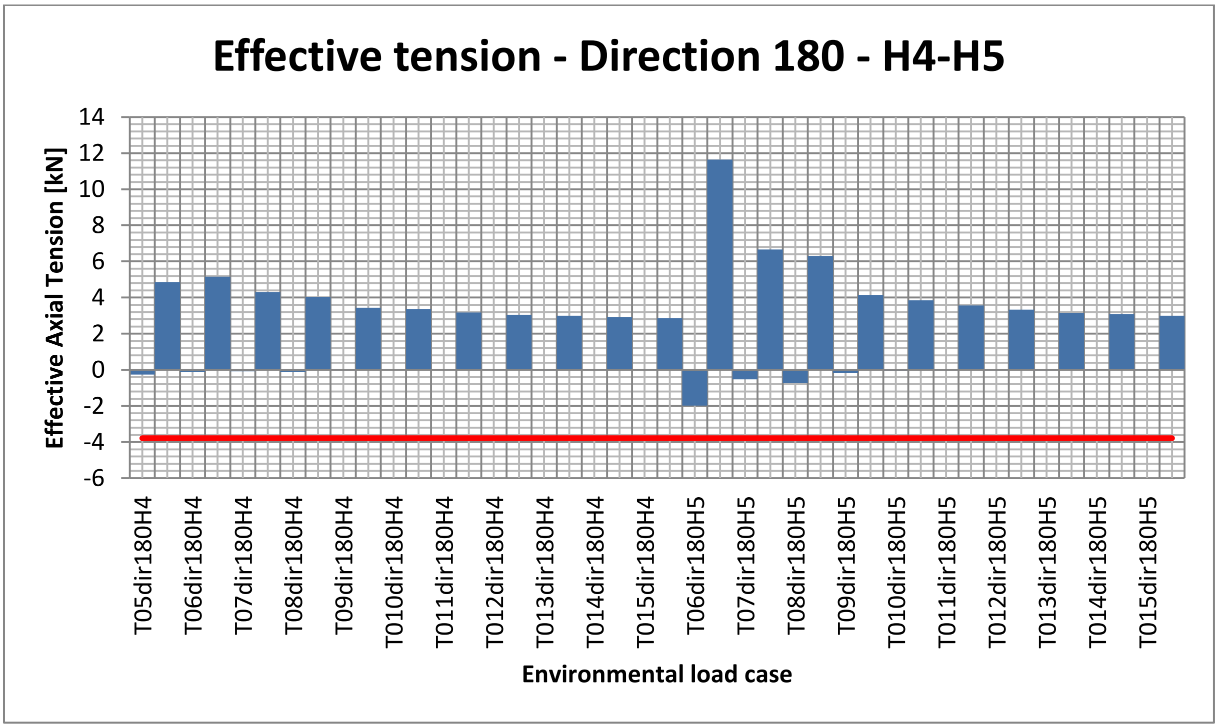

Figure C. 90 - 4” Bunkerflex STH – Lazy wave – 60 m floatation point – Effective tension – Direction 180° - H4-H5

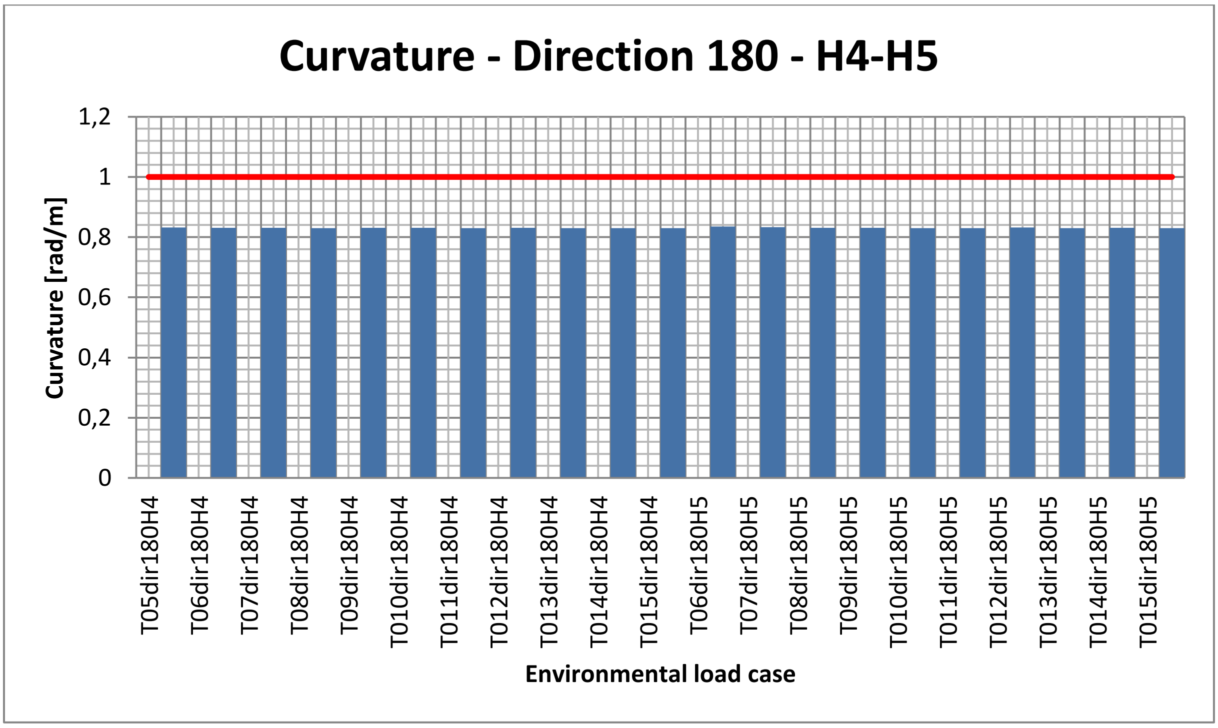

Figure C. 91 - 4” Bunkerflex STH – Lazy wave – 60 m floatation point – Curvature – Direction 180° - H4-H5

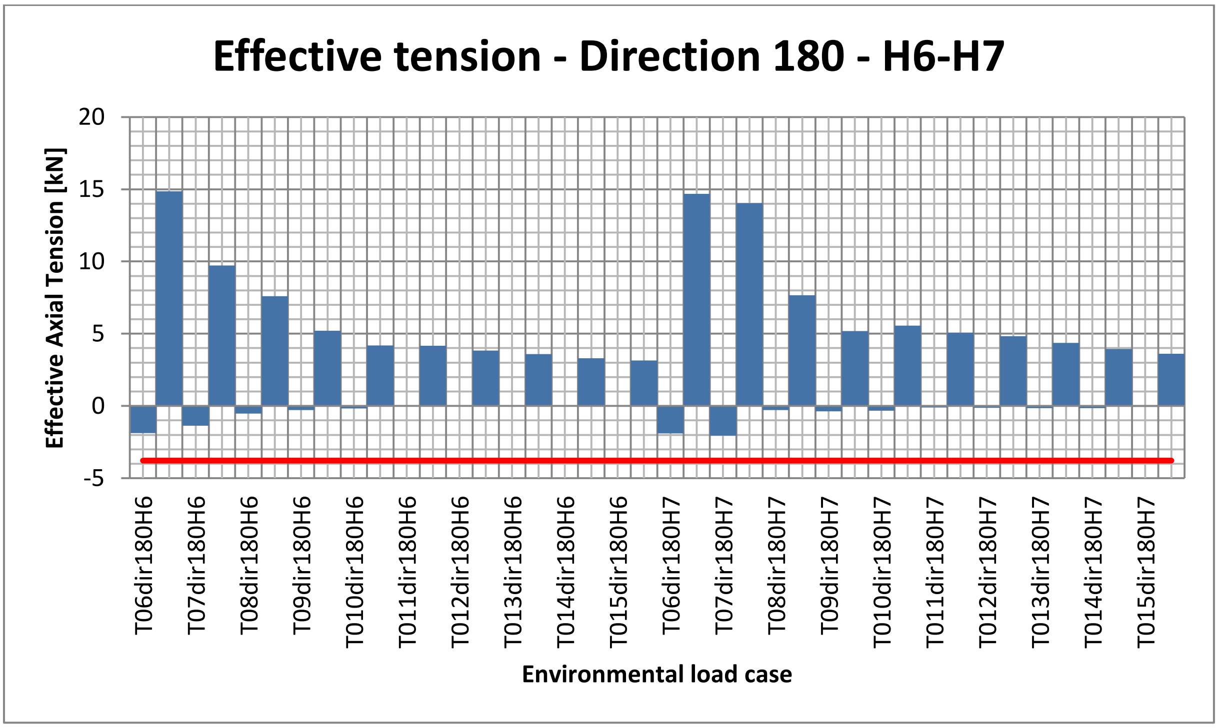

Figure C. 92 - 4” Bunkerflex STH – Lazy wave – 60 m floatation point – Effective tension – Direction 180° - H6-H7

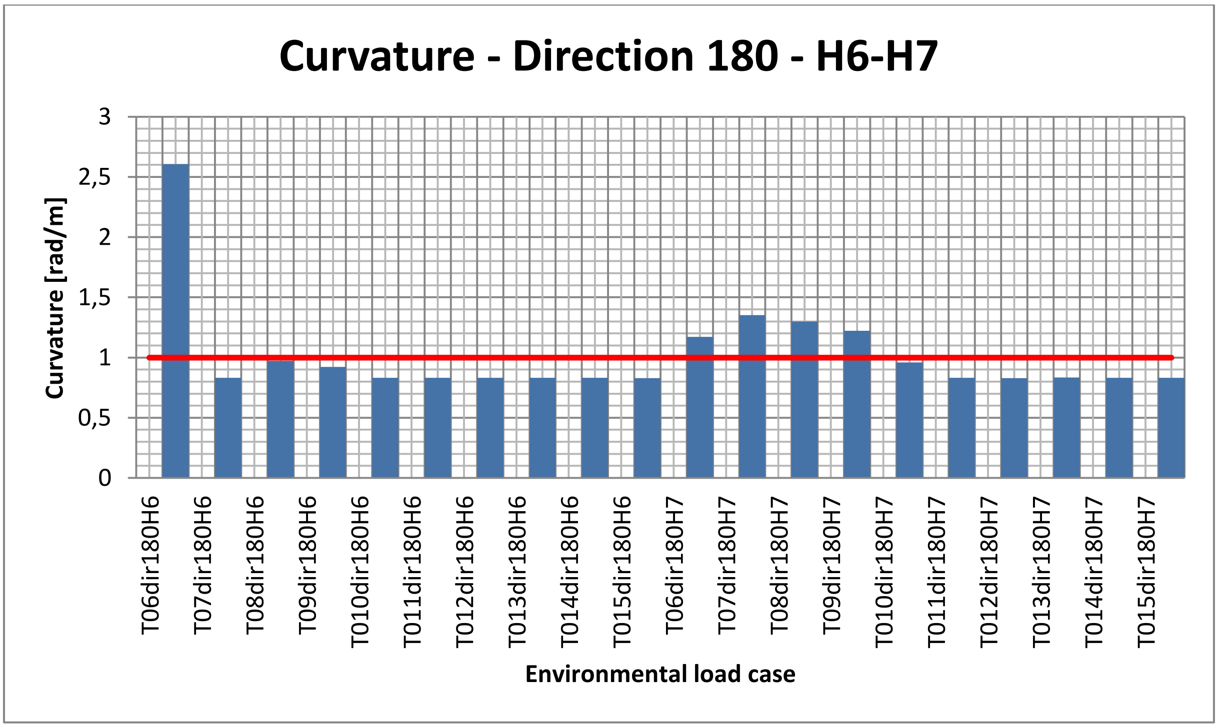

Figure C. 93 - 4” Bunkerflex STH – Lazy wave – 60 m floatation point – Curvature – Direction 180° - H6-H7

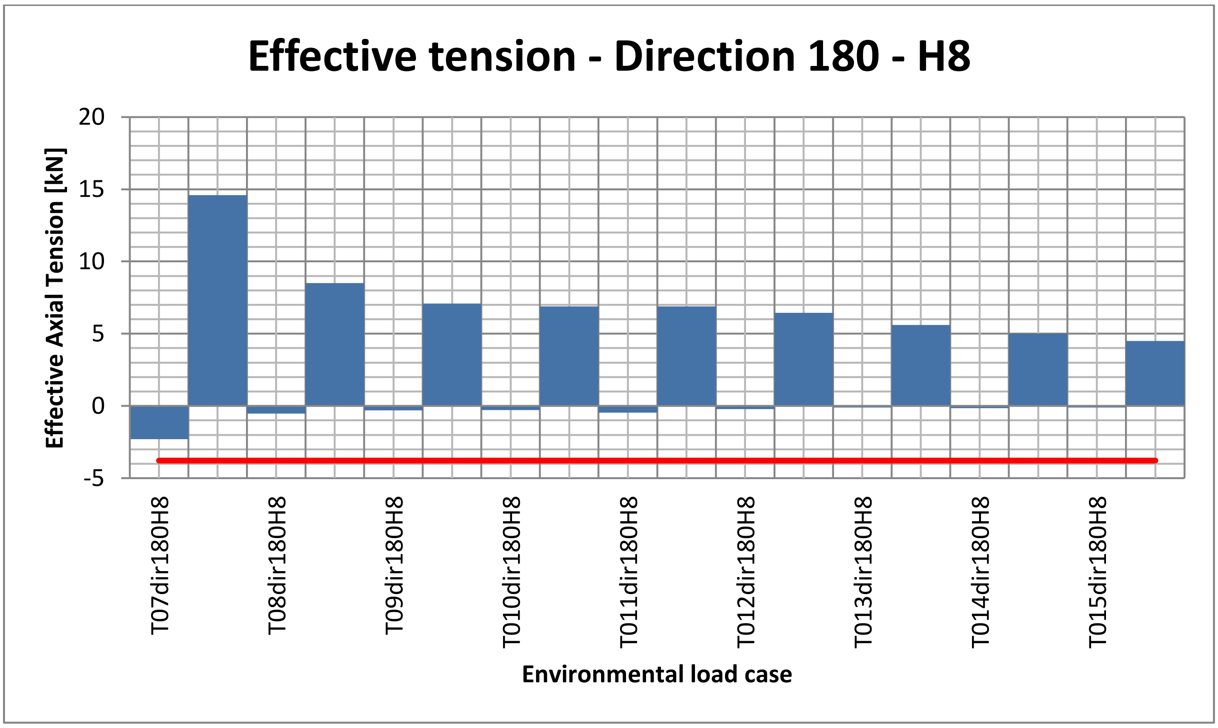

Figure C. 94 - 4” Bunkerflex STH – Lazy wave – 60 m floatation point – Effective tension – Direction 180° - H8

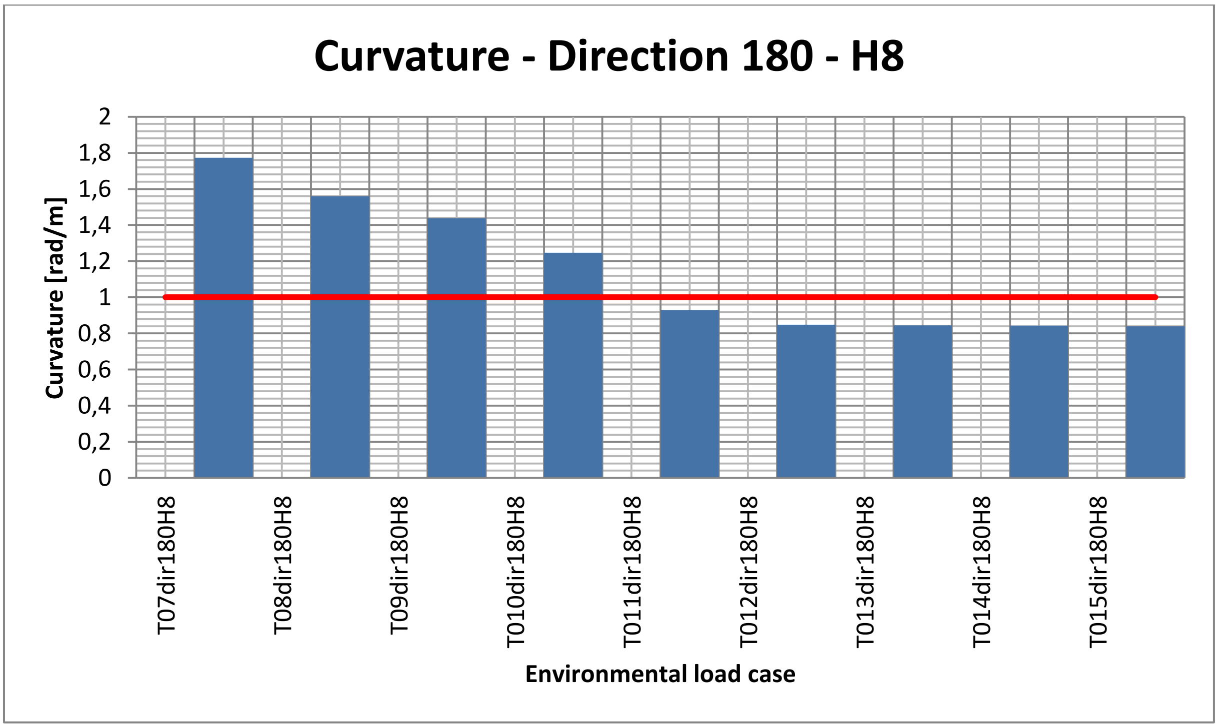

Figure C. 95 - 4” Bunkerflex STH – Lazy wave – 60 m floatation point – Curvature – Direction 180° - H8

Direction 225°

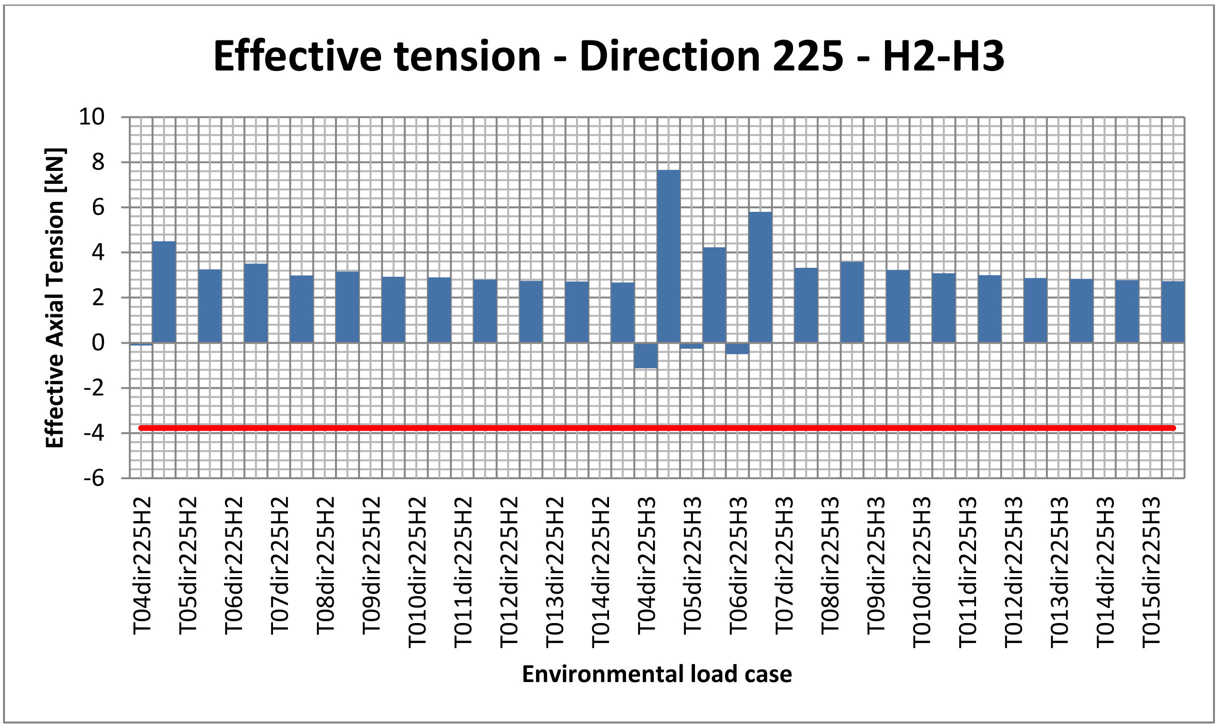

Figure C. 96 - 4” Bunkerflex STH – Lazy wave – 60 m floatation point – Effective tension – Direction 225° - H2-H3

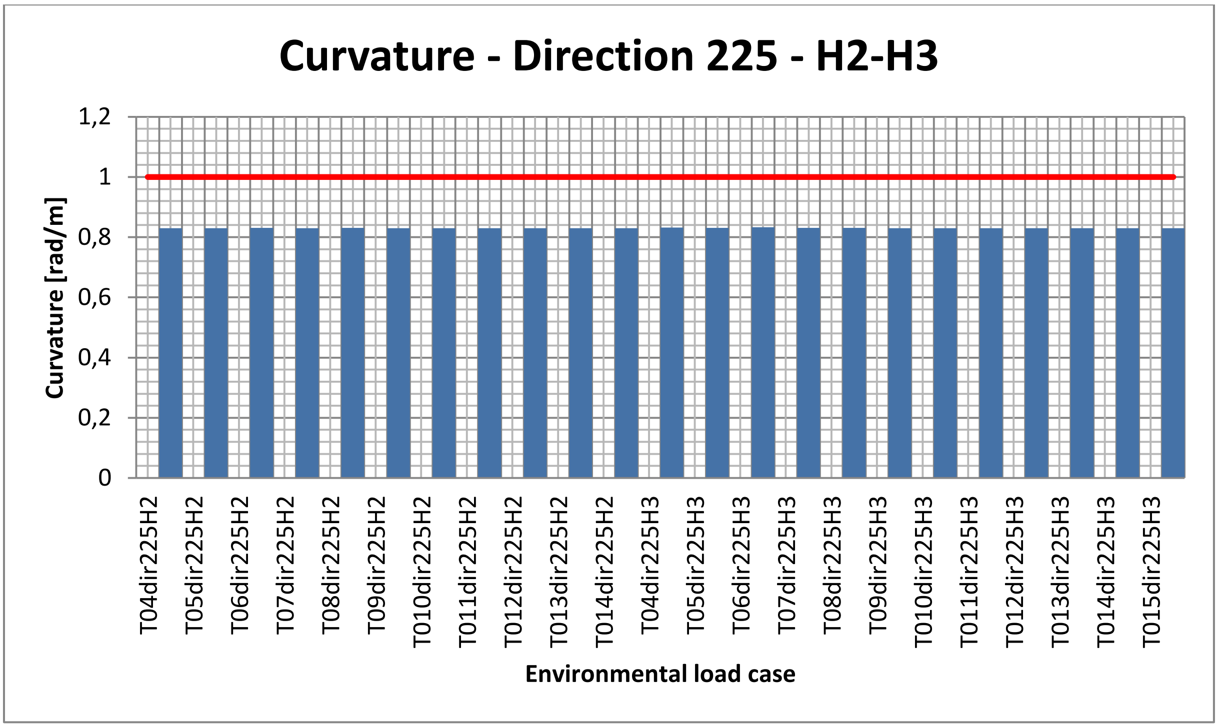

Figure C. 97 - 4” Bunkerflex STH – Lazy wave – 60 m floatation point – Curvature – Direction 225° - H2-H3

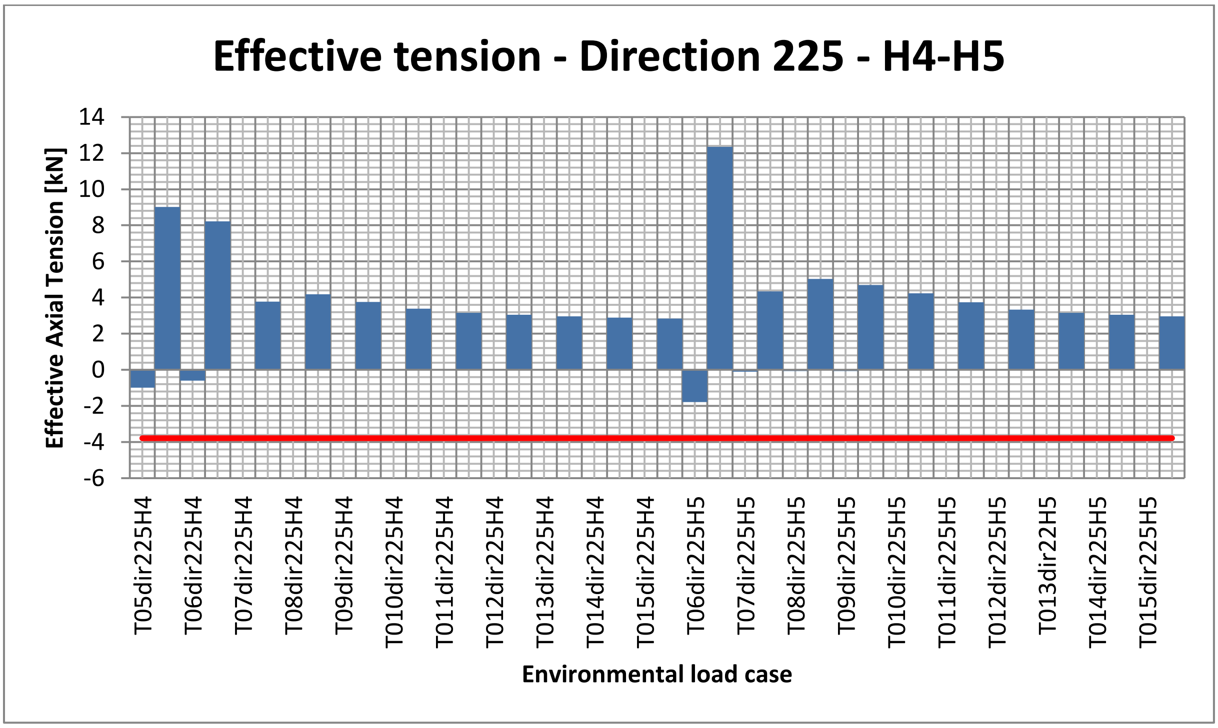

Figure C. 98 - 4” Bunkerflex STH – Lazy wave – 60 m floatation point – Effective tension – Direction 225° - H4-H5

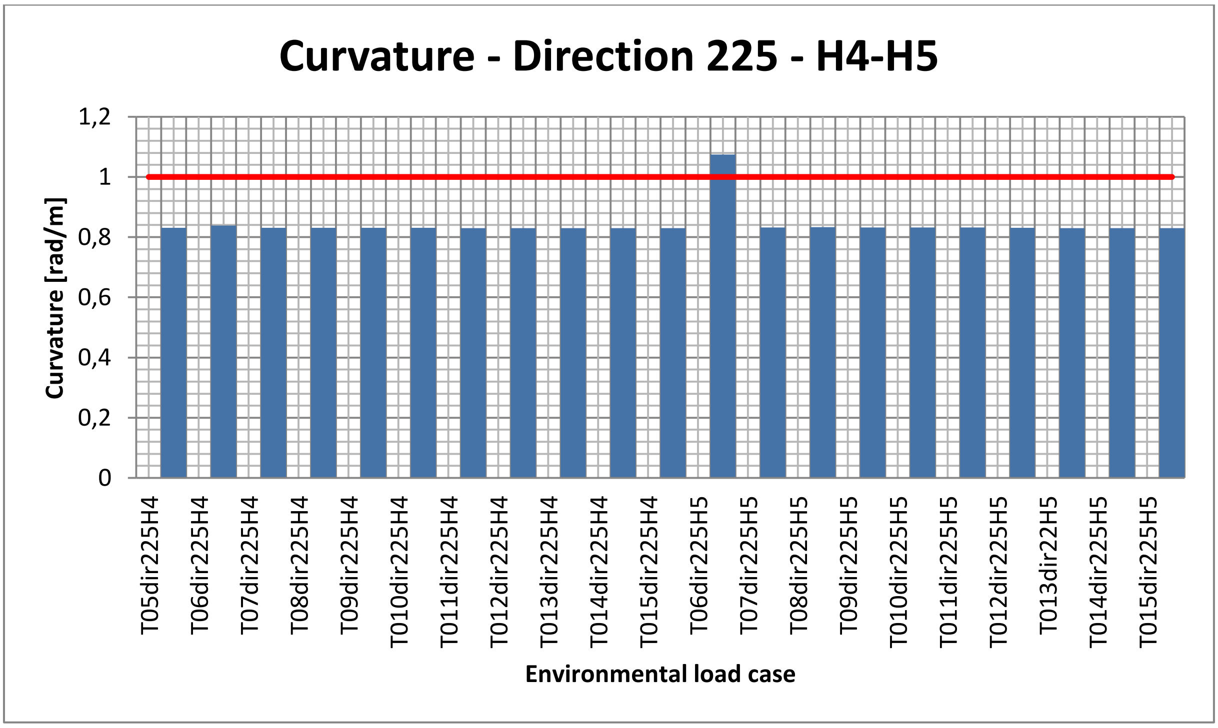

Figure C. 99 - 4” Bunkerflex STH – Lazy wave – 60 m floatation point – Curvature – Direction 225° - H4-H5

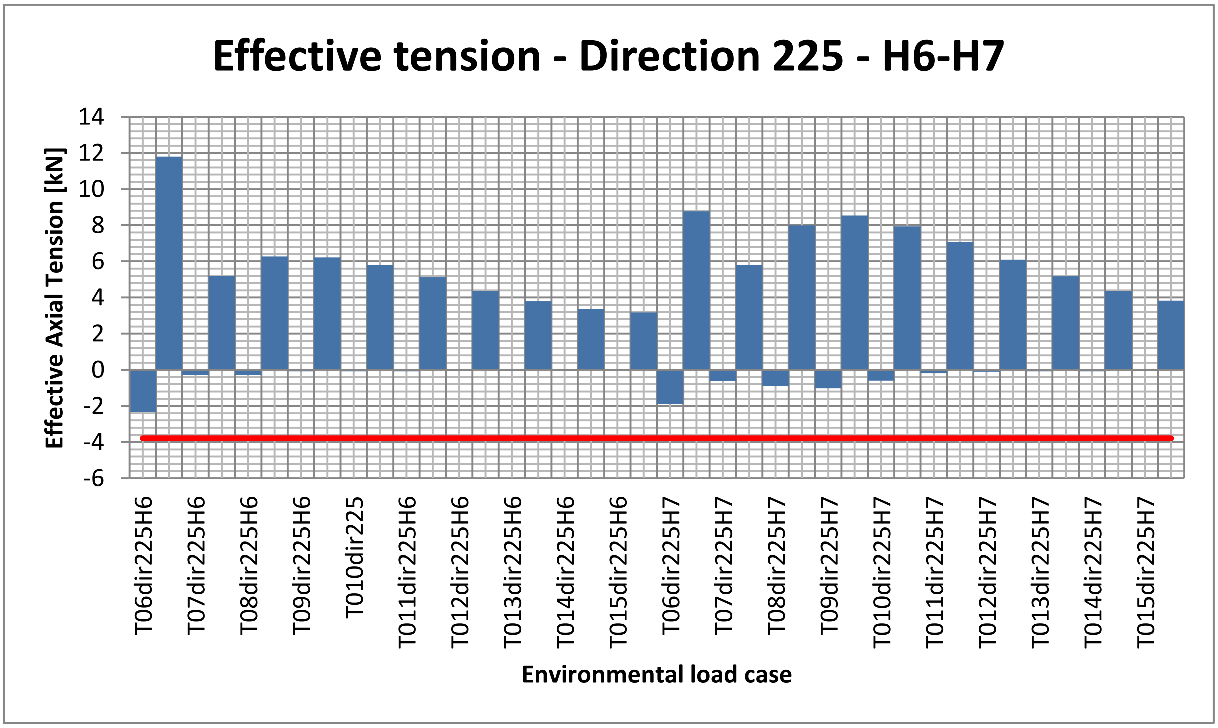

Figure C. 100 - 4” Bunkerflex STH – Lazy wave – 60 m floatation point – Effective tension – Direction 225° - H6-H7

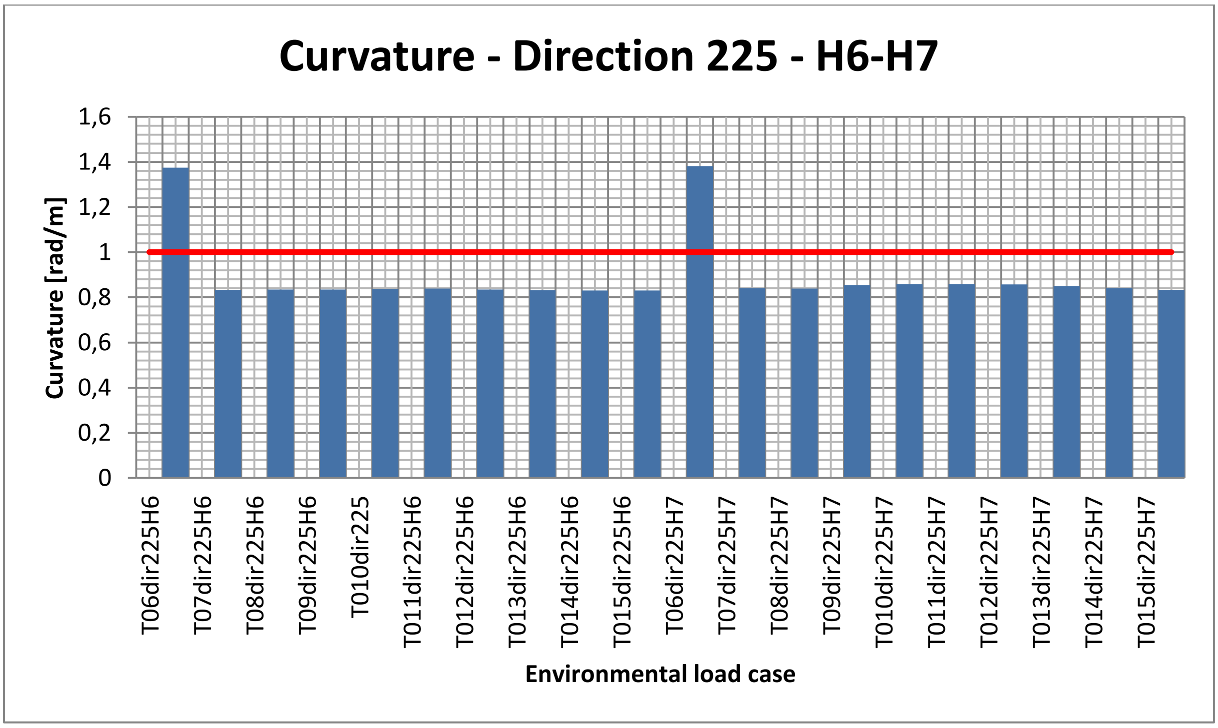

Figure C. 101 - 4” Bunkerflex STH – Lazy wave – 60 m floatation point – Curvature – Direction 225° - H6-H7

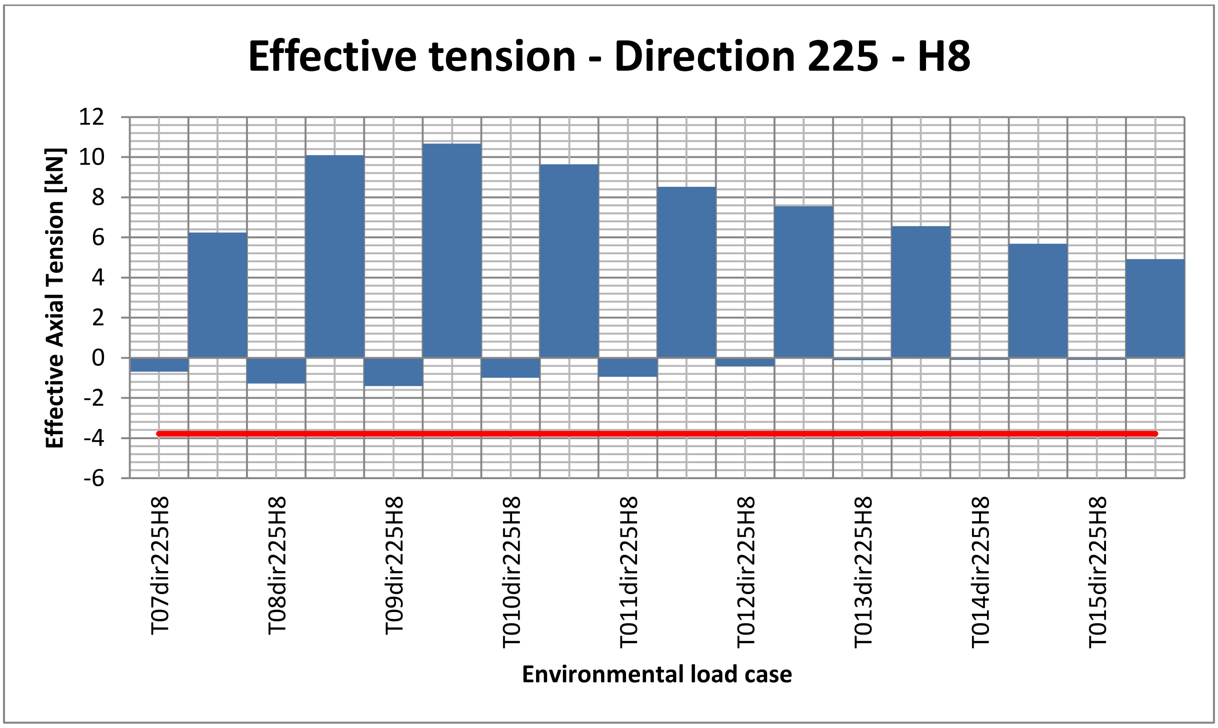

Figure C. 102 - 4” Bunkerflex STH – Lazy wave – 60 m floatation point – Effective tension – Direction 225° - H8

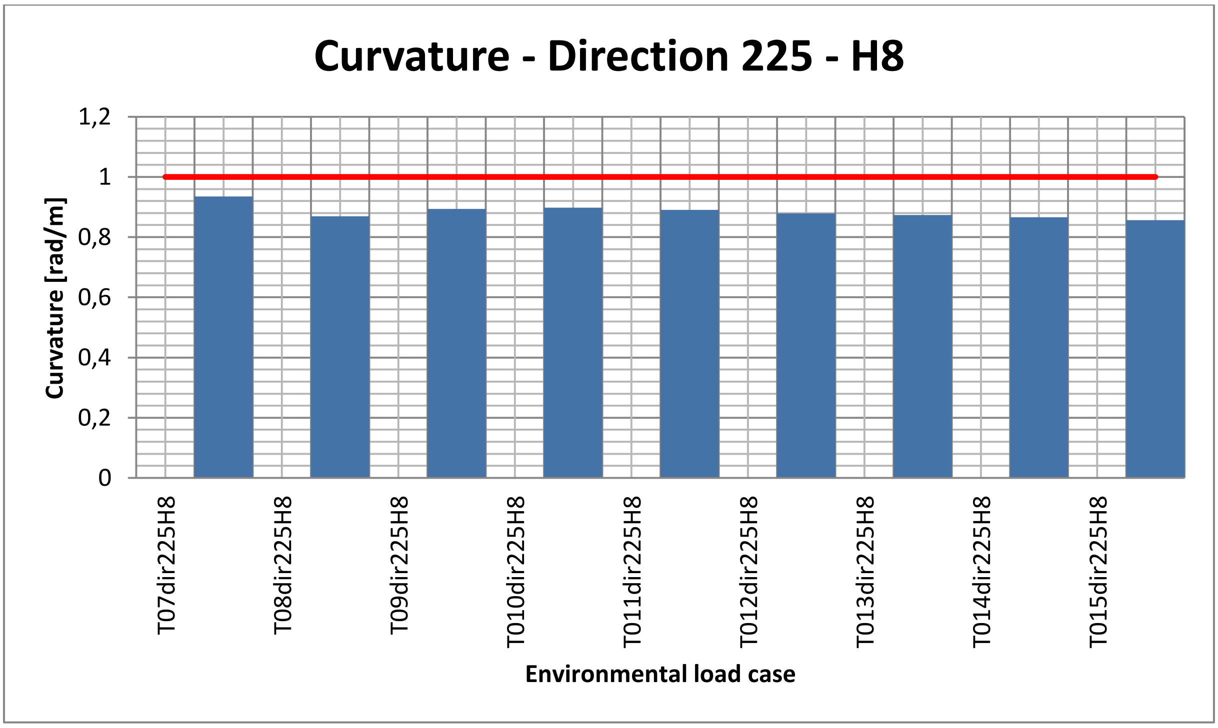

Figure C. 103 - 4” Bunkerflex STH – Lazy wave – 60 m floatation point – Curvature – Direction 225° - H8

Wave rose

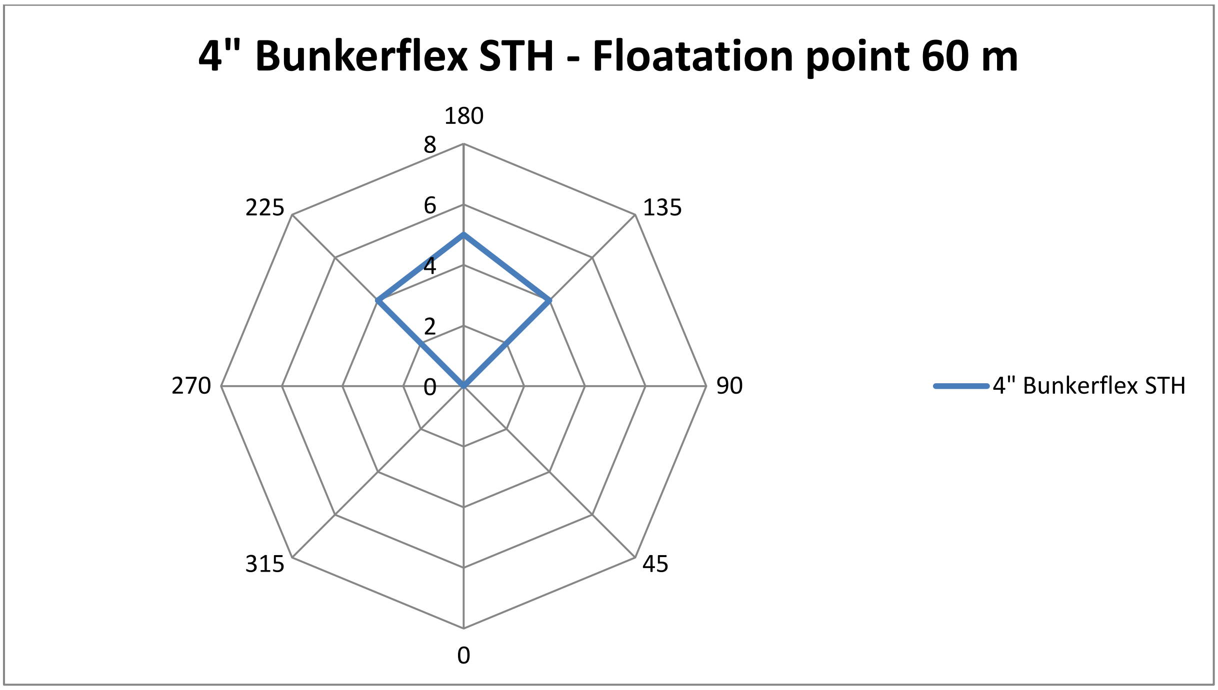

Figure C. 104 - 4" Bunkerflex STH – Lazy wave – 60 m floatation point – Wave rose

Limitation plot

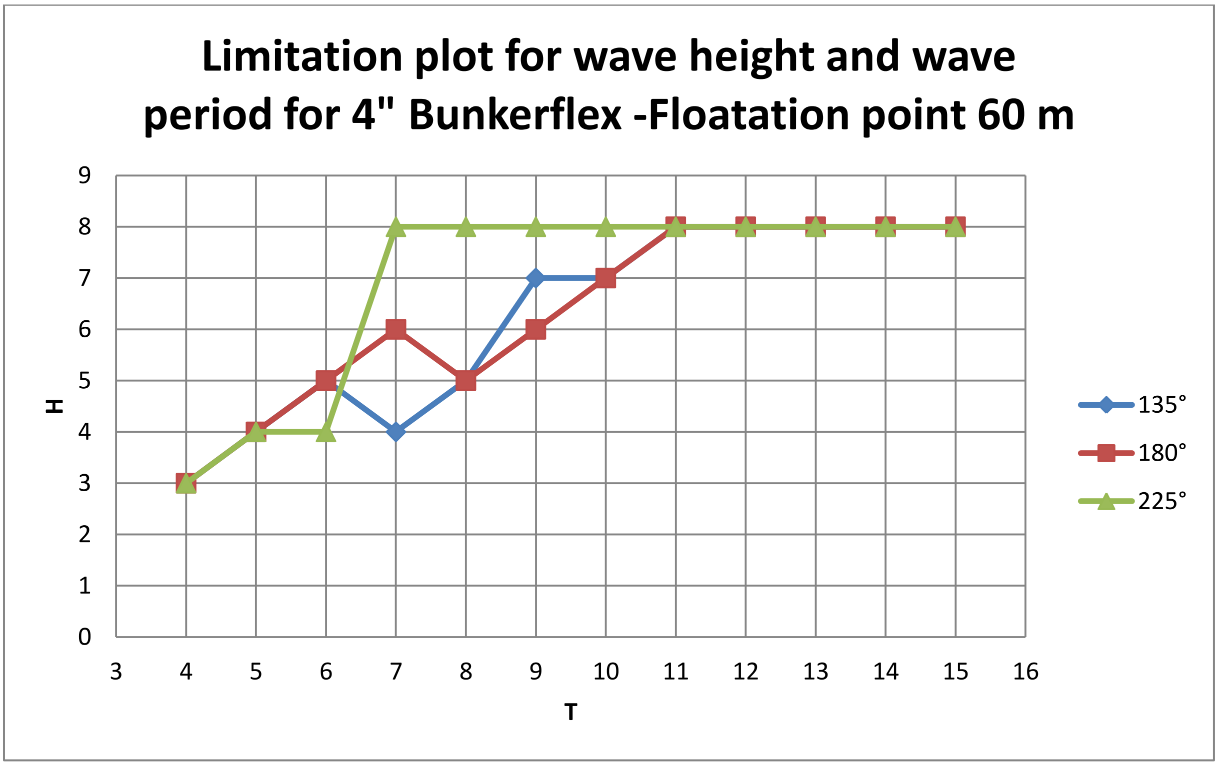

Figure C. 105 - 4" Bunkerflex STH – Lazy wave – 60 m floatation point – Limitation plot

Lazy wave – 80 m floatation point

Direction 135°

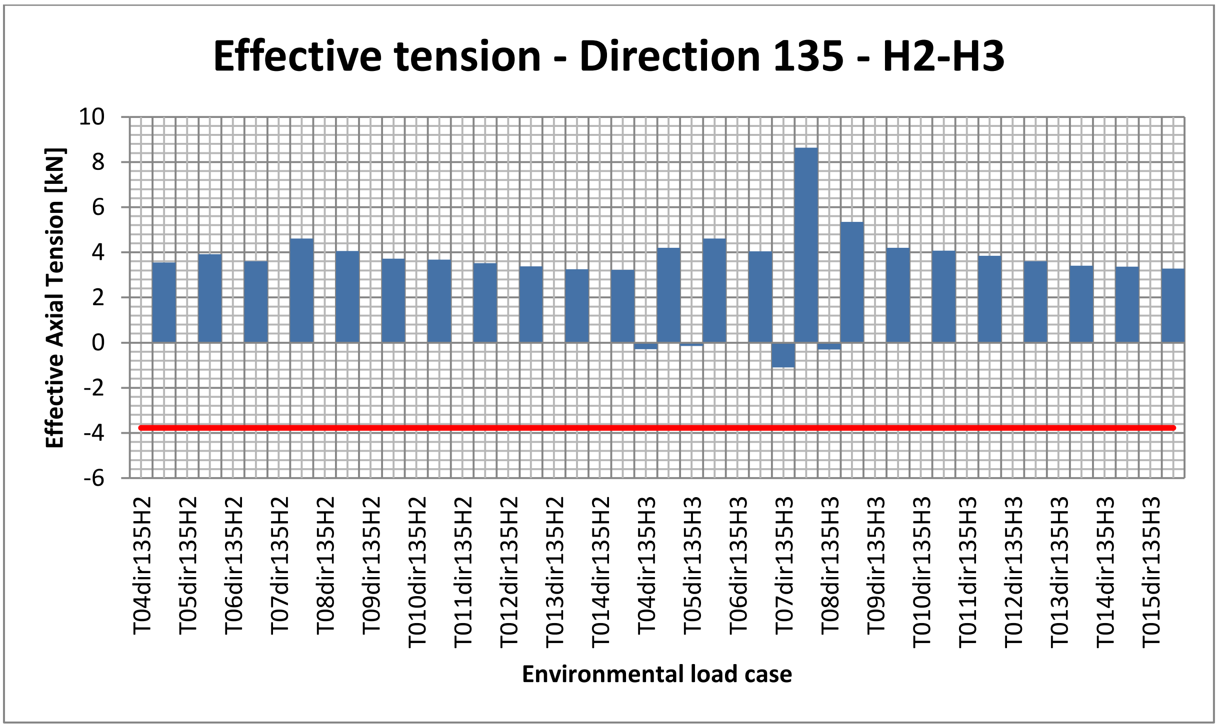

Figure C. 106 - 4” Bunkerflex STH – Lazy wave – 80 m floatation point – Effective tension – Direction 135° - H2-H3

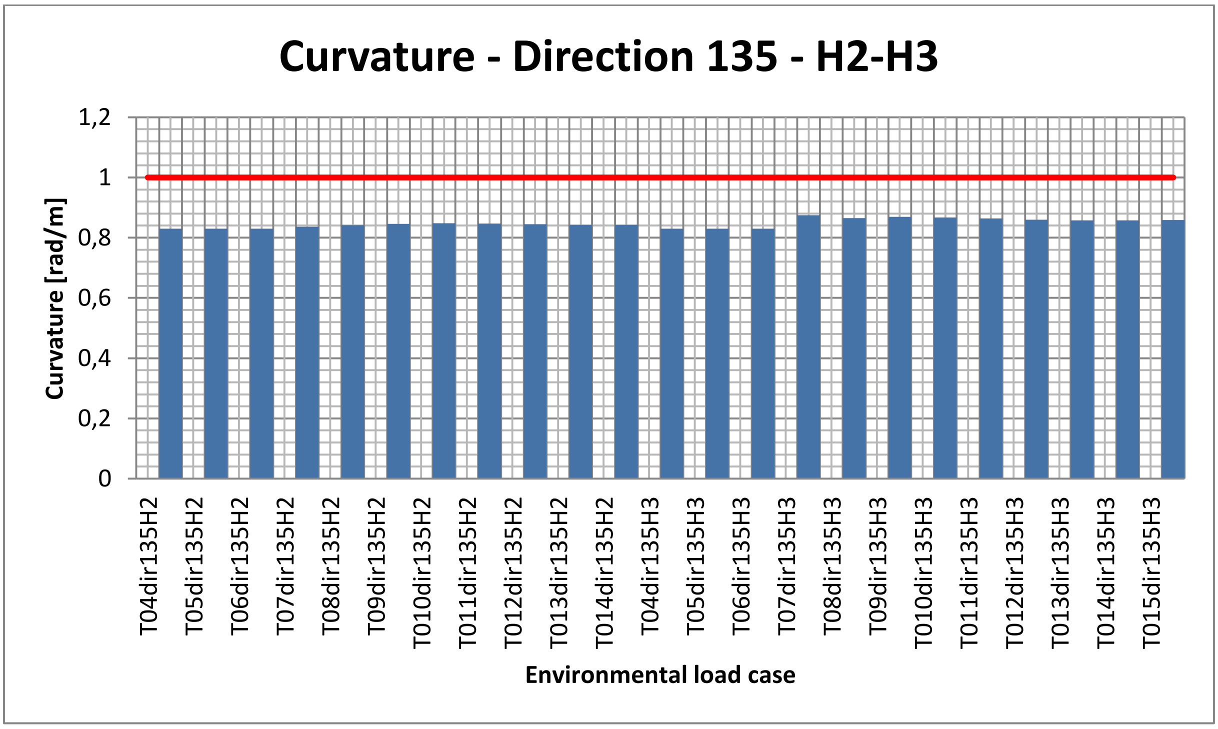

Figure C. 107 - 4” Bunkerflex STH – Lazy wave – 80 m floatation point – Curvature – Direction 135° - H2-H3

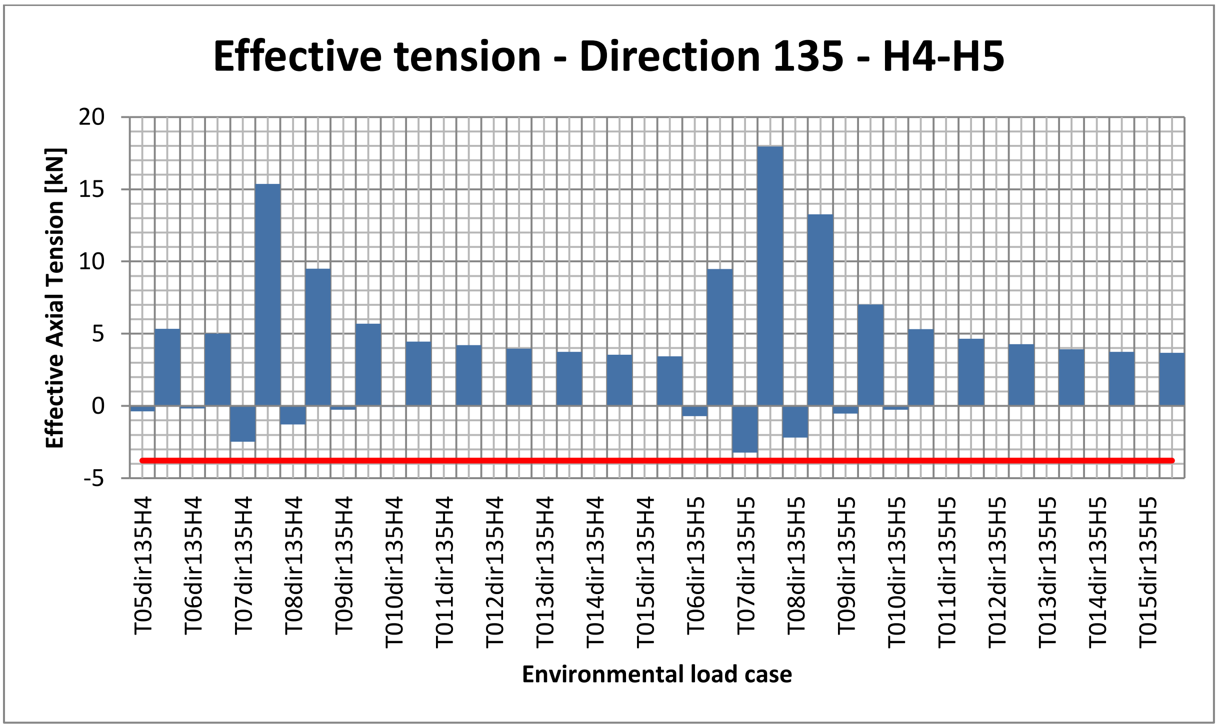

Figure C. 108 - 4” Bunkerflex STH – Lazy wave – 80 m floatation point – Effective tension – Direction 135° - H4-H5

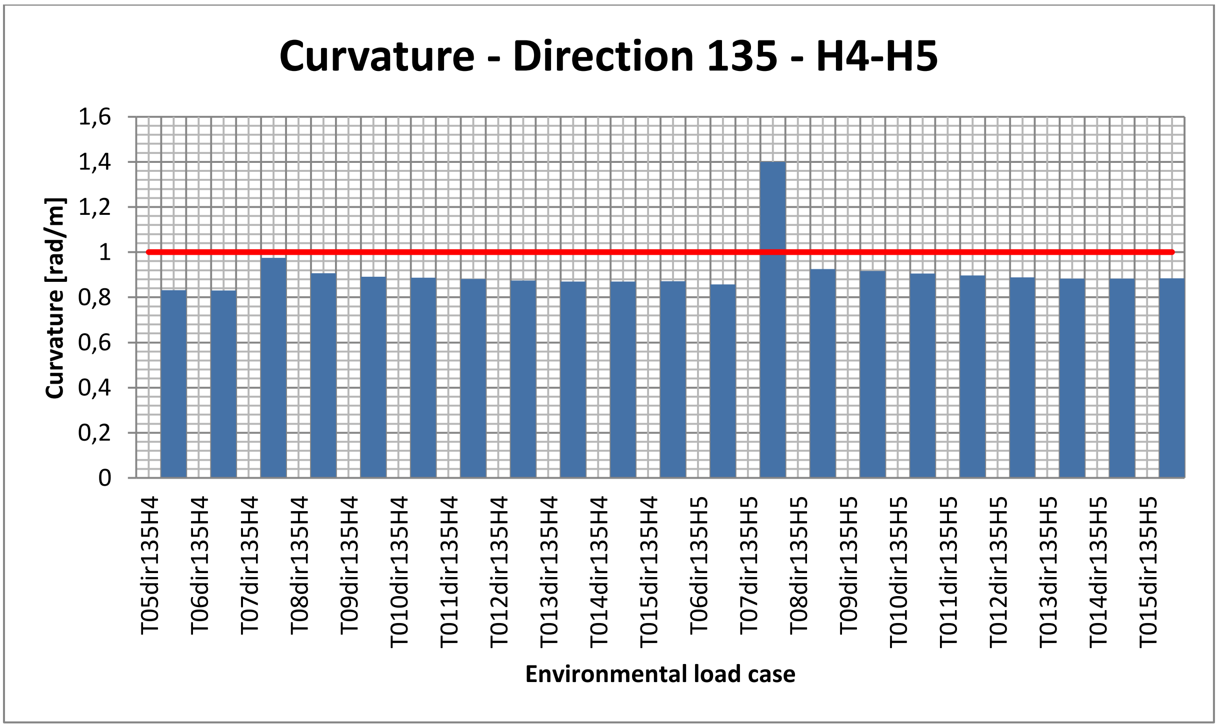

Figure C. 109 - 4” Bunkerflex STH – Lazy wave – 80 m floatation point – Curvature – Direction 135° - H4-H5

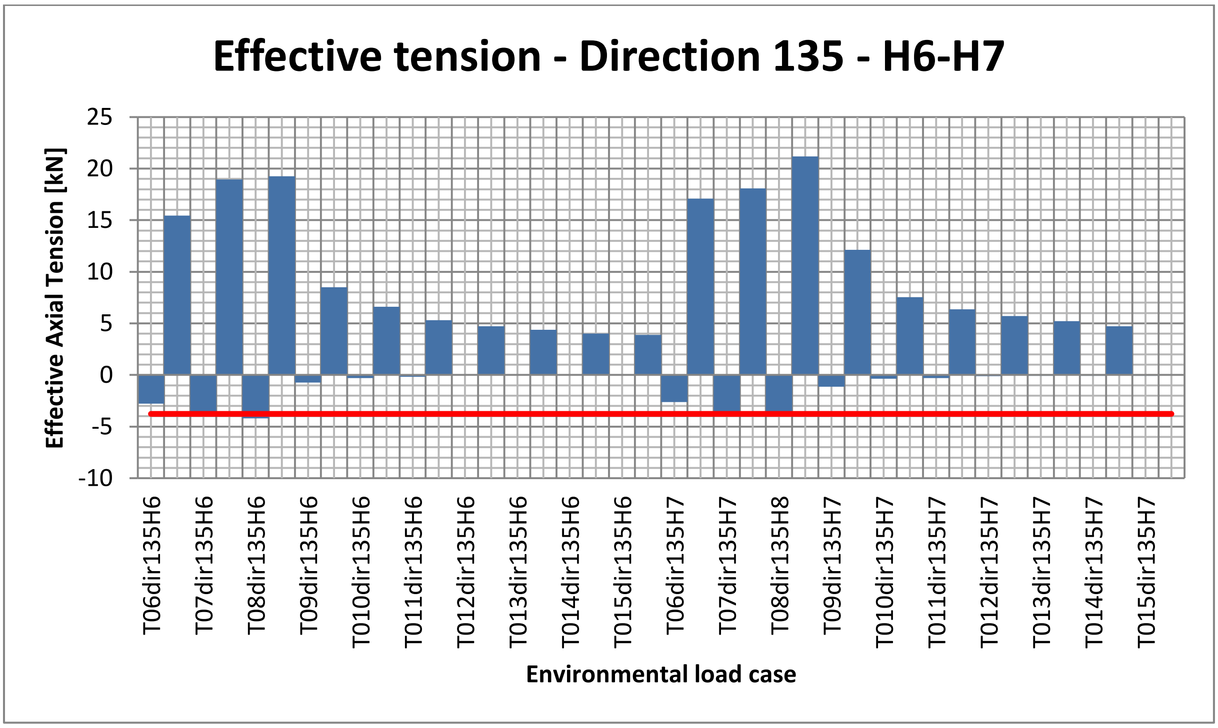

Figure C. 110 - 4” Bunkerflex STH – Lazy wave – 80 m floatation point – Effective tension – Direction 135° - H6-H7

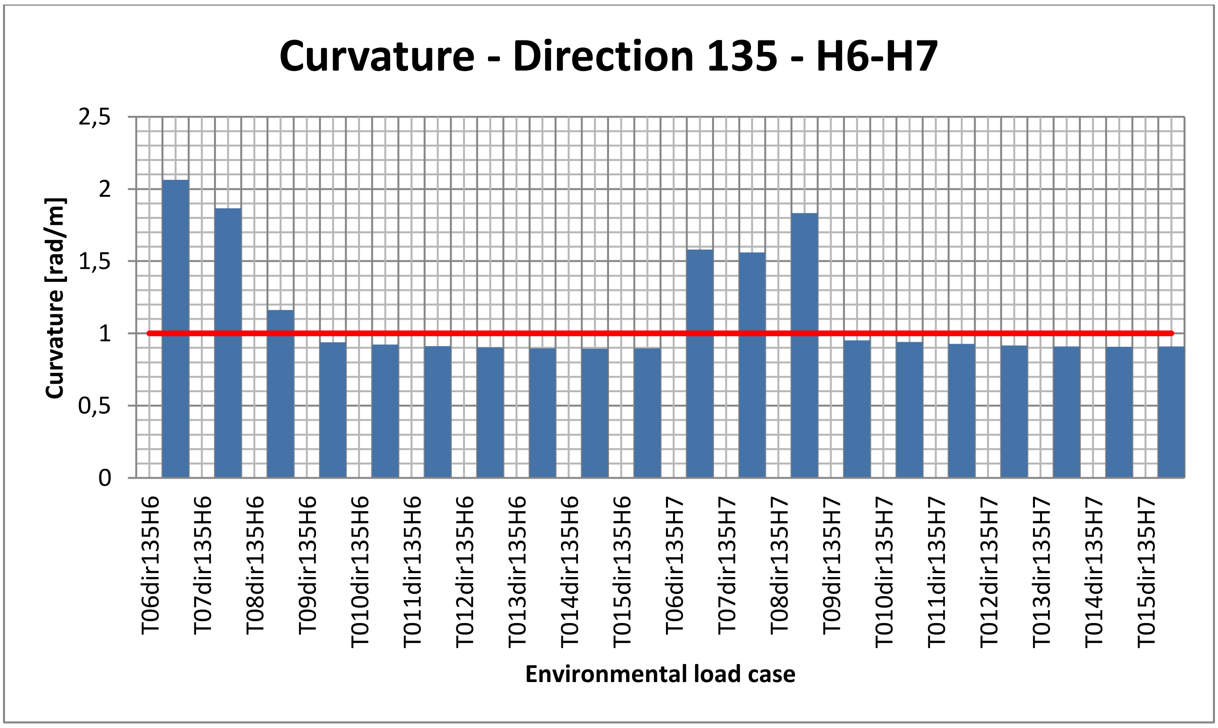

Figure C. 111 - 4” Bunkerflex STH – Lazy wave – 80 m floatation point – Curvature – Direction 135° - H6-H7

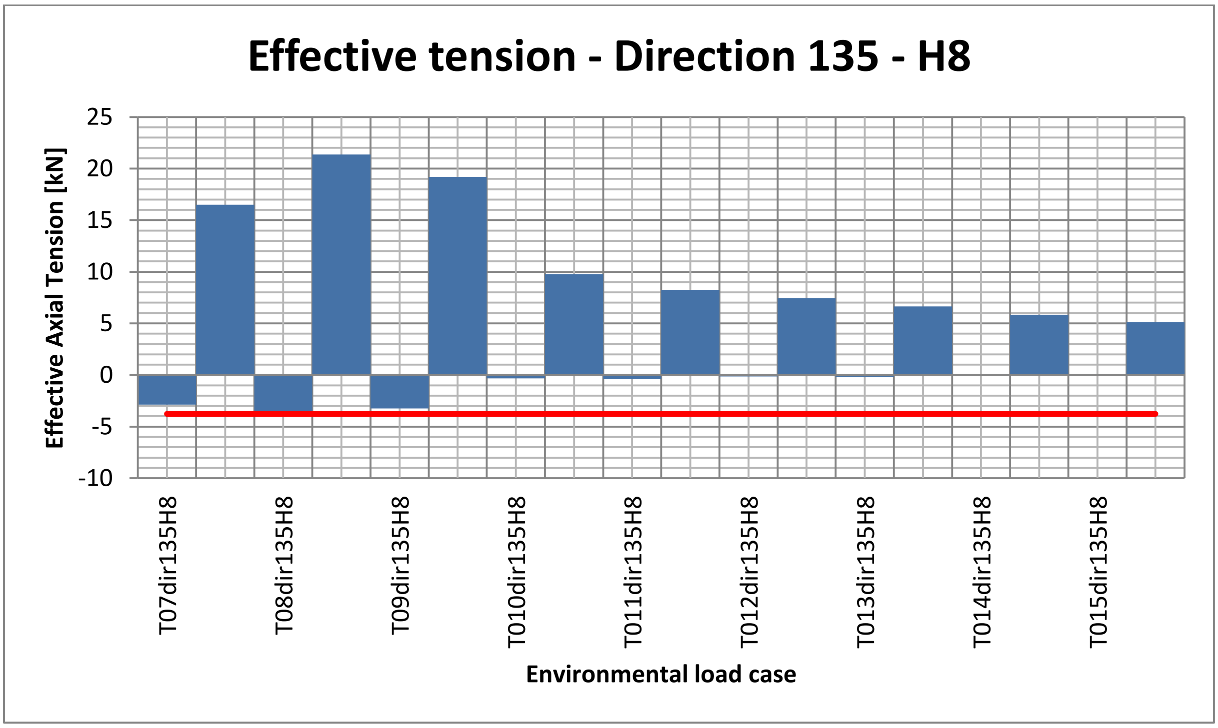

Figure C. 112 - 4” Bunkerflex STH – Lazy wave – 80 m floatation point – Effective tension – Direction 135° - H8

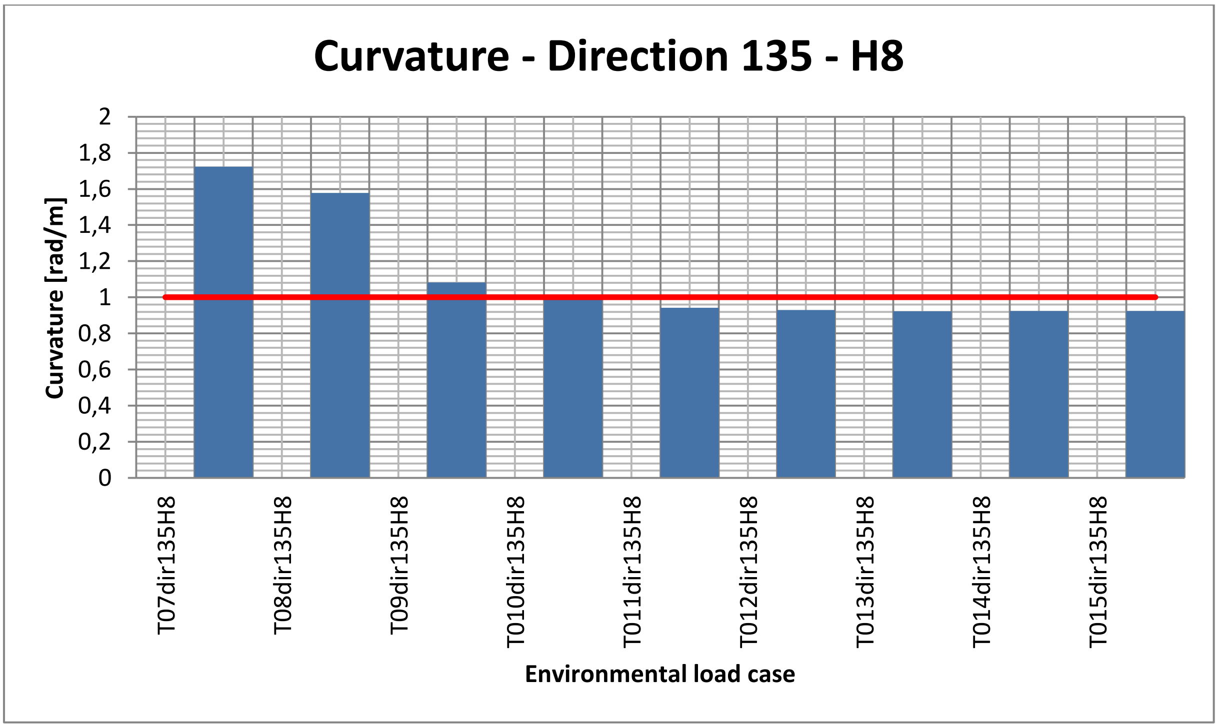

Figure C. 113 - 4” Bunkerflex STH – Lazy wave – 80 m floatation point – Curvature – Direction 135° - H8

Direction 180°

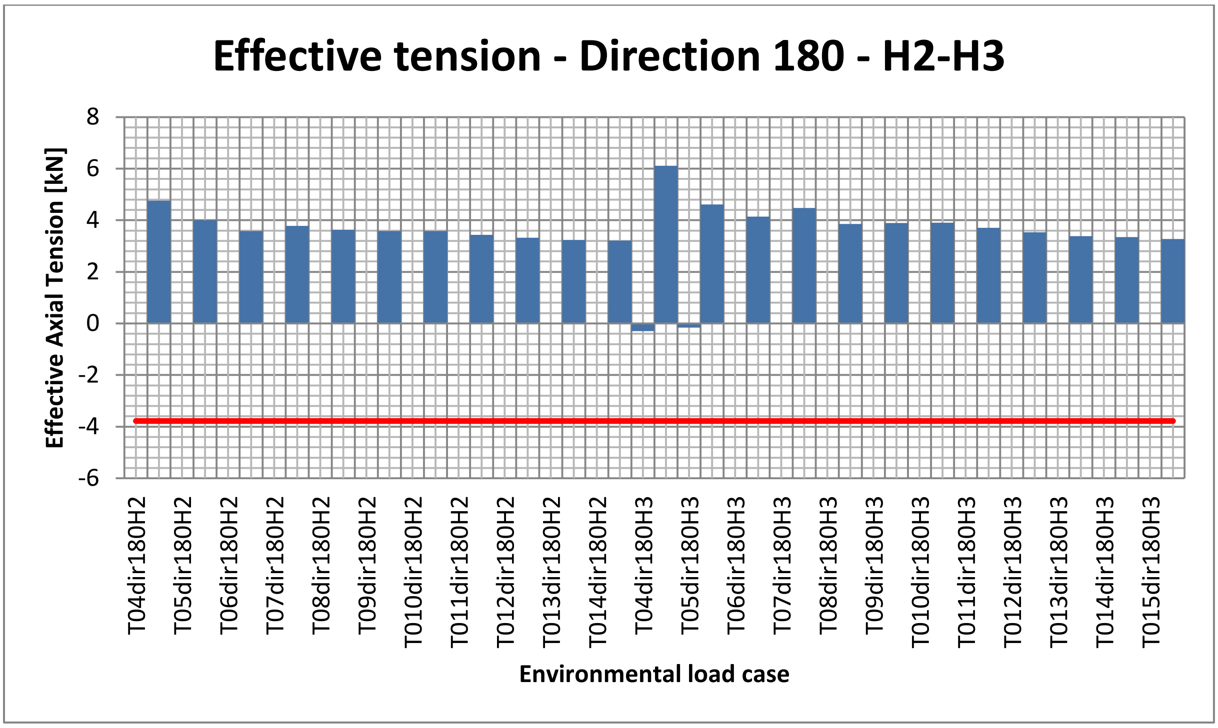

Figure C. 114 - 4" Bunkerflex STH – Lazy wave – 80 m floatation point – Effective tension – Direction 180° - H2-H3

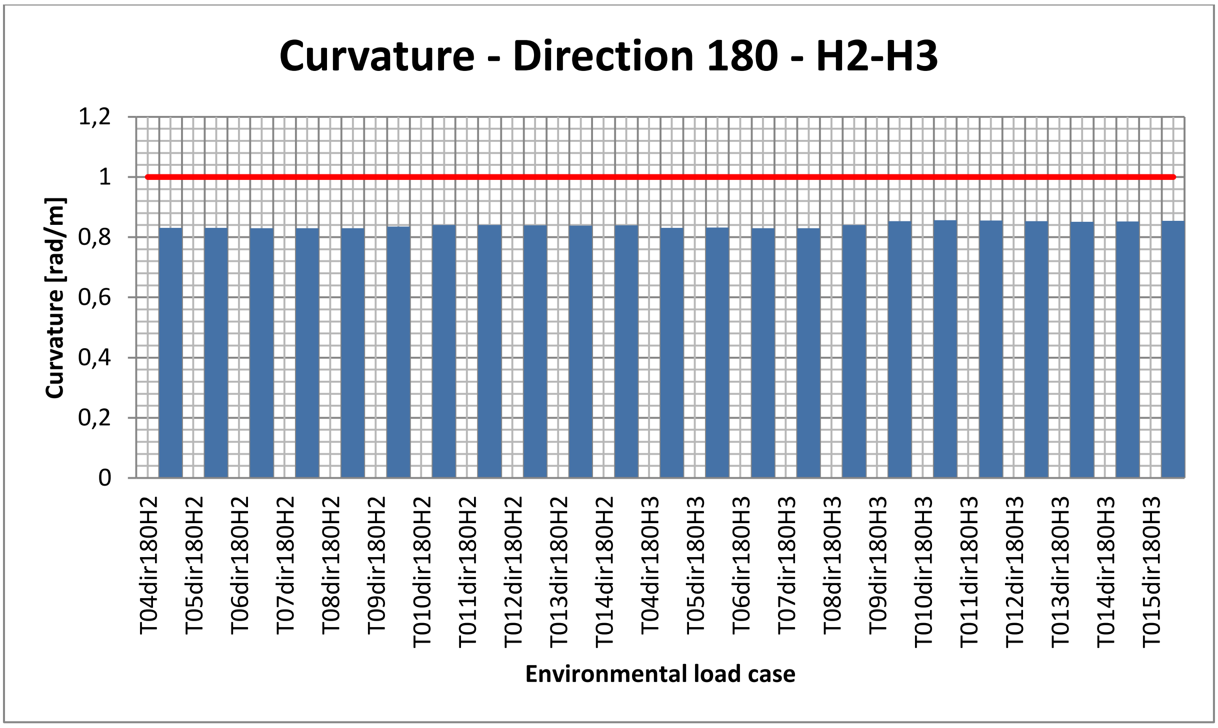

Figure C. 115 - 4" Bunkerflex STH – Lazy wave – 80 m floatation point – Curvature – Direction 180° - H2-H3

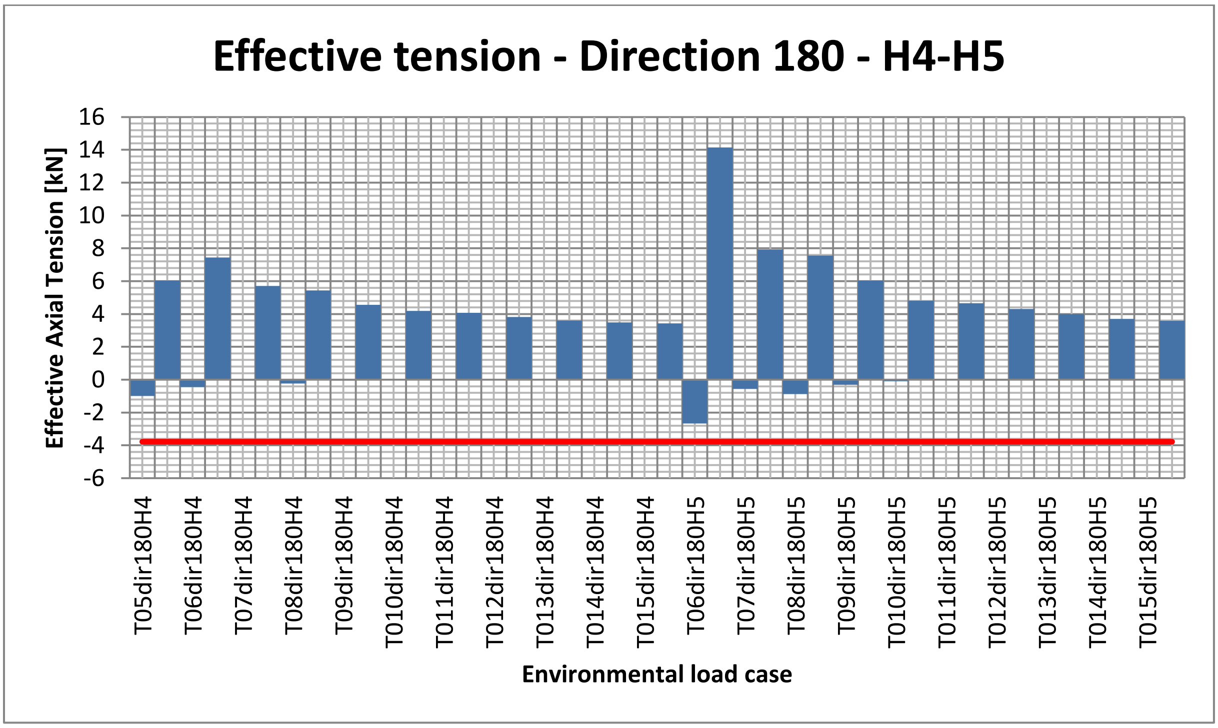

Figure C. 116 - 4” Bunkerflex STH – Lazy wave – 80 m floatation point – Effective tension – Direction 180° - H4-H5

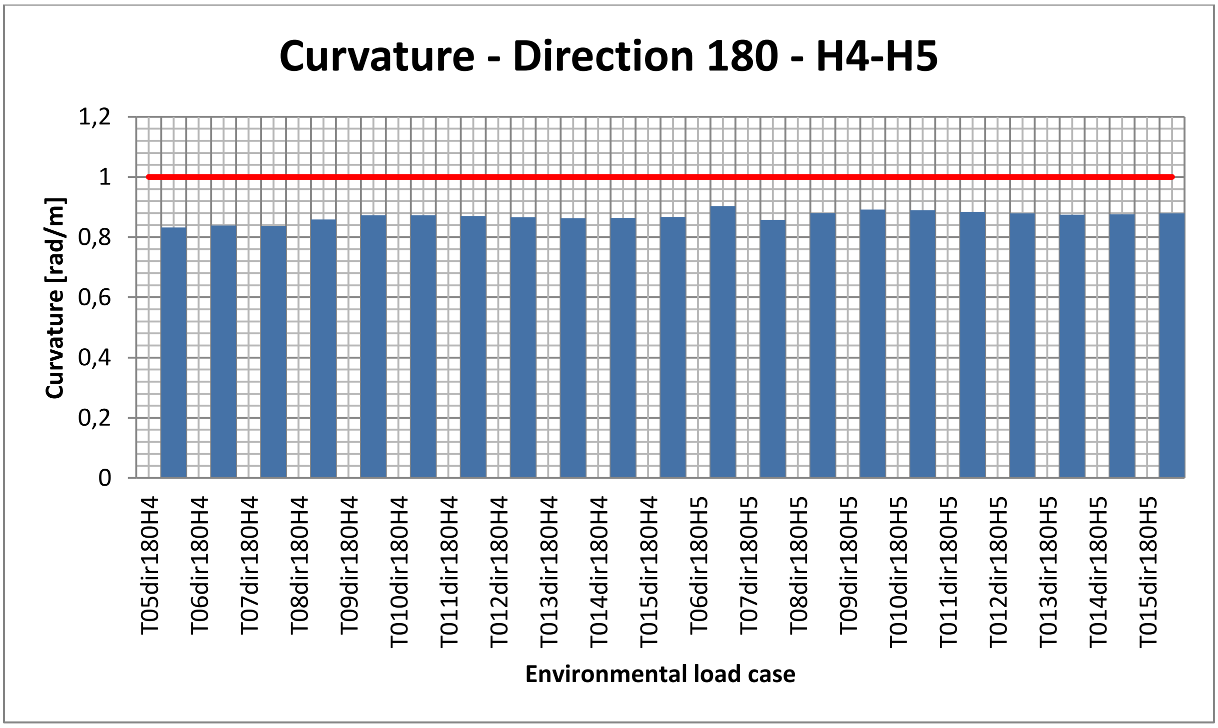

Figure C. 117 - 4” Bunkerflex STH – Lazy wave – 80 m floatation point – Curvature – Direction 180° - H4-H5

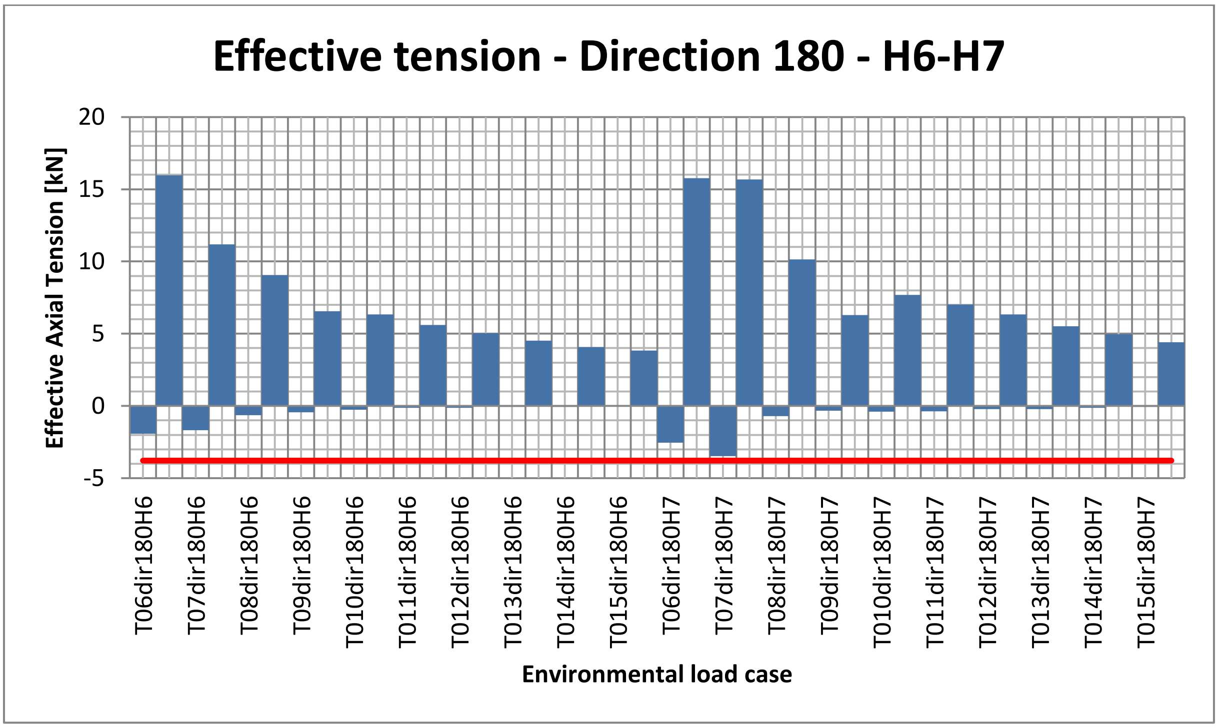

Figure C. 118 - 4” Bunkerflex STH – Lazy wave – 80 m floatation point – Effective tension – Direction 180° - H6-H7

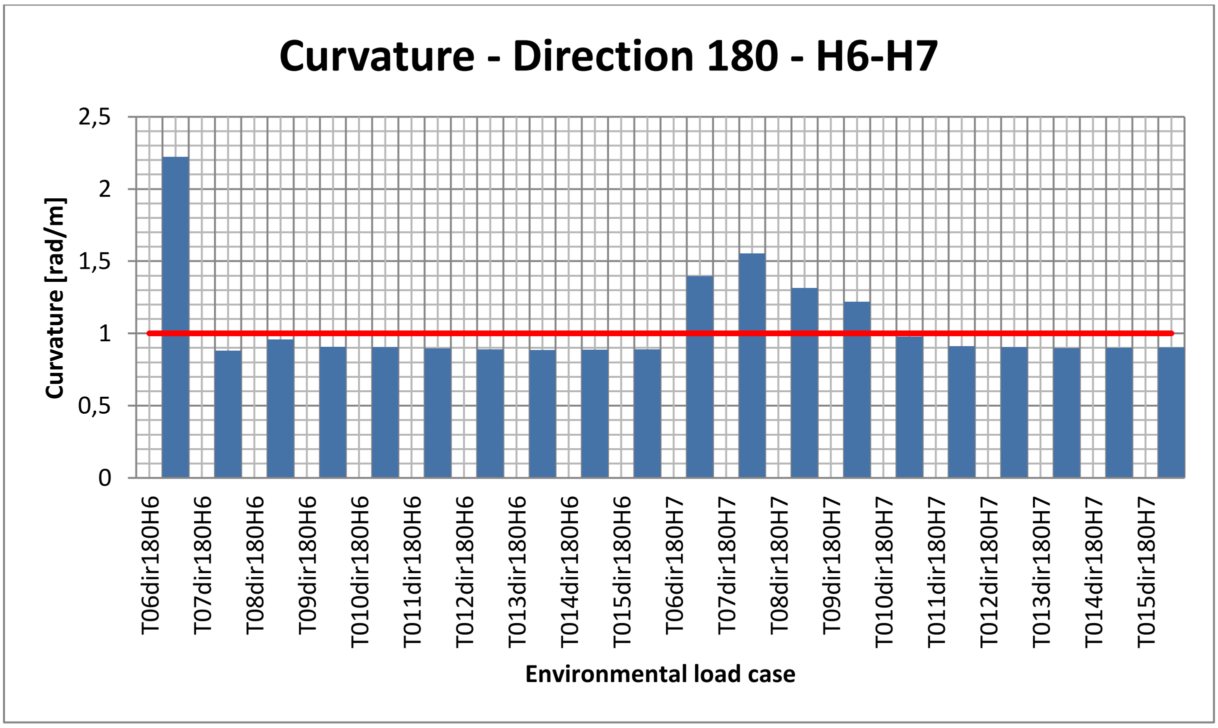

Figure C. 119 - 4” Bunkerflex STH – Lazy wave – 80 m floatation point – Curvature – Direction 180° - H6-H7

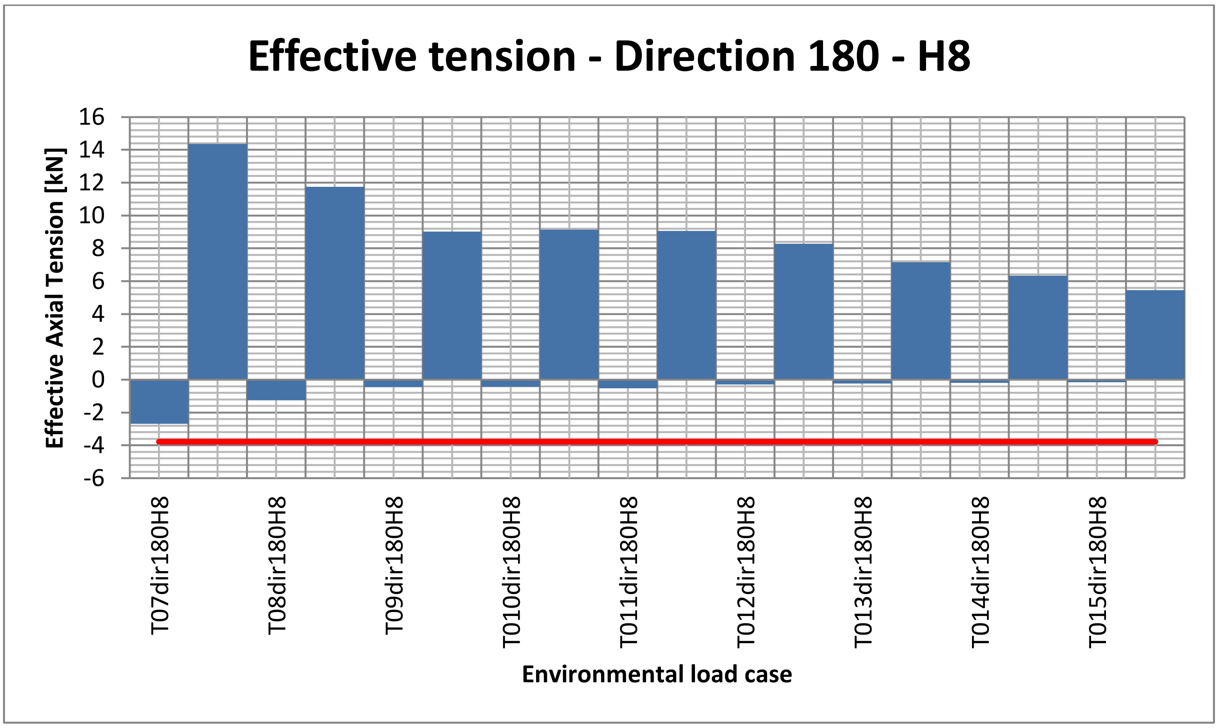

Figure C. 120 - 4” Bunkerflex STH – Lazy wave – 80 m floatation point – Effective tension – Direction 180° - H8

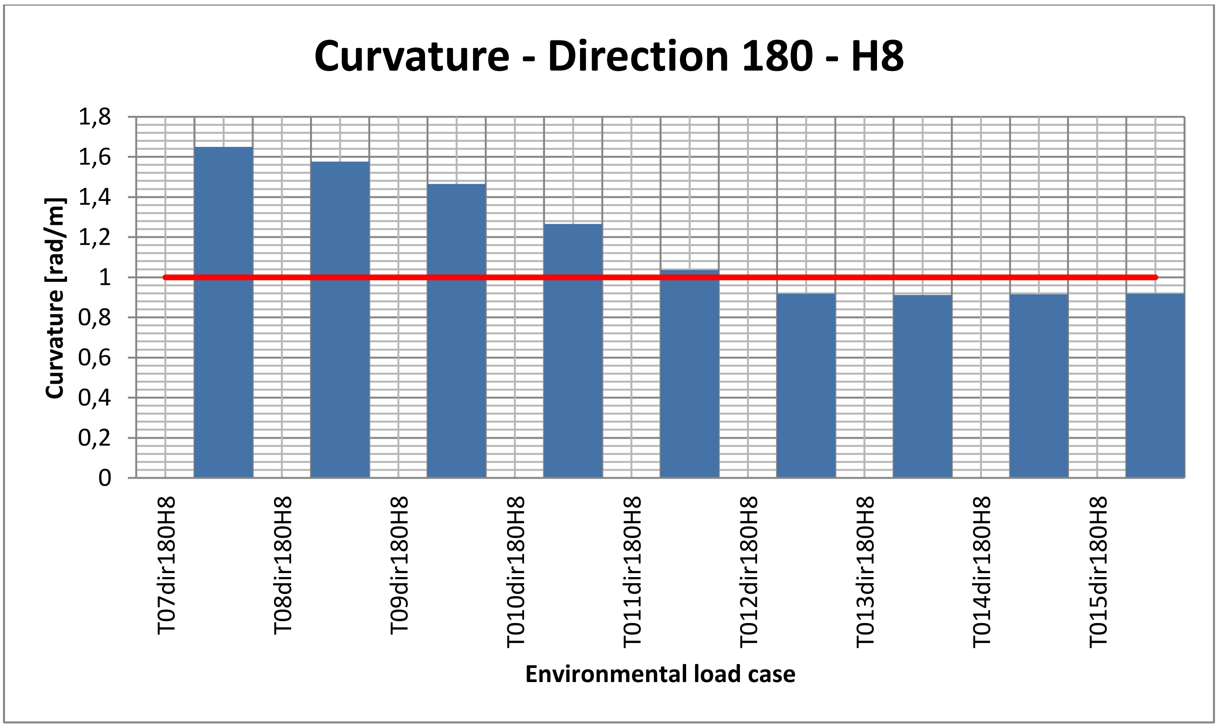

Figure C. 121 - 4” Bunkerflex STH – Lazy wave – 80 m floatation point – Curvature – Direction 180° - H8

Direction 225°

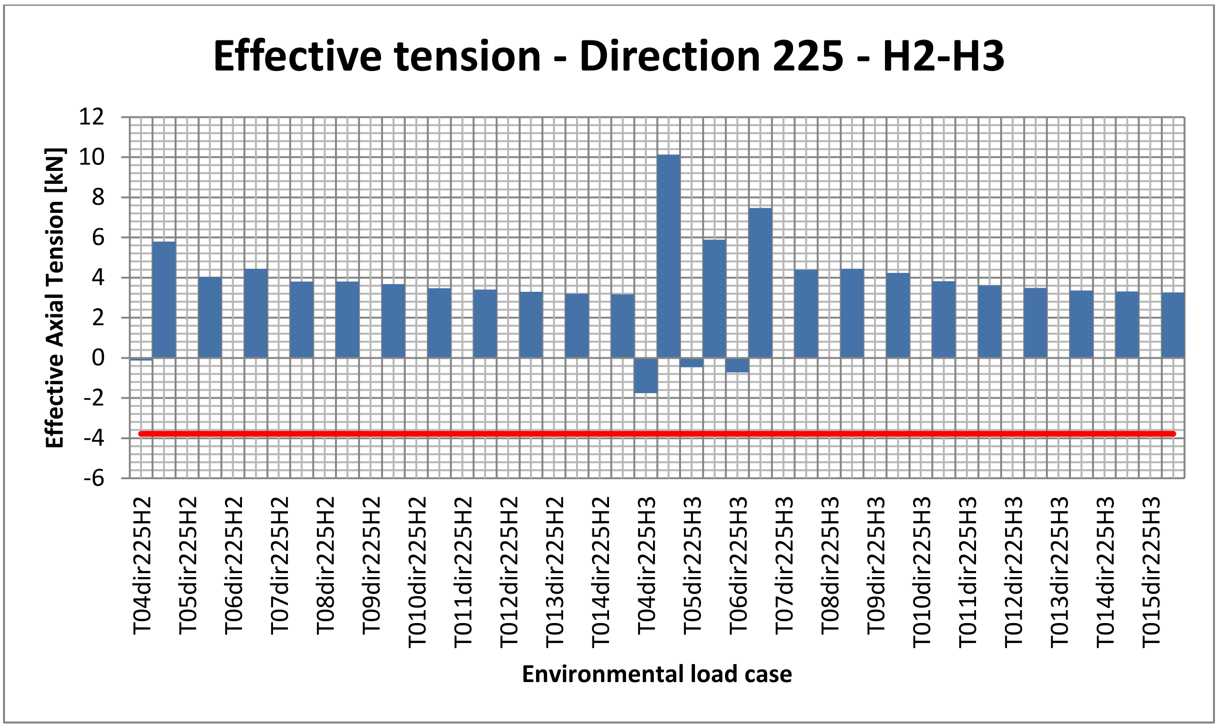

Figure C. 122 - 4” Bunkerflex STH – Lazy wave – 80 m floatation point – Effective tension – Direction 225° - H2-H3

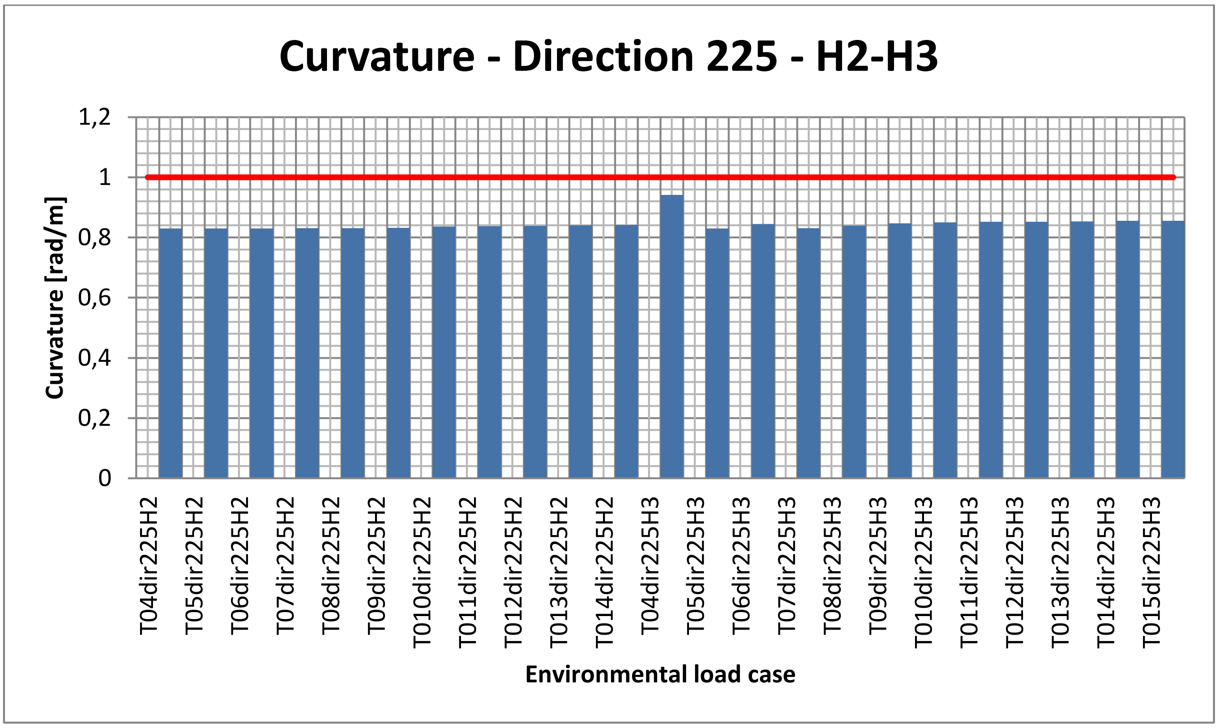

Figure C. 123 - 4” Bunkerflex STH – Lazy wave – 80 m floatation point – Curvature – Direction 225° - H2-H3

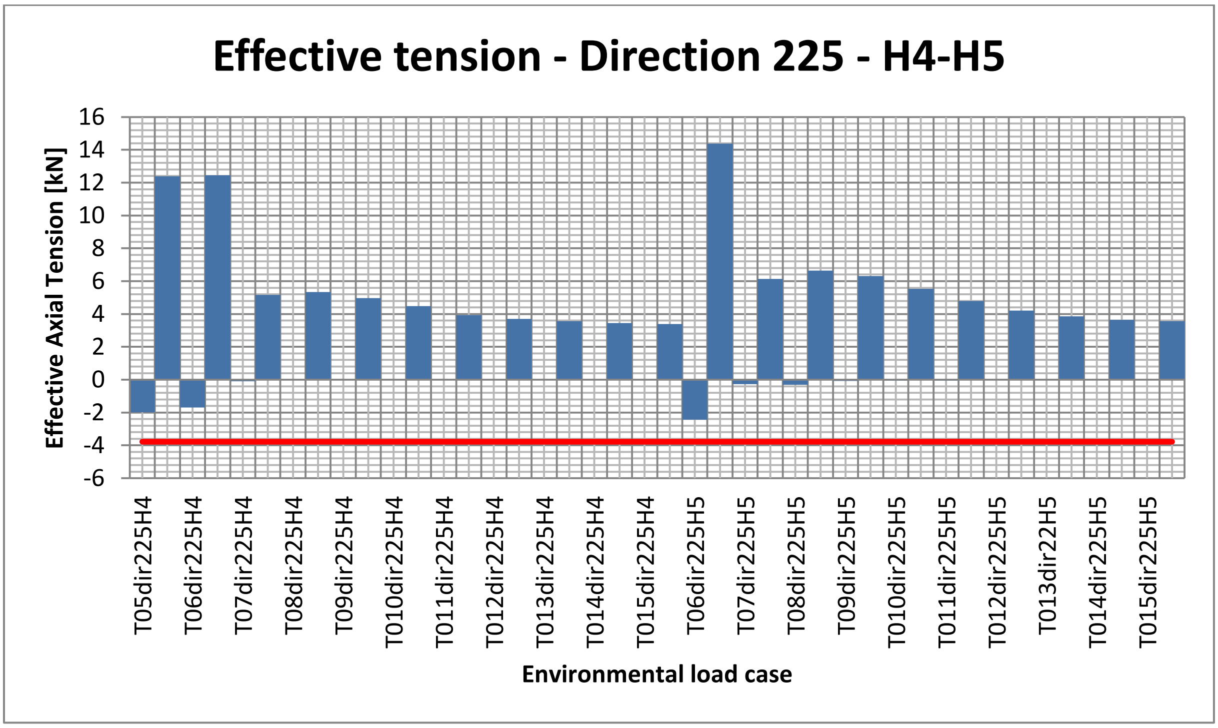

Figure C. 124 - 4” Bunkerflex STH – Lazy wave – 80 m floatation point – Effective tension – Direction 225° - H4-H5

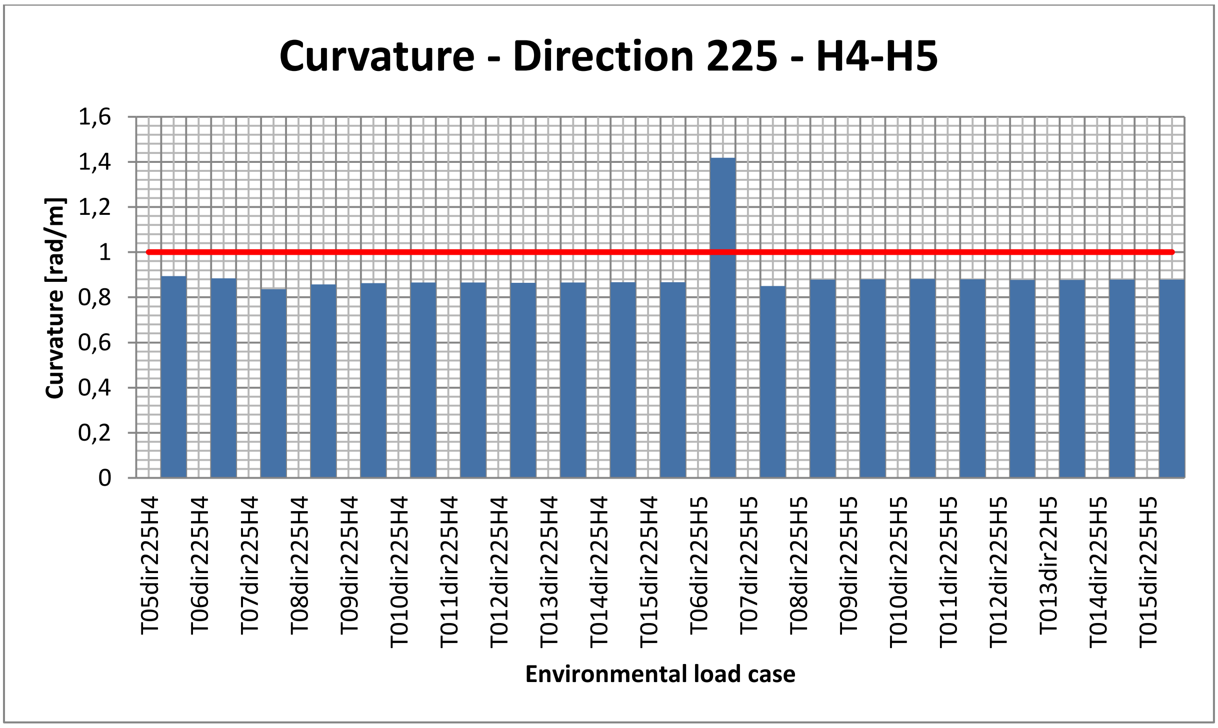

Figure C. 125 - 4” Bunkerflex STH – Lazy wave – 80 m floatation point – Curvature – Direction 225° - H4-H5

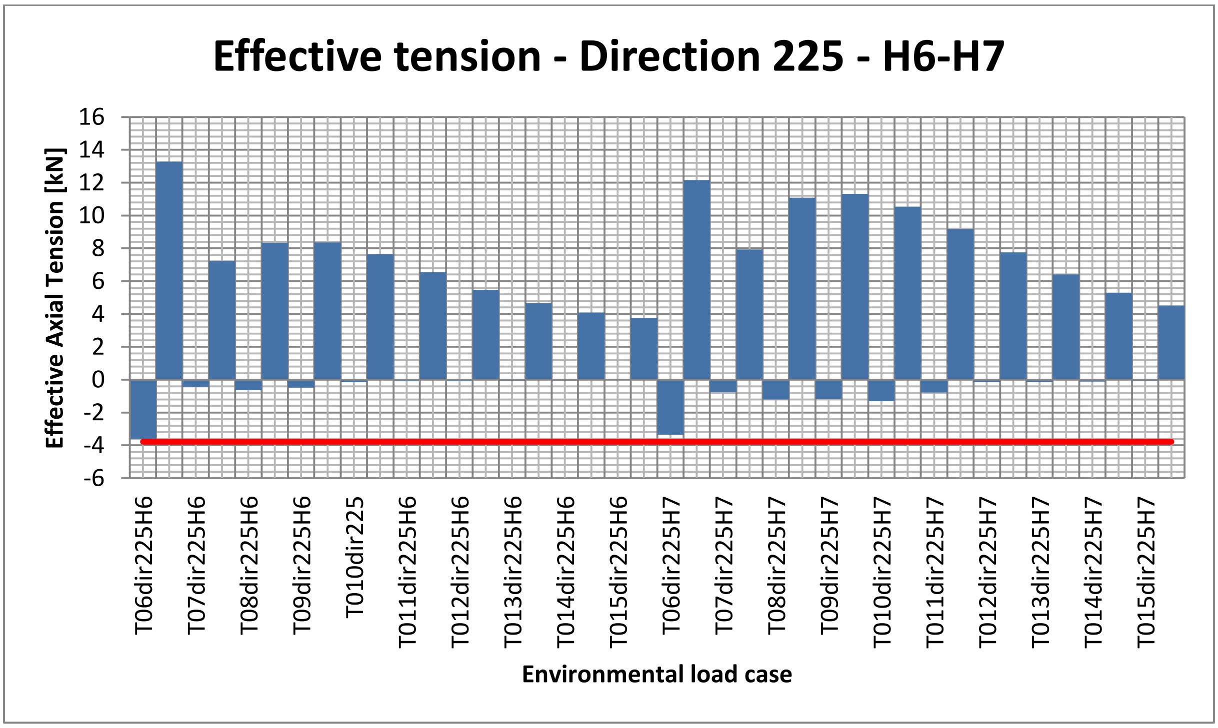

Figure C. 126 - 4" Bunkerflex STH – Lazy wave – 80 m floatation point – Effective tension – Direction 225° - H6-H7

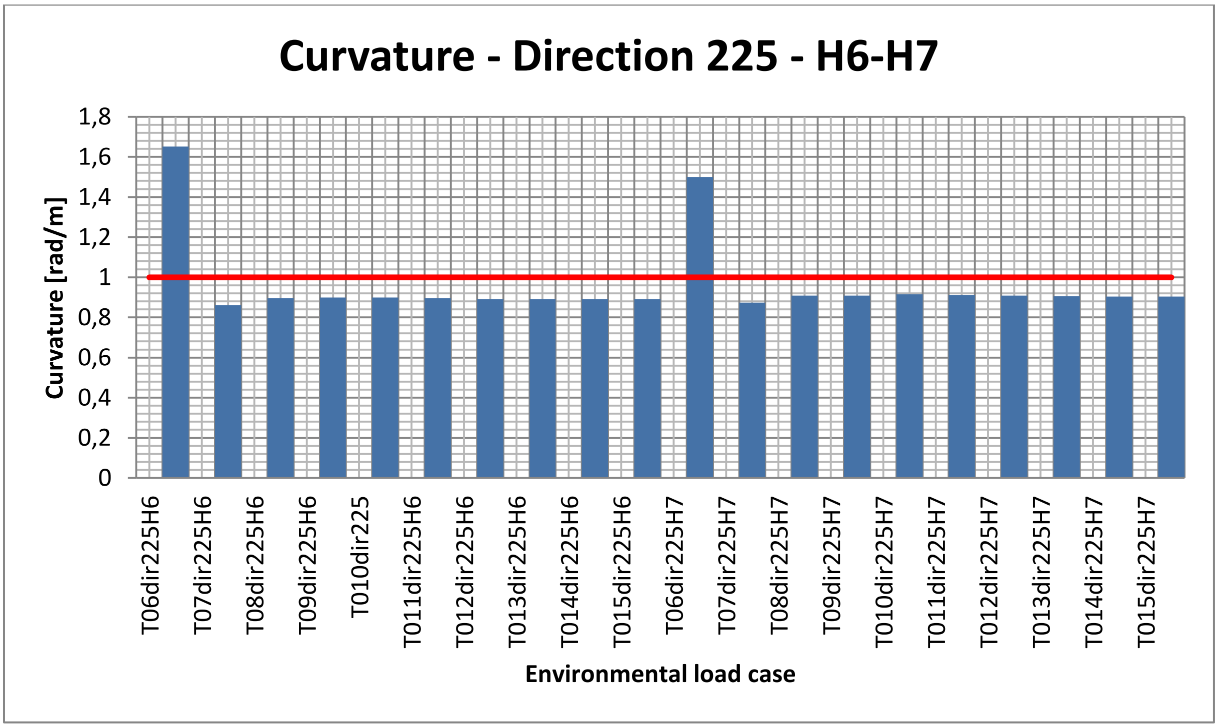

Figure C. 127 - 4" Bunkerflex STH – Lazy wave – 80 m floatation point – Curvature – Direction 225° - H6-H7

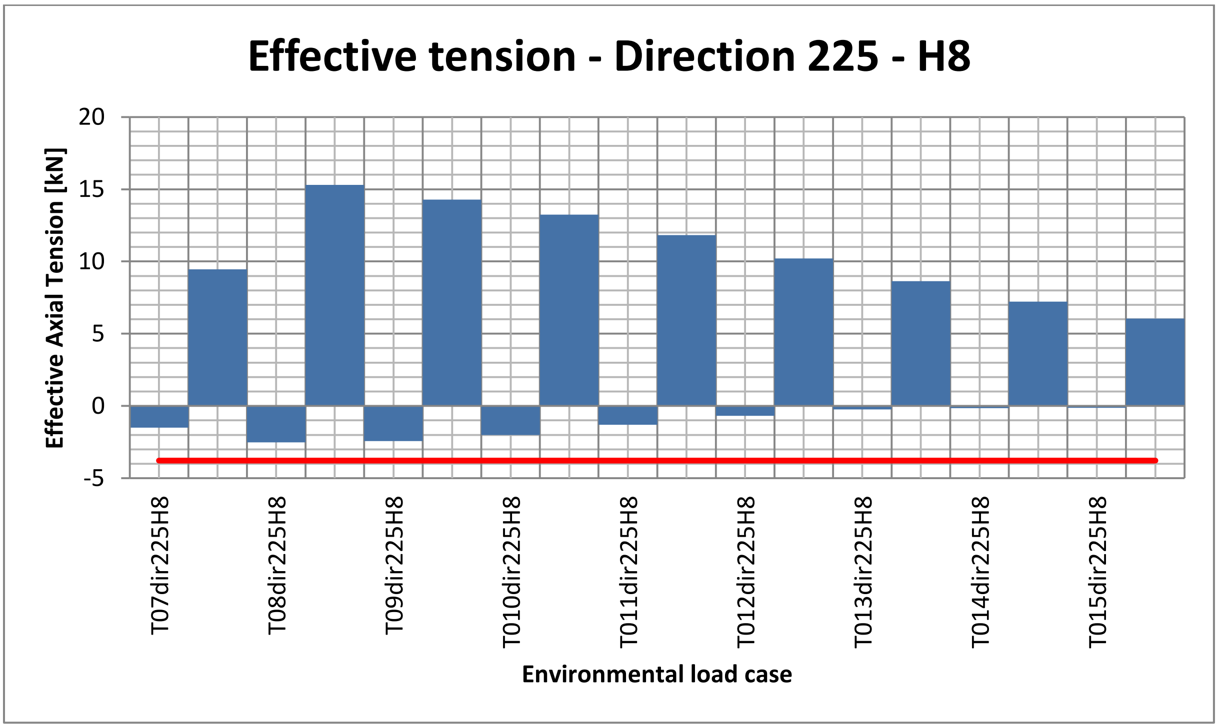

Figure C. 128 - 4” Bunkerflex STH – Lazy wave – 80 m floatation point – Effective tension – Direction 225° - H8

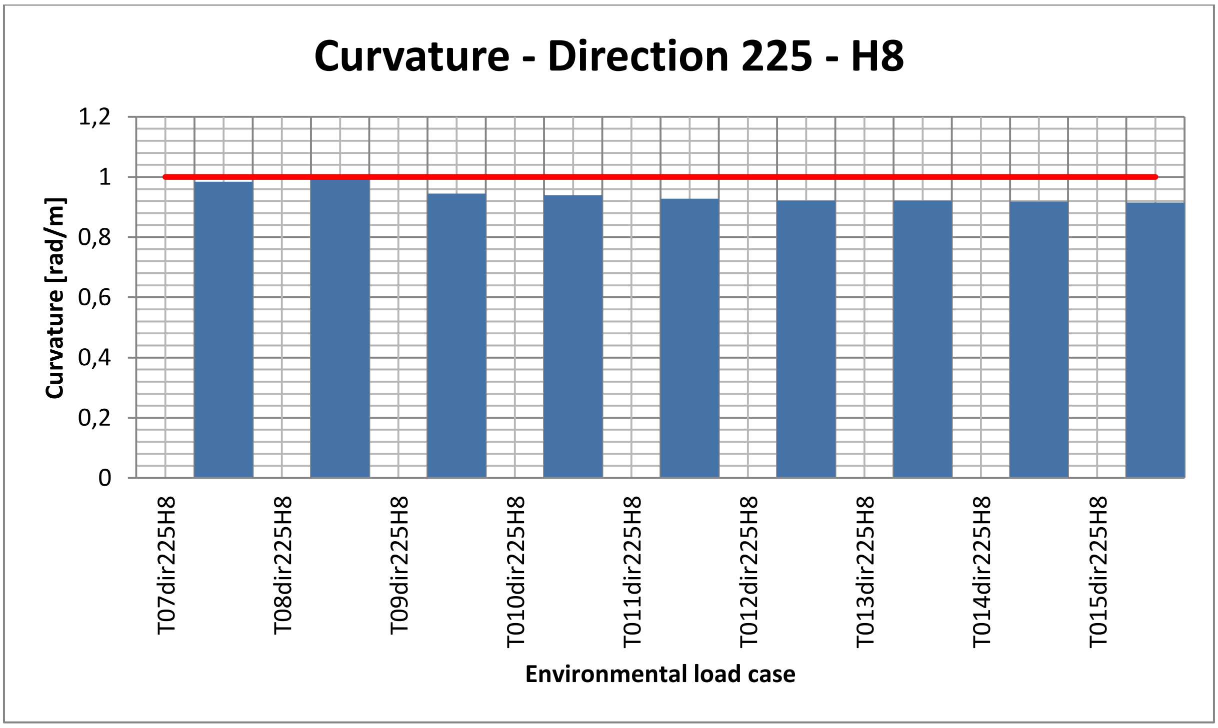

Figure C. 129 - 4” Bunkerflex STH – Lazy wave – 80 m floatation point – Curvature – Direction 225° - H8

Wave rose

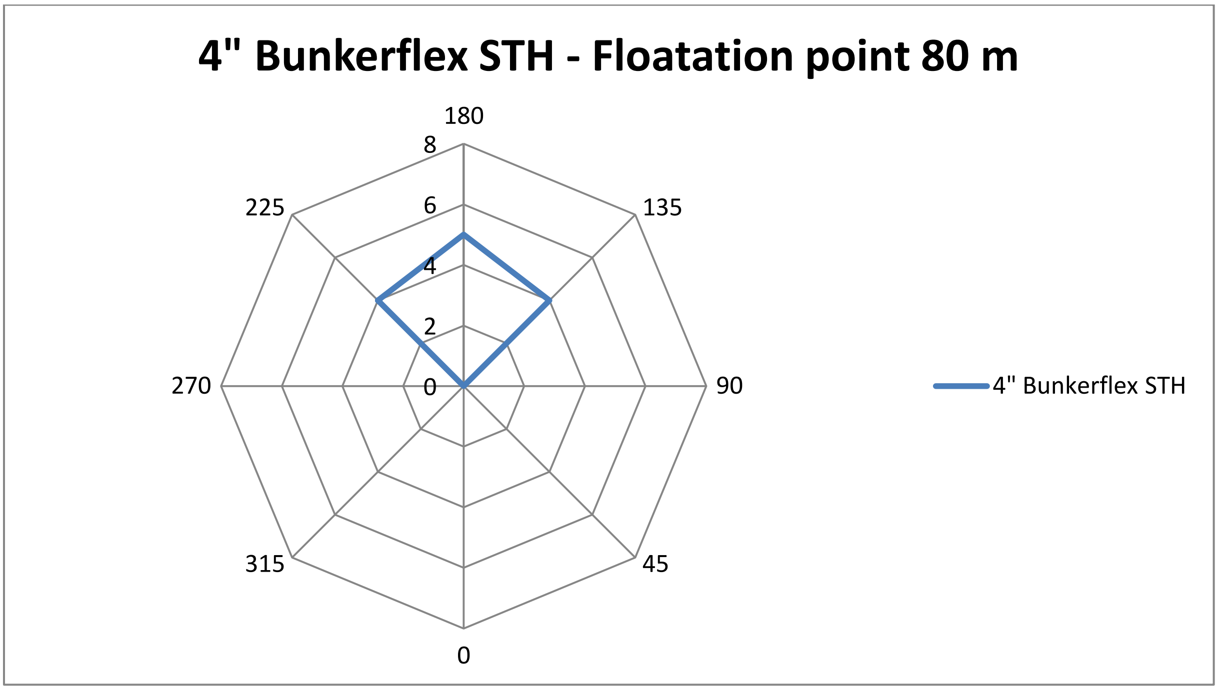

Figure C. 130 - 4” Bunkerflex STH – Lazy wave – 80 m floatation point – Wave rose

Limitation plot

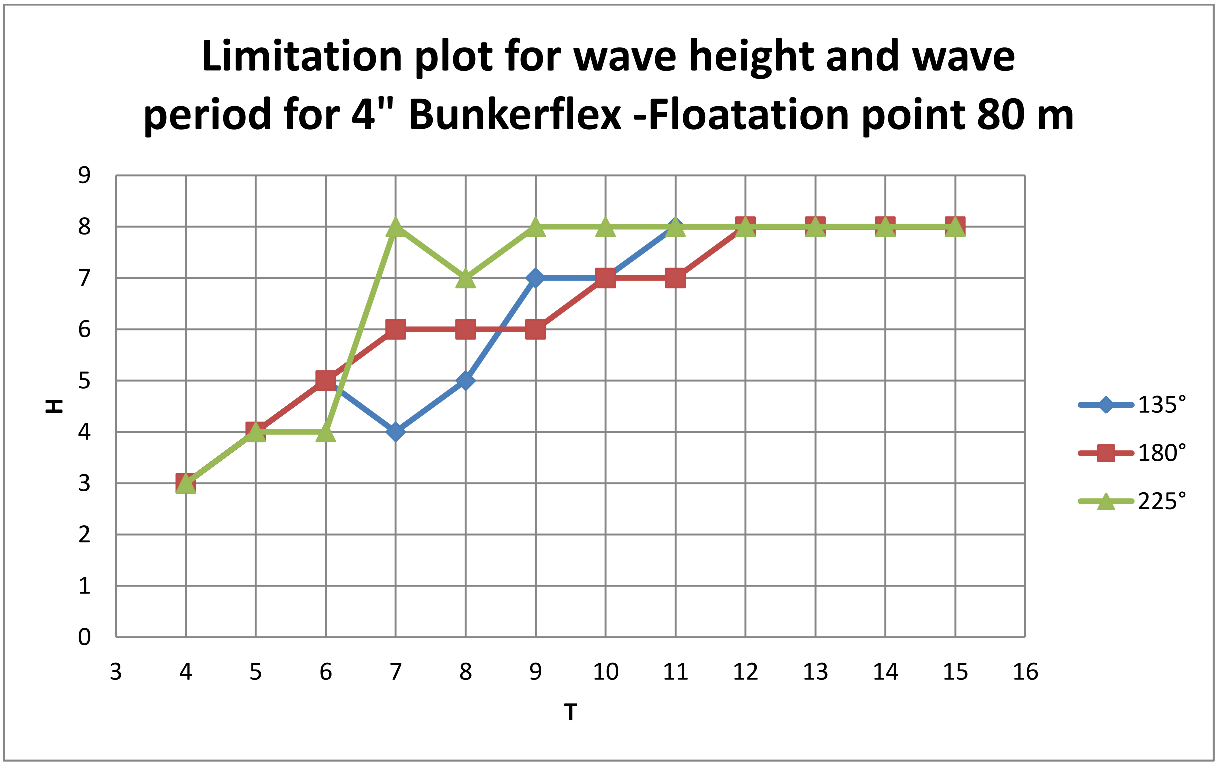

Figure C. 131 - 4” Bunkerflex STH – Lazy wave – 80 m floatation point – Limitation plot

6” Oilflex Super

Free hanging

Direction 135°

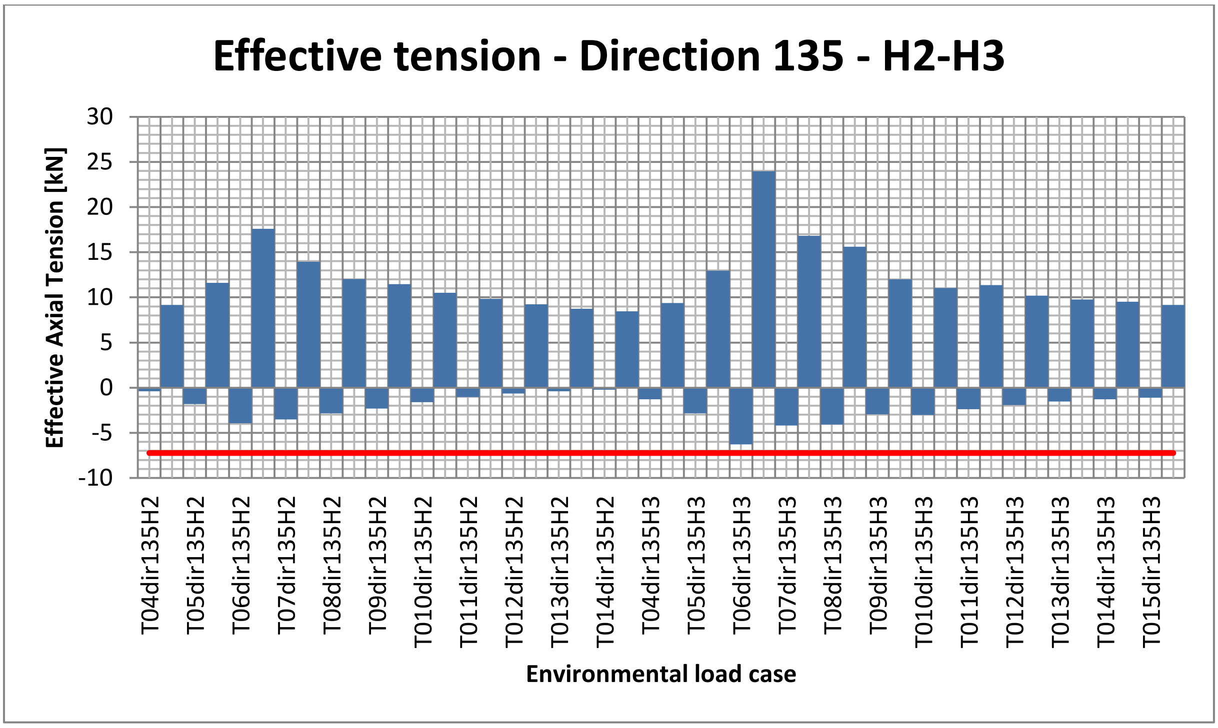

Figure C. 132 - 6” Oilflex Super – Free hanging – Effective tension – Direction 135° - H2-H3

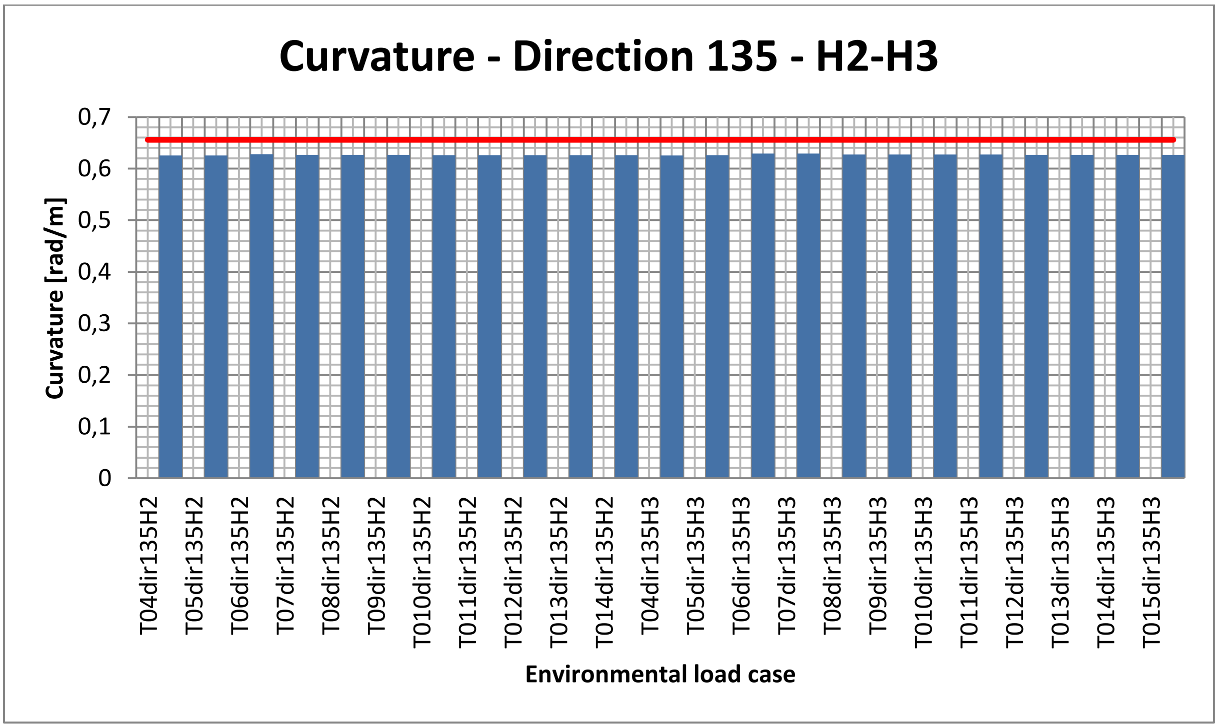

Figure C. 133 - 6” Oilflex Super – Free hanging – Curvature – Direction 135° - H2-H3

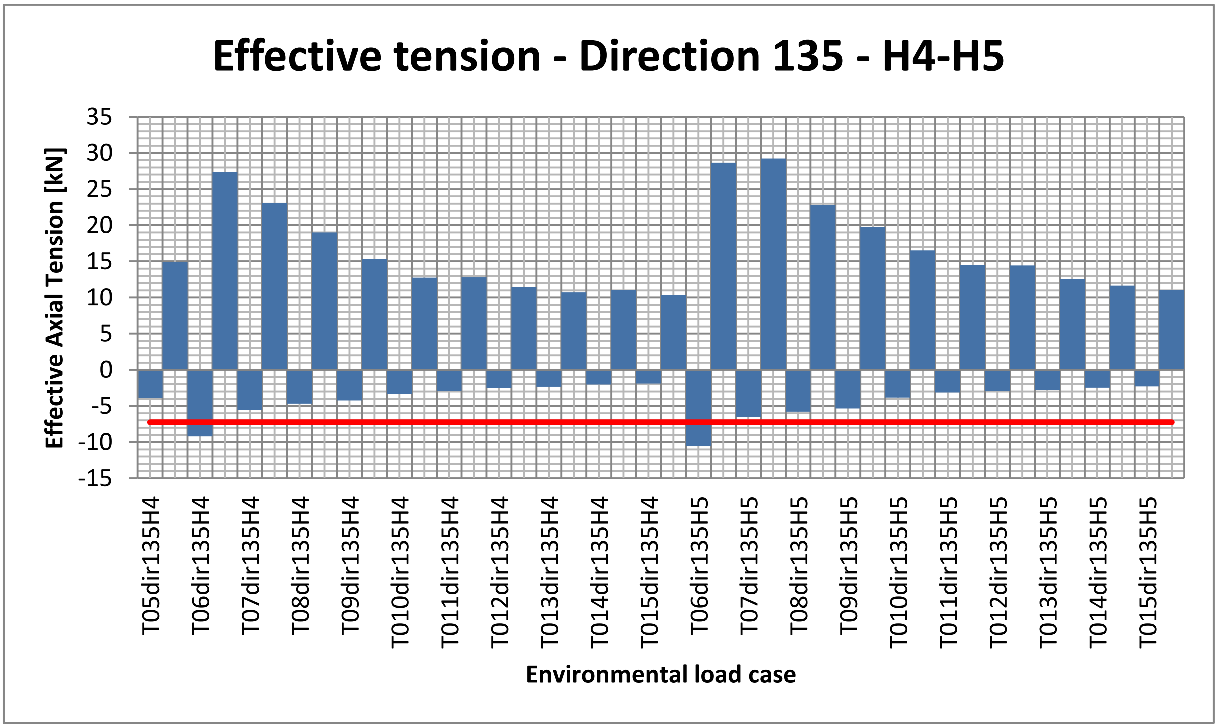

Figure C. 134 - 6" Oilflex Super – Free hanging – Effective tension – Direction 135° - H4-H5

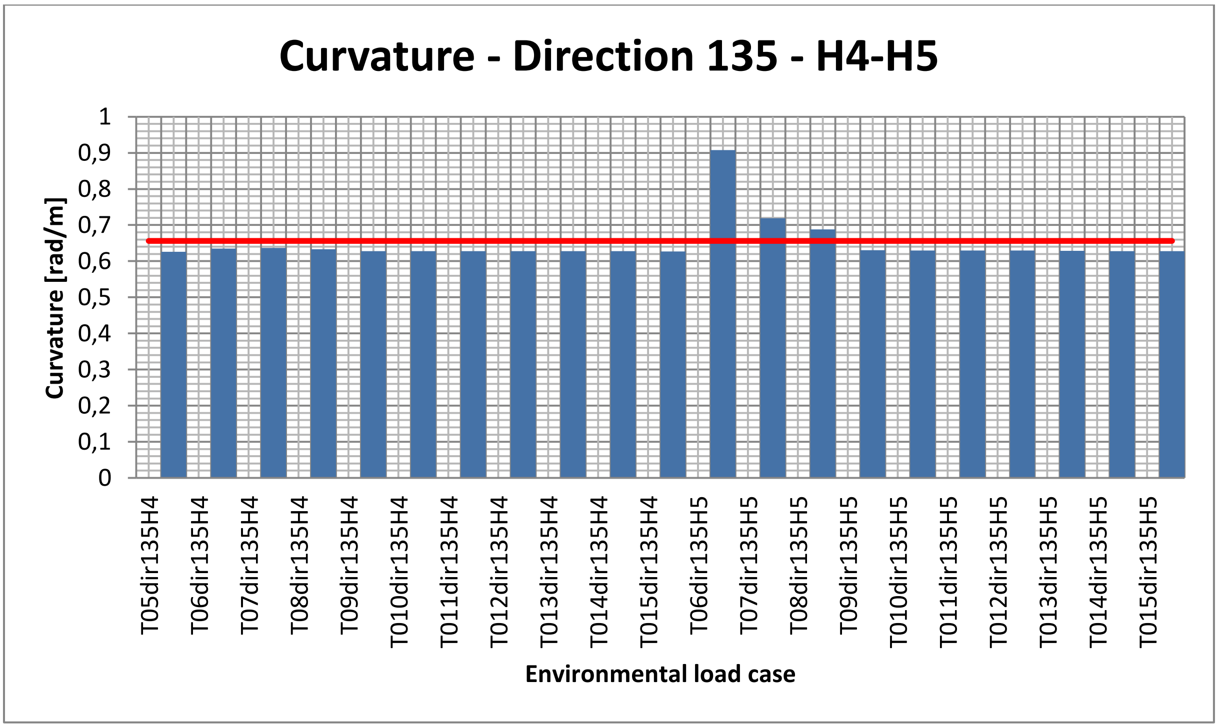

Figure C. 135 - 6" Oilflex Super – Free hanging – Curvature – Direction 135° - H4-H5

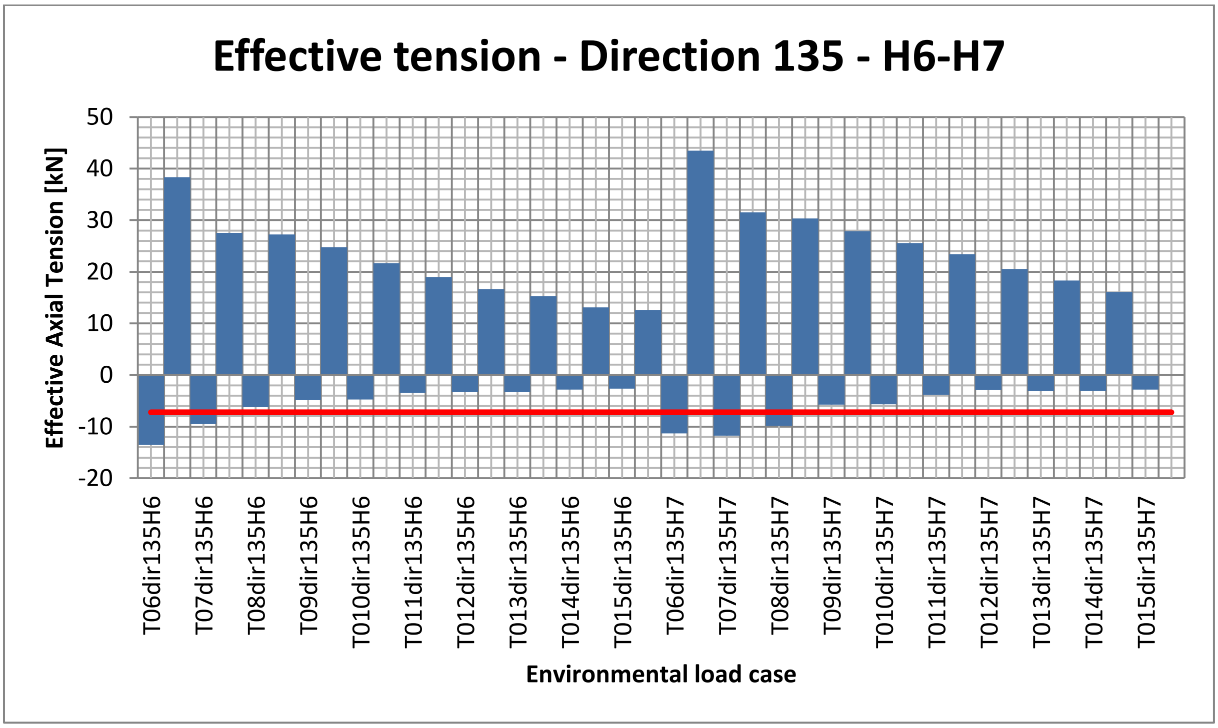

Figure C. 136 - 6” Oilflex Super – Free hanging – Effective tension – Direction 135° - H6-H7

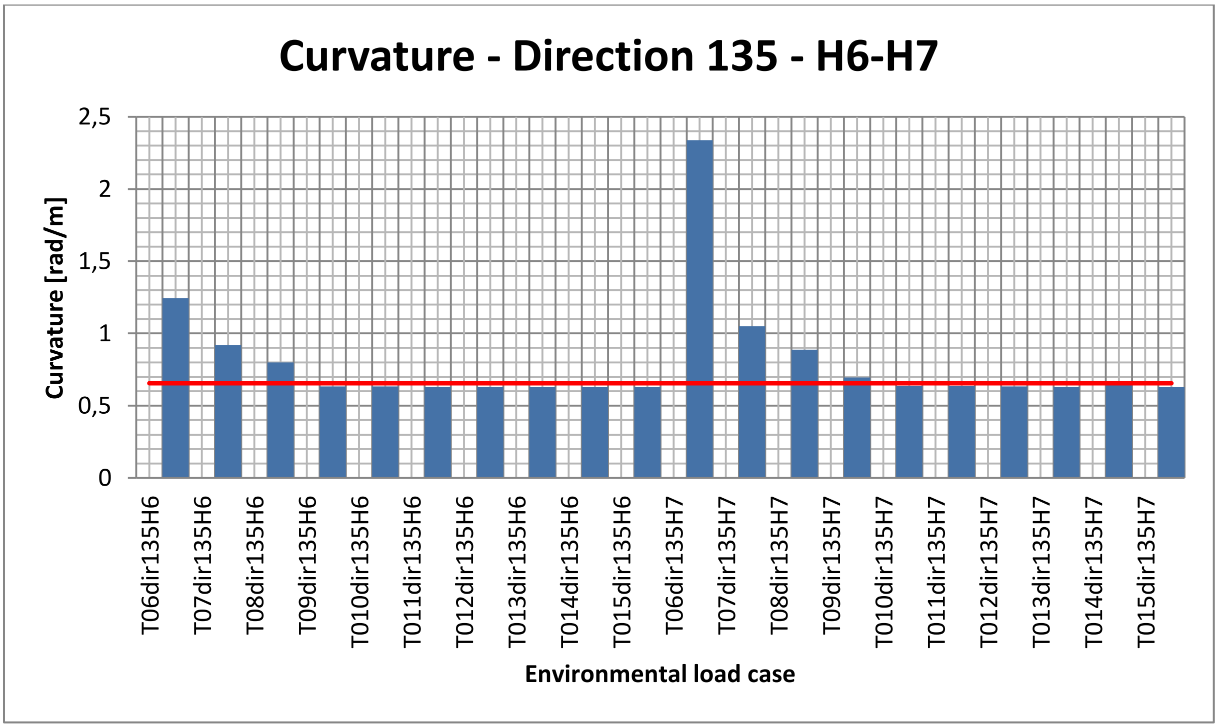

Figure C. 137 - 6” Oilflex Super – Free hanging – Curvature – Direction 135° - H6-H7

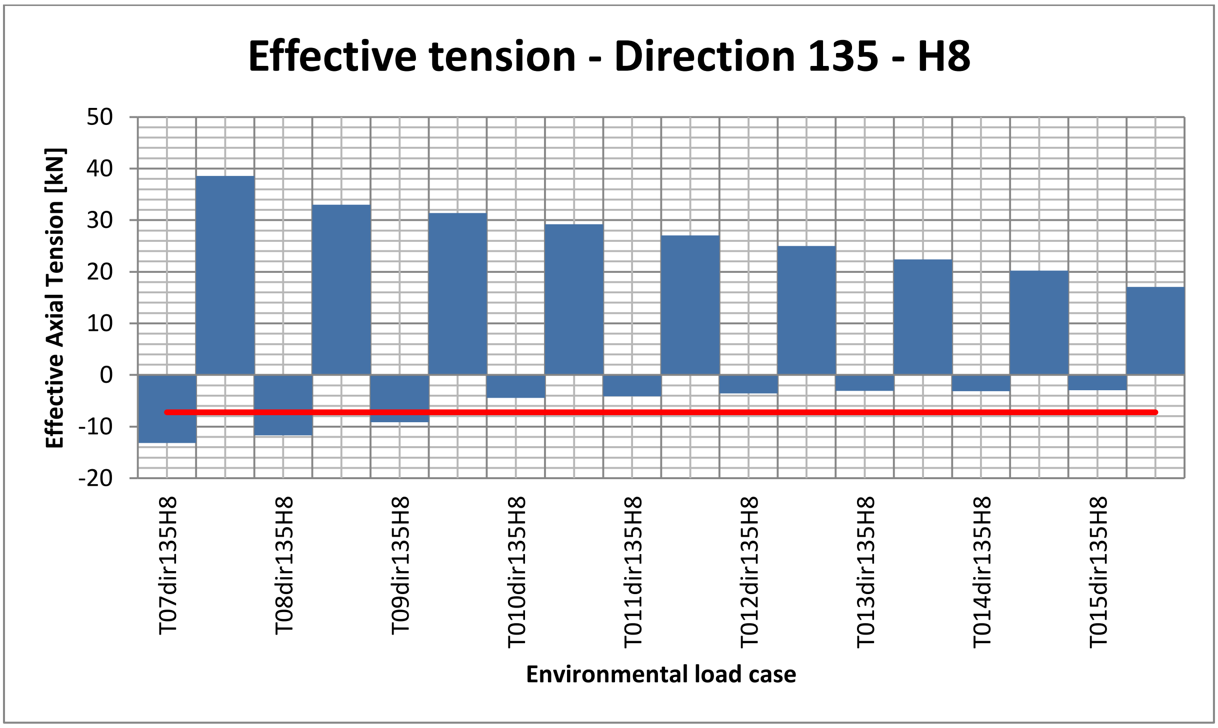

Figure C. 138 - 6” Oilflex Super – Free hanging – Effective tension – Direction 135° - H8

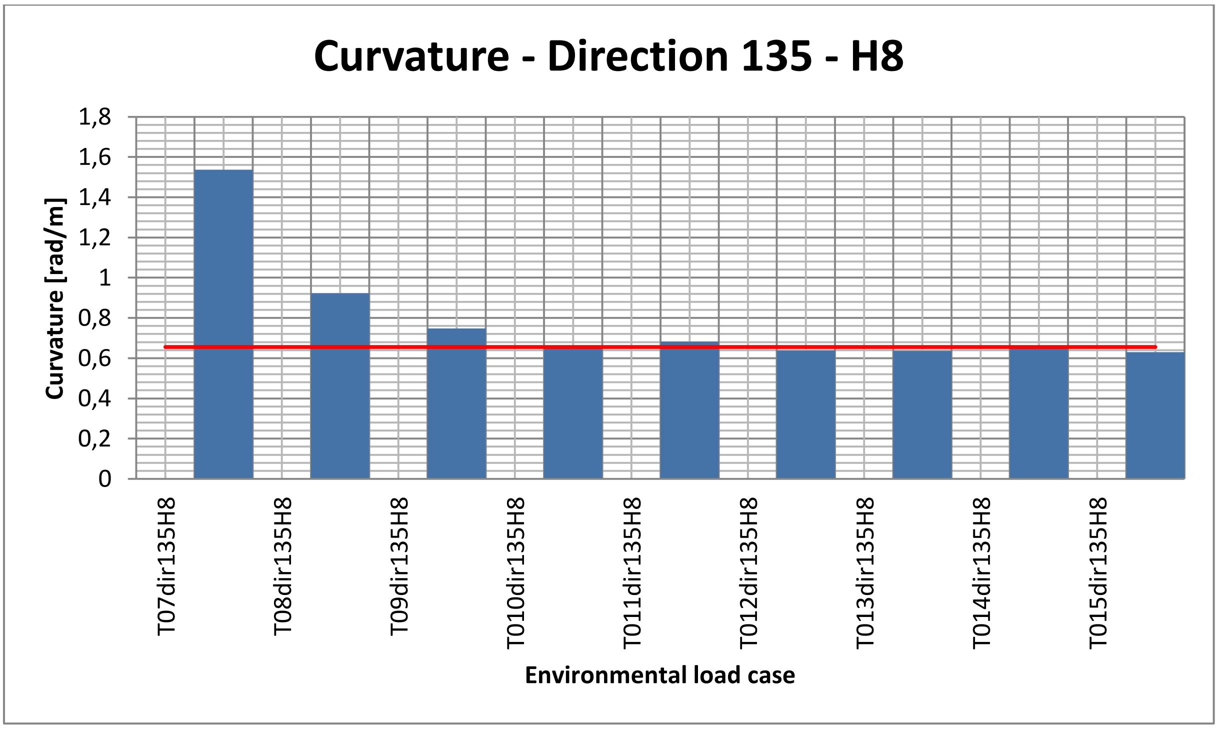

Figure C. 139 - 6” Oilflex Super – Free hanging – Curvature – Direction 135° - H8

Direction 180°

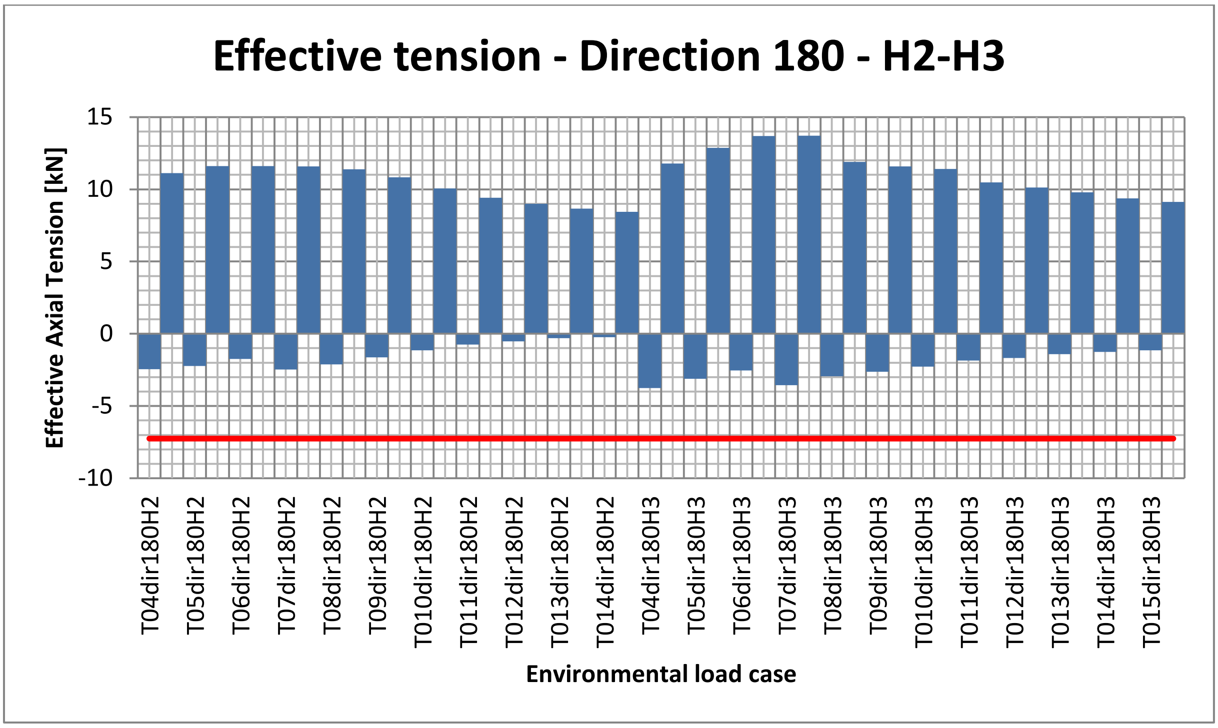

Figure C. 140 - 6” Oilflex Super – Free hanging – Effective tension – Direction 180° - H2-H3

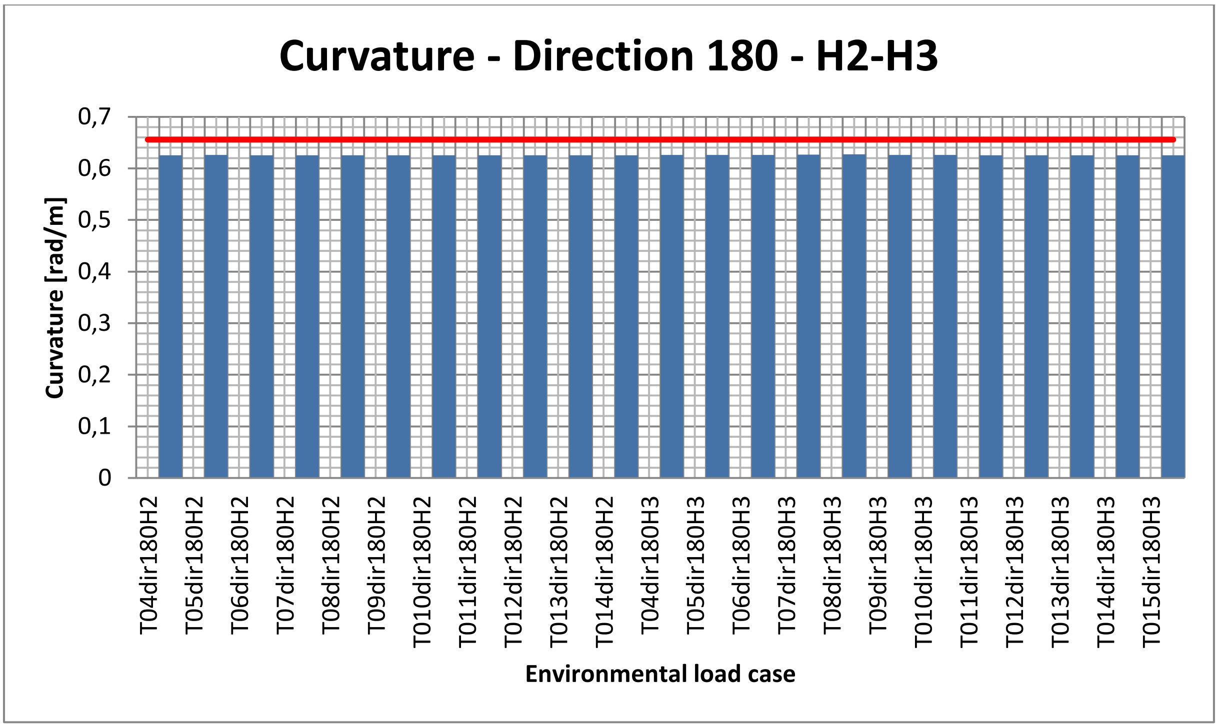

Figure C. 141 - 6” Oilflex Super – Free hanging – Curvature – Direction 180° - H2-H3

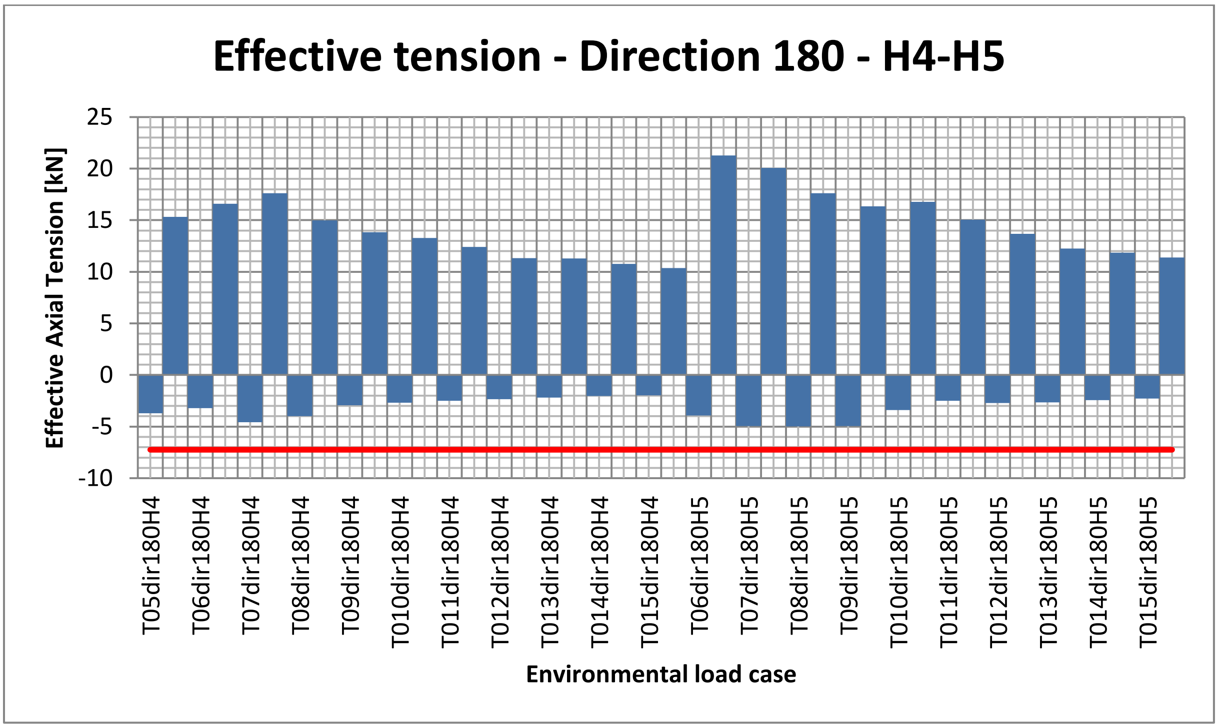

Figure C. 142 - 6" Oilflex Super – Free hanging – Effective tension – Direction 180° - H4-H5

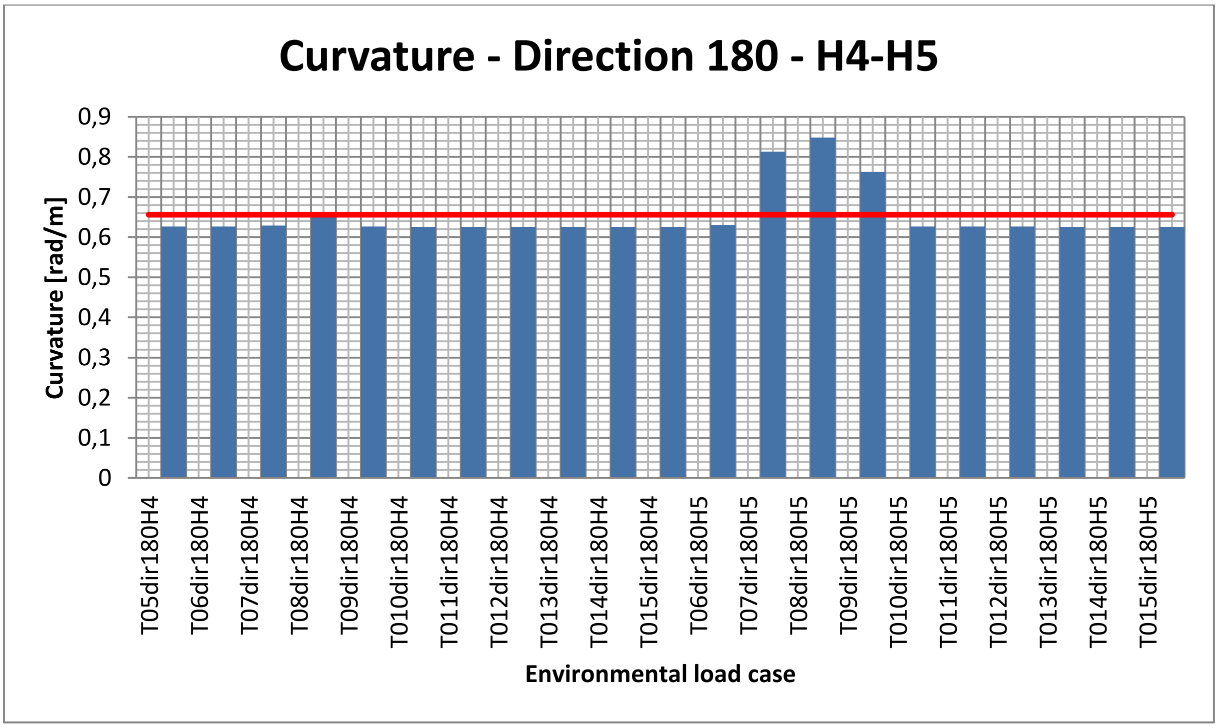

Figure C. 143 - 6" Oilflex Super – Free hanging – Curvature – Direction 180° - H4-H5

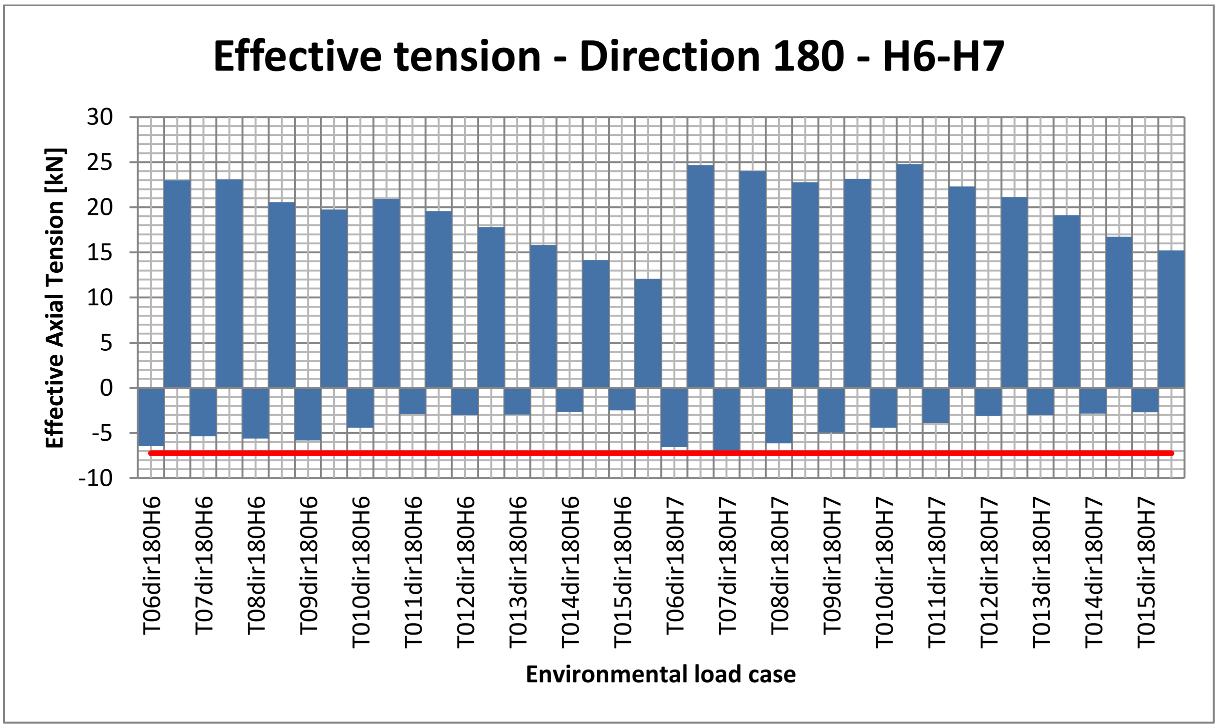

Figure C. 144 - 6" Oilflex Super – Free hanging – Effective tension – Direction 180° - H6-H7

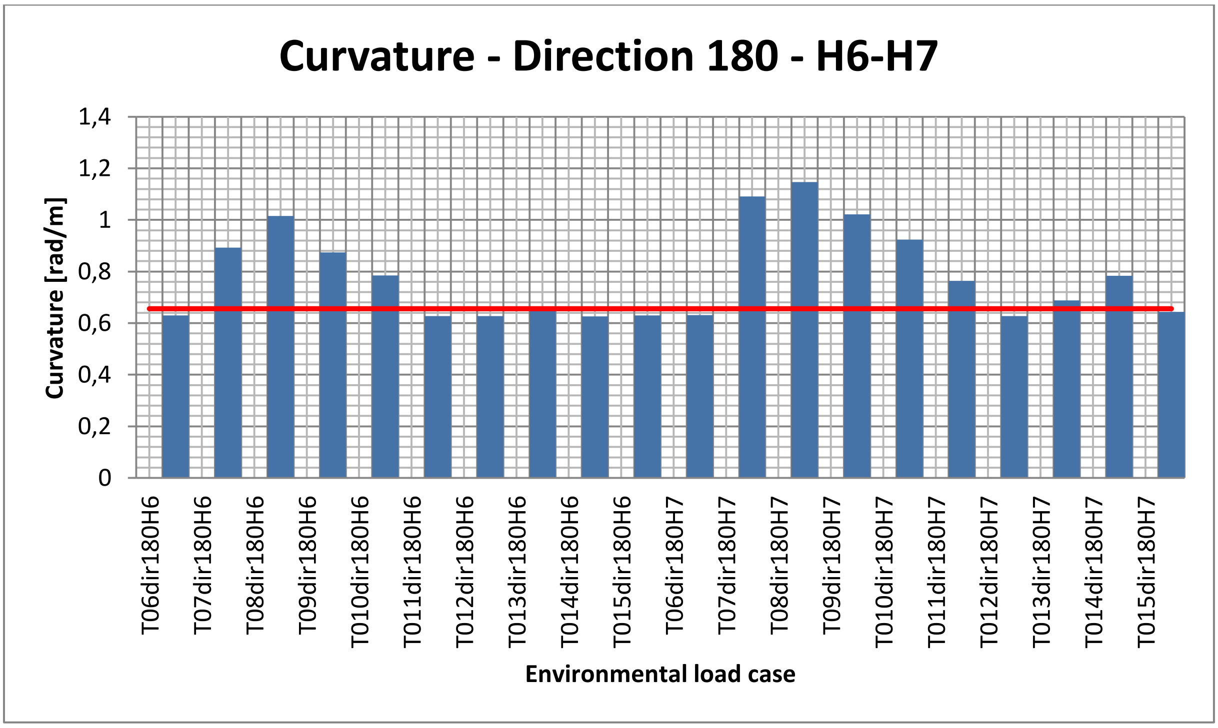

Figure C. 145 - 6" Oilflex Super – Free hanging – Curvature – Direction 180° - H6-H7

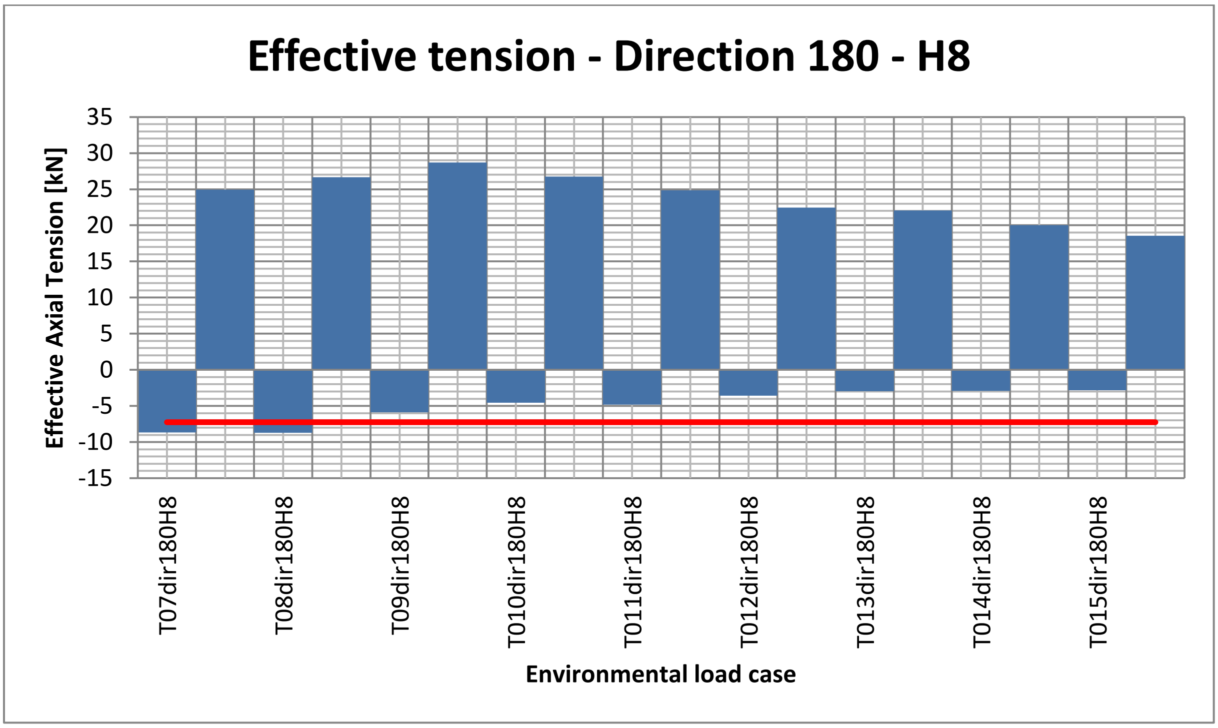

Figure C. 146 - 6” Oilflex Super – Free hanging – Effective tension – Direction 180° - H8

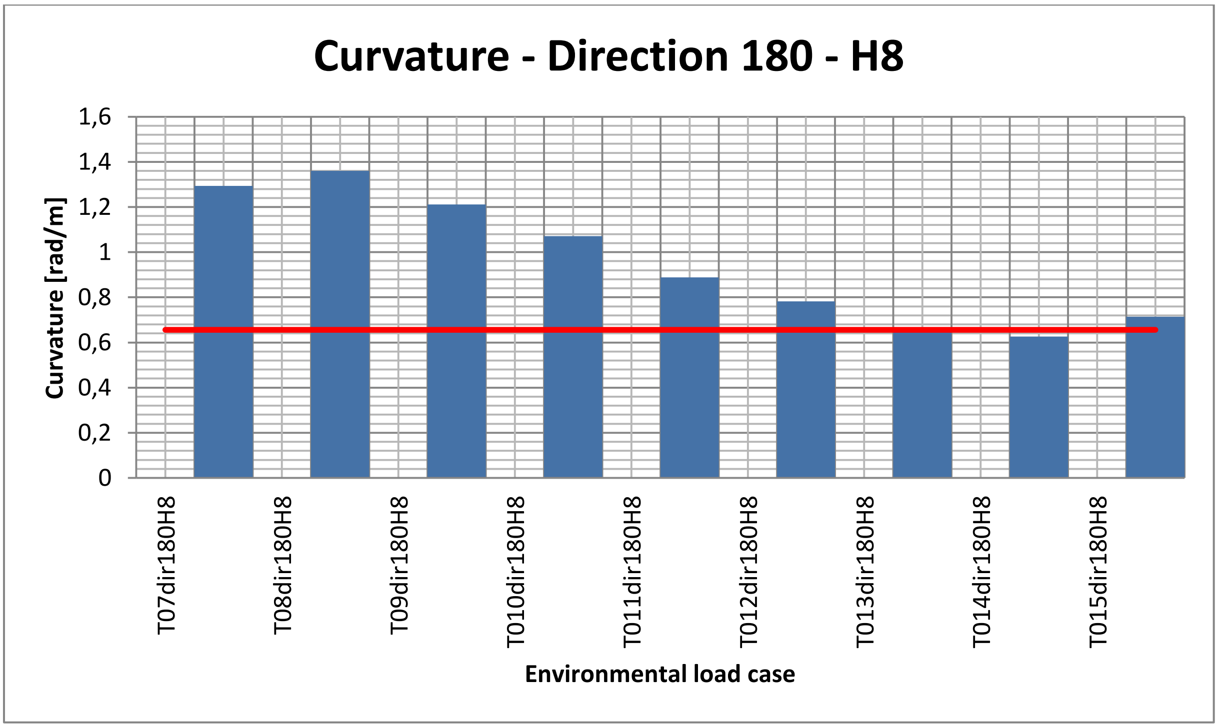

Figure C. 147 - 6” Oilflex Super – Free hanging – Curvature – Direction 180° - H8

Direction 225°

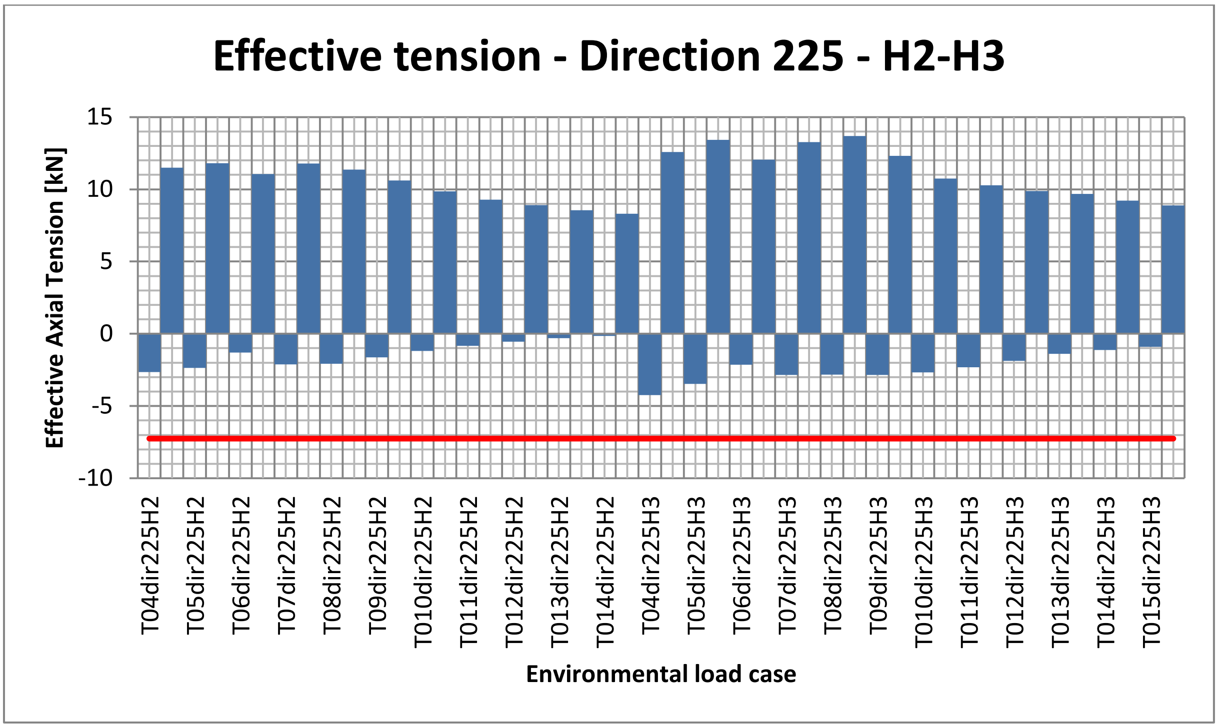

Figure C. 148 - 6" Oilflex Super – Free hanging – Effective tension – Direction 225° - H2-H3

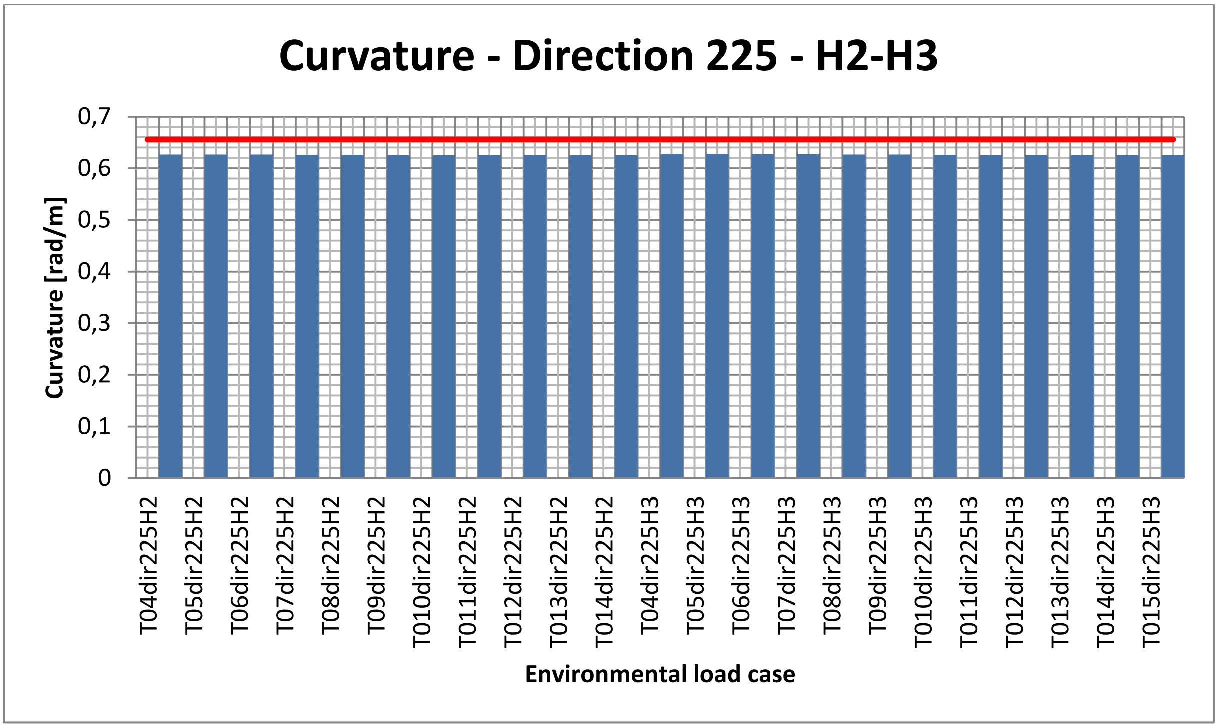

Figure C. 149 - 6" Oilflex Super – Free hanging – Curvature – Direction 225° - H2-H3

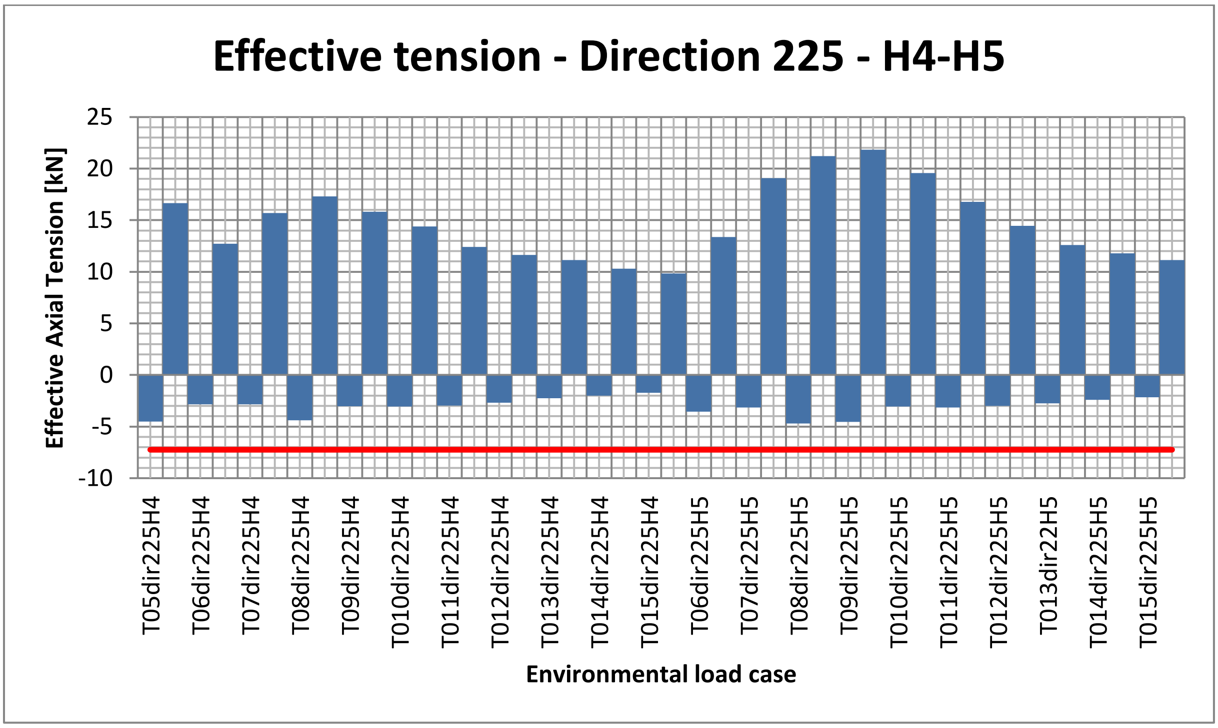

Figure C. 150 - 6” Oilflex Super – Free hanging – Effective tension – Direction 225° - H4-H5

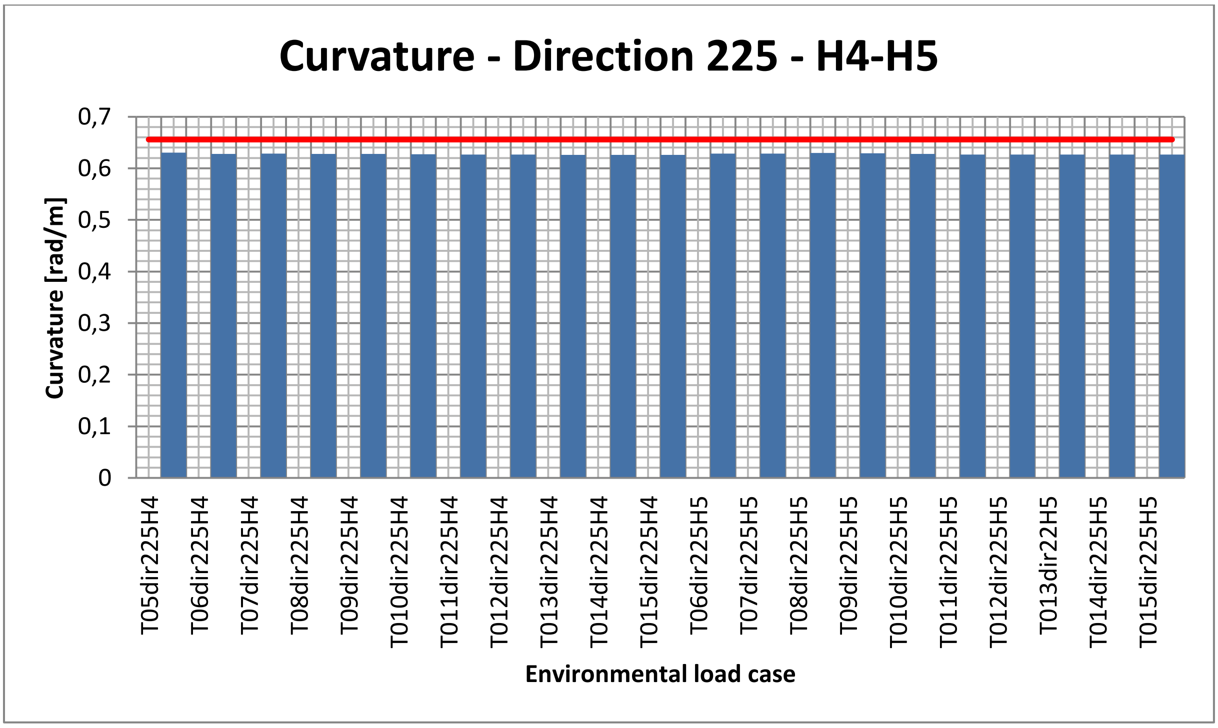

Figure C. 151 - 6” Oilflex Super – Free hanging – Curvature – Direction 225° - H4-H5

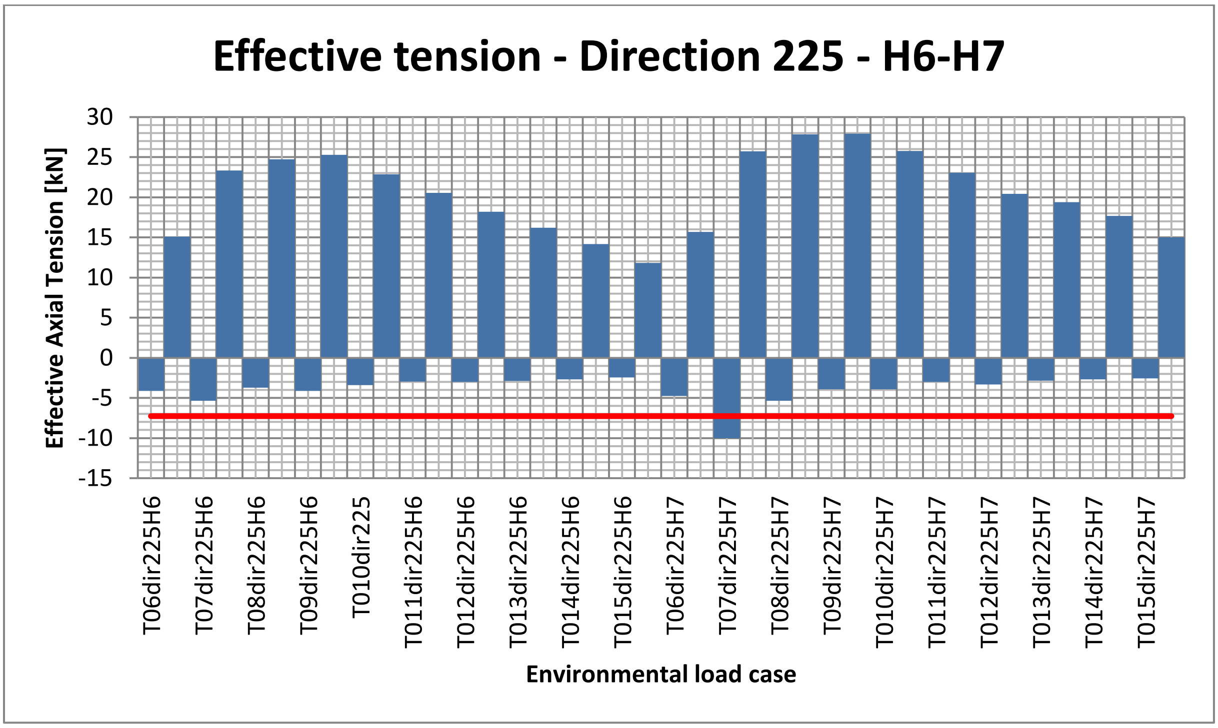

Figure C. 152 - 6" Oilflex Super – Free hanging – Effective tension – Direction 225° - H6-H7

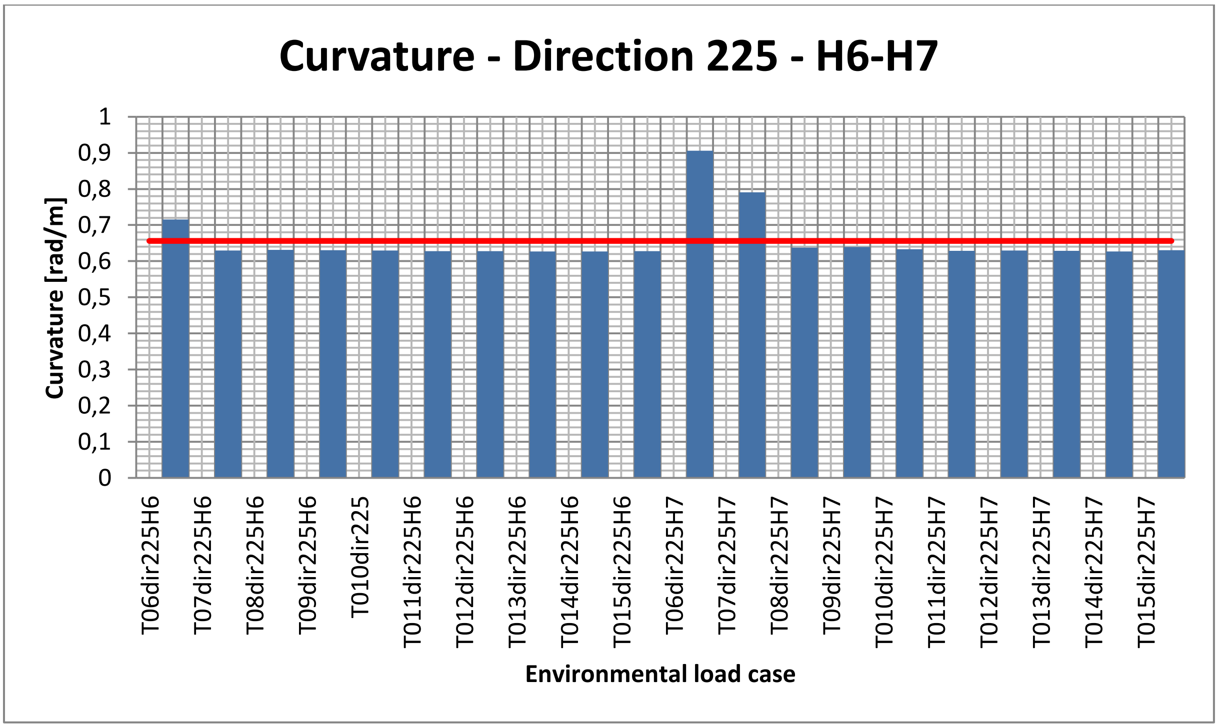

Figure C. 153 - 6" Oilflex Super – Free hanging – Curvature – Direction 225° - H6-H7

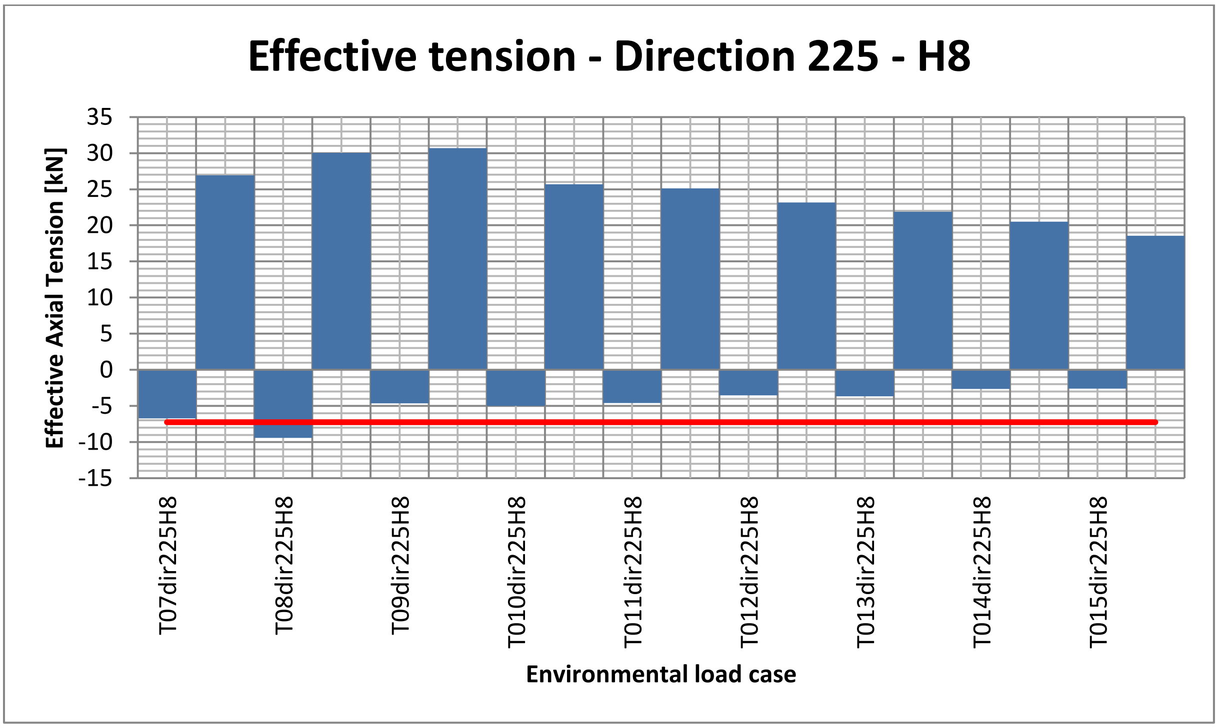

Figure C. 154 - 6" Oilflex Super – Free hanging – Effective tension – Direction 225° - H8

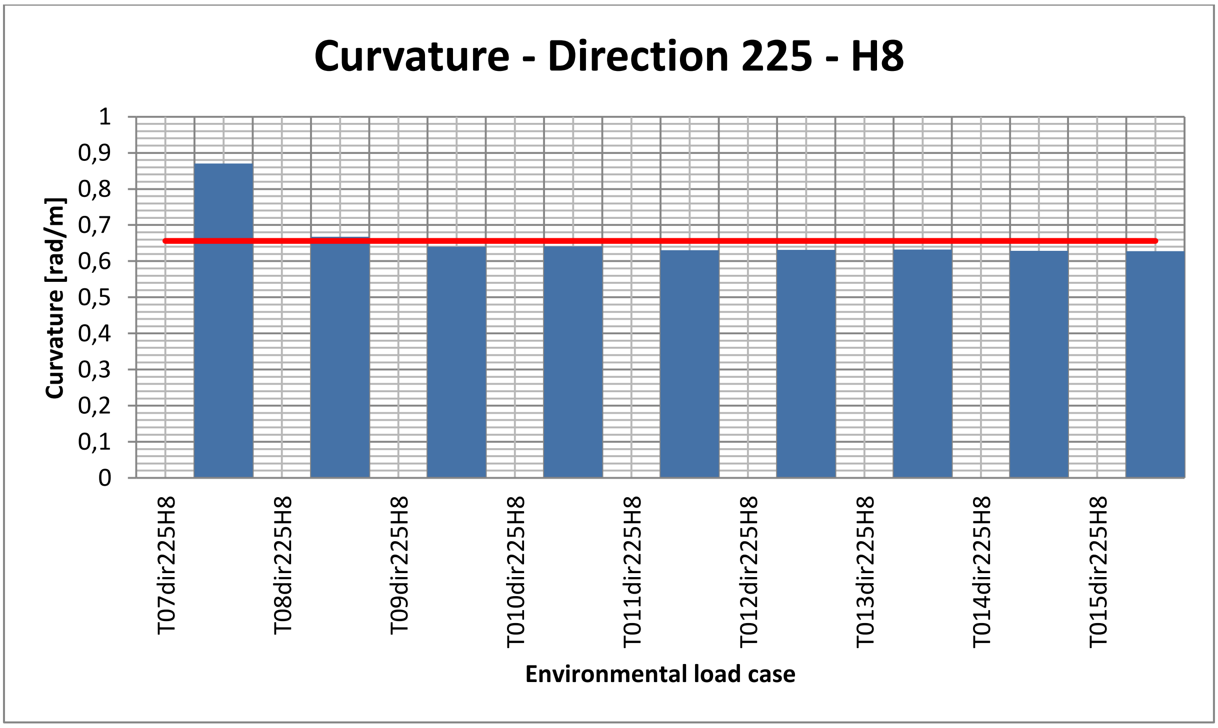

Figure C. 155 - 6" Oilflex Super – Free hanging – Curvature – Direction 225° - H8

Wave rose

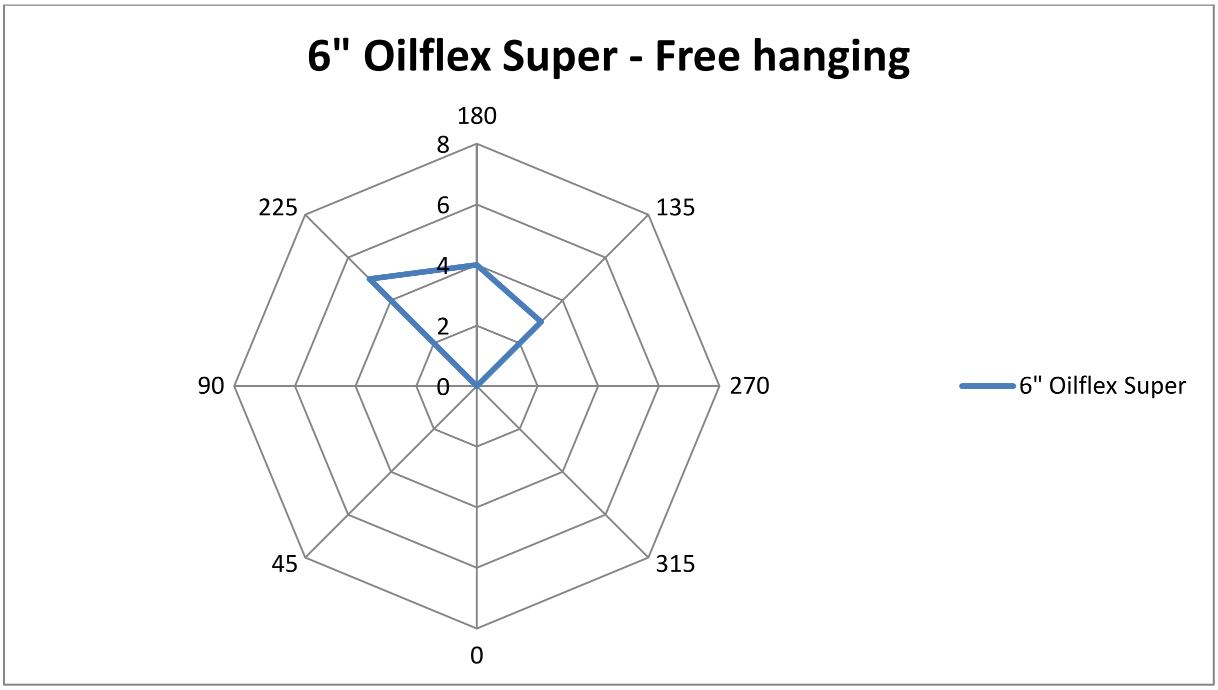

Figure C. 156 - 6” Oilflex Super – Free hanging – Wave rose

Limitation plot

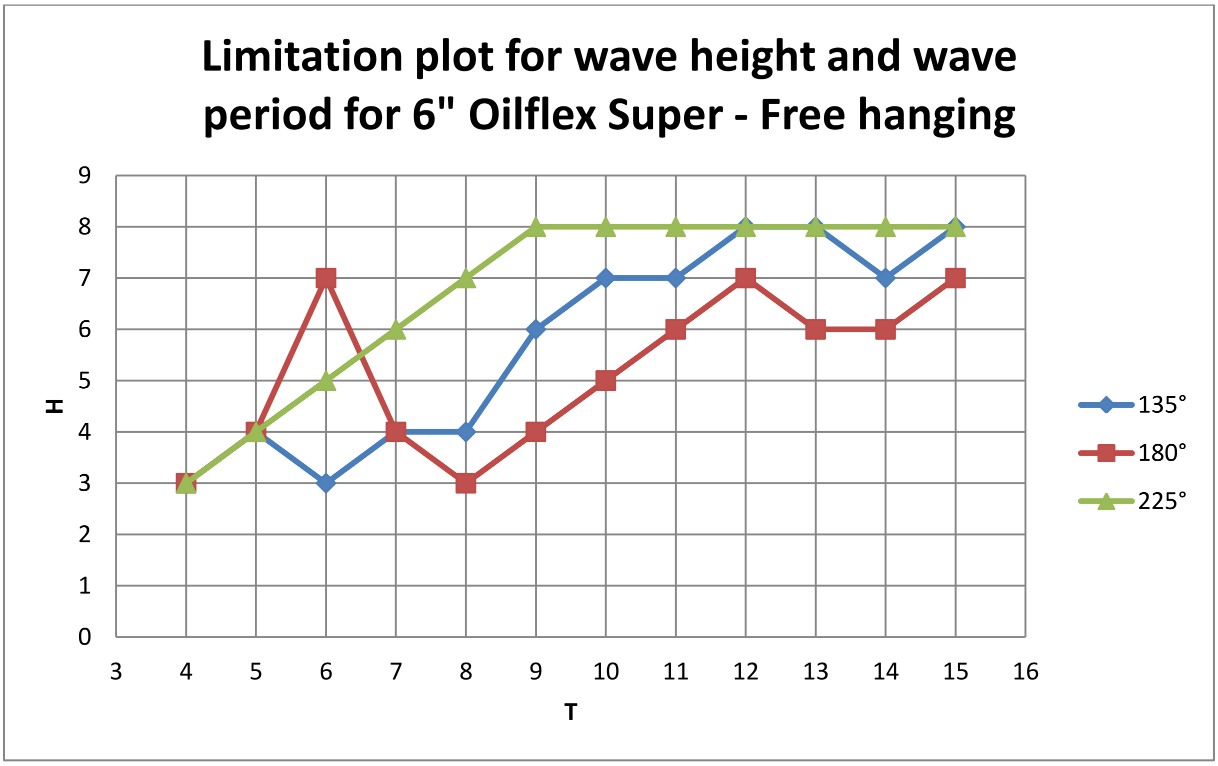

Figure C. 157 - 6” Oilflex Super – Free hanging – Limitation plot

Lazy wave – 20 m floatation point

Direction 135°

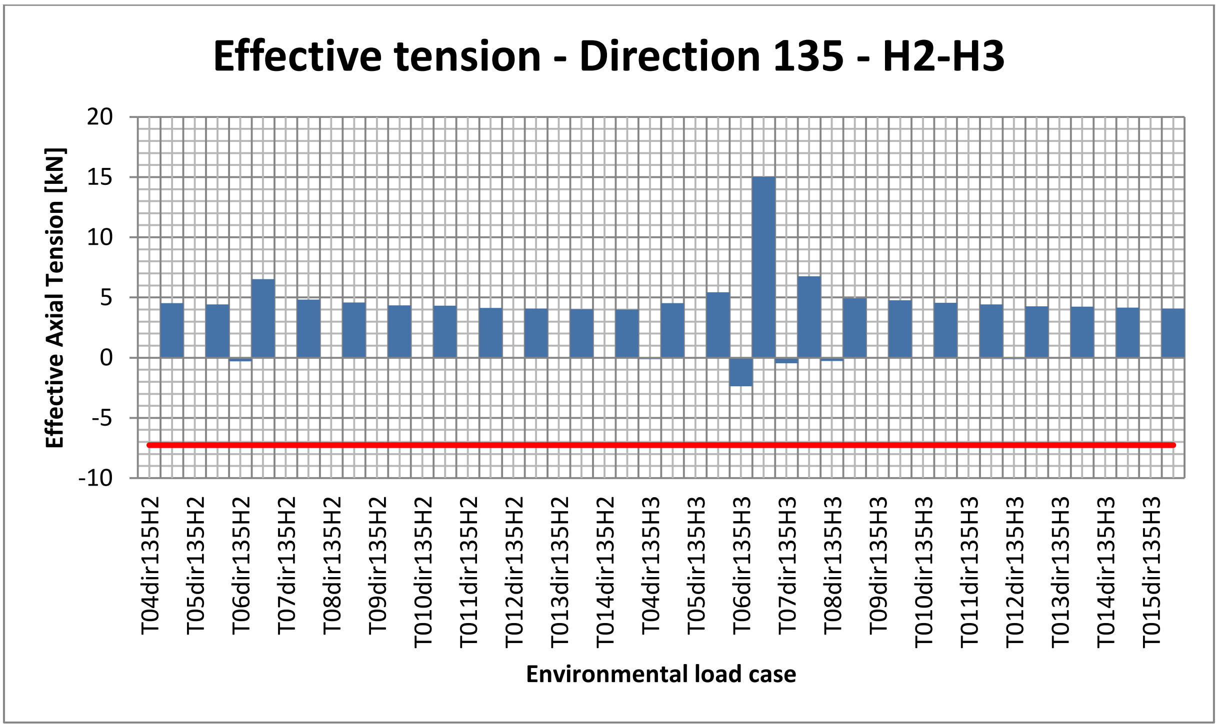

Figure C. 158 - 6" Oilflex Super – Lazy wave – 20 m floatation point – Effective tension – Direction 135° - H2-H3

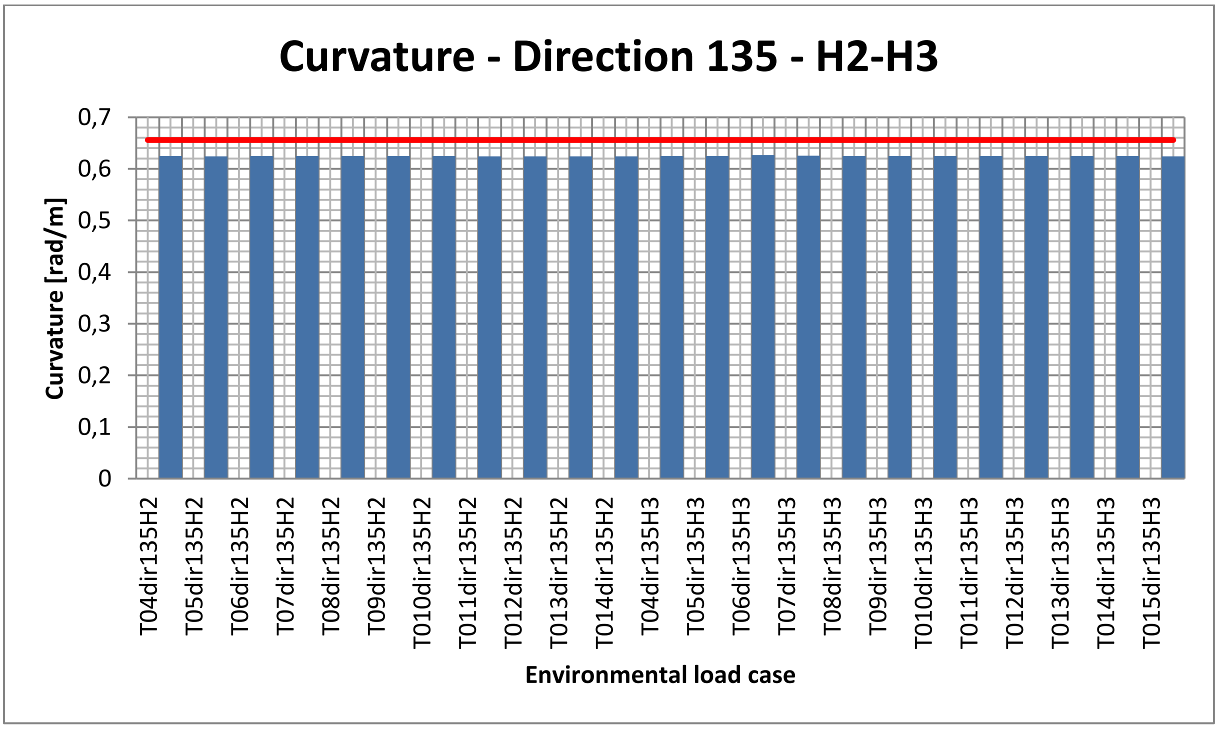

Figure C. 159 - 6" Oilflex Super – Lazy wave – 20 m floatation point – Curvature – Direction 135° - H2-H3

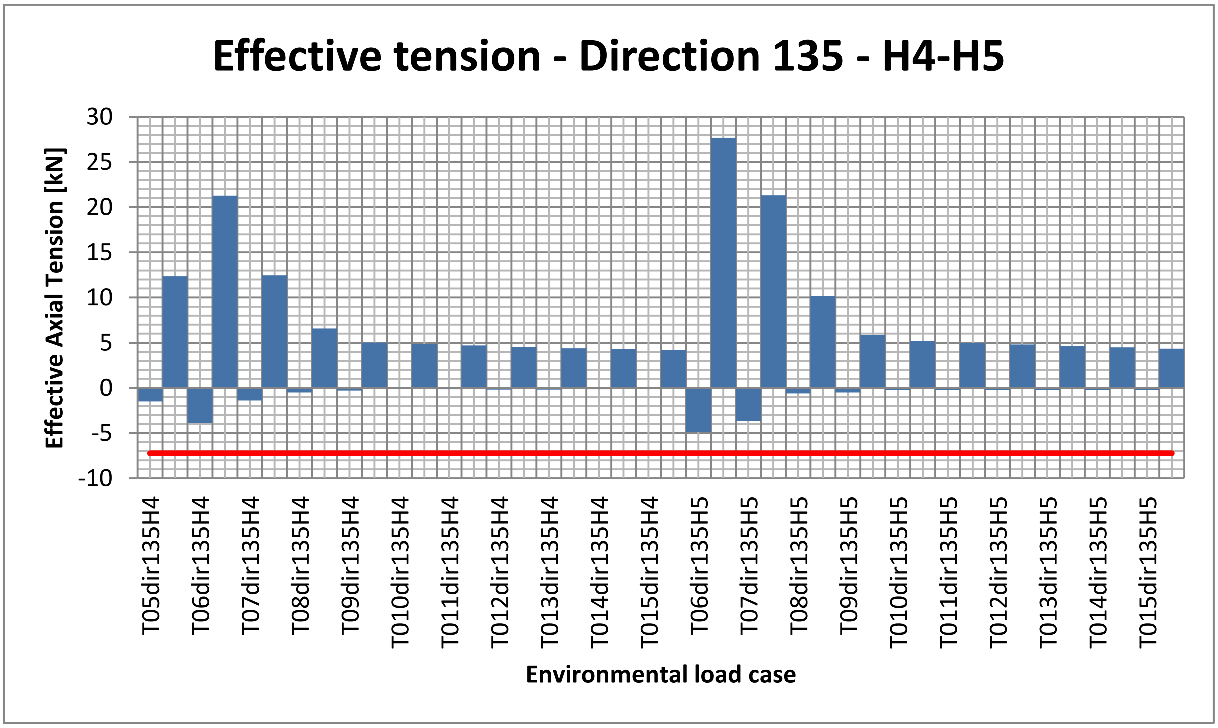

Figure C. 160 - 6" Oilflex Super – Lazy wave – 20 m floatation point – Effective tension – Direction 135° - H4-H5

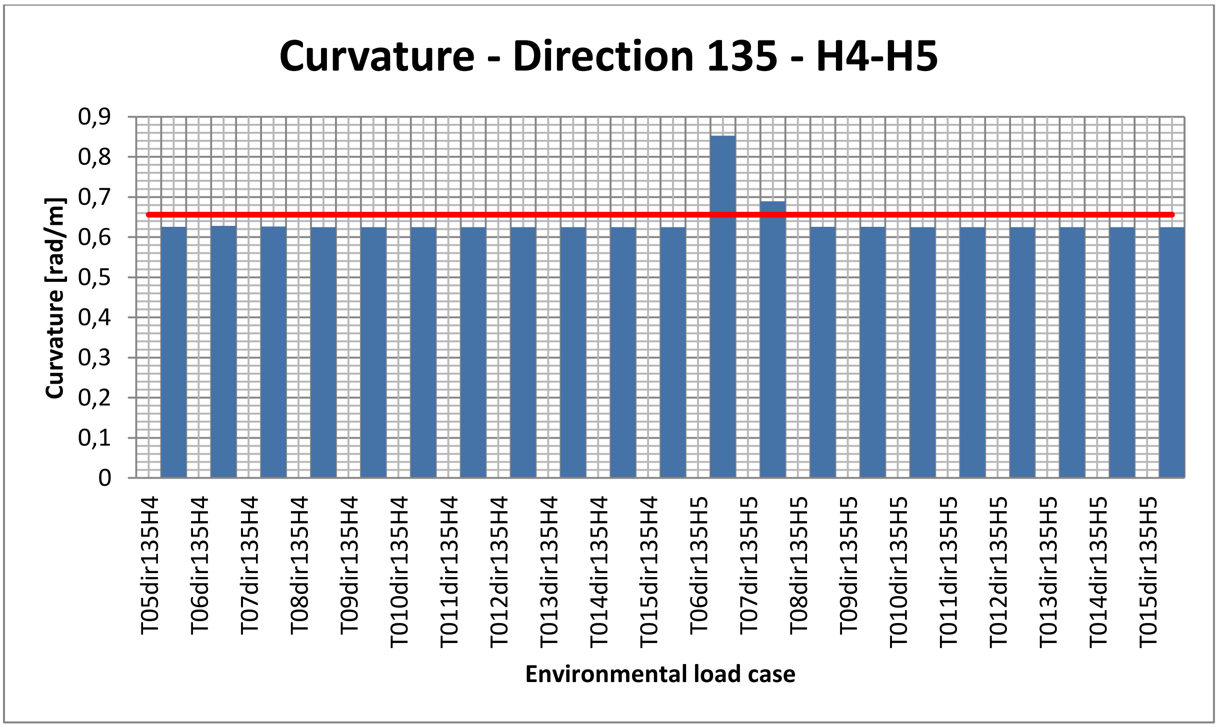

Figure C. 161 - 6" Oilflex Super – Lazy wave – 20 m floatation point – Curvature – Direction 135° - H4-H5

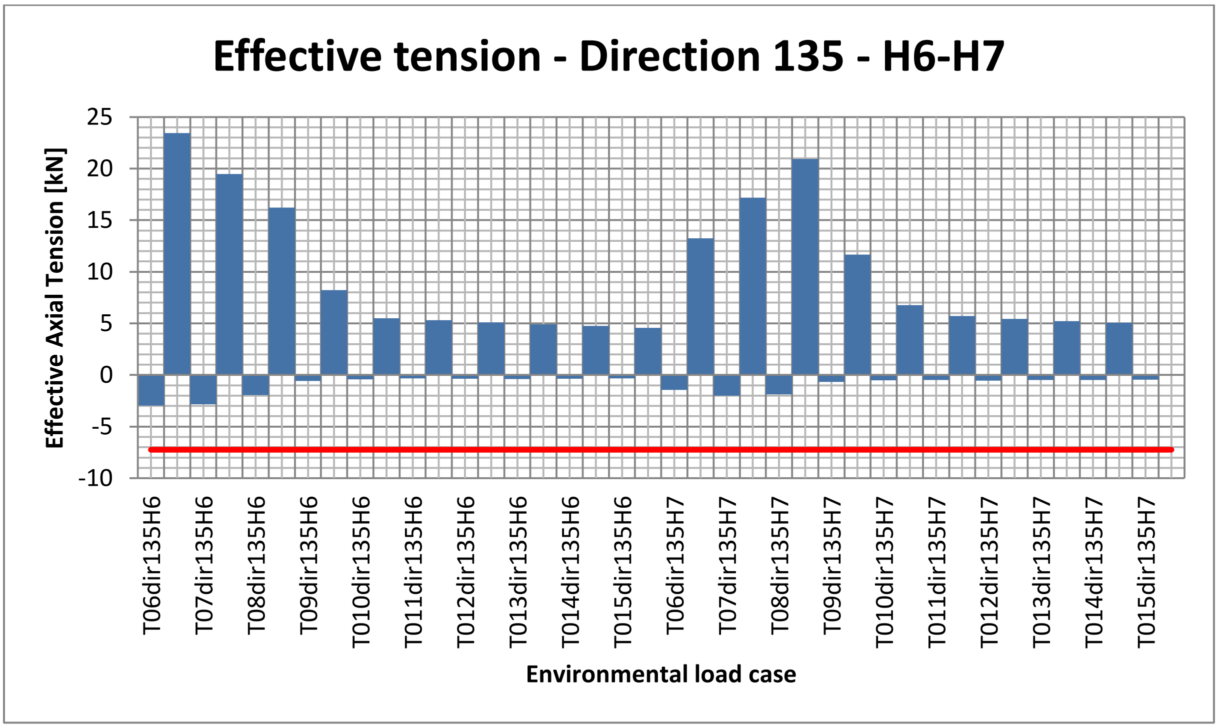

Figure C. 162 - 6” Oilflex Super – Lazy wave – 20 m floatation point – Effective tension – Direction 135° - H6-H7

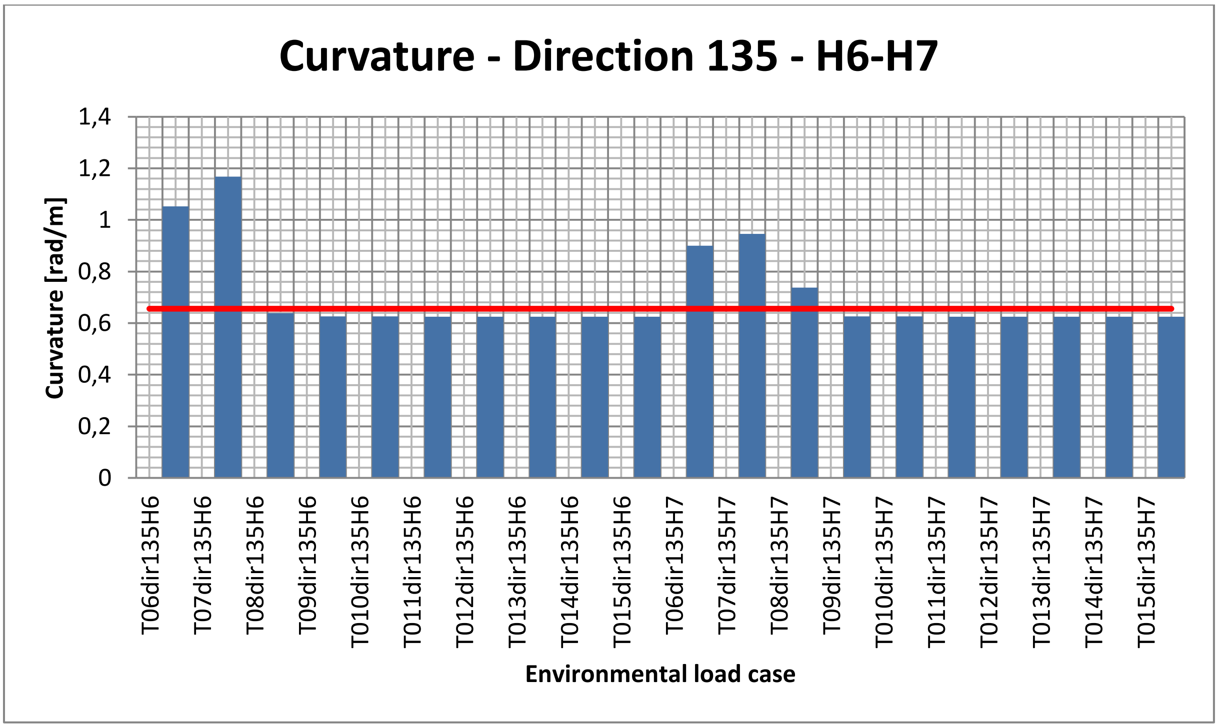

Figure C. 163 - 6” Oilflex Super – Lazy wave – 20 m floatation point – Curvature – Direction 135° - H6-H7

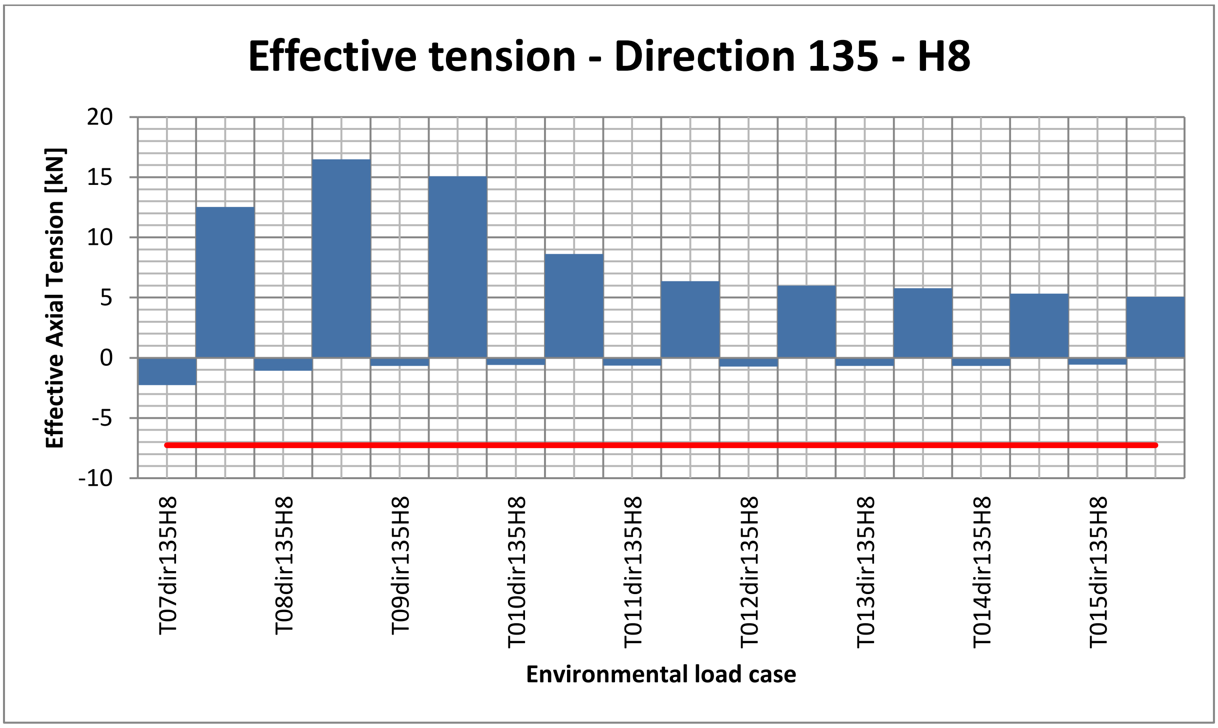

Figure C. 164 - 6” Oilflex Super – Lazy wave – 20 m floatation point – Effective tension – Direction 135° - H8

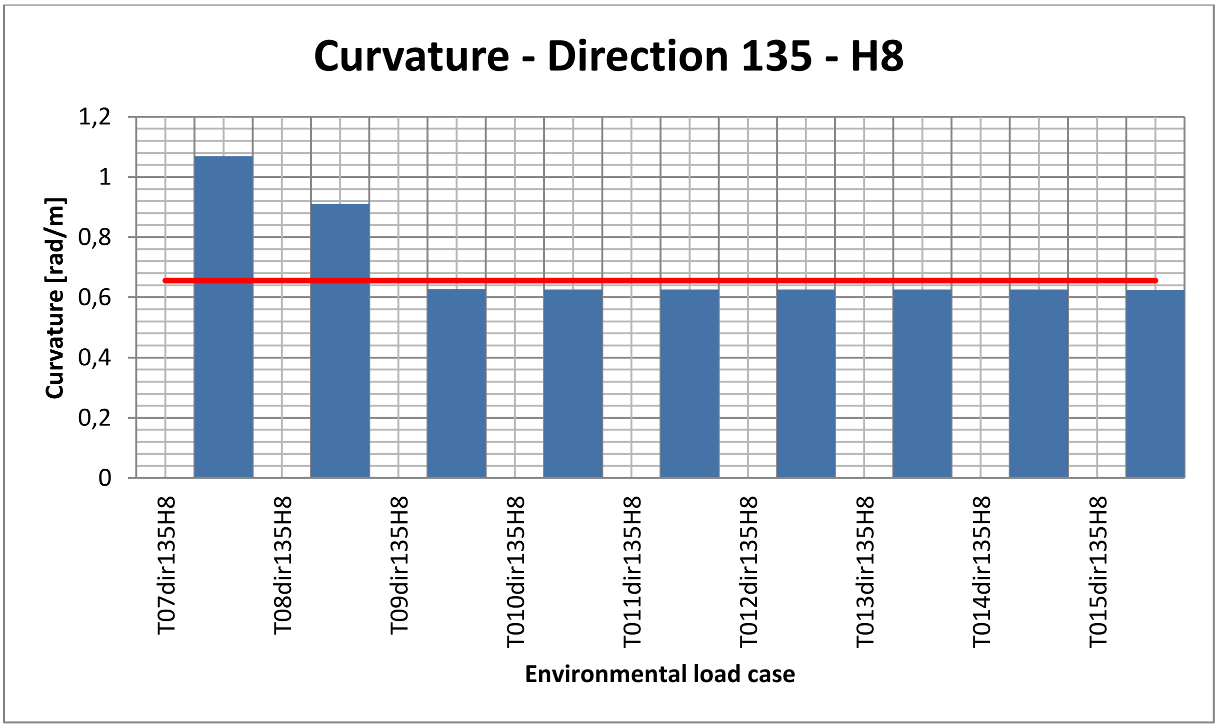

Figure C. 165 - 6” Oilflex Super – Lazy wave – 20 m floatation point – Curvature – Direction 135° - H8

Direction 180°

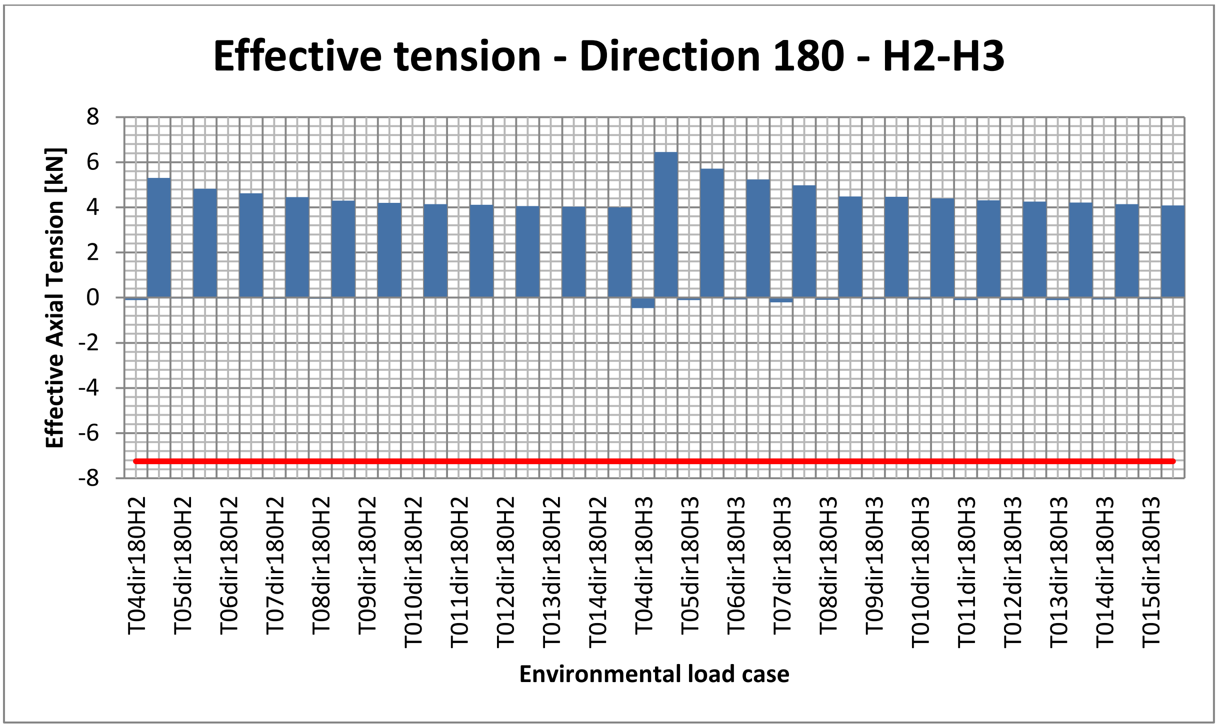

Figure C. 166 - 6" Oilflex Super – Lazy wave – 20 m floatation point – Effective tension – Direction 180° - H2-H3

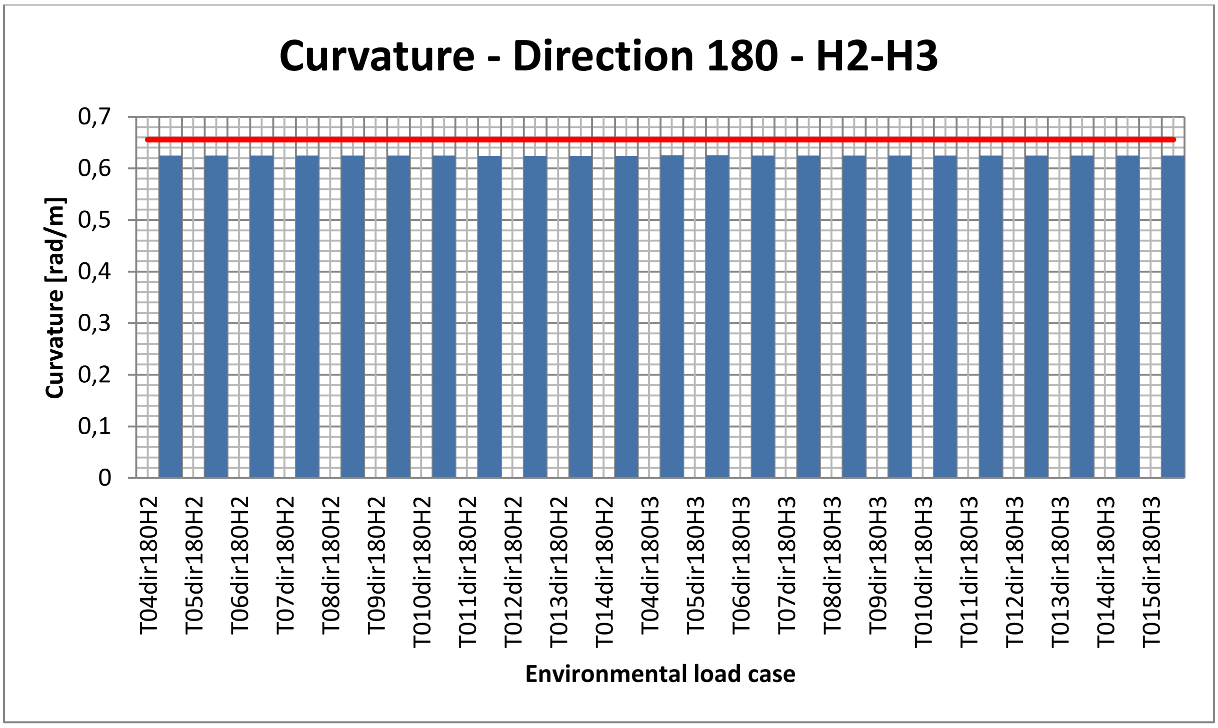

Figure C. 167 - 6" Oilflex Super – Lazy wave – 20 m floatation point – Curvature – Direction 180° - H2-H3

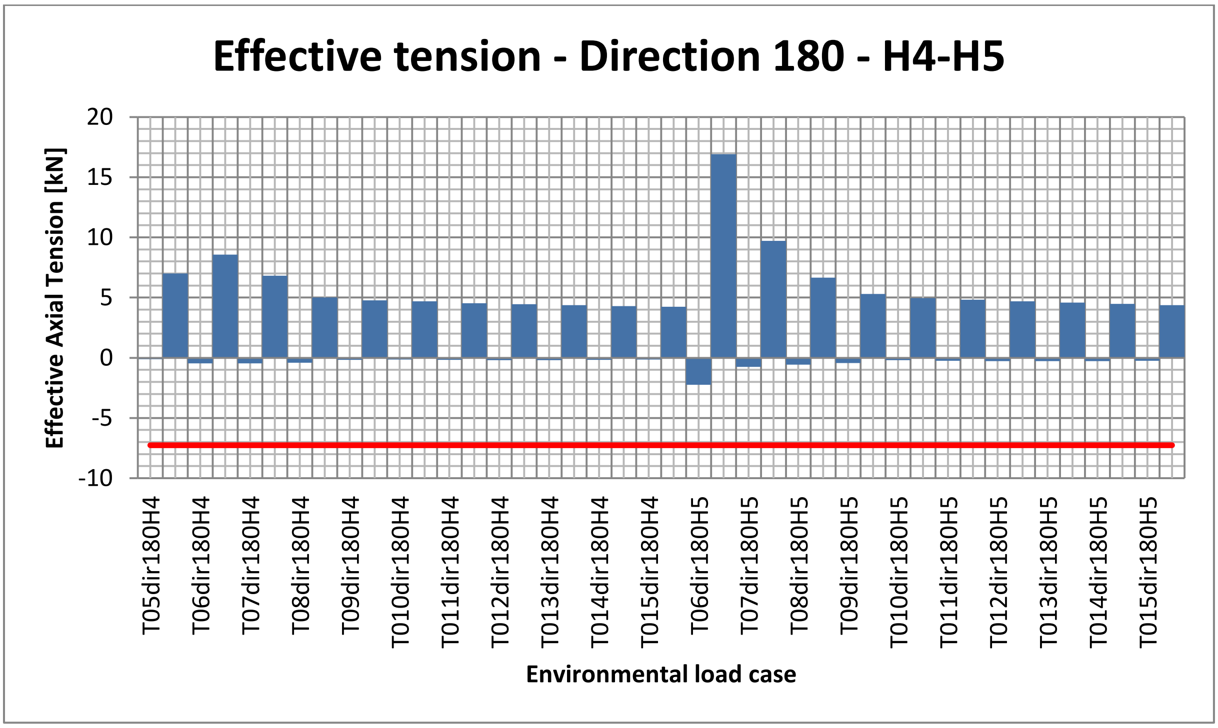

Figure C. 168 - 6" Oilflex Super – Lazy wave – 20 m floatation point – Effective tension – Direction 180° - H4-H5

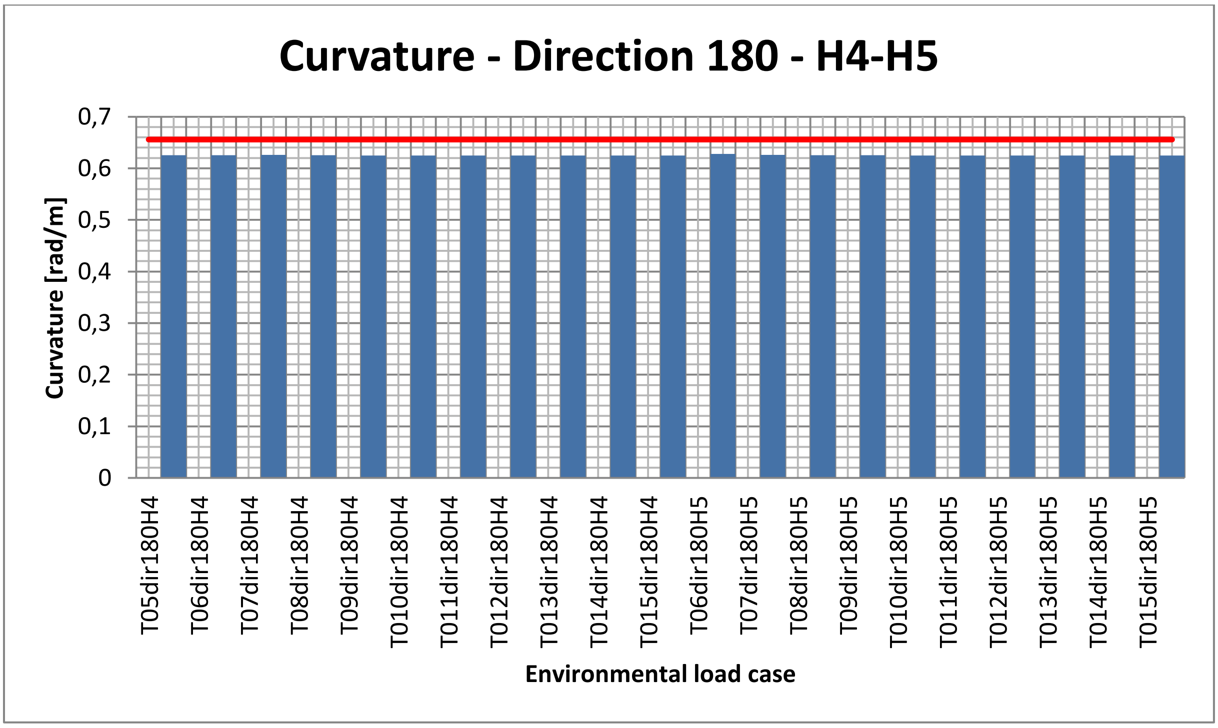

Figure C. 169 - 6" Oilflex Super – Lazy wave – 20 m floatation point – Curvature – Direction 180° - H4-H5

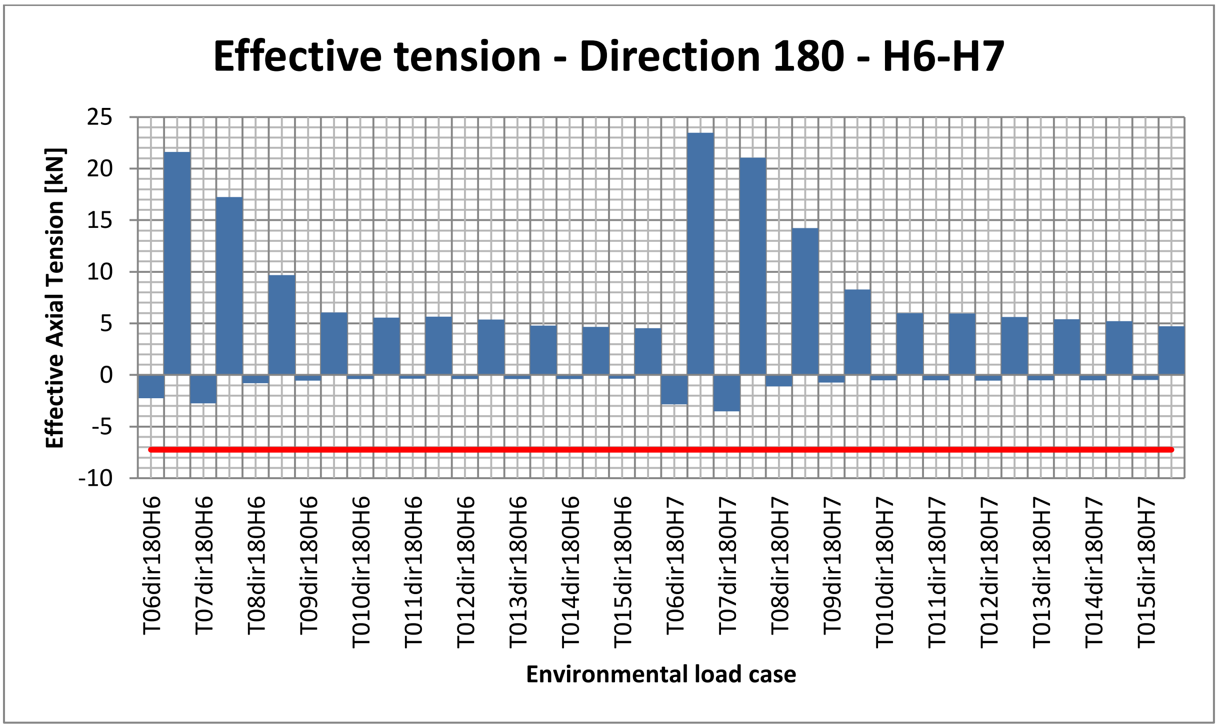

Figure C. 170 - 6” Oilflex Super – Lazy wave – 20 m floatation point – Effective tension – Direction 180° - H6-H7

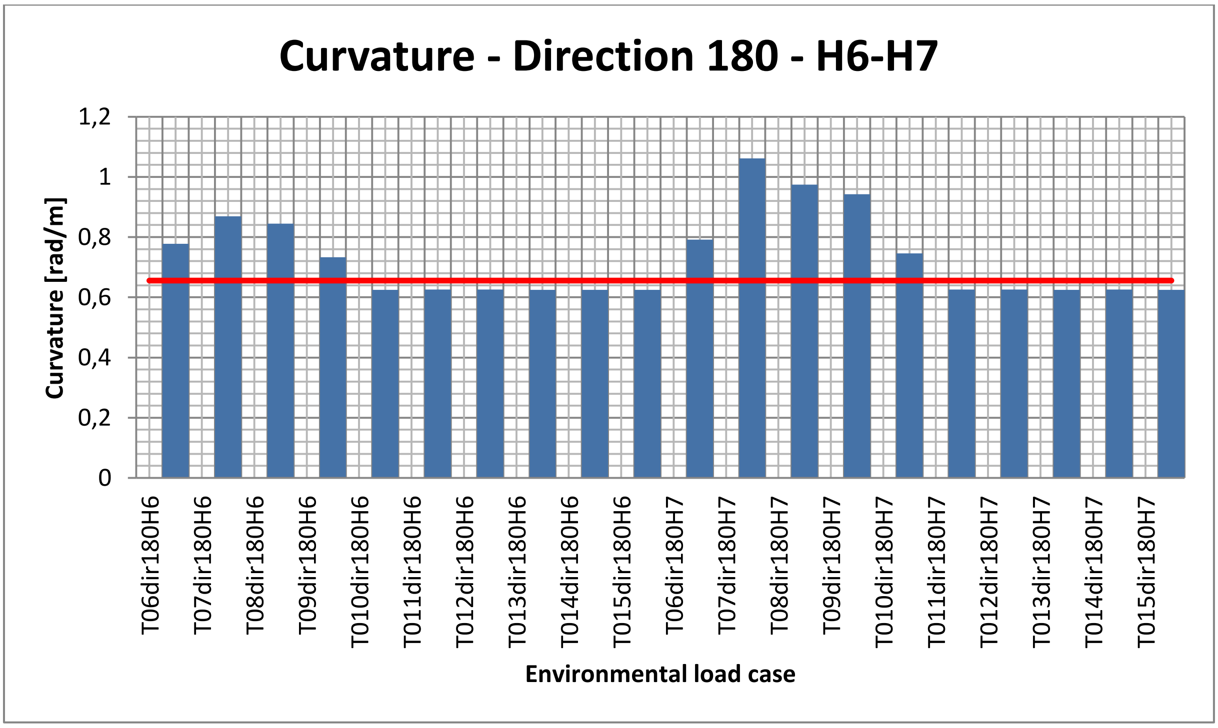

Figure C. 171 - 6” Oilflex Super – Lazy wave – 20 m floatation point – Curvature – Direction 180° - H6-H7

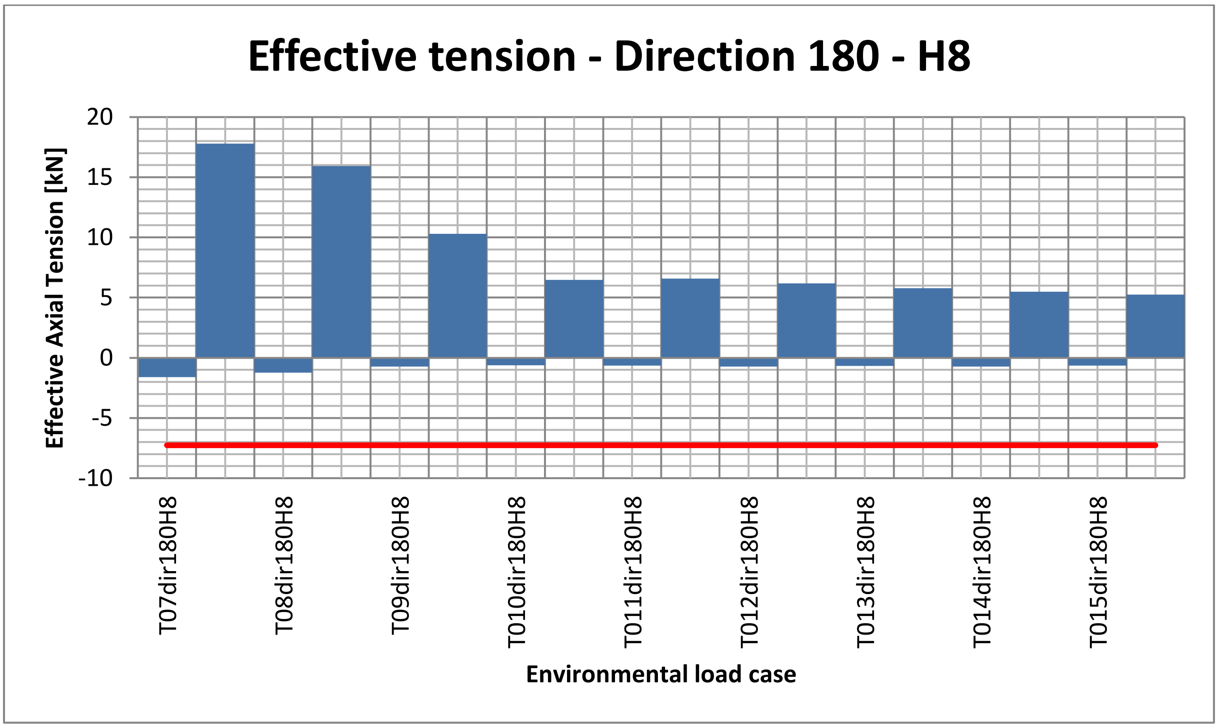

Figure C. 172 - 6” Oilflex Super – Lazy wave – 20 m floatation point – Effective tension – Direction 180° - H8

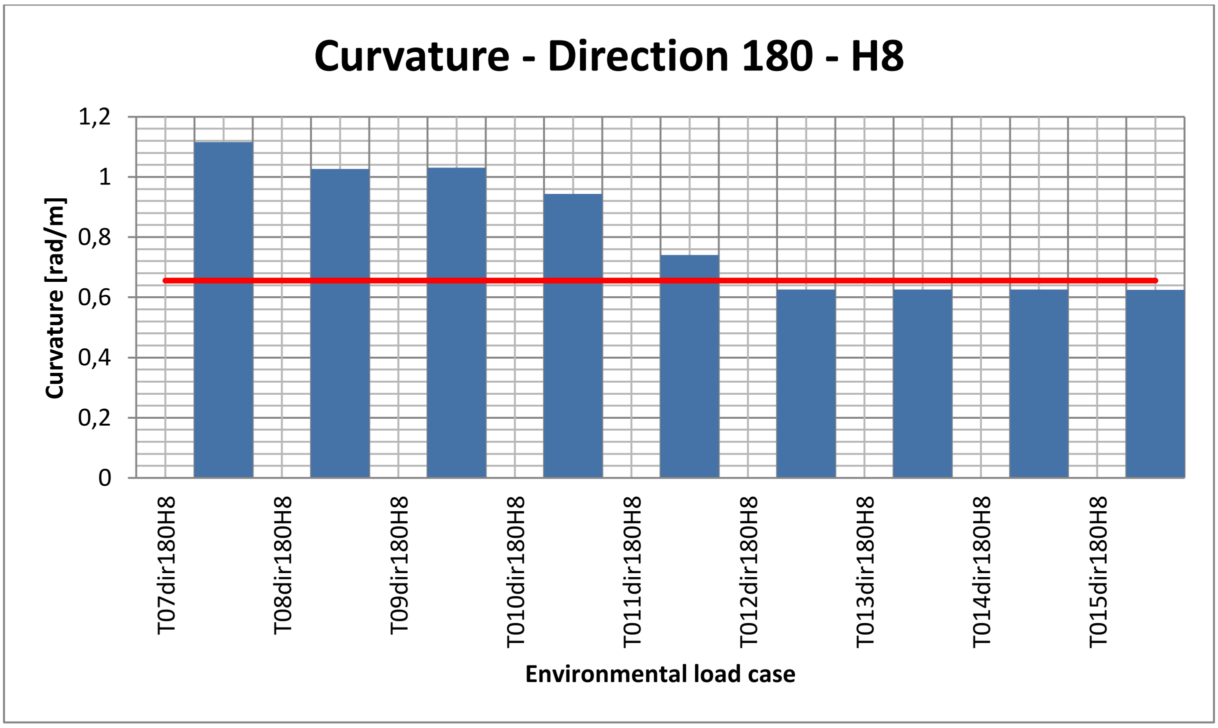

Figure C. 173 - 6” Oilflex Super – Lazy wave – 20 m floatation point – Curvature – Direction 180° - H8

Direction 225°

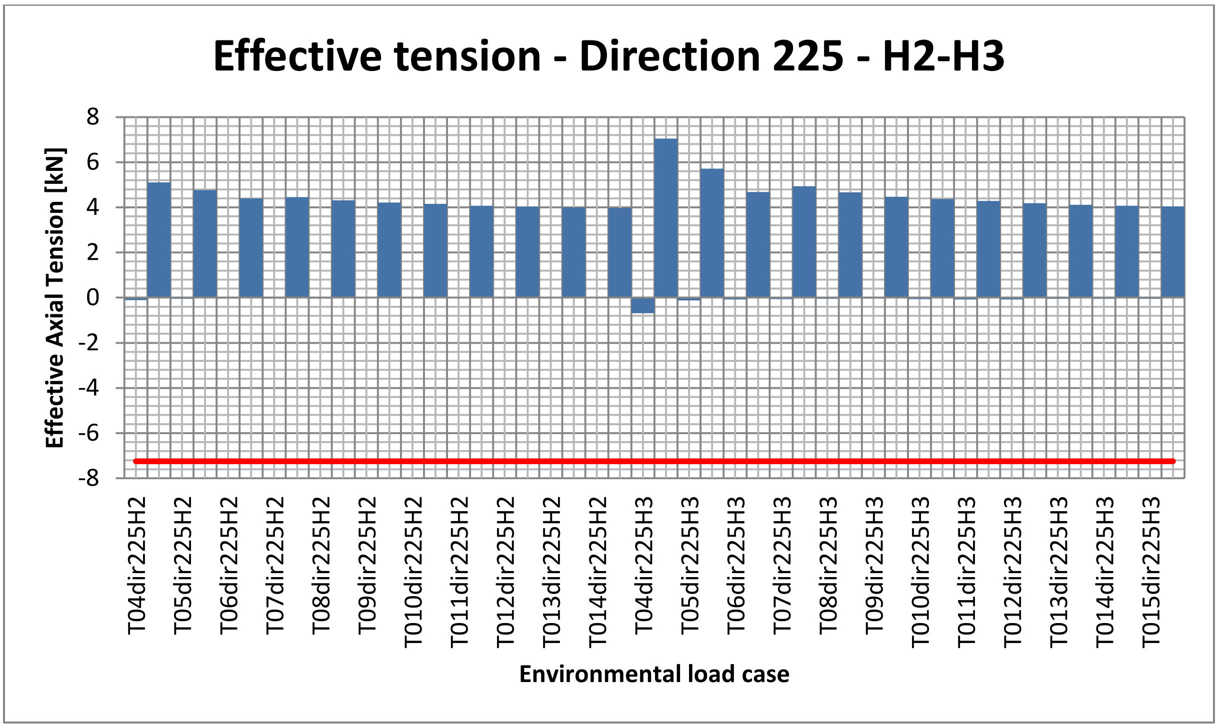

Figure C. 174 - 6” Oilflex Super – Lazy wave – 20 m floatation point – Effective tension – Direction 225° - H2-H3

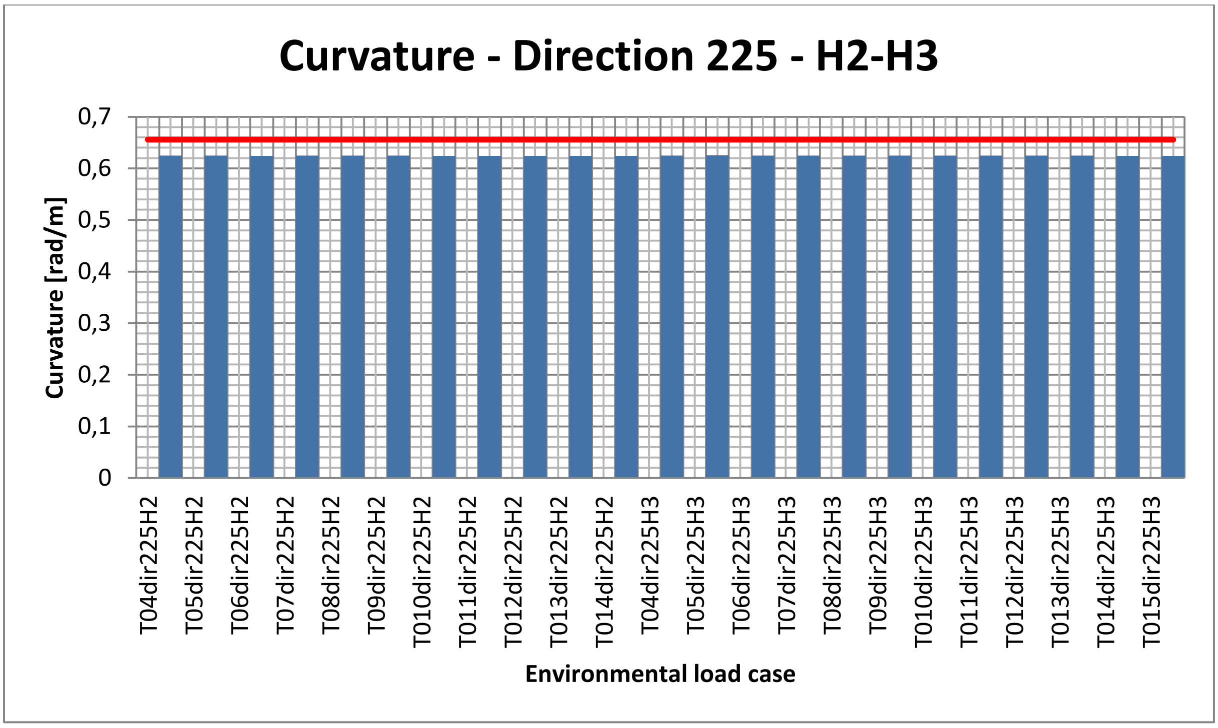

Figure C. 175 - 6” Oilflex Super – Lazy wave – 20 m floatation point – Curvature – Direction 225° - H2-H3

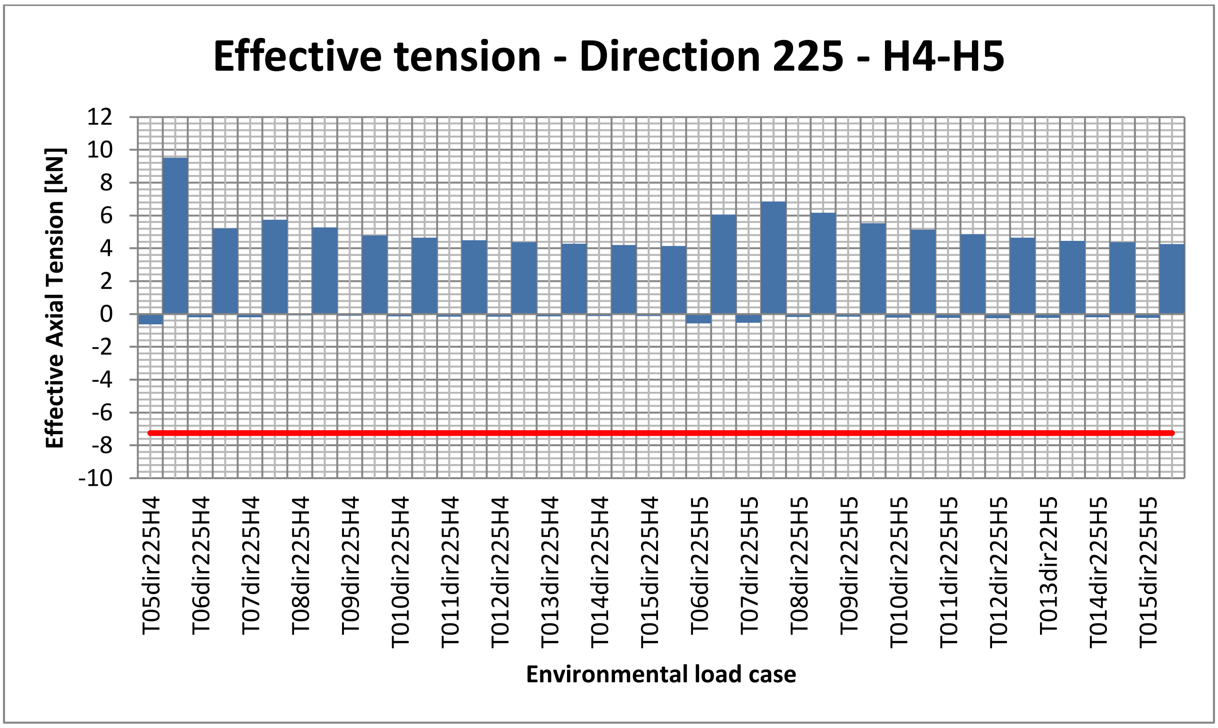

Figure C. 176 - 6” Oilflex Super – Lazy wave – 20 m floatation point – Effective tension – Direction 225° - H4-H5

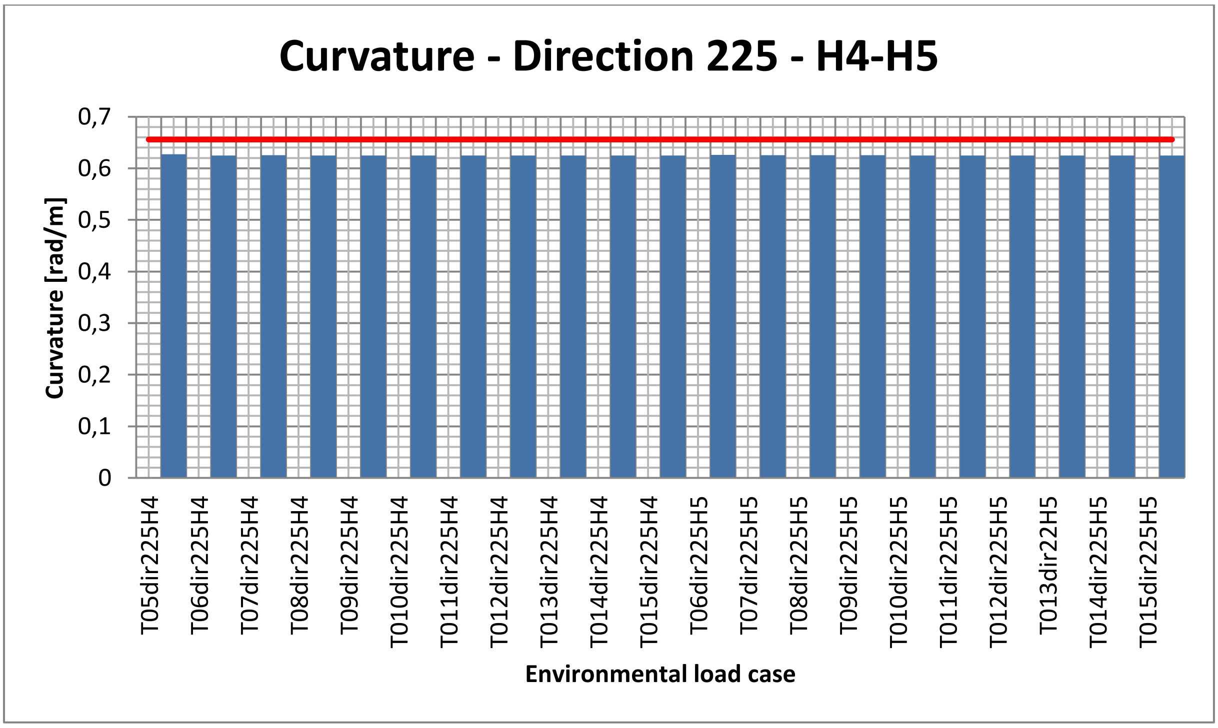

Figure C. 177 - 6” Oilflex Super – Lazy wave – 20 m floatation point – Curvature – Direction 225° - H4-H5

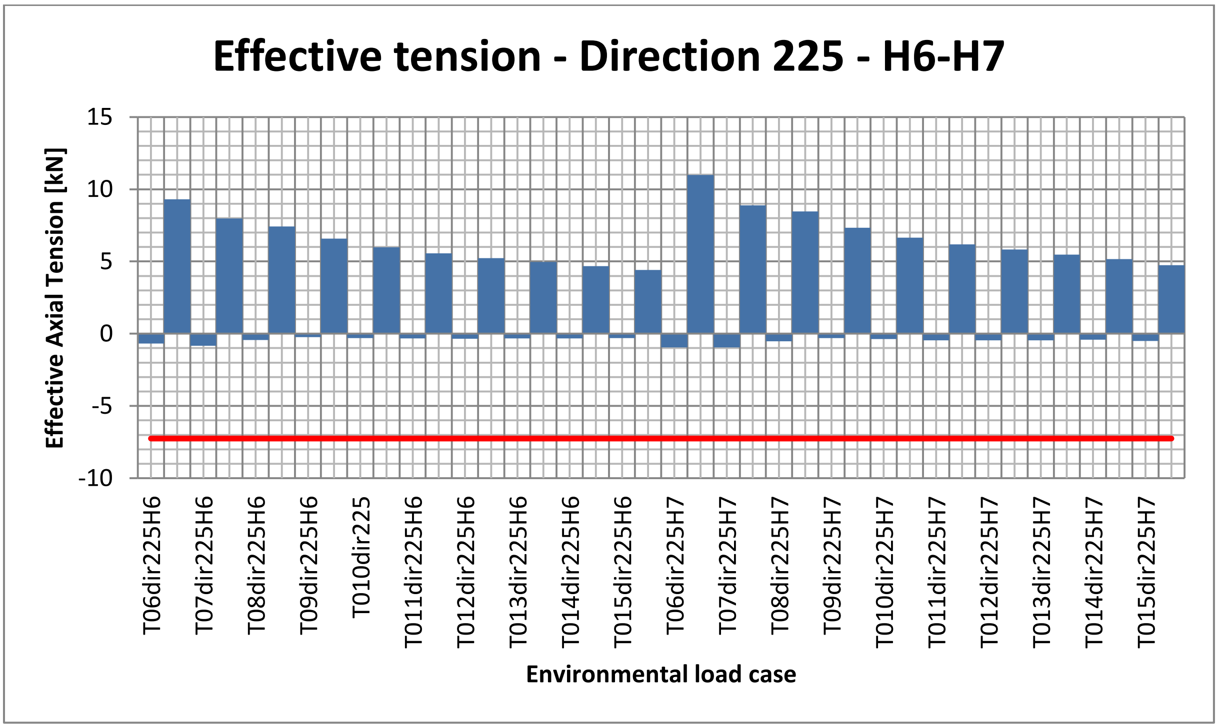

Figure C. 178 - 6" Oilflex Super – Lazy wave – 20 m floatation point – Effective tension – Direction 225° - H6-H7

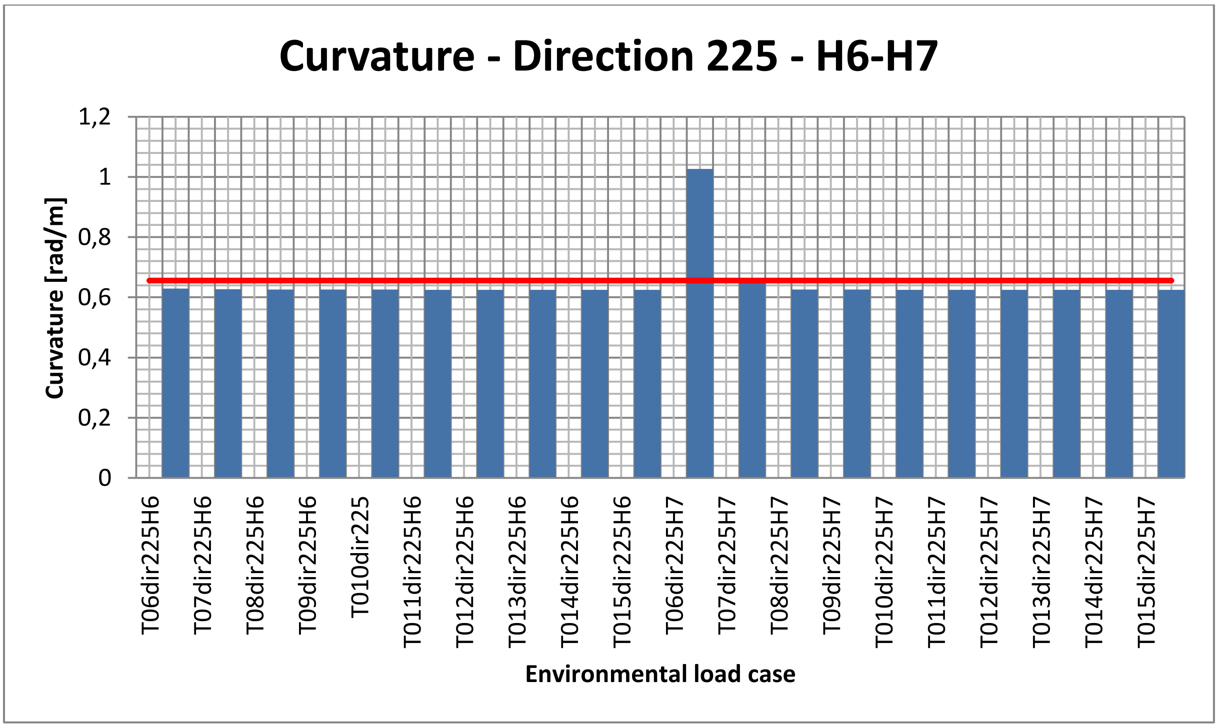

Figure C. 179 - 6" Oilflex Super – Lazy wave – 20 m floatation point – Curvature – Direction 225° - H6-H7

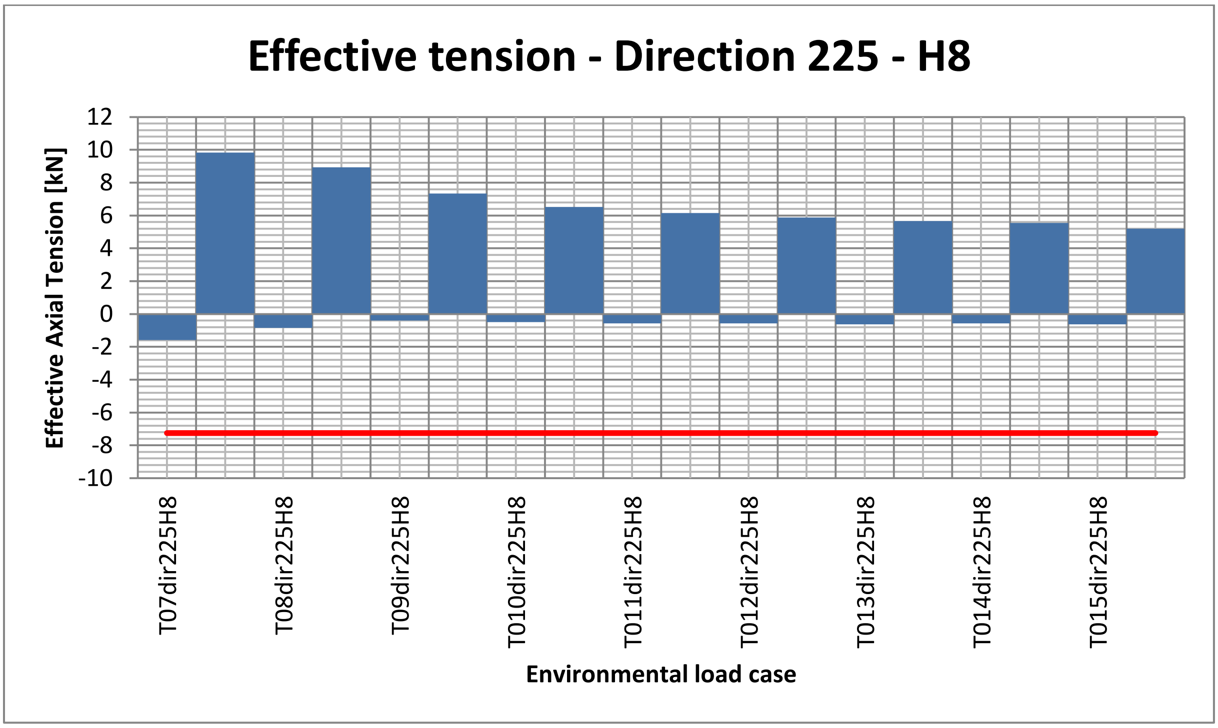

Figure C. 180 - 6" Oilflex Super – Lazy wave – 20 m floatation point – Effective tension – Direction 225° - H8

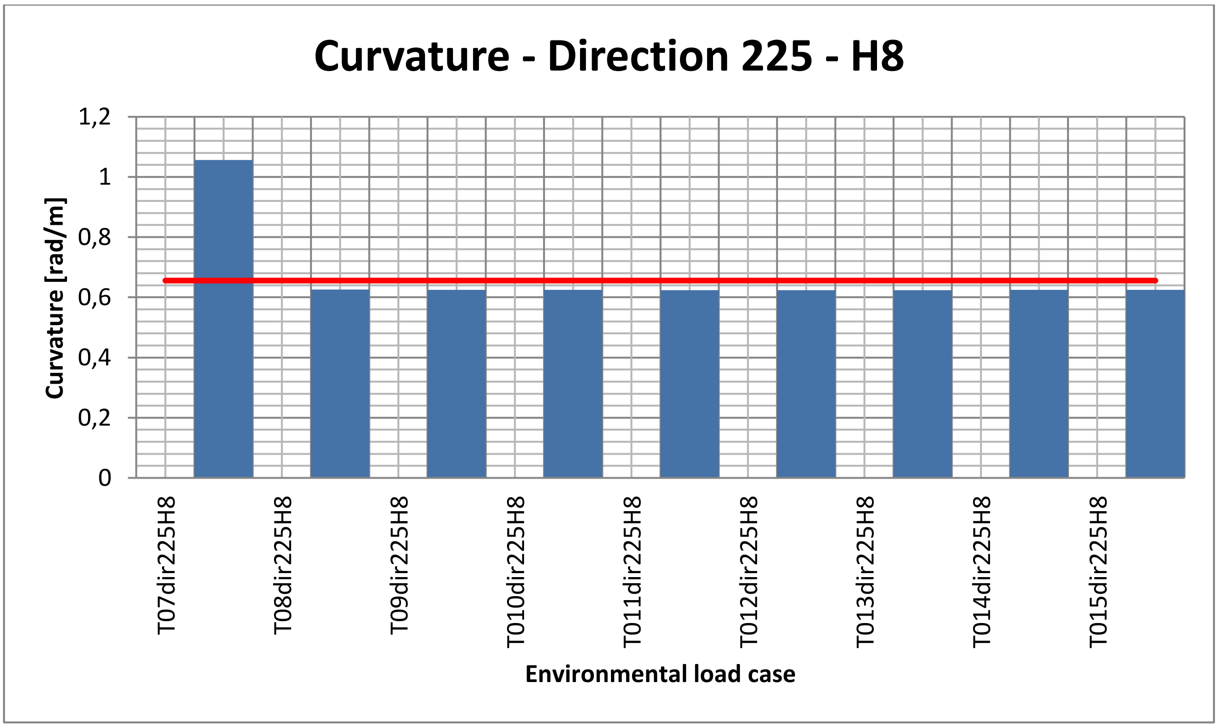

Figure C. 181 - 6" Oilflex Super – Lazy wave – 20 m floatation point – Curvature – Direction 225° - H8

Wave rose

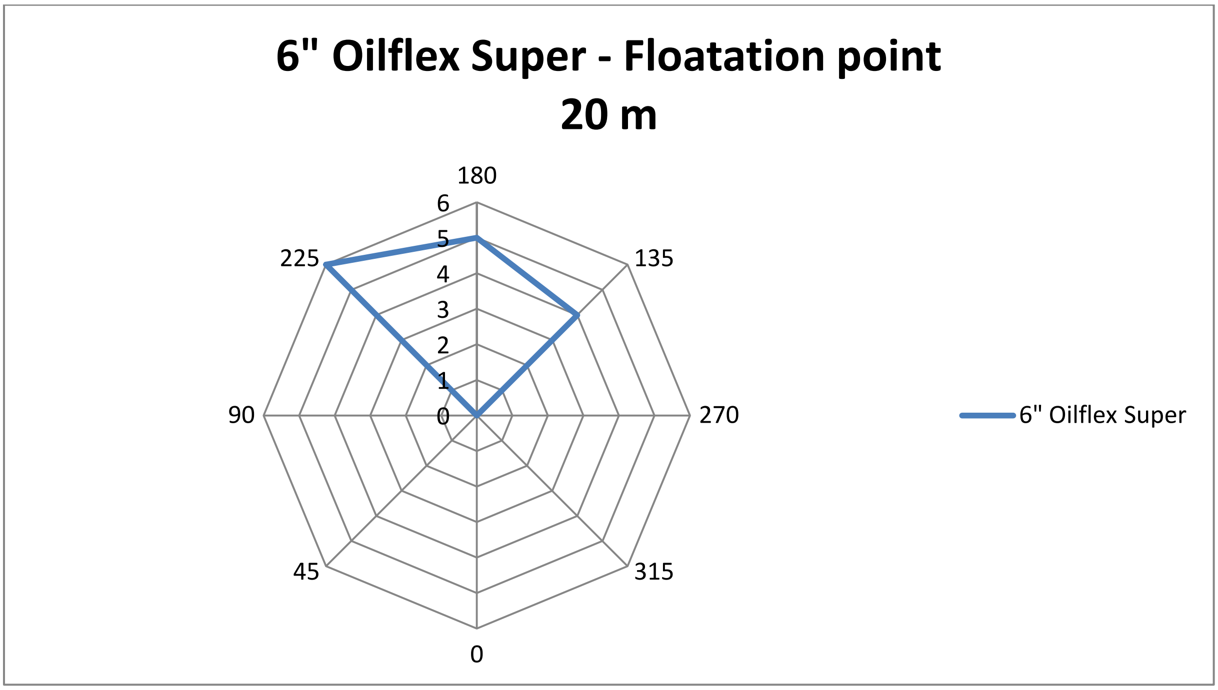

Figure C. 182 - 6" Oilflex Super – Lazy wave – 20 m floatation point – Wave rose

Limitation plot

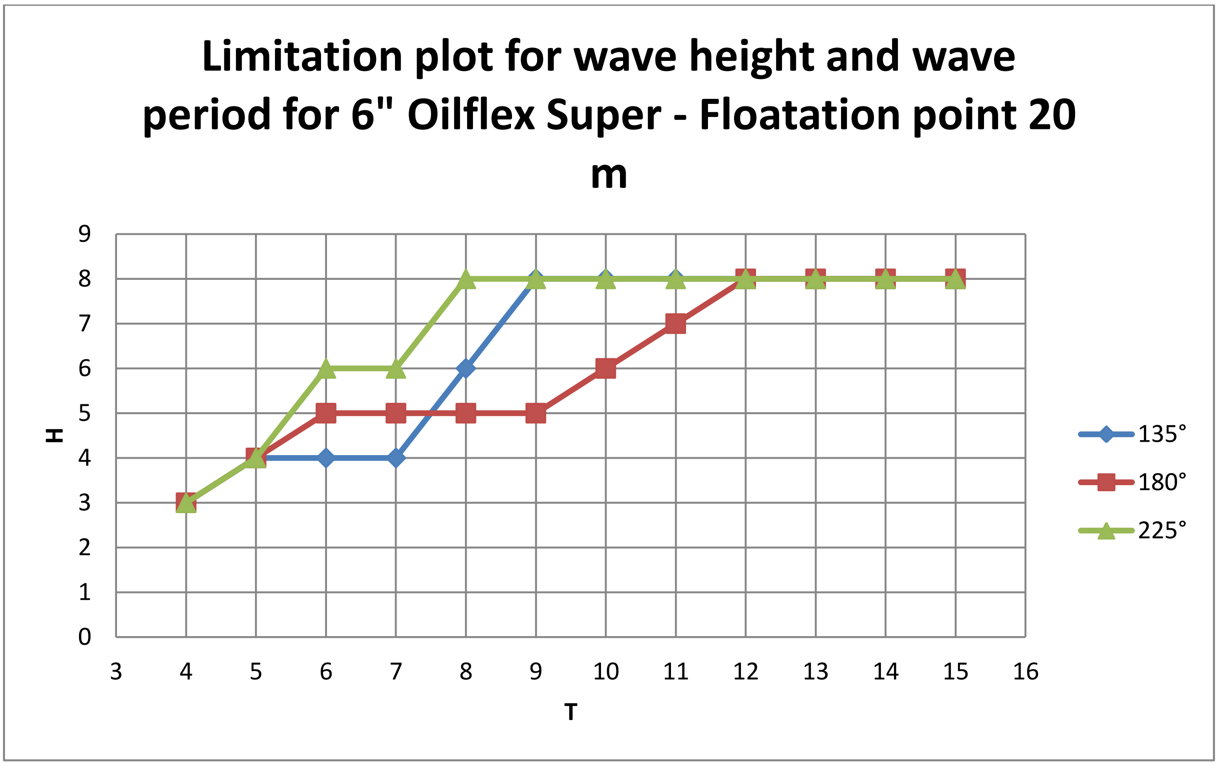

Figure C. 183 - 6" Oilflex Super – Lazy wave – 20 m floatation point – Limitation plot

Lazy wave – 40 m floatation point

Direction 135°

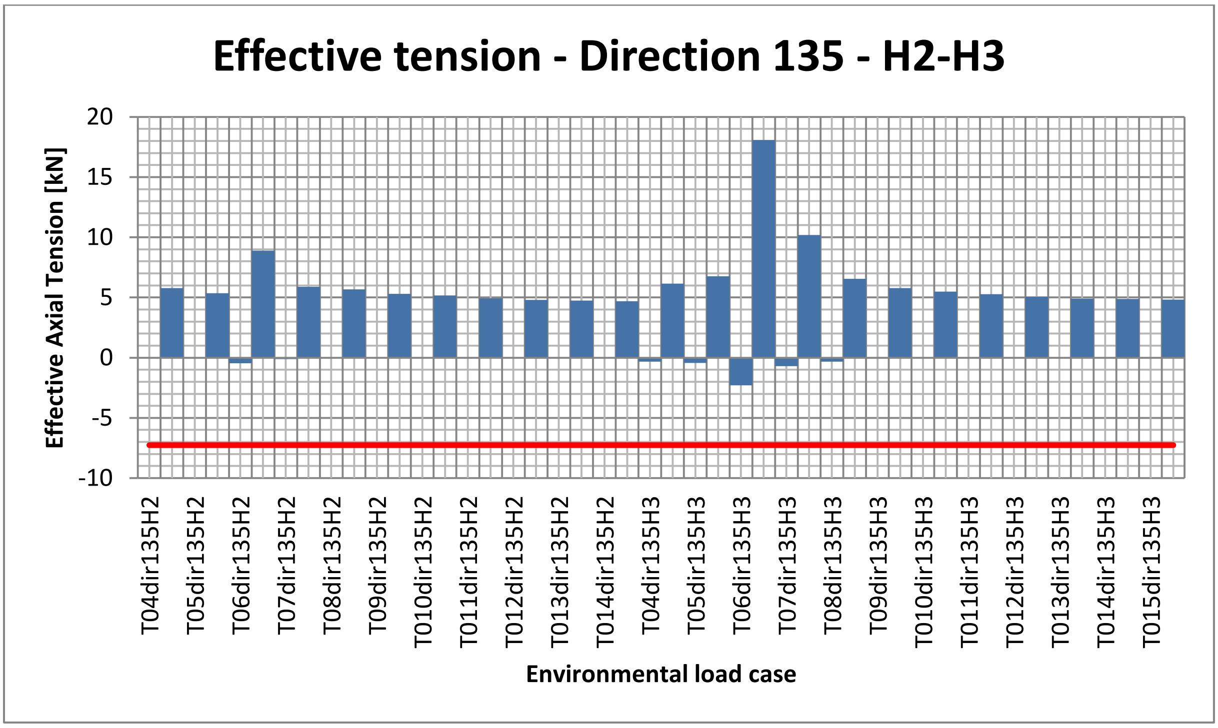

Figure C. 184 - 6" Oilflex Super – Lazy wave – 40 m floatation point – Effective tension – Direction 135° - H2-H3

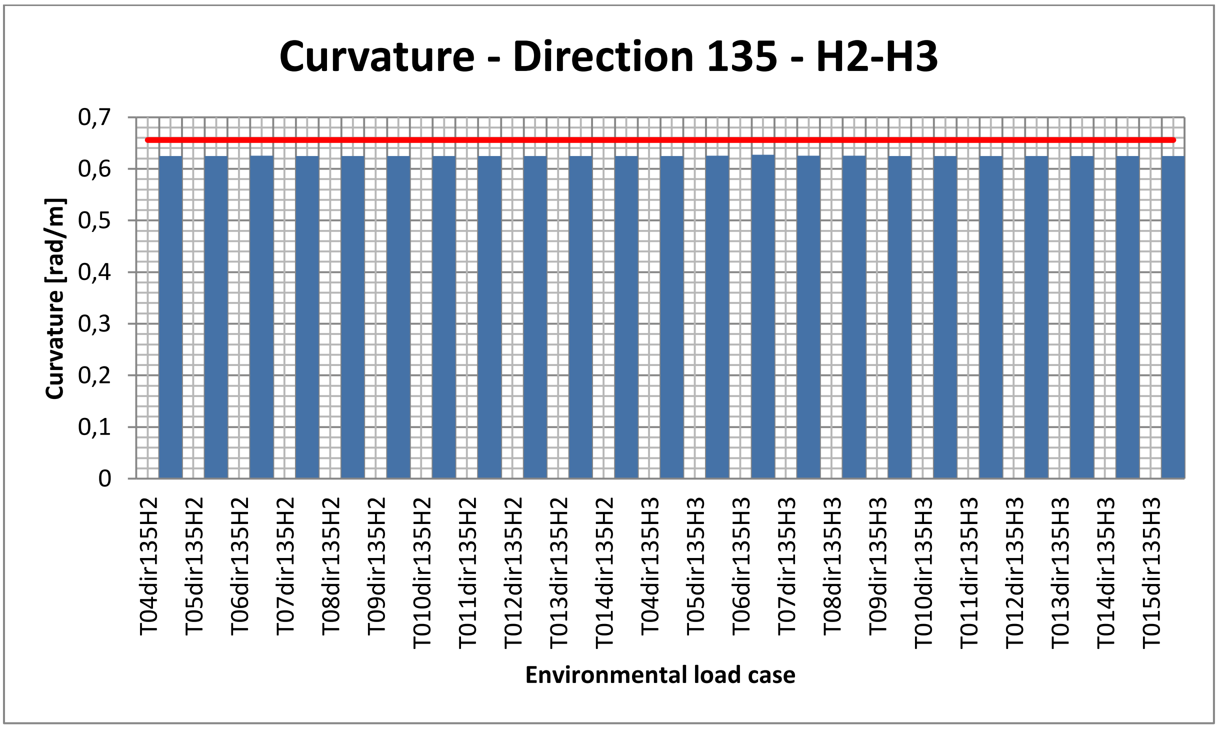

Figure C. 185 - 6" Oilflex Super – Lazy wave – 40 m floatation point – Curvature – Direction 135° - H2-H3

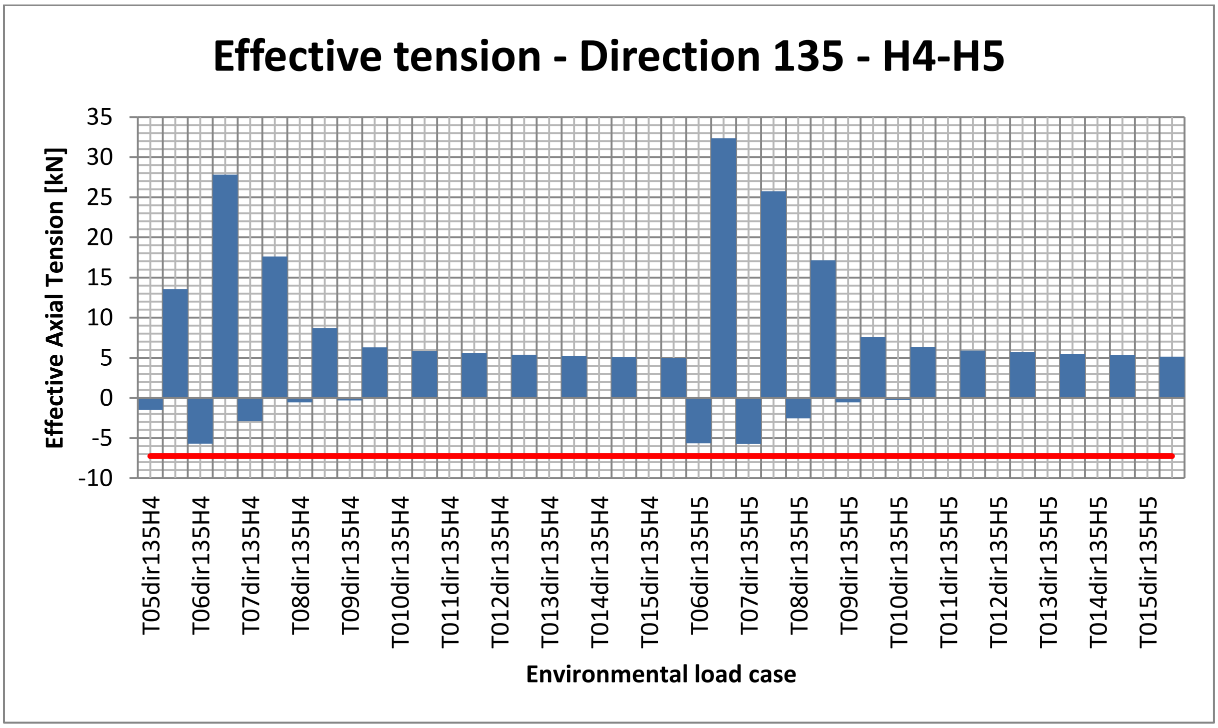

Figure C. 186 - 6” Oilflex Super – Lazy wave – 40 m floatation point – Effective tension – Direction 135° - H4-H5

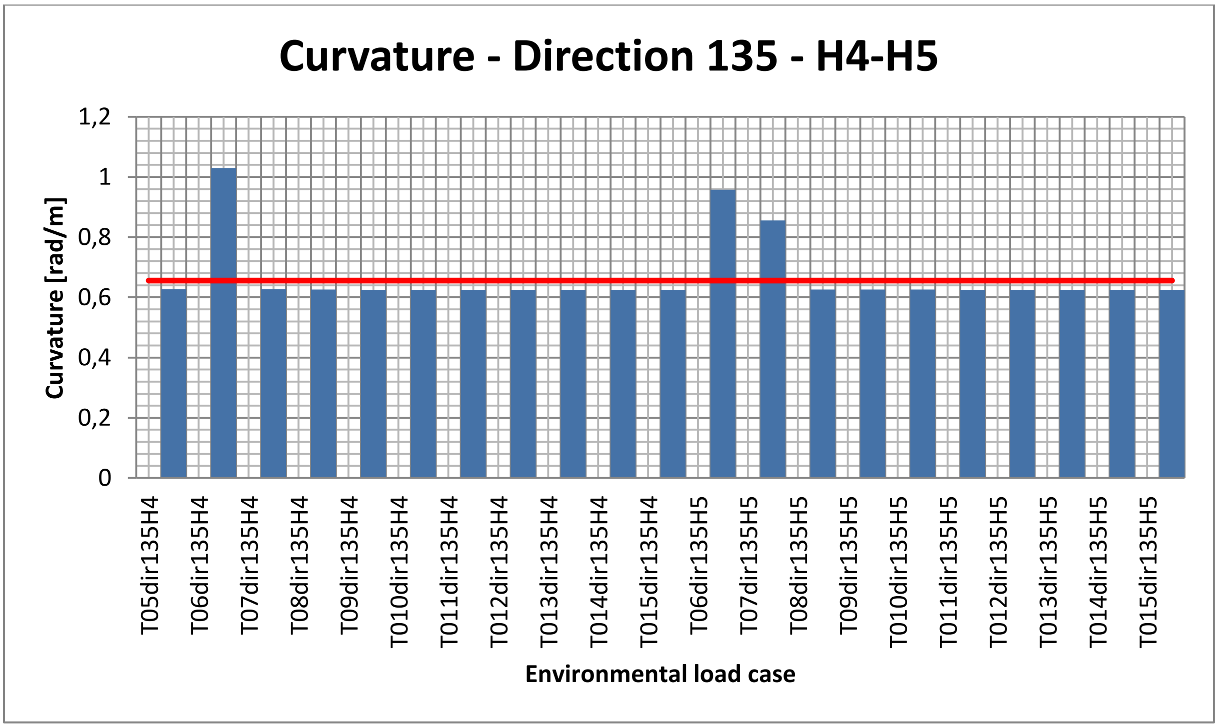

Figure C. 187 - 6” Oilflex Super – Lazy wave – 40 m floatation point – Curvature – Direction 135° - H4-H5

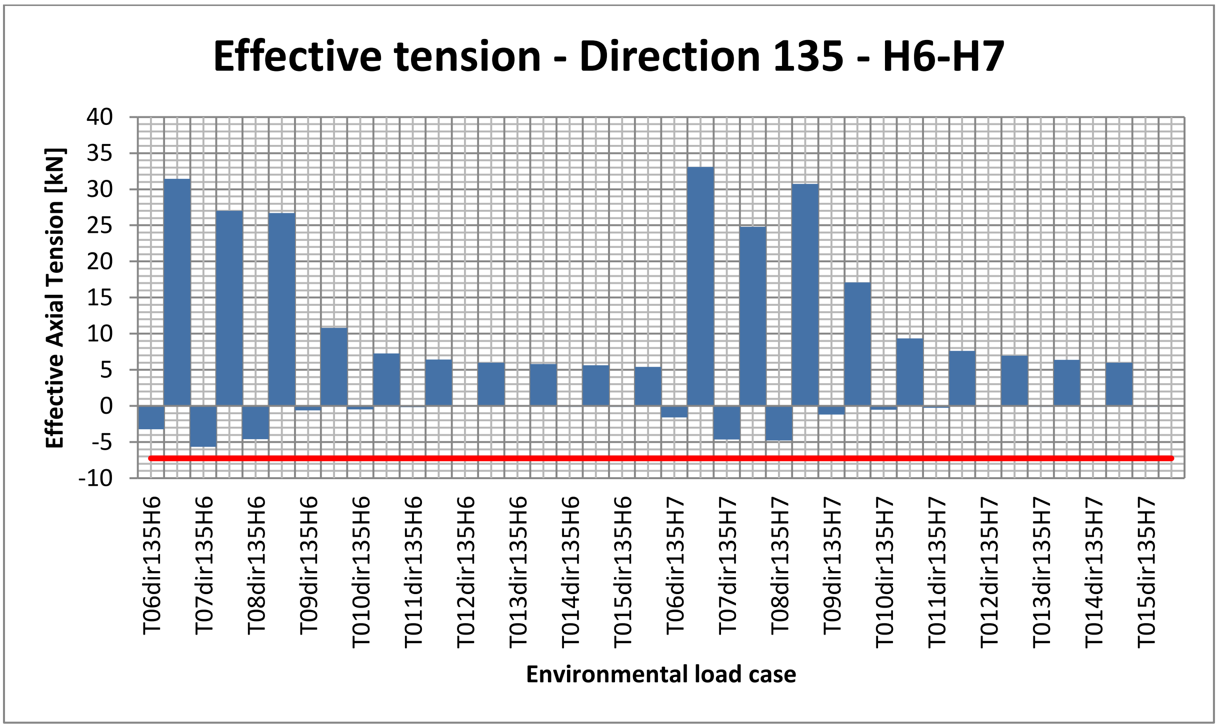

Figure C. 188 - 6" Oilflex Super – Lazy wave – 40 m floatation point – Effective tension – Direction 135° - H6-H7

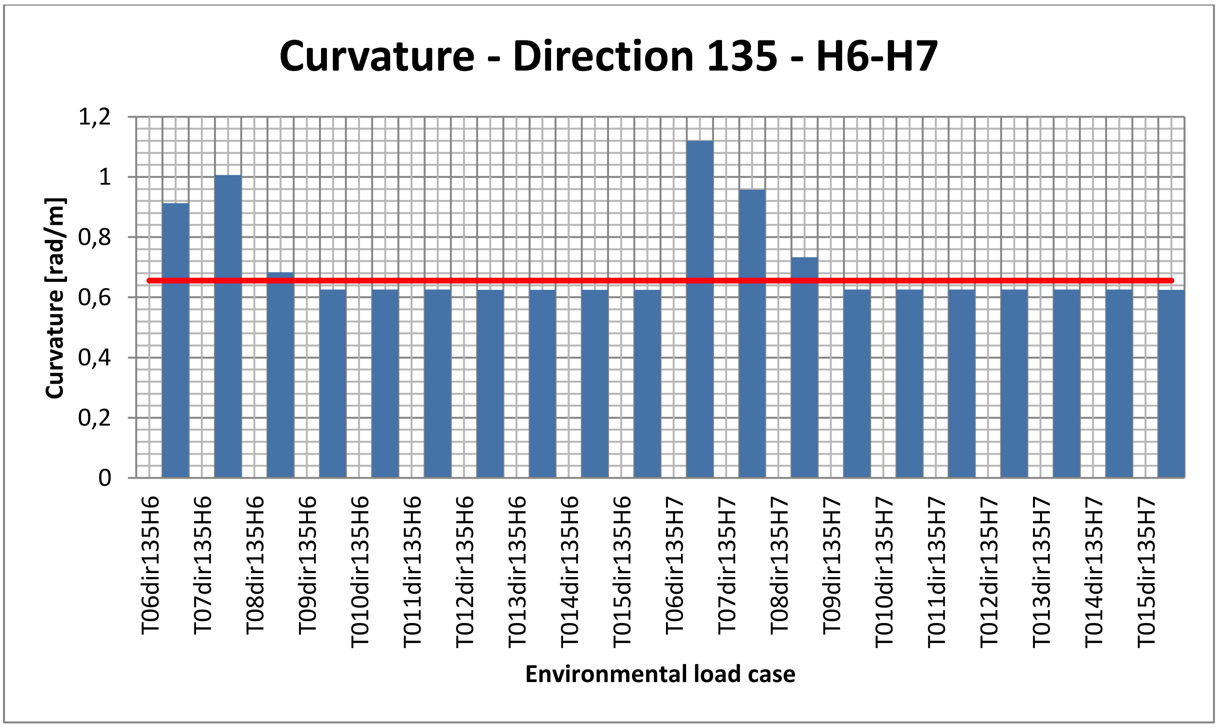

Figure C. 189 - 6" Oilflex Super – Lazy wave – 40 m floatation point – Curvature – Direction 135° - H6-H7

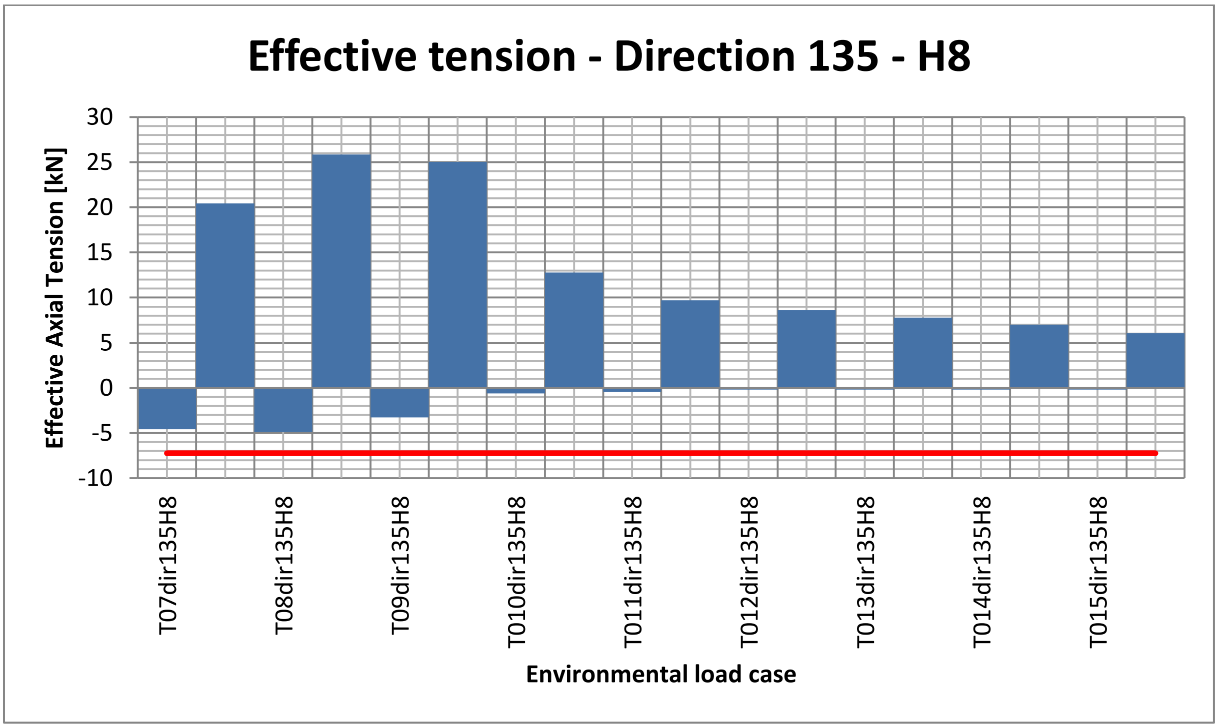

Figure C. 190 - 6” Oilflex Super – Lazy wave – 40 m floatation point – Effective tension – Direction 135° - H8

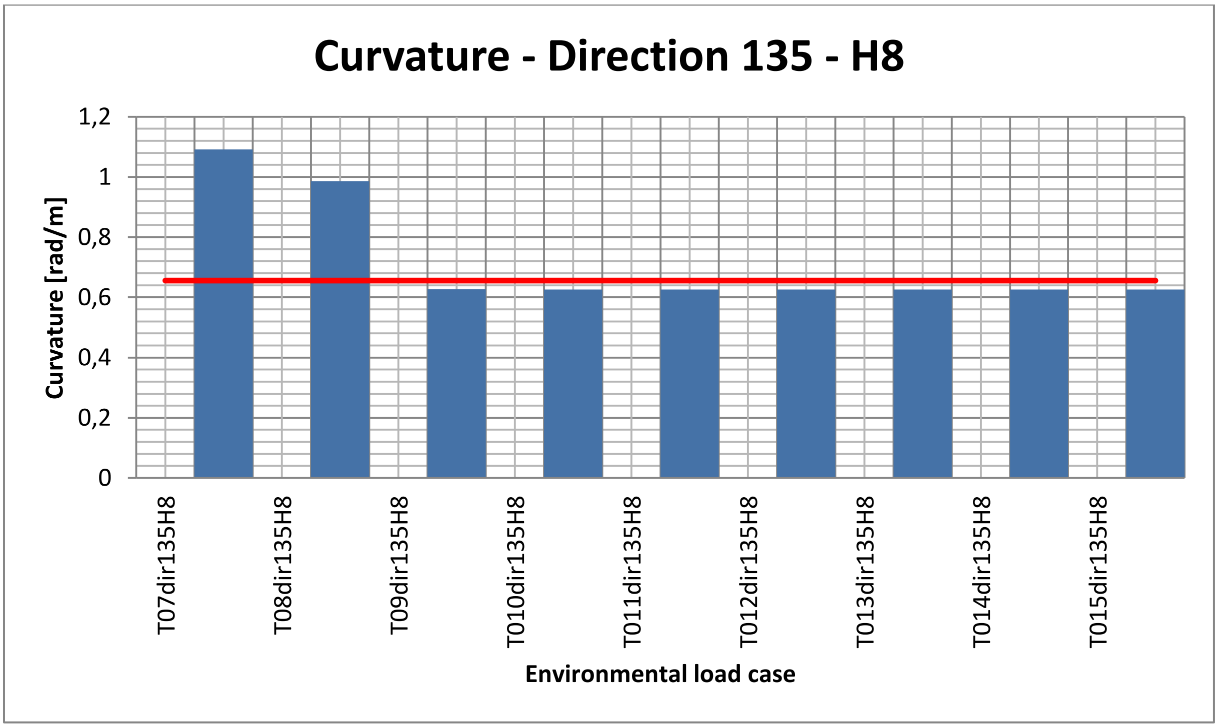

Figure C. 191 - 6” Oilflex Super – Lazy wave – 40 m floatation point – Curvature – Direction 135° - H8

Direction 180°

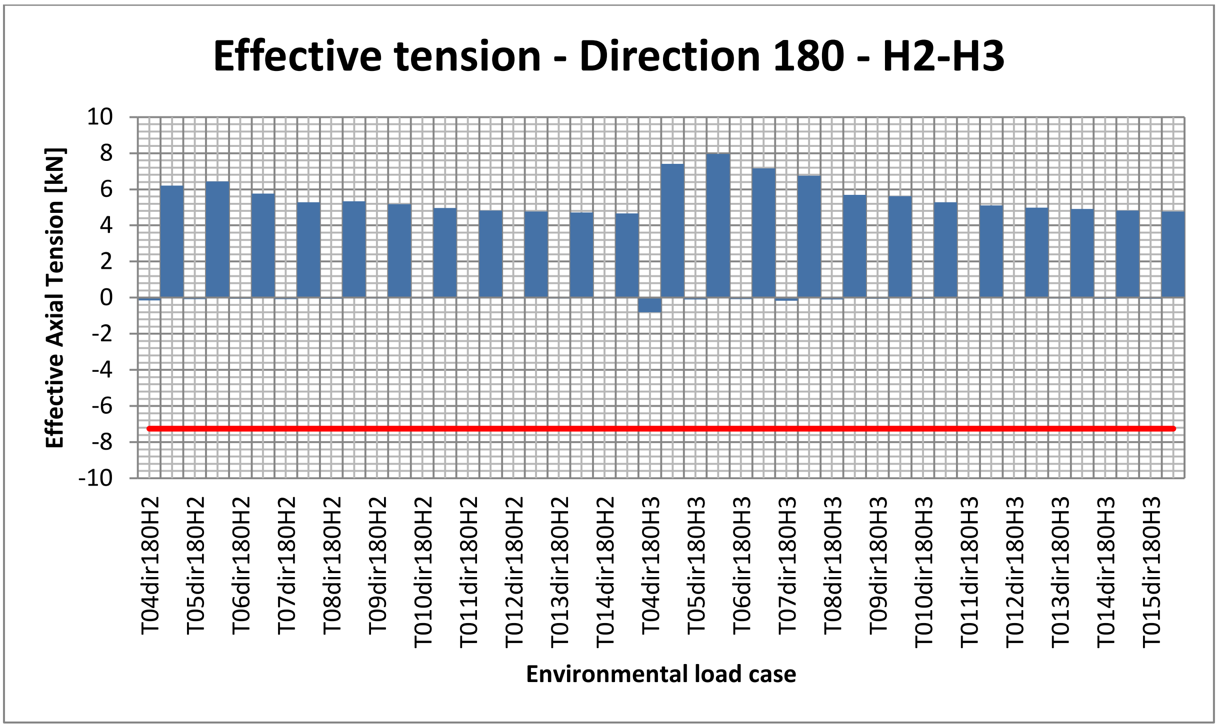

Figure C. 192 - 6" Oilflex Super – Lazy wave – 40 m floatation point – Effective tension – Direction 180° - H2-H3

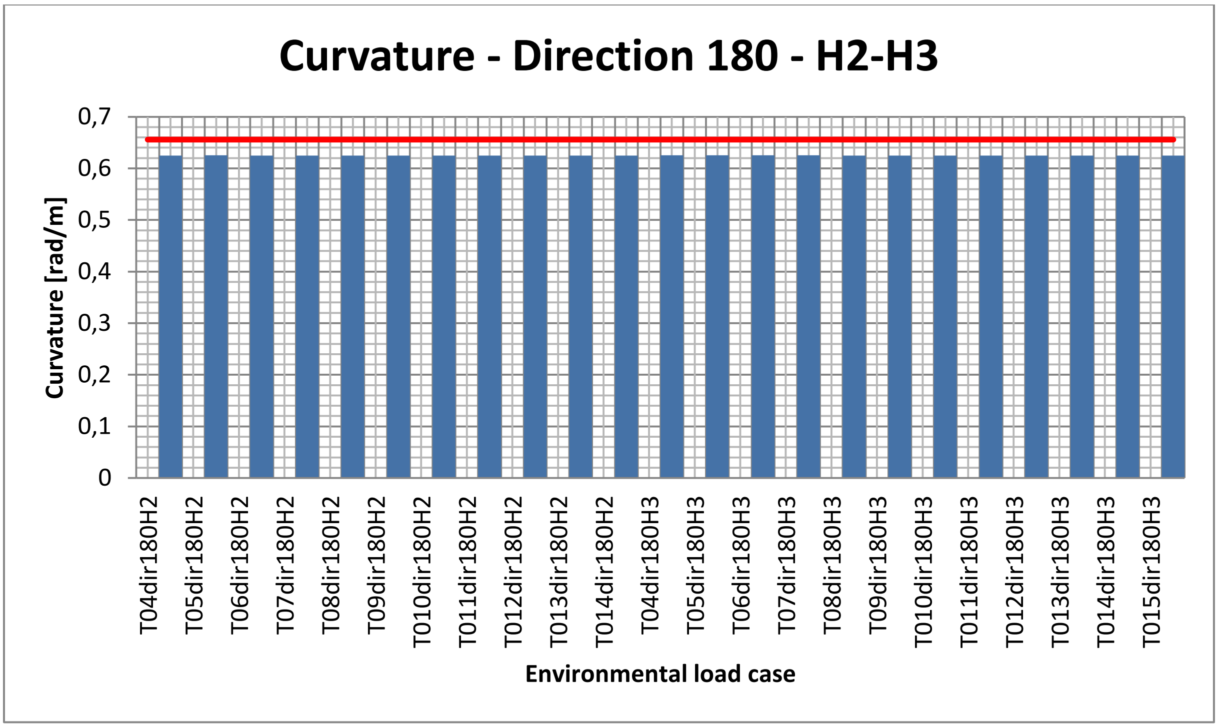

Figure C. 193 - 6" Oilflex Super – Lazy wave – 40 m floatation point – Curvature – Direction 180° - H2-H3

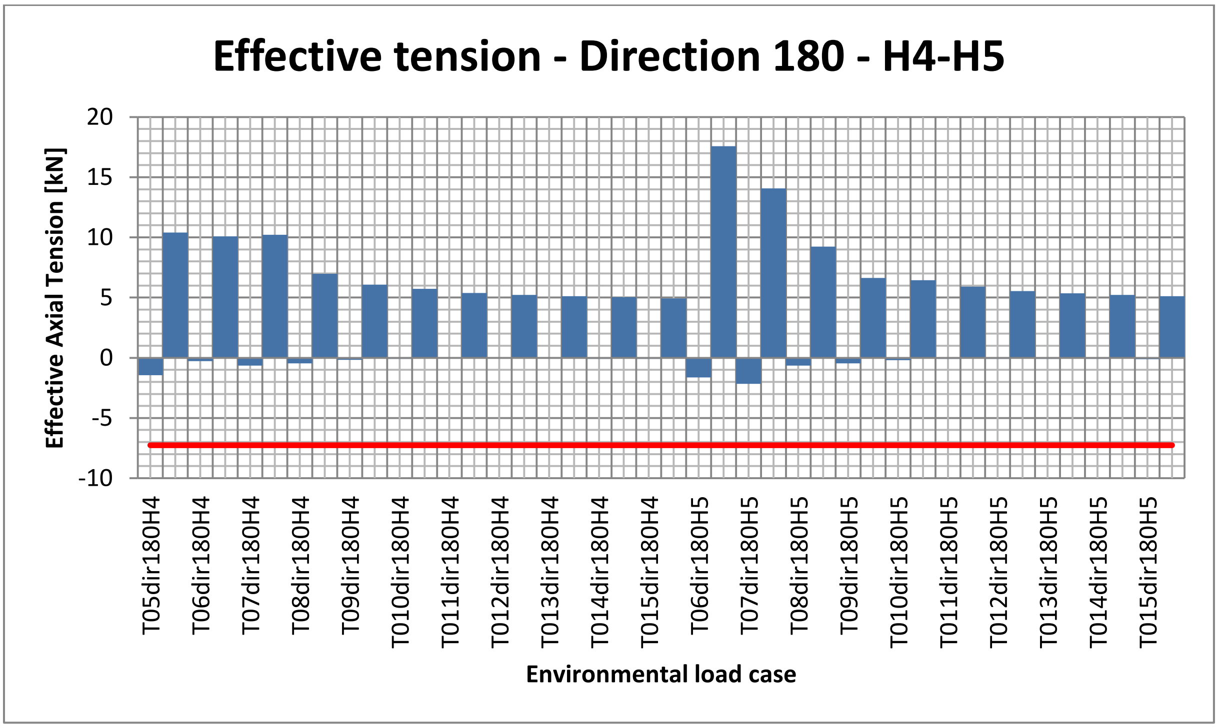

Figure C. 194 - 6" Oilflex Super – Lazy wave – 40 m floatation point – Effective tension – Direction 180° - H4-H5

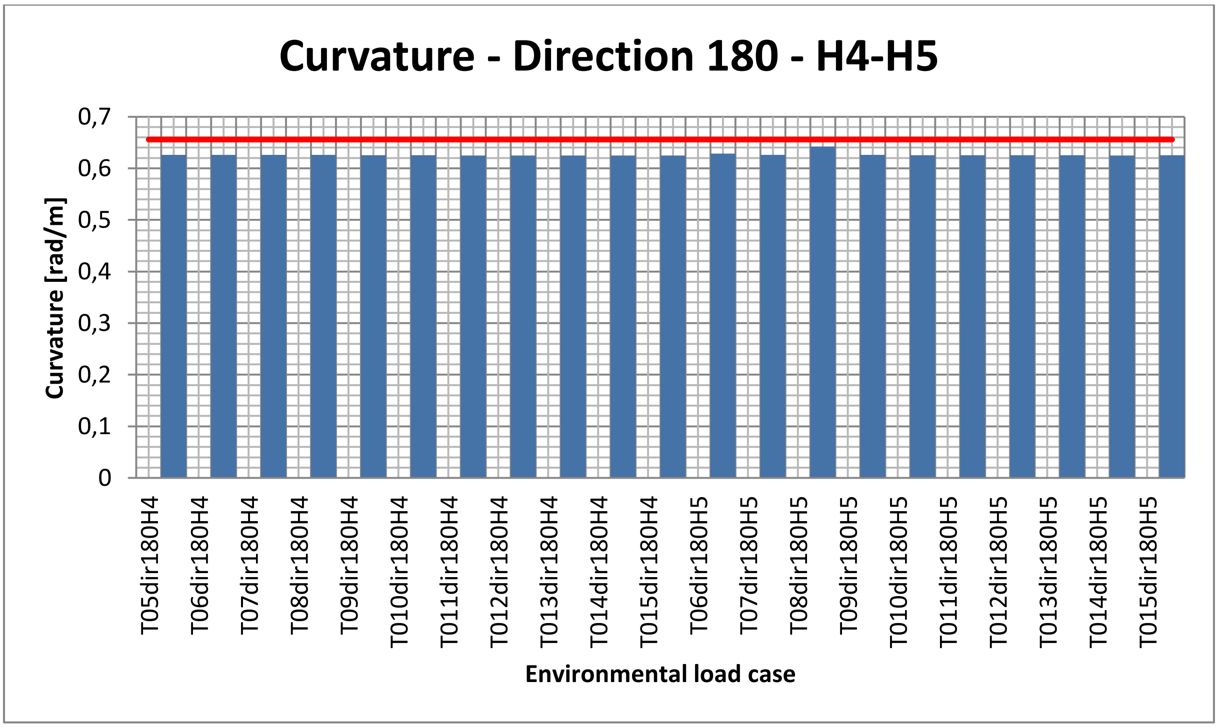

Figure C. 195 - 6" Oilflex Super – Lazy wave – 40 m floatation point – Curvature – Direction 180° - H4-H5

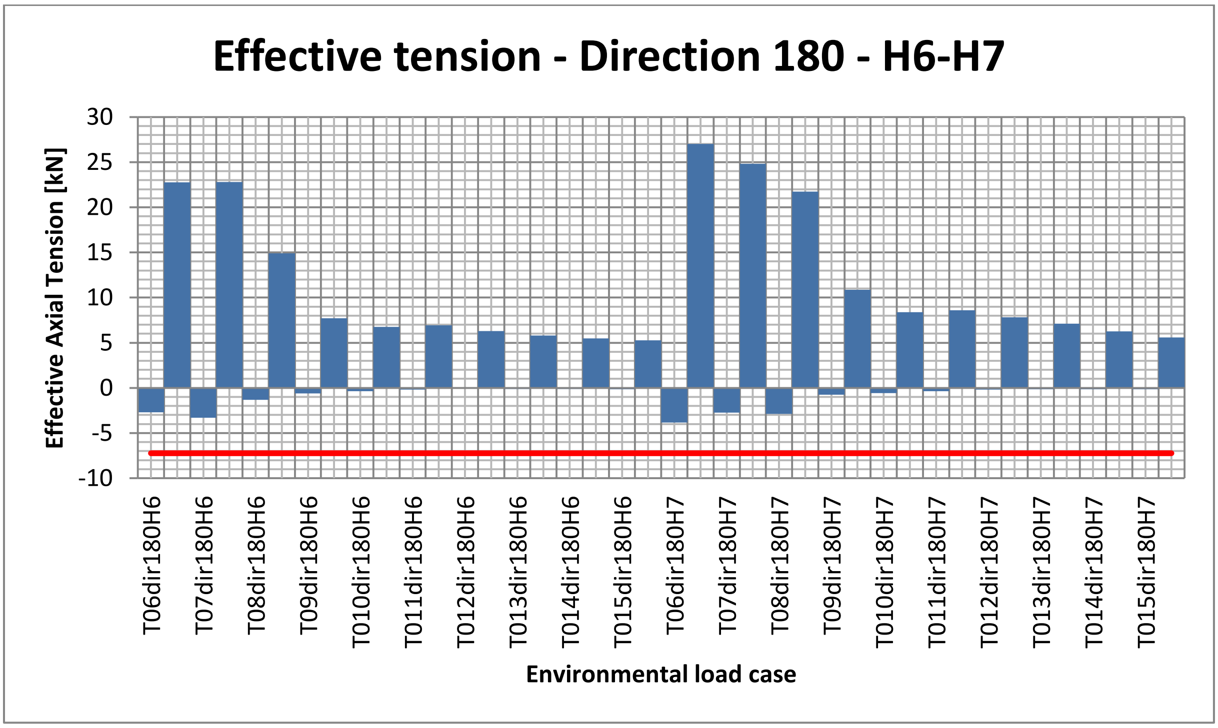

Figure C. 196 - 6” Oilflex Super – Lazy wave – 40 m floatation point – Effective tension – Direction 180° - H6-H7

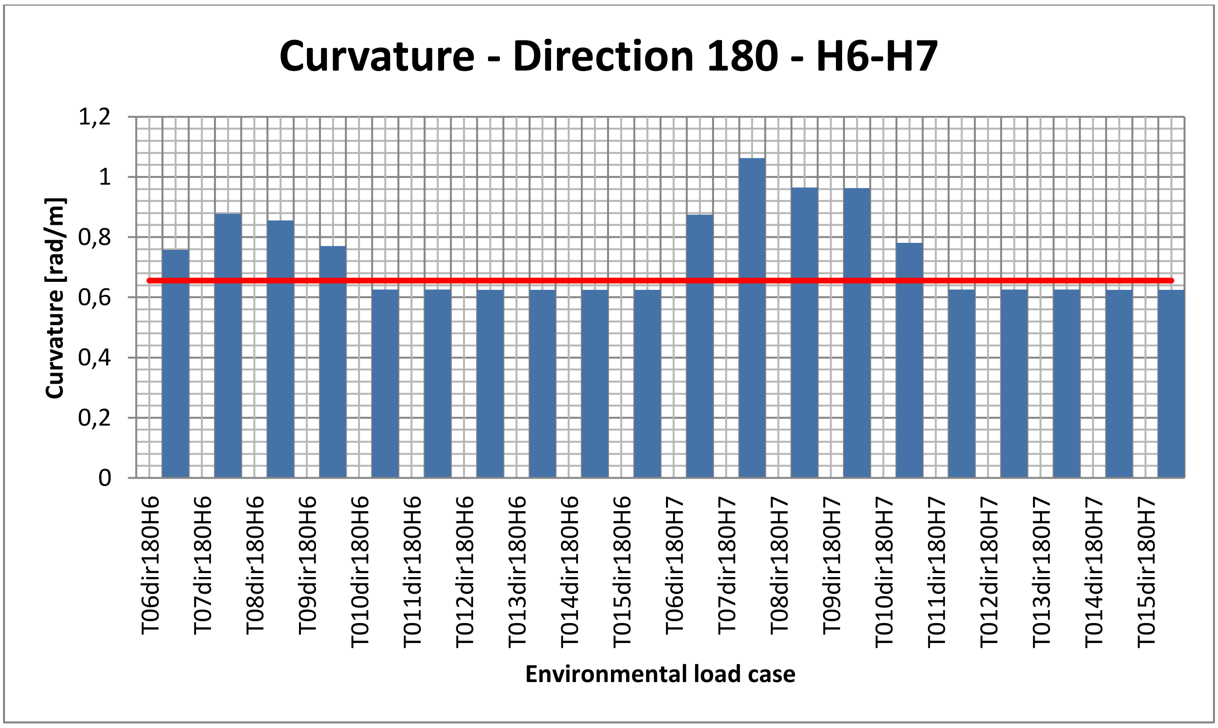

Figure C. 197 - 6” Oilflex Super – Lazy wave – 40 m floatation point – Curvature – Direction 180° - H6-H7

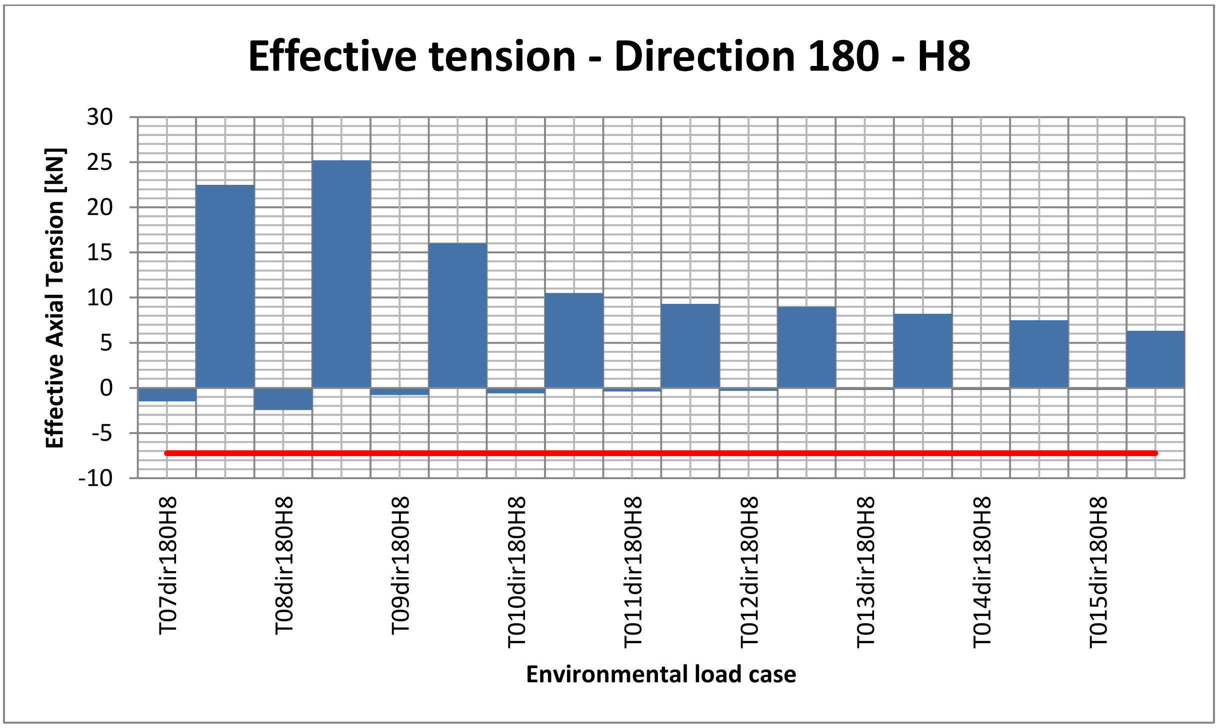

Figure C. 198 - 6” Oilflex Super – Lazy wave – 40 m floatation point – Effective tension – Direction 180° - H8

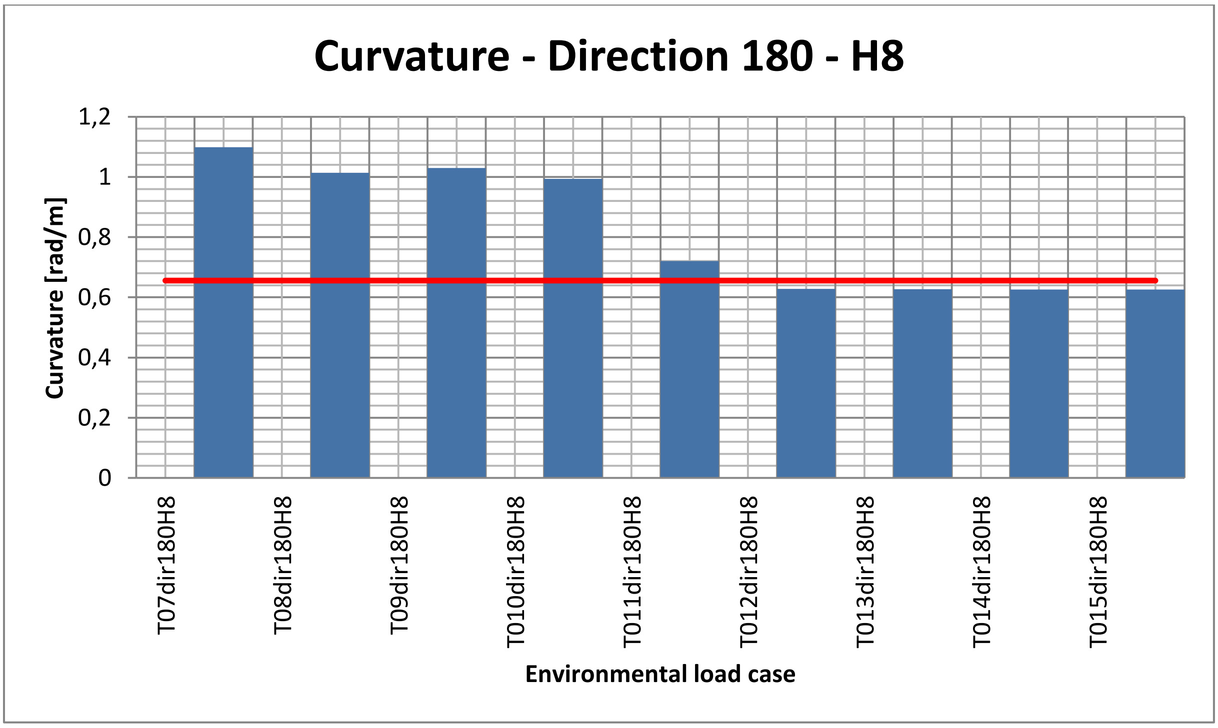

Figure C. 199 - 6” Oilflex Super – Lazy wave – 40 m floatation point – Curvature – Direction 180° - H8

Direction 225°

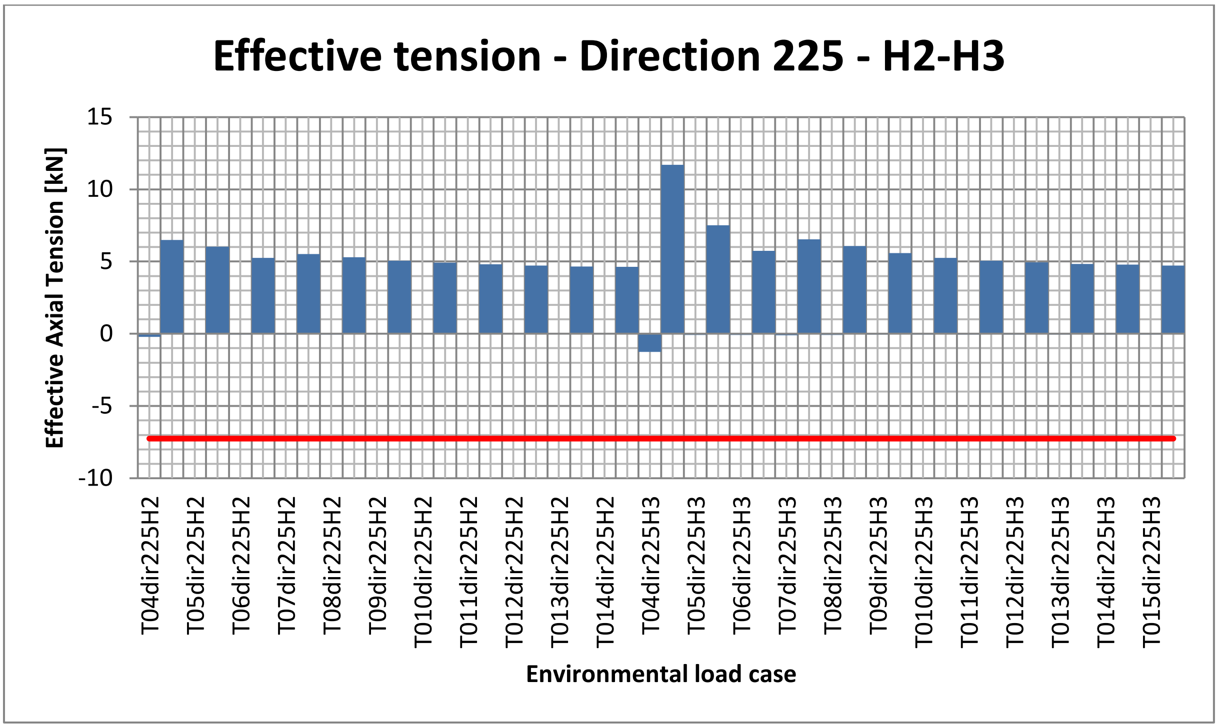

Figure C. 200 - 6” Oilflex Super – Lazy wave – 40 m floatation point – Effective tension – Direction 225° - H2-H3

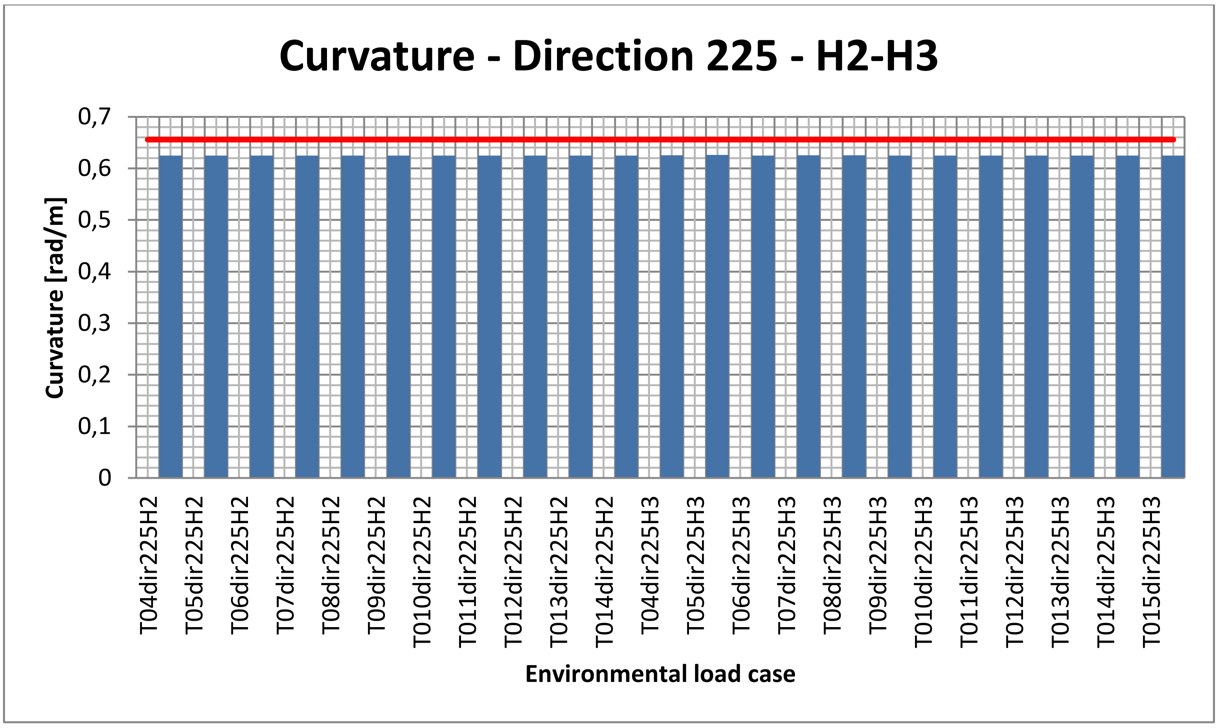

Figure C. 201 - 6” Oilflex Super – Lazy wave – 40 m floatation point – Curvature – Direction 225° - H2-H3

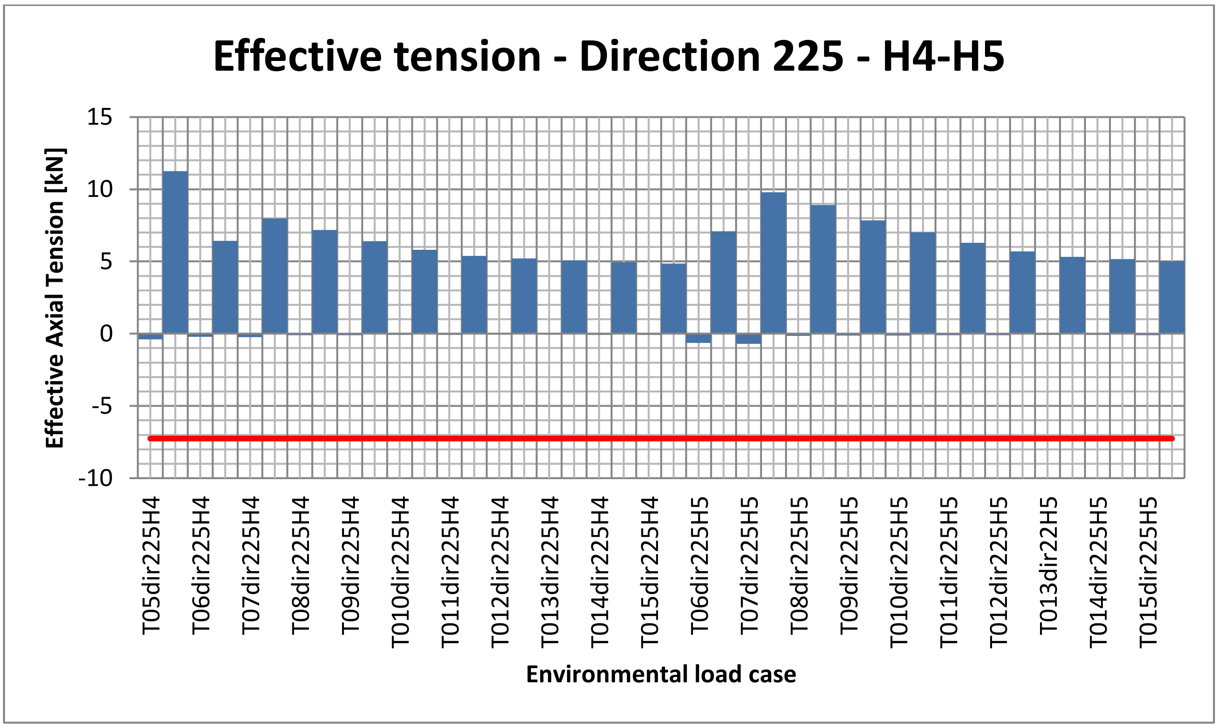

Figure C. 202 - 6” Oilflex Super – Lazy wave – 40 m floatation point – Effective tension – Direction 225° - H4-H5

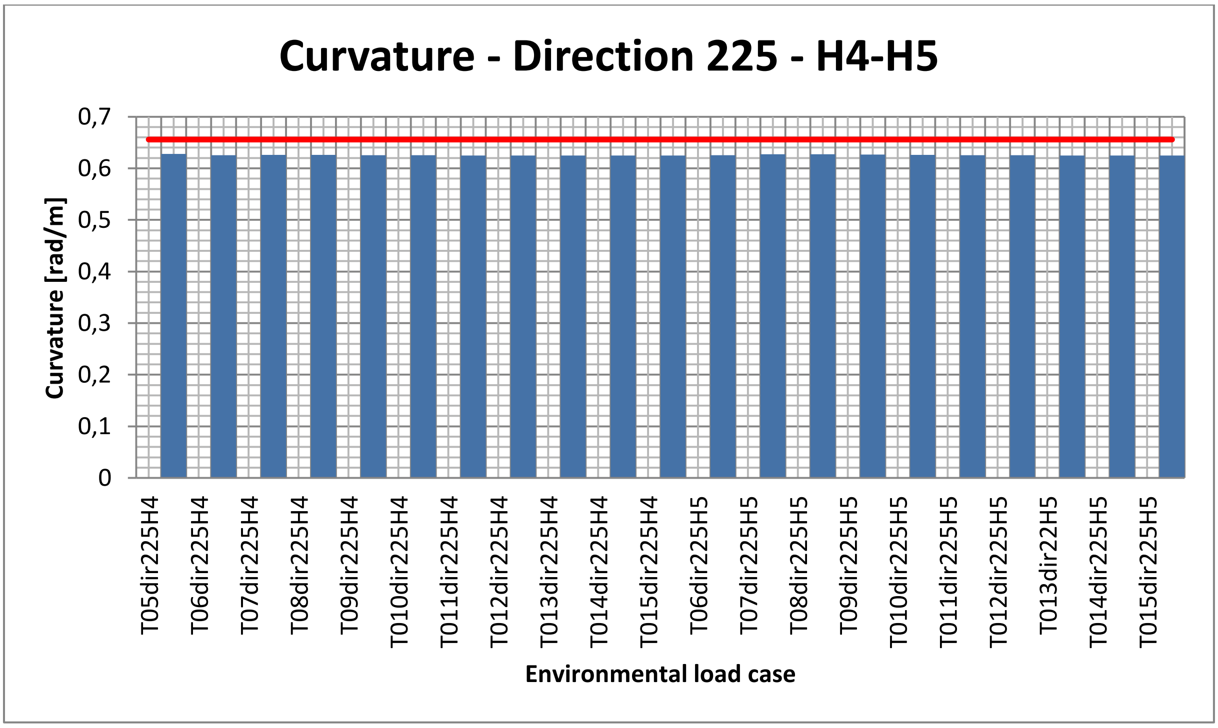

Figure C. 203 - 6” Oilflex Super – Lazy wave – 40 m floatation point – Curvature – Direction 225° - H4-H5

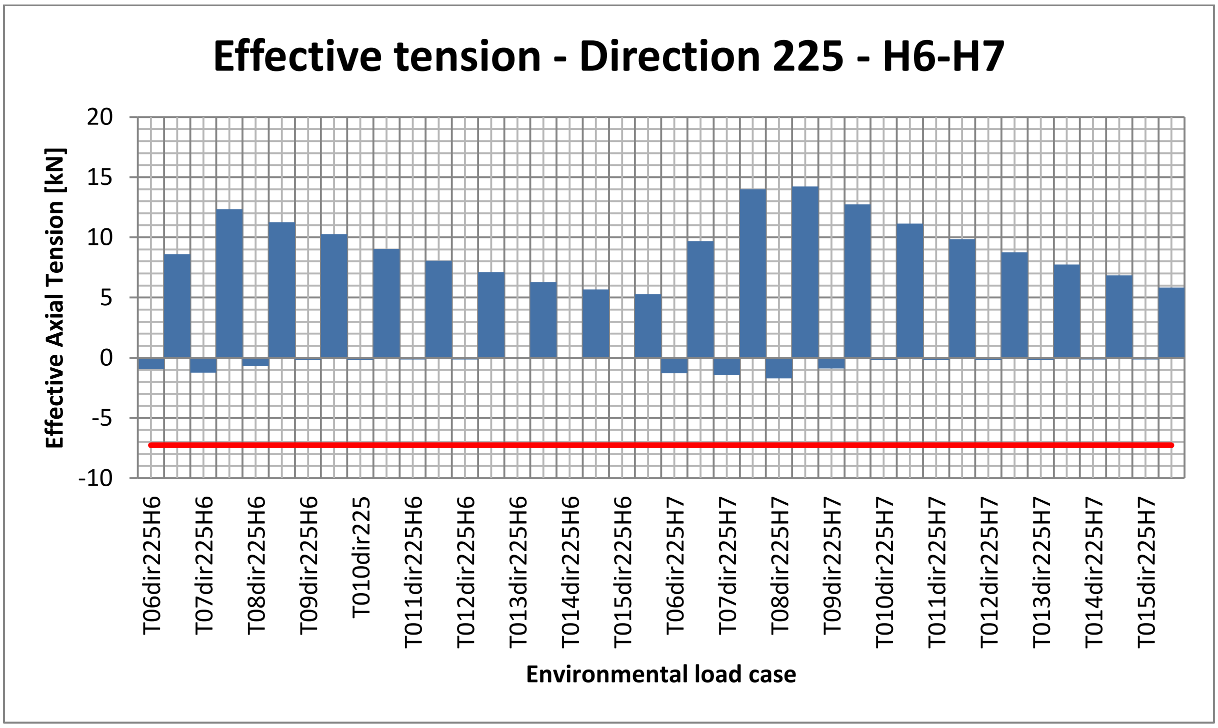

Figure C. 204 - 6” Oilflex Super – Lazy wave – 40 m floatation point – Effective tension – Direction 225° - H6-H7

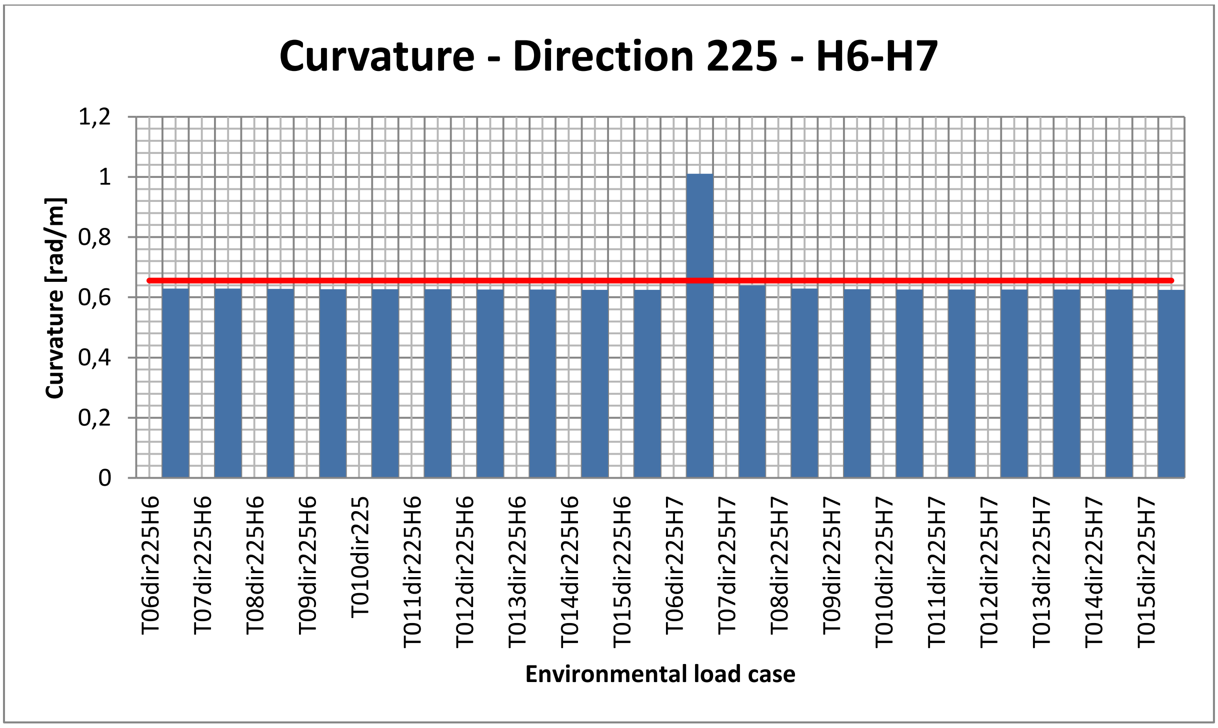

Figure C. 205 - 6” Oilflex Super – Lazy wave – 40 m floatation point – Curvature – Direction 225° - H6-H7

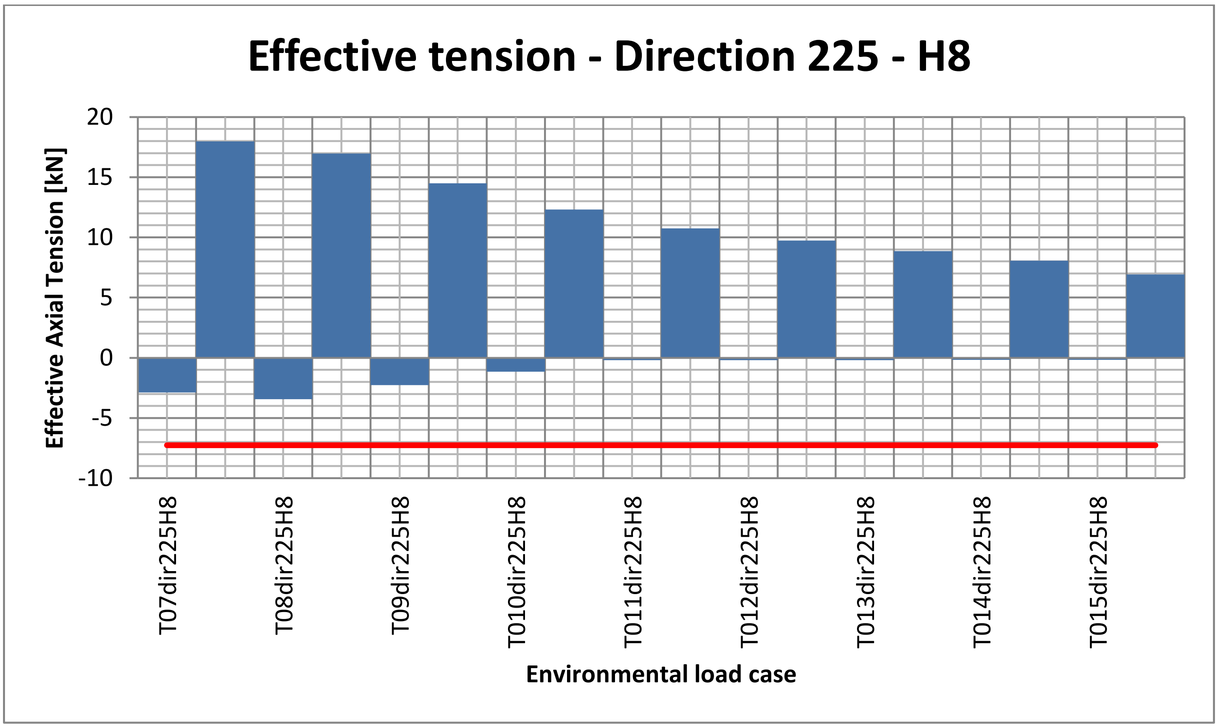

Figure C. 206 - 6” Oilflex Super – Lazy wave – 40 m floatation point – Effective tension – Direction 225° - H8

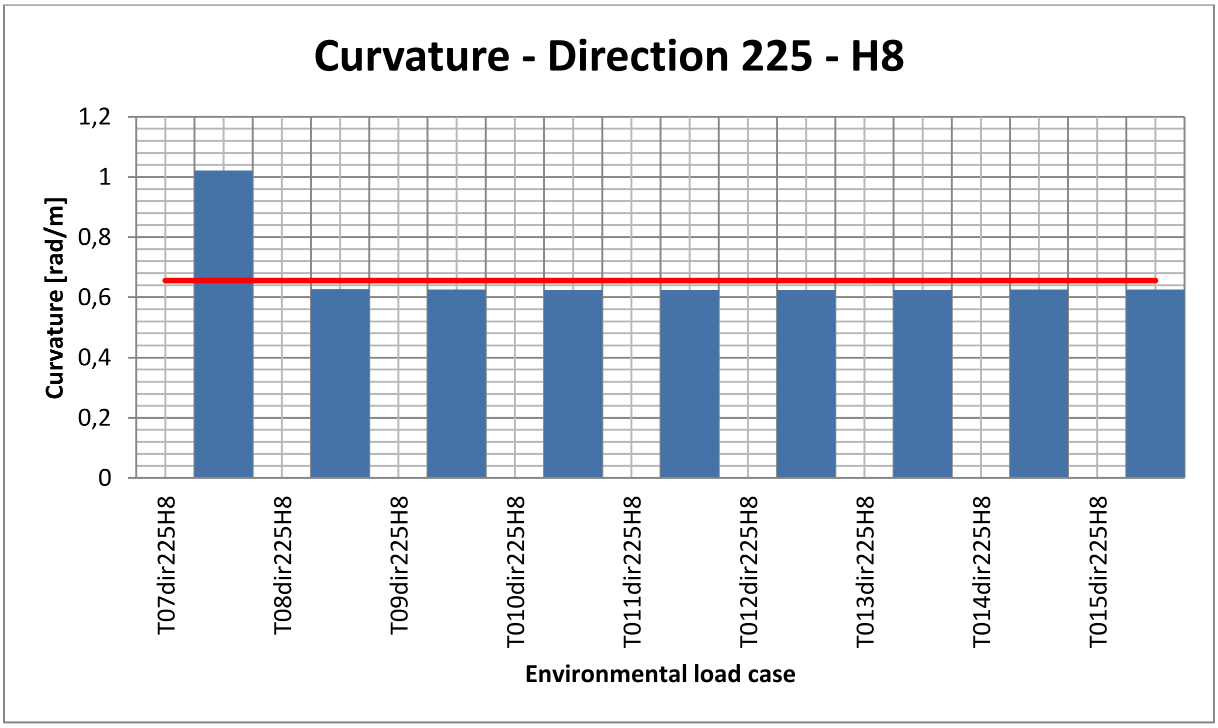

Figure C. 207 - 6” Oilflex Super – Lazy wave – 40 m floatation point – Curvature – Direction 225° - H8

Wave rose

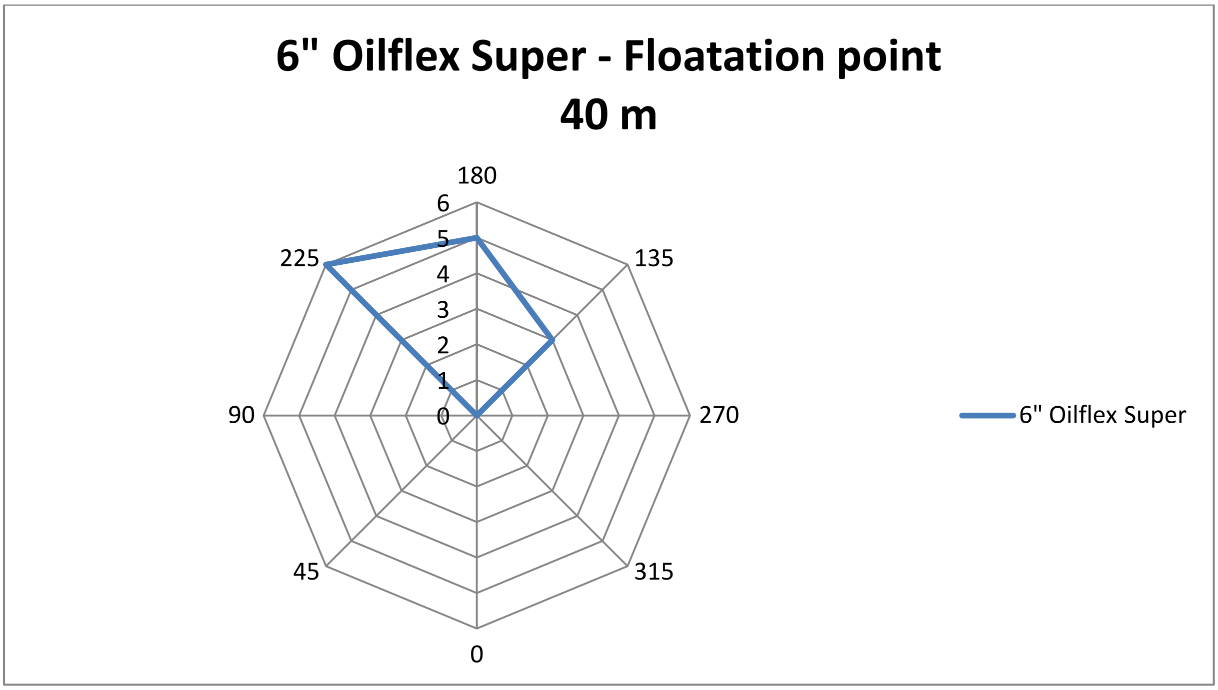

Figure C. 208 - 6" Oilflex Super – Lazy wave – 40 m floatation point – Wave rose

Limitation plot

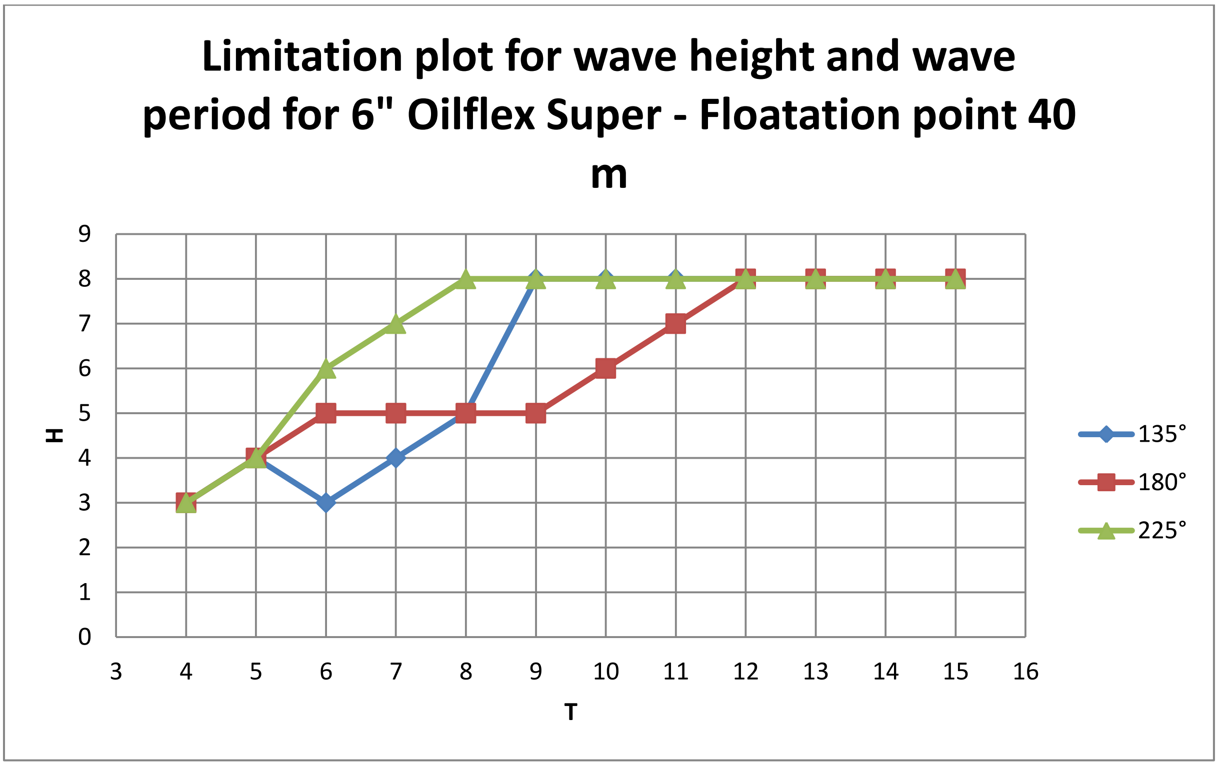

Figure C. 209 - 6" Oilflex Super – Lazy wave – 40 m floatation point – Limitation plot

Lazy wave – 60 m floatation point

Direction 135°

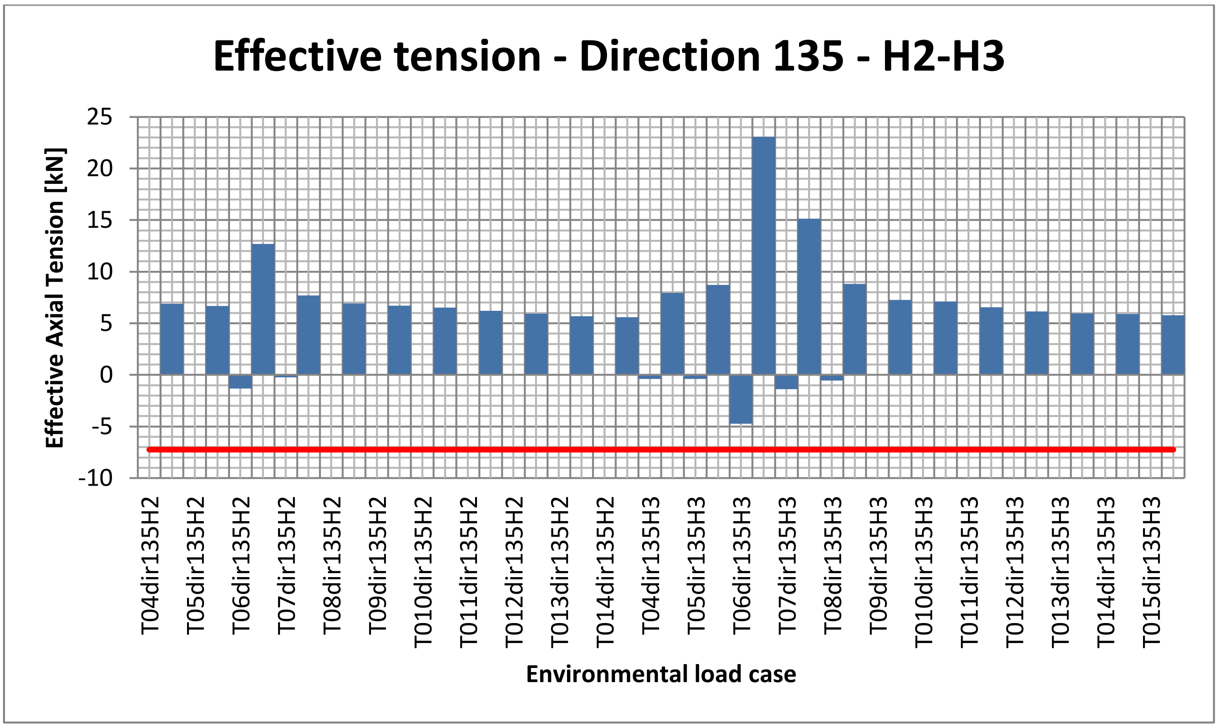

Figure C. 210 - 6” Oilflex Super – Lazy wave – 60 m floatation point – Effective tension – Direction 135° - H2-H3

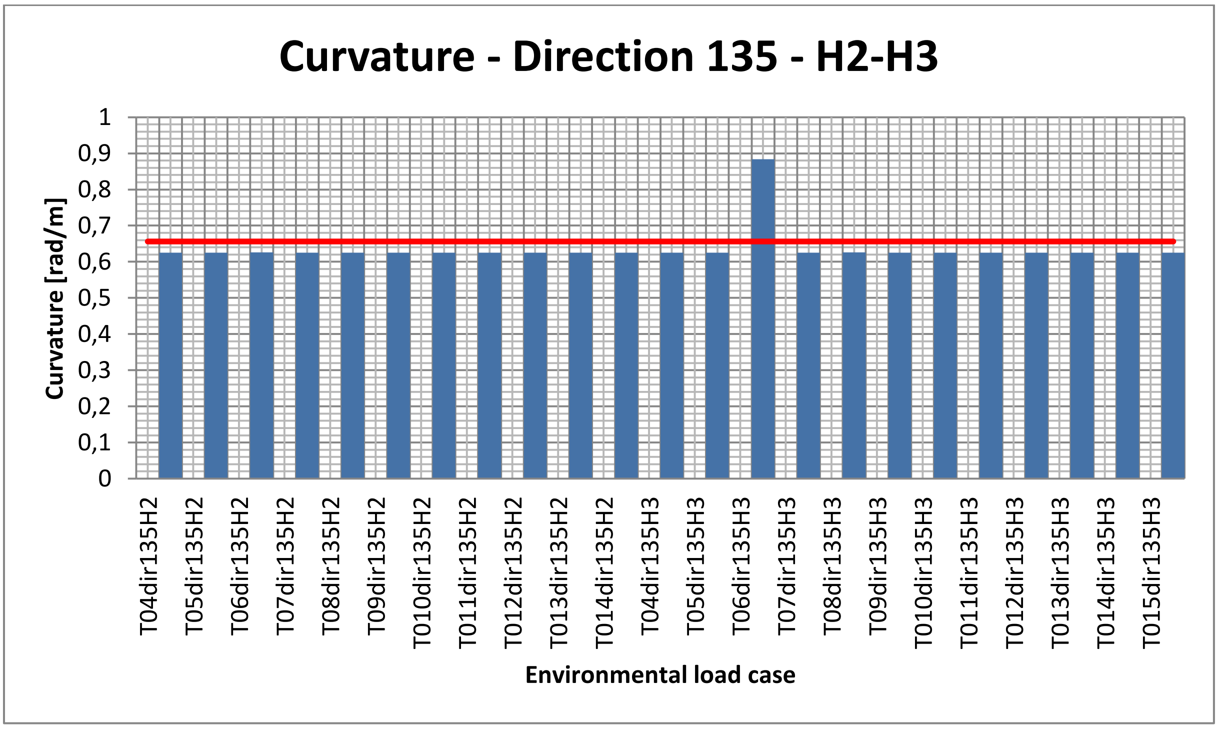

Figure C. 211 - 6” Oilflex Super – Lazy wave – 60 m floatation point – Curvature – Direction 135° - H2-H3

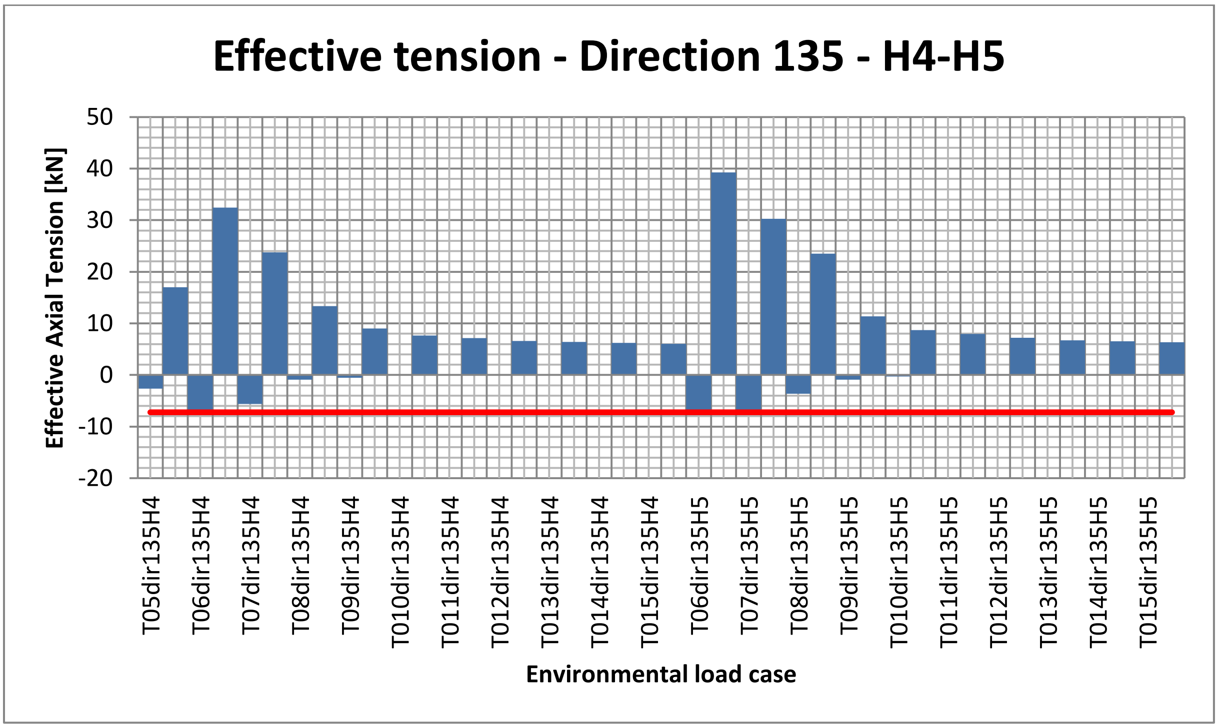

Figure C. 212 - 6” Oilflex Super – Lazy wave – 60 m floatation point – Effective tension – Direction 135° - H4-H5

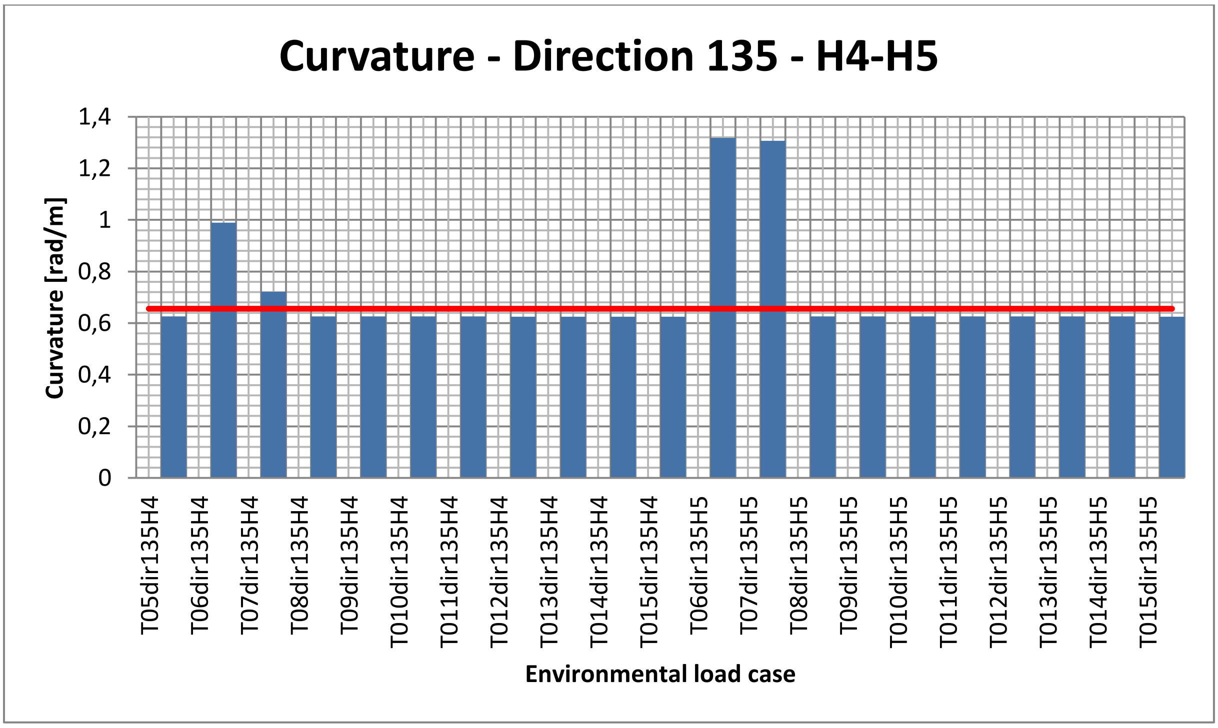

Figure C. 213 - 6” Oilflex Super – Lazy wave – 60 m floatation point – Curvature – Direction 135° - H4-H5

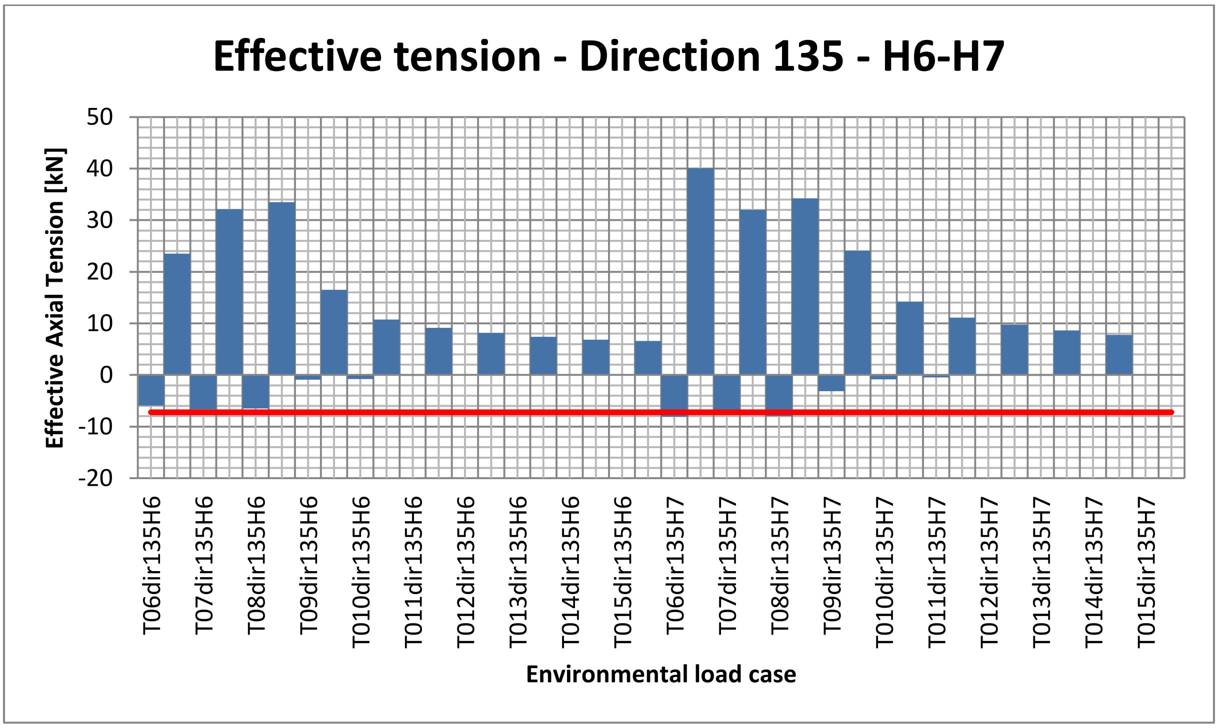

Figure C. 214 - 6" Oilflex Super – Lazy wave – 60 m floatation point – Effective tension – Direction 135° - H6-H7

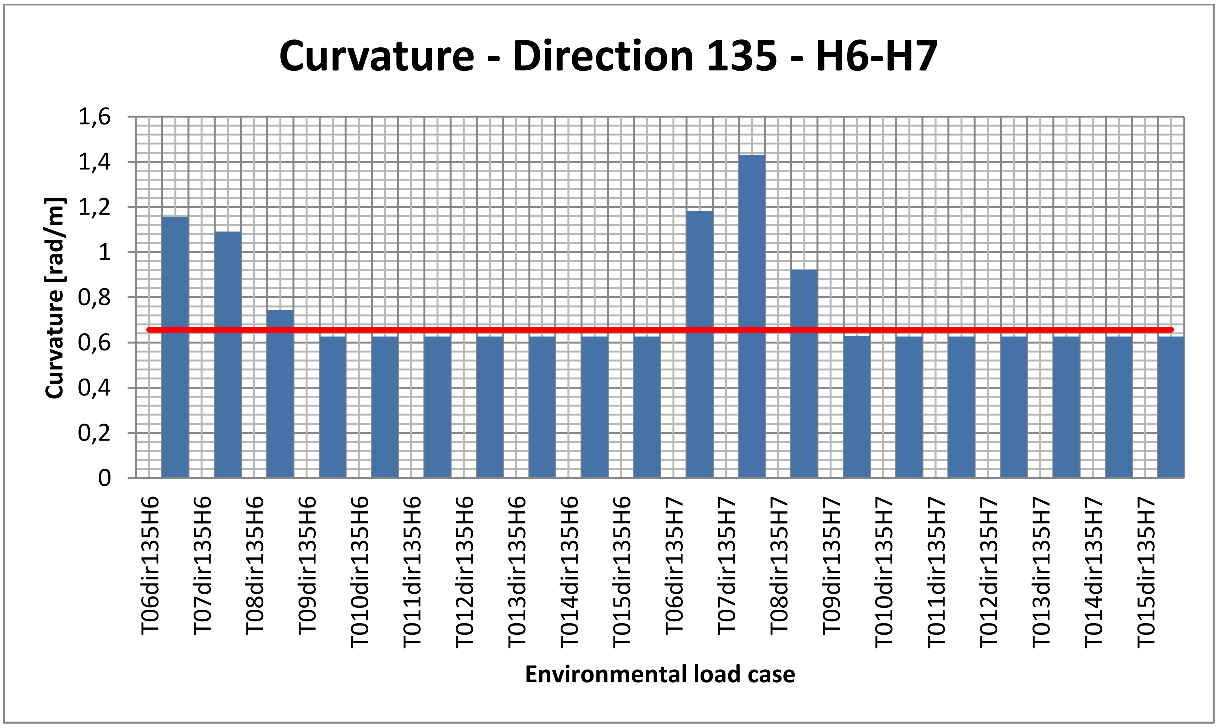

Figure C. 215 - 6" Oilflex Super – Lazy wave – 60 m floatation point – Curvature – Direction 135° - H6-H7

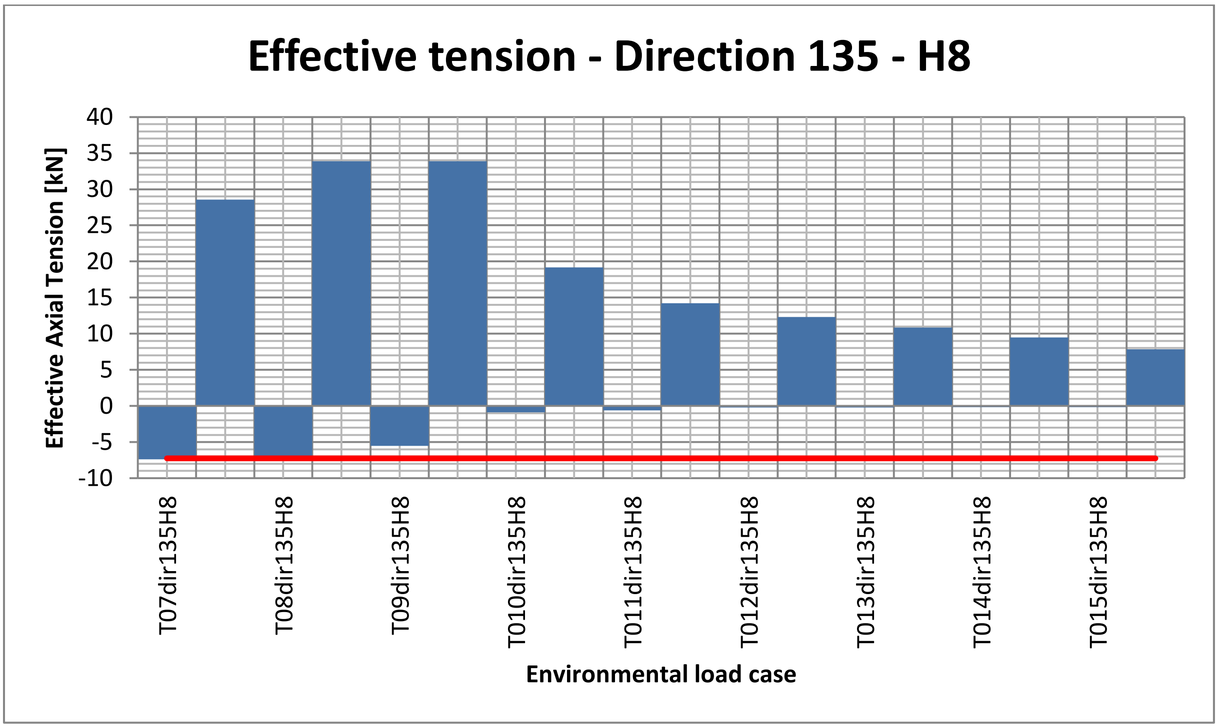

Figure C. 216 - 6" Oilflex Super – Lazy wave – 60 m floatation point – Effective tension – Direction 135° - H8

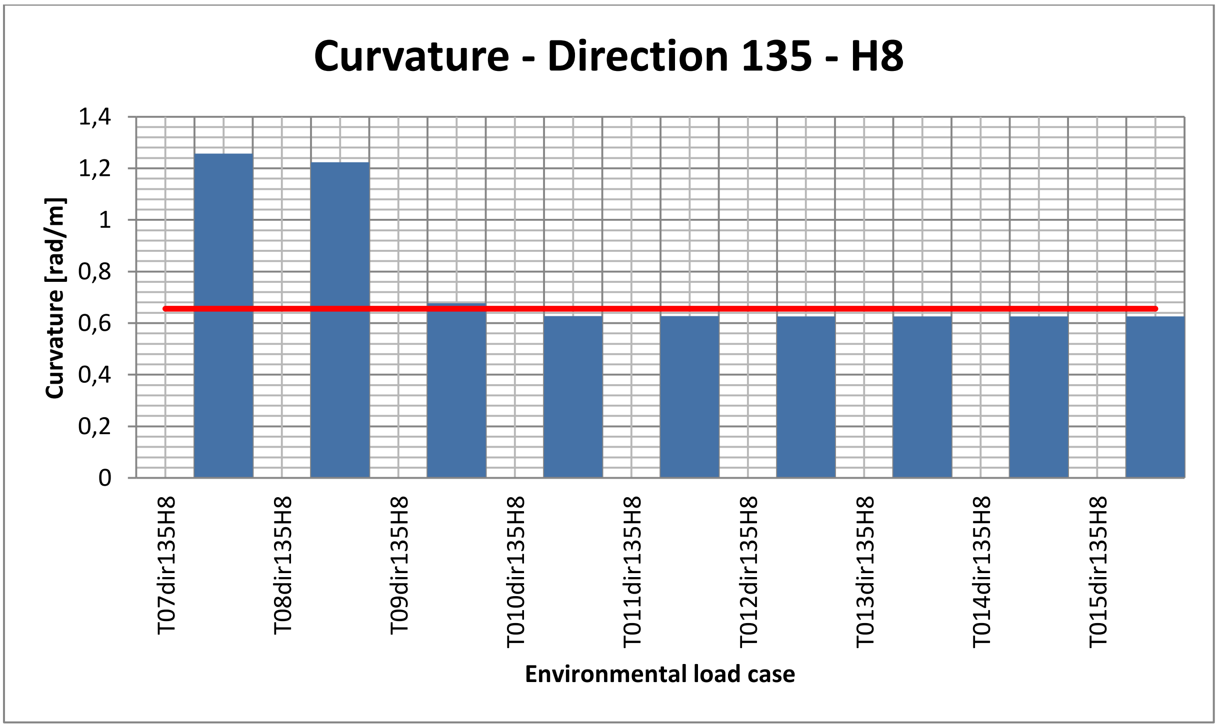

Figure C. 217 - 6" Oilflex Super – Lazy wave – 60 m floatation point – Curvature – Direction 135° - H8

Direction 180°

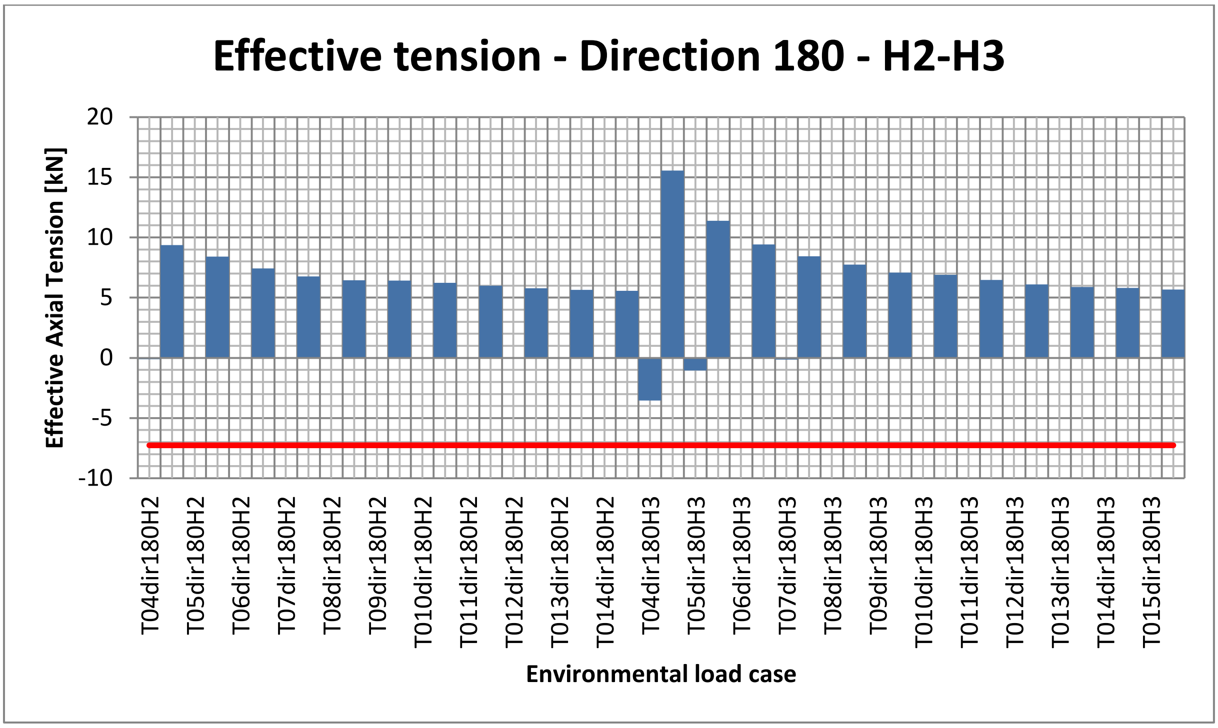

Figure C. 218 - 6" Oilflex Super – Lazy wave – 60 m floatation point – Effective tension – Direction 180° - H2-H3

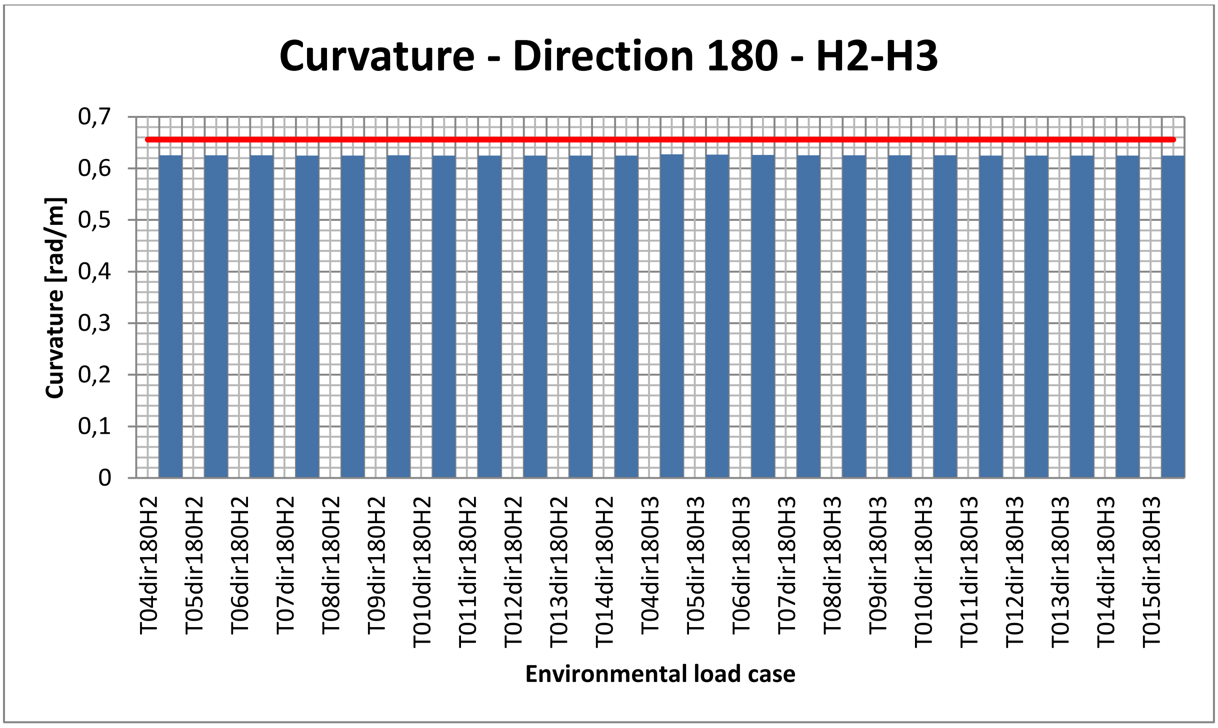

Figure C. 219 - 6" Oilflex Super – Lazy wave – 60 m floatation point – Curvature – Direction 180° - H2-H3

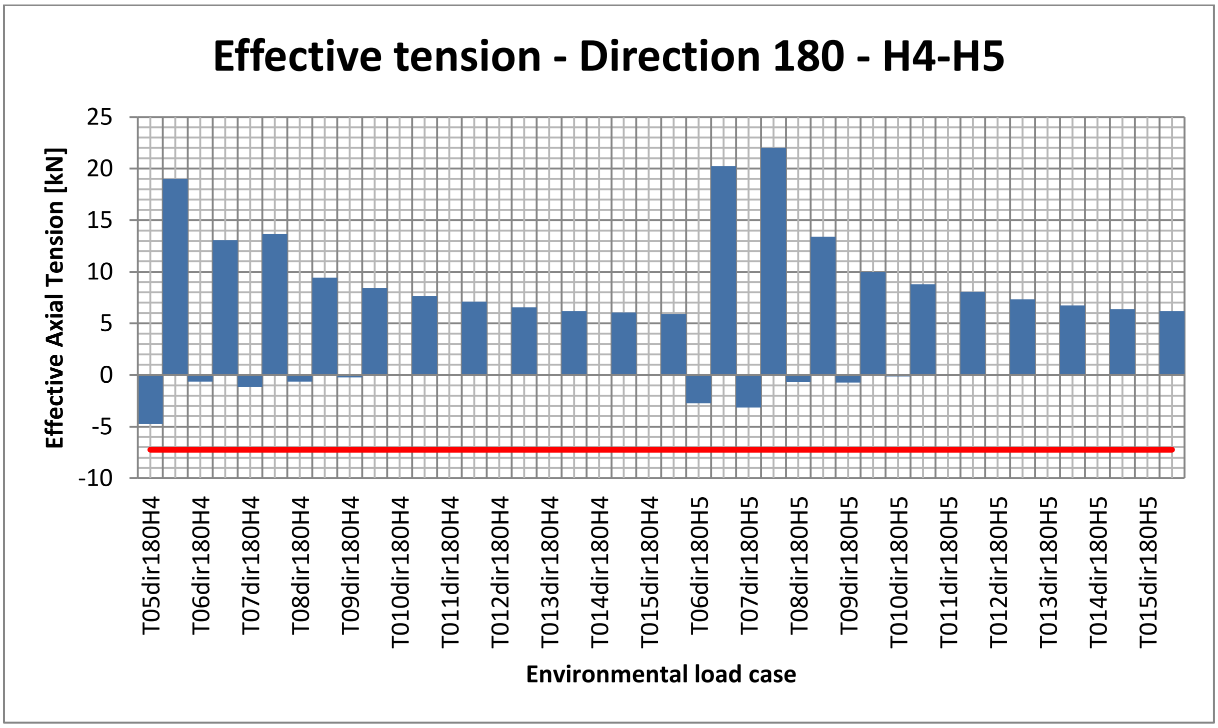

Figure C. 220 - 6” Oilflex Super – Lazy wave – 60 m floatation point – Effective tension – Direction 180° - H4-H5

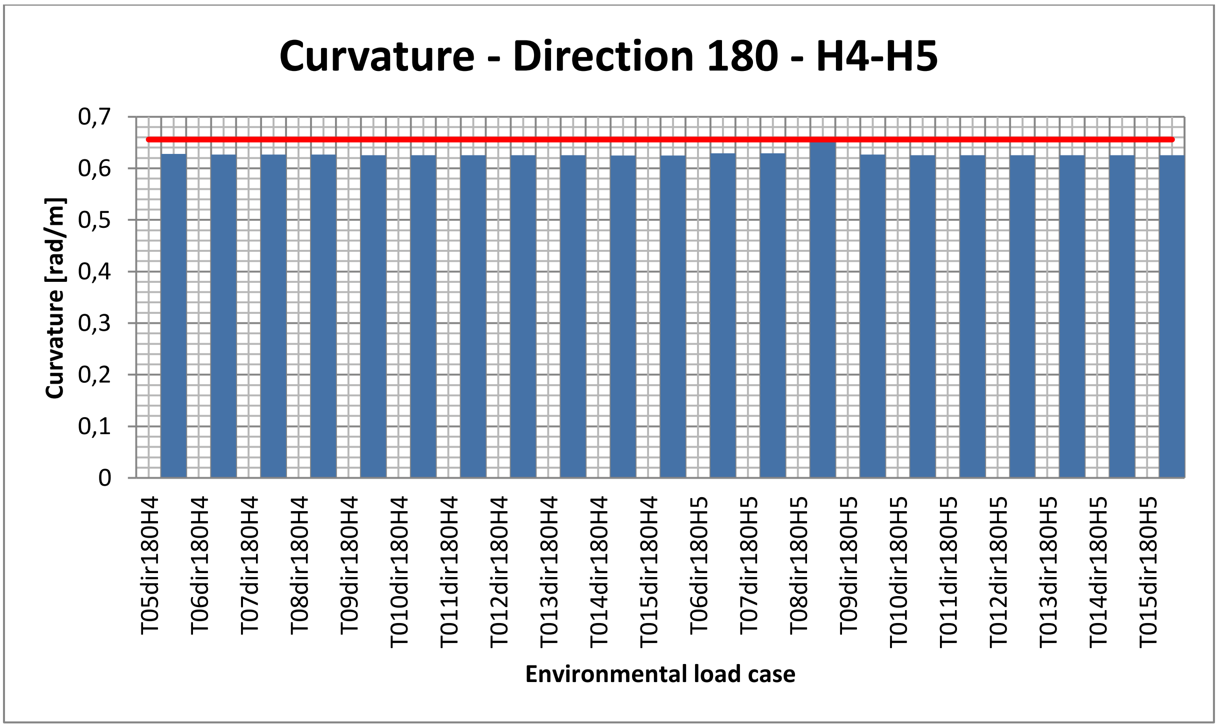

Figure C. 221 - 6” Oilflex Super – Lazy wave – 60 m floatation point – Curvature – Direction 180° - H4-H5

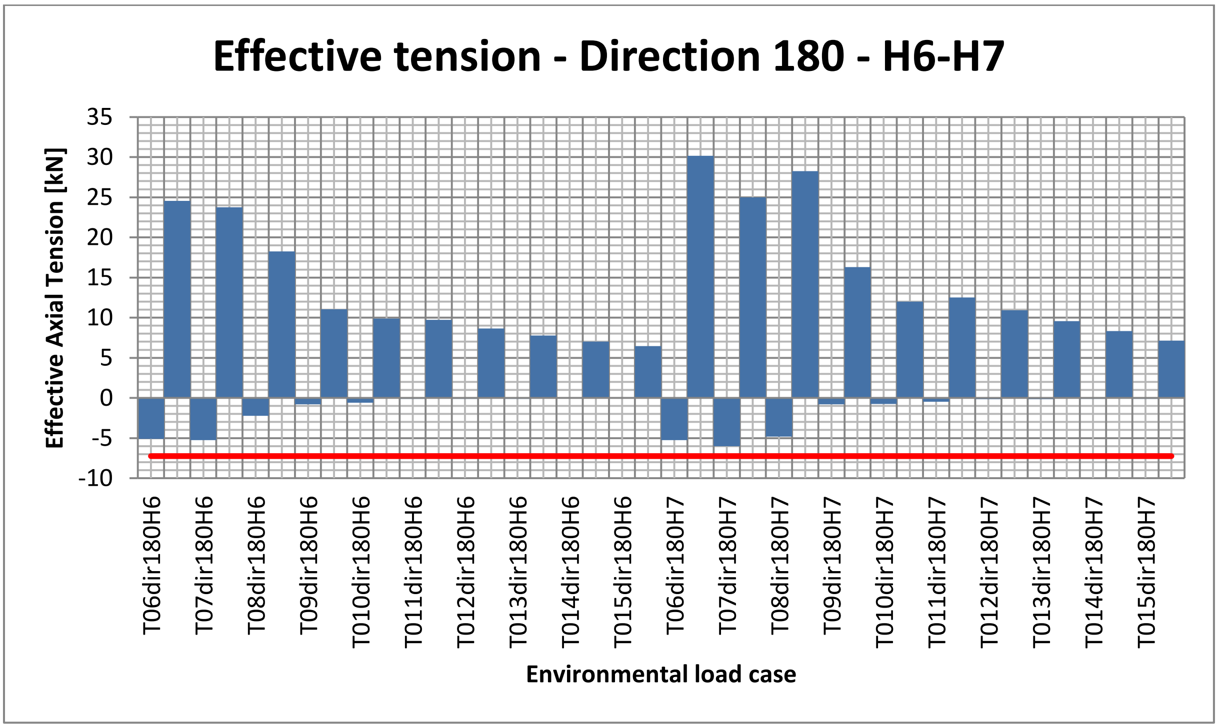

Figure C. 222 - 6” Oilflex Super – Lazy wave – 60 m floatation point – Effective tension – Direction 180° - H6-H7

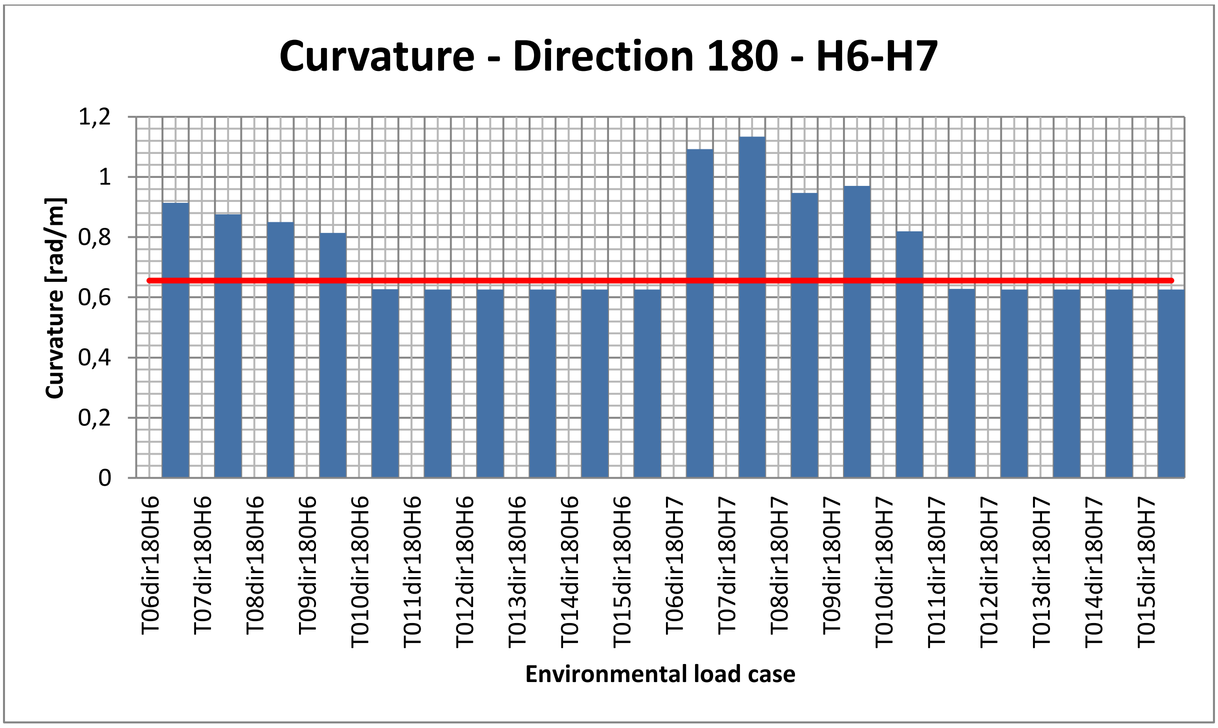

Figure C. 223 - 6” Oilflex Super – Lazy wave – 60 m floatation point – Curvature – Direction 180° - H6-H7

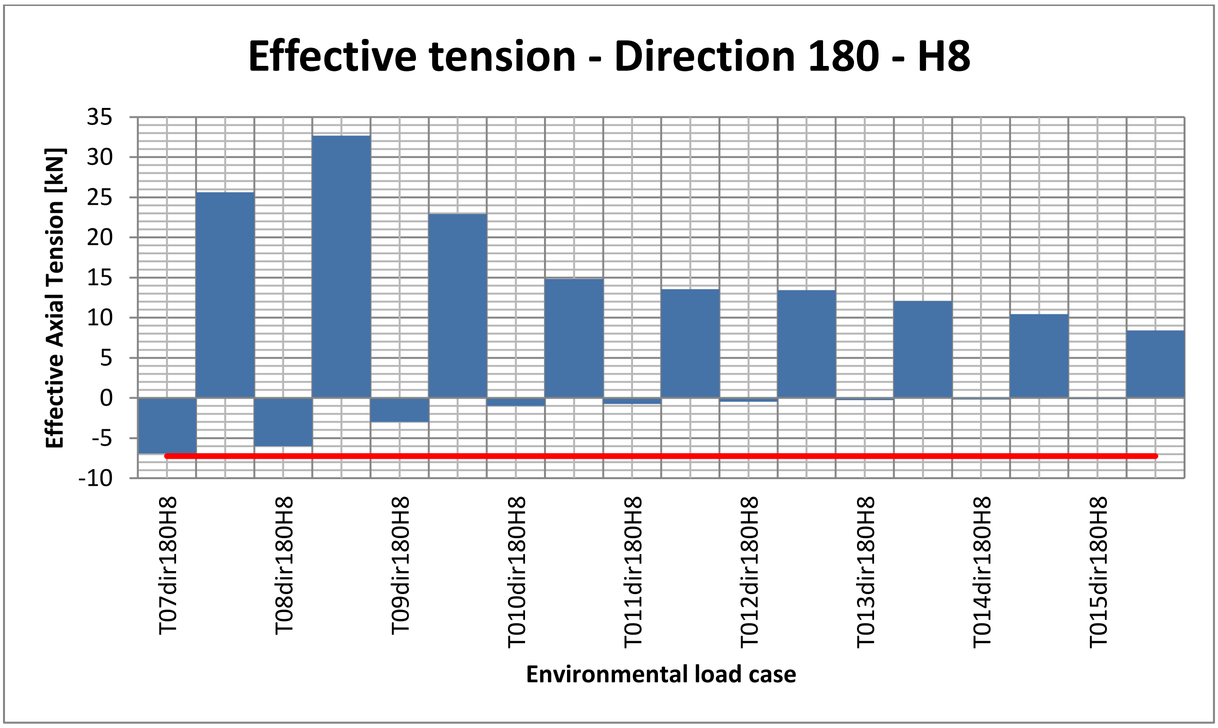

Figure C. 224 - 6" Oilflex Super – Lazy wave – 60 m floatation point – Effective tension – Direction 180° - H8

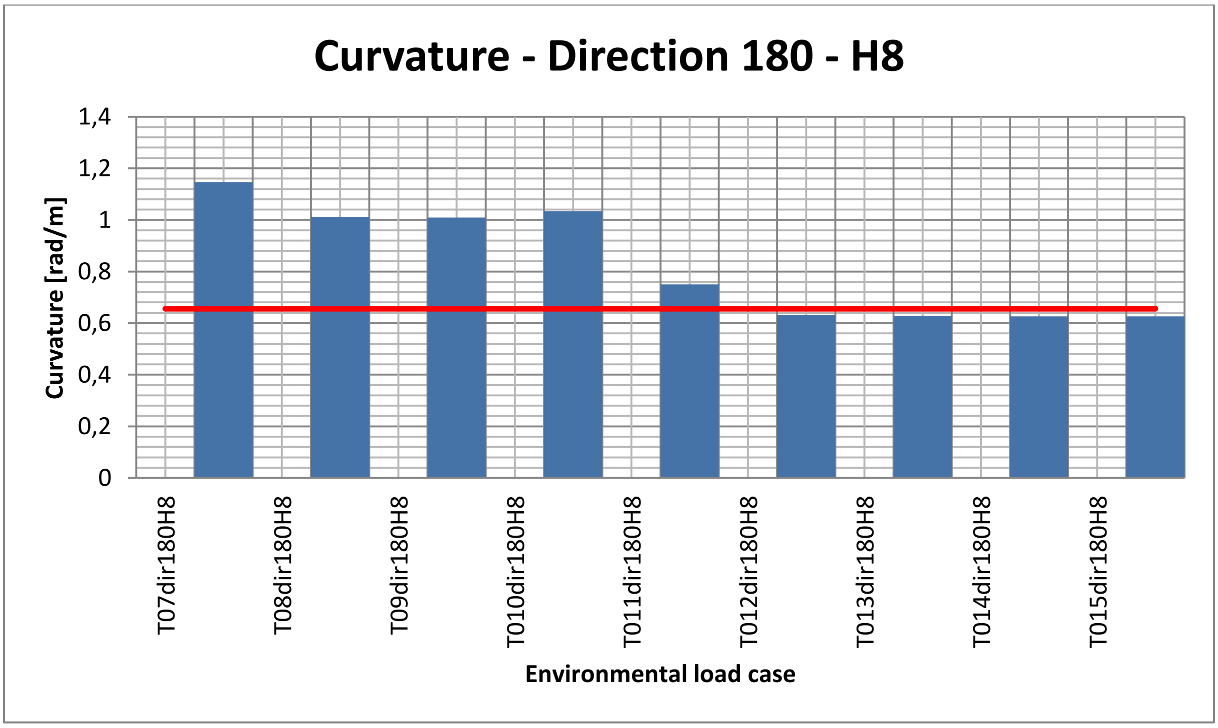

Figure C. 225 - 6" Oilflex Super – Lazy wave – 60 m floatation point – Curvature – Direction 180° - H8

Direction 225°

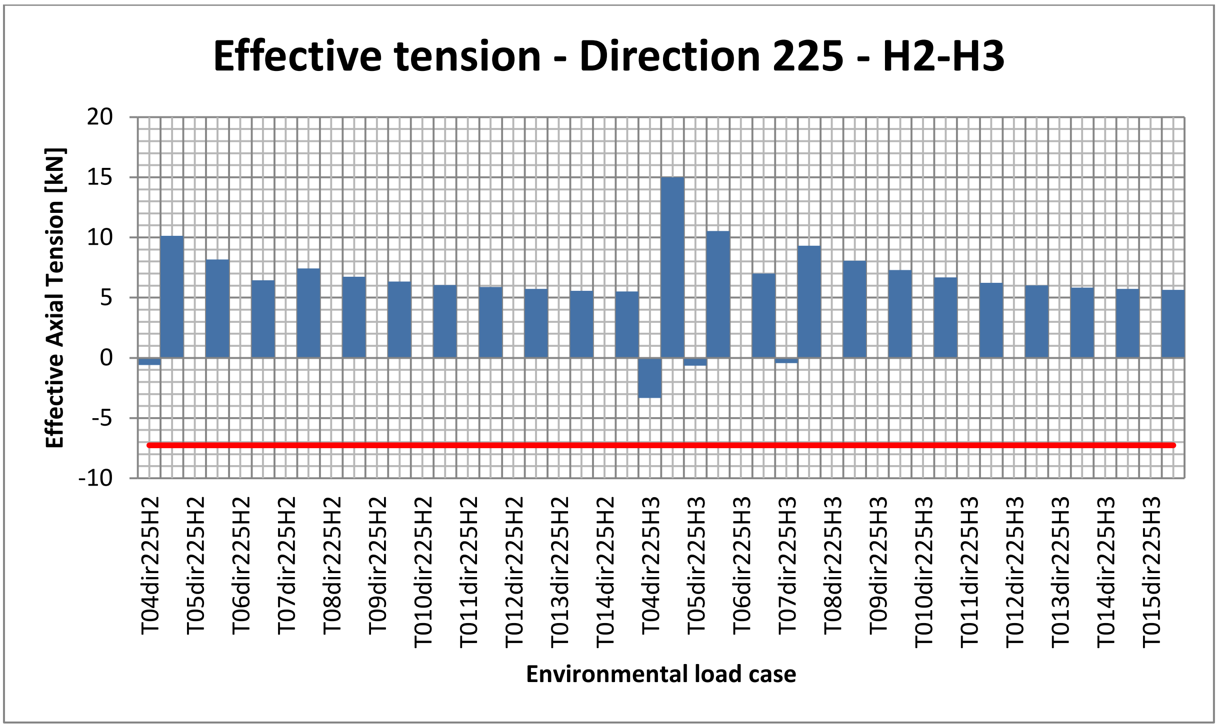

Figure C. 226 - 6” Oilflex Super – Lazy wave – 60 m floatation point – Effective tension – Direction 225° - H2-H3

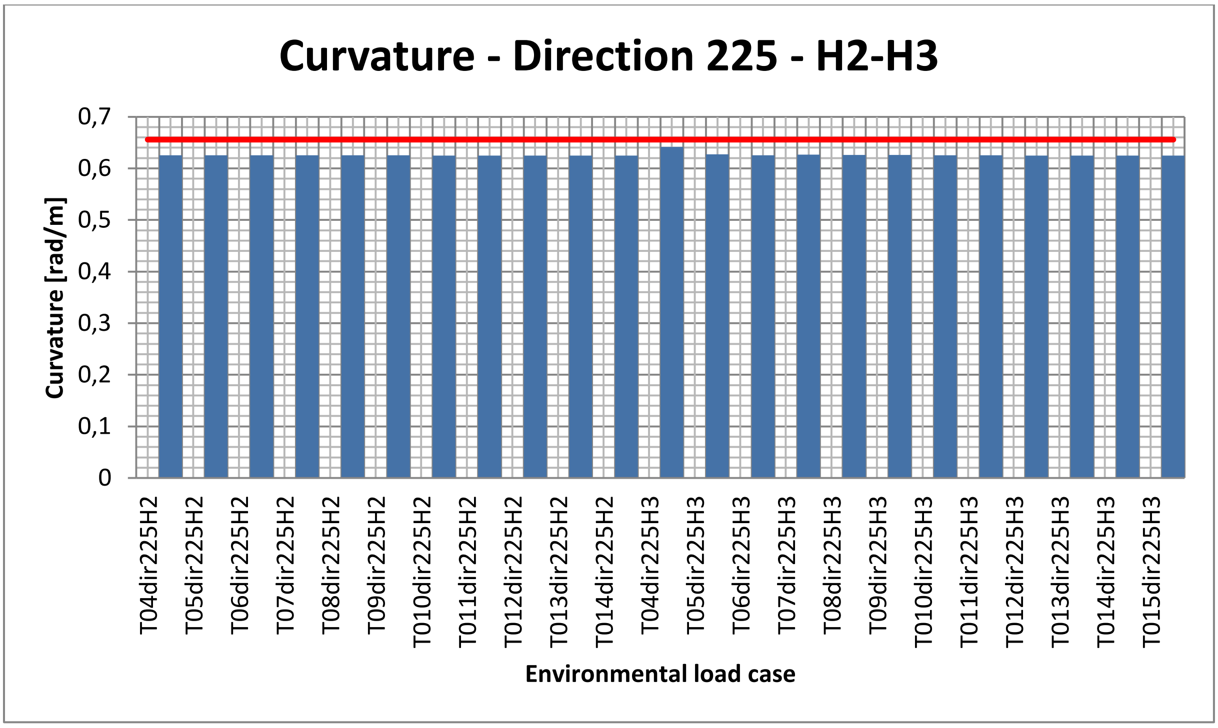

Figure C. 227 - 6” Oilflex Super – Lazy wave – 60 m floatation point – Curvature – Direction 225° - H2-H3

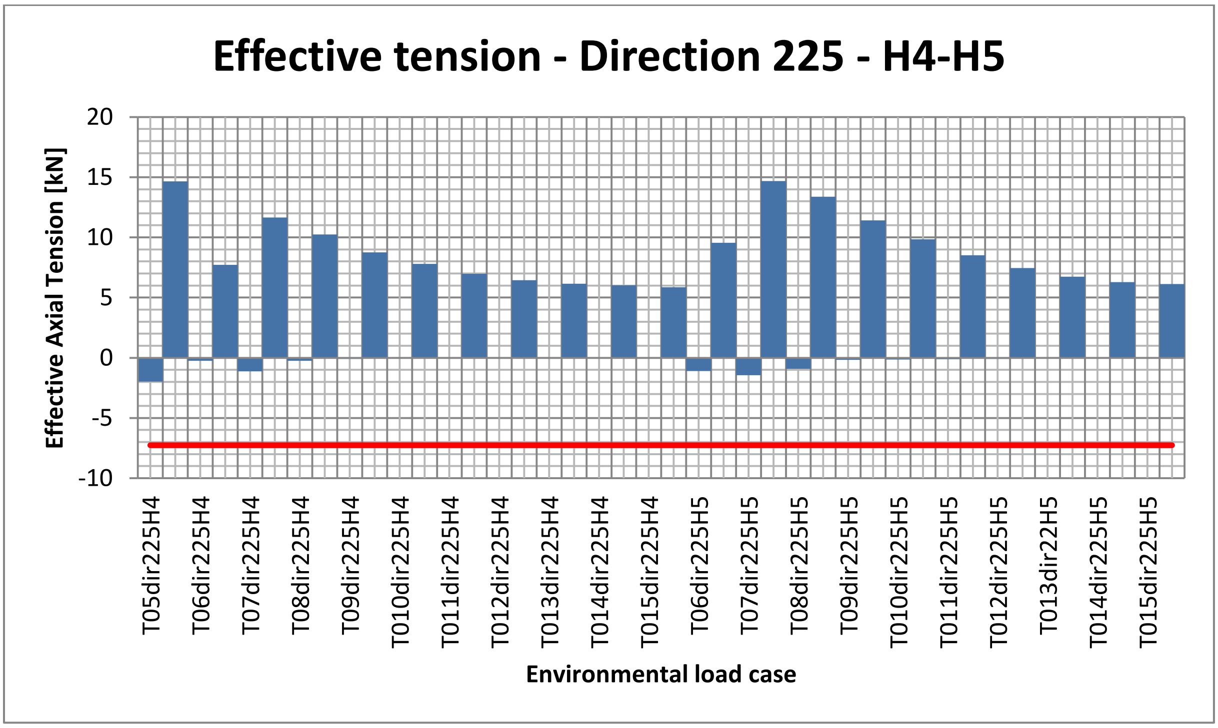

Figure C. 228 - 6” Oilflex Super – Lazy wave – 60 m floatation point – Effective tension – Direction 225° - H4-H5

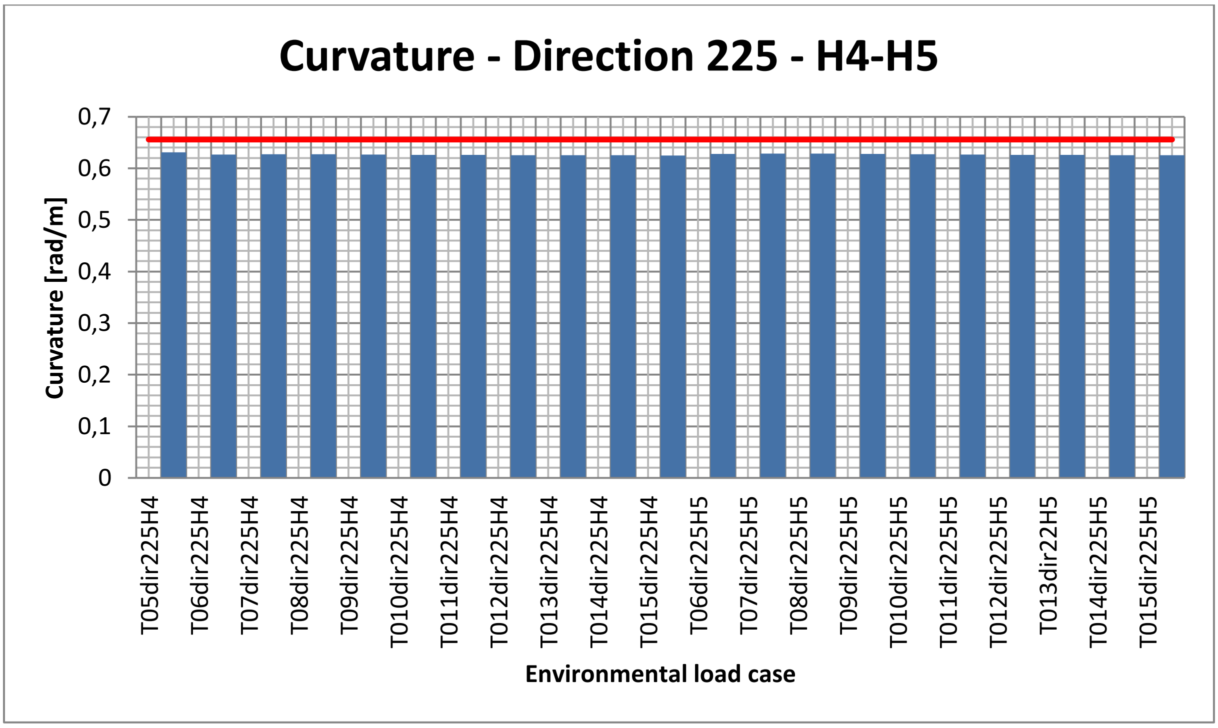

Figure C. 229 - 6” Oilflex Super – Lazy wave – 60 m floatation point – Curvature – Direction 225° - H4-H5

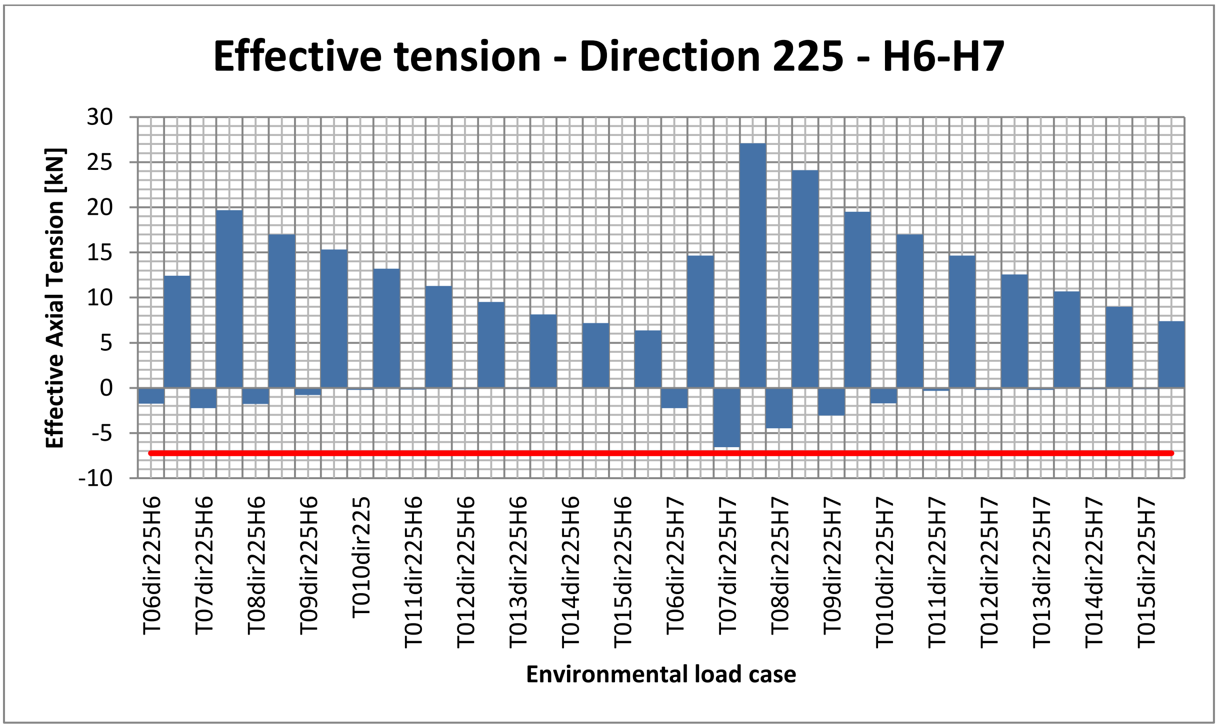

Figure C. 230 - 6” Oilflex Super – Lazy wave – 60 m floatation point – Effective tension – Direction 225° - H6-H7

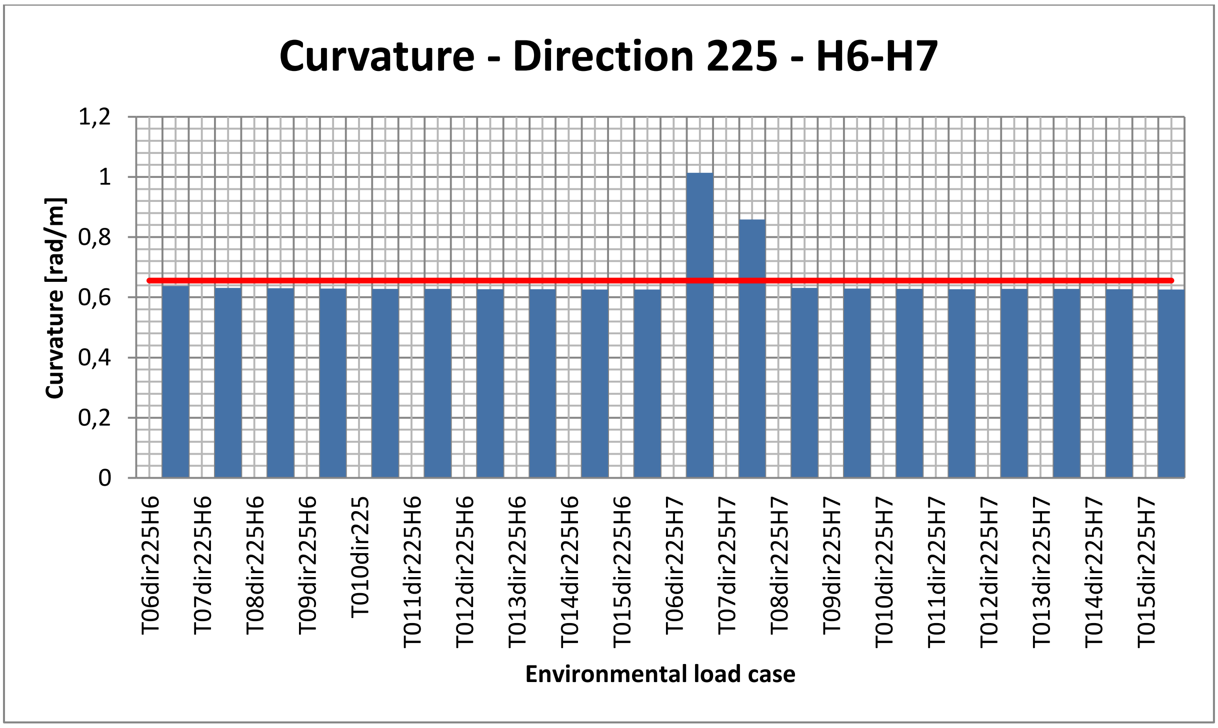

Figure C. 231 - 6” Oilflex Super – Lazy wave – 60 m floatation point – Curvature – Direction 225° - H6-H7

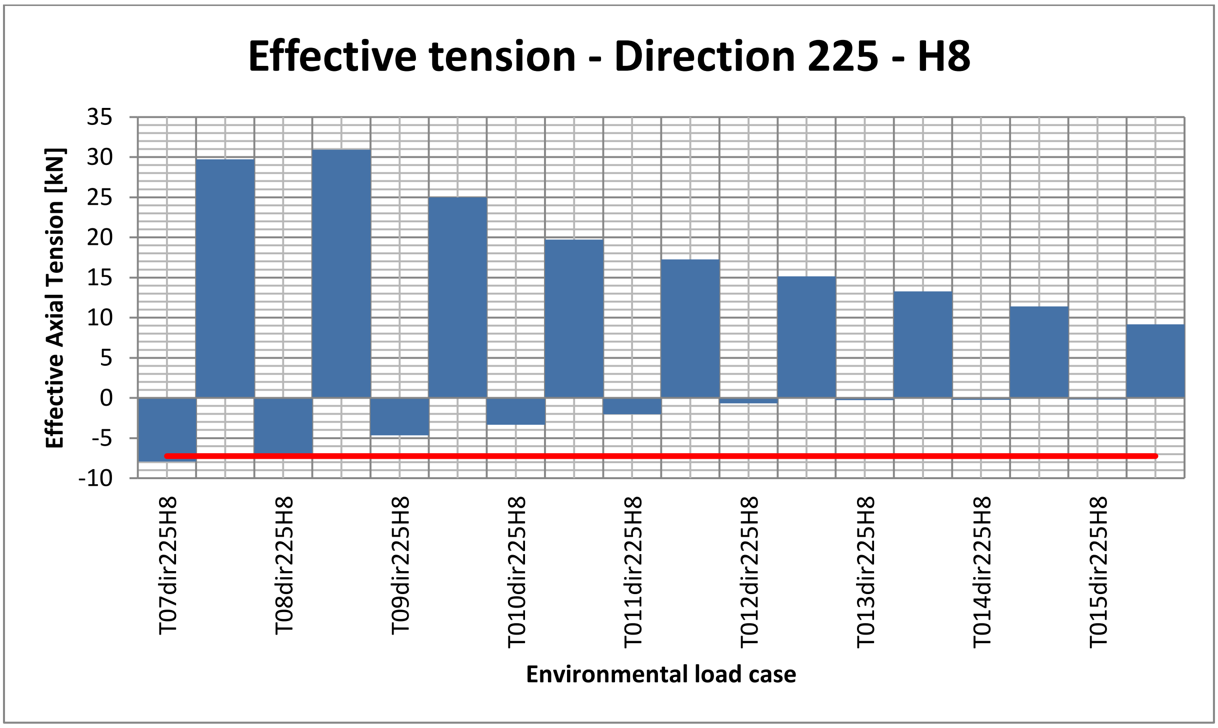

Figure C. 232 - 6” Oilflex Super – Lazy wave – 60 m floatation point – Effective tension – Direction 225° - H8

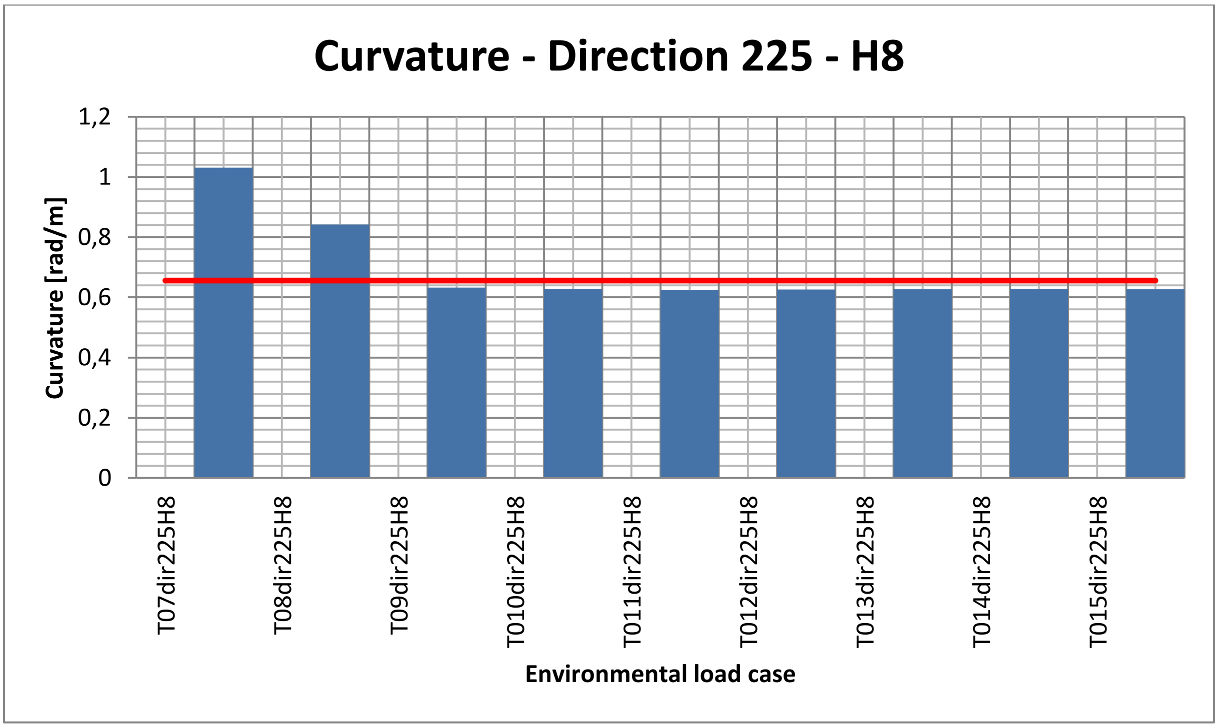

Figure C. 233 - 6” Oilflex Super – Lazy wave – 60 m floatation point – Curvature – Direction 225° - H8

Wave rose

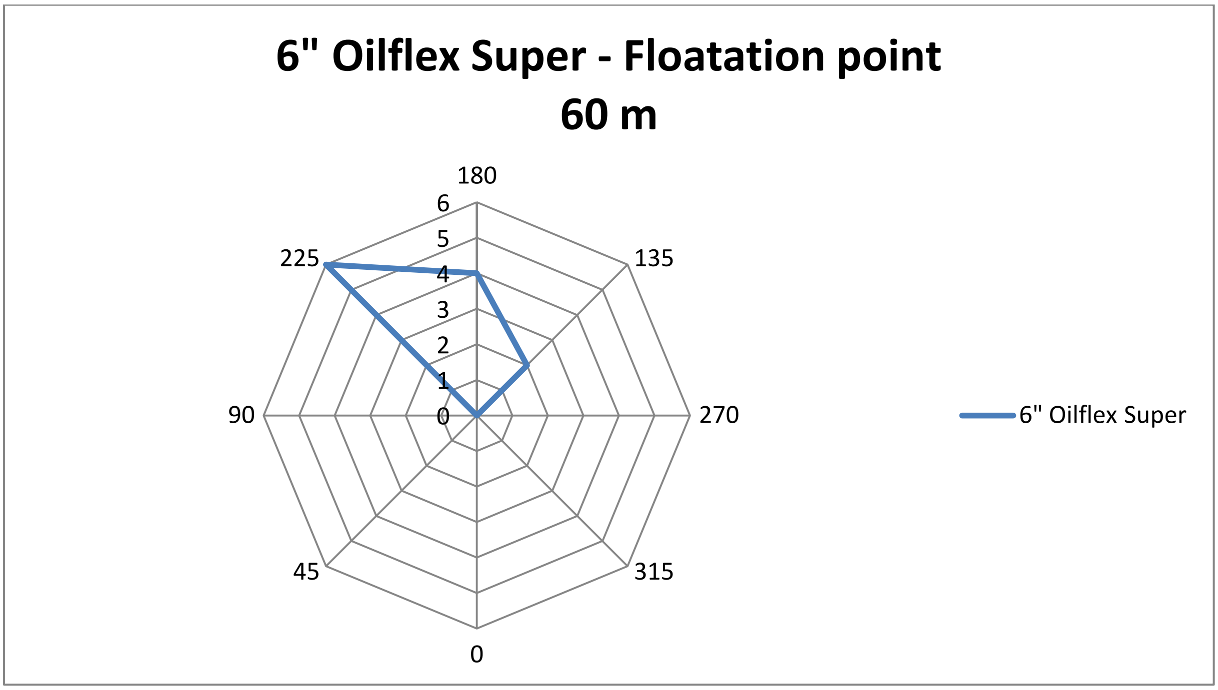

Figure C. 234 - 6" Oilflex Super – Lazy wave – 60 m floatation point – Wave rose

Limitation plot

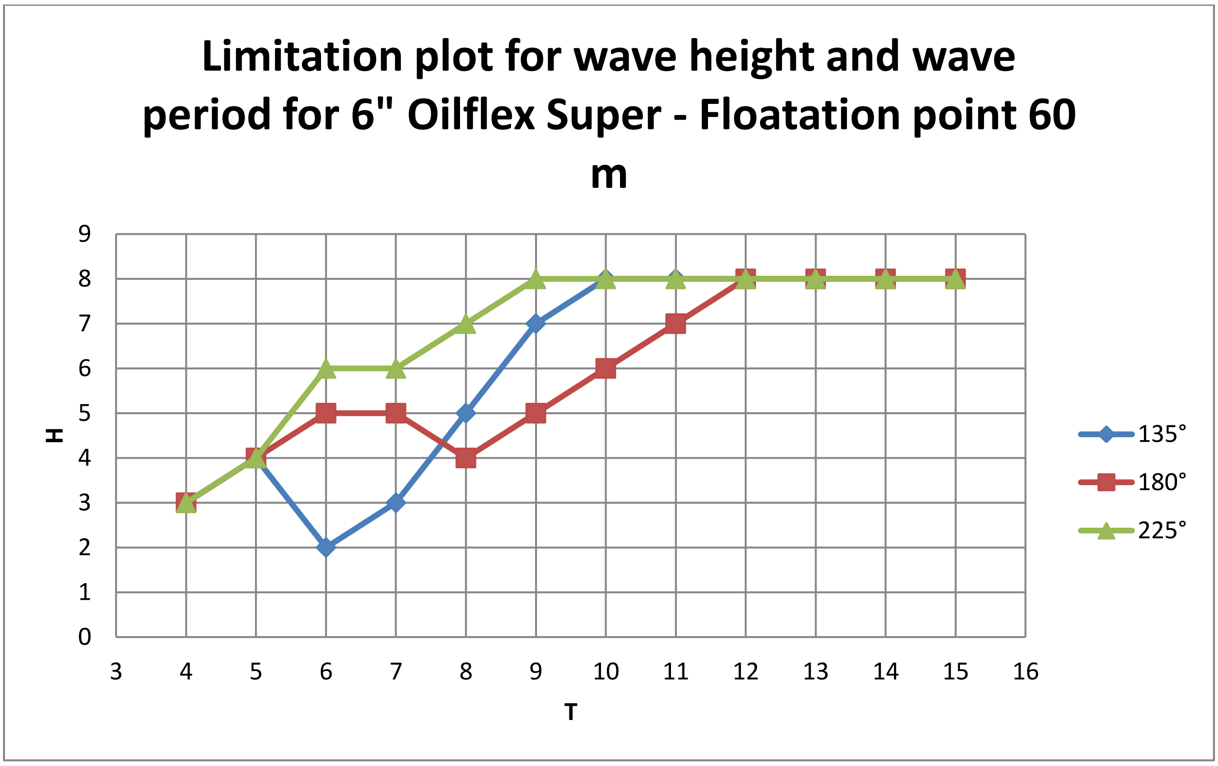

Figure C. 235 - 6" Oilflex Super – Lazy wave – 60 m floatation point – Limitation plot

Lazy wave – 80 m floatation point

Direction 135°

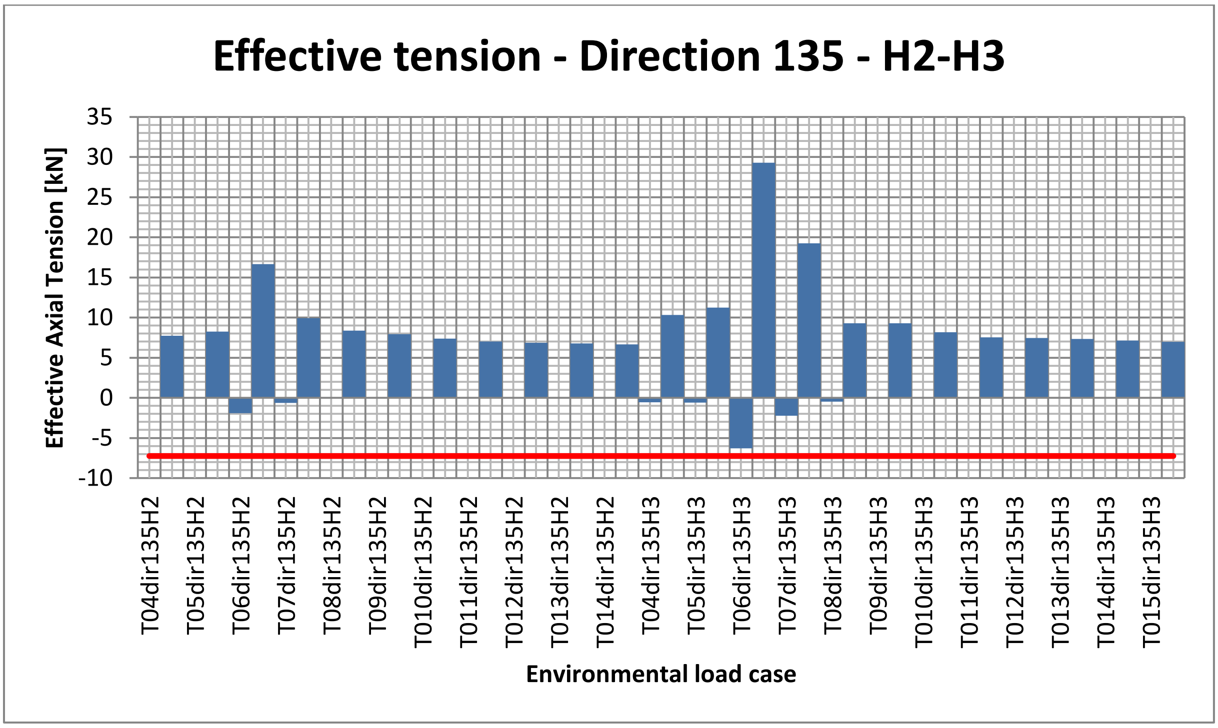

Figure C. 236 - 6” Oilflex Super – Lazy wave – 80 m floatation point – Effective tension – Direction 135° - H2-H3

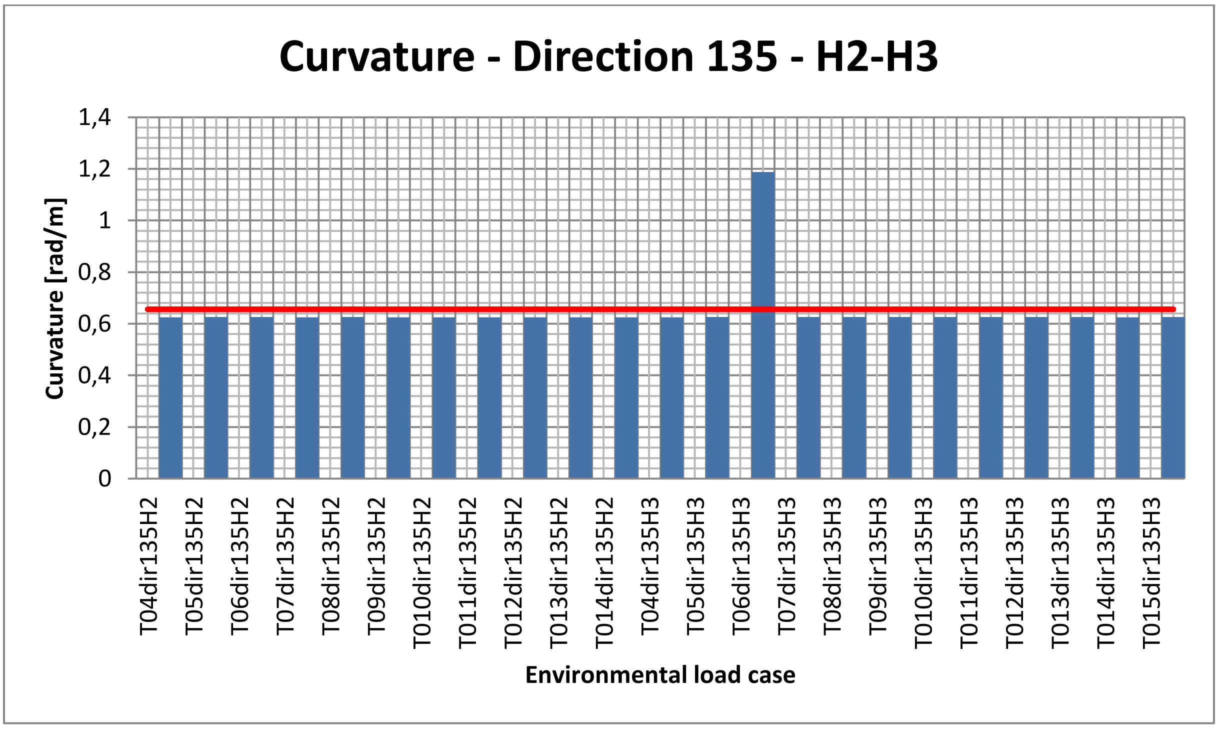

Figure C. 237 - 6” Oilflex Super – Lazy wave – 80 m floatation point – Curvature – Direction 135° - H2-H3

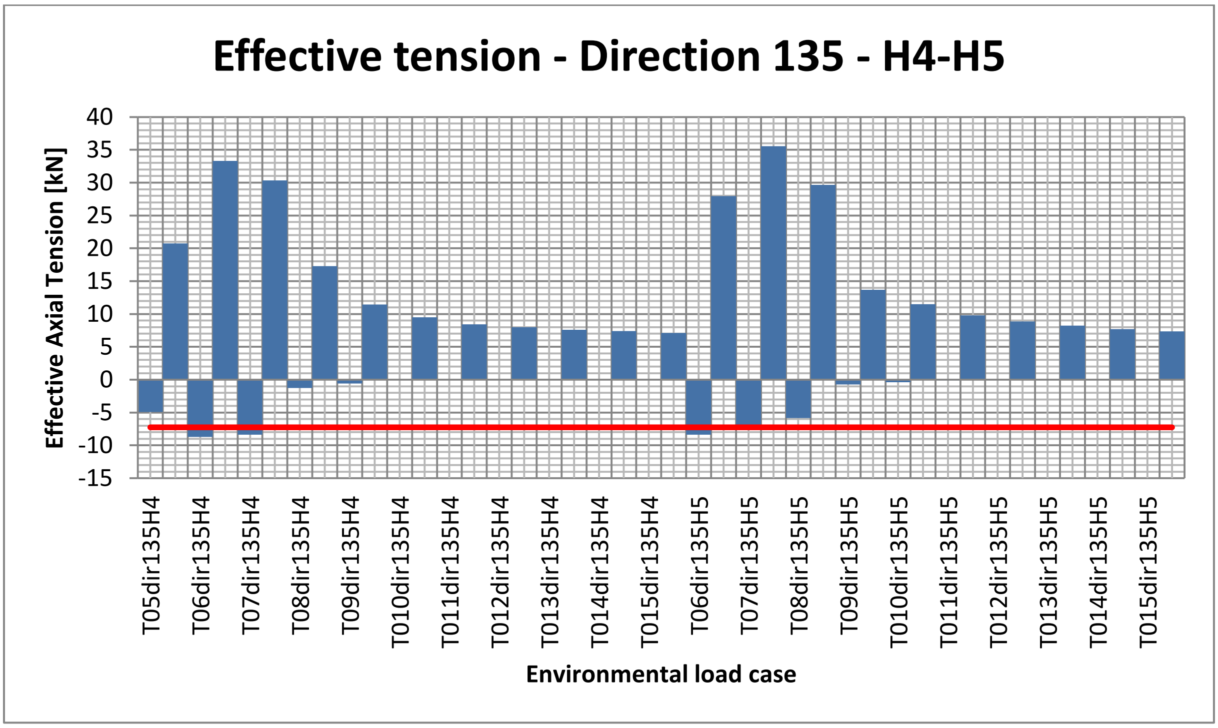

Figure C. 238 - 6” Oilflex Super – Lazy wave – 80 m floatation point – Effective tension – Direction 135° - H4-H5

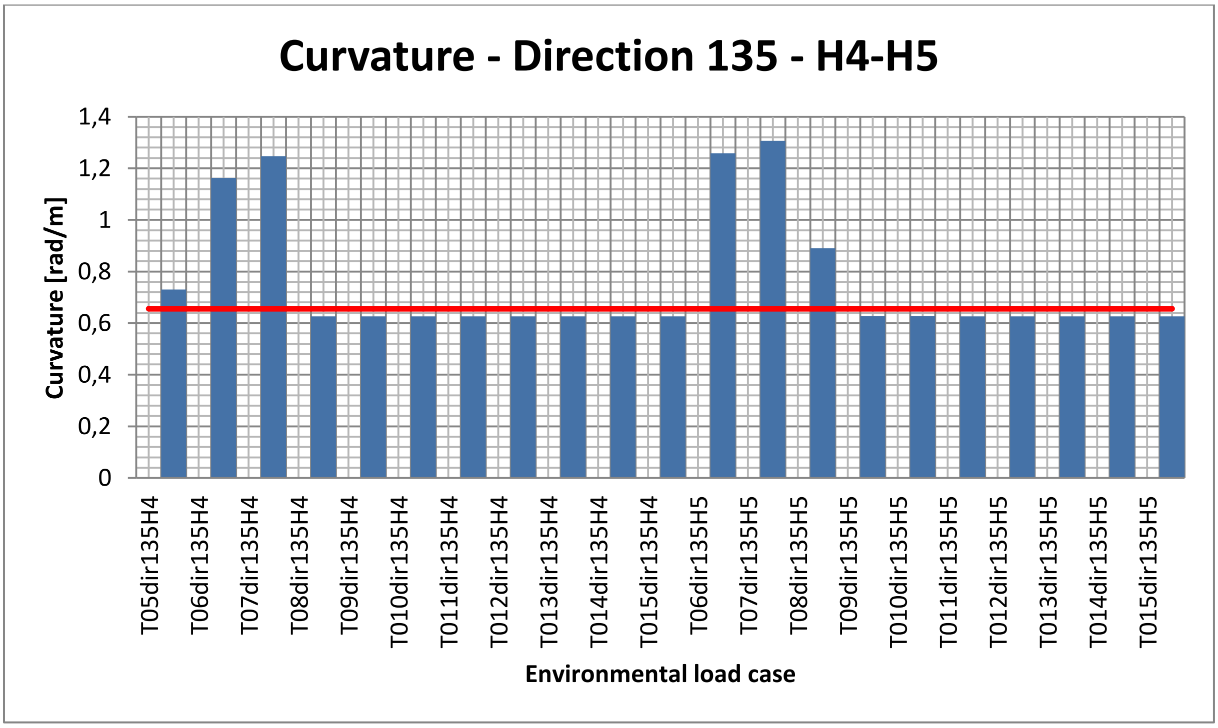

Figure C. 239 - 6” Oilflex Super – Lazy wave – 80 m floatation point – Curvature – Direction 135° - H4-H5

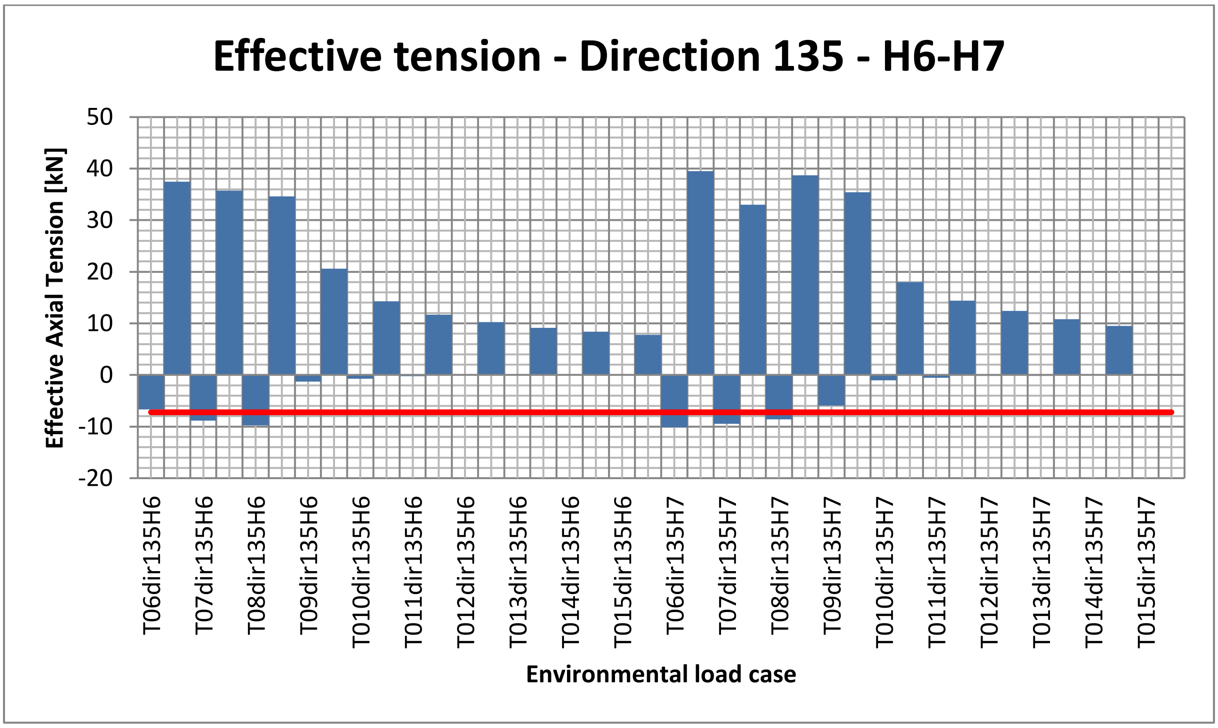

Figure C. 240 - 6" Oilflex Super – Lazy wave – 80 m floatation point – Effective tension – Direction 135° - H6-H7

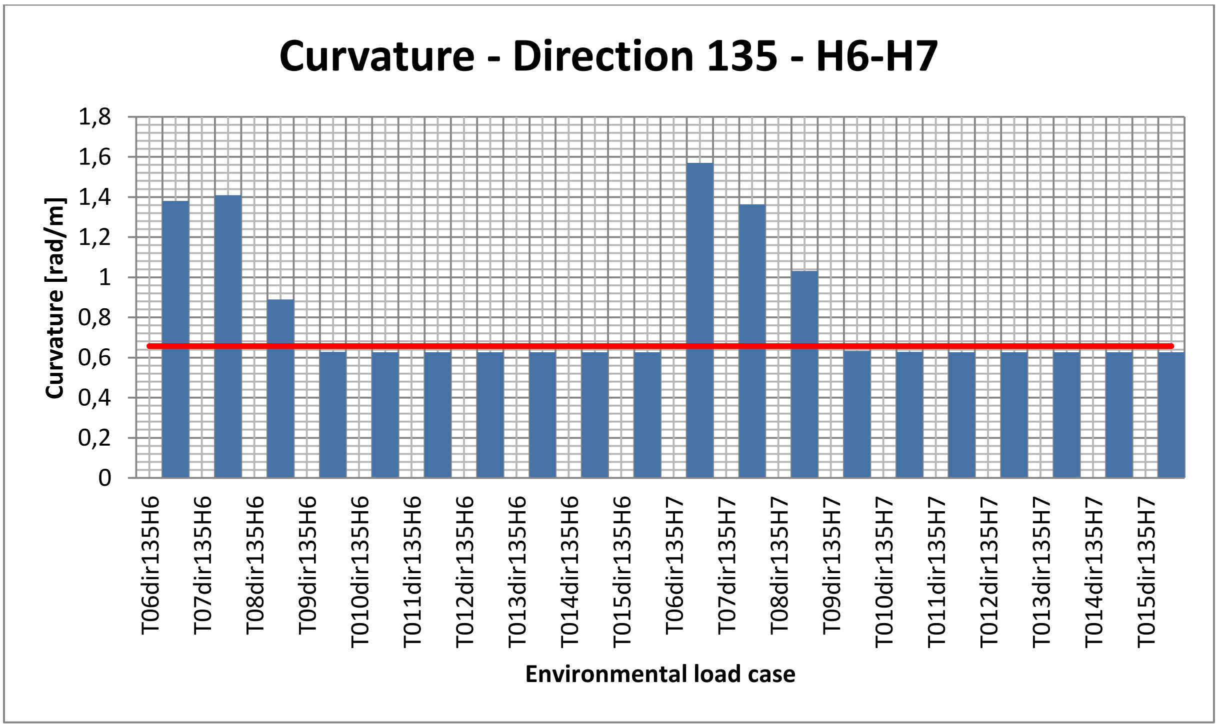

Figure C. 241 - 6" Oilflex Super – Lazy wave – 80 m floatation point – Curvature – Direction 135° - H6-H7

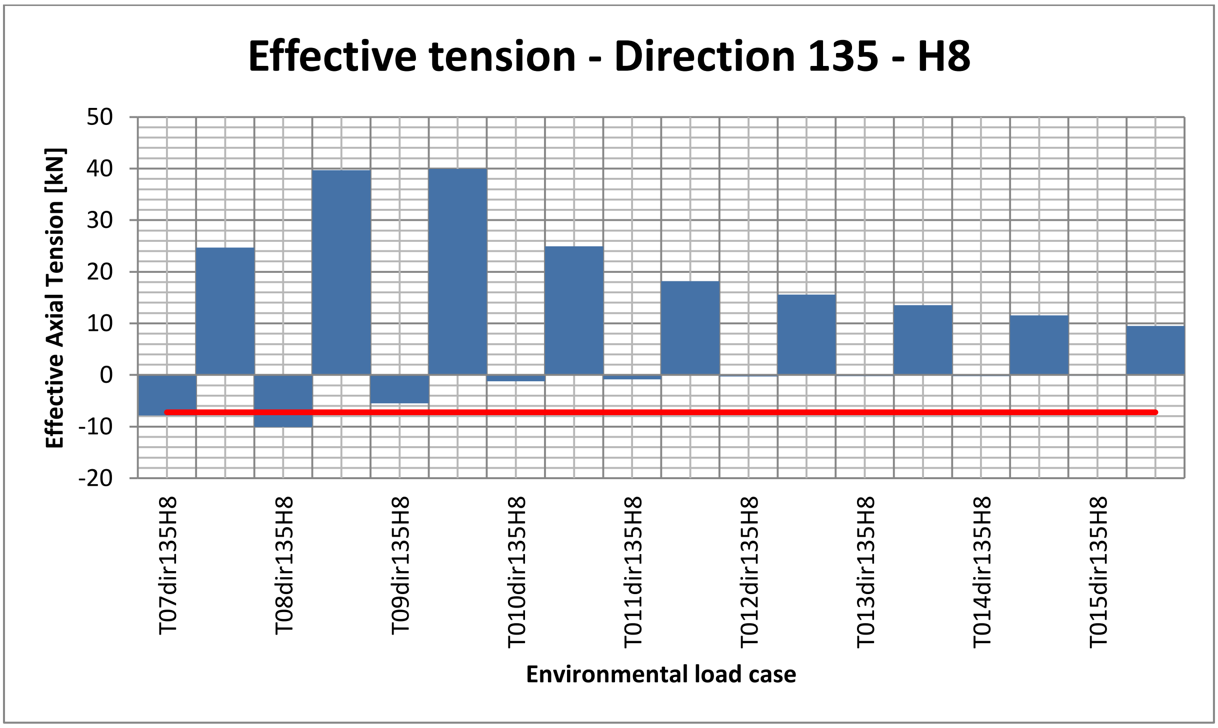

Figure C. 242 - 6” Oilflex Super – Lazy wave – 80 m floatation point – Effective tension – Direction 135° - H8

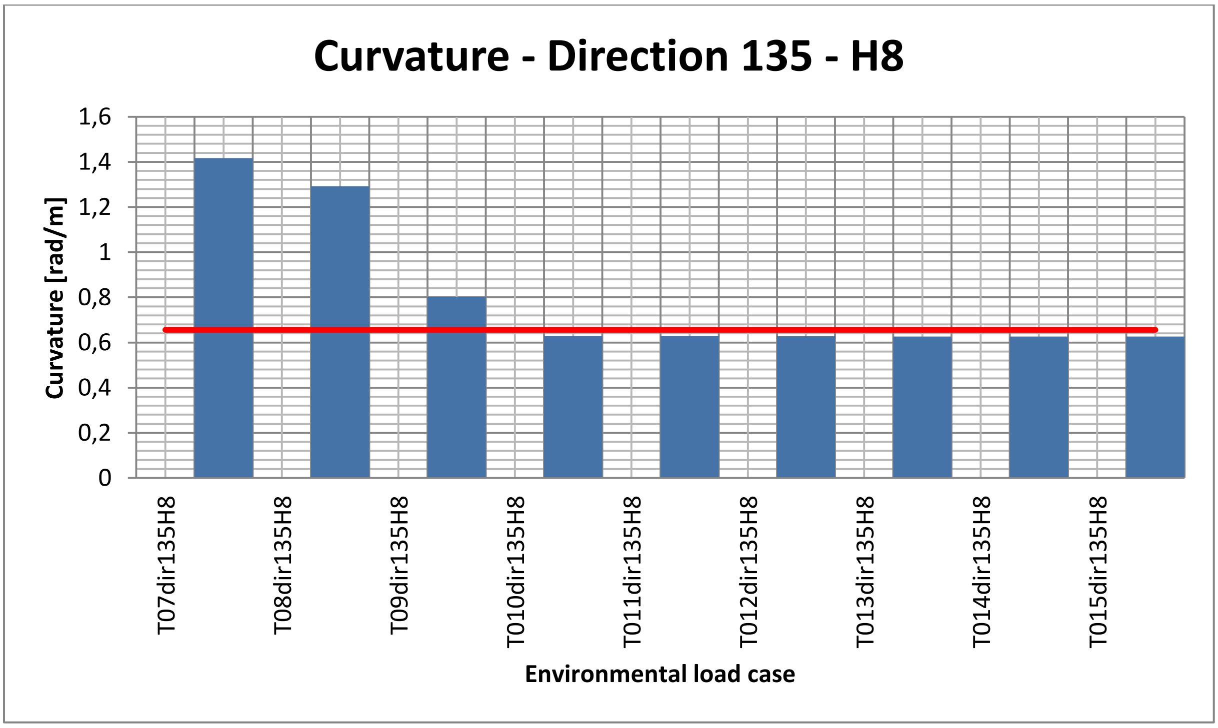

Figure C. 243 - 6” Oilflex Super – Lazy wave – 80 m floatation point – Curvature – Direction 135° - H8

Direction 180°

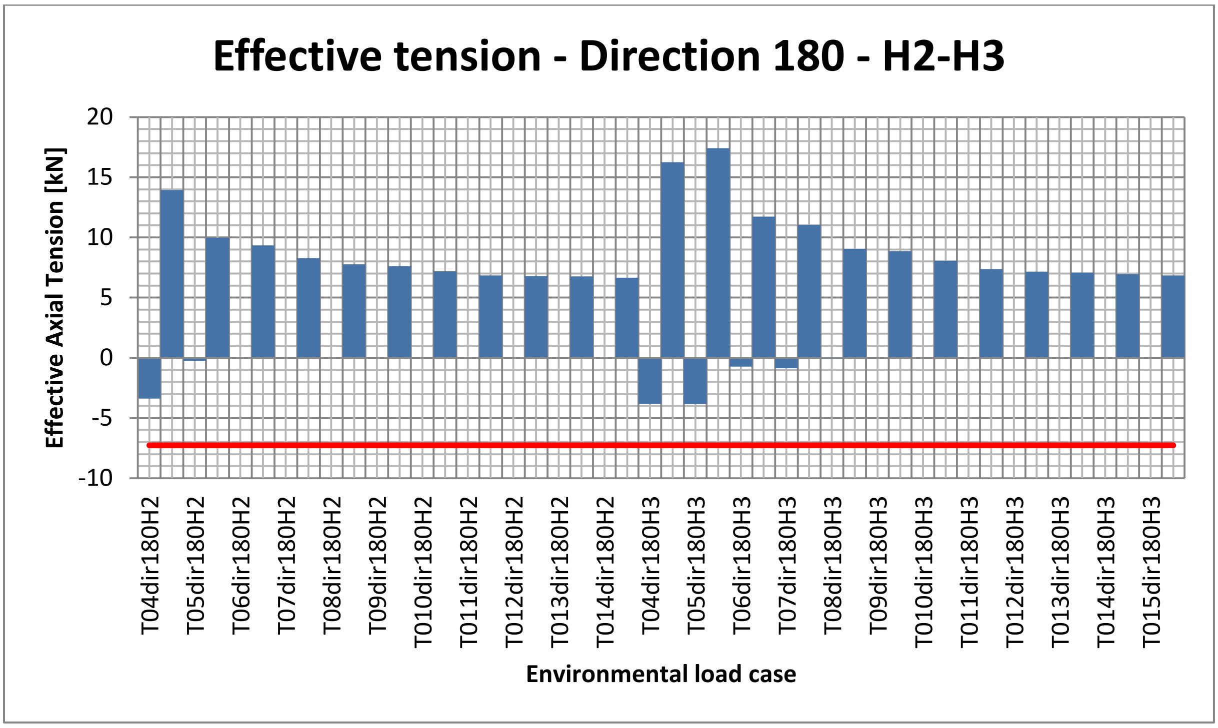

Figure C. 244 - 6" Oilflex Super – Lazy wave – 80 m floatation point – Effective tension – Direction 180° - H2-H3

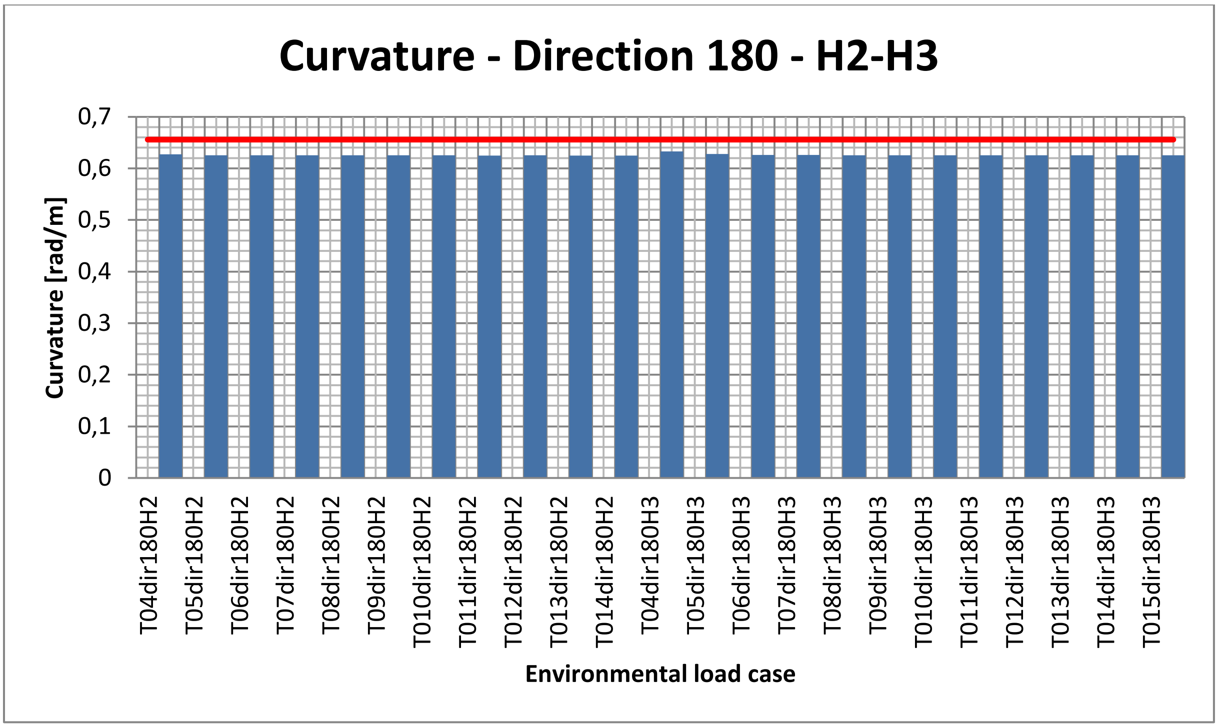

Figure C. 245 - 6" Oilflex Super – Lazy wave – 80 m floatation point – Curvature – Direction 180° - H2-H3

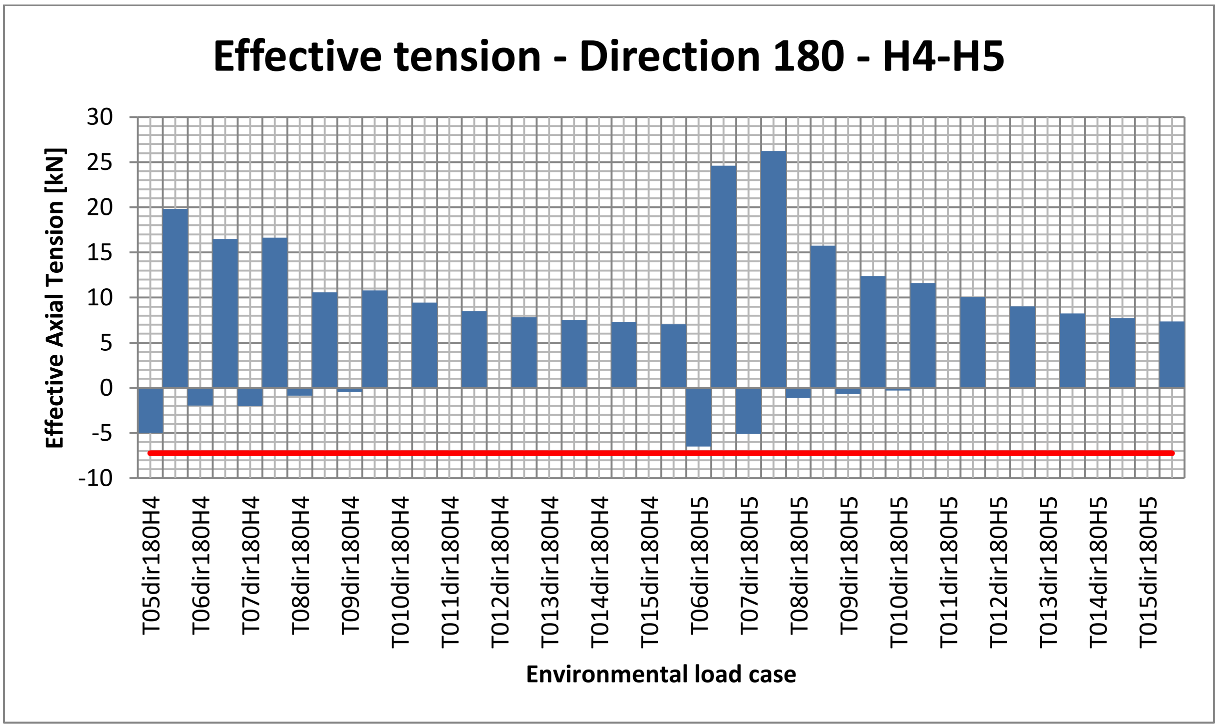

Figure C. 246 - 6” Oilflex Super – Lazy wave – 80 m floatation point – Effective tension – Direction 180° - H4-H5

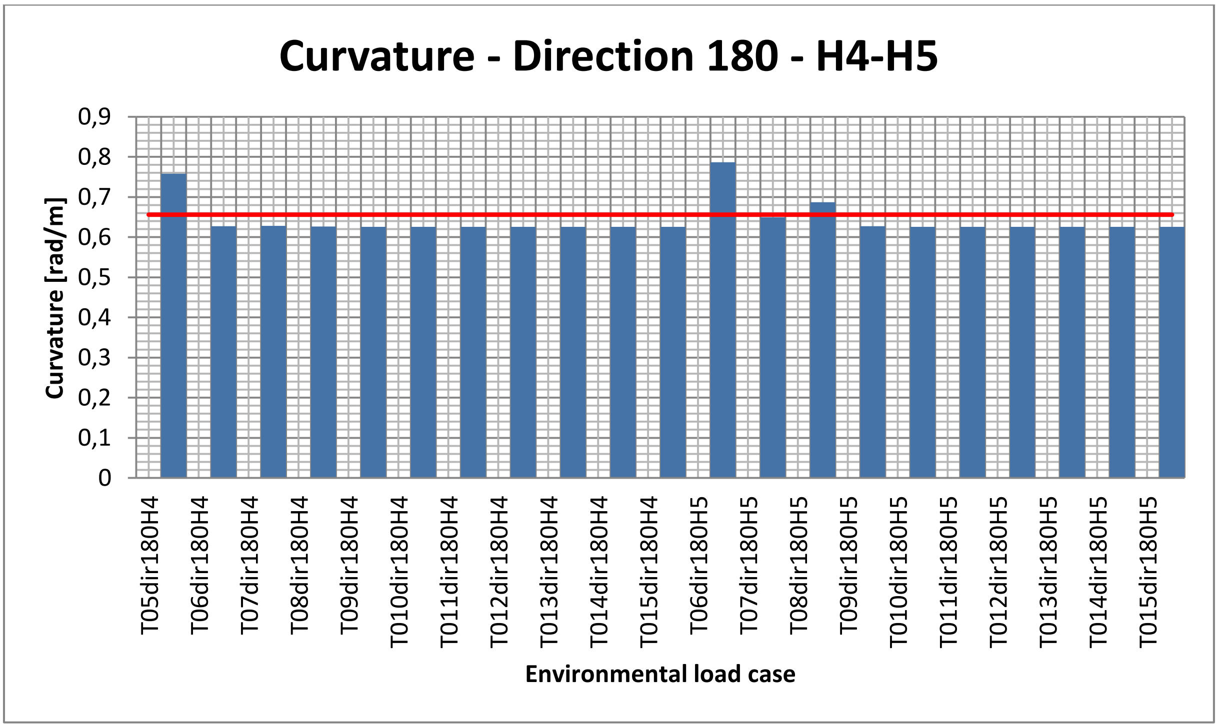

Figure C. 247 - 6” Oilflex Super – Lazy wave – 80 m floatation point – Curvature – Direction 180° - H4-H5

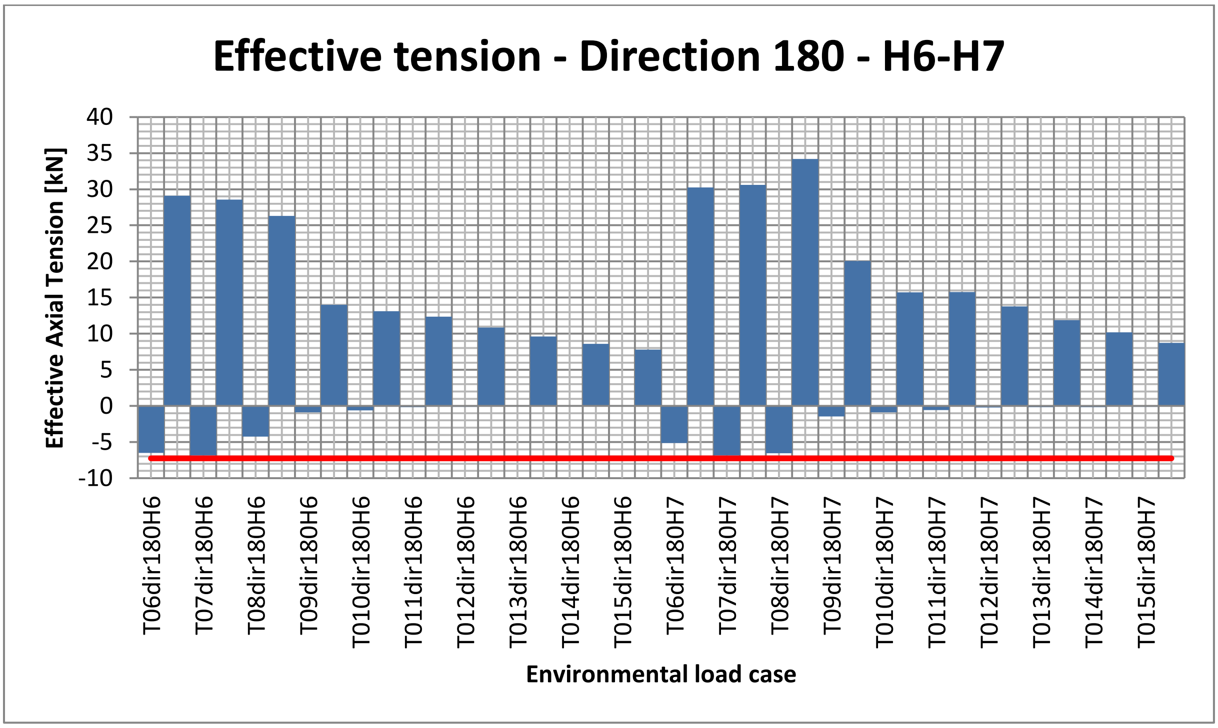

Figure C. 248 - 6” Oilflex Super – Lazy wave – 80 m floatation point – Effective tension – Direction 180° - H6-H7

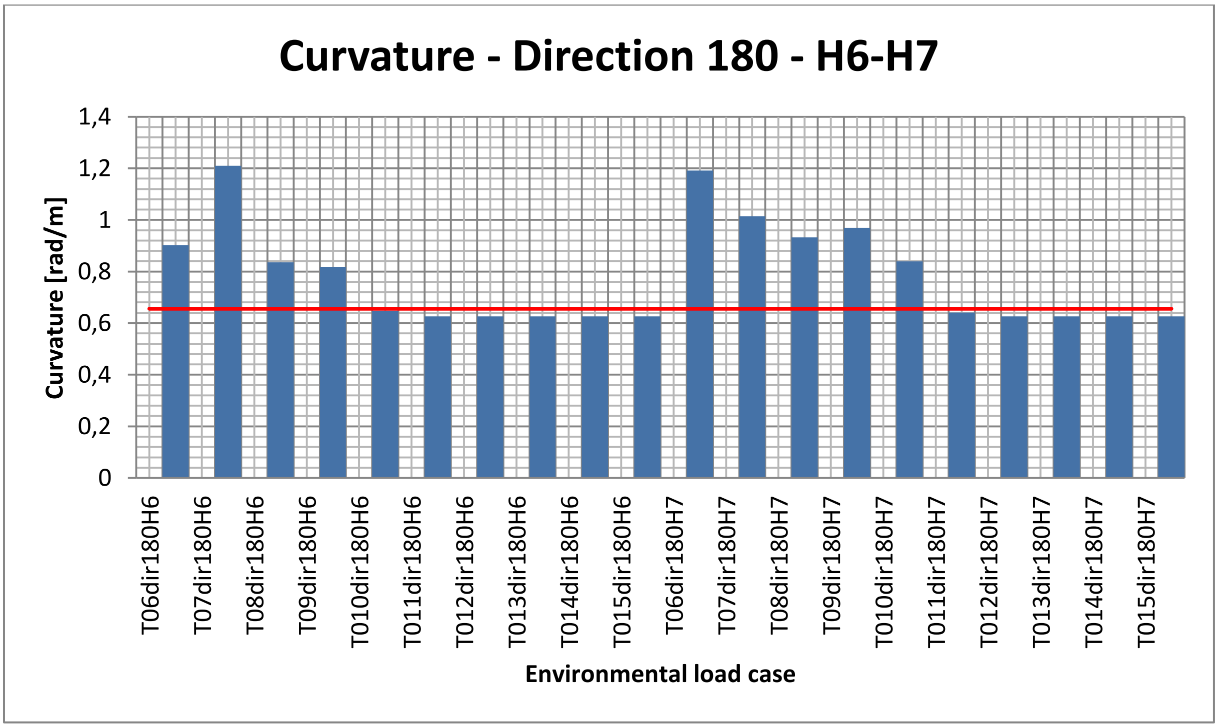

Figure C. 249 - 6” Oilflex Super – Lazy wave – 80 m floatation point – Curvature – Direction 180° - H6-H7

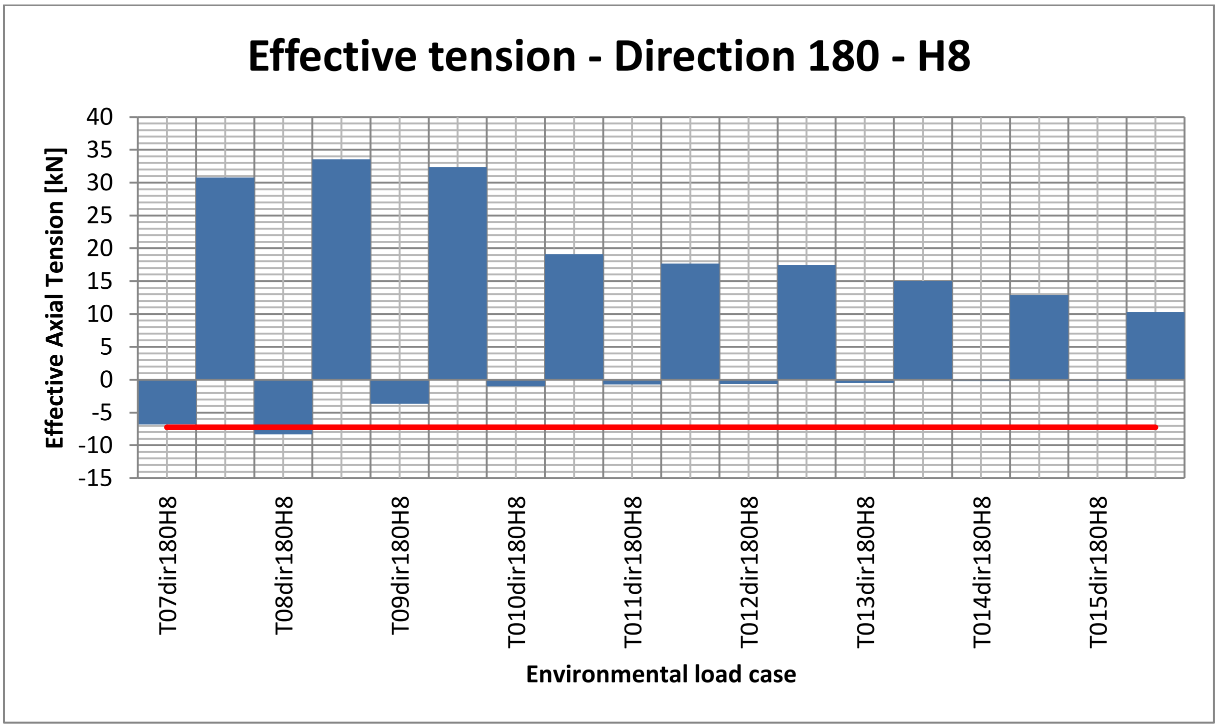

Figure C. 250 - 6" Oilflex Super – Lazy wave – 80 m floatation point – Effective tension – Direction 180° - H8

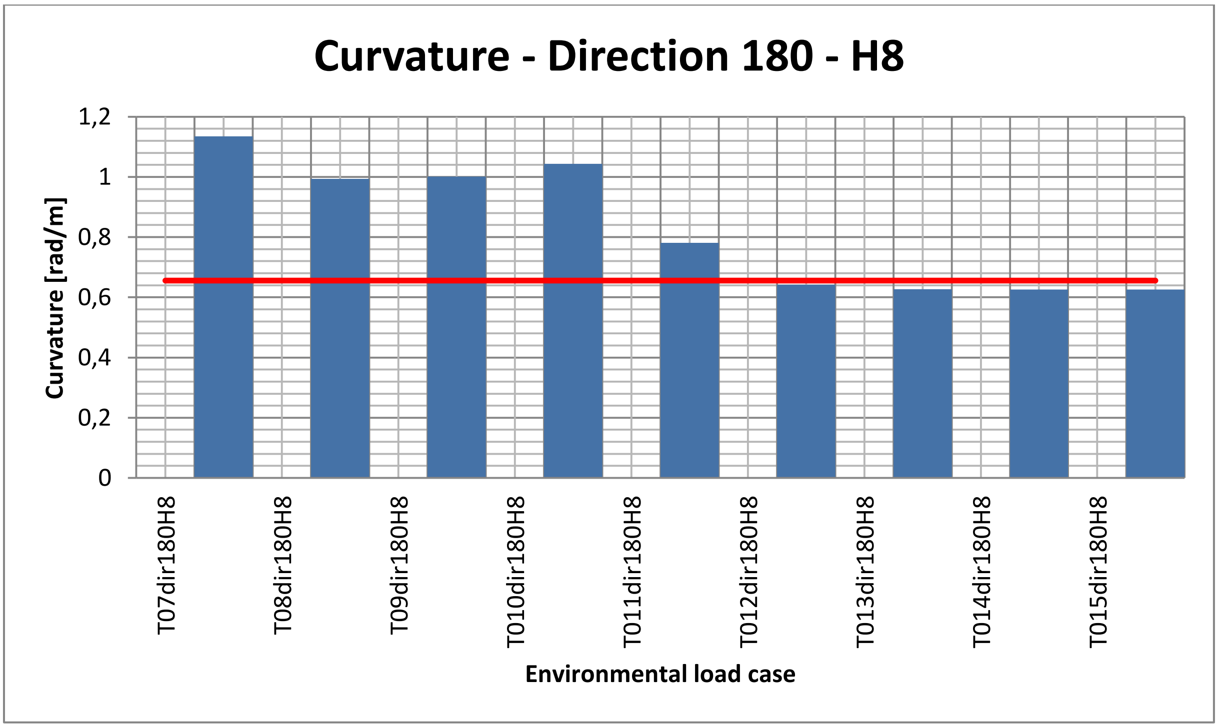

Figure C. 251 - 6" Oilflex Super – Lazy wave – 80 m floatation point – Curvature – Direction 180° - H8

Direction 225°

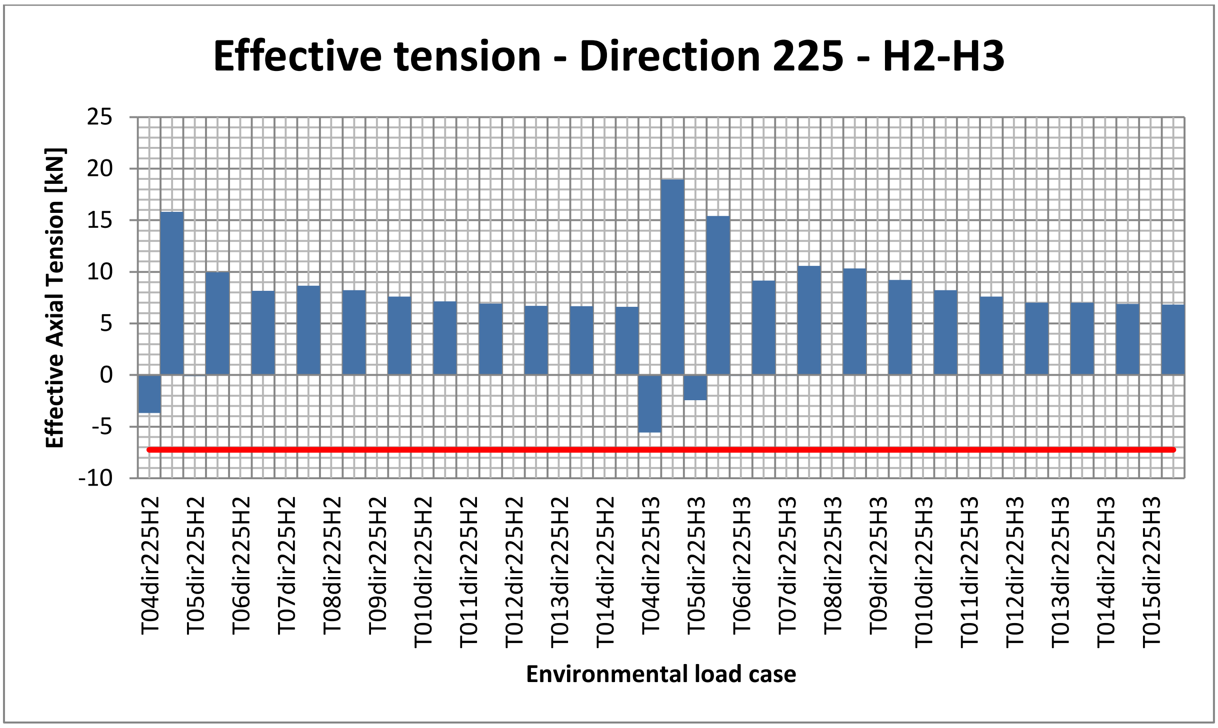

Figure C. 252 - 6” Oilflex Super – Lazy wave – 80 m floatation point – Effective tension – Direction 225° - H2-H3

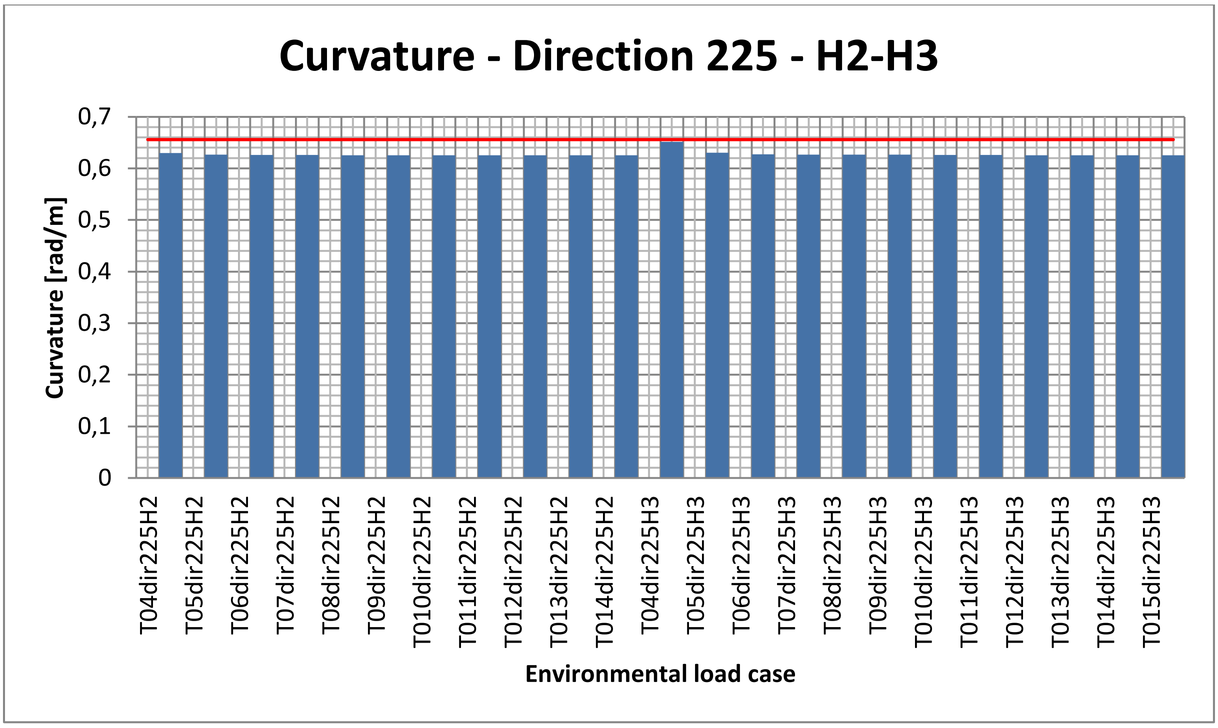

Figure C. 253 - 6” Oilflex Super – Lazy wave – 80 m floatation point – Curvature – Direction 225° - H2-H3

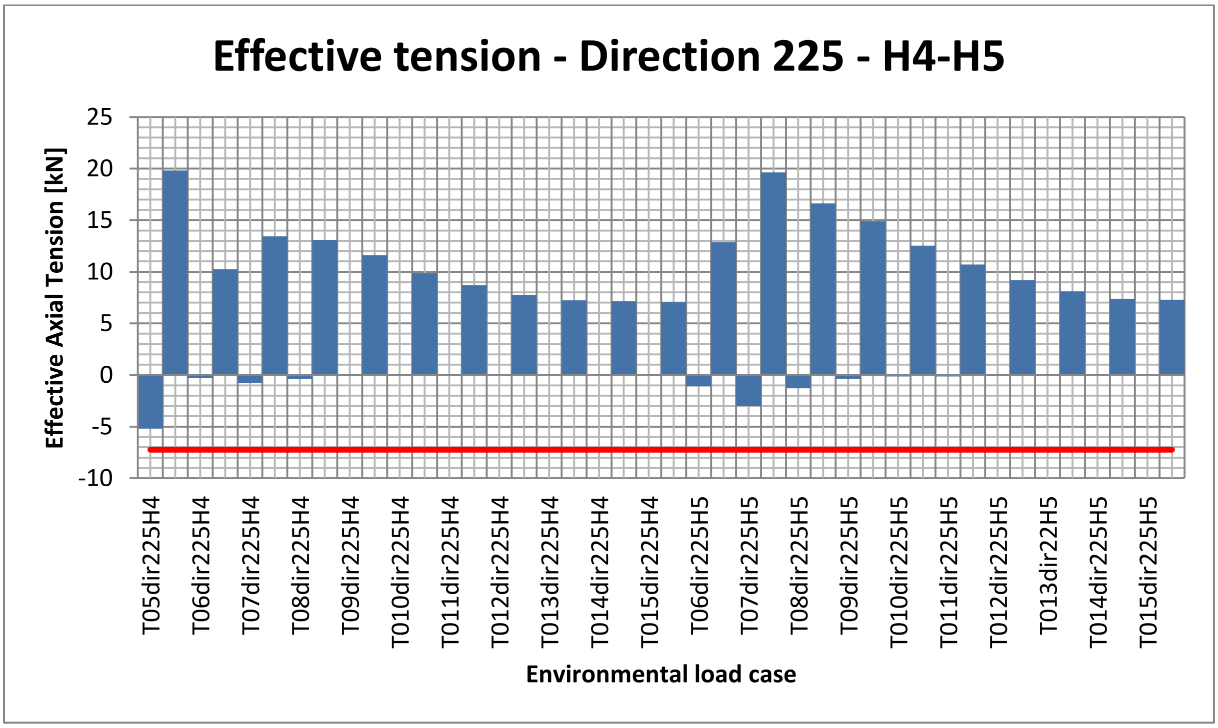

Figure C. 254 - 6” Oilflex Super – Lazy wave – 80 m floatation point – Effective tension – Direction 225° - H4-H5

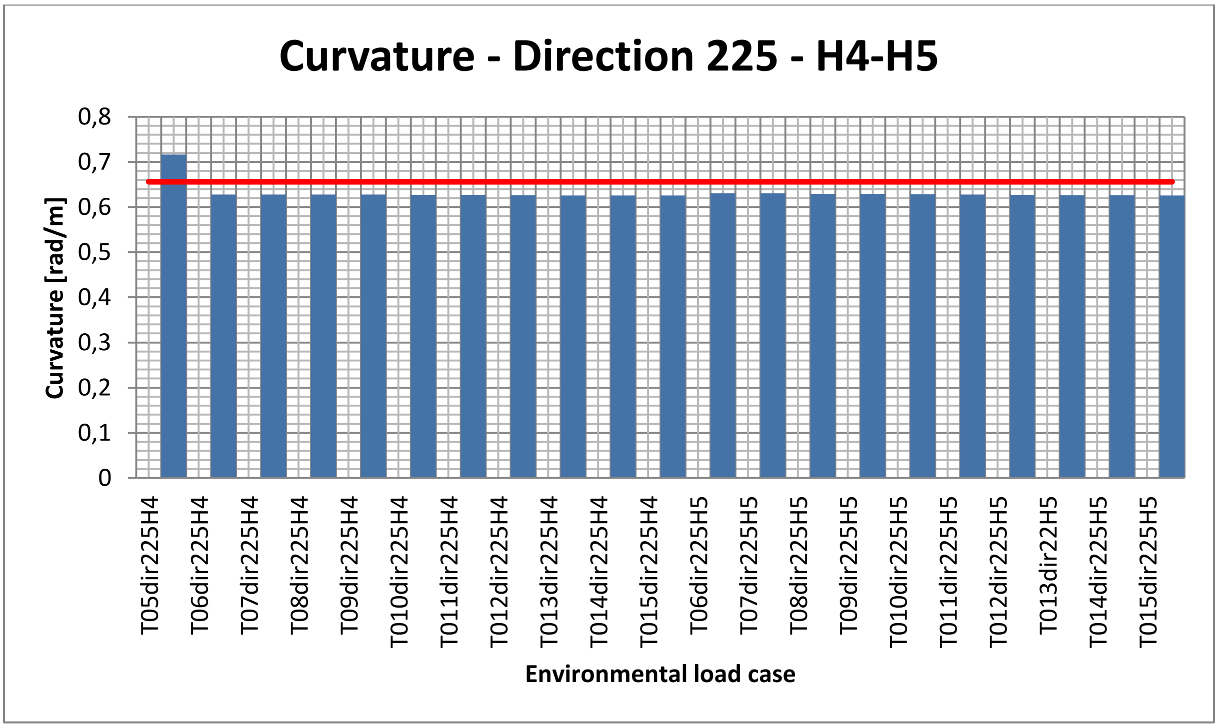

Figure C. 255 - 6” Oilflex Super – Lazy wave – 80 m floatation point – Curvature – Direction 225° - H4-H5

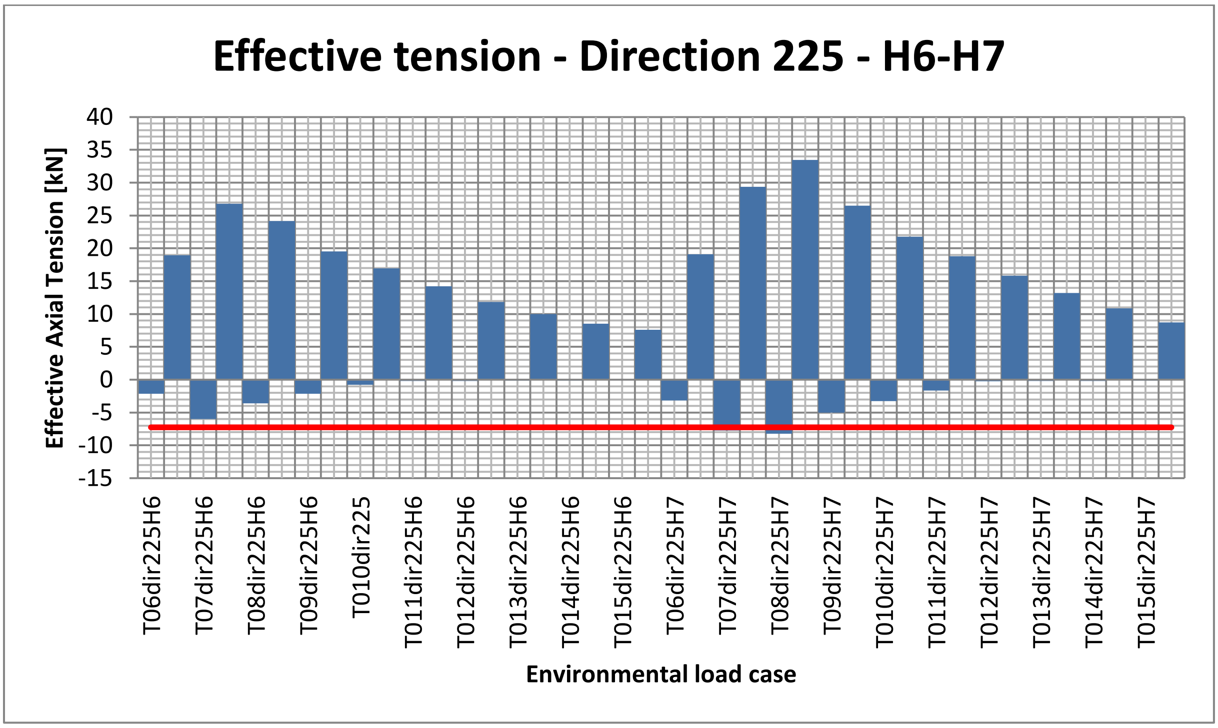

Figure C. 256 - 6” Oilflex Super – Lazy wave – 80 m floatation point – Effective tension – Direction 225° - H6-H7

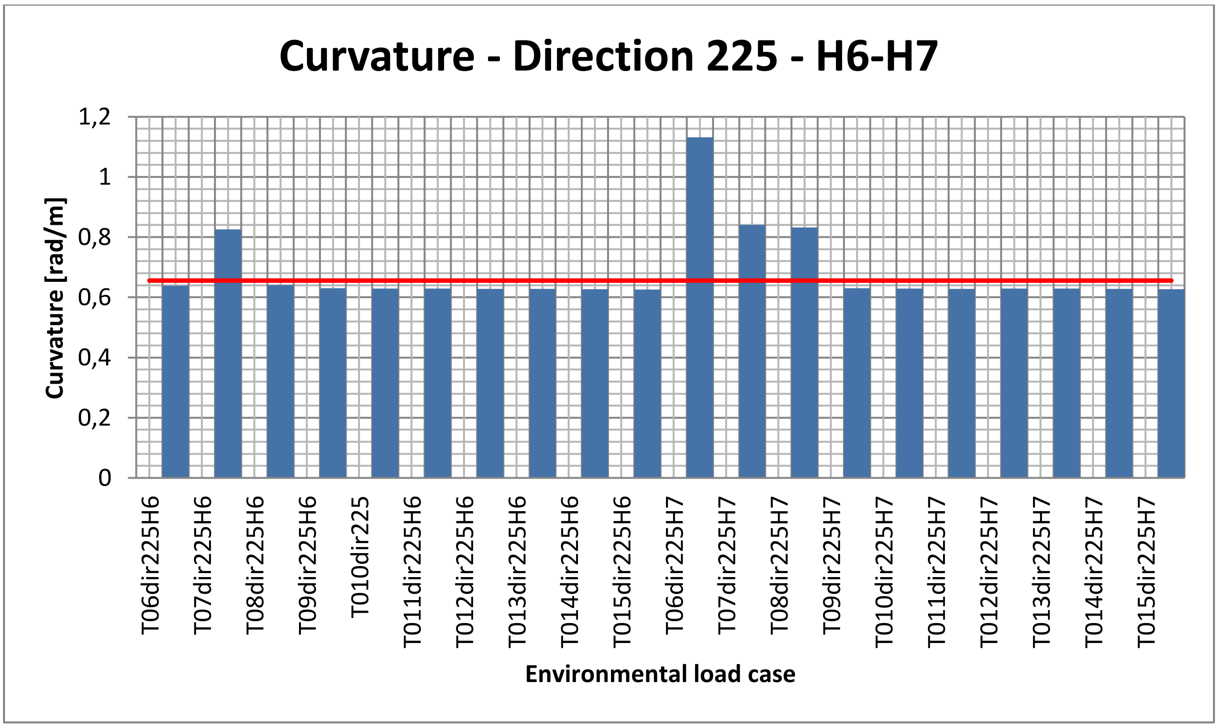

Figure C. 257 - 6” Oilflex Super – Lazy wave – 80 m floatation point – Curvature – Direction 225° - H6-H7

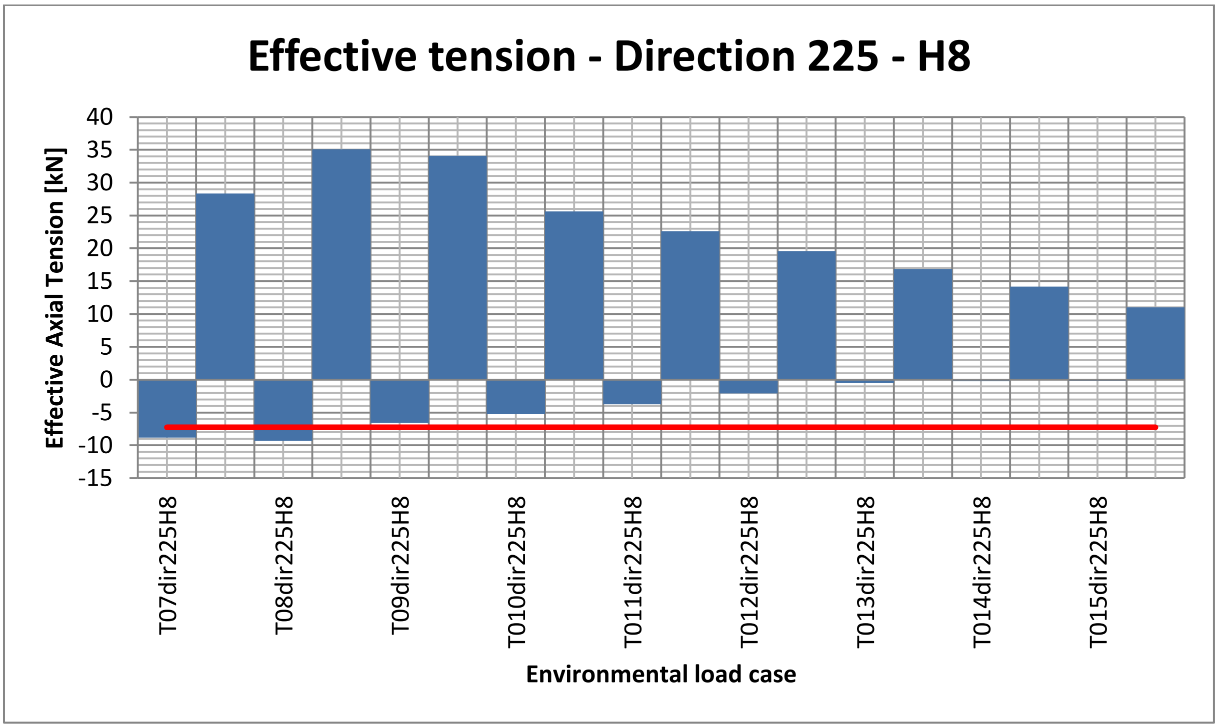

Figure C. 258 - 6" Oilflex Super – Lazy wave – 80 m floatation point – Effective tension – Direction 225° - H8

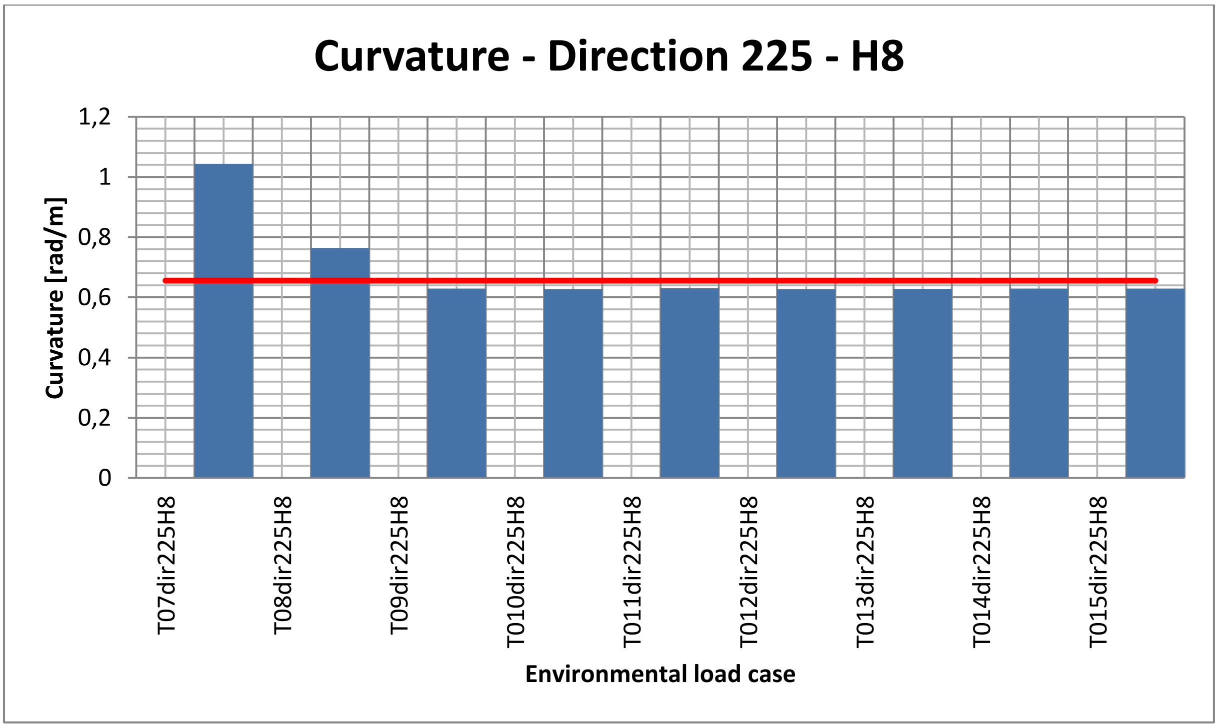

Figure C. 259 - 6" Oilflex Super – Lazy wave – 80 m floatation point – Curvature – Direction 225° - H8

Wave rose

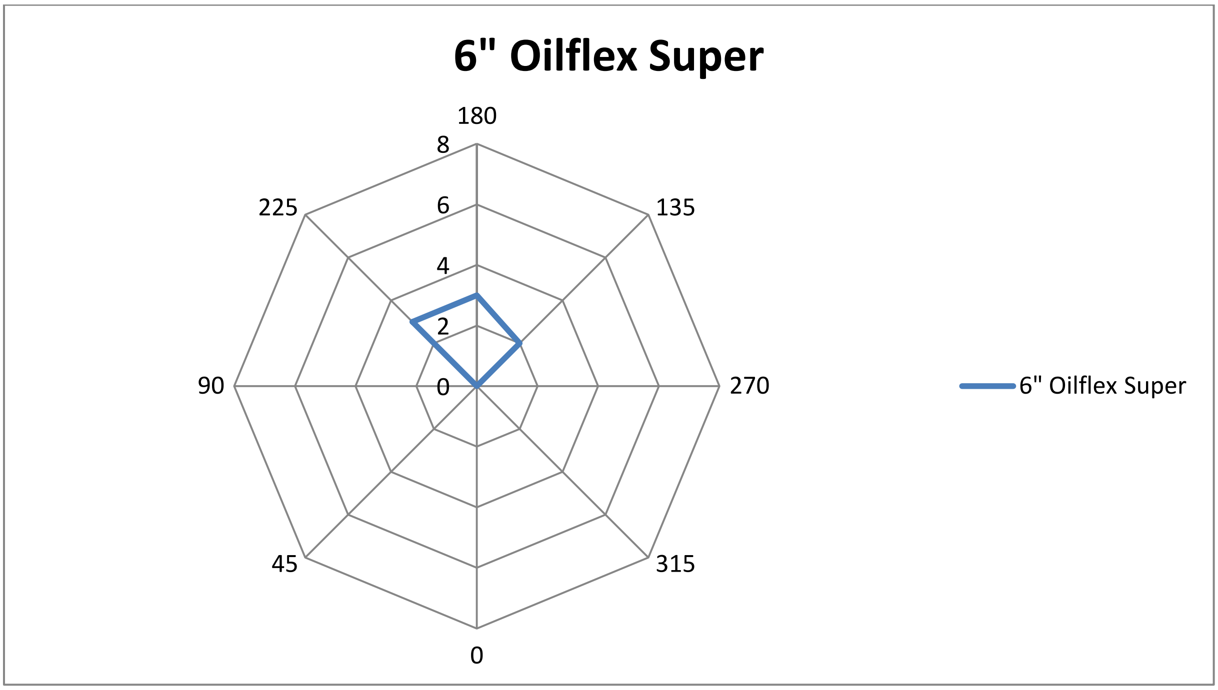

Figure C. 260 - 6” Oilflex Super – Lazy wave – 80 m floatation point – Wave rose

Limitation plot

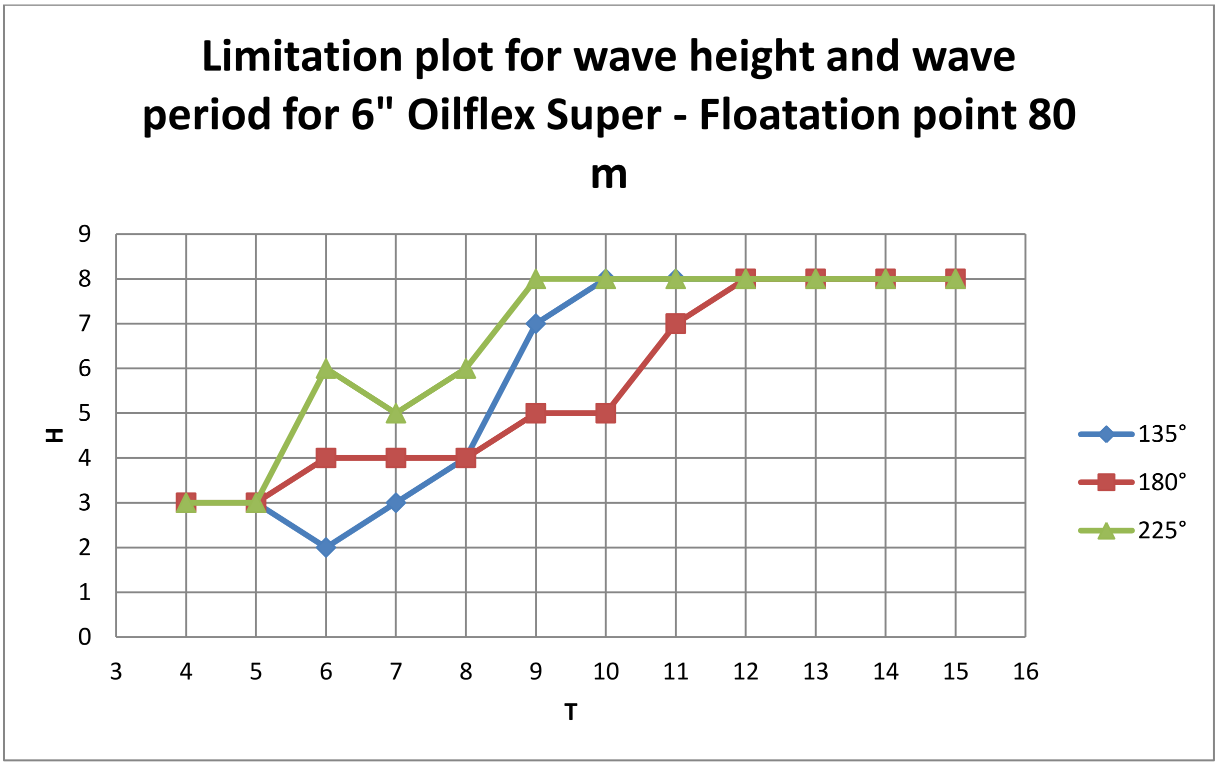

Figure C. 261 - 6” Oilflex Super – Lazy wave – 80 m floatation point – Limitation plot

Appendix D – Dynamic results - current

Table of Contents

List of Figures

Introduction

A detailed description of the graphs used in this Appendix is found Chapter 6.5.1 in the main report. In addition to the description in the main report, the current direction is included in the description at the end of each environmental load case.

However, the direction conventions for the vessel are shown in Figure D. 1 below.

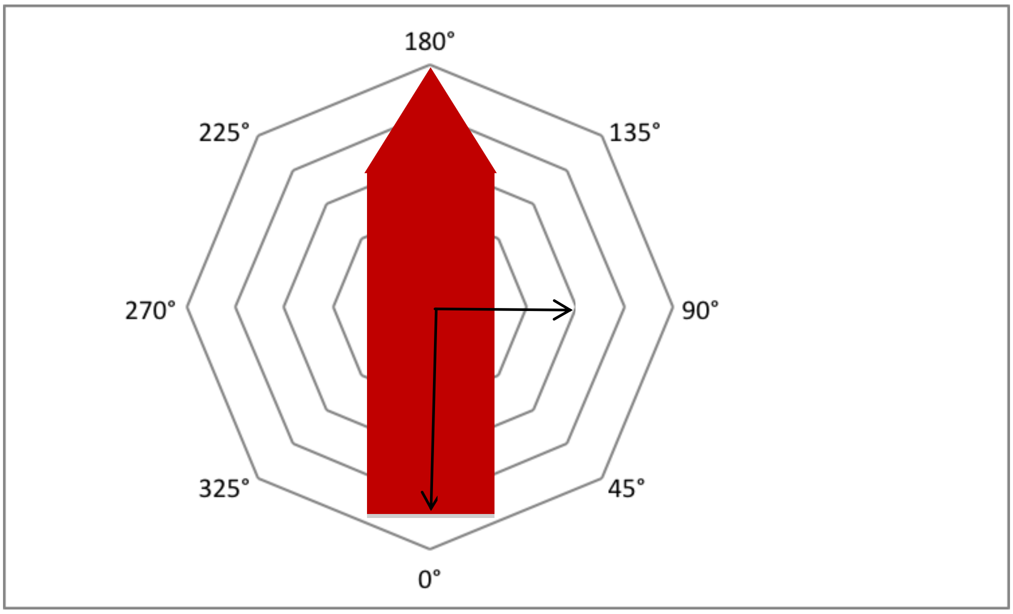

Figure D. 1 Direction conventions for the vessel

4” Bunkerflex STH

Free hanging - 0° direction current

Wave direction 135°

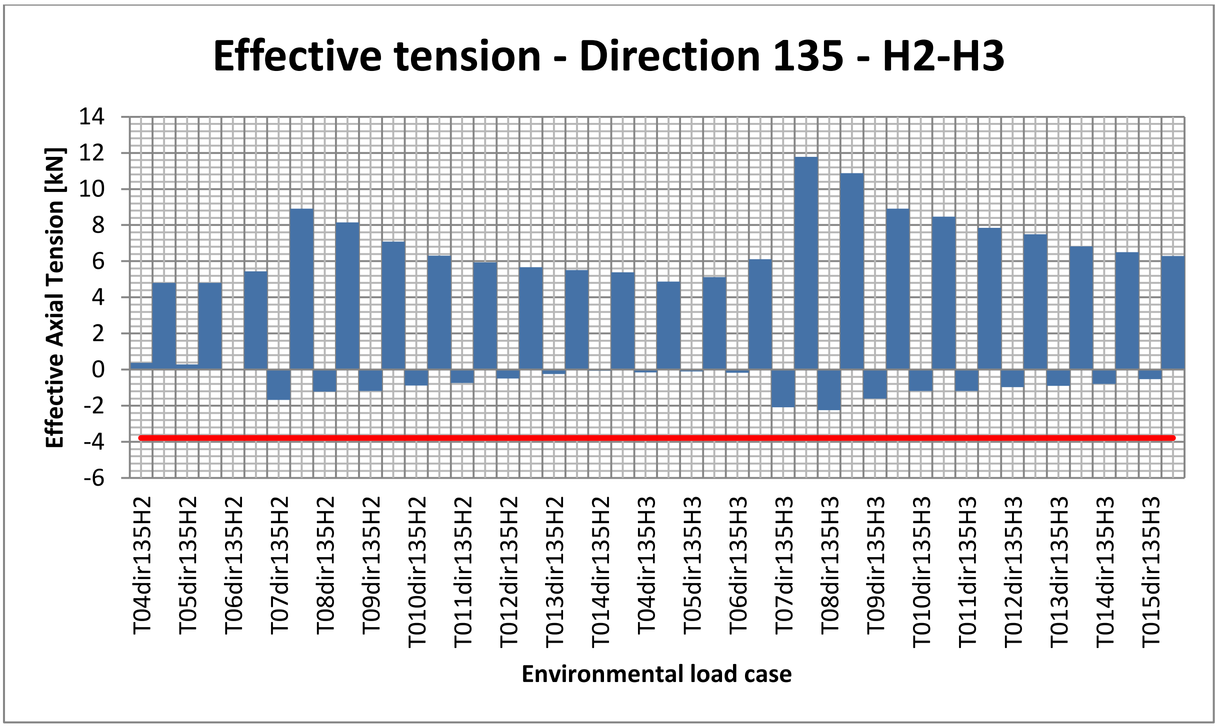

Figure D. 2 - 4"Bunkerflex STH - Free hanging - Effective tension - Direction 135° - H2-H3 - Current 0°

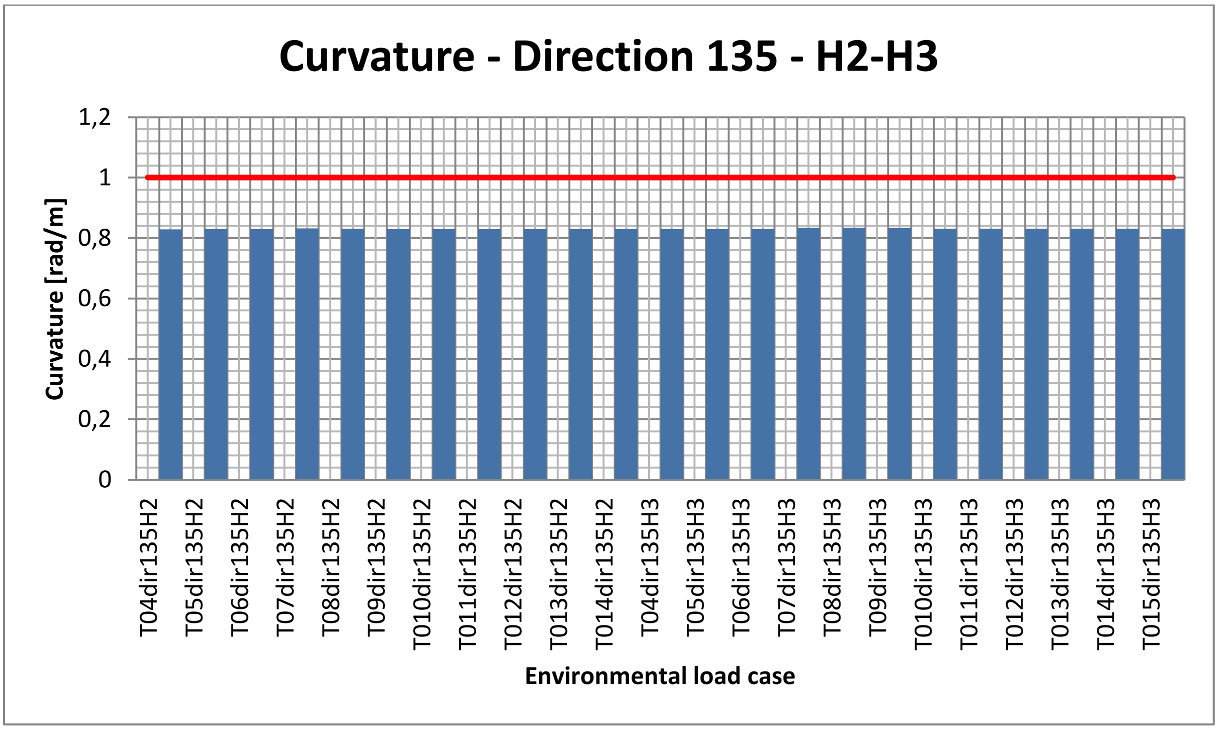

Figure D. 3 - 4"Bunkerflex STH - Free hanging - Curvature - Direction 135° - H2-H3 - Current 0°

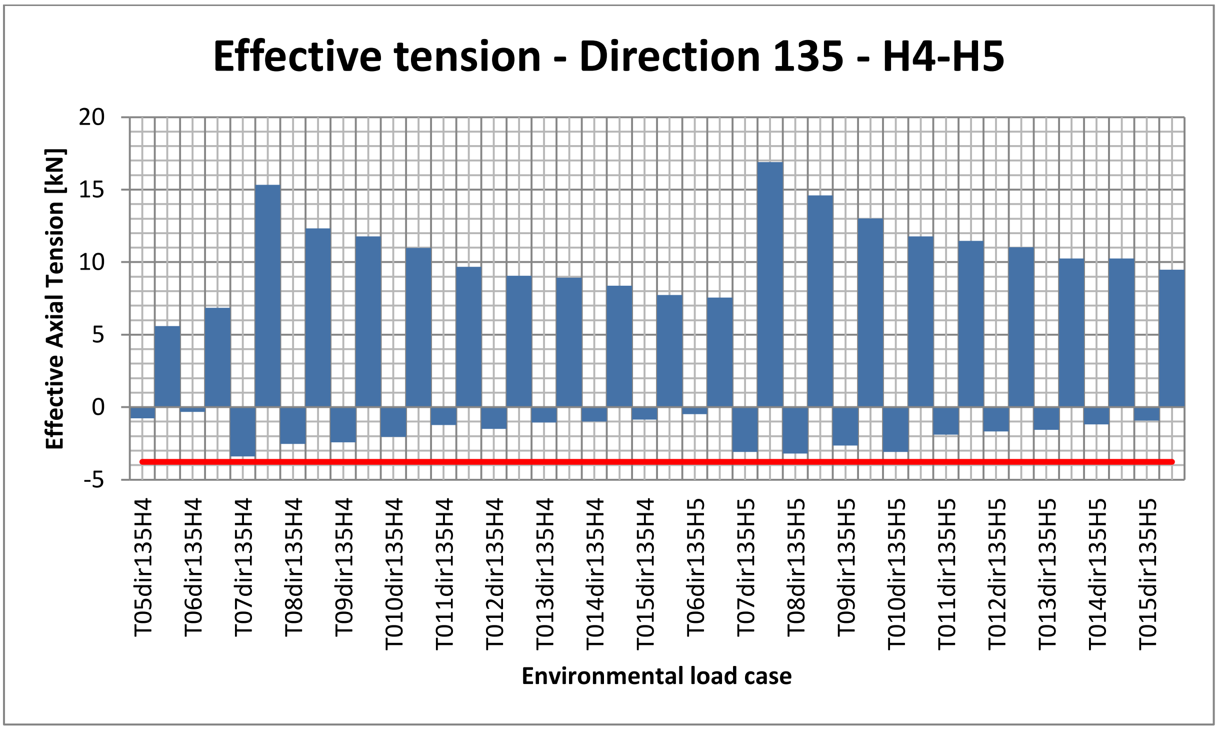

Figure D. 4 - 4"Bunkerflex STH - Free hanging - Effective tension - Direction 135° - H4-H5 - Current 0°

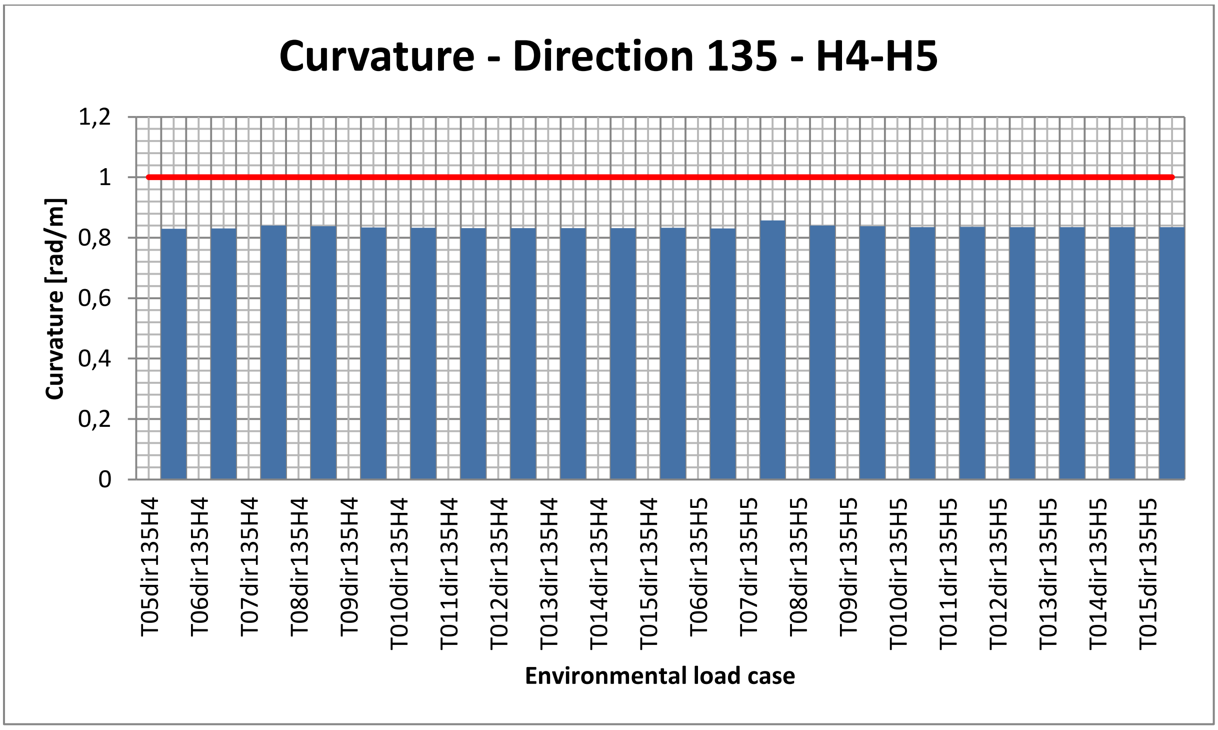

Figure D. 5 - 4"Bunkerflex STH - Free hanging - Curvature - Direction 135° - H4-H5 - Current 0°

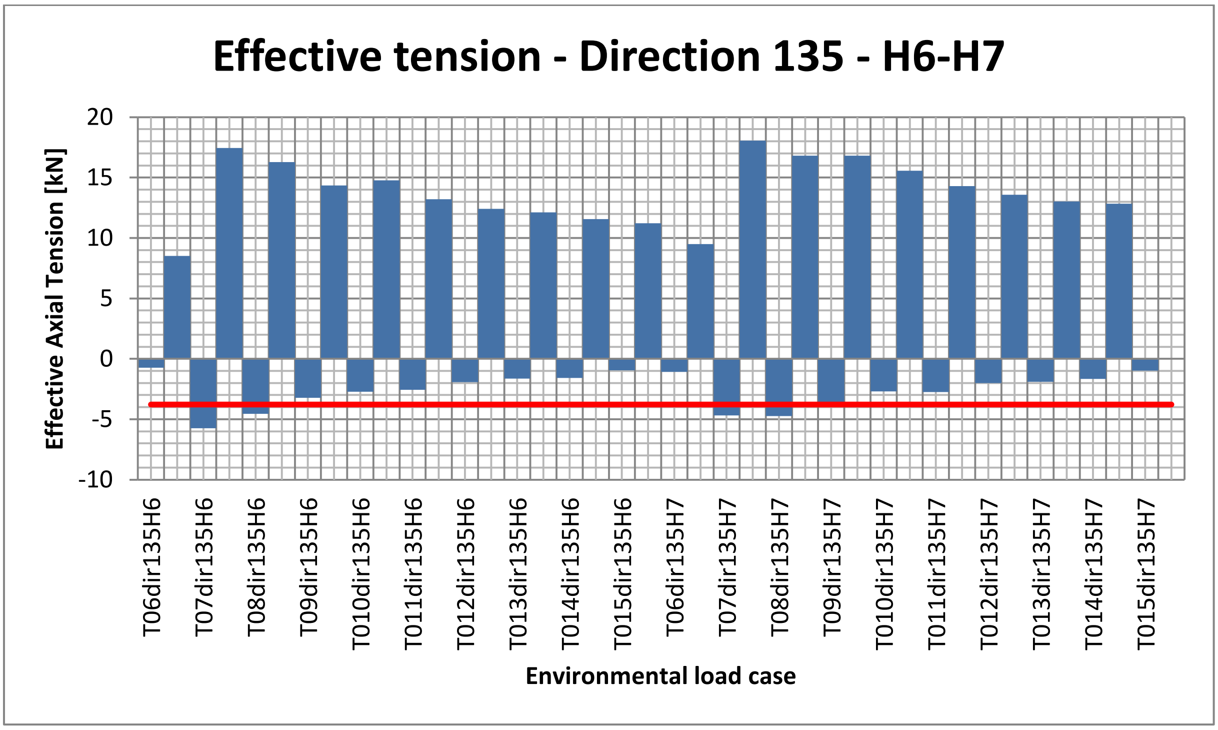

Figure D. 6 - 4"Bunkerflex STH - Free hanging - Effective tension - Direction 135° - H6-H7 - Current 0°

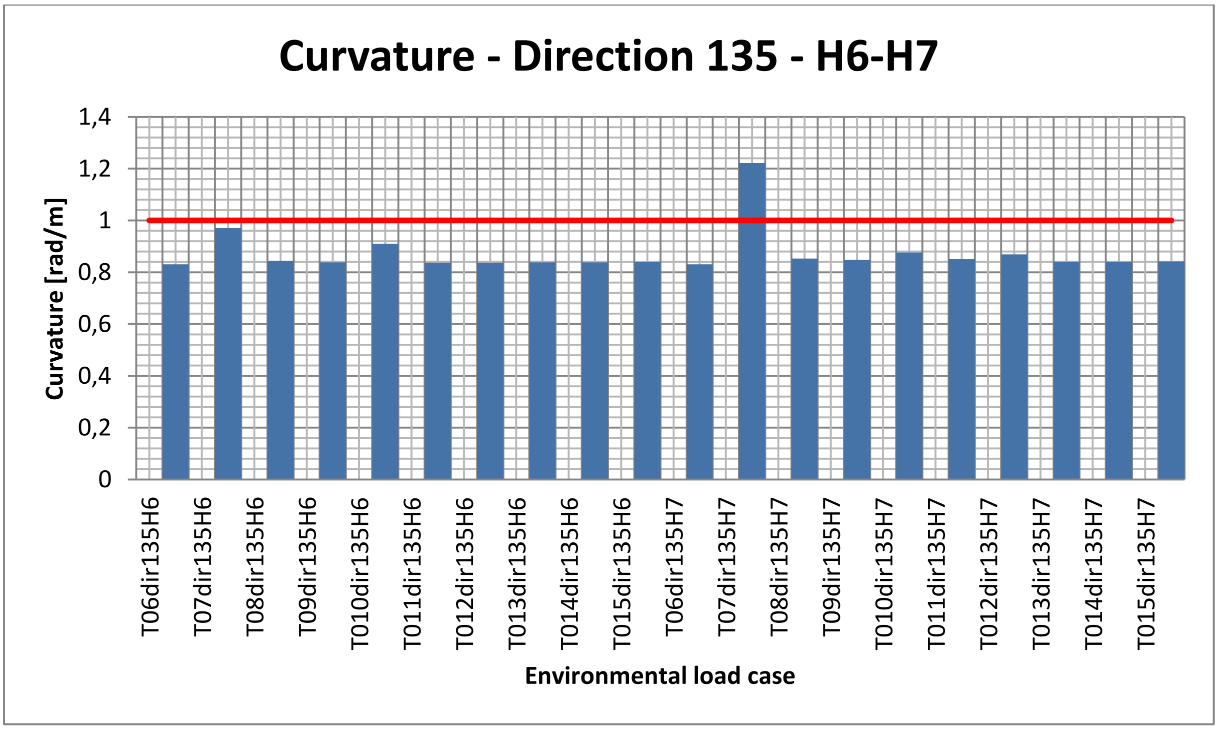

Figure D. 7 - 4"Bunkerflex STH - Free hanging - Curvature - Direction 135° - H6-H7 - Current 0°

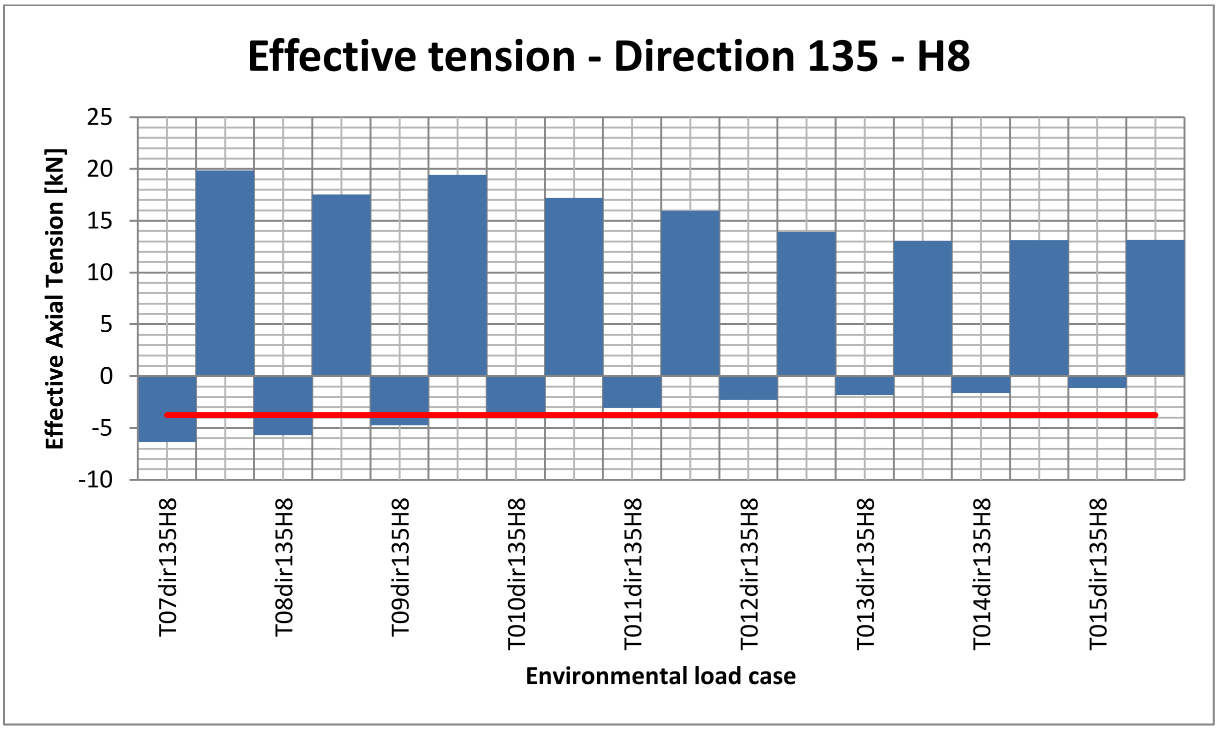

Figure D. 8 - 4"Bunkerflex STH - Free hanging - Effective tension - Direction 135° - H8 - Current 0°

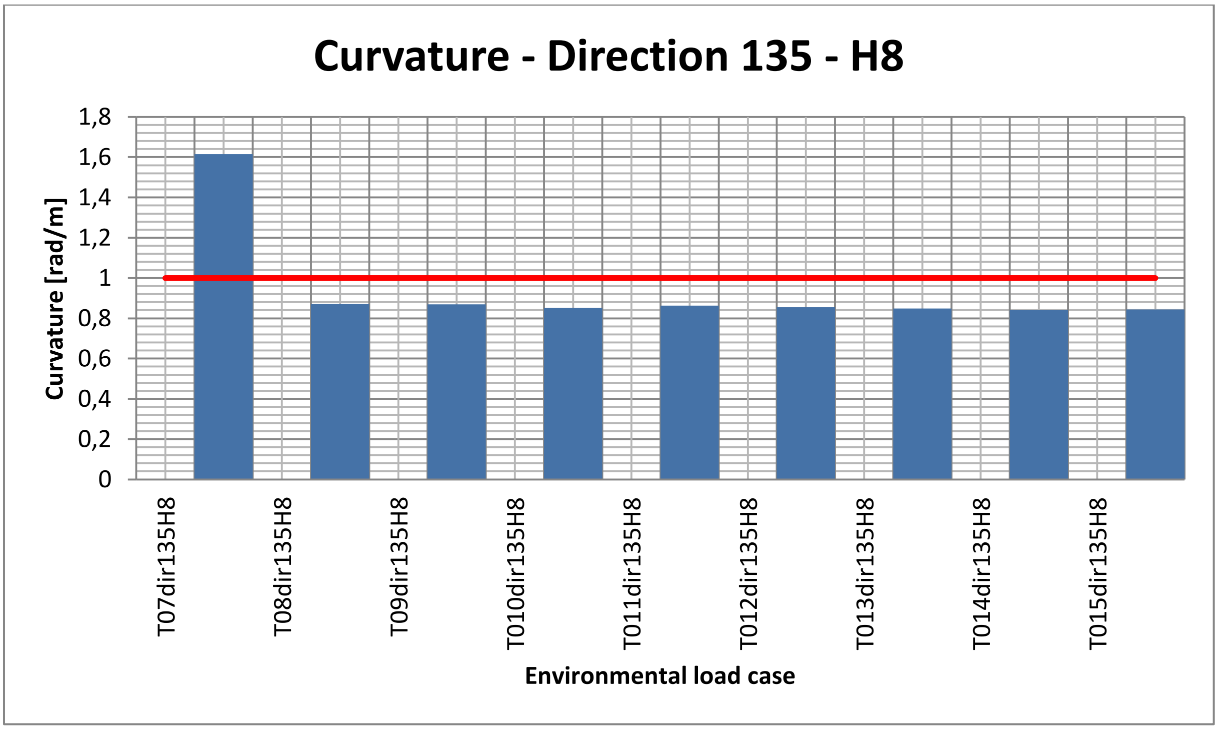

Figure D. 9 - 4"Bunkerflex STH - Free hanging - Curvature - Direction 135° - H8 - Current 0°

Direction 180°

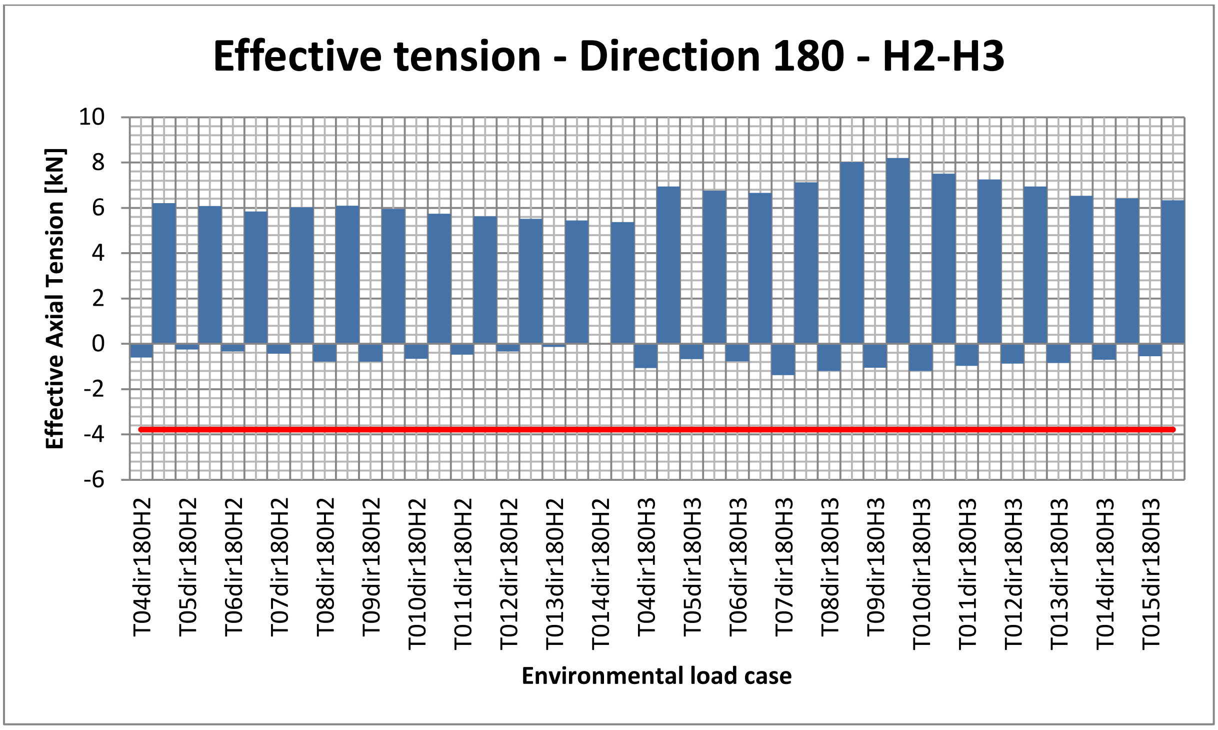

Figure D. 10 - 4"Bunkerflex STH - Free hanging - Effective tension - Direction 180° - H2-H3 - Current 0°

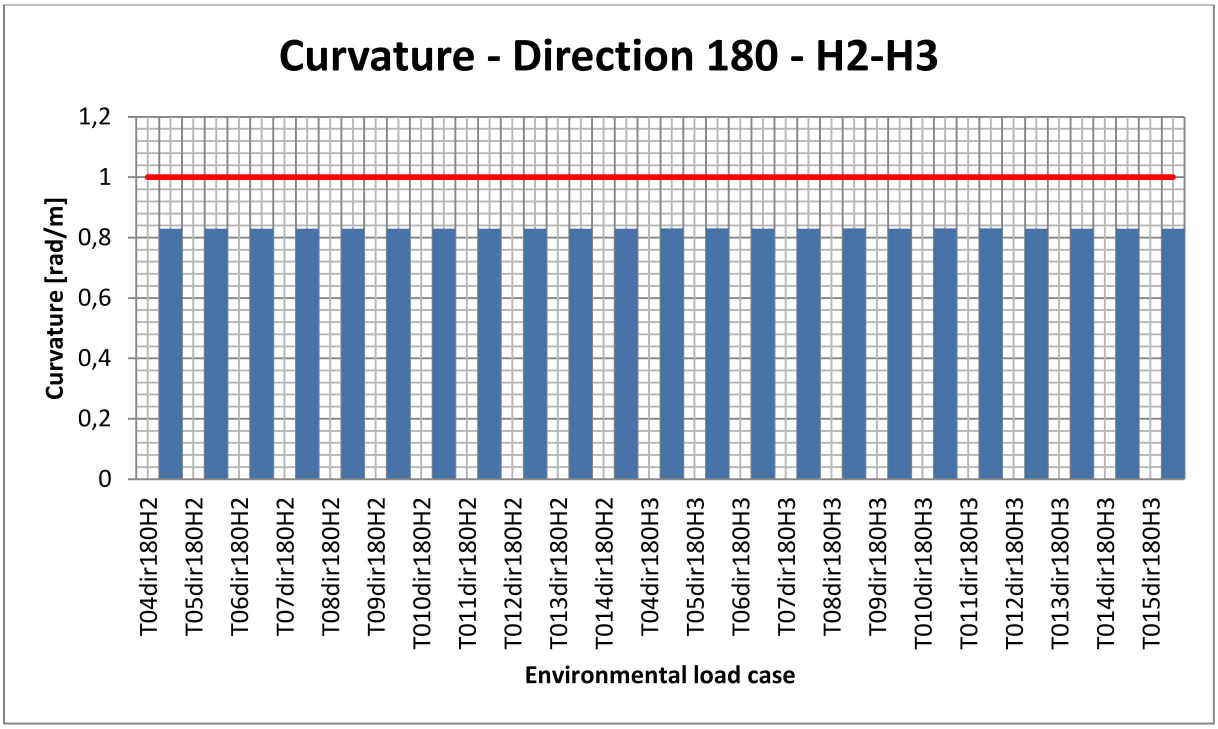

Figure D. 11 - 4"Bunkerflex STH - Free hanging - Curvature - Direction 180° - H2-H3 - Current 0°

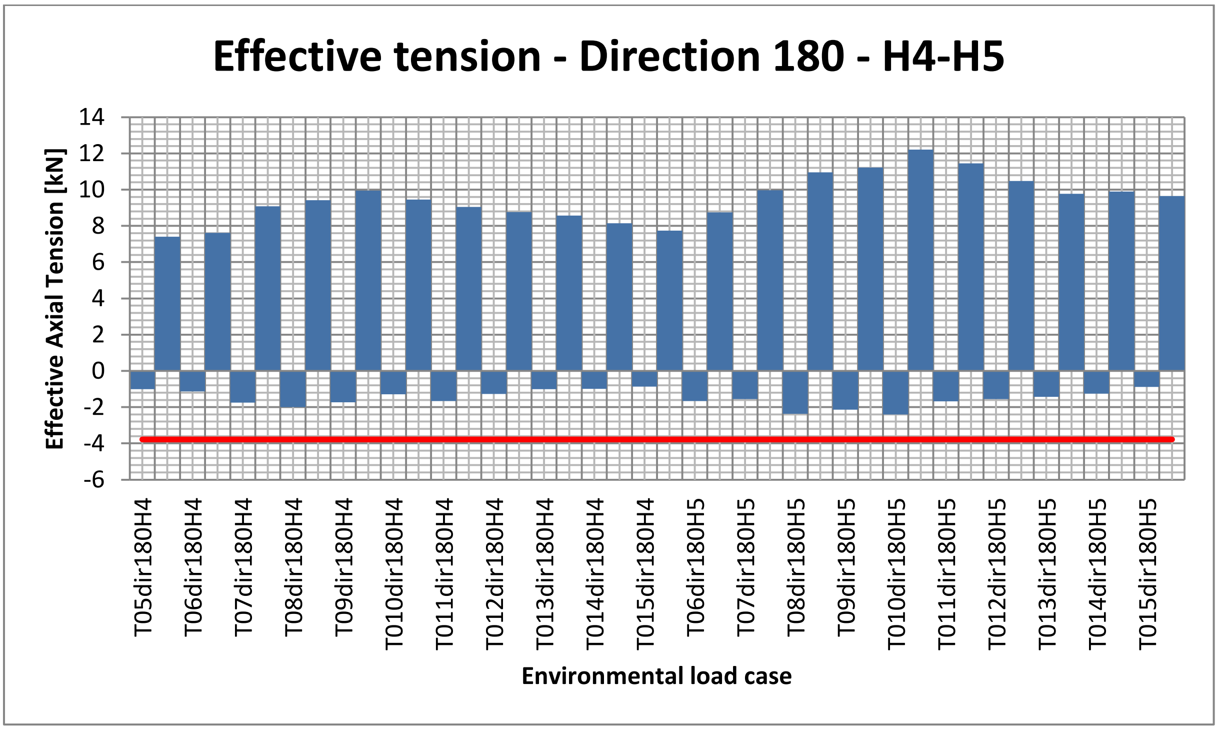

Figure D. 12 - 4"Bunkerflex STH - Free hanging - Effective tension - Direction 180° - H4-H5 - Current 0°

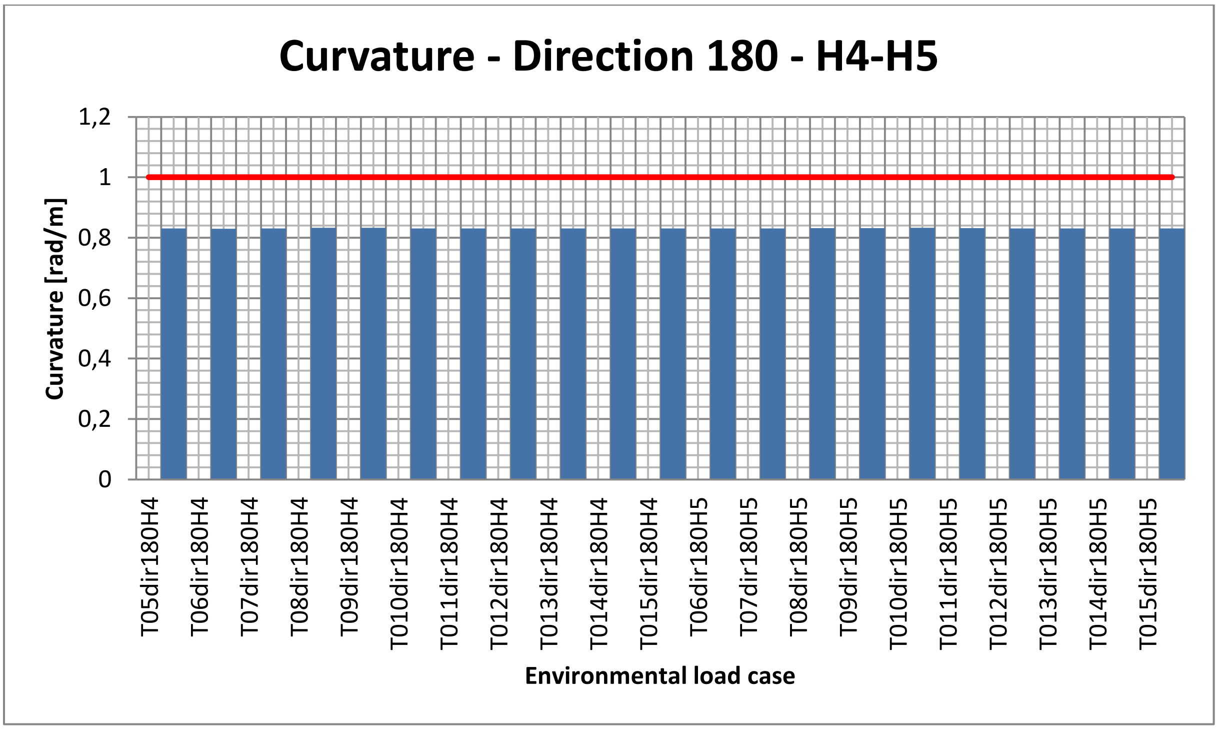

Figure D. 13 - 4"Bunkerflex STH - Free hanging - Curvature - Direction 180° - H4-H5 - Current 0°

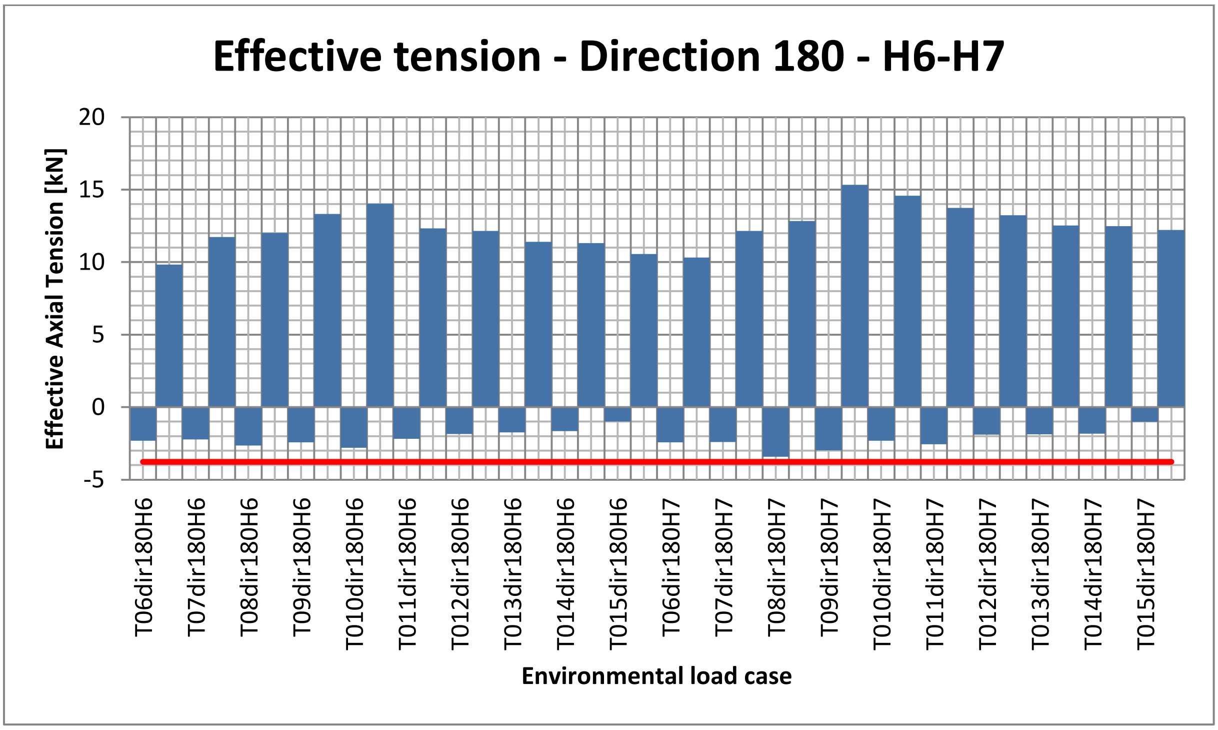

Figure D. 14 - 4"Bunkerflex STH - Free hanging - Effective tension - Direction 180° - H6-H7 - Current 0°

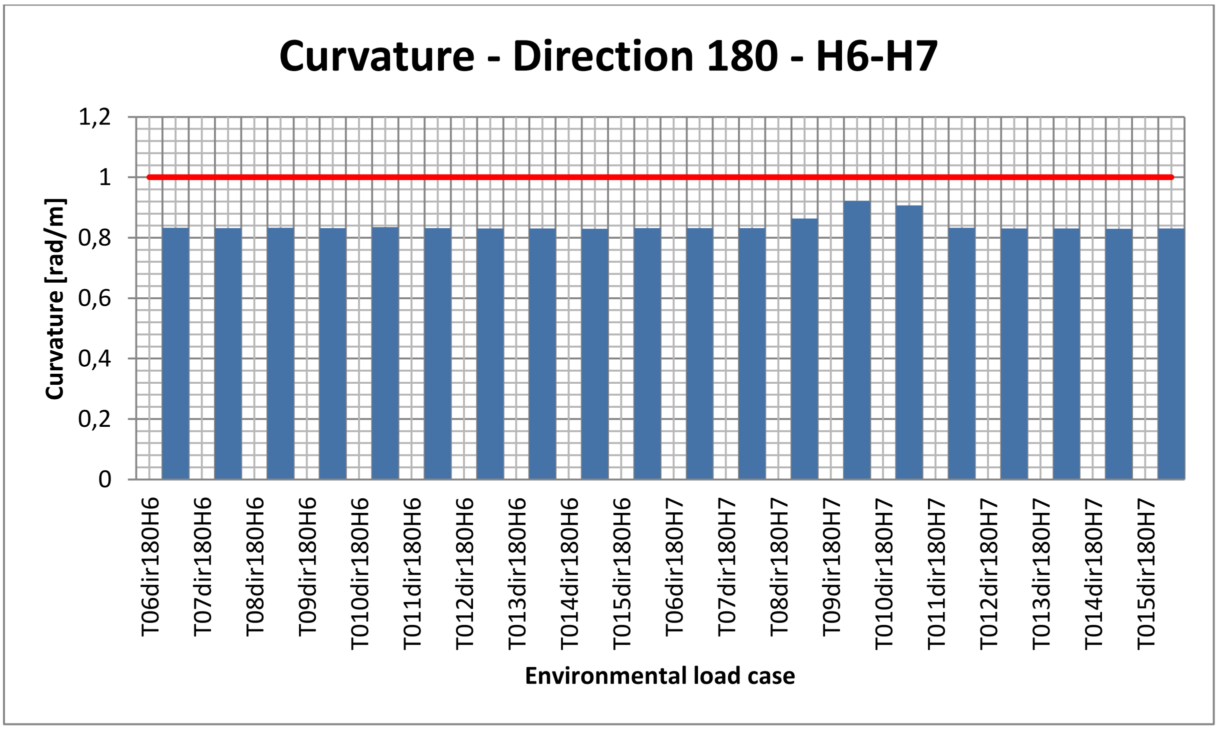

Figure D. 15 - 4"Bunkerflex STH - Free hanging - Curvature - Direction 180° - H6-H7 - Current 0°

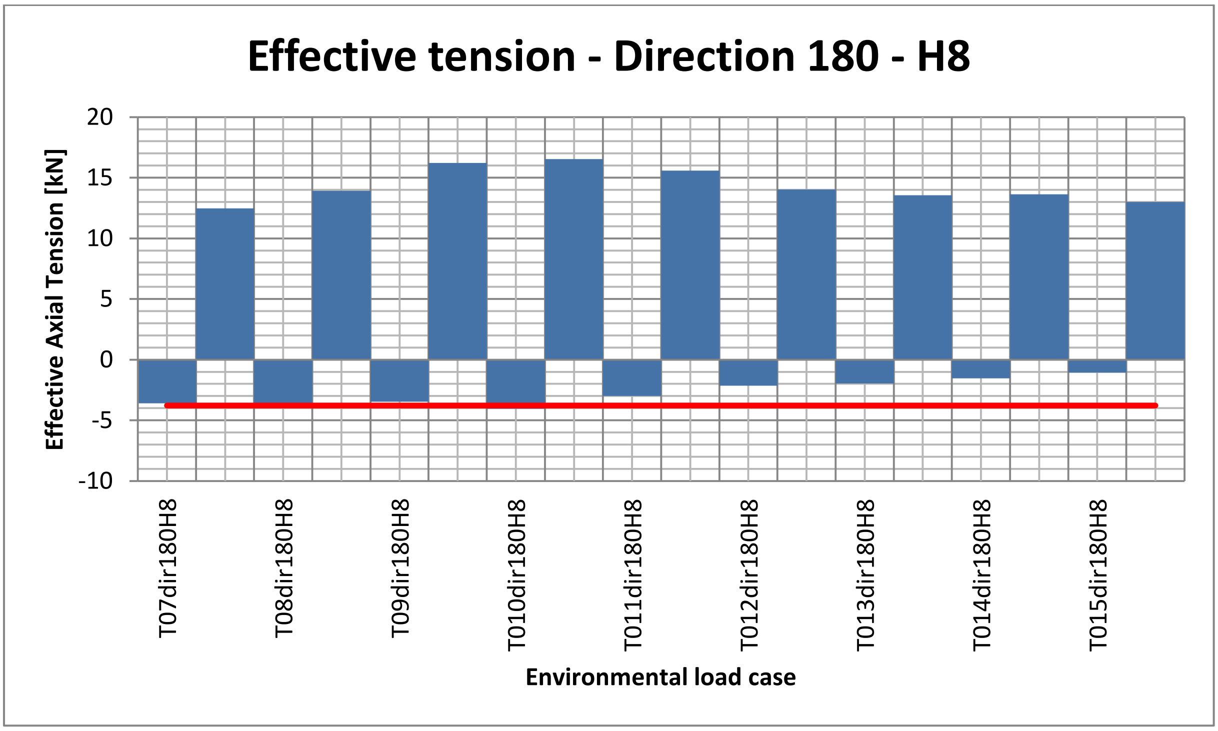

Figure D. 16 - 4"Bunkerflex STH - Free hanging - Effective tension - Direction 180° - H8 - Current 0°

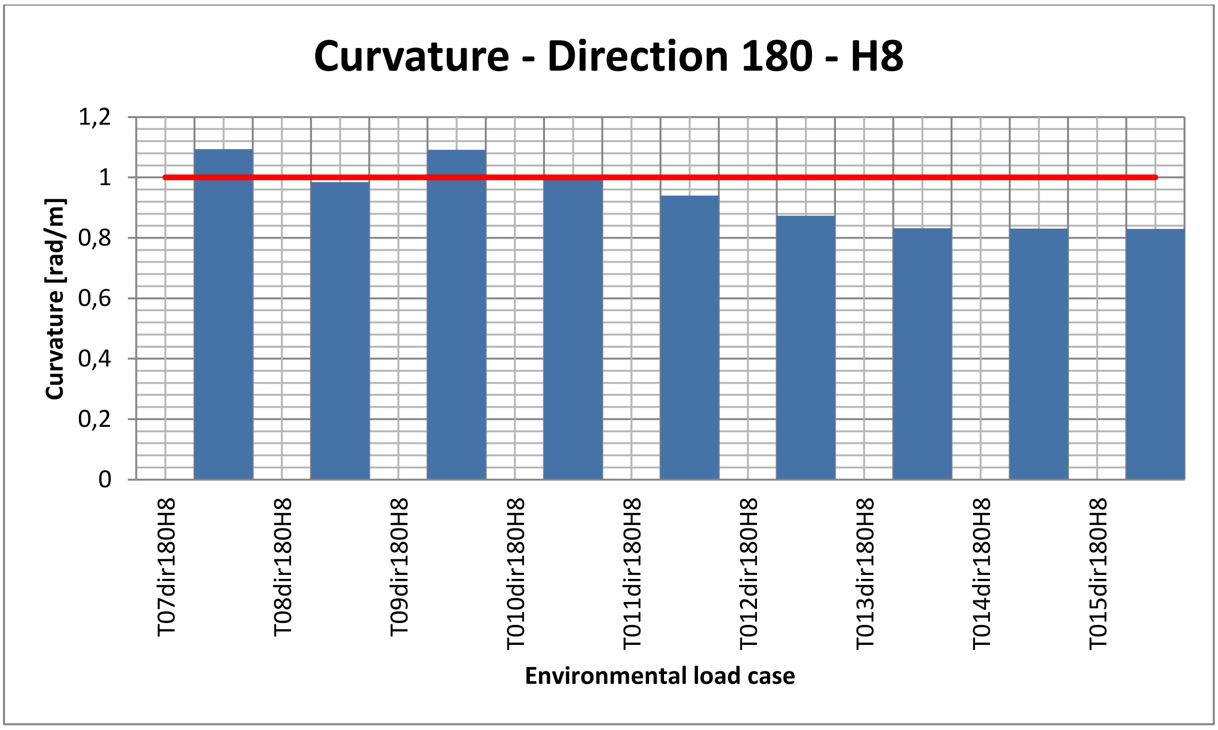

Figure D. 17 - 4"Bunkerflex STH - Free hanging - Curvature - Direction 180° - H8 - Current 0°

Direction 225°

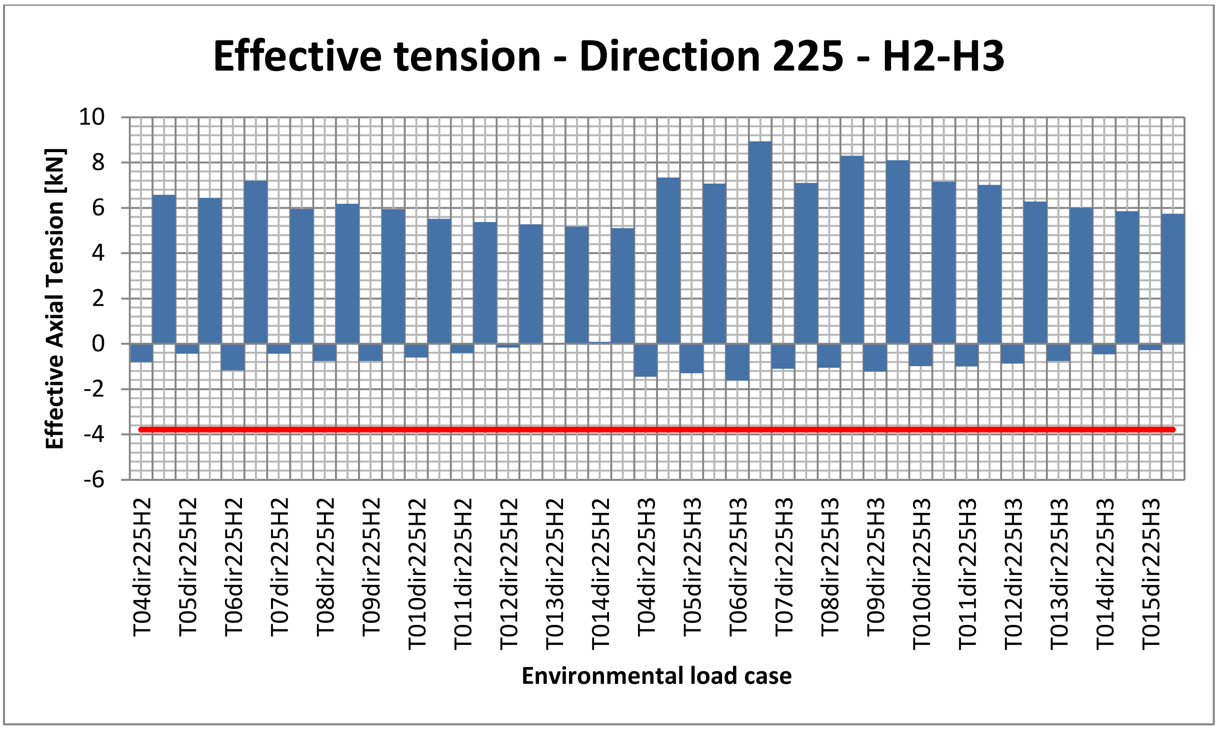

Figure D. 18 - 4"Bunkerflex STH - Free hanging - Effective tension - Direction 225° - H2-H3 - Current 0°

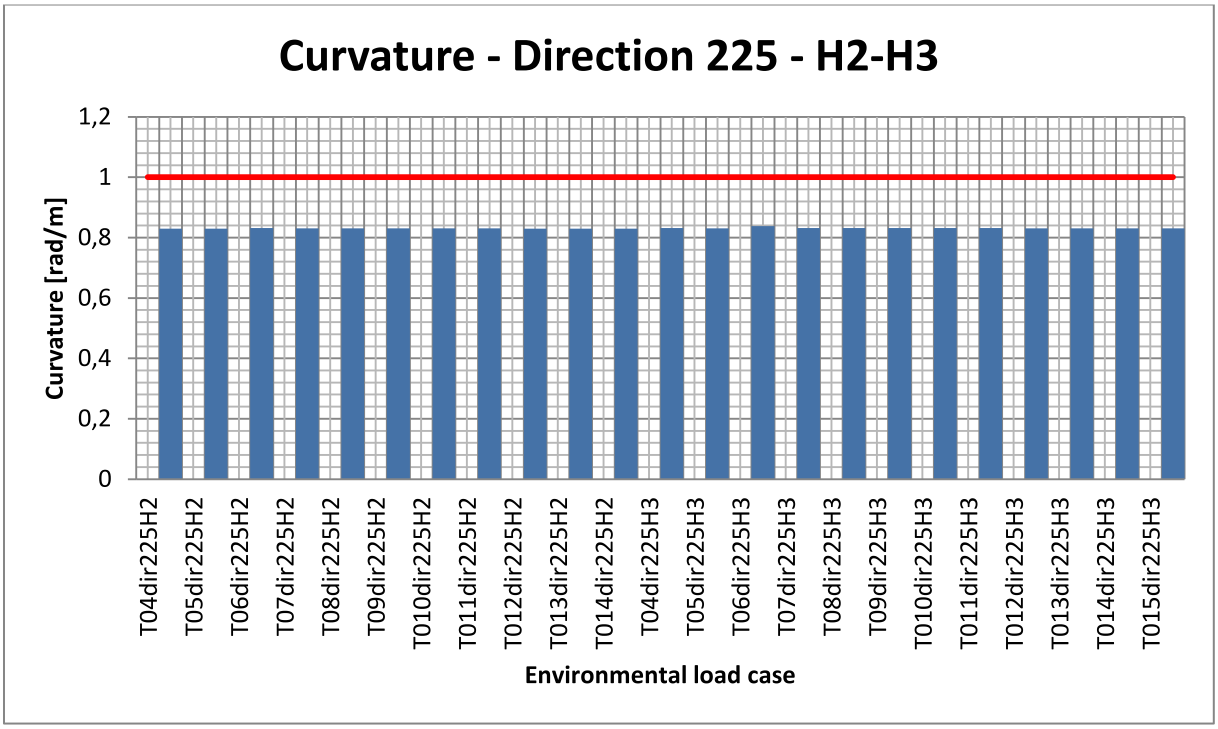

Figure D. 19 - 4"Bunkerflex STH - Free hanging - Curvature - Direction 225° - H2-H3 - Current 0°

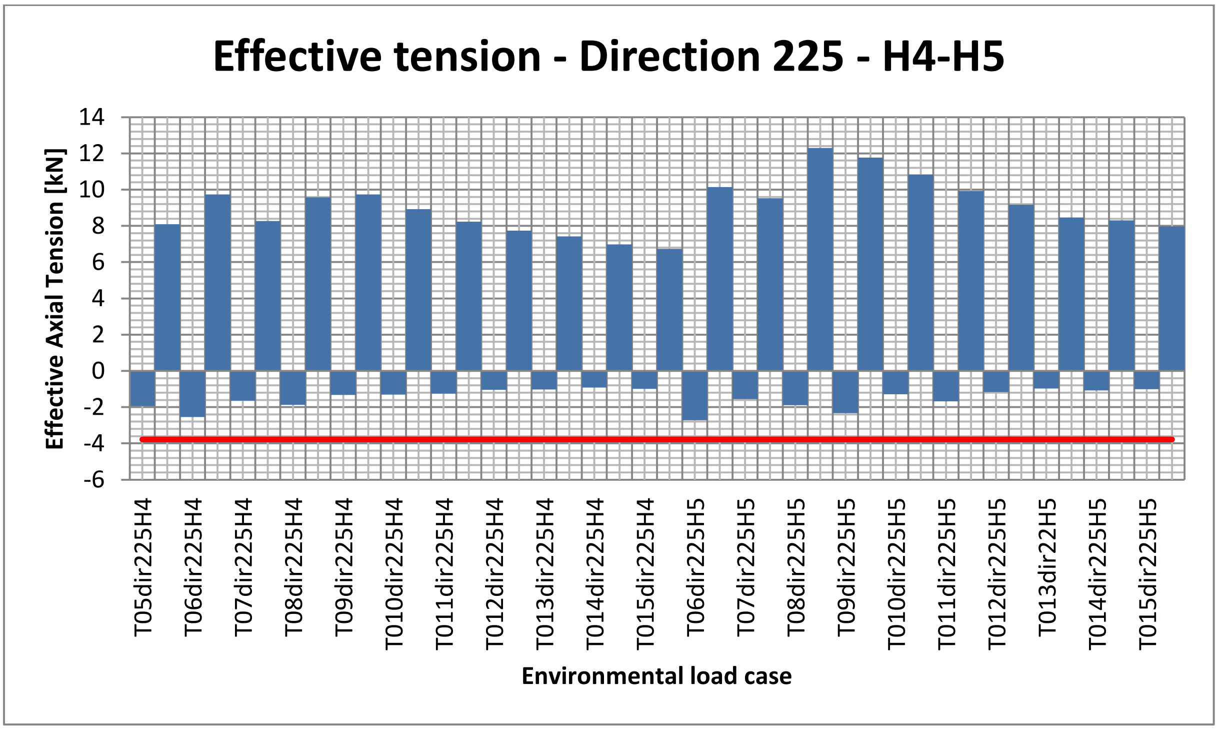

Figure D. 20 - 4"Bunkerflex STH - Free hanging - Effective tension - Direction 225° - H4-H5 - Current 0°

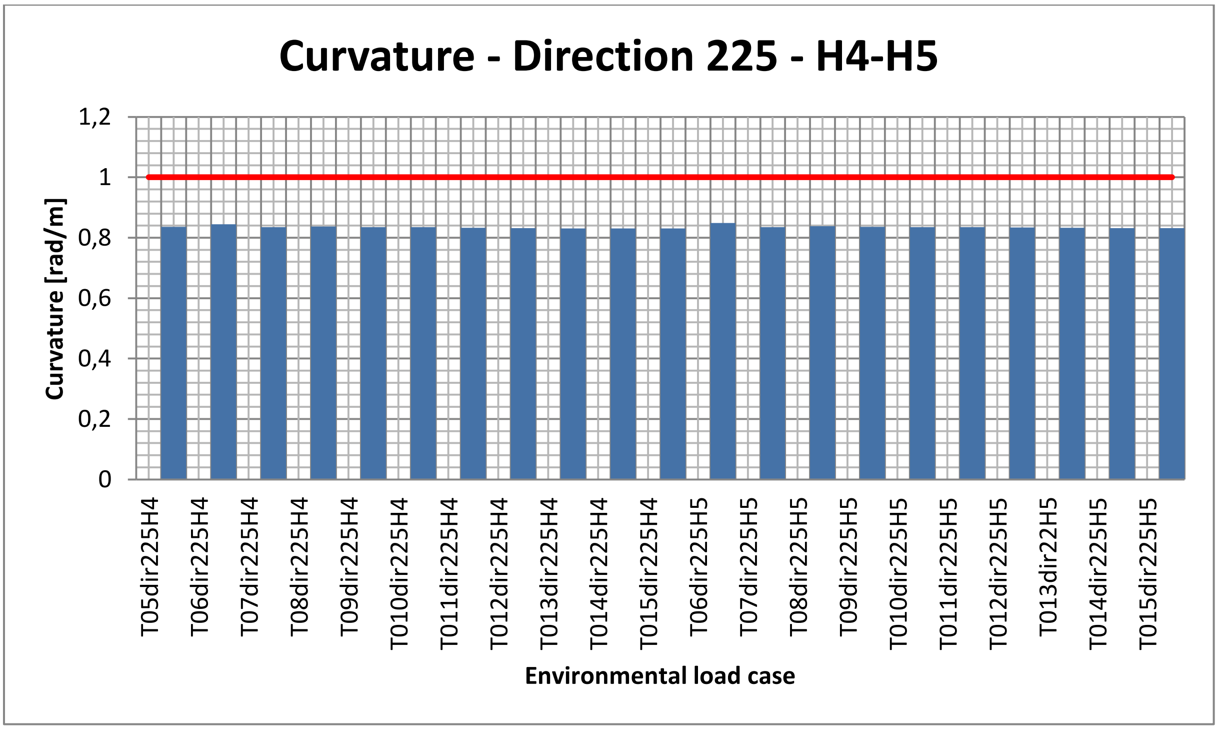

Figure D. 21 - 4"Bunkerflex STH - Free hanging - Curvature - Direction 225° - H4-H5 - Current 0°

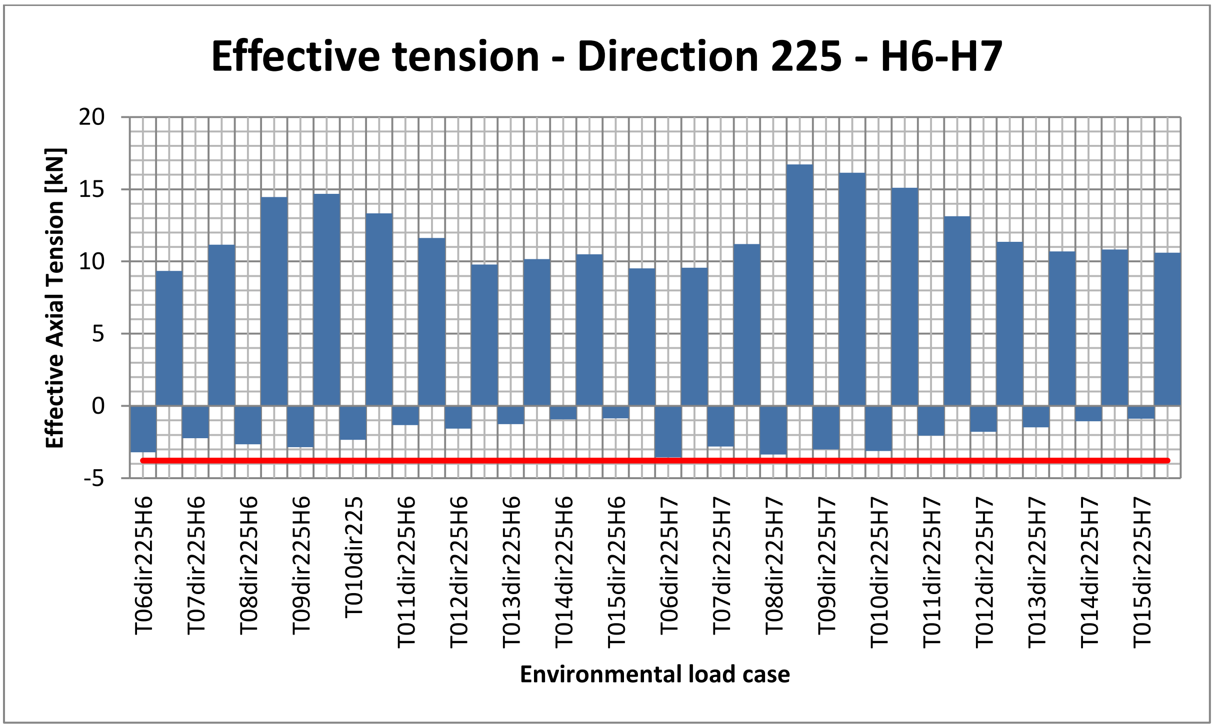

Figure D. 22 - 4"Bunkerflex STH - Free hanging - Effective tension - Direction 225° - H6-H7 - Current 0°

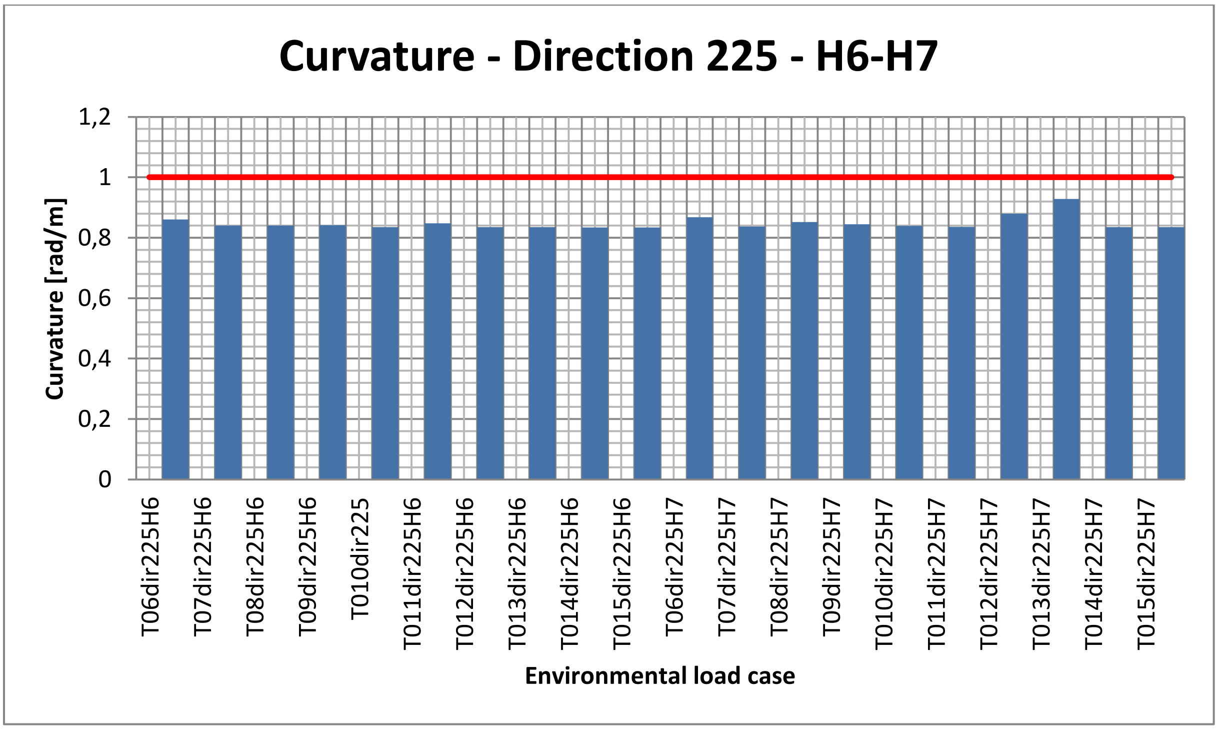

Figure D. 23 - 4"Bunkerflex STH - Free hanging - Curvature - Direction 225° - H6-H7 - Current 0°

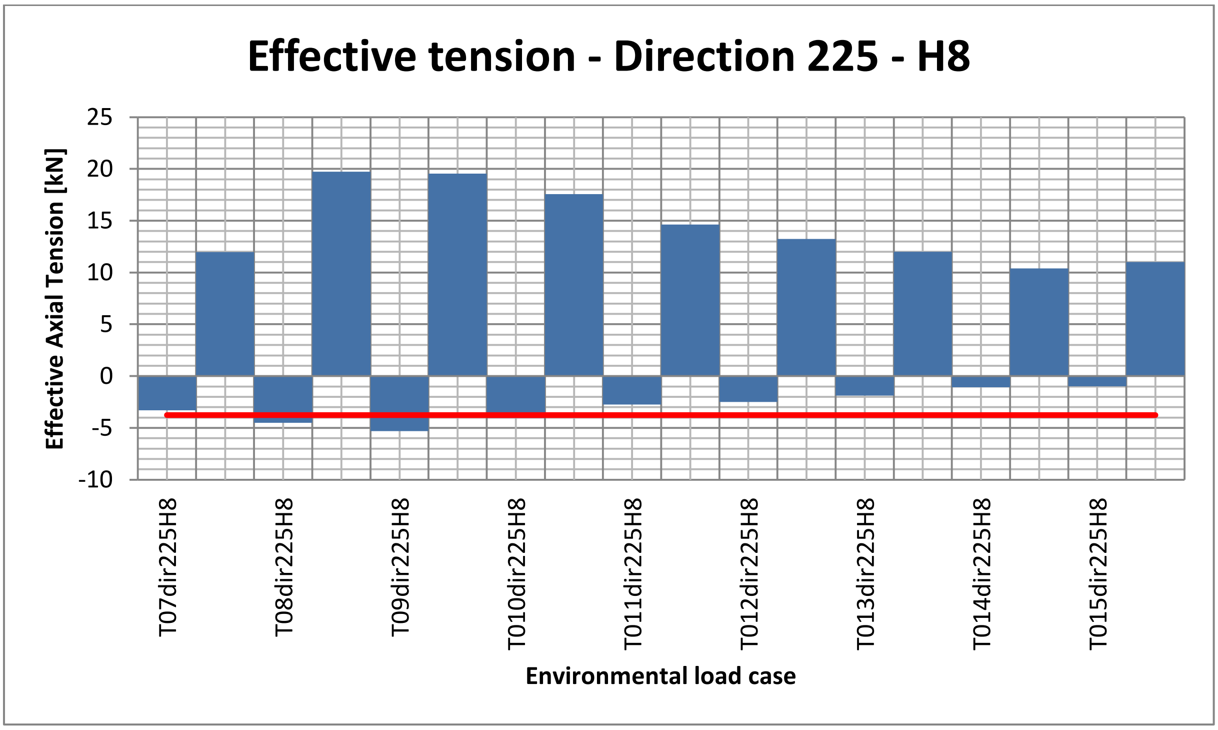

Figure D. 24 - 4"Bunkerflex STH - Free hanging - Effective tension - Direction 225° - H8 - Current 0°

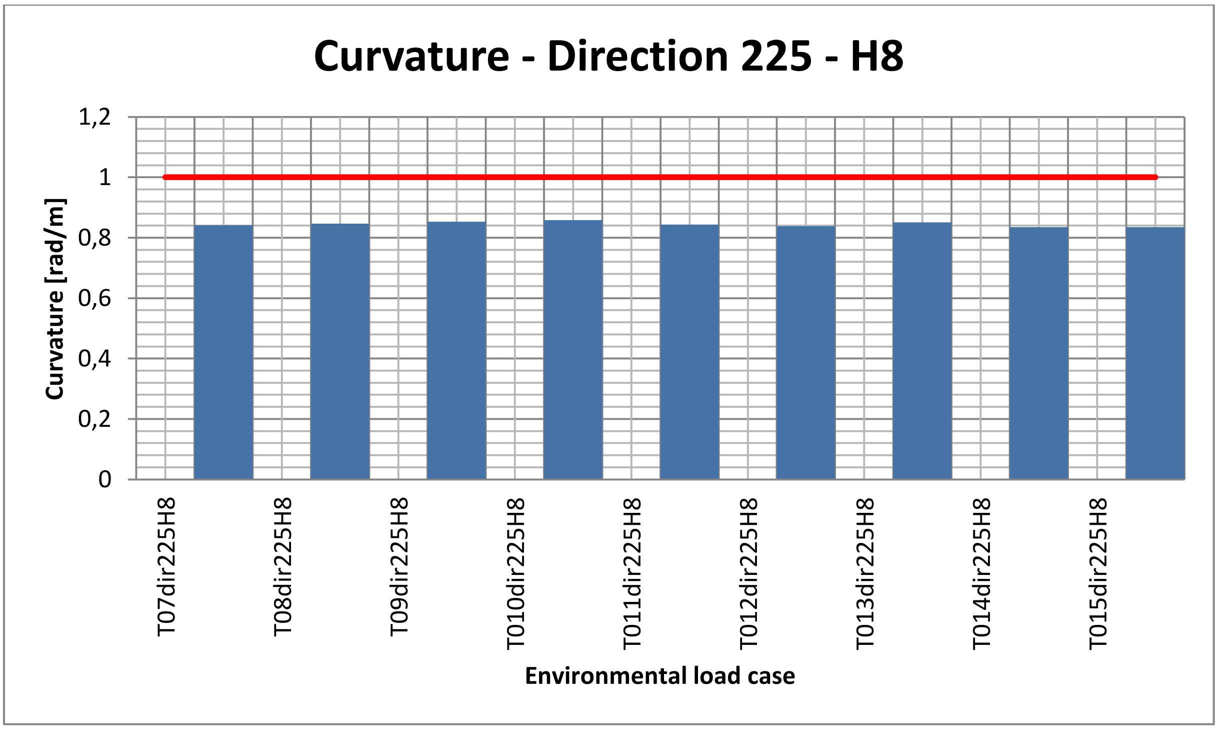

Figure D. 25 - 4"Bunkerflex STH - Free hanging - Curvature - Direction 225° - H8 - Current 0°

Wave rose

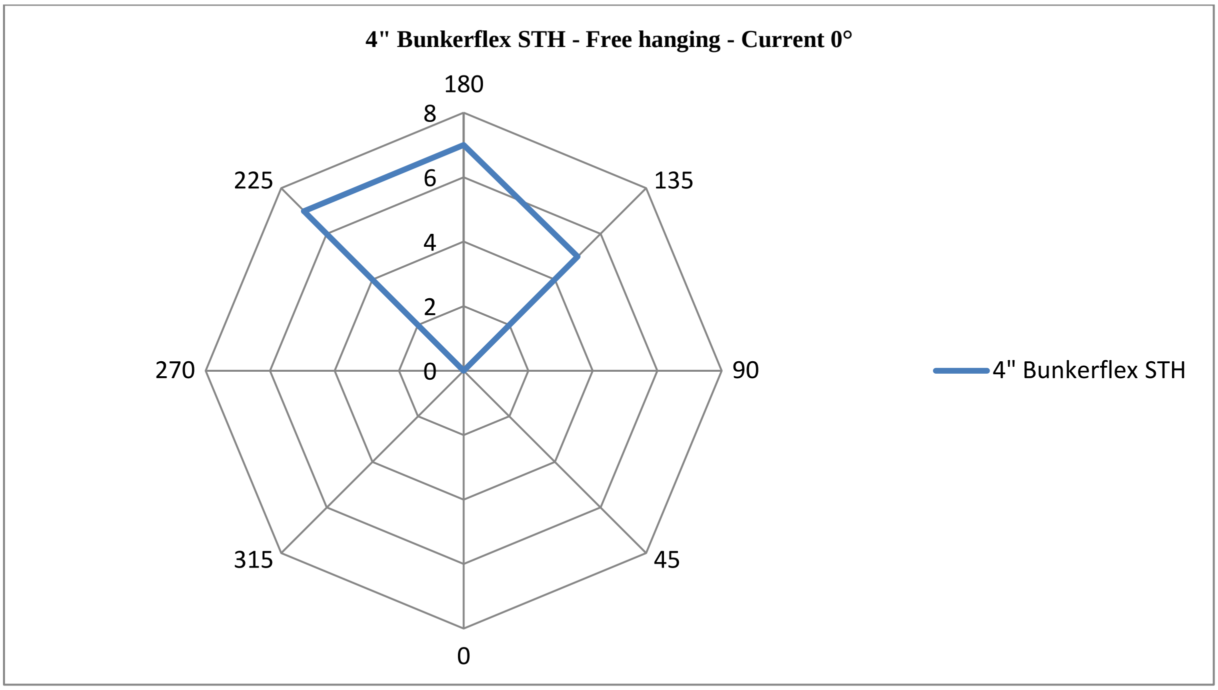

Figure D. 26 - 4” Bunkerflex STH - Free hanging - Wave rose - Current 0°

Free hanging - 90° direction current

Wave direction 135°

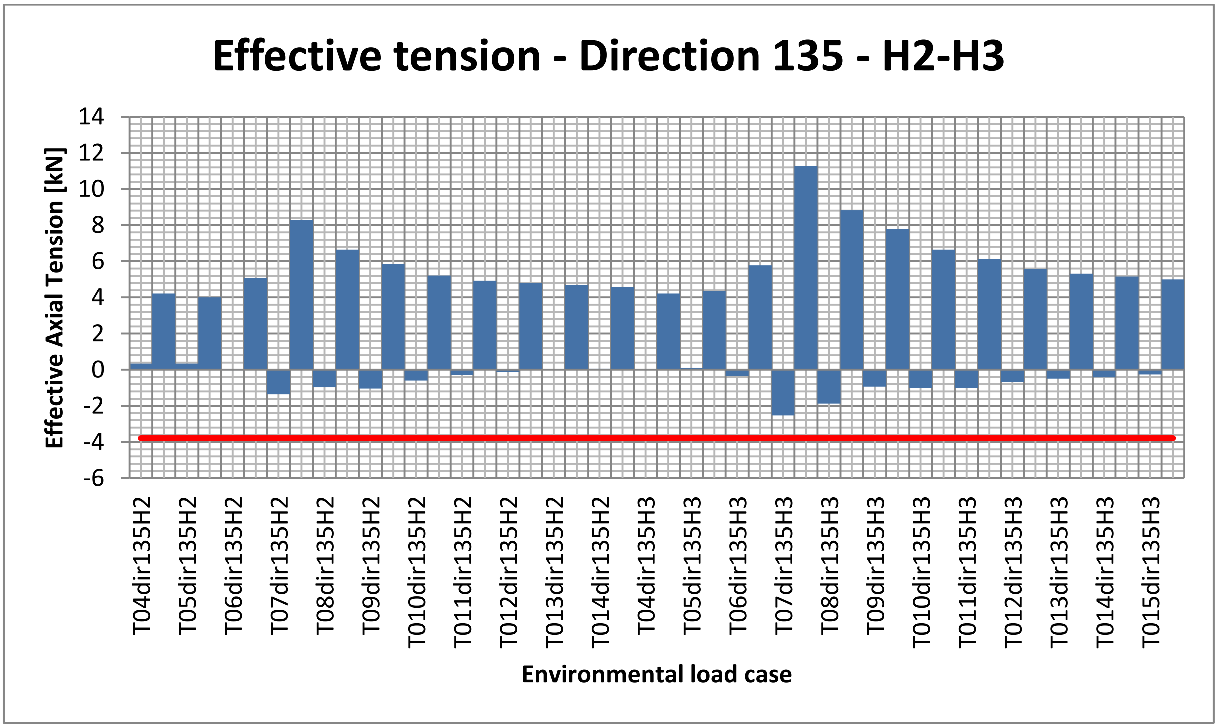

Figure D. 27 - 4"Bunkerflex STH - Free hanging - Effective tension - Direction 135° - H2-H3 - Current 90°

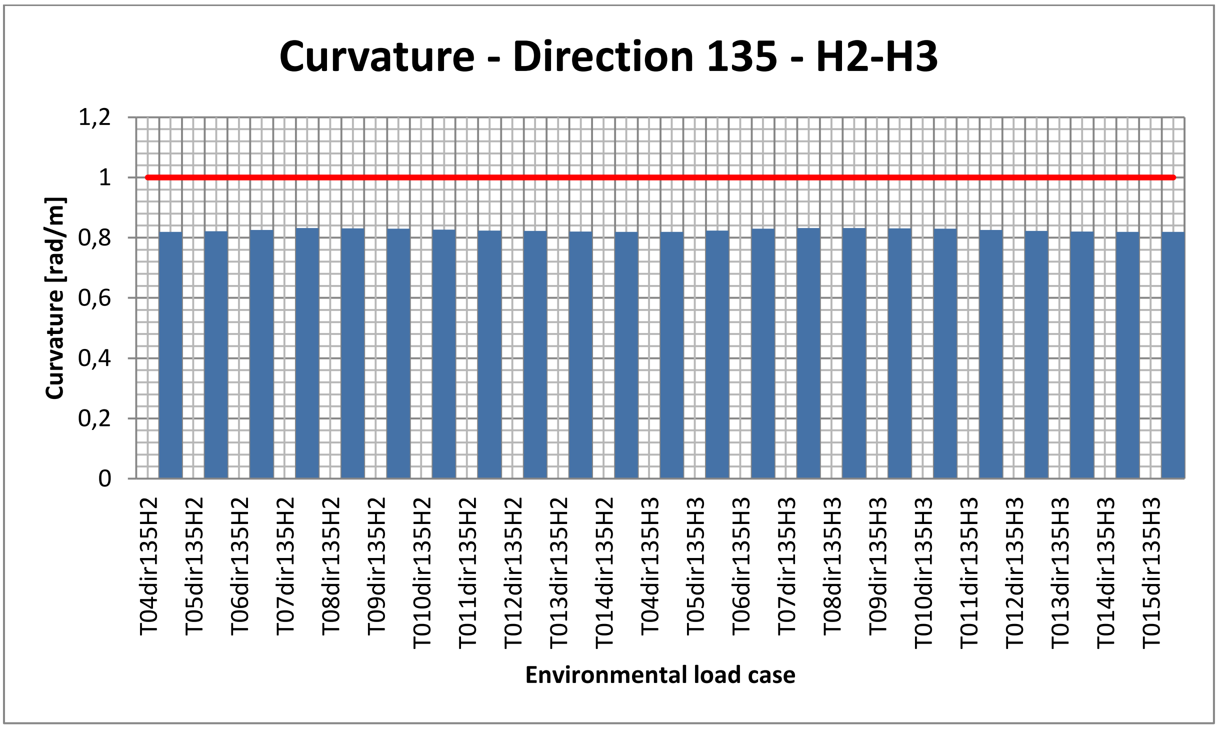

Figure D. 28 - 4"Bunkerflex STH - Free hanging - Curvature - Direction 135° - H2-H3 - Current 90°

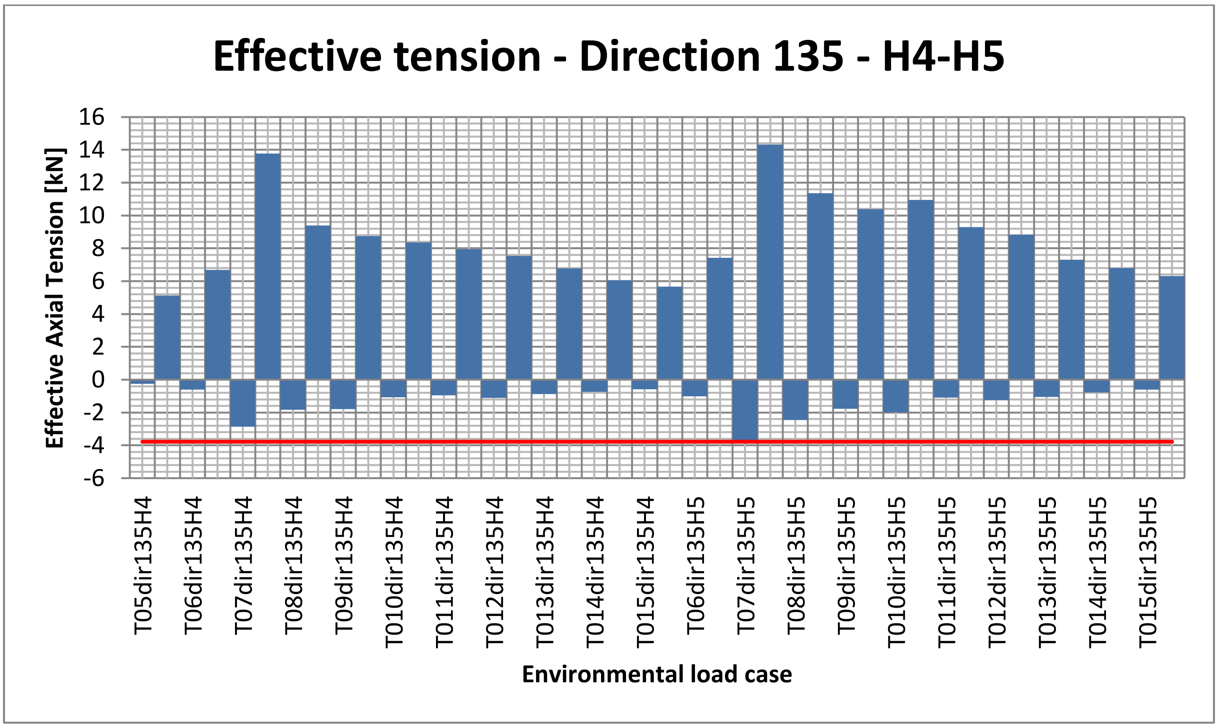

Figure D. 29 - 4"Bunkerflex STH - Free hanging - Effective tension - Direction 135° - H4-H5 - Current 90°

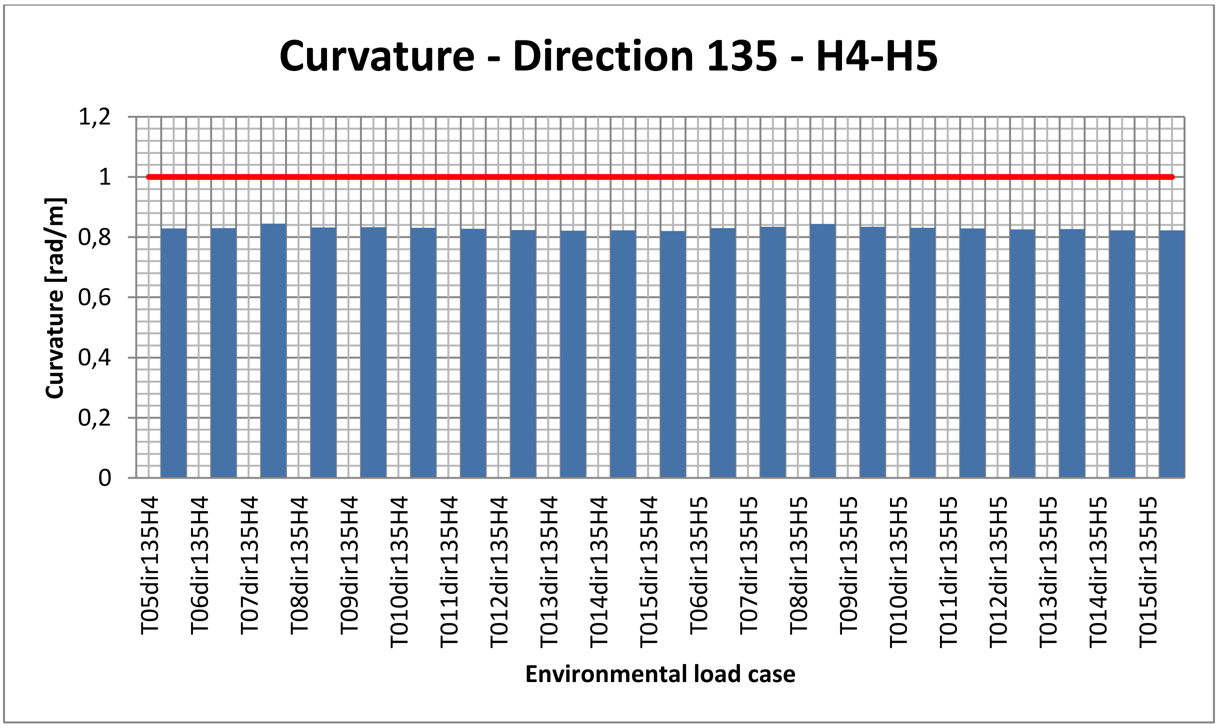

Figure D. 30 - 4"Bunkerflex STH - Free hanging - Curvature - Direction 135° - H4-H5 - Current 90°

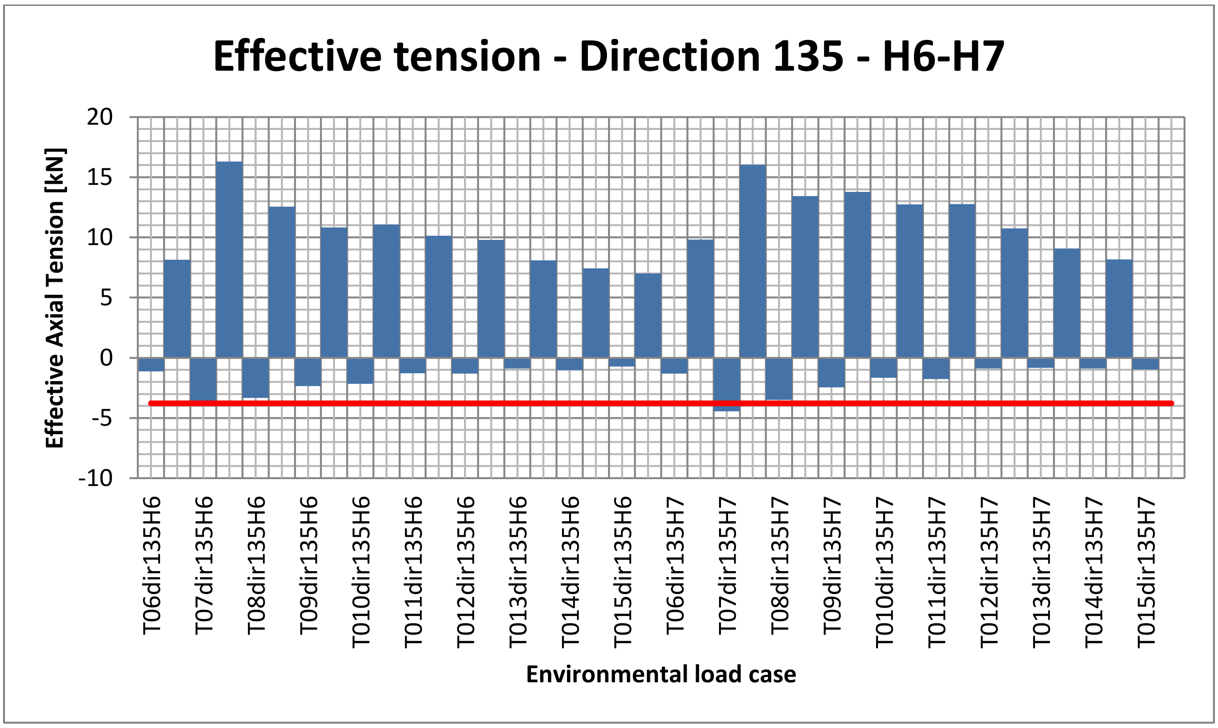

Figure D. 31 - 4"Bunkerflex STH - Free hanging - Effective tension - Direction 135° - H6-H7 - Current 90°

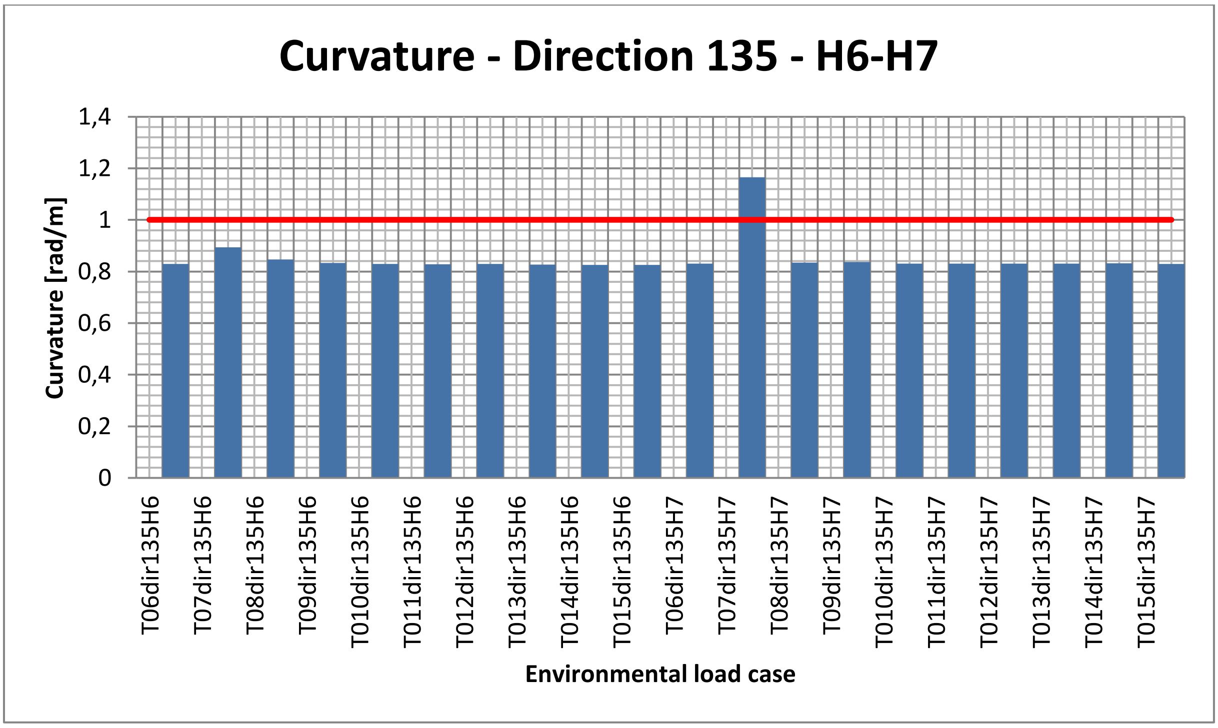

Figure D. 32 - 4"Bunkerflex STH - Free hanging - Curvature - Direction 135° - H6-H7 - Current 90°

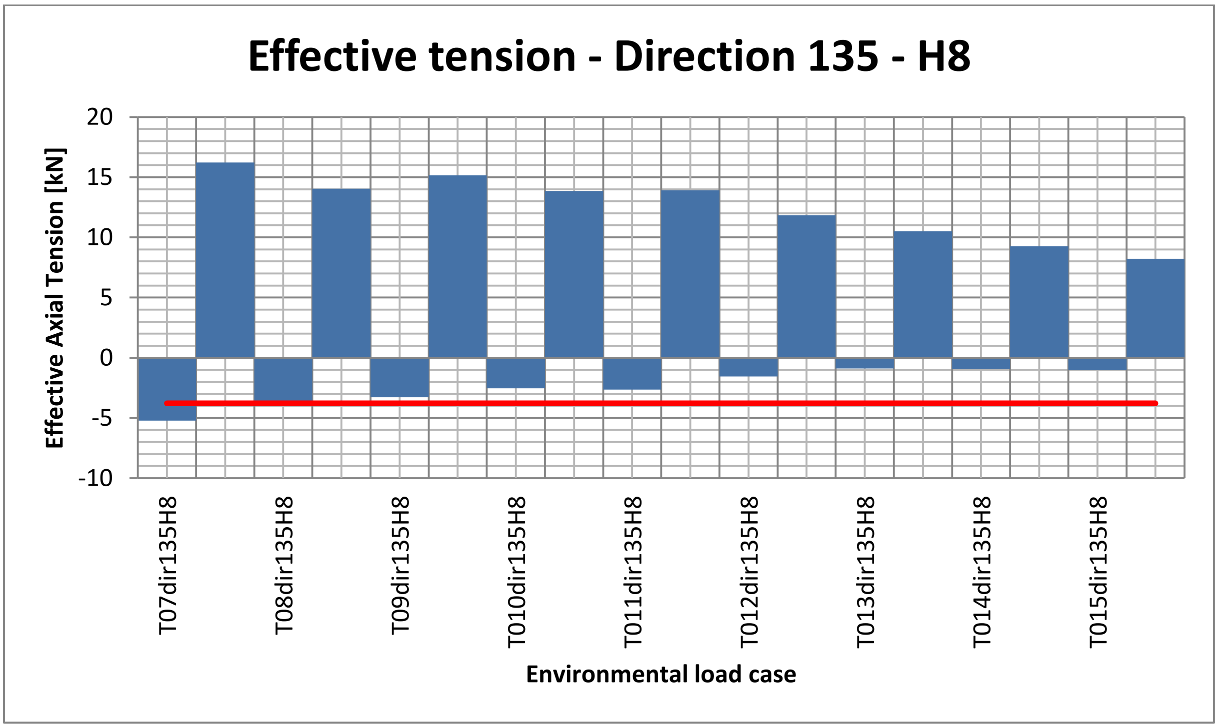

Figure D. 33 - 4"Bunkerflex STH - Free hanging - Effective tension - Direction 135° - H8 - Current 90°

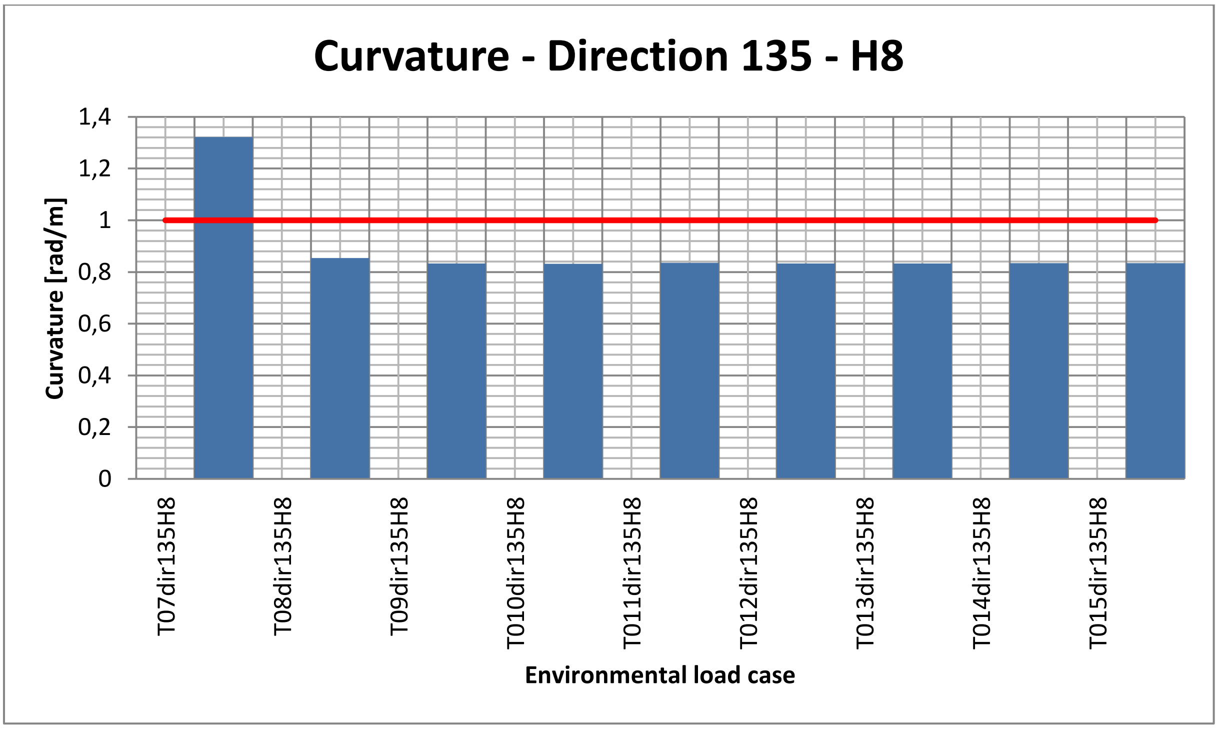

Figure D. 34 - 4"Bunkerflex STH - Free hanging - Curvature - Direction 135° - H8 - Current 90°

Direction 180°

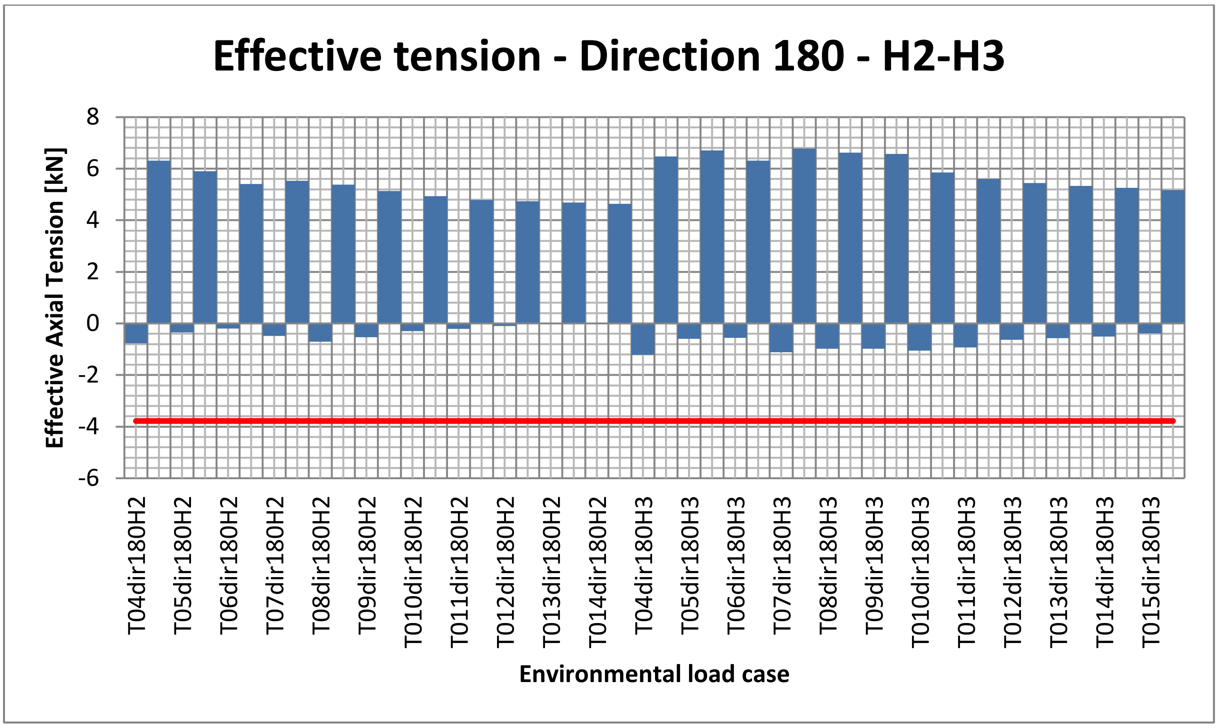

Figure D. 35 - 4"Bunkerflex STH - Free hanging - Effective tension - Direction 180° - H2-H3 - Current 90°

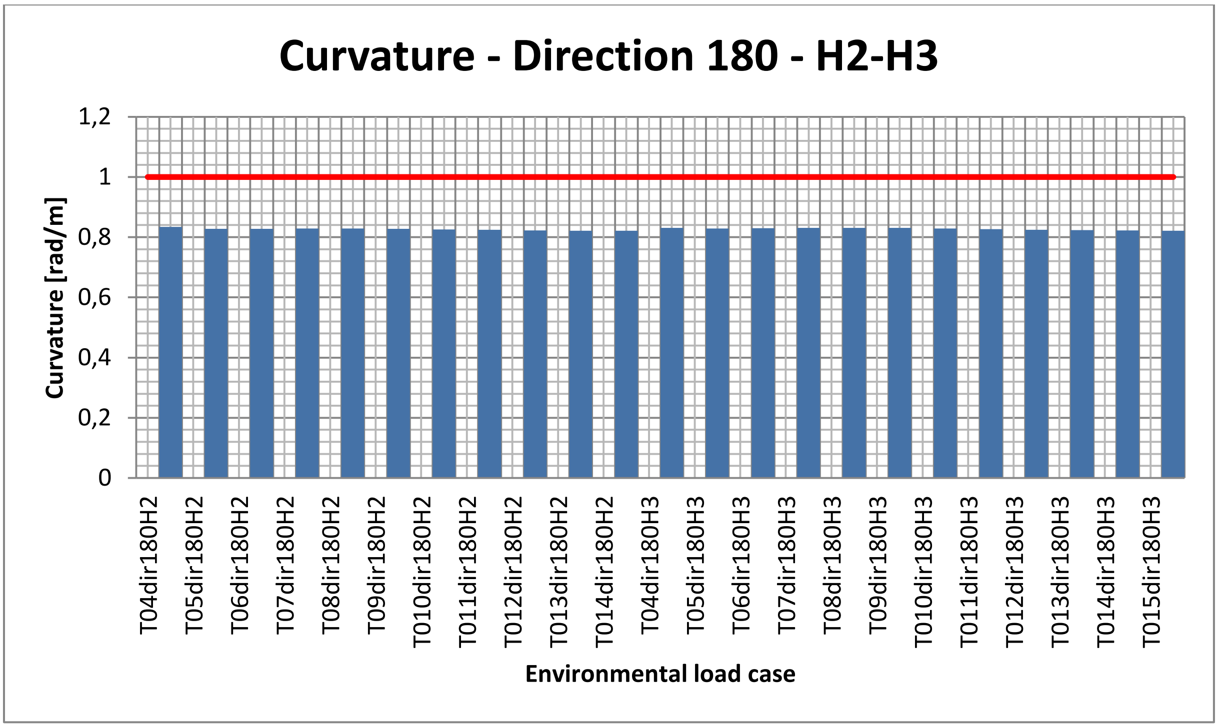

Figure D. 36 - 4"Bunkerflex STH - Free hanging - Curvature - Direction 180° - H2-H3 - Current 90°

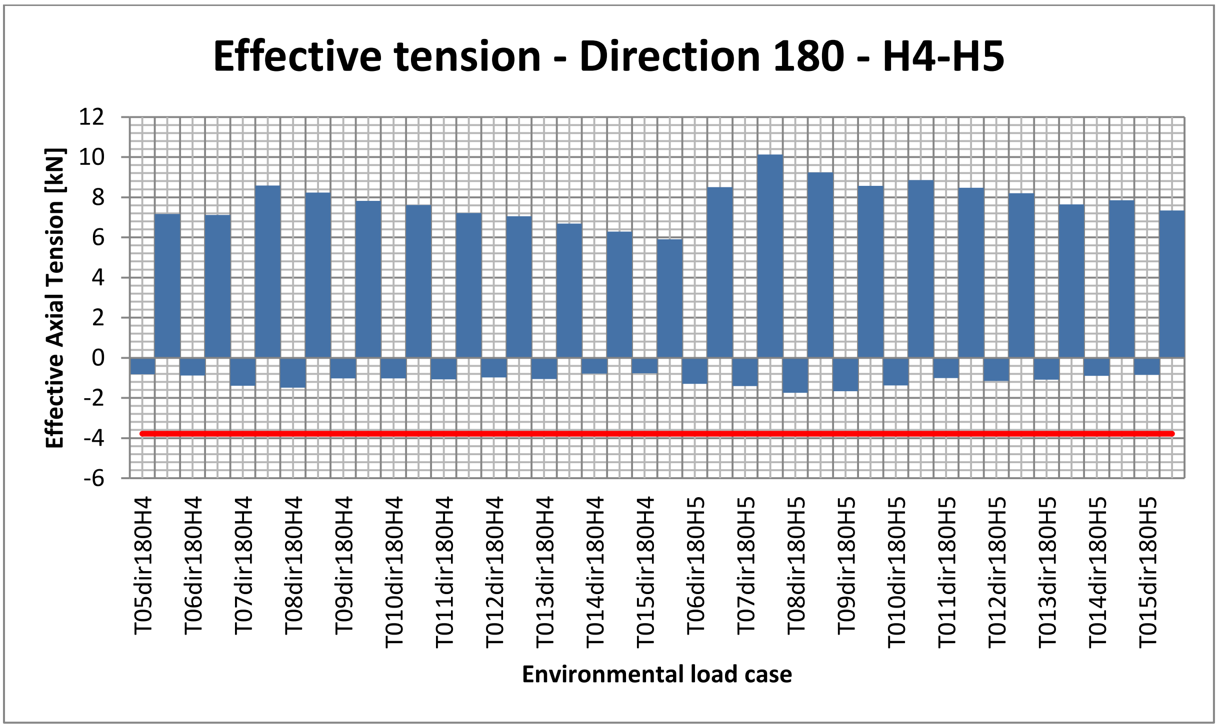

Figure D. 37 - 4"Bunkerflex STH - Free hanging - Effective tension - Direction 180° - H4-H5 - Current 90°

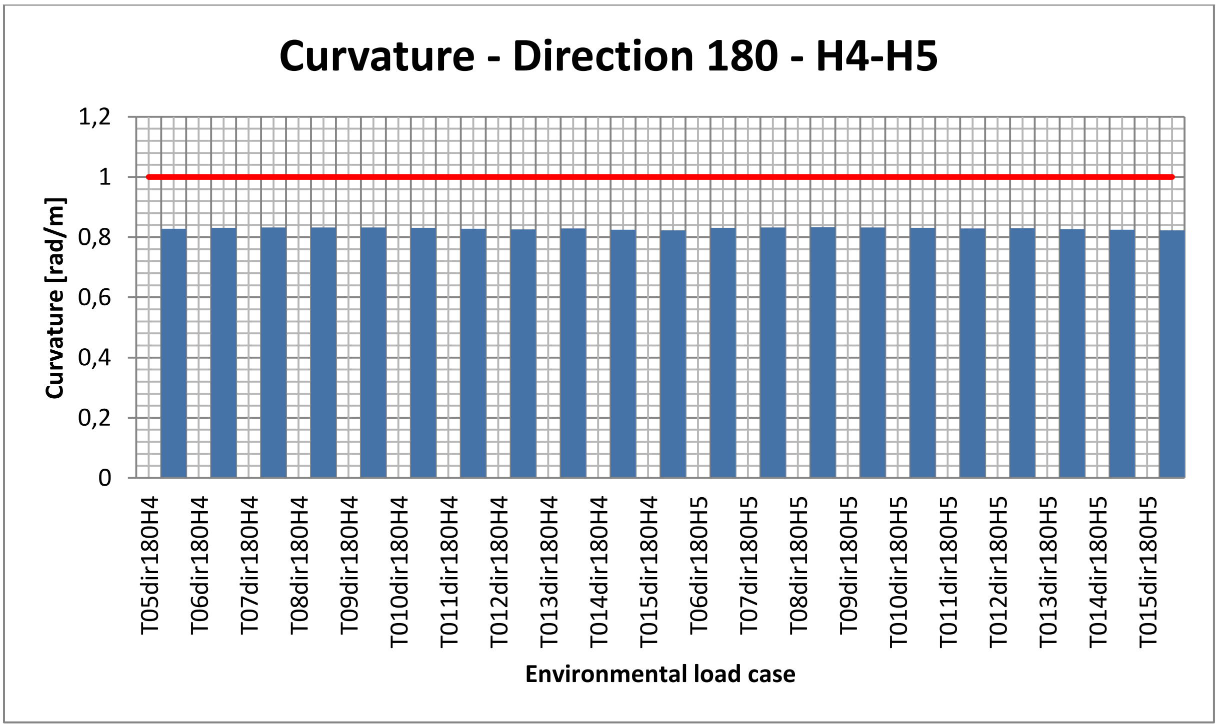

Figure D. 38 - 4"Bunkerflex STH - Free hanging - Curvature - Direction 180° - H4-H5 - Current 90°

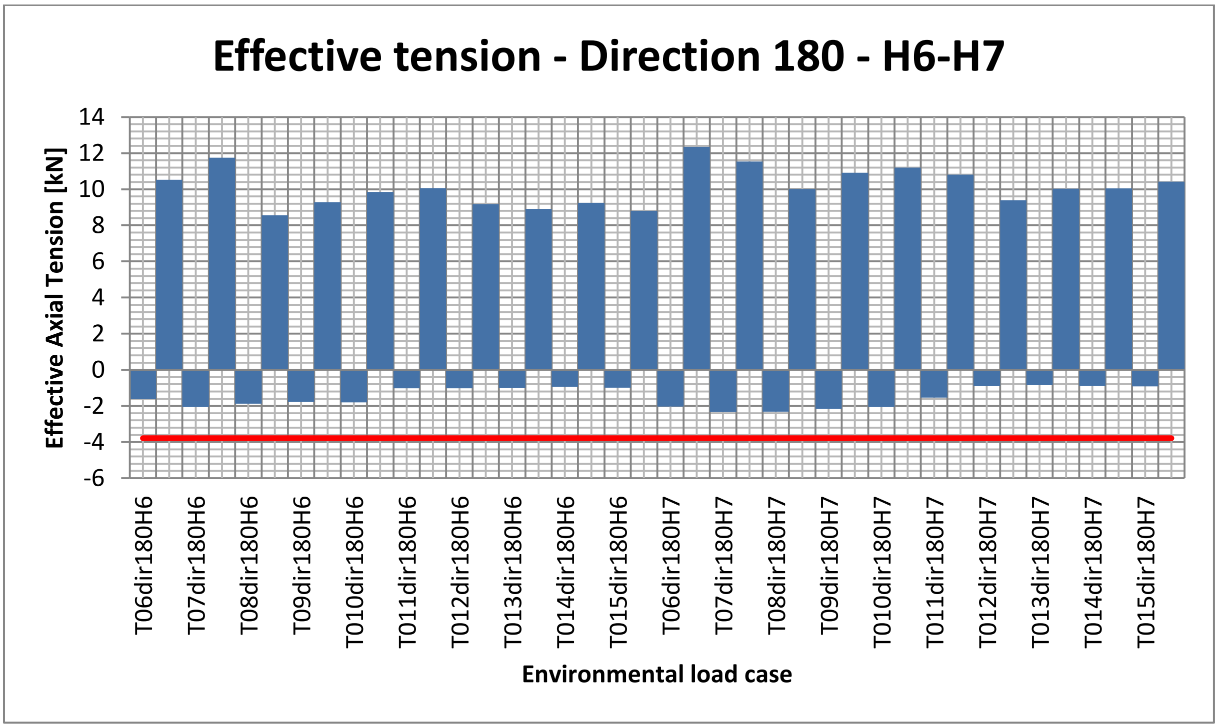

Figure D. 39 - 4"Bunkerflex STH - Free hanging - Effective tension - Direction 180° - H6-H7 - Current 90°

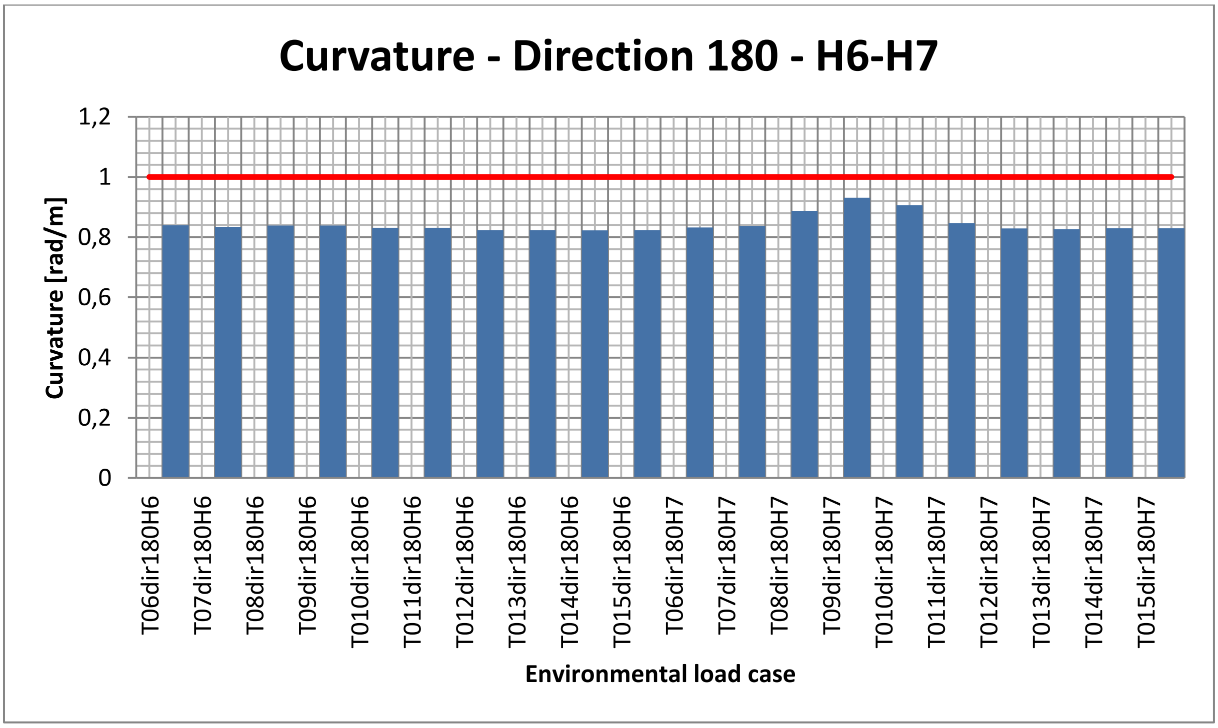

Figure D. 40 - 4"Bunkerflex STH - Free hanging - Curvature - Direction 180° - H6-H7 - Current 90°

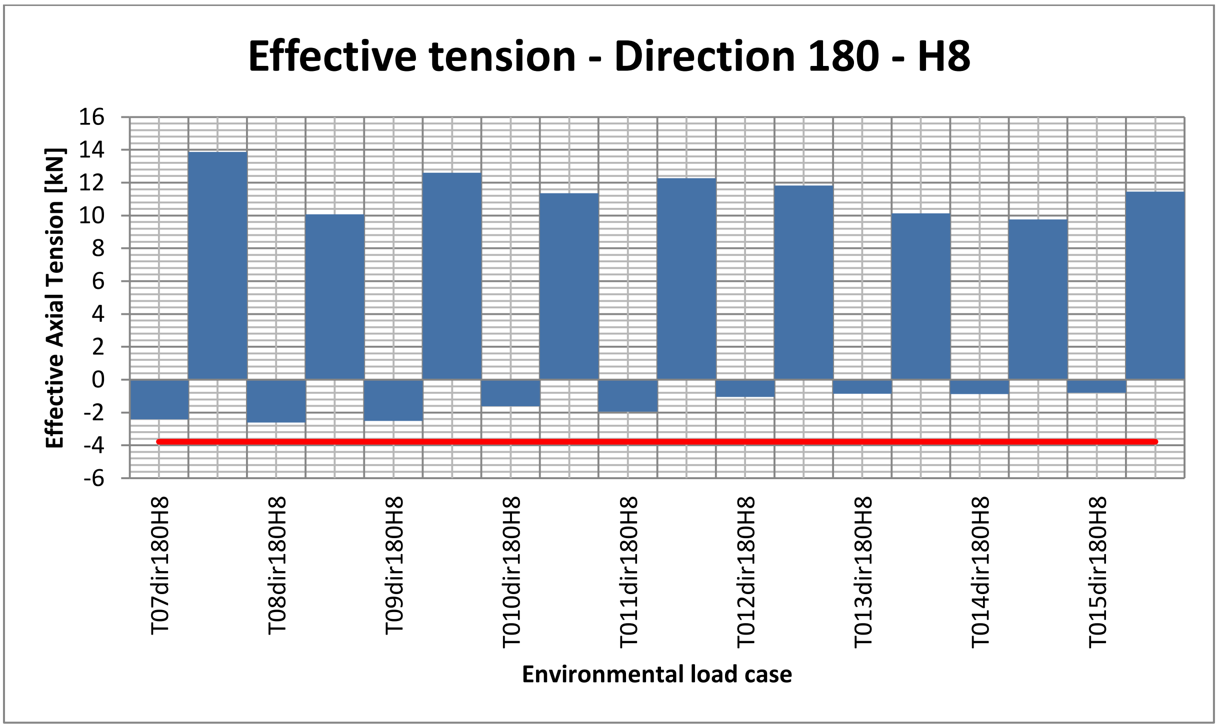

Figure D. 41 - 4"Bunkerflex STH - Free hanging - Effective tension - Direction 180° - H8 - Current 90°

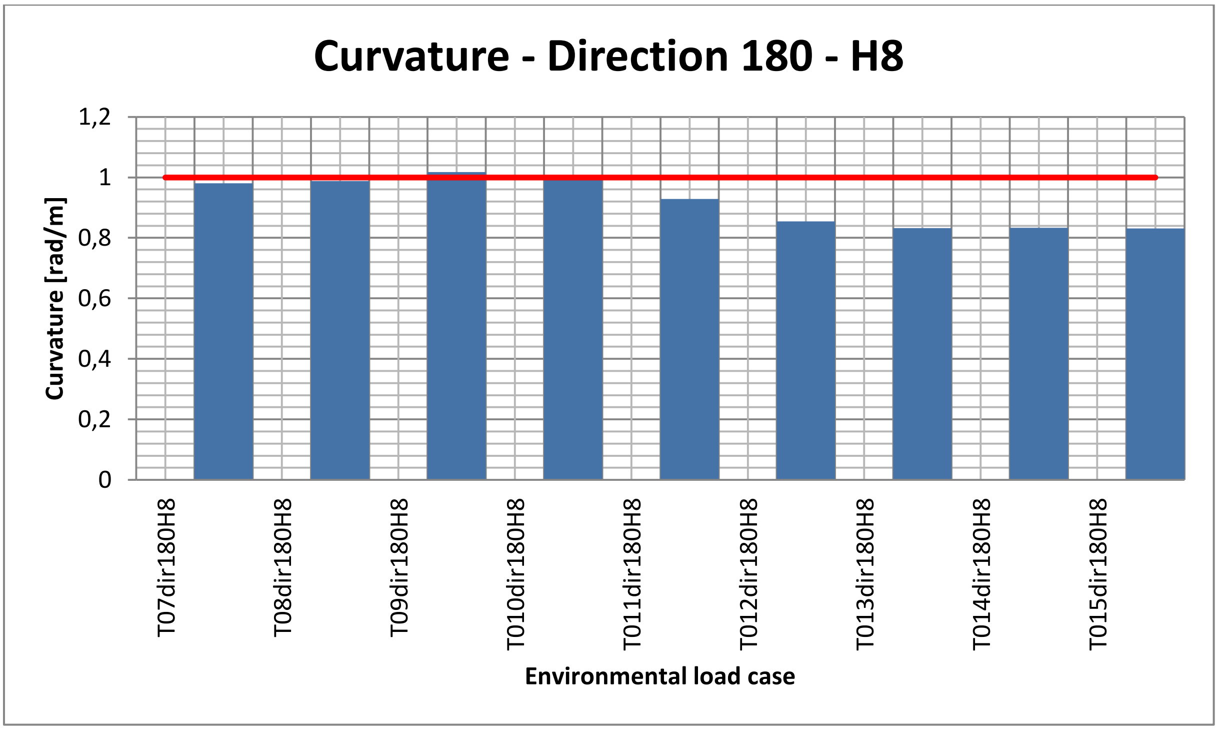

Figure D. 42 - 4"Bunkerflex STH - Free hanging - Curvature - Direction 180° - H8 - Current 90°

Direction 225°

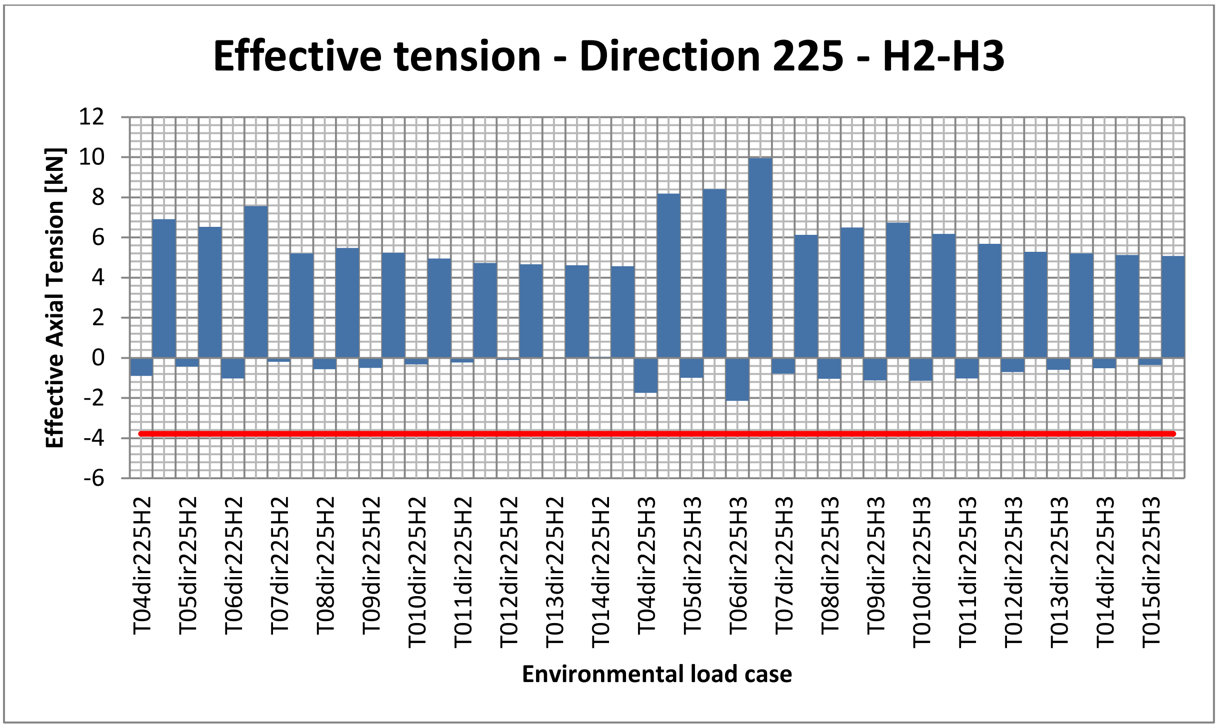

Figure D. 43 - 4"Bunkerflex STH - Free hanging - Effective tension - Direction 225° - H2-H3 - Current 90°

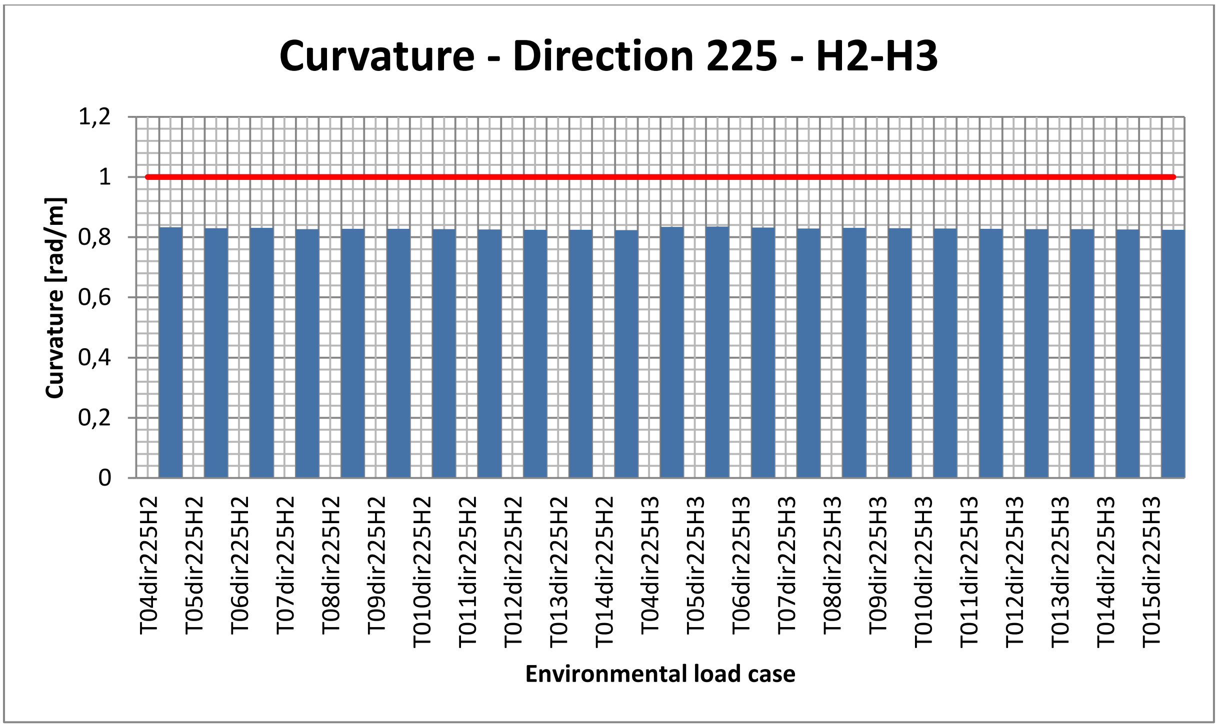

Figure D. 44 - 4"Bunkerflex STH - Free hanging - Curvature - Direction 225° - H2-H3 - Current 90°

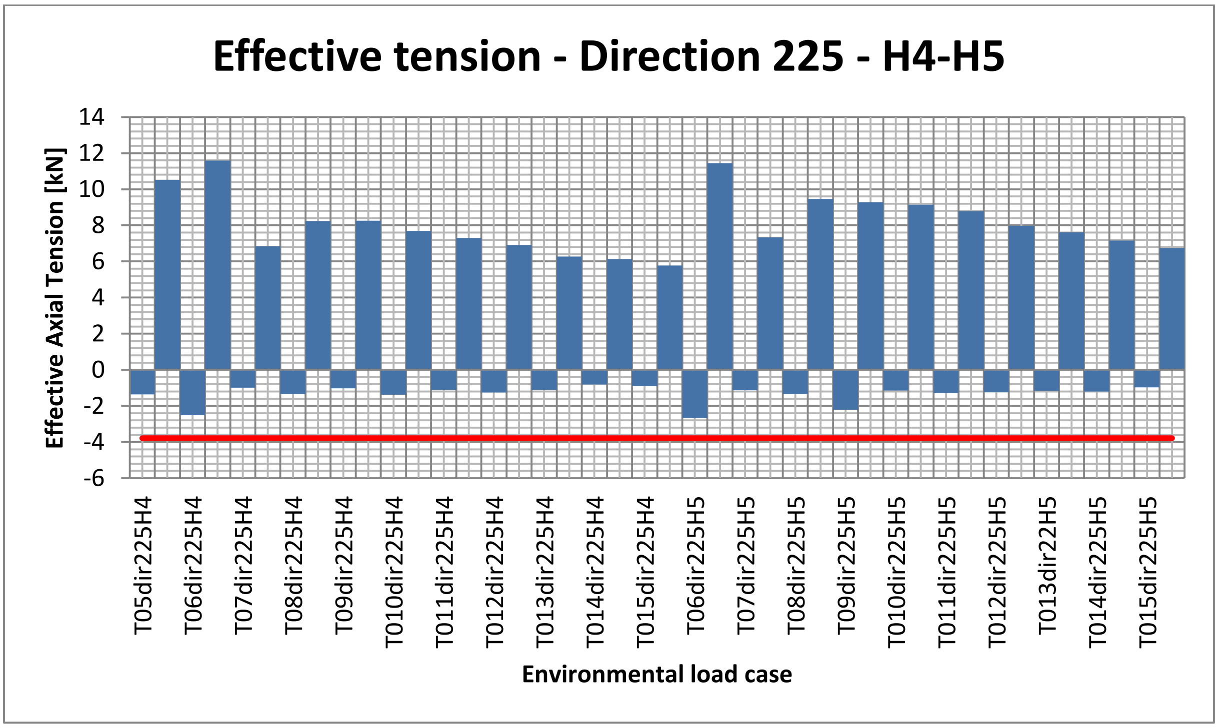

Figure D. 45 - 4"Bunkerflex STH - Free hanging - Effective tension - Direction 225° - H4-H5 - Current 90°

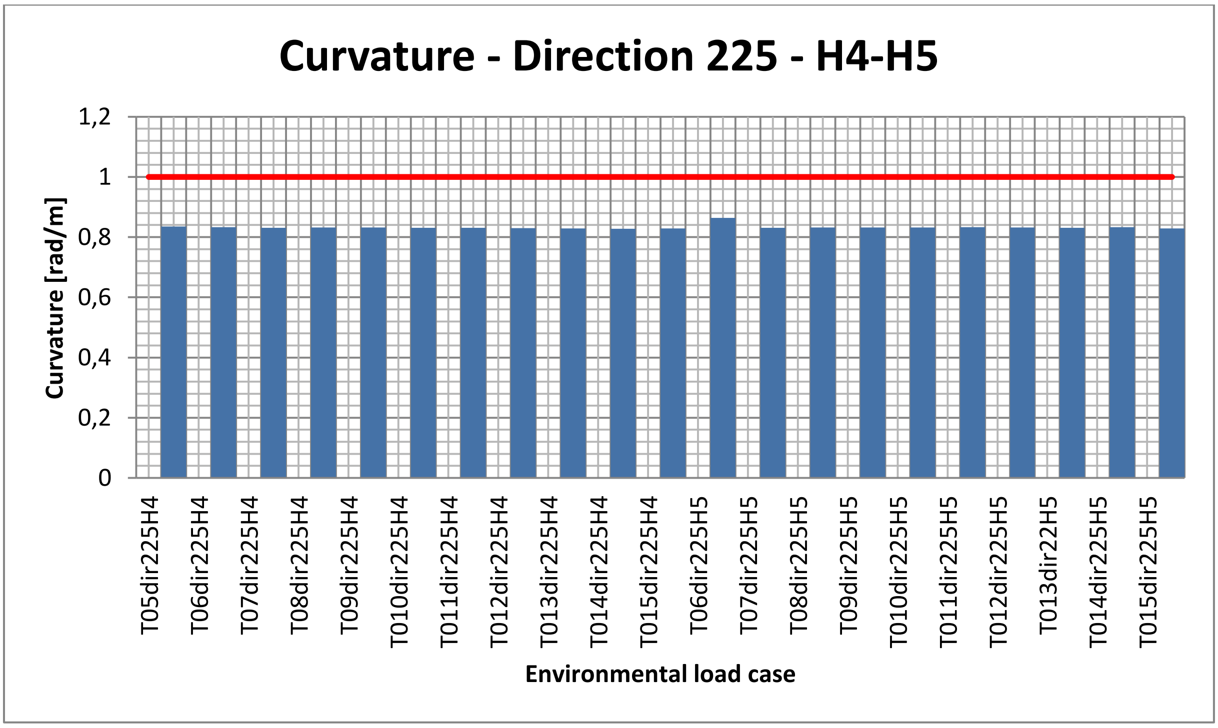

Figure D. 46 - 4"Bunkerflex STH - Free hanging - Curvature - Direction 225° - H4-H5 - Current 90°

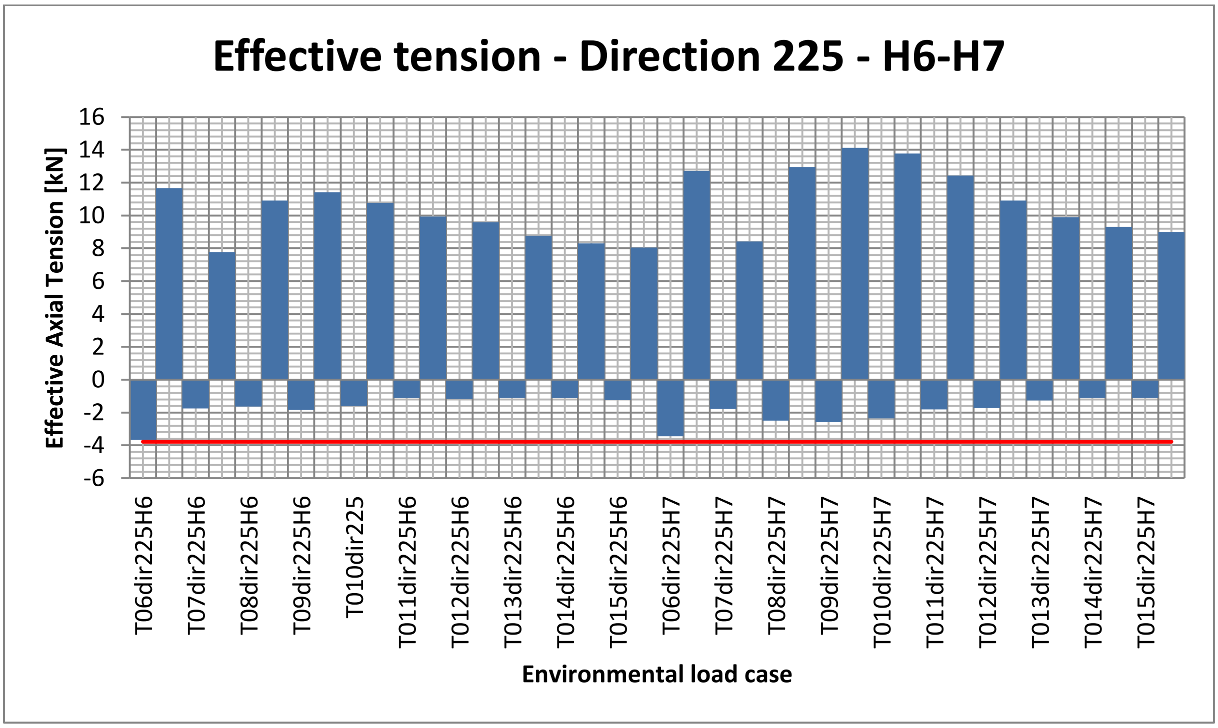

Figure D. 47 - 4"Bunkerflex STH - Free hanging - Effective tension - Direction 225° - H6-H7 - Current 90°

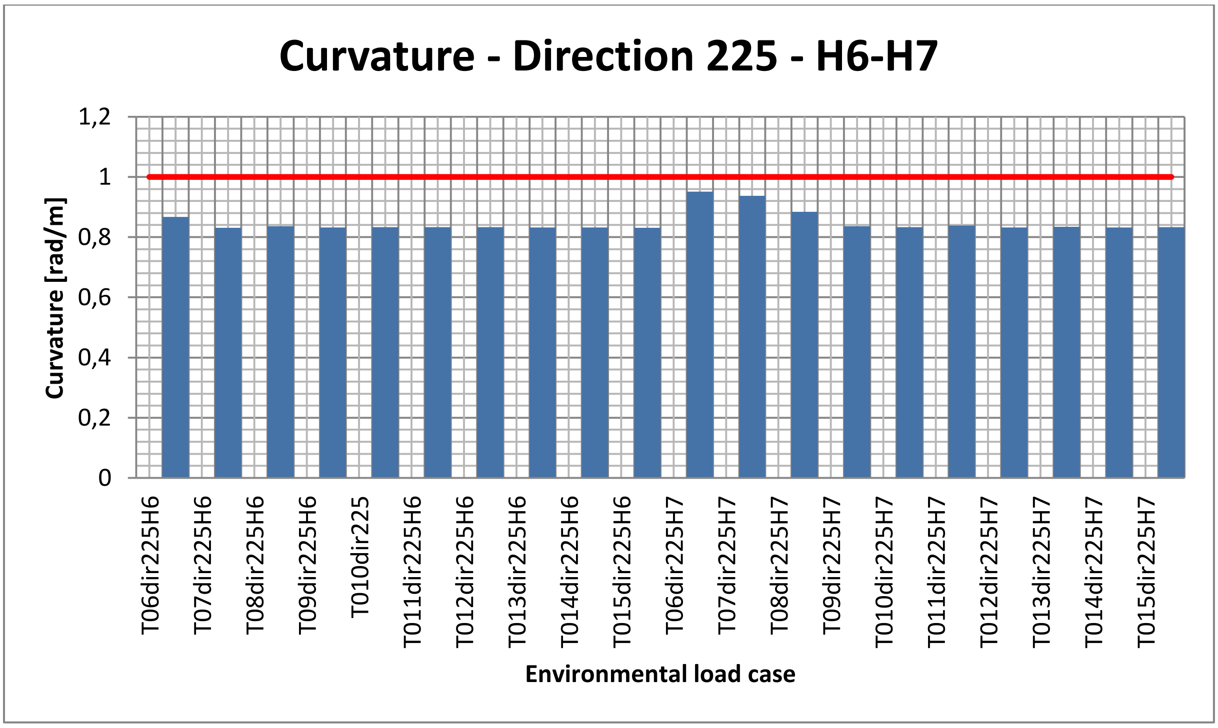

Figure D. 48 - 4"Bunkerflex STH - Free hanging - Curvature - Direction 225° - H6-H7 - Current 90°

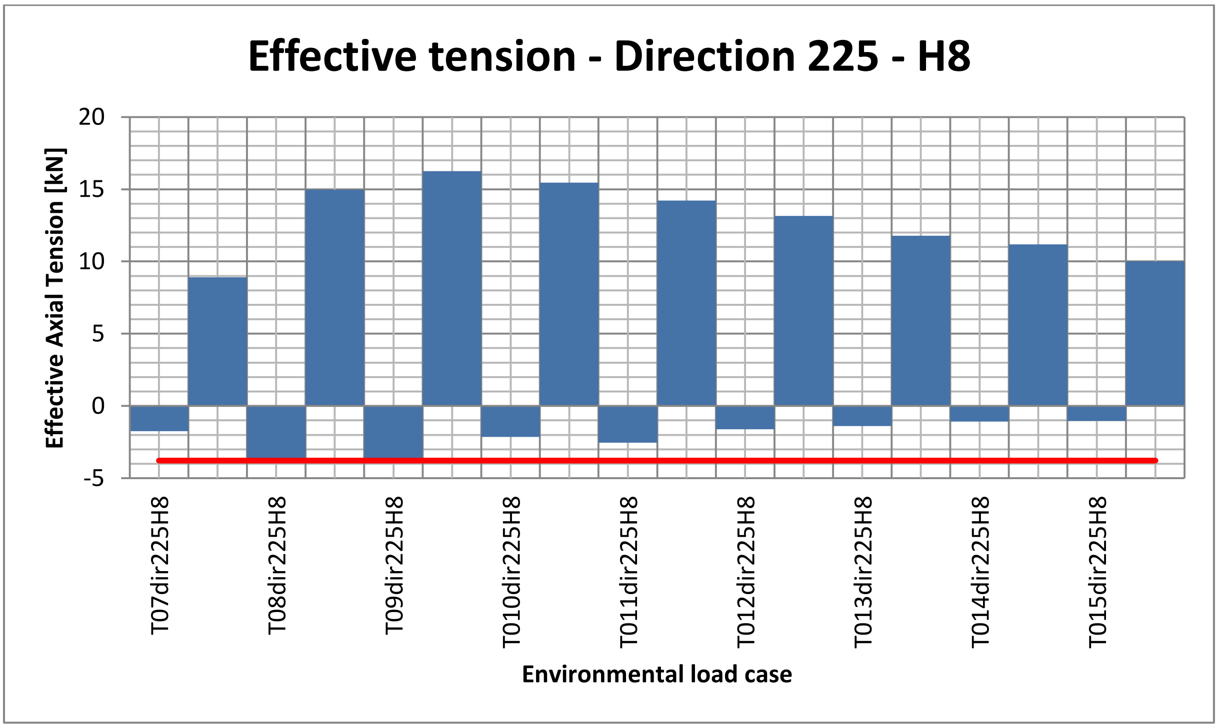

Figure D. 49 - 4"Bunkerflex STH - Free hanging - Effective tension - Direction 225° - H8 - Current 90°

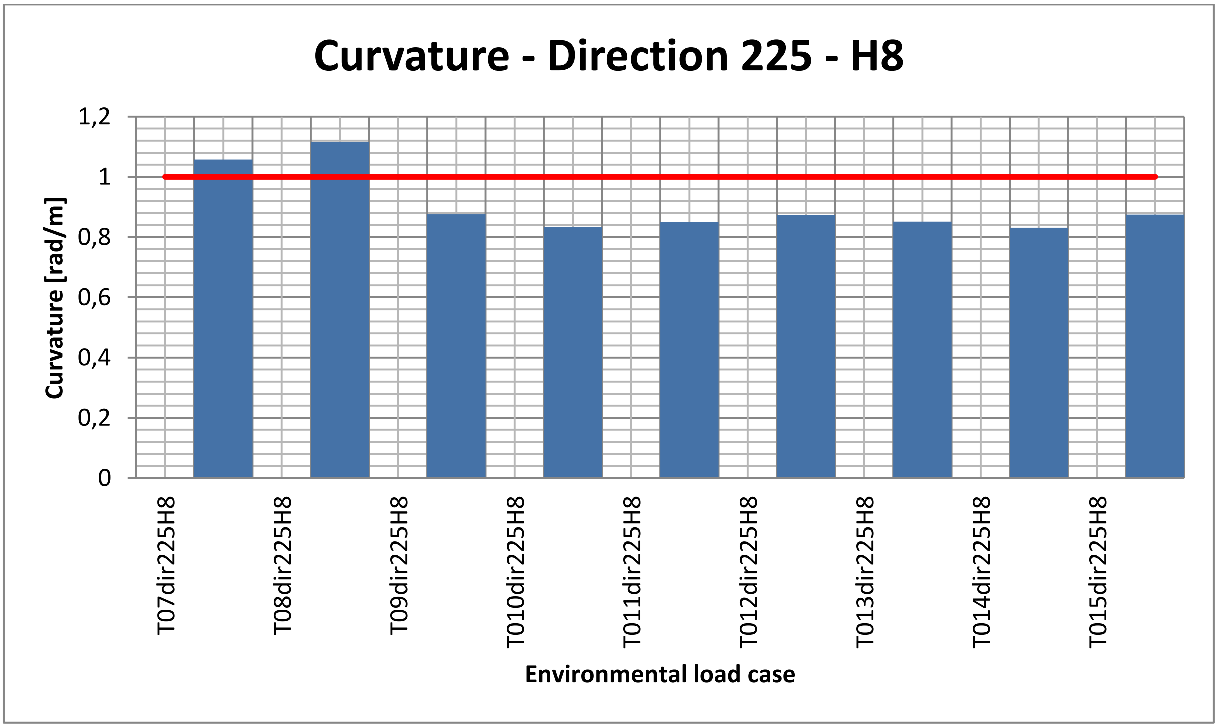

Figure D. 50 - 4"Bunkerflex STH - Free hanging - Curvature - Direction 225° - H8 - Current 90°

Wave rose

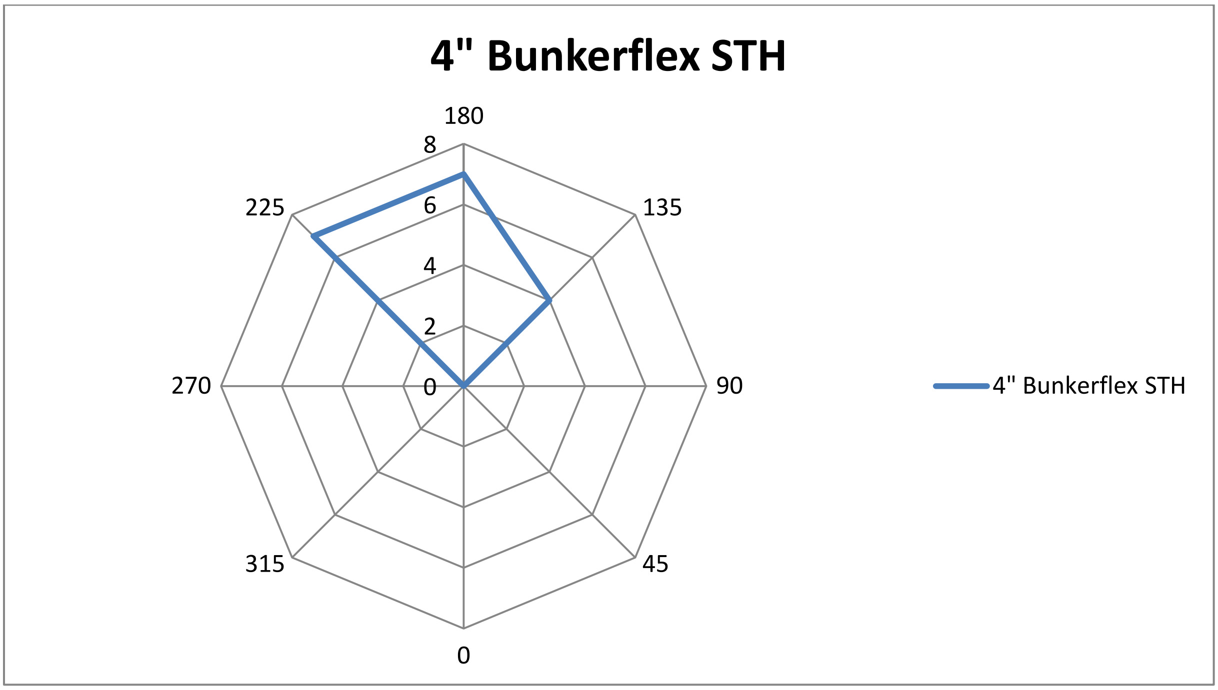

Figure D. 51 - 4" Bunkerflex STH - Free hanging - Wave rose - Current 90°

Free hanging - 180° direction current

Wave direction 135°

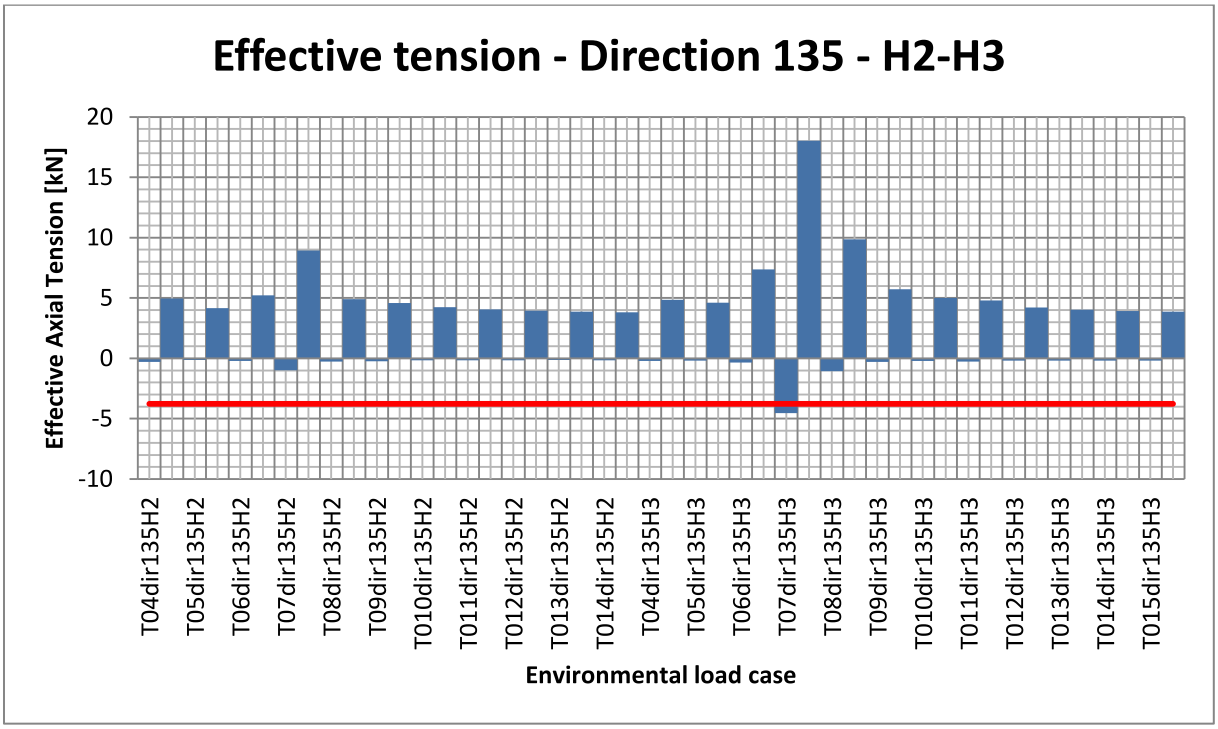

Figure D. 52 - 4"Bunkerflex STH - Free hanging - Effective tension - Direction 135° - H2-H3 - Current 180°

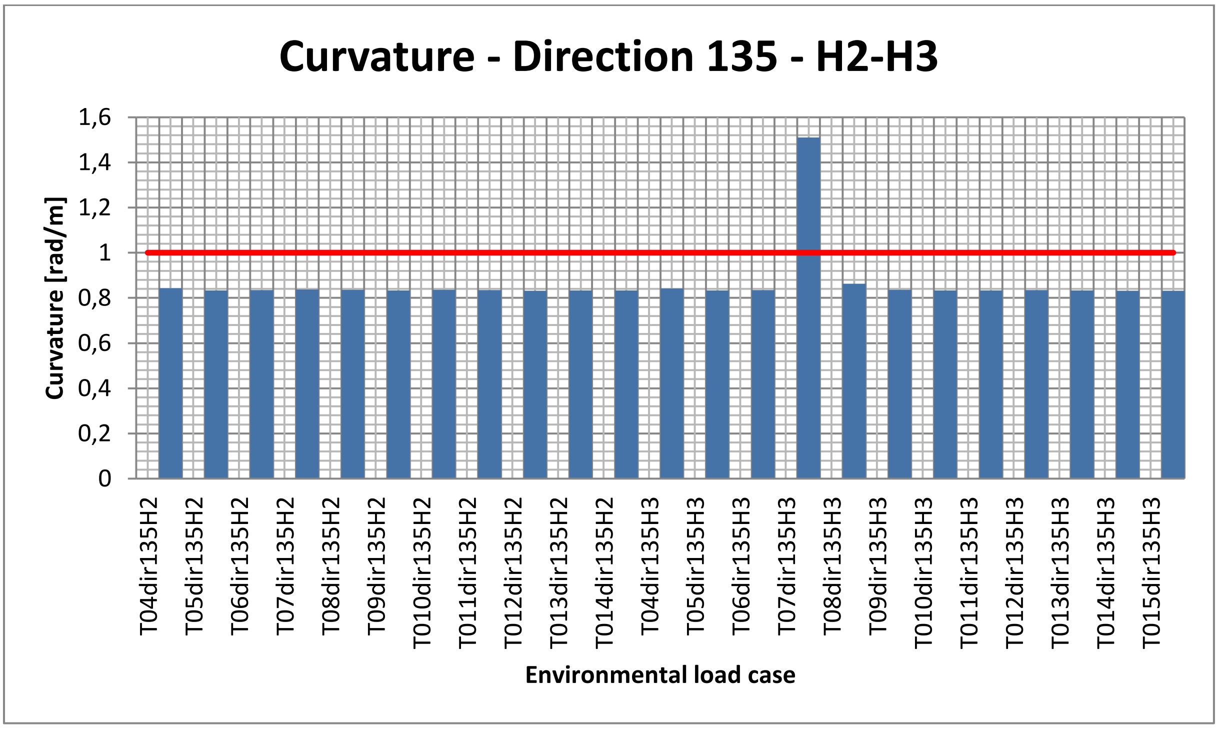

Figure D. 53 - 4"Bunkerflex STH - Free hanging - Curvature - Direction 135° - H2-H3 - Current 180°

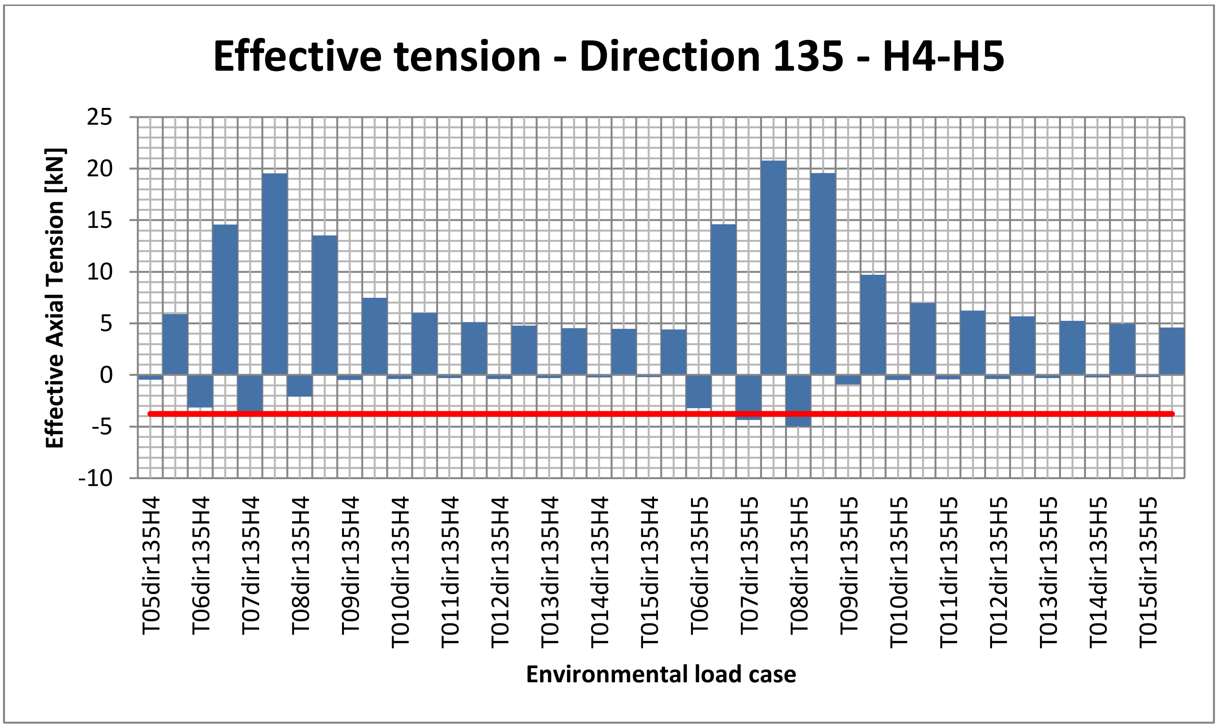

Figure D. 54 - 4"Bunkerflex STH - Free hanging - Effective tension - Direction 135° - H4-H5 - Current 180°

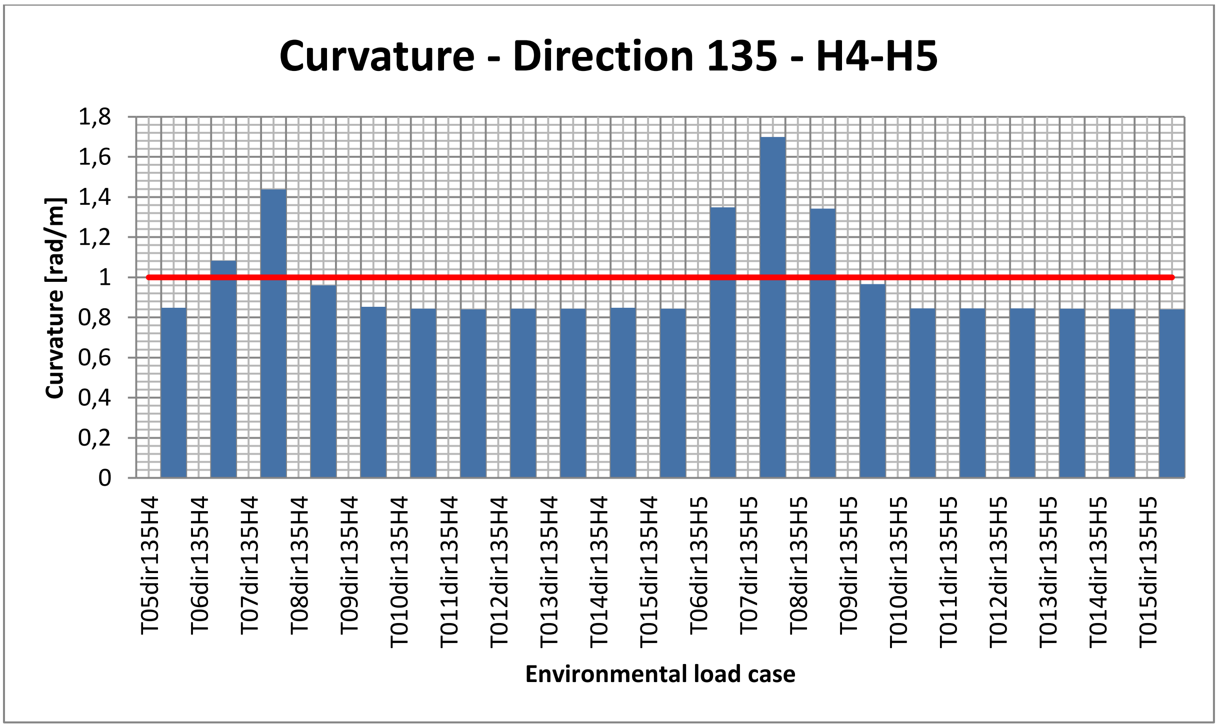

Figure D. 55 - 4"Bunkerflex STH - Free hanging - Curvature - Direction 135° - H4-H5 - Current 180°

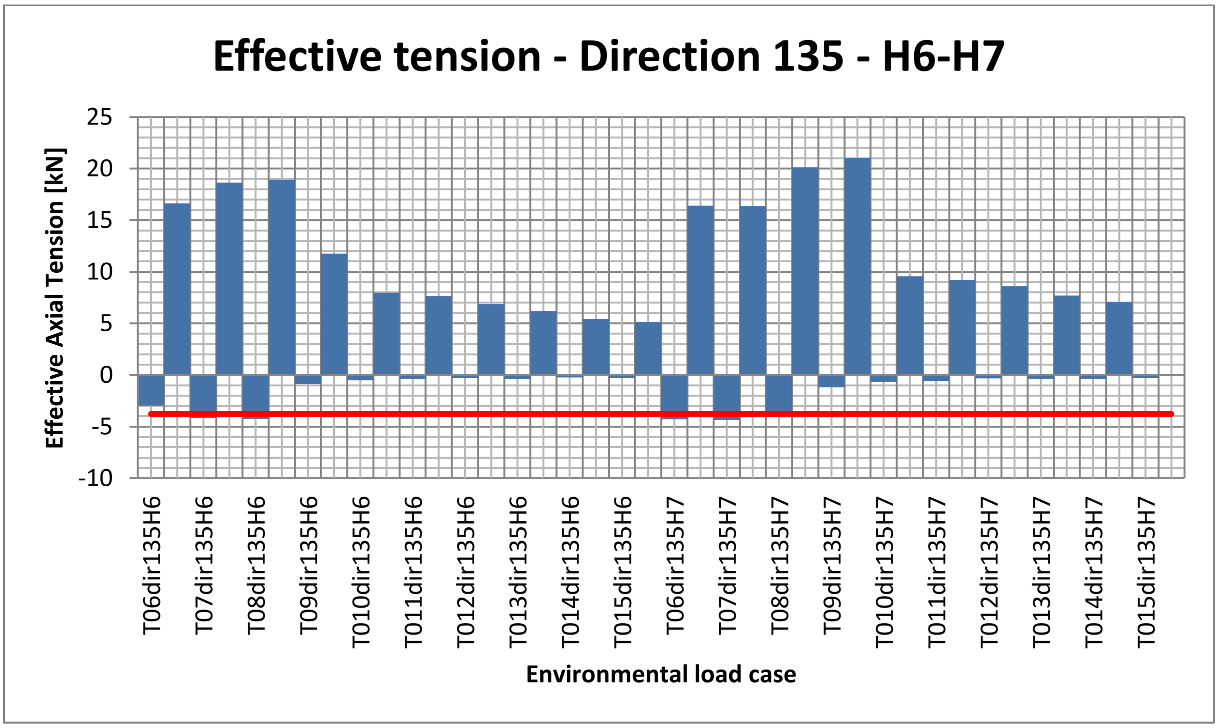

Figure D. 56 - 4"Bunkerflex STH - Free hanging - Effective tension - Direction 135° - H6-H7 - Current 180°

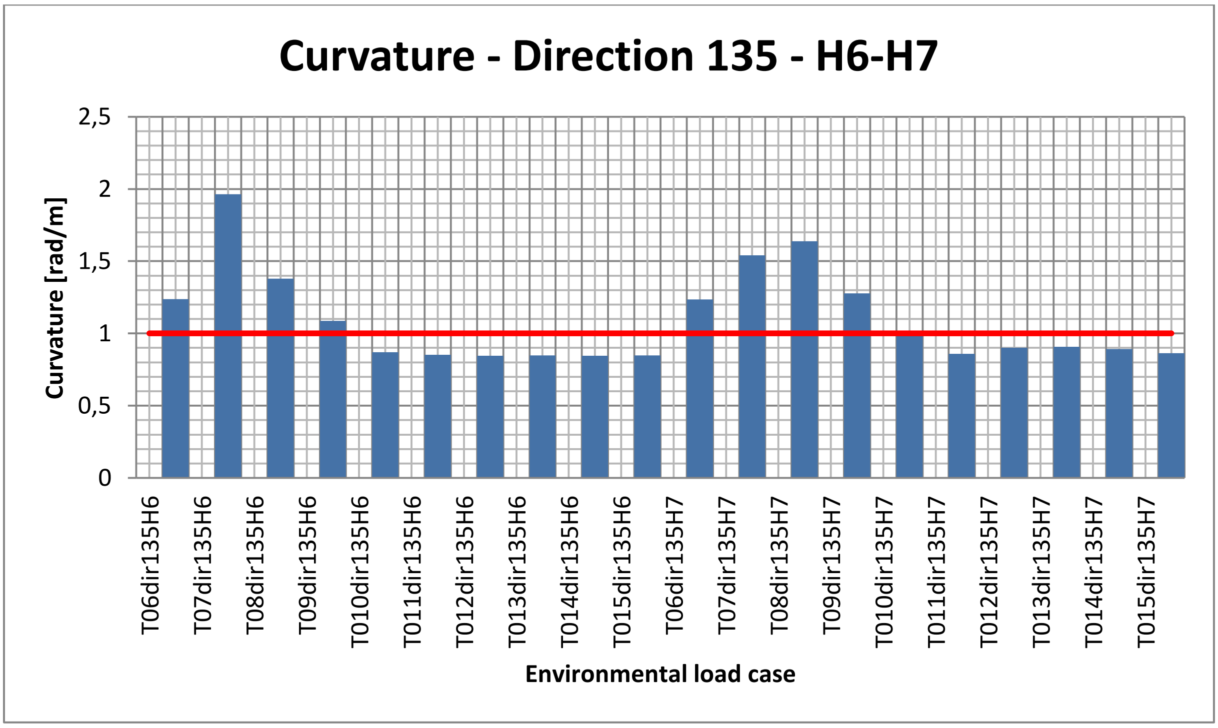

Figure D. 57 - 4"Bunkerflex STH - Free hanging - Curvature - Direction 135° - H6-H7 - Current 180°

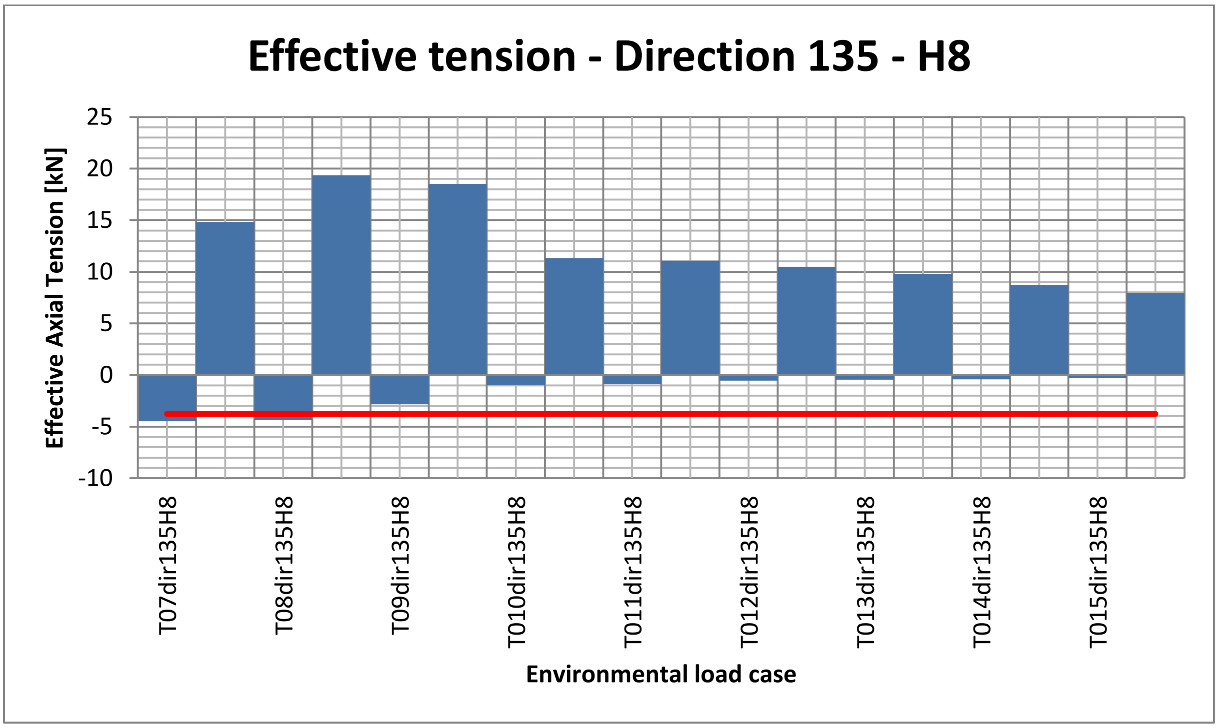

Figure D. 58 - 4"Bunkerflex STH - Free hanging - Effective tension - Direction 135° - H8 - Current 180°

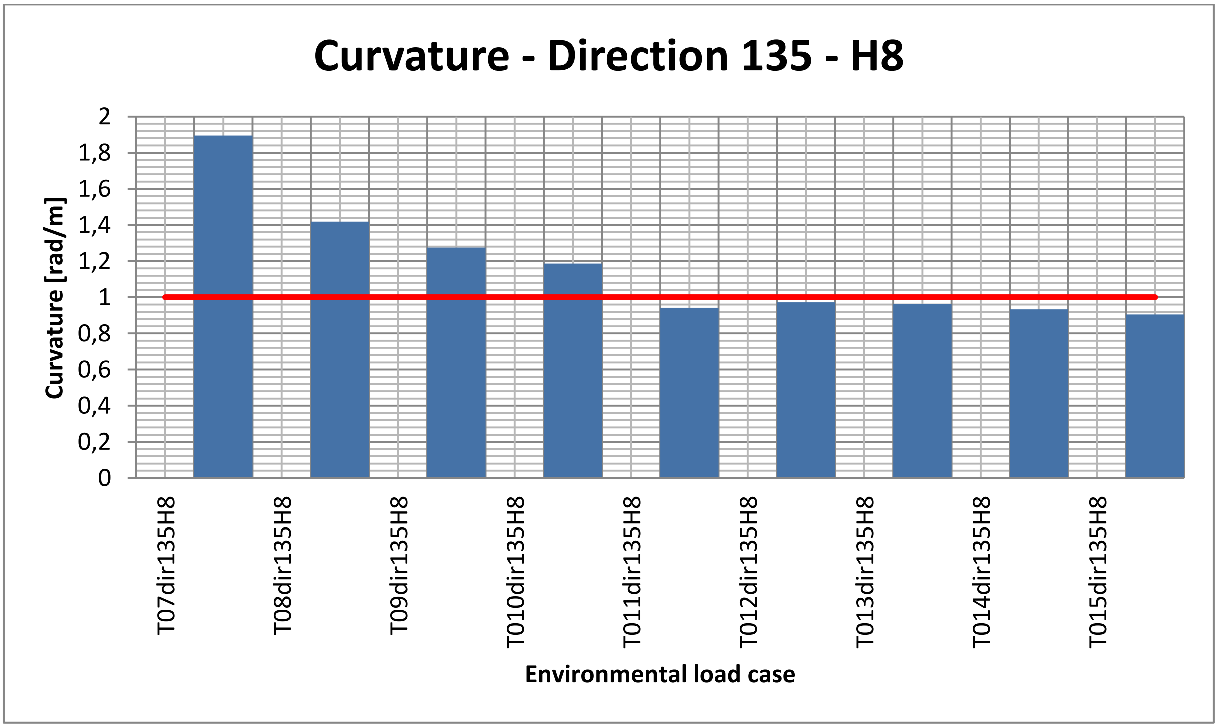

Figure D. 59 - 4"Bunkerflex STH - Free hanging - Curvature - Direction 135° - H8 - Current 180°

Direction 180°

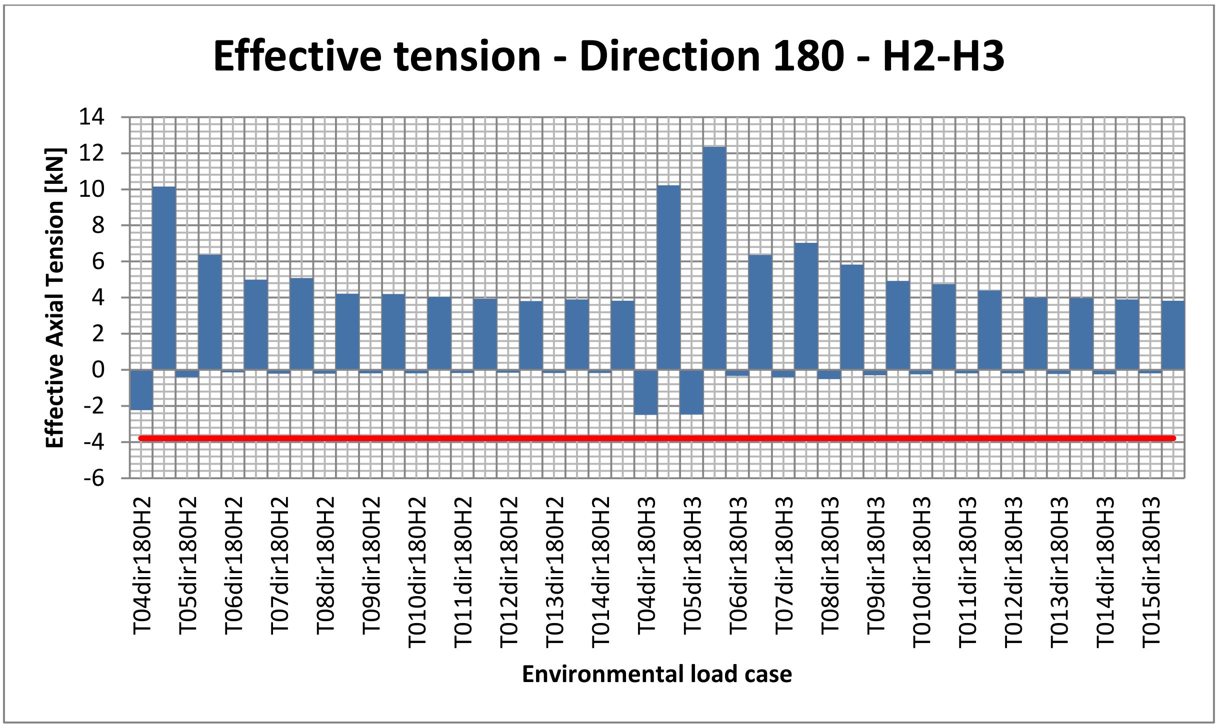

Figure D. 60 - 4"Bunkerflex STH - Free hanging - Effective tension - Direction 180° - H2-H3 - Current 180°

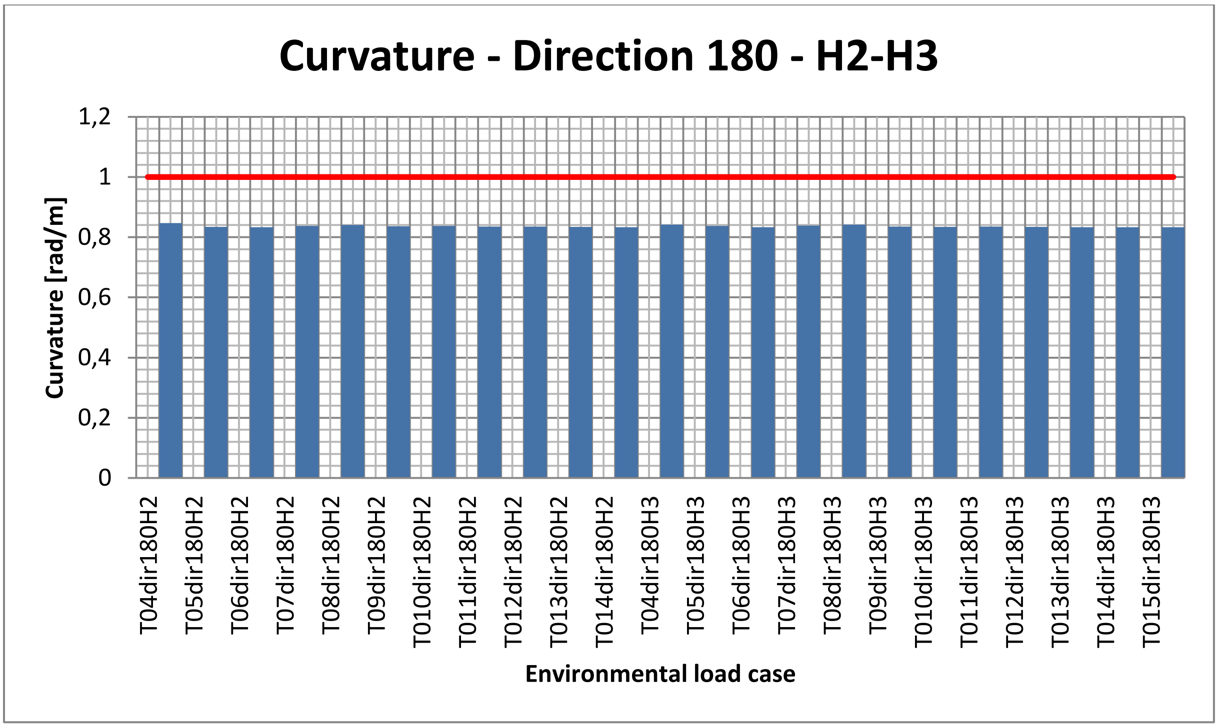

Figure D. 61 - 4"Bunkerflex STH - Free hanging - Curvature - Direction 180° - H2-H3 - Current 180°

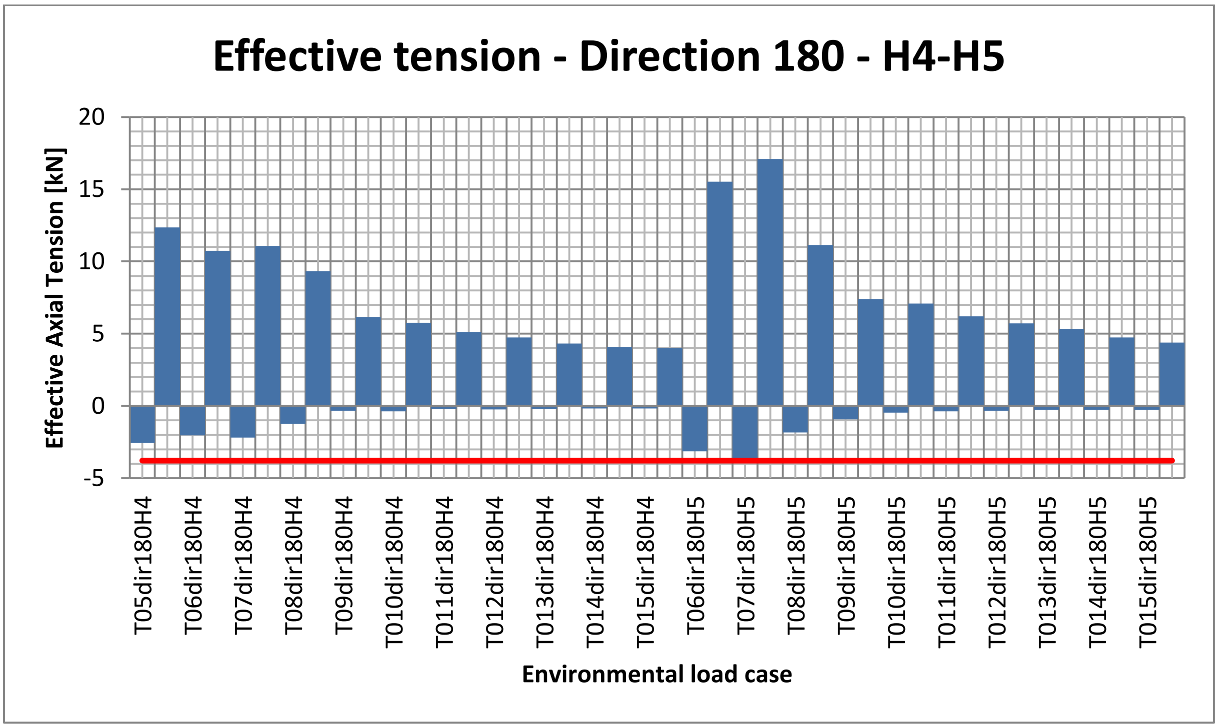

Figure D. 62 - 4"Bunkerflex STH - Free hanging - Effective tension - Direction 180° - H4-H5 - Current 180°

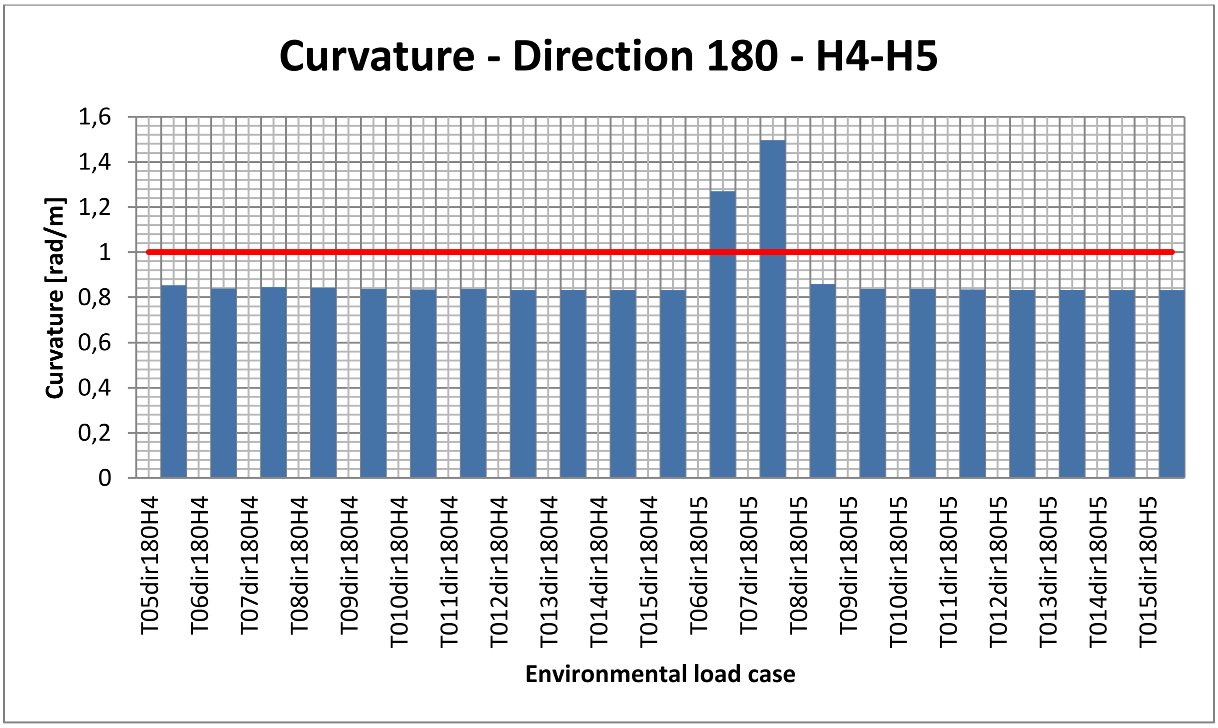

Figure D. 63 - 4"Bunkerflex STH - Free hanging - Curvature - Direction 180° - H4-H5 - Current 180°

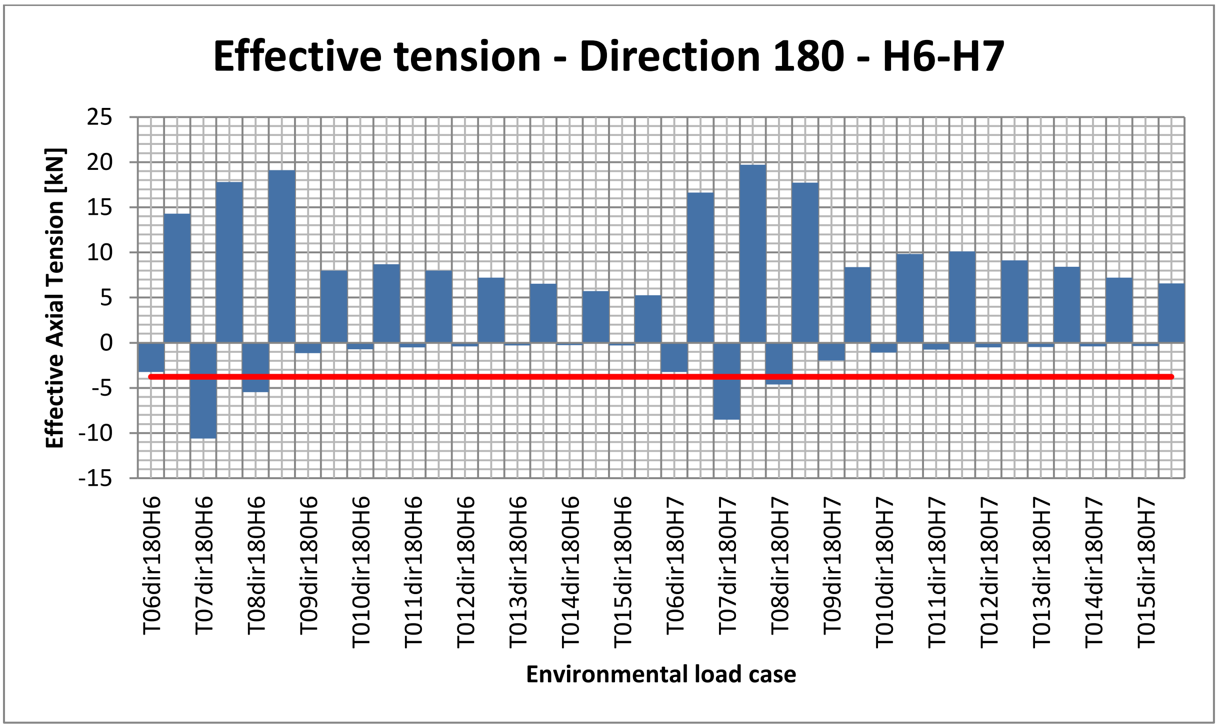

Figure D. 64 - 4"Bunkerflex STH - Free hanging - Effective tension - Direction 180° - H6-H7 - Current 180°

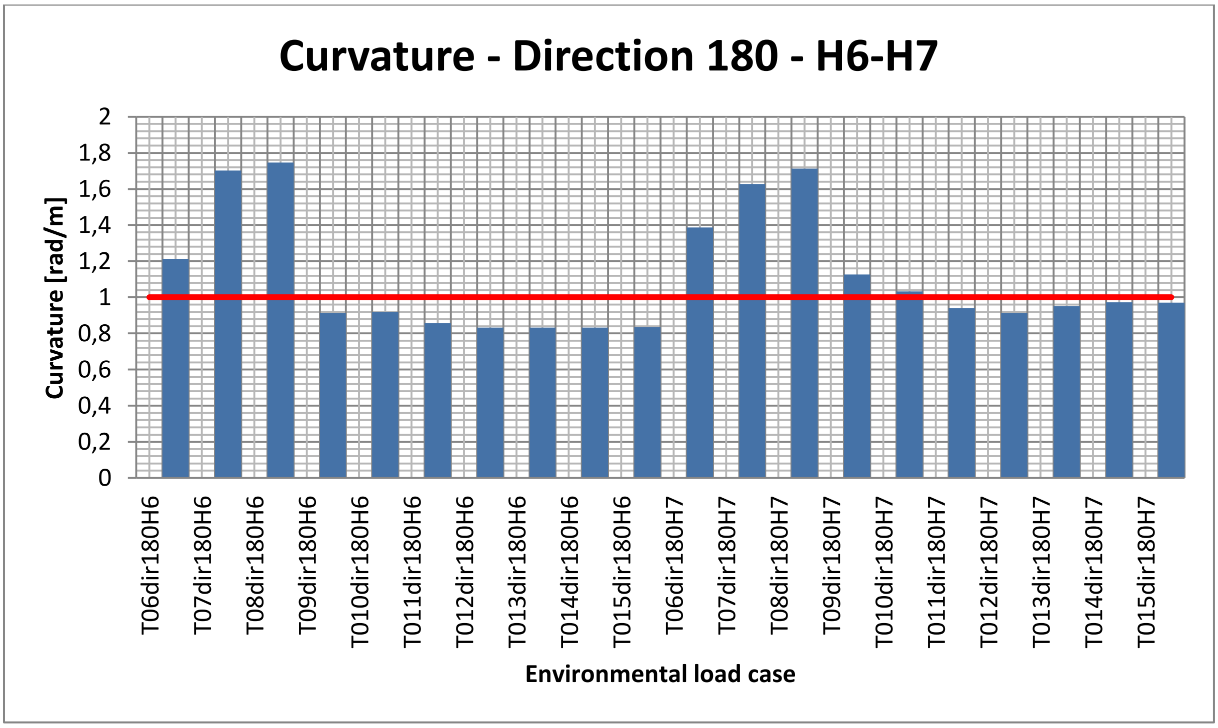

Figure D. 65 - 4"Bunkerflex STH - Free hanging - Curvature - Direction 180° - H6-H7 - Current 180°

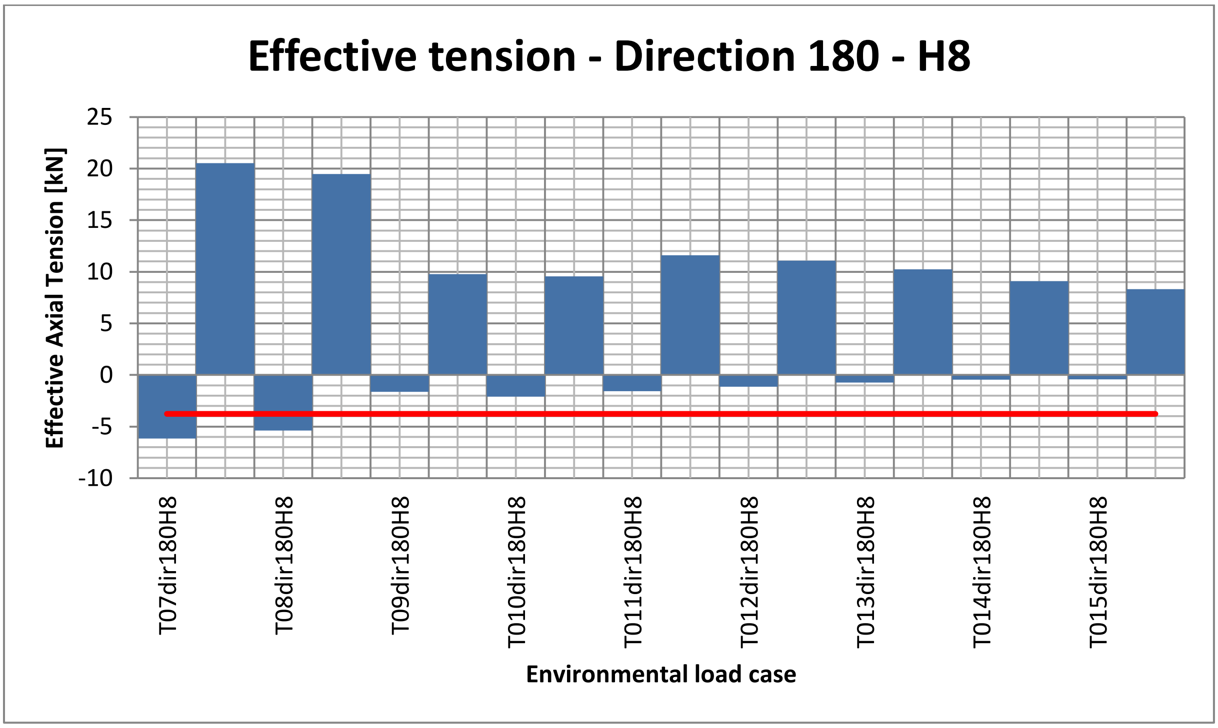

Figure D. 66 - 4"Bunkerflex STH - Free hanging - Effective tension - Direction 180° - H8 - Current 180°

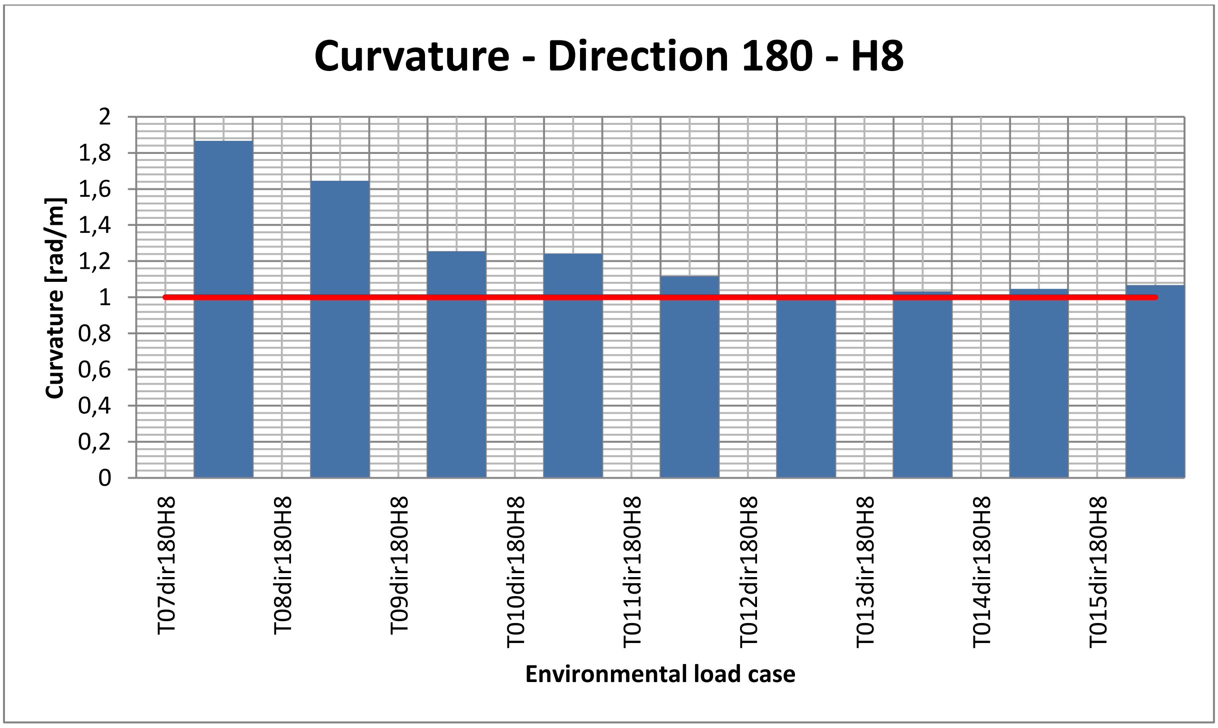

Figure D. 67 - 4"Bunkerflex STH - Free hanging - Curvature - Direction 180° - H8 - Current 180°

Direction 225°

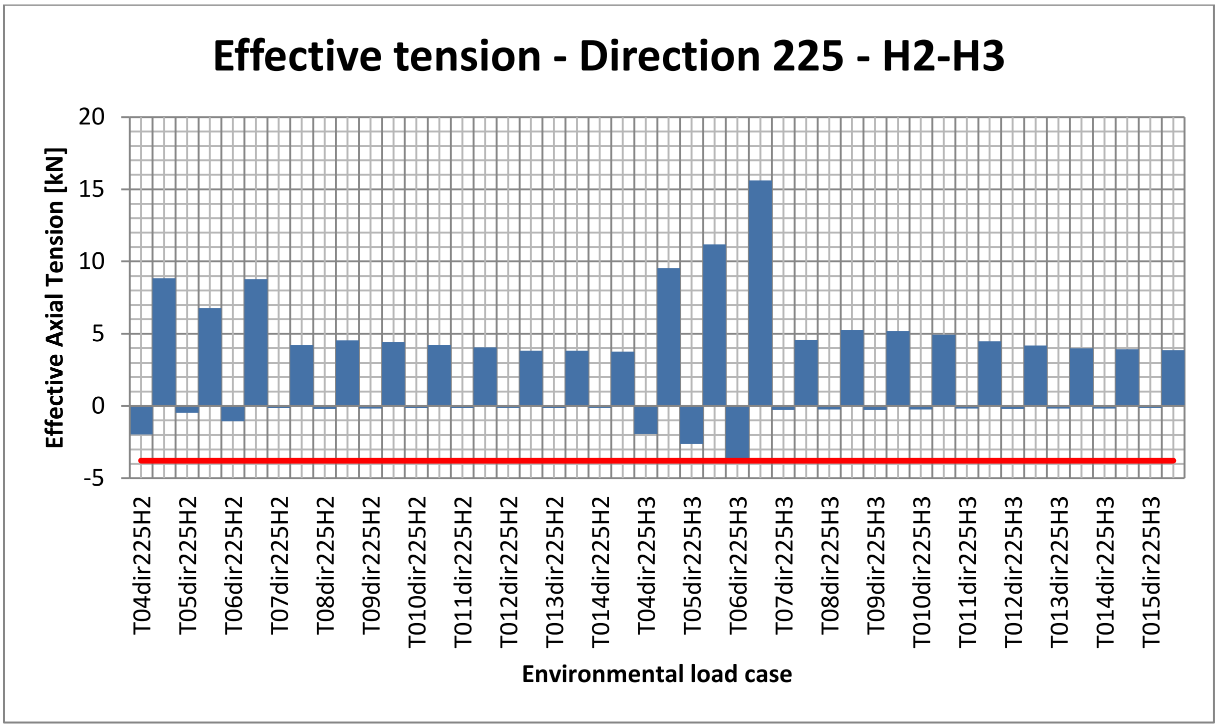

Figure D. 68 - 4"Bunkerflex STH - Free hanging - Effective tension - Direction 225° - H2-H3 - Current 180°

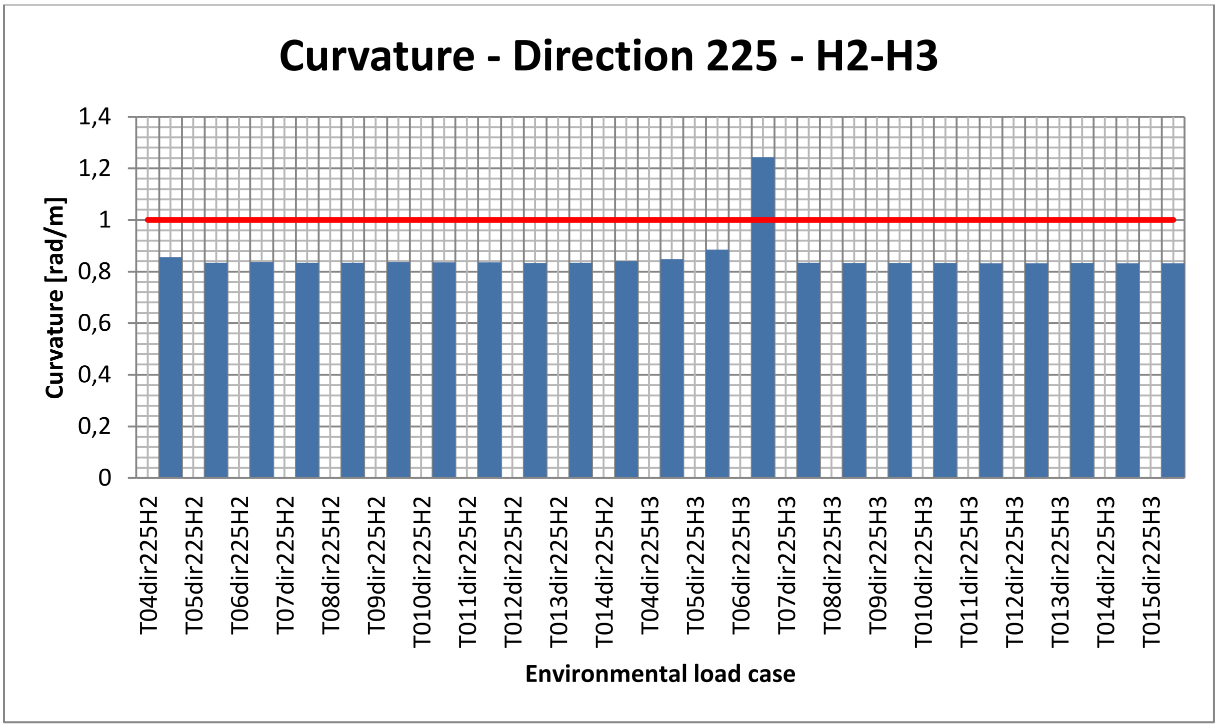

Figure D. 69 - 4"Bunkerflex STH - Free hanging - Curvature - Direction 225° - H2-H3 - Current 180°

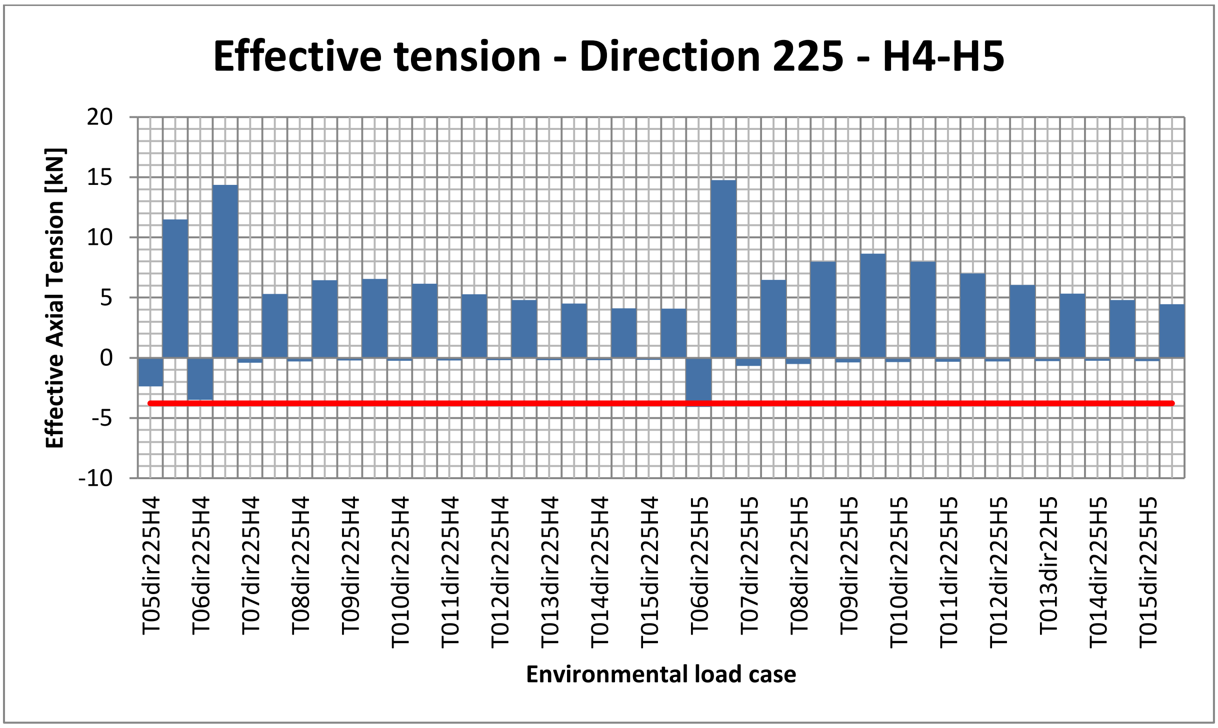

Figure D. 70 - 4"Bunkerflex STH - Free hanging - Effective tension - Direction 225° - H4-H5 - Current 180°

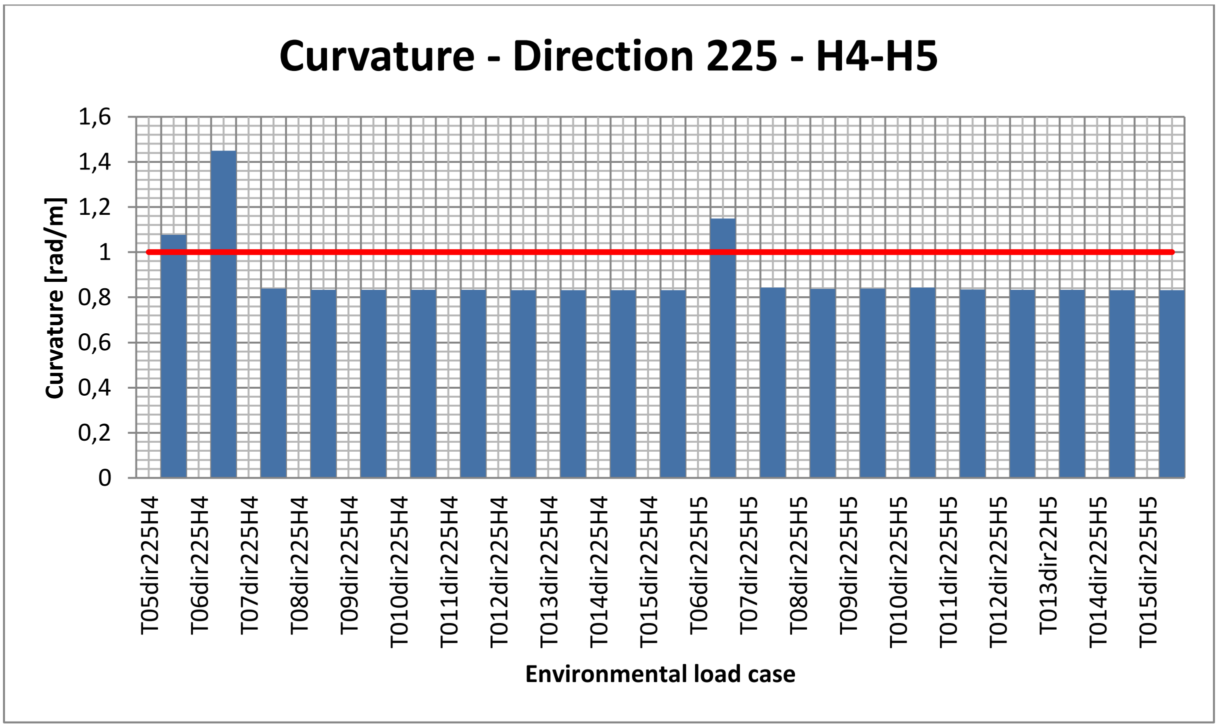

Figure D. 71 - 4"Bunkerflex STH - Free hanging - Curvature - Direction 225° - H4-H5 - Current 180°

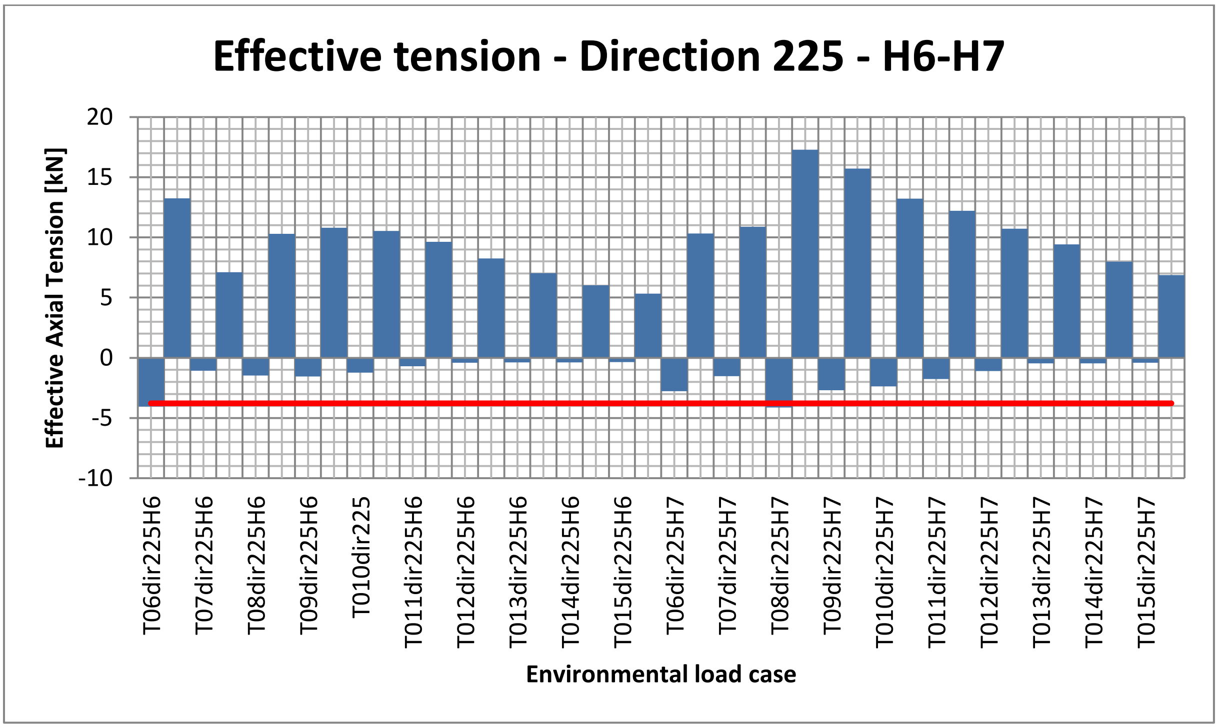

Figure D. 72 - 4"Bunkerflex STH - Free hanging - Effective tension - Direction 225° - H6-H7 - Current 180°

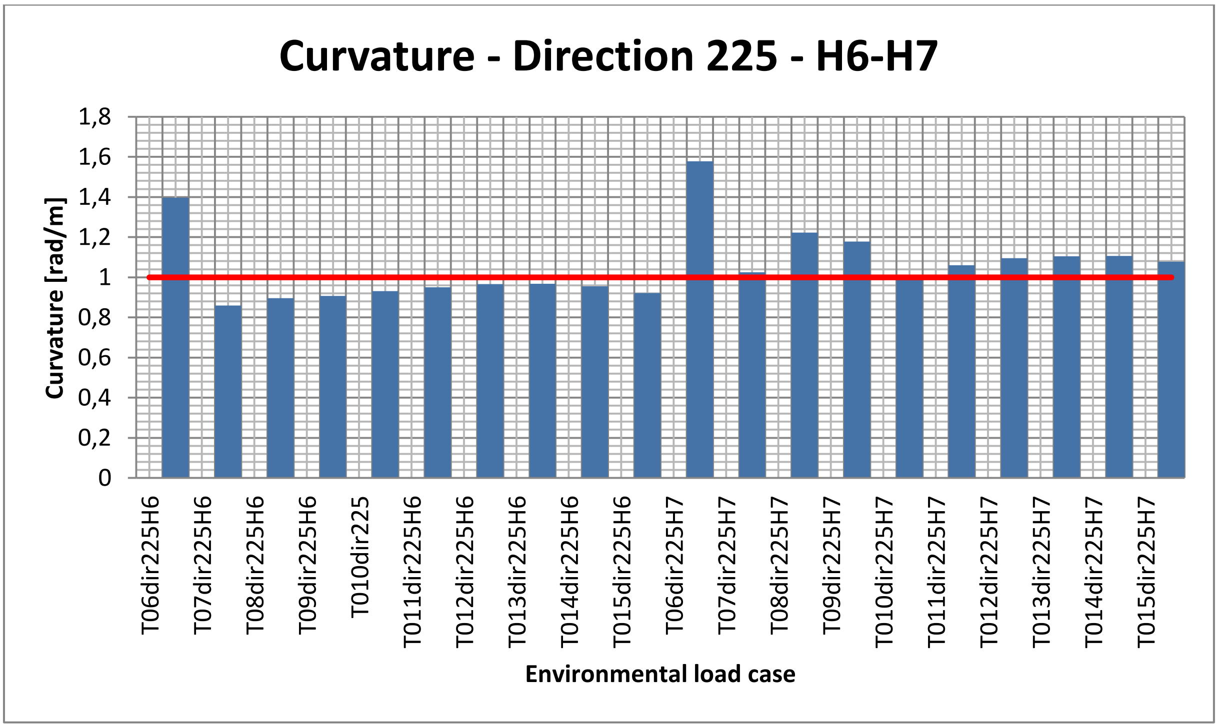

Figure D. 73 - 4"Bunkerflex STH - Free hanging - Curvature - Direction 225° - H6-H7 - Current 180°

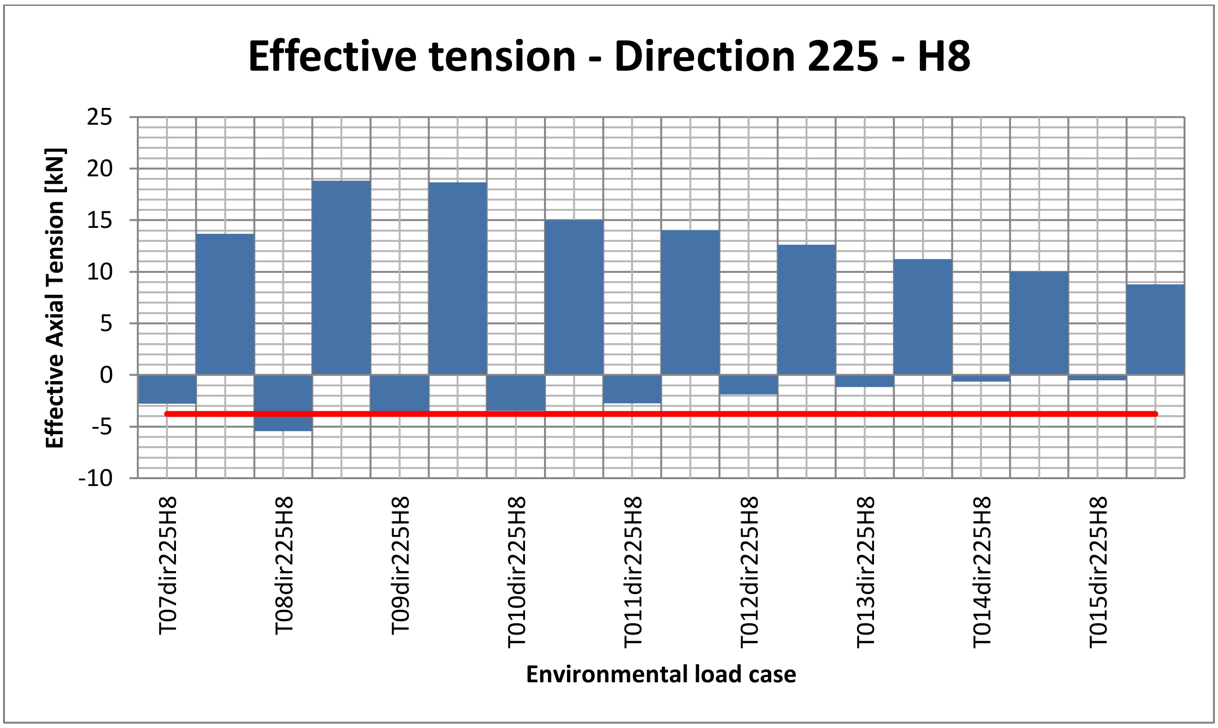

Figure D. 74 - 4"Bunkerflex STH - Free hanging - Effective tension - Direction 225° - H8 - Current 180°

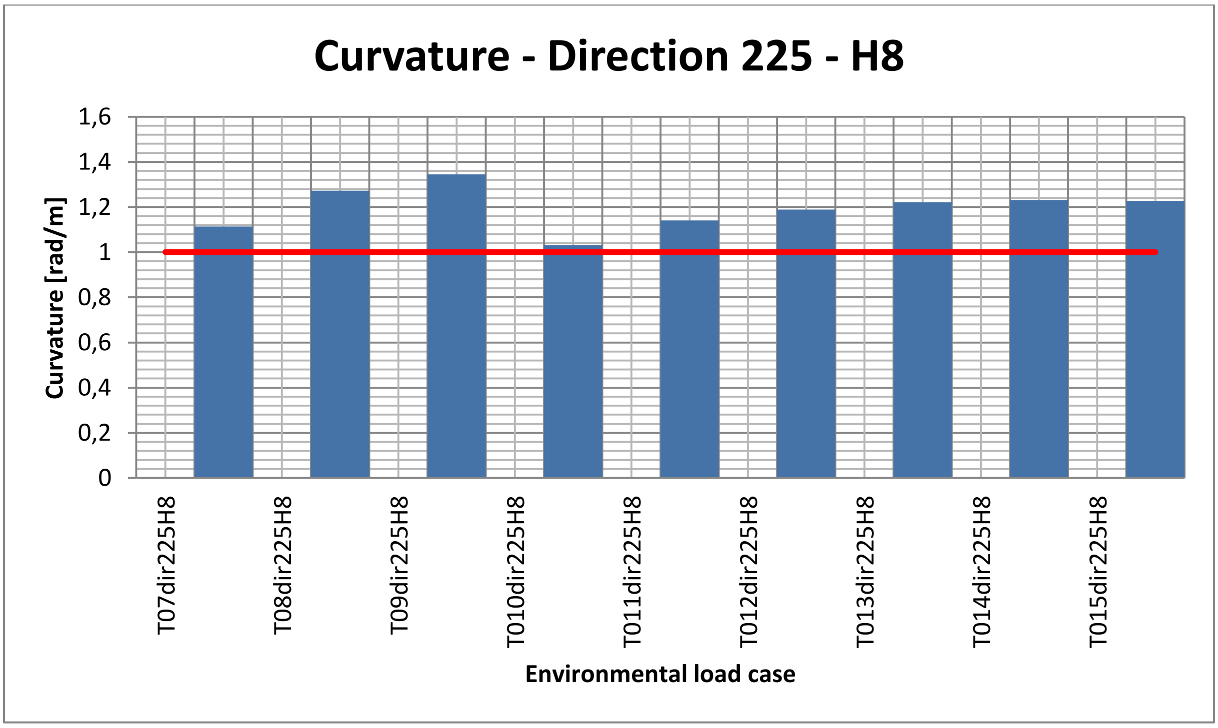

Figure D. 75 - 4"Bunkerflex STH - Free hanging - Curvature - Direction 225° - H8 - Current 180°

Wave rose

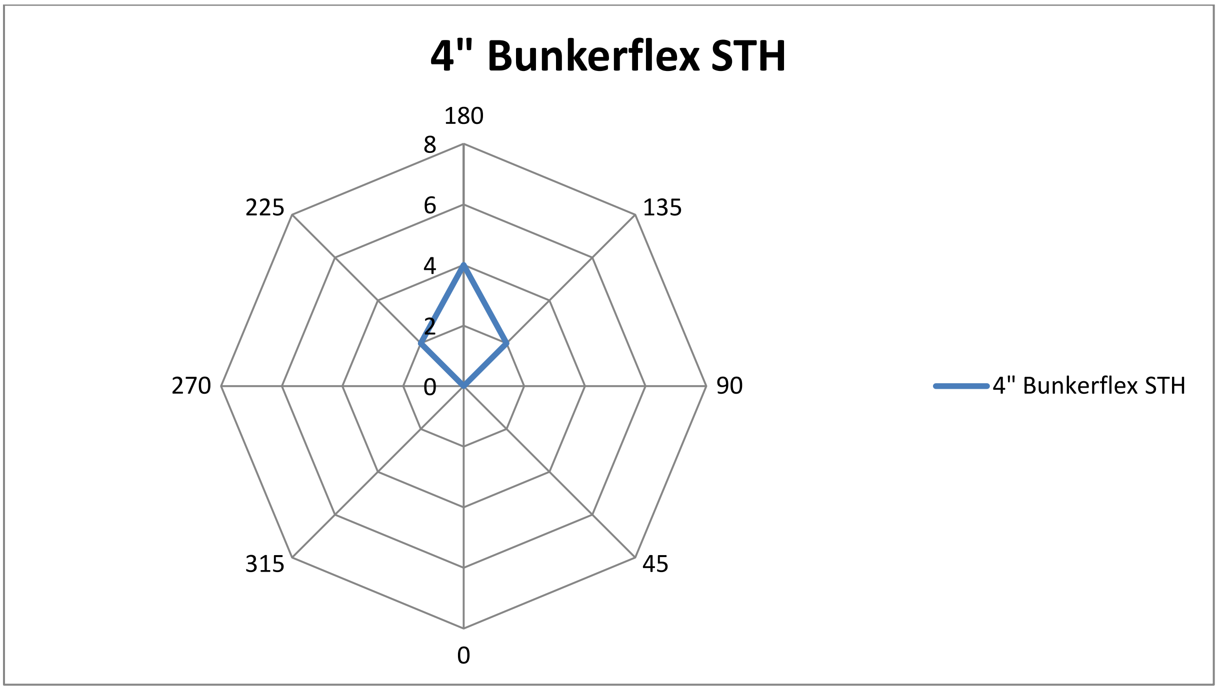

Figure D. 76 - 4” Bunkerflex STH - Free hanging - Wave rose - Current 180°

Free hanging - 270° direction current

Wave direction 135°

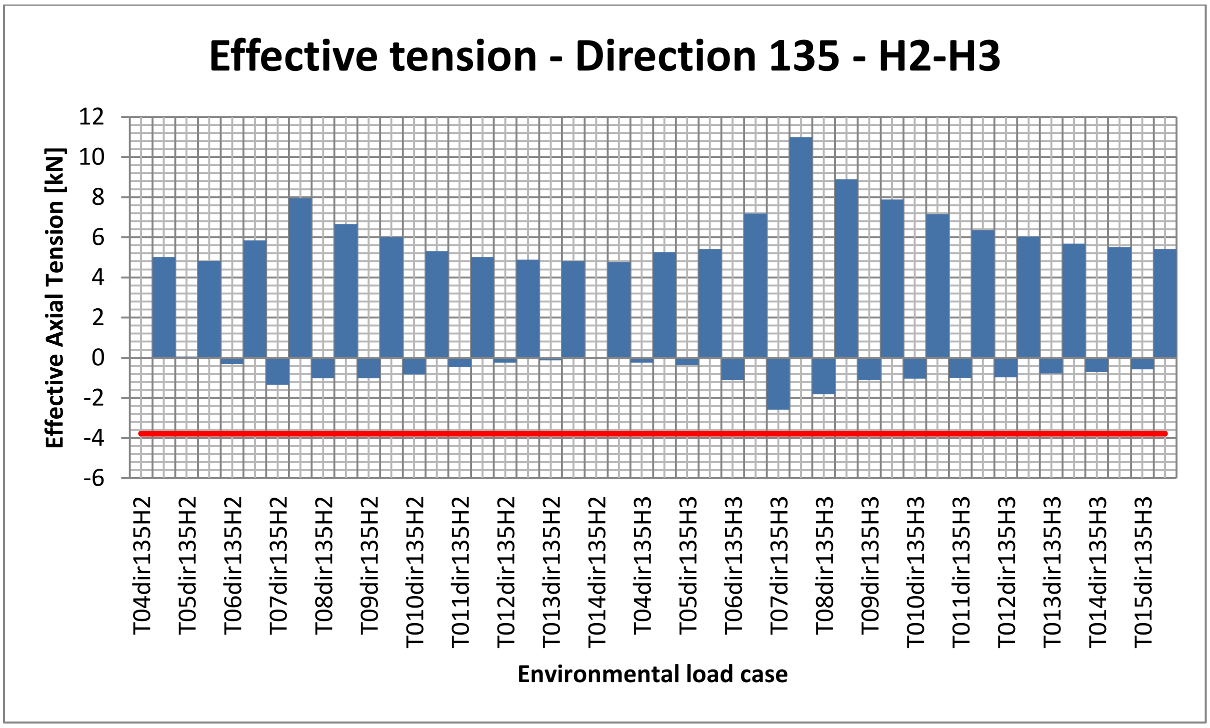

Figure D. 77 - 4"Bunkerflex STH - Free hanging - Effective tension - Direction 135° - H2-H3 - Current 270°

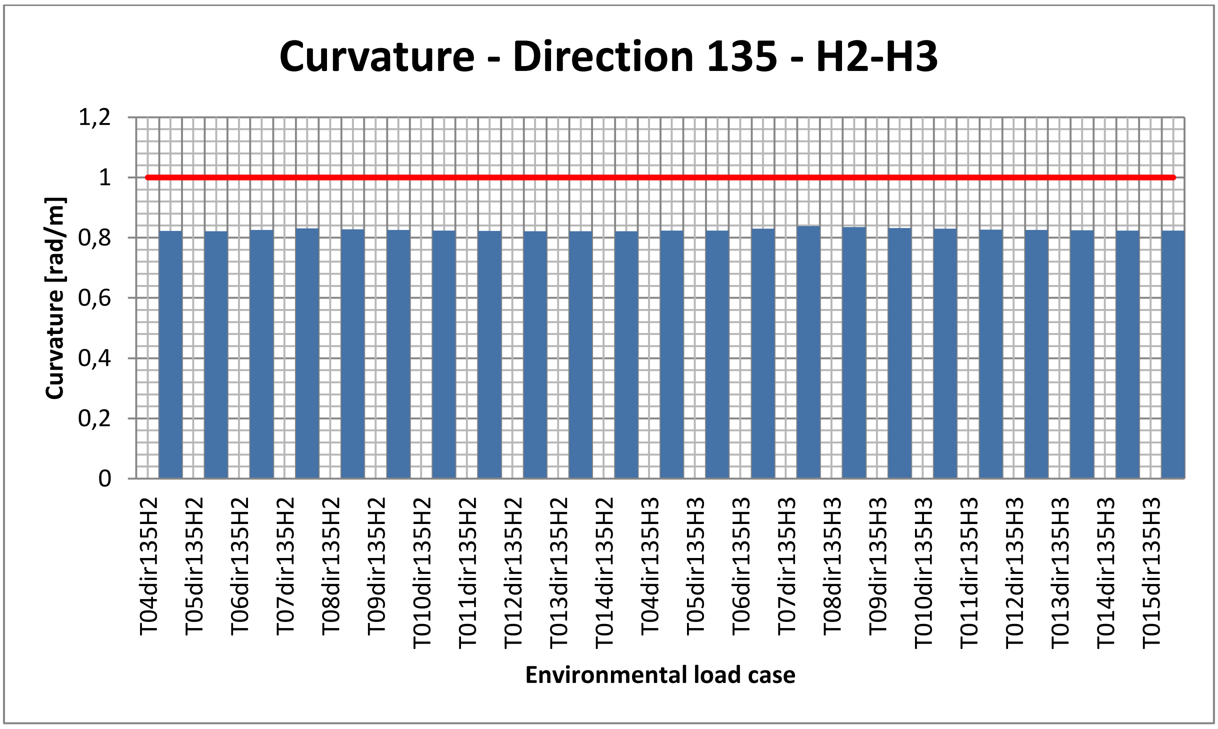

Figure D. 78 - 4"Bunkerflex STH - Free hanging - Curvature - Direction 135° - H2-H3 - Current 270°

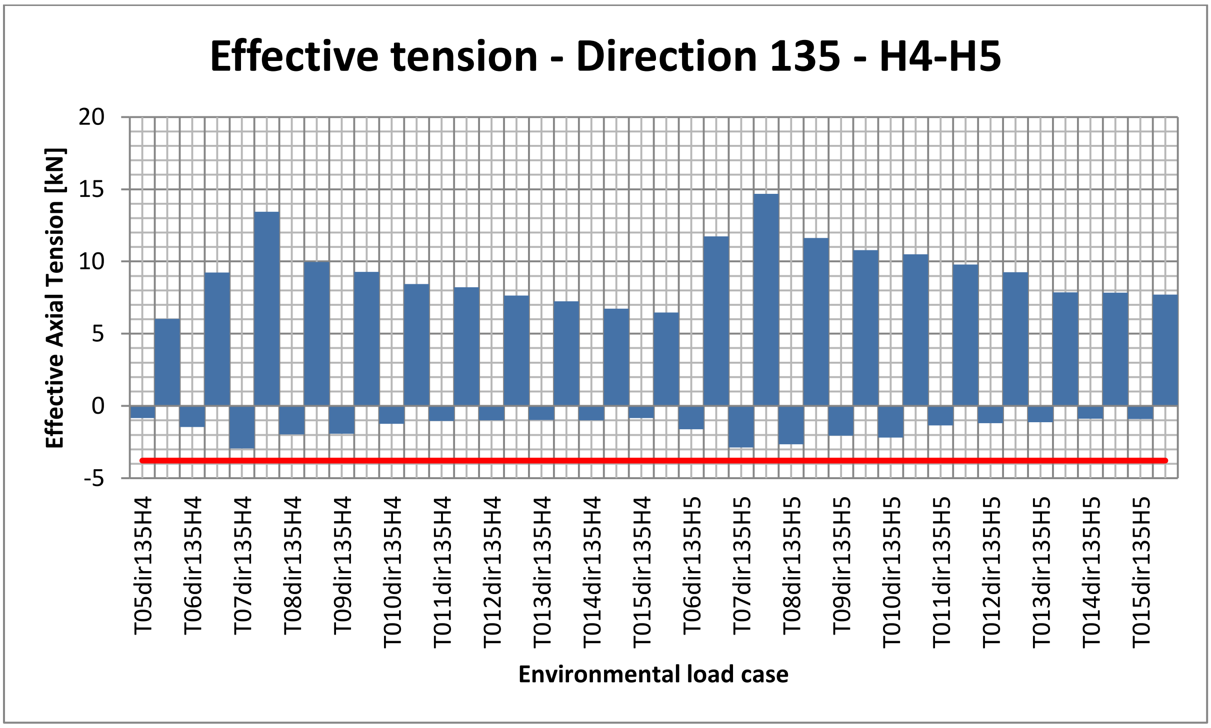

Figure D. 79 - 4"Bunkerflex STH - Free hanging - Effective tension - Direction 135° - H4-H5 - Current 270°

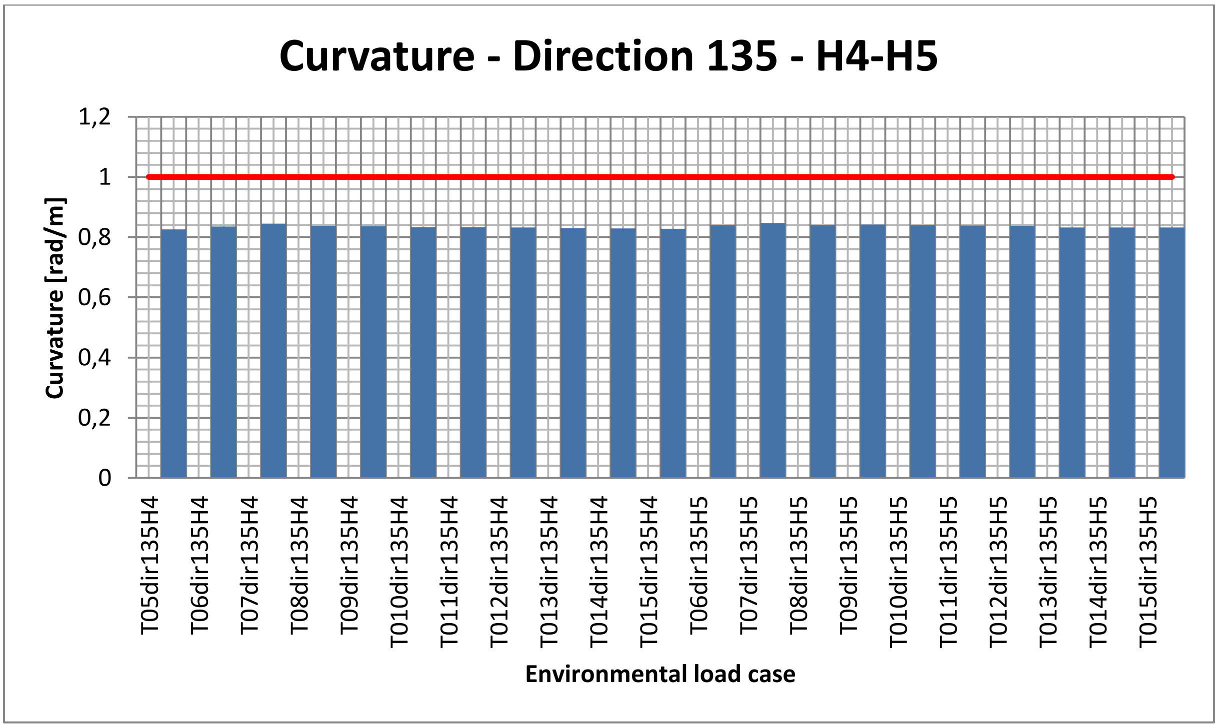

Figure D. 80 - 4"Bunkerflex STH - Free hanging - Curvature - Direction 135° - H4-H5 - Current 270°

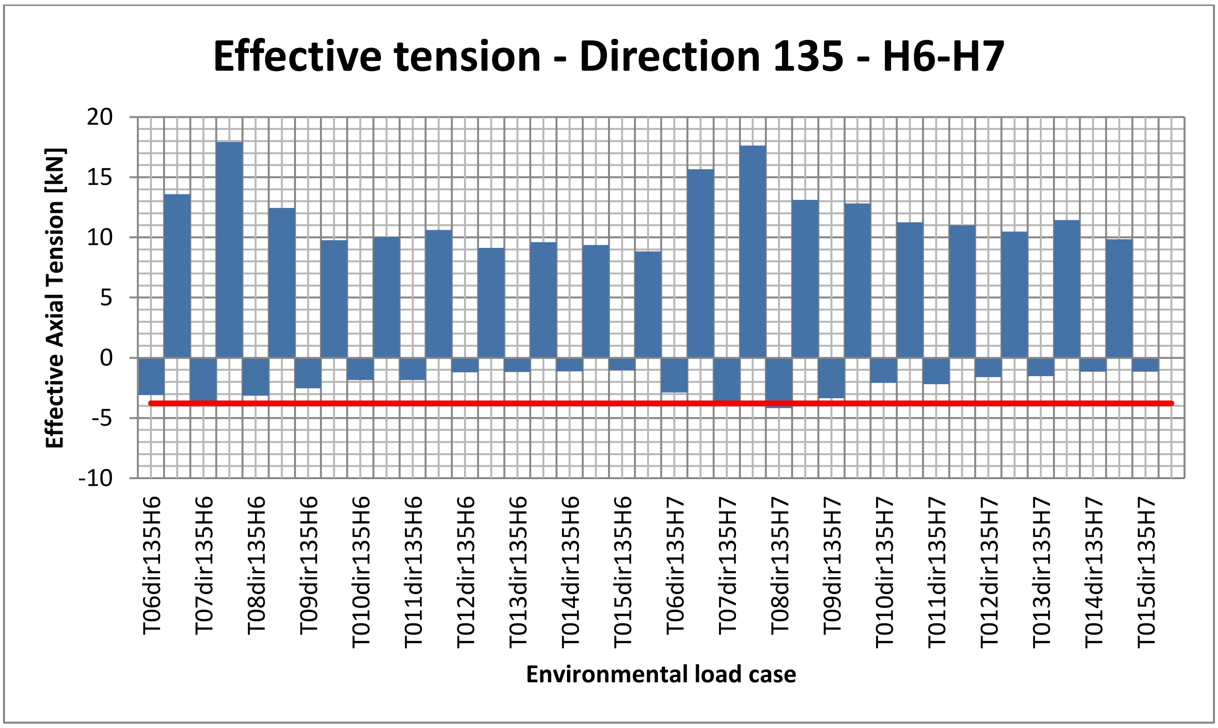

Figure D. 81 - 4"Bunkerflex STH - Free hanging - Effective tension - Direction 135° - H6-H7 - Current 270°

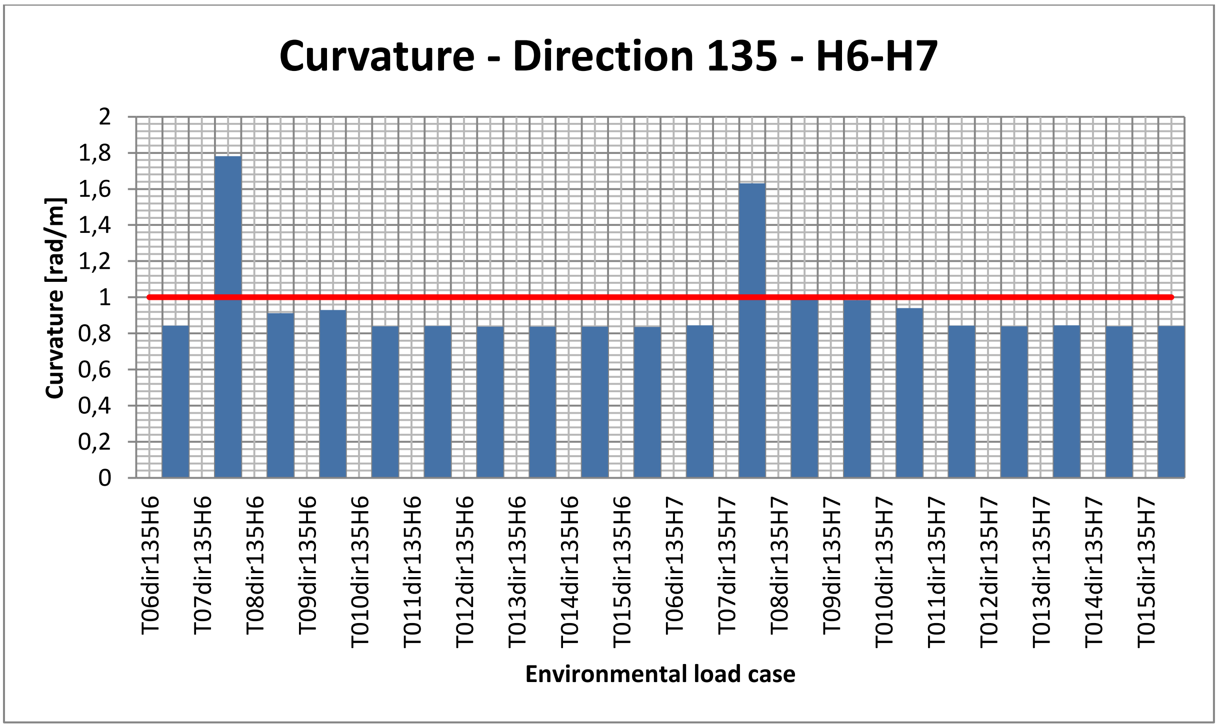

Figure D. 82 - 4"Bunkerflex STH - Free hanging - Curvature - Direction 135° - H6-H7 - Current 270°

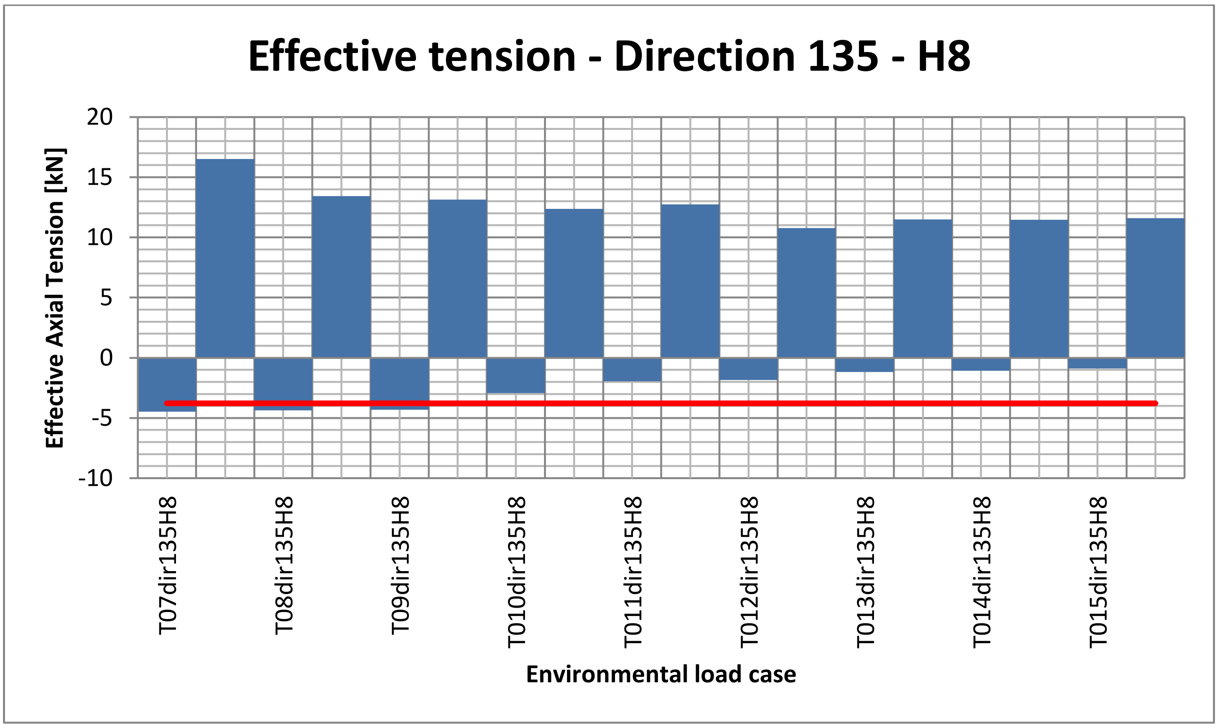

Figure D. 83 - 4"Bunkerflex STH - Free hanging - Effective tension - Direction 135° - H8 - Current 270°

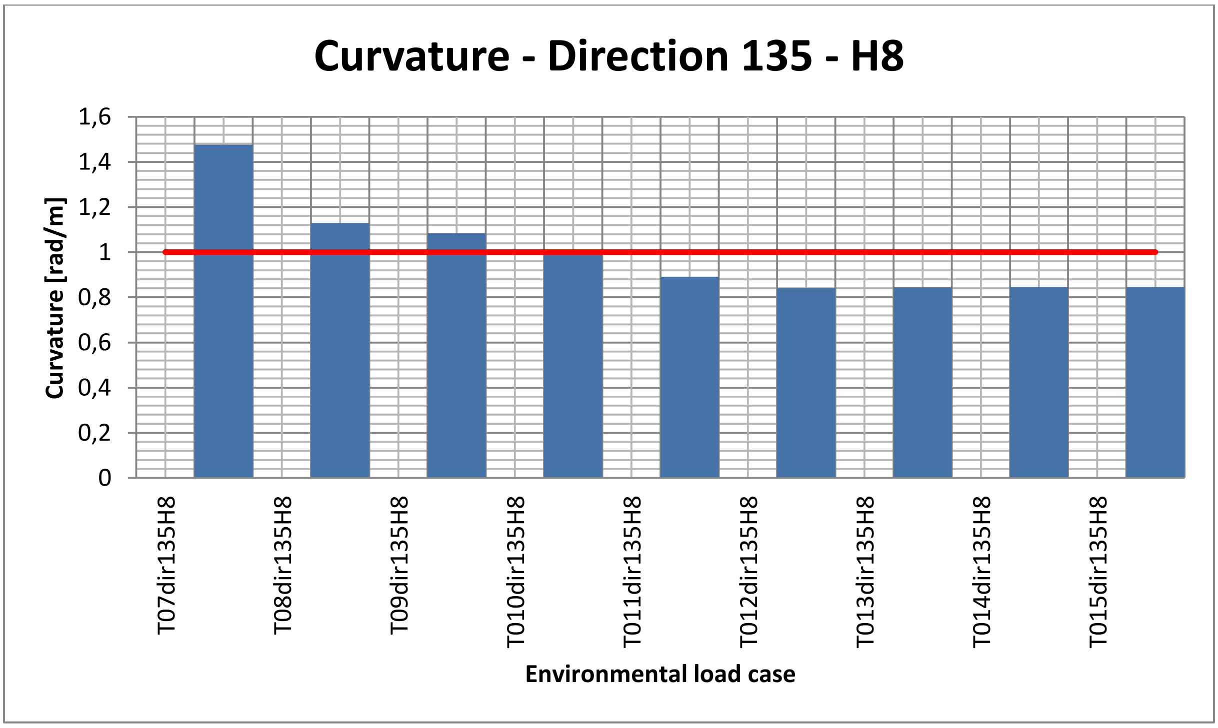

Figure D. 84 - 4"Bunkerflex STH - Free hanging - Curvature - Direction 135° - H8 - Current 270°

Direction 180°

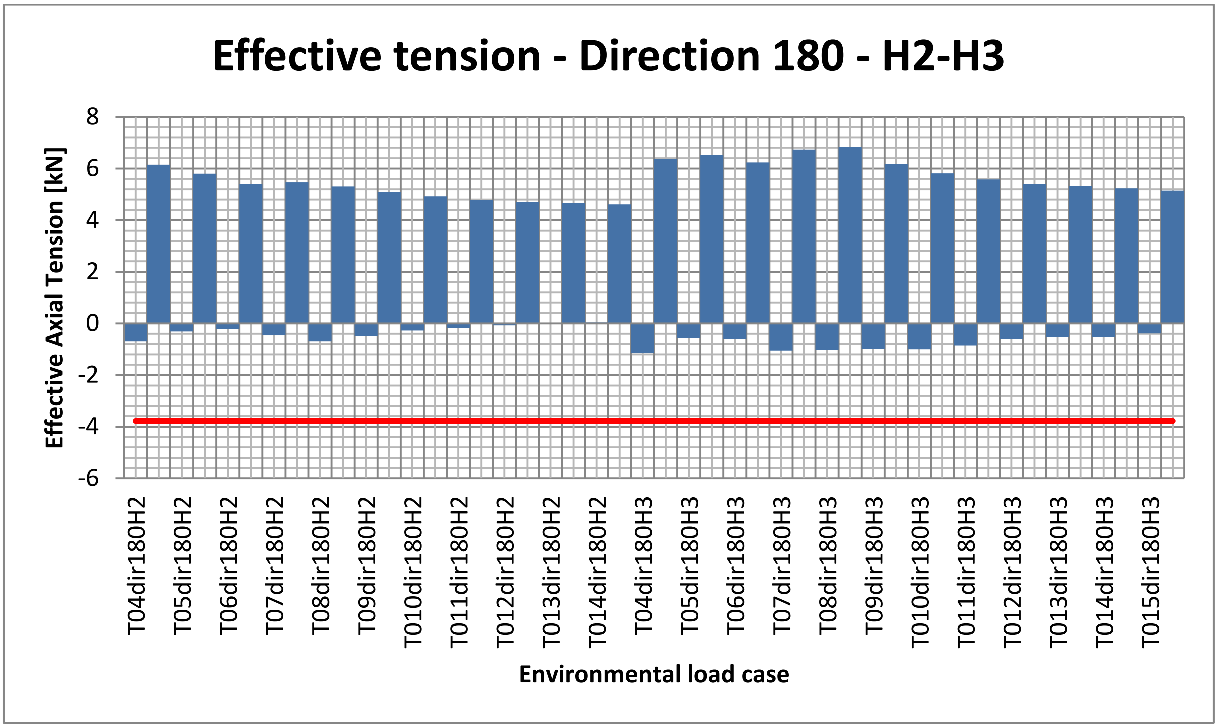

Figure D. 85 - 4"Bunkerflex STH - Free hanging - Effective tension - Direction 180° - H2-H3 - Current 270°

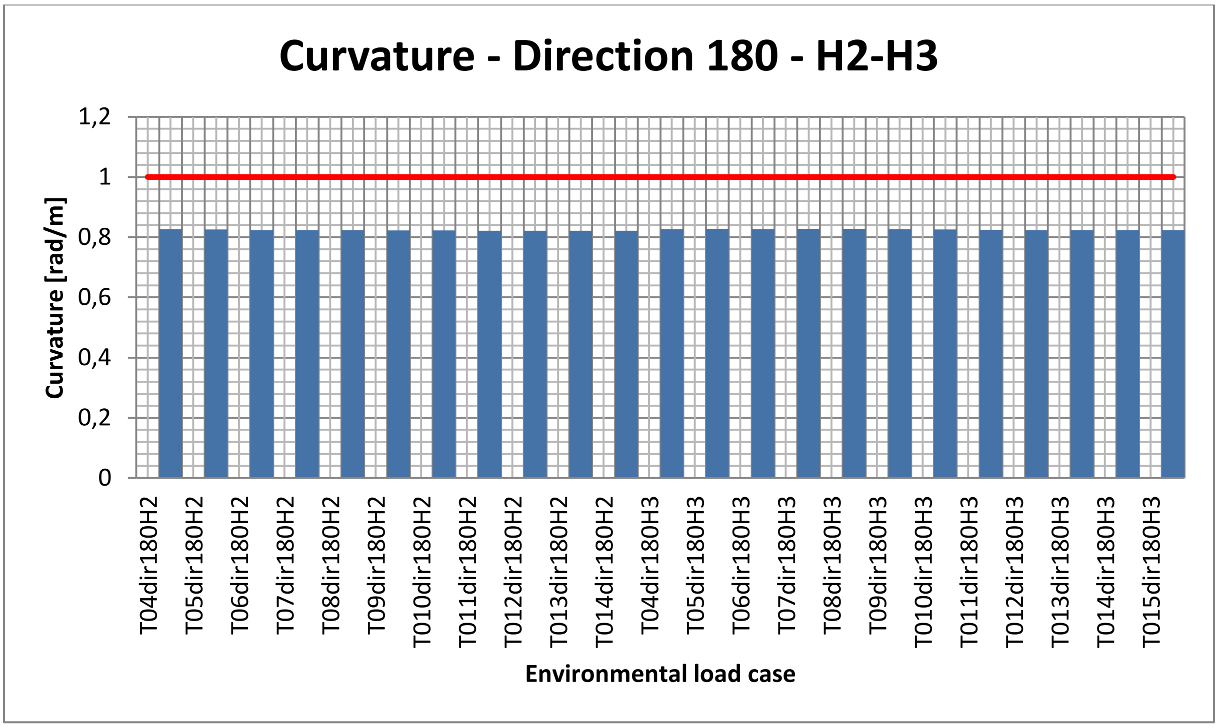

Figure D. 86 - 4"Bunkerflex STH - Free hanging - Curvature - Direction 180° - H2-H3 - Current 270°

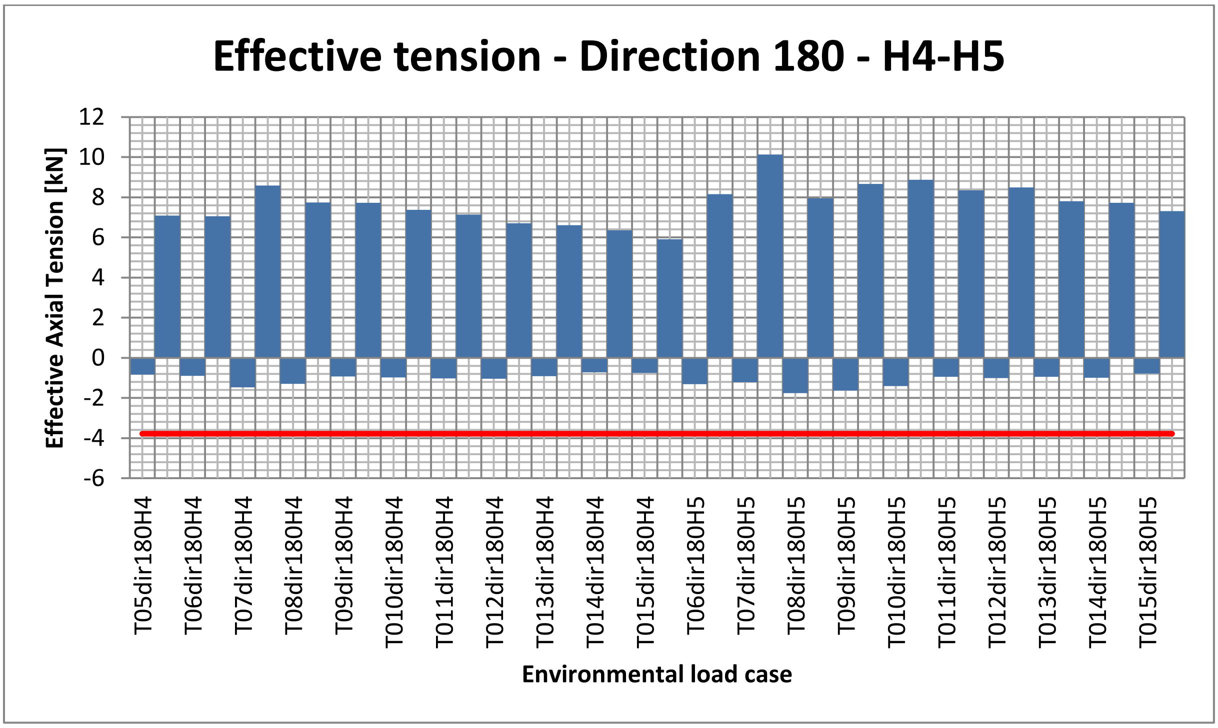

Figure D. 87 - 4"Bunkerflex STH - Free hanging - Effective tension - Direction 180° - H4-H5 - Current 270°

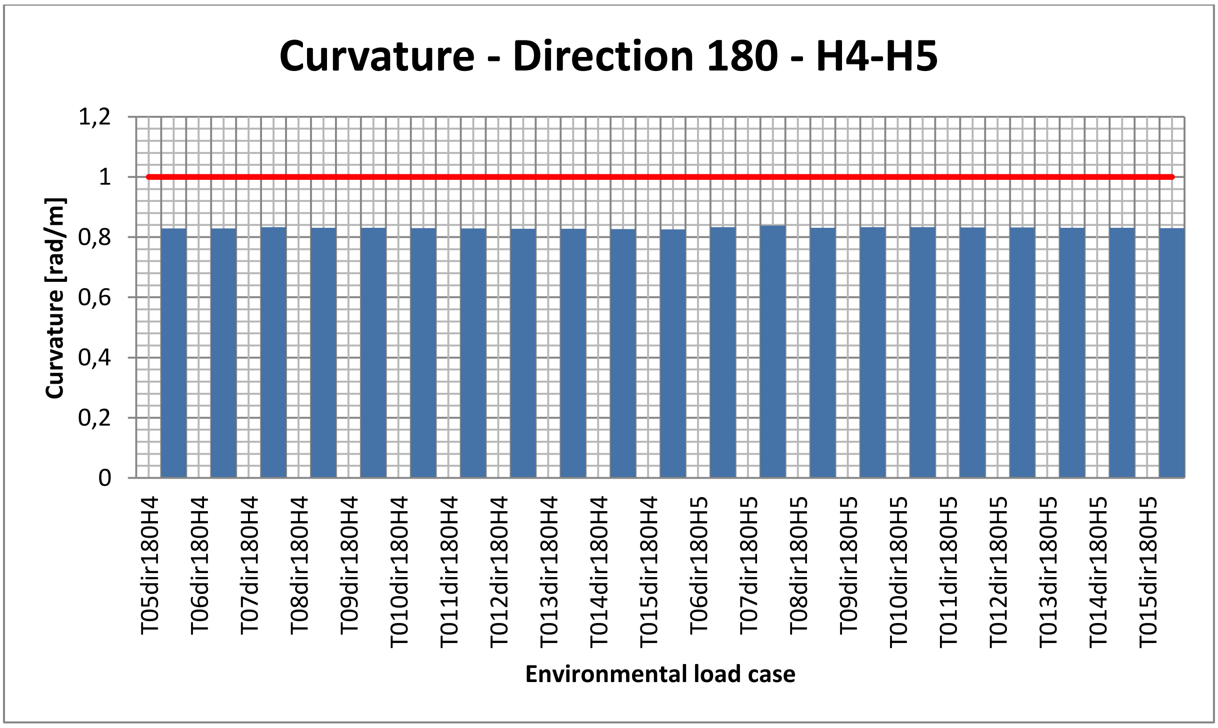

Figure D. 88 - 4"Bunkerflex STH - Free hanging - Curvature - Direction 180° - H4-H5 - Current 270°

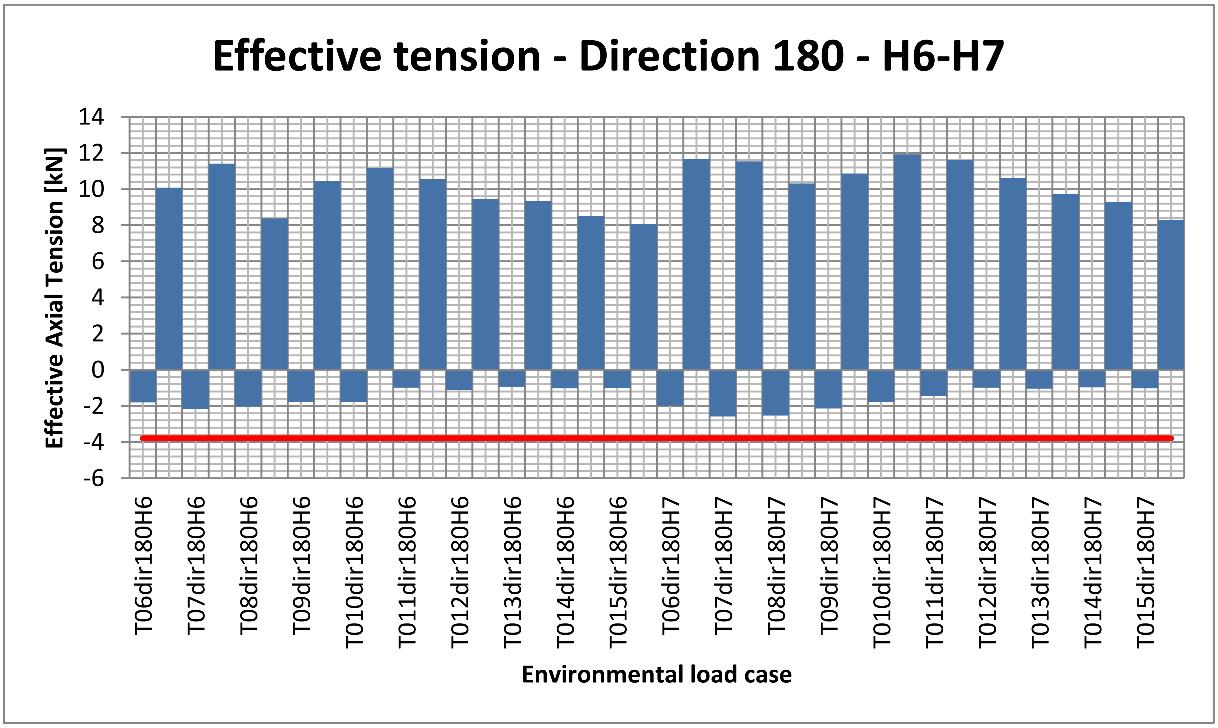

Figure D. 89 - 4"Bunkerflex STH - Free hanging - Effective tension - Direction 180° - H6-H7 - Current 270°

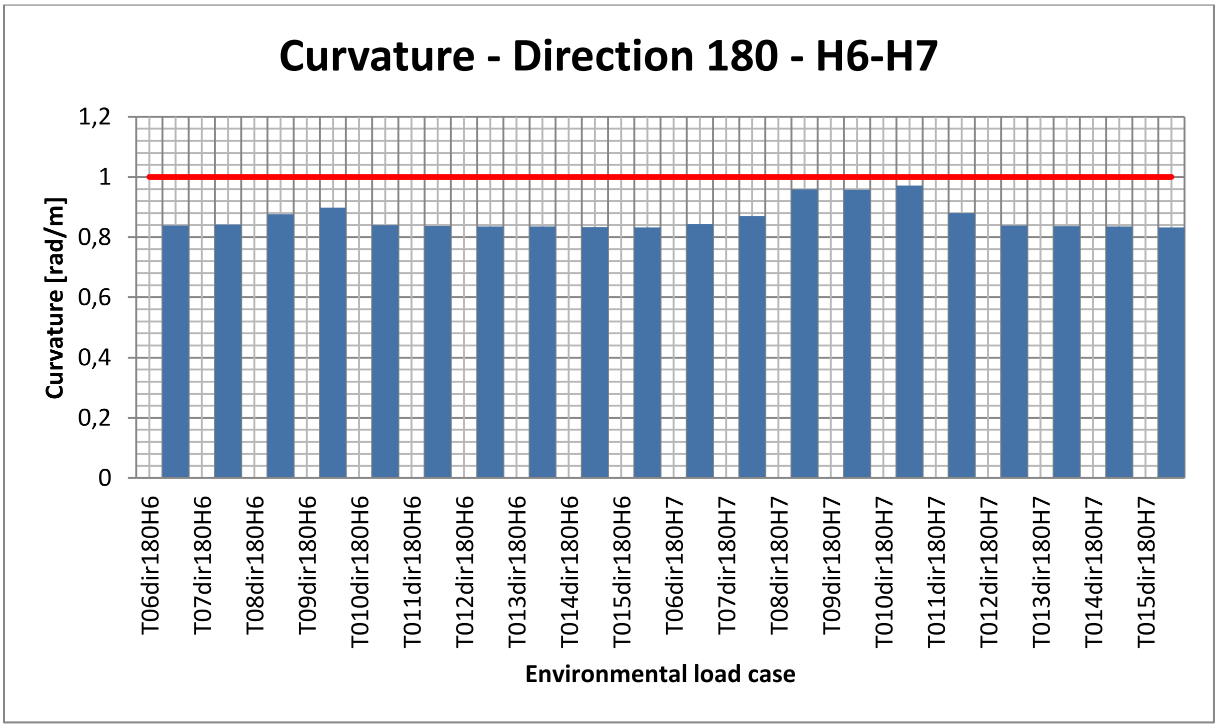

Figure D. 90 - 4"Bunkerflex STH - Free hanging - Curvature - Direction 180° - H6-H7 - Current 270°

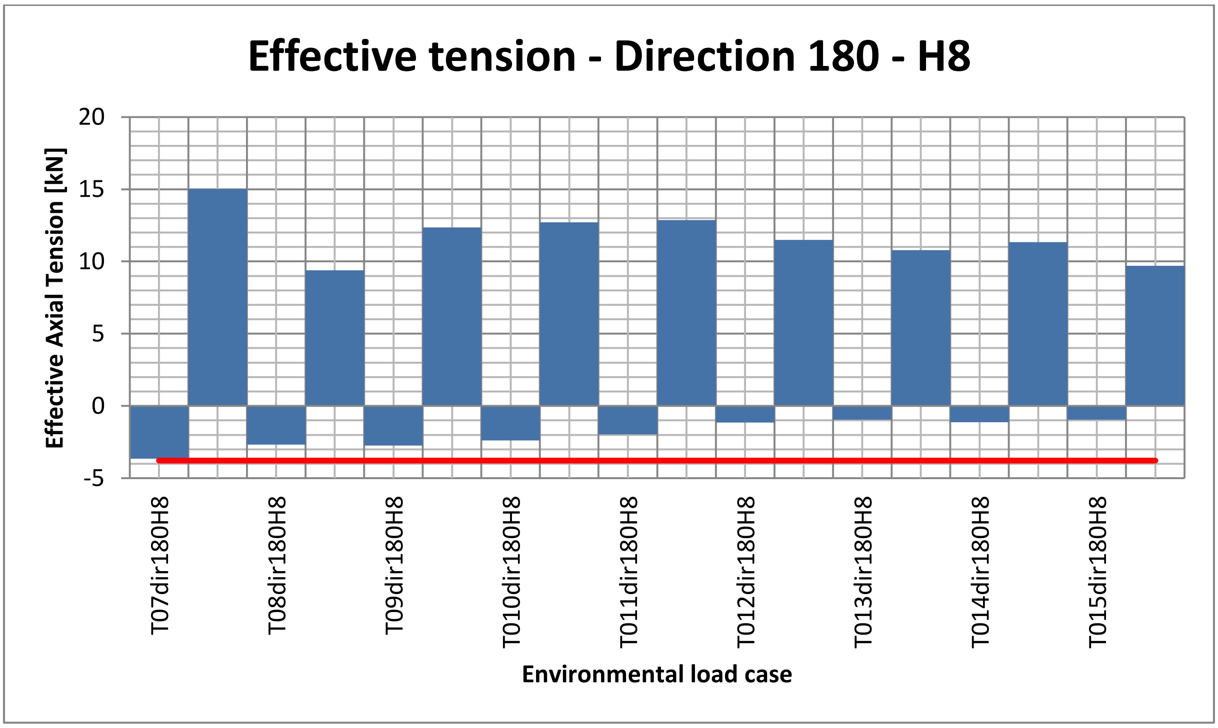

Figure D. 91 - 4"Bunkerflex STH - Free hanging - Effective tension - Direction 180° - H8 - Current 270°

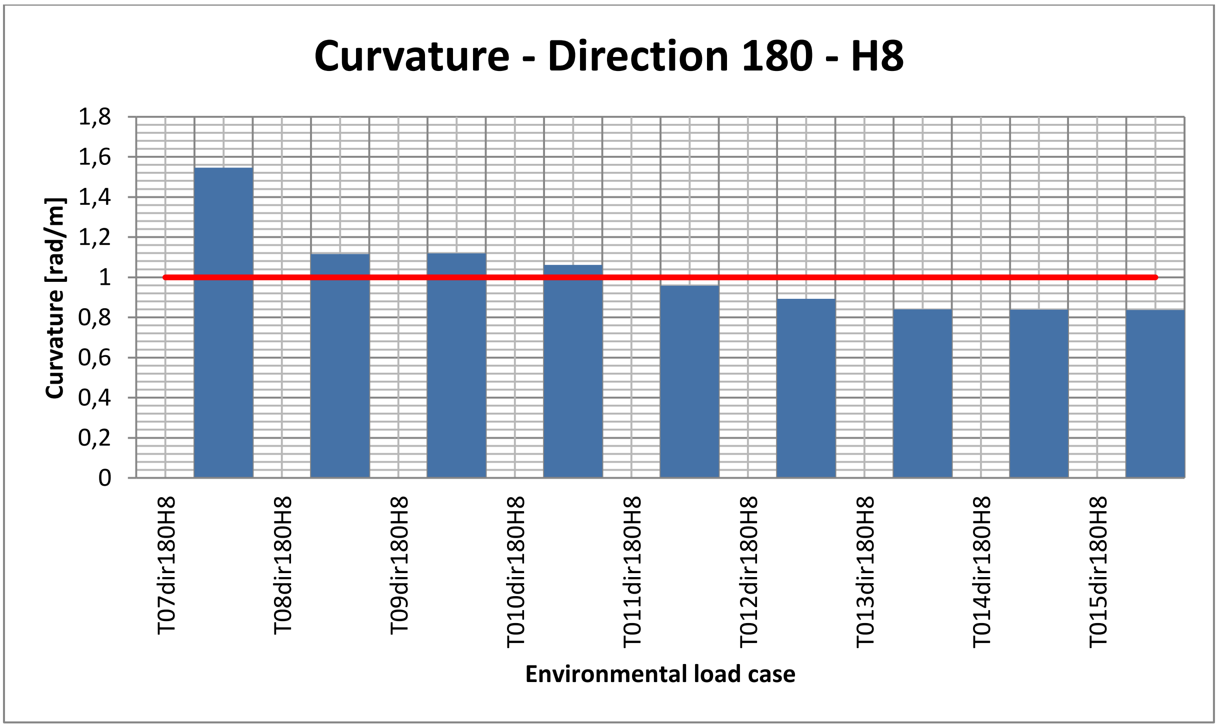

Figure D. 92 - 4"Bunkerflex STH - Free hanging - Curvature - Direction 180° - H8 - Current 270°

Direction 225°

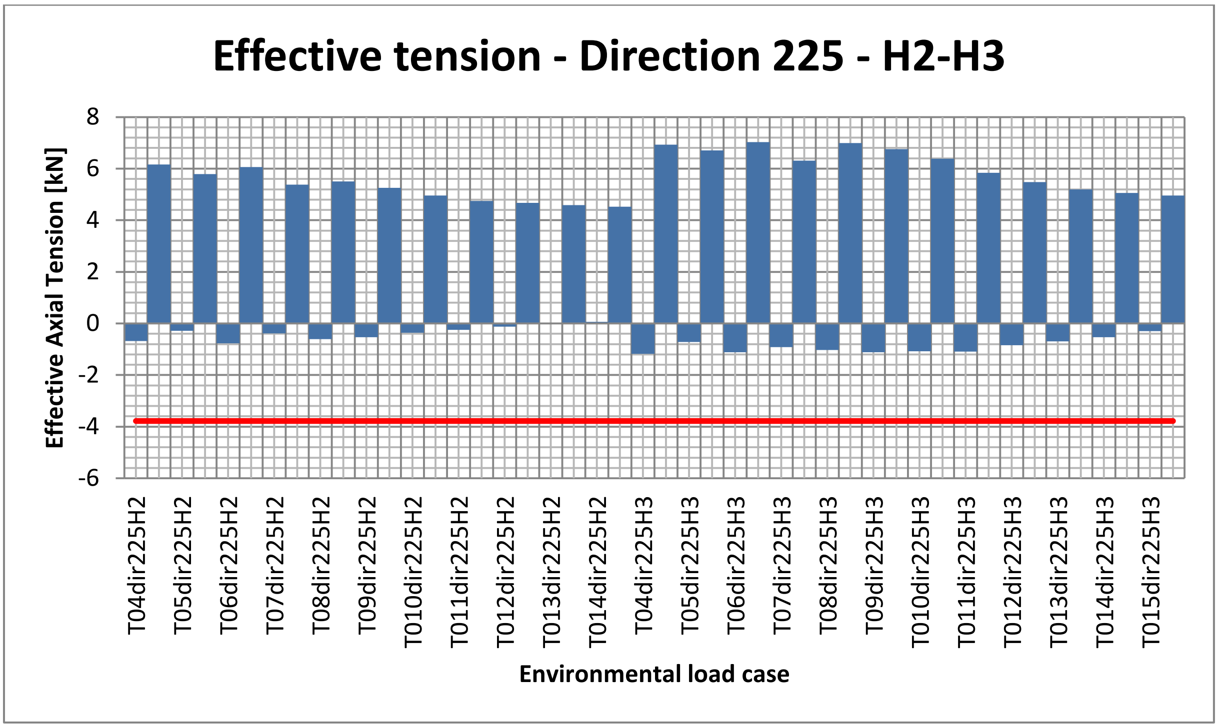

Figure D. 93 - 4"Bunkerflex STH - Free hanging - Effective tension - Direction 225° - H2-H3 - Current 270°

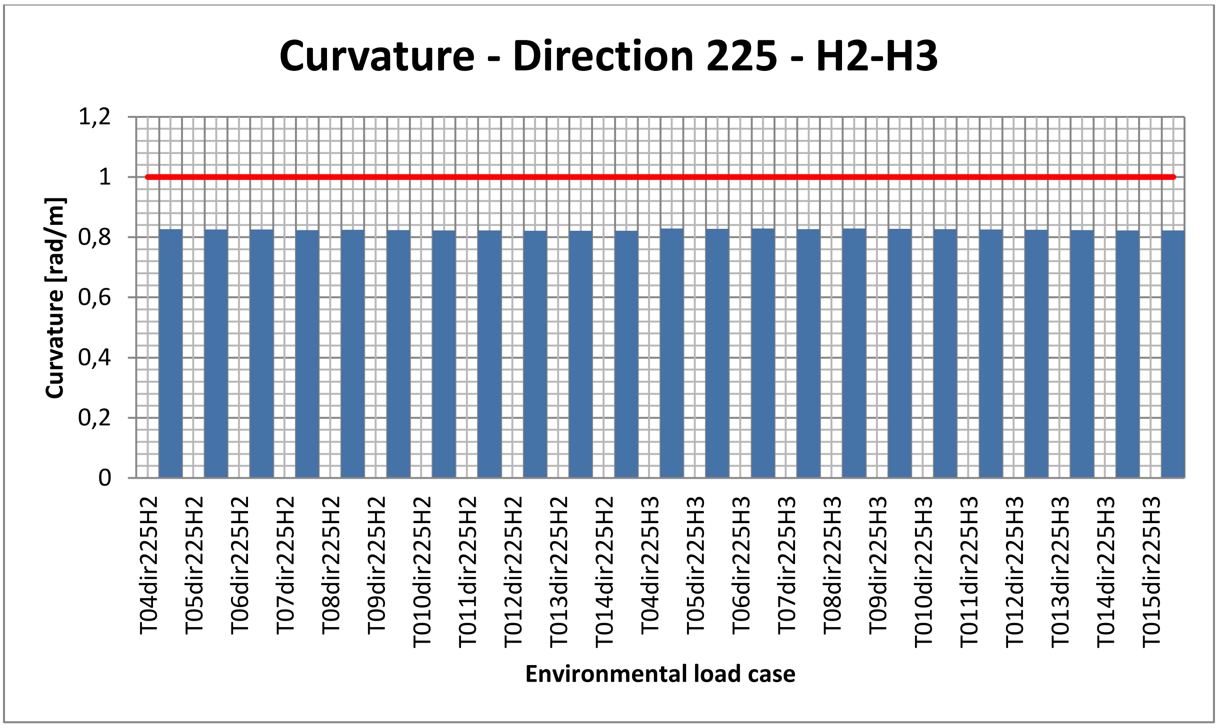

Figure D. 94 - 4"Bunkerflex STH - Free hanging - Curvature - Direction 225° - H2-H3 - Current 270°

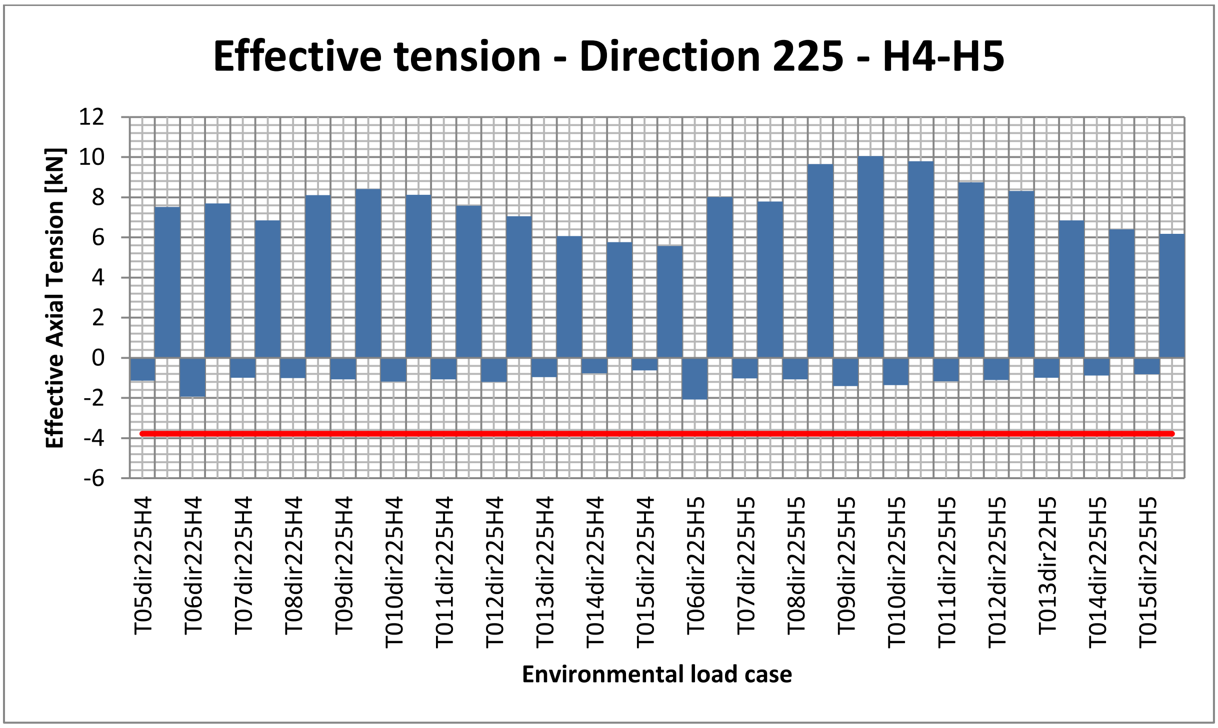

Figure D. 95 - 4"Bunkerflex STH - Free hanging - Effective tension - Direction 225° - H4-H5 - Current 270°

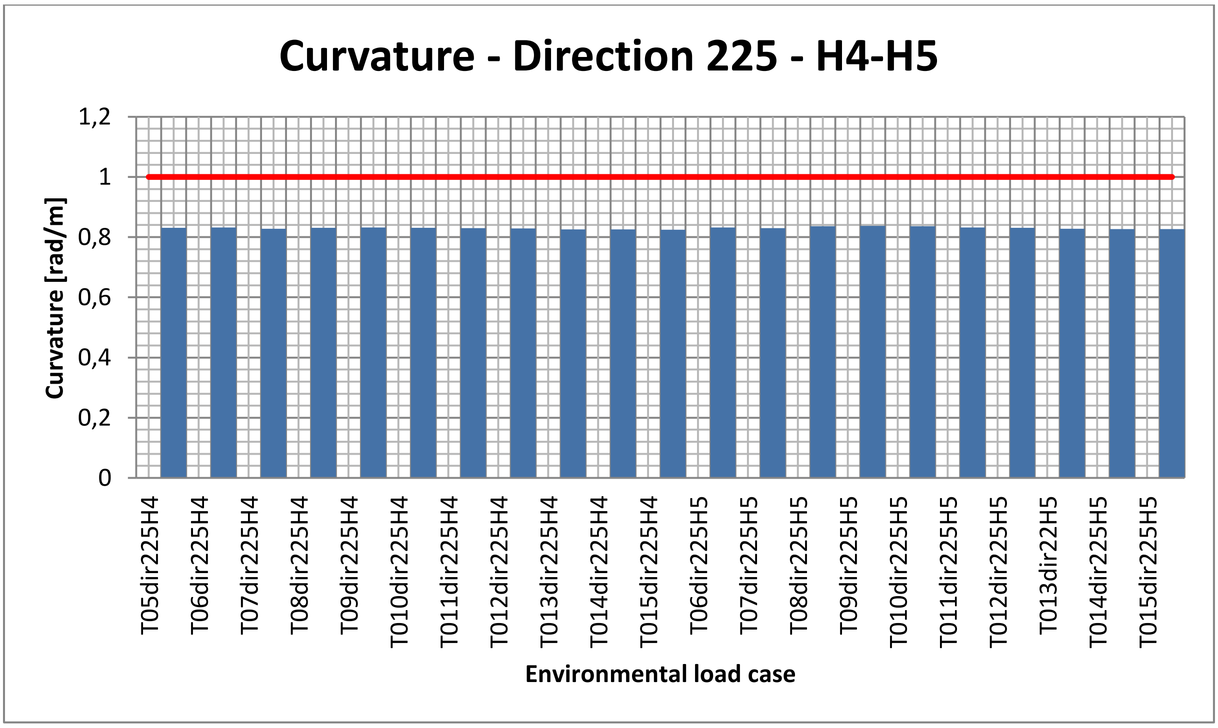

Figure D. 96 - 4"Bunkerflex STH - Free hanging - Curvature - Direction 225° - H4-H5 - Current 270°

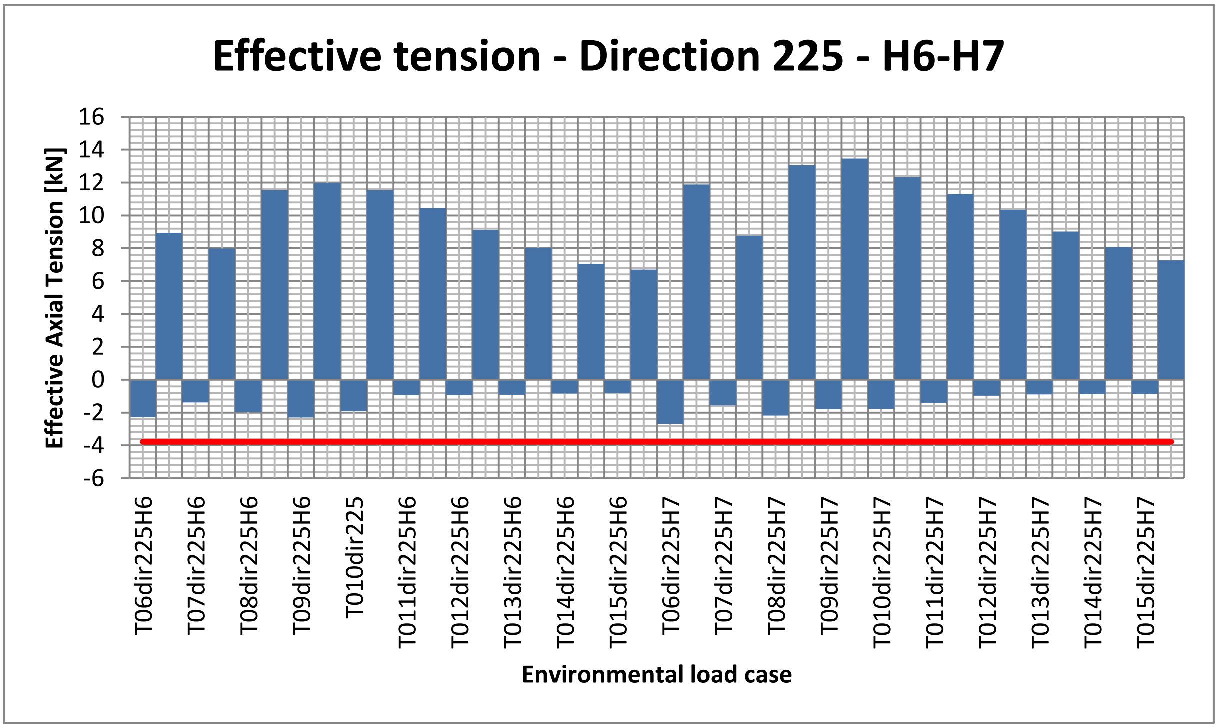

Figure D. 97 - 4"Bunkerflex STH - Free hanging - Effective tension - Direction 225° - H6-H7 - Current 270°

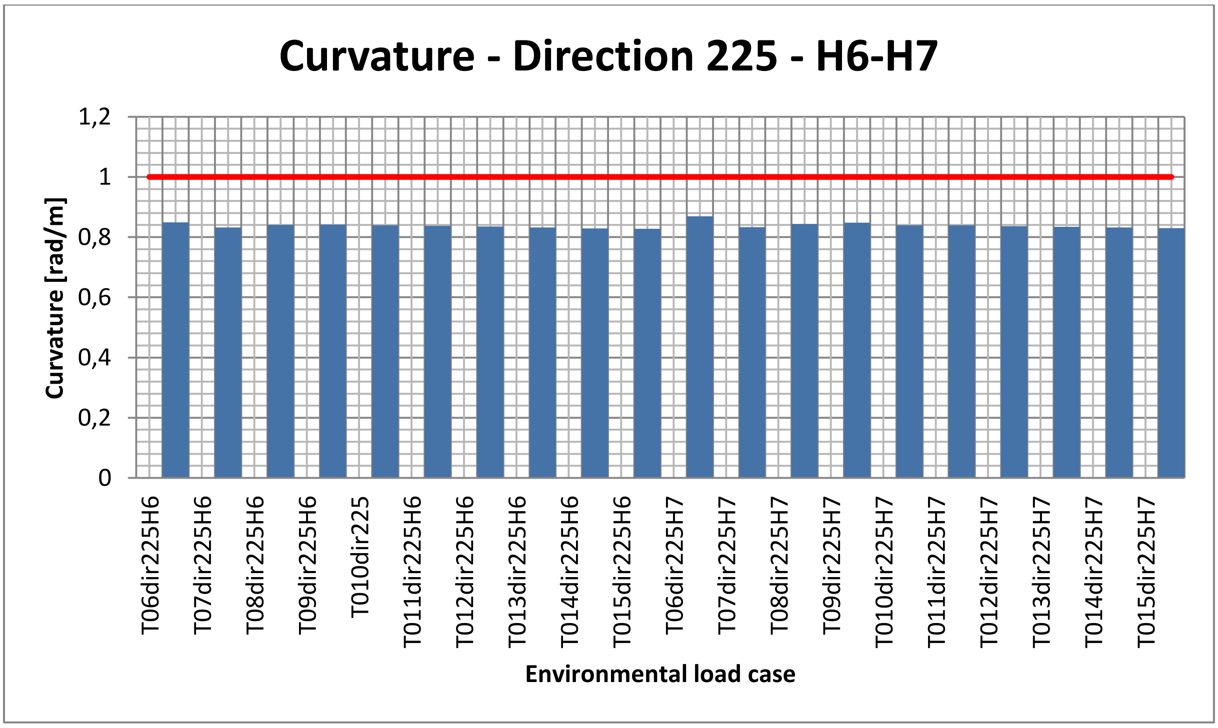

Figure D. 98 - 4"Bunkerflex STH - Free hanging - Curvature - Direction 225° - H6-H7 - Current 270°

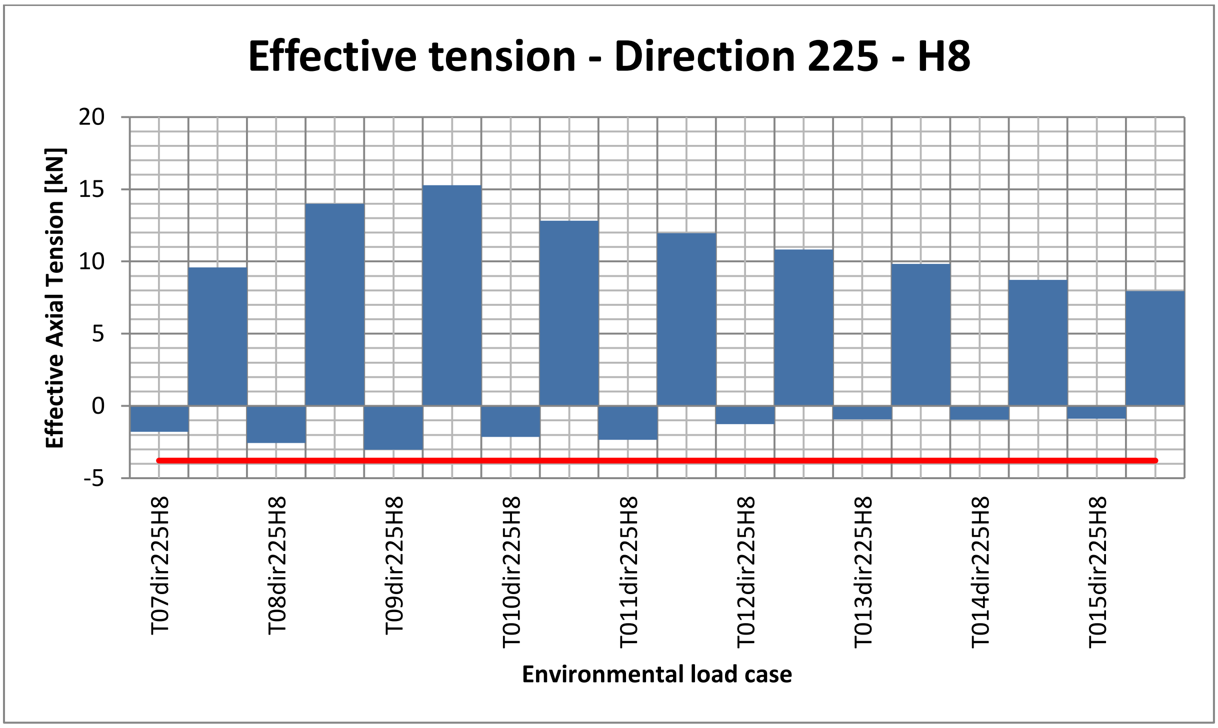

Figure D. 99 - 4"Bunkerflex STH - Free hanging - Effective tension - Direction 225° - H8 - Current 270°

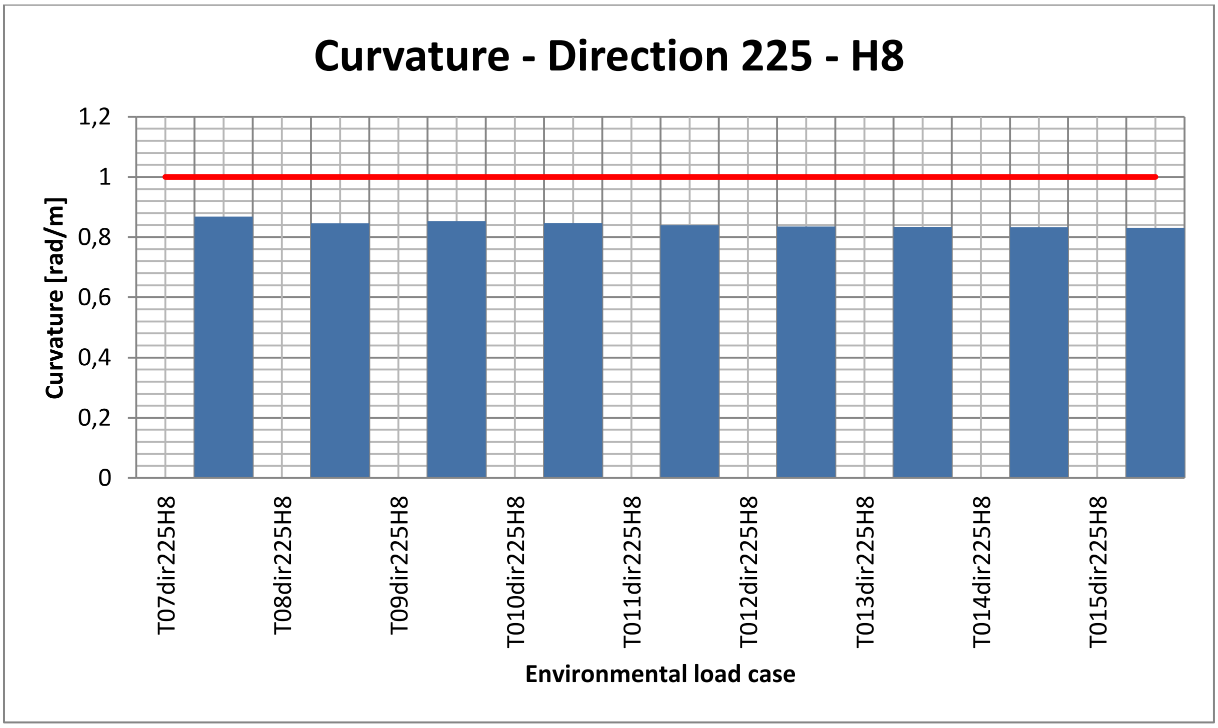

Figure D. 100 - 4"Bunkerflex STH - Free hanging - Curvature - Direction 225° - H8 - Current 270°

Wave rose

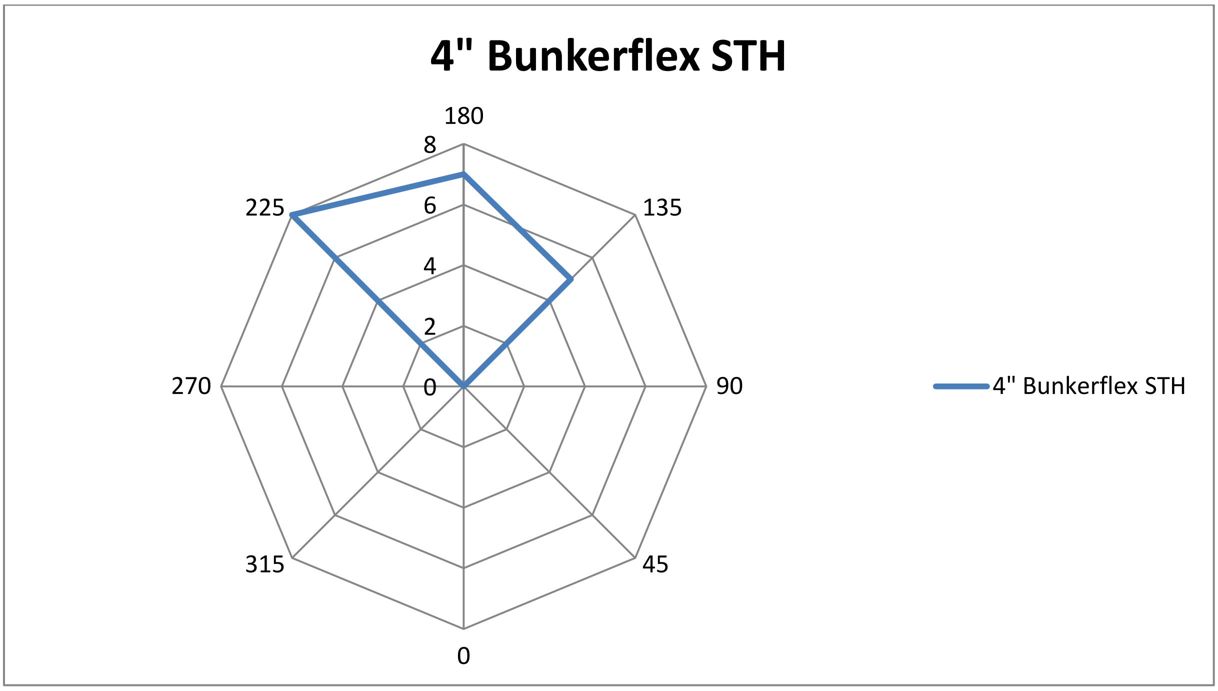

Figure D. 101 - 4” Bunkerflex STH - Free hanging - Wave rose - Current 270°